

AD-A244 869



AGARD-CP-509



AGARD-CP-509

AGARD

ADVISORY GROUP FOR AEROSPACE RESEARCH & DEVELOPMENT

7 RUE ANCELLE 92200 NEUILLY SUR SEINE FRANCE

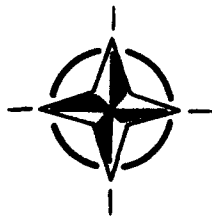
AGARD CONFERENCE PROCEEDINGS 509

Aircraft Ship Operations

(Le Couple Aéronef-Navire dans les Opérations)

DTIC
ELECTE
S D
JAN 23 1992
D

Copies of papers presented at the Flight Mechanics Panel Symposium held in Seville, Spain from 20th-23rd May 1991.



NORTH ATLANTIC TREATY ORGANIZATION

This document has been approved for public release and sale; its distribution is unlimited.

Published November 1991

Distribution and Availability on Back Cover

AGARD

ADVISORY GROUP FOR AEROSPACE RESEARCH & DEVELOPMENT
7 RUE ANCELLE 92200 NEUILLY SUR SEINE FRANCE

AGARD CONFERENCE PROCEEDINGS 509

Aircraft Ship Operations
(Le Couple Aéronef-Navire dans les Opérations)



Accession For	
NTIS GRA&I	<input checked="" type="checkbox"/>
DTIC TAB	<input type="checkbox"/>
Unannounced	<input type="checkbox"/>
Justification	
By	
Distribution	
Availability Codes	
Dist	Avail and/or Special
A-1	

Copies of papers presented at the Flight Mechanics Panel Symposium held in Seville, Spain from 20th—23rd May 1991.



North Atlantic Treaty Organization
Organisation du Traité de l'Atlantique Nord

92 1 22 049

92-01815
■■■■■■■■

The Mission of AGARD

According to its Charter, the mission of AGARD is to bring together the leading personalities of the NATO nations in the fields of science and technology relating to aerospace for the following purposes:

- Recommending effective ways for the member nations to use their research and development capabilities for the common benefit of the NATO community;
- Providing scientific and technical advice and assistance to the Military Committee in the field of aerospace research and development (with particular regard to its military application);
- Continuously stimulating advances in the aerospace sciences relevant to strengthening the common defence posture;
- Improving the co-operation among member nations in aerospace research and development;
- Exchange of scientific and technical information;
- Providing assistance to member nations for the purpose of increasing their scientific and technical potential;
- Rendering scientific and technical assistance, as requested, to other NATO bodies and to member nations in connection with research and development problems in the aerospace field.

The highest authority within AGARD is the National Delegates Board consisting of officially appointed senior representatives from each member nation. The mission of AGARD is carried out through the Panels which are composed of experts appointed by the National Delegates, the Consultant and Exchange Programme and the Aerospace Applications Studies Programme. The results of AGARD work are reported to the member nations and the NATO Authorities through the AGARD series of publications of which this is one.

Participation in AGARD activities is by invitation only and is normally limited to citizens of the NATO nations.

The content of this publication has been reproduced directly from material supplied by AGARD or the authors.

Published November 1991

Copyright © AGARD 1991
All Rights Reserved

ISBN 92-835-0641-3



Printed by Specialised Printing Services Limited
40 Chigwell Lane, Loughton, Essex IG10 3TZ

Preface

The interest in the use of shipborne aircraft is widespread among NATO countries. Major weapons systems like aircraft carriers with conventional fixed-wing aircraft, VSTOL aircraft or helicopters embarked, are operated by the United States, the United Kingdom, France, Italy and Spain. Nearly all NATO countries employ various classes of smaller ships as helicopter platforms for amphibious assault, anti-submarine warfare or search and rescue.

The deployment of aircraft on board ships presents unusual and difficult technical and operational problems. Considering the multi-national interest in aircraft/ship operations it was considered meaningful and timely for the Flight Mechanics Panel to sponsor a symposium on this topic. This symposium considered problems of mutual interest connected with fixed and rotary wing aircraft operations from ships, and the application of new technology to enhance such operations.

The Symposium reviewed and assessed the current problems and possible future progress in:

- The ship environment in terms of wind, temperature, precipitation, turbulence and deck motion.
- Guidance, Controls and Displays, primarily in the approach and landing phase.
- Flight Test and Simulation Techniques.
- Launch, Recovery and Handling Systems Developments.
- Operational/Pilot Views.
- Future Developments.

Préface

La mise en oeuvre d'aéronefs embarqués suscite un vif intérêt dans les différents pays membres de l'OTAN. Les systèmes d'armes majeurs que sont les porte-avions dotés soit de chasseurs conventionnels à voilure fixe, soit d'avions VSTOL, soit d'hélicoptères embarqués, sont en service aux Etats-Unis, au Royaume-Uni, en France, en Italie et en Espagne. La quasi-totalité des pays membres de l'OTAN utilise divers type de navires de moindre tonnage en tant que porte-hélicoptères pour l'assaut amphibie, la guerre anti-sous-marine et les missions de recherche et sauvetage.

Le déploiement d'avions embarqués à partir de bâtiments de guerre pose des problèmes techniques et opérationnels spécifiques et difficiles. Etant donné l'intérêt multi-national manifesté pour les opérations aéronef-navire, le Panel a jugé opportun et positif d'organiser un symposium sur ce sujet. Le symposium a examiné certains problèmes d'intérêt mutuel concernant la mise en oeuvre de aéronefs embarqué à voilure fixe et à voilure tournante, ainsi que les applications possibles des nouvelles technologies pour accroître l'efficacité de telles opérations.

Le symposium a examiné et évalué les problèmes actuels qui se posent et une évolution future possible dans les domaines suivants:

- l'environnement navire, sous les aspects vent, température, précipitations, turbulence et mouvements du pont.
- le guidage, les commandes et la visualisation, principalement lors des phases de d'approche et d'atterrissage.
- les techniques de simulation et d'essais en vol.
- le développement de systèmes de lancement, de recueil et de manutention.
- les aspects opérationnels/points de vue des pilotes.
- les développements futurs.

Flight Mechanics Panel

Chairman: ICA J.-M. Duc
Directeur
Affaires Internationales
ONERA
29, Avenue de la Division Leclerc
92322 Châtillon-sous-Bagneux
France

Deputy Chairman: Prof. L.M.B. da Costa Campos
Pavilhao de Maquinas
Instituto Superior Tecnico
1096 Lisboa Codex
Portugal

TECHNICAL PROGRAMME COMMITTEE

Mr R.A. Russell
Technical Director
Force Warfare
Aircraft Test Directorate
Naval Air Test Center
Code TP02B
Patuxent River
MD 20670-5304
United States

Ir J.T.M. van Doorn
Deputy Director
National Aerospace Laboratory
P.O. Box 90502
1006 BM Amsterdam
The Netherlands

HOST NATION COORDINATOR

Prof. J.L. Lopez Ruiz
SENER, Ingeniera & Sistemas S.A.
C/ Raimundo Fernandez Villaverde, 65
28003 Madrid
Spain

PANEL EXECUTIVE

Mr M.K. Foster

Mail from Europe:
AGARD—OTAN
Attn: FMP Executive
7, rue Ancelle
92200 Neuilly sur Seine
France

Mail from US and Canada:
AGARD—NATO
Attn: FMP Executive
Unit 21551
APO AE 09777

Tel: 33(1) 47 38 57 70
Telex: 610176 (France)
Telefax: 33(1) 47 38 57 99

ACKNOWLEDGEMENT

The Flight Mechanics Panel wishes to express its thanks to the National Authorities of Spain for the invitation to hold this meeting in Seville, and for the facilities and personnel which made the meeting possible.

Le Panel du Mécanique du Vol tient à remercier les Autorités Nationales de l'Espagne pour leur invitation à tenir cette réunion à Séville ainsi que des installations et du personnel mis à sa disposition.

Contents

	Page
Preface/Préface	iii
Flight Mechanics Panel	iv
	Reference
Fixed Wing/Carrier Operations Perspective by P.W. Parcels	1
Helicopter/VSTOL Ship Operations Perspective by R.H. Burn	2
Deck Motion Criteria for Carrier Aircraft Operations by J.H. Pattison and R.R. Bushway	3
The Aerodynamics of Ship Superstructures by J.V. Healey	4
Ship Airwake Measurement and Modeling Options for Rotorcraft Applications by D. Carico, B. Reddy and C. Dimarzio	5
Measurement of the Flow Distribution over the Flight Deck of an Aircraft Carrier by M. Mulero and F. Gomez Portabella	6
A New Method for Simulating Atmospheric Turbulence for Rotorcraft Applications by J. Riaz, J.V.R. Prasad, D.P. Schrage and G.H. Gaonkar	7
Enhanced Displays, Flight Controls and Guidance Systems for Approach and Landing by R.W. Huff and G.K. Kessler	8
Paper 9 withdrawn	
Intégration du Pilotage et des Systèmes d'Aide à l'Appontage pour les Opérations Embarquées par B. Dang Vu, T. Le Moing et P. Costes	10F
Integration of Flight and Carrier Landing Aid Systems for Shipboard Operations by B. Dang Vu, T. Le Moing and P. Costes	10E
Approche et Appontage Assistés par Traitement d'Image Embarqué sur Aéronef par Y. Le Guilloux et R. Feuilloy	11
Approach and Landing Guidance by A.J. Smith and E.J. Guiver	12
Analytical Modeling of SH-2F Helicopter Shipboard Operation by Fu-Shang Wei, E. Baitis and W. Myers	13
Paper 14 withdrawn	
Helicopter/Ship Analytic Dynamic Interface by B. Ferrier, H. Polvi and F.A. Thibodeau	15
Evaluating Fixed Wing Aircraft in the Aircraft Carrier Environment by C.P. Senn	16

	Reference
EH 101 Ship Interface Trials – Flight Test Programme and Preliminary Results by R. Longobardi, G. Vismara and B. Paggi	17
Determination of Limitations for Helicopter Ship-Borne Operations by R. Fang	18
United Kingdom Approach to Deriving Military Ship Helicopter Operating Limits by B.A. Finlay	19
A Review of Australian Activity on Modelling the Helicopter/Ship Dynamic Interface by A.M. Arney, J. Blackwell, L.P. Erm and N.E. Gilbert	20
United States Navy Ski Jump Experience and Future Applications by T.C. Lea, III, J.W. Clark, Jr and C.P. Senn	21
Helicopter Handling: Experience and New Developments by W.R.M. Reimering and T. Craig	22
Comportement Dynamique d'un Avion sur ses Atterrisseurs: Expérimentation et Validation par Franchissement d'un Dièdre par D. Fleygnac et E. Bourdais	23
Some Implications of Advanced STOVL Operation from Invincible Class Ships by K. Ainscow and P.G. Knott	24
Paper 25 withdrawn	
Fixed Wing Night Carrier Aeromedical Considerations by J.C. Antonio	26
Limitation des Opérations des Hélicoptères dans le Milieu Aéronaval par D. Falcinelli	27
Revolution at Sea: Aircraft Options for the Year 2030 by J.C. Biggers and P.A. Silvia	28

KEYNOTE ADDRESS
FIXED WING/CARRIER OPERATIONS PERSPECTIVE

by

RADM P.W. Parcels, USN
 Commander, Tactical Wings, Atlantic Fleet
 Naval Air Station Oceana
 Virginia Beach, Virginia 23456-5125
 United States

I. INTRODUCTION

Good morning ladies and Gentlemen. I'm RADM "Wick" Parcels of the United States Navy, and I will be speaking on behalf of VADM Jack Ready, Commander, Naval Air Force Atlantic Fleet. His extremely heavy schedule precluded his being here to address you today, but that workload has given me this unexpected pleasure.

It is an honor to participate in this symposium, and I'm particularly pleased to be asked to address a topic which has been my professional life for over 30 yers. The subject of fixed wing carrier operations covers a field that is as broad as it is deep, touching so many interesting subcategories and evoking so many memories that it is probably fortunate for you that my time is restricted. I will address four specific areas: Carrier and Carrier Battle Group structure, organization, and function; carrier air wing structure and missions; flight operations; and future developments in fixed wing carrier operations.

In post-world War II Terms, the greatest conflict in fixed wing

carrier philosophy has been the extend to which aircraft design must be compromised to enable it to be flown successfully from a ship of reasonable size and cost. Pre-world II aircraft could, in general, be launched and recovered without significant help from anything but the wind. The Royal Navy's evacuation of RAF aircraft from Norway during the early stages of the war comes to mind. As combat requirements increased, the flying machines necessarily became more sophisticated - heavier being a useful equivalent to more sophisticated. Toward the end of that war, many combat loaded aircraft required catapulting, and virtually all needed arresting gear to recover. Thus, at that time, limits to the size and complexity of the combat aircraft were frequently defined by the capability of shipboard catapult and arresting gear machinery, and to a lesser extent, by the size of the flight deck. Therefore, at that stage, land based aircraft built without the heavy modification required of a combat carrier aircraft threatened to outclass the seaborne types. In addition, aircraft in development at that time - 1944 -46 - required catapult and

arresting gear specifications beyond those existing even on the excellent "Essex" class heavy fleet carrier.

Aircraft technology grew by leaps and bounds in the post World War II era. With the shrinking budgets after the war, cost became more and more of a limiting factor - a factor which basically did not even have to be considered during the war. The cost factor generated another philosophical conflict which continues in one form or another to this day: Do we build a carrier to exploit aircraft capabilities, or design aircraft to live within the carrier's limitations. What pushes what? This energetic debate had and has many ramifications that are familiar to anyone who has fought a budget battle. The question revolves around the ever present questions: How much do we need; how much can we afford; and how much is enough, but not too much; i.e., too costly?

The U.S. defines a Carrier Battle Group (CVBG) as a strike force, since it contains the preponderance of the U.S. Navy's conventional war fighting capability. To protect that strike capability, our battle groups contain a large "sunk cost" in fighter and early warning aircraft. That sunk cost may threaten to be too expensive, hence the trend toward true multi-role aircraft. Multi-role aircraft, of course, cost more and we get back to the question of how expensive is too expensive? The cost versus effectiveness debate has encompassed the building of carriers, with the added dimension of

survivability. Given the number and complexity of carrier aviation missions, aircraft carriers have necessarily become large and more expensive. The large versus small carrier debate in the U.S. has become muted in recent years, as most realize that little is gained in numbers or costs of deployable carriers by down scaling their size, while a significant potential loss is evident in capability, sustainability, and survivability. While much of the debate is emotional and conjectural, perhaps the most telling argument is the physics of ship design, which essentially dictate that ships half the size of the NIMITZ will still require about 2/3 of the power plant, and a half size carrier may not allow even half as many aircraft or mission capabilities, and will almost certainly not mean half the crew, shop space, support equipment, etc. It is also doubtful that a half size attack carrier would be less of an inviting target, or would be equally effective in combat, or survivable while under attack. We believe that we have arrived at the optimum size carrier with optimum capabilities and potential, but more on that in a moment.

CARRIERS AND CARRIER BATTLE GROUPS

As I mentioned, the Navy's conventional war fighting capability resides in the Carrier Battle Group (CVBG). This potent force is composed of at least one large deck carrier (with an air wing of 70 to 90 aircraft), 1-3 AEGIS Cruisers, 1-3 Guided Missile Destroyers, 103 Fast Frigates, 102 Attack Submarines, and 1-3

Combat Oilers and Stores ships.

The main battery of the mobile and versatile battle group is the people - the crews who man the ships and aircraft.

However, our purpose at AGARD is to discuss the machines that those people will operate. Not only aircraft, but tomahawk and harpoon cruise missiles in their surface-to-surface modes give the force nearly unprecedented long range striking power, though the cruise missiles come at a much higher unit cost and are constrained by limited numbers.

The basic carrier battle group plans and trains as a single force, able to conduct simultaneous operations in our four basic combined warfare groups: Anti-Air (AAW), Anti-Surface (ASU), Anti-Submarine (ASW), Electronic Warfare (EW) as well as Airborne Logistics/Supply and Coordination (ARE). Significant synergistic economies of scale are achieved when two or more carrier battle groups conduct combined operations. These economies are particularly useful in multiplying available strike aircraft and reducing the number of anti-air assets required to cover a given area. How, Where, and When this synergism becomes useful is dependent on the level and complexity of the threat to the force.

The aircraft carrier itself is the centerpiece, heart and soul, and most expensive item in the battle group. All of the problems and opportunities inherent in a discussion of the fixed wing carrier perspective necessarily revolve around the

"Bird Farm." The United States presently operates five classes of big-deck, fixed wing fleet carriers: The Midway, The Forrestal Class (four ships), the Kitty Hawk Class (four ships), the Enterprise (a nuclear powered Kitty Hawk Class), and the Nimitz Class (five ships). Our Navy has settled on the Nimitz class as our deck of choice, the debates on size, cost, and complexity continuing apace of course. All carriers are organized and equipped in a standardized fashion, based on the lessons of over 60 years of large fleet carrier work and warfare. They embark up to 100 aircraft of differing types. The carrier's fixed wing aircraft can reach approximately 90 percent of the earth's surface. Using internal assets only, they can detect, target, and attack airborne, surface or subsurface hostile forces; support ground forces and interdict enemy forces at the beach or inland; and provide an ever present nuclear deterrent. The carrier is the heart of our naval force, and is as modern as its aircraft and air wing. Its size, mobility, endurance, structural strength, compartmentalization, protective armor and sophisticated damage control systems make it the most effective and least vulnerable surface warship ever constructed.

The aircraft carrier is commanded by a highly experienced designated naval aviator. The ship is divided into departments and divisions for maximum efficiency in administration and training, as well as combat operations. A

modern carrier with its air wing embarked may include a crew of over 6000. Incidentally, of these, about 1/3 turn over every year and the average age of the crew is less than 20 years.

III. THE CARRIER AIR WING

As mentioned, the battle group contains potent strike and defensive armament in all its combatants. However, the main striking force remains the air wing. Although we operate several classes of aircraft carriers, the air wing is standardized in aircraft and equipment.

The air wing is composed of seven to nine fixed wing squadrons of differing types and one helicopter squadron, all with overlapping missions. This aircraft mix allows simultaneous search, surveillance and attack operations as well as fighter protection for the battle group and strike aircraft. Included in the capabilities of a modern air wing are airborne early warning, electronic warfare, in-flight refueling, photo reconnaissance, anti-submarine warfare, and combat search and rescue.

The primary fighter aircraft is the F-14 Tomcat, of Hollywood fame. A thirty ton, variable wing sweep fighter, its speed, versatility, and agility belie its size as it brings the most powerful fighter radar in the world into combat, as well as four different air-to-air weapons, the 50 mile phoenix, the 15 mile sparrow, the 3 mile sidewinder, and a six barrel, 2000 rounds/minute 20mm

cannon.

The primary attack aircraft in the air wing's arsenal is the A-6E Intruder, a long range, combat proven workhorse which is perhaps the premier all-weather land attack aircraft in the world. Sophisticated avionics, a two man crew, and large internal fuel load enable it to attack targets at long range, in any weather with a wide variety of guided and gravity weapons. Older model A-6's provide air-to-air refueling.

The F/A-18 is the newest addition to carrier aviation's tactical punch. Designed to accomplish both fighter and attack roles, its modern and ultra-sophisticated avionics suite, airborne agility, and ability to deliver most air-to-air and air-to-ground weaponry make it the most versatile in the inventory.

Fixed wing anti-submarine warfare is conducted by the fan jet powered S-3 Viking and is complemented by the SH-3 Sea King Helicopter for close in work. The Viking also possesses long range surveillance and anti-shipping capabilities, while the Sea King also performs search and rescue.

One of the most critical missions in carrier warfare is early warning and command/control. The E-2 Hawkeye is the platform of choice for these. A high endurance TurboProp, the E-2 is equipped with sophisticated search radar and a complex communications suite. Able to control fighters, coordinate search, and vector attack

aircraft, the contributions of this platform cannot be overrated.

The late Admiral Gorshkov of the Russian Navy once stated that he who controls the electromagnetic spectrum will control the war. All carrier aircraft have inherent defensive/active ECM suites, and may have offensive/passive capabilities as well. The EA-6 Prowler is the air wing's highest performance electronic countermeasures (ECM) aircraft. Able to conduct offensive or defensive jamming, and with excellent radar attack capabilities, it is an integral part of all airpower plans as well as CVBG defense/counter targeting.

As air warfare becomes ever more demanding, the aircraft and tactics involved with it require improvement also. While always subject to debates on affordability and capability, upgrades are in work or in planning for all our fixed wing carrier aircraft and most systems. For instance, the F-14 is beginning strike warfare; the F/A-18 will be modified to increase range and payload; and the E-2, A-6, and S-3 are receiving upgrades even as follow on aircraft are being examined. The key point again: an aircraft carrier is as modern and capable as its air wing.

IV. FLIGHT OPERATIONS

Aircraft carriers are floating cities with thousands of inhabitants, trained to fight and work together with incredible coordination. The entire purpose of this huge leviathan is to launch and

recover aircraft - a process which can go on for many hours or days without stop. Preparations for flight operations usually begin the night before with the distribution of the air plan. An outline of the coming day's events, it includes launch and recovery times and information about the mission, number of sorties, fuel and ordnance loads, and tactical frequencies.

Flight quarters are announced to all hands over the ship's announcing system and manned as prescribed by the watch, quarter, and station bill. Crew members not directly involved in flight operations are not permitted on or near the flight deck. Those who are have specific, clearly defined functions are recognizable at a glance by the colored helmets and jerseys that denote their roles.

Pilots and aircrews, meanwhile, have received comprehensive briefings and man their aircraft forty-five minutes prior to launch. Before word is given to start engines they conduct preflight inspections of their aircraft to ensure that all is in order.

Flight-deck and squadron-maintenance personnel have also been busy readying their equipment and conducting a "FOD (Foreign Object Damage) walkeown" in which they systematically comb every inch of the deck for loose material that could be blown about by jet engines or prop wash and cause injury to personnel or aircraft engines. Only after the FOD walkdown is the order given to start engines.

By this time the carrier has been turned to a course that will provide approximately 30 knots of wind over the flight deck for launch. Aircraft are directed forward by yellow-shirted plane directors and precisely positioned on the steam catapults. As an aircraft is "spotted" on the "CAT," a blast deflector rises from the deck behind it to protect personnel and aircraft aft of the catapult.

A green-shirted hookup man attaches the aircraft to the catapult shuttle. When all is ready the pilot, on signal from the yellow shirt, releases his brakes and applies full power. At this time the catapult officer signals with a rotating hand motion, two fingers extended. After a final check to see if the aircraft is functioning correctly, the pilot salutes to indicate he is ready and braces himself for the shot. The catapult officer makes final checks on the CAT'S readiness and confirms from other on-deck personnel that the aircraft is ready for flight. He then touches the deck, signaling to a crewman in the catwalk to press the steam-catapult firing button. The aircraft is shot into the air, accelerating from zero to a normal "end speed" of 150 knots. The acceleration from zero to safe flying speed puts tremendous pressure on the aircraft and its crew. This spectacular achievement, which is usually duplicated more than one hundred times a day during peacetime carrier operations, is the product of brilliant engineering, careful and skilled maintenance of equipment, effective training of intelligent and motivated

personnel, and complete attention to detail and safety.

As the aircraft becomes airborne, the catapult crews are already scrambling to position and hook up the next plane. A proficient team of four catapult crews can launch an aircraft every twenty to thirty seconds. In a matter of six minutes the ship can launch twenty aircraft and commence recovery operations.

The airborne aircraft, meanwhile, are under the control of the Carrier-Air-Traffic Control Center (CATCC), which guides them in the carrier control area. As planes are launched, they join up at designed rendezvous areas and proceed to carry out various missions as directed by the air plan.

When the aircraft return to the ship and weather precludes a visual approach, CATCC controls their arrival and clears each aircraft for approach at one-minute intervals. It is the Landing Signal Officer (LSO) who becomes the key player in assisting the pilot in his final approach to landing. The LSO is a carefully selected, seasoned carrier pilot - A "Tailhooker" - who has had extensive training in this specialized field. He operates from a well-equipped platform above the landing area on the aft port side of the ship. He and his assistants correlate factors such as wind, weather, aircraft characteristics, deck motion, and pilot experience to help aid the pilot as his aircraft makes its final approach. The LSO is an expert, his judgement fine-tuned and rarely questioned.

For recovery in visual conditions, the aircraft return to an overhead "stack" at altitudes prescribed by air-wing doctrine. Individual flight leaders "take interval" on the flights at lower altitudes in the stack. Aircraft, in formations of two to four, normally enter the break for landing from astern of the ship, on the same heading and slightly to the starboard side, at an altitude of eight hundred feet. The flight leader will break left when he has reached a position projected ahead of the ship, establish himself in the downwind leg, descend to six hundred feet, and complete his landing checklist in preparation for landing. For his final approach, he will normally use the Fresnel Lens Optical Landing System (FLOLS), a combination of lenses and lights located on the port edge of the angled deck. This is an automatic, gyrostabilized system. It is interesting to note that this entire operation - the recovery of approximately twenty aircraft - routinely is conducted without radio communication.

As the aircraft lines up for its final approach at somewhere between 120 and 150 knots, depending on the type of aircraft, the pilot will observe and fly the "meatball." The "meatball" is an amber light that appears at the center of the lens or "mirror." If the aircraft is properly positioned on the glide path, the "meatball" will be aligned with a horizontal line of green reference lights on either side of the center lens. If it is above the glide path, the "ball" will appear high; if

below, it will appear low. The pilot's objective is to keep the ball centered all the way to touchdown and to engage the "three wire" - the third of four cross-deck pendants (wires) extending up the deck from the fantail, or the ramp, as "tailhookers" refer to the stern of the ship.

While it is the pilot's responsibility to fly the ball, the LSO may also give light signals or voice instructions until touchdown. If the approach is unsafe or the deck not ready, the LSO will activate flashing red lights ordering a wave-off. The pilot has no option in this situation; he must comply with the order to take his aircraft around the landing pattern again for another approach.

The aircraft will normally land on the angled deck, catch a wire, and be brought to a halt within a few hundred feet. The cross-deck wires are attached to cables that are weaved through pulleys and around the drums of the ship's four arresting-gear engines. Hydraulic dampeners are adjusted for each aircraft according to its weight, so that the arrestment does not exceed the aircraft's structural limits but does stop the aircraft within the landing area.

As the landing aircraft makes contact with the deck, the pilot moves his throttle to the full-power position. If his aircraft's tailhook engages one of the cross-deck wires, he immediately retards the power so the engines idle after the aircraft is brought to an abrupt stop. This is an

arrested landing - a "trap." If the landing aircraft does not engage one of the four cables, the throttle remains in the full-power position, the engine accelerates, and the aircraft becomes airborne again for another try. This event, called a "bolter," is the principal reason for designing the carrier with an angled deck. For this and other carrier innovations such as steam catapults, the "mirror" landing aid, and hurricane bows we owe thanks to our British colleagues. If the aircraft has been successfully trapped the hook is raised and the aircraft is then taxied forward to clear the landing area. The arresting gear is quickly reset for the next aircraft. During recovery operations a proficient carrier air wing team will complete the recovery of twenty aircraft in 15 to 18 minutes.

A pilot making a good approach snags either the number two or number three wire. If he catches the number four, he was probably high or fast on the glidescope; a trap on the number one indicates that he was low or slow. The LSO grades every approach on a carrier trend analysis form so that there is a continuing record of each pilot's performance. Competition among pilots is extremely keen.

When necessary, aircraft are recovered in bad weather. A variety of systems are available to aid foul-weather landings, including the instrument landing system, Tactical Air Navigation System (TACAN), Carrier Controlled Approach (CCA), and the Automatic Carrier Landing

System (ACLS).

The ACLS is capable of bringing an aircraft to touch down when a pilot does not have visual contact with the landing area. A computer takes information from the ship's precision radar and sends signals to the aircraft's automatic pilot, which in turn flies the aircraft and executes the approach. In ACLS landings the pilot does not have to touch the controls.....but his hands are close.

Flight operations, then, is the essence of fixed wing carrier aviation: The launch and recovery of warplanes; the rapid repair, refueling, rearming, and launch again; the sustaining of these combat cycles for infinite periods of time.

V. FUTURE DEVELOPMENTS

A brief discourse on emerging technologies as they relate to fixed wing carrier aviation is almost a contradiction in terms. Many of the AGARD speakers will deal with these subjects far more effectively than I. But perhaps an overview is in order. The rapidly changing world geopolitical scene makes it more and more difficult to accurately predict operational requirements 10 or even 5 years hence. Since it takes 4-7 years for even a rapid weapons system development, the effect of a bad guess or analysis could be catastrophic at worst or expensive at a minimum. Events in the USSR and Central Europe are familiar to all here, and lend themselves to even more uncertain prophecies. A good guess would

be that the enormous soviet military establishment will not change very much or very fast. Even if the USSR is able to proceed on the path of liberalization and democracy, its need for hard cash will at least lead to the export of many if not most of their non-nuclear military technology. Thus, soviet military hardware will remain a reasonable benchmark on which to measure wester requirements.

I have spoken a bit on the systems and interfaces of the carrier, the battle group and the air wing. Research and development as it affects fixed wing carrier aviation drives toward greater simplification in all areas. Aboard ship, we are working toward lighter, cheaper and less labor-intensive catapults and arresting gear. Within the air wing, we seek to "neck-down" the number of types of aircraft and weapons. The air wing of the future could well have only three basic airframes (F-14), F/A-18, S-3 for example) performing all tactical missions. Air-to-air weaponry could very conceivably be reduced to one weapon from three. Commonality in guided or "Smart" air-to-ground weapons is also being pursued, with one or two airframe/power plant types being fitted with a variety of warheads and guidance systems. This commonality will yield obvious benefits in procurement costs, maintenance, training and manning.

As far as the battle groups as a whole, increased efficiency and effectiveness is being pursued in: ASW; search, surveillance and targeting;

command, control and communications; battle management; and reconnaissance.

VI. CONCLUDING REMARKS

In conclusion, the launch and recovery of our heavy, sophisticated, high performance fixed wing aircraft is at the same time the source of the greatest utility of carrier and the root of all its complexities and much of the cost. Great strides have been made in recent years with vertical or short take off and landing aircraft. I look forward to our next speaker to learn more about these fascinating and emerging aircraft. Yet, for the foreseeable future, fixed wing aircraft still are the only airframes capable of the speed, range, and payload demanded of seaborne power projection. These modern fixed wing aircraft - necessarily fairly large and heavy - will continue to require the big deck carriers with which we have become familiar. Carriers can be defended, and carrier aircraft can continue to penetrate dense and complex defenses to deliver their weapons - they have done it in the recent past. But in truth, this capability comes at an ever increasing cost. The challenge to fixed wing carrier aviation is to maintain and improve its combat effectiveness without pricing itself out of existence. Utility must balance cost; cost must translate into combat potential, combat potential must equal battle success. The challenge then is improvement, not necessarily replacement.

In closing, let me state that I

In closing, let me state that I consider it a personal honor to have been a part of 1991 AGARD. Thank you.

I'd be happy to entertain any questions.

KEYNOTE ADDRESS

HELICOPTER/VSTOL SHIP OPERATIONS PERSPECTIVE

by

Rear Admiral R.H. Burn, AFC
 Director General Aircraft (Navy)
 United Kingdom Ministry of Defence
 Room 337, St George's Court
 14, New Oxford Street
 London WC1A 1EJ
 United Kingdom

My intention this morning is to comment very briefly on the first helicopter and Short Take-Off and Vertical Landing (STOVL) operations in the Royal Navy to consider whether defence policy has a place for these alternative forms of naval aviation, to look at the roles they can perform, and finally to highlight those areas which concern the chaps who are lucky enough to be out there flying from ships today, to allow your minds to complete transition from last night's paella to the purpose of this week's symposium, thinking of ways to make aircraft operations from ships easier.

This picture hangs in my office in London and shows HMS AFRICA in January 1912 launching a short S27 from a ramp over the bow. I don't know whether this was the first ever ski jump launch, but it must certainly have been a very early one. Unfortunately the S27 did not have a vertical landing capability so there was in fact no way of recovering the aircraft and strictly it falls outside my brief for today, but it is astonishing that nearly 80 years ago the Navy was experimenting with these techniques.

The first British Navy helicopter to fly operationally from a ship was in January 1944 when a Sikorsky Hoverfly deployed on convoy escort duty aboard the DAGHESTAN a converted merchant ship. Weight was a serious problem limiting fuel to 20 gallons and crew to the single pilot. No weapon could be carried and the pilot even discarded his radio in exchange for more fuel.

The first jet STOVL operation from a ship at sea was on the 8th of February 1963 when Bill Bedford operated the P1127 from the deck of HMS ARK ROYAL, leading in the 1970s first to the USMC taking the AV-8A to sea, followed soon after by the Spanish Navy.

The British Navy, following the government's decision to scrap our fixed wing carriers, developed the 20,000 ton Invincible class carrier to operate ASW helicopters and to exploit STOVL aircraft for air defence in the form of the Sea Harrier which first deployed operationally in 1980. At the same time the improvement in helicopter capability led to a growing realisation that fighting effectiveness of frigates and destroyers could be much enhanced with the addition of a helicopter carried on board. So the Royal Navy has specialised in helicopter and STOVL aircraft and has worked hard to develop both the capability and safety of operation from ships.

Now that the cold war is over, the Warsaw Pact dissolved and the Soviet Union is in disarray, the politicians are clamouring for the Peace Dividend redirecting tax revenues into health and education and beating swords into plough shares. Of course allocation of resources must be political decisions, but as a military man looking around the world at the growing instability and turmoil in so many areas and seeing the growing divide between the US and Europe on the one hand, and Third World countries on the other, it makes no sense at all to me to lay down our arms. The end of super power confrontation together with economic recession has inevitably caused belt tightening, but I believe that governments in the West will in the end find support to maintain an adequate defence capability, although this must evolve from a design for confrontation in well-prepared positions, to one equipped to deal with trouble spots anywhere in the world. The British Government last year declared its policy for smaller but better forces and has emphasised the need for flexibility and mobility. This is the emerging change in policy to which I would draw your attention. Air power and sea power can provide this flexibility and mobility and I believe that the future will see a growing requirement for naval air power to support military operations in whatever corner of the globe trouble looms.

The Gulf crisis demonstrated the essential need for countries to work together to enforce United Nations resolutions. By joining an alliance countries can contribute as they did earlier this year by sending whatever warships they can make available. Not many nations can afford large aircraft carriers and airgroups, but more are equipping their ships with helicopters and the USMC, Spain, UK, India and the Soviet Union operate STOVL aircraft at sea and others are showing a growing interest. These shipborne helicopters and STOVL aircraft can make vital contributions in a wide range of roles and I would like to take a couple of minutes to look at those roles.

The Lynx, operated by 10 Navies, is probably the most capable small ship helicopter in the world. Control of the sea during the period of tension, before the outbreak of hostilities, necessitates the ability to detect, identify and monitor surface contacts with the aid of radar and passive vision aids, such as this SANDPIPER. It may be necessary to

investigate ships cargoes and to send in boarding parties using fast roping techniques demonstrated here by British Marines.

In the event of hostilities helicopters can play a significant part in the electronic war of deception and jamming, or in surface attack using guns, or air to surface missiles such as the Sea Skua employed so effectively against small Iraqi missile boats. They can also be used for mine hunting, for detection and destruction of submarines using homing torpedoes. Covert operations could also be mounted from ships using helicopters penetrating far into hostile territory.

In the British Navy we use the Sea King both in the ASW role and as a support helicopter for casualty evacuation, working with Fleet Auxiliaries moving supplies, or for supporting Marines in the mountains. We also have a Sea King in the air early warning role developed during the Falklands campaign. And we should not forget rescue, a task which helicopters are regularly called up to perform. So there is a very wide range of tasks which naval helicopters can take on.

I think I have made the point that shipborne helicopters provide great flexibility and are now an integral and indeed essential part of the ship's weapon system. In fact they contribute so much that their availability on task is frequently crucial to the successful execution of the task group's objectives.

STOVL aircraft allow Navies that cannot afford one of Admiral READY's Battle Groups to provide a naval force with fixed wing organic air defence and attack capability. The Falklands campaign demonstrated the capability of a small force of Sea Harriers. Of course they can also perform a valuable reconnaissance and air to surface missile attack using Sea Eagle or similar weapons. The Indian Navy is equipped with a very similar aircraft to the Royal Navy.

The USMC and the Spanish Navy have developed the STOVL concept in support of ground forces, allowing the aircraft to operate from the ship or deploy to forward ground bases ashore.

The AV-8B is a highly capable ground attack aircraft and was used to good effect in the Gulf. The Italian Navy has also ordered AV 8B.

Operation of STOVL aircraft from ships is still relatively novel but it has matured sufficiently to have successfully demonstrated its potential and I have no doubt whatsoever that this concept will eventually replace conventional fixed wing aircraft at sea. I say eventually, it may take quite a long time, but large aircraft carriers and air groups are very expensive to buy and to operate and STOVL offers a cheaper alternative.

I hope that I have said enough about the contribution that helicopters and STOVL aircraft now make to naval operations through the many roles they perform, to make you appreciate that if the command is deprived of their services by rough seas, or by fog, or by some other factor, the effective capability of the force will be seriously downgraded. Thus the ability to operate, to launch and recover in high and low temperatures, by day and by night in the hostile weather conditions frequently encountered at sea is of key importance.

If we can expand the operating envelope at low cost and gain an increase in aircraft availability we have realised a significant increase in the ship's fighting effectiveness; a high return for a small investment. A rather simple example would be the ability to operate by night which approximately doubles availability and may present a significant tactical advantage. I believe it is a fact that neither the US Navy nor the Japanese had an effective night flying capability from their ships until quite late in World War II.

Faced with conditions endangering safety of operation the command will on occasion be under great pressure to take a chance. Almost exactly 50 years ago on the night of 24 May three Fulmars were launched from HMS VICTORIOUS in appalling weather in the search for the Bismark in the full knowledge that their recovery was at best going to be difficult. Two of these aircraft sighted and reported the Bismark but only one of the three was successfully recovered on board. On their return the other two failed to make visual contact with VICTORIOUS and subsequently ditched and were lost.

Another example of poor aircraft availability was seen in the 1950s before steam catapults were developed when high ambient temperatures and low natural wind states frequently precluded the launch of jet aircraft from conventional carriers. These days STOVL aircraft also have to watch high ambient temperatures very carefully particularly with respect to hover weights for landing.

It has often been said that 9/10ths of success in war is all about getting the right thing in the right place at the right time, but if you cannot use it when you get there it could be crucial, so ability to operate in almost any conditions is of key importance if full operational capability is to be exploited. So what are the factors which limit availability? Let me first consider helicopters and then move on to STOVL aircraft.

It may seem a rather obvious thing to say, but launching aircraft is intrinsically easier than recovering them back on board first and foremost because the aircraft starts with the ship and does not have the problem of locating it in the fog or reducing relative motion to zero in high sea states.

Problems for helicopters begin with high wind speeds which can damage blades during spreading and rotor engagement. Perhaps this is more engineering than flight mechanics,

but the take off manoeuvre itself can be limited by wind particularly if required to take off out of wind when tail rotor control power can become critical. If a pilot chooses the wrong moment in the ship/wave cycle to unstick then there is risk of an expensive gearbox over torque while attempting to establish an initial rate of climb to clear the deck quickly. This boils down to a need for adequate vertical agility or the product of engine response and specific excess power. Life would also become easier if transmissions were more damage tolerant to overload. But in general if you can spread and engage the rotor and if you can predict ship motion quiescent periods, take off should not present a problem, even without plenty of excess power.

To get the most out of the aircraft ship combination the command needs real time information on relative wind and on ship motion presented in a user friendly form against a plot of operating limitations. Coupled with computer prediction of ship motion this would allow selection of the most favourable launch condition and would represent a significant step forward.

Once safely airborne, transition to the climb and transfer from outside visual references to flight instruments is a manoeuvre involving risk particularly for single pilot operations at night. How nice it would be to engage autopilot for the transition away.

Now after 4 hours out there over the cold grey stormy sea it is time to think about recovery, something to eat, and a warm bed when safely back aboard. Finding the ship in these days of satellite navigation and other extraordinarily accurate systems should not be a problem, but its worth a mention, if nothing else in tribute to those bold Fulmar pilots of 50 years ago who failed on a dark stormy night to locate the VICTORIOUS.

Even these days, tired and uncomfortable after a long sortie transferring from instruments to visual contact with the ship in low visibility, or in heavy turbulence, its not difficult to lose concentration on altitude and fly into the water. Surely if we can arrange automatic transition to the dunk to operate sonar, it should not be difficult, knowing the wind direction and relative position of the ship, to organise automatic transition to the hover alongside, where visual contact with the deck can be established. This must be an early and I would have thought easily achievable objective with today's technology. Only the decision to specify the requirement and to fund system development is needed. Helicopters like the MERLIN are expensive and sophisticated machines. After a long sortie in adverse conditions we must ensure that the pilot has every assistance in successfully completing his recovery which in some circumstances can present a high work load.

Whether we have autopilot control to the hover or not, a ship mounted visual aid giving the pilot glide path information during final approach and transition to the hover is an essential requirement for safe recovery. With attention divided between cockpit instruments and the outside world, glide path information is of key importance and in the British Navy we are currently working on an improved stabilised device with modern optics.

Having arrived in the hover with good visual contact with the deck, what problems remain. We need to position the aircraft over the landing spot and make a controlled descent and touchdown. Sounds easy, but in a heavy sea landing on a small deck in a gusty wind especially at night can be quite an interesting challenge.

First the pilot needs to be able to identify the correct hover position over the deck and to assist him he needs some visual alignment aids. Most landings especially at night are done facing in the same direction as the ship so that the pilot can use the ship's structure and any lighting aids mounted on the structure for reference. Of course it is not just a question of finding the right position, but of being able to detect relative motion between the aircraft and the ship so that the pilot can instinctively determine what control inputs to make to hold the required position for touch down.

Some Navies prefer a haul down system of recovery. The British approach is to leave the pilot in full control but whatever technique is employed the pilot needs to have good visual cues to tell him where he is in relation to his target landing spot and to provide guidance in a way which will make it as easy as possible to maintain a good position in the presence of ship motion. There is plenty of scope here for inventive minds to improve visual aids.

Given that the pilot knows where he should be, the next problem is having sufficient control power to hover safely in close quarters with the ship and this is where the strength and direction of the wind become particularly relevant. The ship helicopter operating limitations or SHOLs shown on this diagram will be familiar to most of you and depict the limiting wind strength and direction. Add to this the agility required to hold position with ship motion, and the envelope gets smaller, and at night it gets smaller again.

Only the ship can know the relative wind and ship motion at the landing sight and must make the decision to attempt recovery. But is the command provided with accurate information and can he assist the pilot by predicting quiescent periods of ship motion. The facts are that British Navy ships are not equipped with adequate ship motion sensors, or computers to aid prediction and this deficiency will lead either to excessive caution with loss of aircraft availability or to limit exceedencies and risk of accidents.

And what about aircraft agility to maintain position in free hover over a pitching, rolling and heaving deck. In the Sea King and Lynx we have two very different helicopters. The Sea King is basically slow to respond particularly to collective demands and this poor

vertical agility is a major limitation when operating from small ships in heavy weather. The Lynx on the other hand has excellent agility and it is perhaps this characteristic more than any other which has made it the popular choice as a small ship helicopter for a large number of navies. However we must keep an eye on weight growth over the 20 or even 30 years that our aircraft are now required to remain in service. Progressive increase in weight will erode vertical thrust margin, and if engines are uprated we can run into gearbox overtorque problems.

Touch down at last: I am sure that designers in the 1990s will provide landing gear capable of absorbing heavy vertical loads and will not overlook the lateral loads that will from time to time be experienced in difficult conditions. Pilots are not always completely fool proof.

Having arrived on deck it is important to stay there and not to start sliding towards danger, so we must have a well engineered retention system to ensure safe operation with high winds and deck motion. In limiting conditions the final hover and landing is a demanding task involving response through aircraft controls to a complex system of ship motion, wind and turbulence. Its asking much of a tired pilot, perhaps with a poor field of view and peering out through salt spray on the windshield to get it right every time. Would it not be possible to automate the landing phase? As a pilot this idea makes me nervous, both because a good landing is very satisfying to achieve and I would not want to be out performed by a flight control system and because I wonder whether it would be possible to make it really reliable. Could we afford to develop such a system? I don't know the answers, but question must certainly be asked.

Summarising the areas that need to be addressed for helicopters, recovery is the limiting task, the aircraft needs to know the relative position of the ship and the required final approach heading. Good visual aids should be provided both for glide path control during transition to the hover and to enable accurate positioning for touch-down. Aircraft agility, particularly in the vertical needs to be adequate to maintain the required position over a moving deck and automation of transition to the climb, of final approach and transition to the hover and of the final landing phase should be considered. An ability to predict quiescent periods during heavy ship motion would also be most helpful.

Moving on to STOVL aircraft one is inclined to think immediately of Harrier derivatives, which is why I have chosen this picture of Russian Forgers and then of course we should also recognise the tilt-rotor Osprey, shown here during recent trials in USS Wasp.

But the Harrier in the form of the Matador, AV-8A and B, Indian FRS Mk 51 and the Sea Harrier have given us the experience on which my comments are based.

In the early days we were quite concerned that free take off might produce handling difficulties at the deck end, where the pilot rotated the nozzles and took control of aircraft attitude simultaneously. In practice these fears proved to be unfounded. The aircraft is in fact quite tolerant, especially off the ski jump where on more than one occasion pilots have been known, instead of rotating the nozzles, to confuse the controls and to close the throttle, albeit briefly and still to fly away safely.

For take off these aircraft do require three or four hundred feet of deck run to get airborne with a full weapon load and keeping straight, if the ship is rolling, can be a concern and a pitching deck can reduce performance safety margins if you leave the ramp at the wrong time in the cycle.

STOVL operations depend heavily on thrust to weight ratio and the community is always hungry for more thrust especially in high ambient temperatures where engine performance falls off. Thrust is a must, lift is a gift' they say, but of course as soon as you give them more engine thrust they bolt on more weapons or bigger fuel tanks and you are back to where you started.

The difficulty of recovery in adverse weather is where the main cause of lost aircraft availability can be found. Out at sea with no diversion or alternate to fly to, failure to recover means a lost aircraft and perhaps a lost pilot as well and jet fighters cannot afford to allocate very much fuel, by which I mean very much time to missed approaches. This makes the command rather cautious about launching Harriers if the weather is likely to be at all marginal for recovery. So if we could approach a zero/zero recovery capability, aircraft availability to meet operational priorities would be enhanced quite significantly.

Like a helicopter the STOVL aircraft must slow from its approach speed to the hover alongside the ship. Aircraft handling characteristics during this manoeuvre are such that it is best to make the transition in visual contact with the ship, transferring from cockpit flight instruments to external ship mounted visual aids at about half a mile, but still keeping one eye on engine temperature, attitude and rate of descent. It should not be difficult to provide the aircraft with continuous information regarding the relative position of the ship and thus throughout the approach to enable the aircraft system to compute and display approach guidance. Indeed MADGE in the Sea Harrier does this very well. To give a zero/zero capability the final approach and transition would need to be automated, bringing the aircraft to the hover alongside the ship at which time the pilot would take control using visual guidance from the ship. Those unfamiliar with the Sea Harrier might be surprised to know that it has very low authority stability augmentation making it difficult, or should I say expensive to automate the transition, but for a future design the message is clear - automated transition to the hover.

In the hover and landing phase jet-borne flight does not provide the same agility as rotor-borne flight. But of course the bigger ships from which Harriers operate do not jump around like frigates. Provided the ship holds a course which gives minimal turbulence over the landing spot, control margins are generally adequate, although there is sometimes insufficient power available to compensate for a late ship heave and this can lead to damage to the landing gear.

However, at night it gets more difficult. Ship motion is hard to deal with and tends to drive the pilot to over control in the hover. Here is an interesting challenge, to devise visual guidance which will compensate for ship motion. Or maybe we should go for fully automated hover and landing. But we would need to be able to justify the considerable expense involved by demonstrating a very considerable expansion in operating envelope. But would this be value for money, would we really gain very much for the cost - another interesting question.

I will not be forgiven if I fail to comment on engine thrust. The most important things in a Harrier pilot's life are launch weight and hover weight and of course more thrust makes all fighter pilots happy. But the facts are that engine power is very expensive and experience over the last 10 years suggests that additional thrust will quickly be consumed by the overriding requirement for additional operational capability in the form of extra weight and the unfortunate pilot is left with much the same thrust to weight ratio. Harrier operation is regulated to ensure that adequate thrust margins are preserved both for launch and for vertical landing in all conditions. Yes of course we want better thrust to weight ratio and I am sure that advances in engine technology will be able to deliver improved performance. I would be surprised however if power to weight ratios emerged as a central issue in your deliberations this week.

To conclude, I remember my closest encounter with an early end to my naval career was when trying to get back aboard at night in bad weather. Glide path control went to pieces and I got too low when trying to identify visual cues from the ship. Reduction of workload on final approach remains a priority today both for helicopters and STOVL, automation to the hover alongside would be a real advance. Coping with ship motion with better visual aids and the ability to predict quiescent periods are also capabilities which we need. Perhaps ships should be designed with landing spots positioned where ship motion is least and perhaps more use should be made of ship stabilisers. But if we are to extract the maximum ship/aircraft operating capability with safety, the command must know what the actual prevailing weather conditions are in terms of the limiting parameters and this information needs to be displayed to him in a user friendly form.

I believe naval aviation will continue to attract funding in the troubled world in which we now live. Helicopters and STOVL aircraft can perform many essential roles and provide affordable alternatives to conventional aircraft and big aircraft carriers. But operations from small ships especially in bad weather, can present a number of difficulties and limit fighting effectiveness.

Ladies and Gentlemen there is plenty of scope for your skills and inventive powers to find ways of reducing pilot workload, of extending operational limitations and of ensuring the safe recovery of our crews. I wish you a productive and successful symposium.

DECK MOTION CRITERIA FOR CARRIER AIRCRAFT OPERATIONS

J.H. Pattison

Hull Form and Hydrodynamic Performance Division
Naval Sea Systems Command
Washington, DC 20362-5101, USA

R.R. Bushway

Ship and Shore Installations Division
Naval Air Systems Command
Washington, DC 20361-5510, USA

1. **SUMMARY.** Updated ship motion criteria for conventional fixed wing aircraft launch, recovery and handling operations are presented. The criteria were required to evaluate the effectiveness of proposed hull modifications for USS MIDWAY (CV 41). A balanced approach was used to develop the criteria; including a review of existing criteria, an air department workshop, motion measurements during aircraft operations aboard USS MIDWAY and USS CONSTELLATION, flight simulations of aircraft recovery, and a study of the sensitivity of operability calculations to changes in the criteria. Deck attitude (list and trim) and wind limitations are discussed. Sample results are presented to show how the criteria are used to evaluate the effects of hull improvements in a typical operating area of the ocean. It is shown how the criteria may be used in on board motion displays to guide the ship operator to best speeds and headings to avoid deck motion effects on operations.

2. **INTRODUCTION.** At the heart of a U. S. Navy carrier battle group is a large deck carrier that must support aircraft operations in all kinds of weather. To assure interoperability in a joint North Atlantic Treaty Organization (NATO) task force, other navies have similar requirements for all weather aircraft operations. In this paper, we focus on how level the flight and hangar decks must be and how much deck motion and wind over deck are allowed before aircraft launch, recovery, handling and maintenance become degraded. Quantified criteria for deck motion, deck attitude and wind over deck are essential for the design of ships which will fully support aircraft opera-

tions.

3. **DEFINING THE INTERFACE.** The aircraft-ship interface is defined in terms of ship motions and airflow around the flight deck and their effects on aircraft operations. Referring to Figure 1, the ship motion responses to a seaway can be broken down into six components; three translational (surge, sway and heave) and three rotational (roll, pitch and yaw) about a center of motion. The center of motion is assumed to be the center of gravity (CG) of the ship. For the typical aircraft carrier, the center of gravity is located somewhat aft of amidships and a small distance below the waterline.

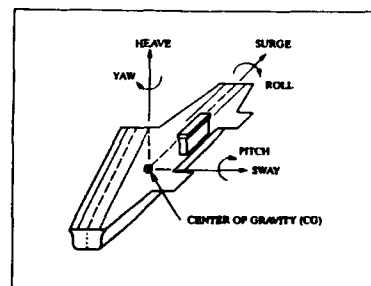


FIGURE 1. BASIC SHIP MOTION COMPONENTS

The rotational motion components at any other point

on the ship are the same as those at the CG; but the longitudinal, transverse and vertical components of the translational motions contain algebraic combinations of surge, sway, heave, roll, pitch and yaw depending on how far the point is from the CG. The motions are typically defined in terms of displacement amplitudes, although velocity and acceleration figure in some of the criteria discussed below. Also important to aircraft operations are the steady deck attitude and wind over the flight deck. The steady deck attitude is defined in terms of trim (bow down or stern down) or list (port or starboard down). The effect of heel when the ship is in a turn is similar to that of list. Wind over the deck is defined in terms of relative wind, which is the vector sum of the true wind and the ship speed and direction, as shown in Figure 2.

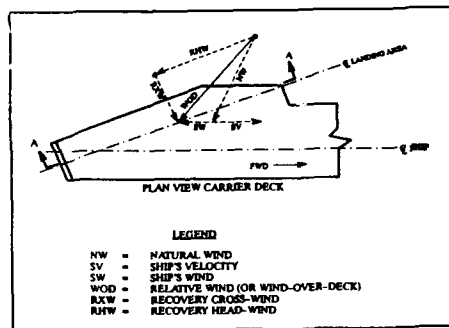


FIGURE 2. WIND OVER DECK

4. EVOLUTION OF DECK MOTION CRITERIA PRIOR TO 1986. The evolution of seakeeping performance evaluation in the design of aircraft carriers was closely linked to the development of computational methods for assessing the performance. The methodology that evolved is depicted in Figure 3.

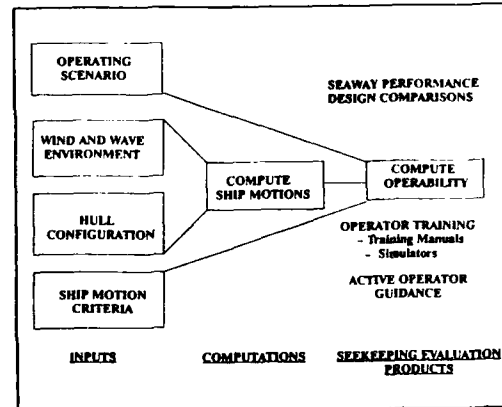


FIGURE 3. SEA KEEPING EVALUATION METHODOLOGY

For aircraft carriers the OPERATING SCENARIO relates to what the ship is required to do to support aircraft operations. The WIND AND WAVE ENVIRONMENT is defined by the statistics of occurrence of various wind speeds and directions and various wave spectra. The U.S. Navy relies on wind and wave occurrence statistics that were hindcast using a Global Spectral Ocean Wave Model (GSOWM) (1). HULL CONFIGURATION comes from an extensive data base on hull shapes for active ship classes and many concept designs. For seakeeping analysis, weight distribution data and appendage shapes, sizes and locations are also included.

In the 1970s, the U.S. Navy turned its attention to designing smaller, less expensive aircraft carriers and air capable ships. The design community looked at the operational characteristics of several aircraft types, including those that were capable of vertical and short takeoffs and landings. They developed generic wind over deck and motion limits associated with aircraft handling, weapons loading and maintenance for a wide range of hull sizes and types. The resulting SHIP MOTION CRITERIA are summarized in a paper by Comstock, Bales and Gentile (2) and are listed in Table I and Figure 4 (2). These criteria were assumed to be complete and adequate. The motion lim-

its were defined in terms of the average of the highest one-third (or significant) single amplitudes, and represented the highest levels at which performance effectiveness was still believed to be 100 percent.

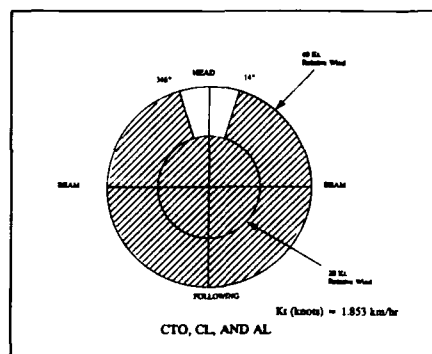


FIGURE 4. GENERIC RELATIVE WIND ENVELOPE

Table I. Summary of 1970s Ship Subsystem Criteria

SUBSYSTEM	PERFORMANCE LIMITATIONS		
	MOTION	LIMIT*	LOCATION
Hull	Slamming	20/hr	Opposite
Elevator	Wetness	5/hr	Bottom, Inner Loading Elevator Edge
Personnel	Roll	8 deg	CG
	Pitch	3 deg	CG
	Vertical Acceleration	0.4 g	Bridge
	Lateral Acceleration	0.2 g	Bridge
Support Equipment	Roll	3.5 deg	CG
	Pitch	3.5 deg	CG
Conventional Takeoff (CTO)	Roll	5 deg	CG
	Pitch	1 deg	CG
	Relative Wind	(Generic CTO Envelope)	
Conventional (CL) and Arrested (AL) Landing Aircraft	Roll	5 deg	CG
	Pitch	1 deg	CG
	Vertical Displacement	2.2 m (7.1 ft)	Ramp
	Vertical Velocity	1.4 m/sec (4.7 ft/s)	Touch Down Point
	Relative Wind	(Generic CL and AL Envelope)	

* Motion limits are significant single amplitude values.

Slender ship theory, as programmed into the U.S. Navy Standard Ship Motion Program (SMP) (3), is used to compute ship motions for all headings and speeds into all anticipated combinations of wave height and modal period. This information is incorporated in the U.S. Navy Seakeeping Evaluation Program (SEP) (4) to COMPUTE OPERABILITY based on the computed ship motions, the statistics of wind and wave occurrence, the specified operating

scenarios and the ship motion criteria.

5. **USS MIDWAY ROLL MOTION PROBLEM.** In 1986, USS MIDWAY was fitted with a blister that extended 2/3 the length of the hull and from the flight deck to well below the waterline, as shown in Figure 5. The beam at the waterline was increased by 6 meters (20 feet) to 43 meters (141 feet). An earlier blister had been installed in 1965-67 to accommodate an angled flight deck. The 1986 blister was installed to bring the hull up to strength standards needed to support a flight deck that had grown significantly in size over the years and to meet standards for surviving hull damage. Also, the blister extended below the waterline to increase buoyancy and, thereby, reduce draft in hopes that lowered aircraft elevators would be less subjected to wetness. At the same time a centerline fin was added at the stern to give the ship better directional stability for aircraft recovery.

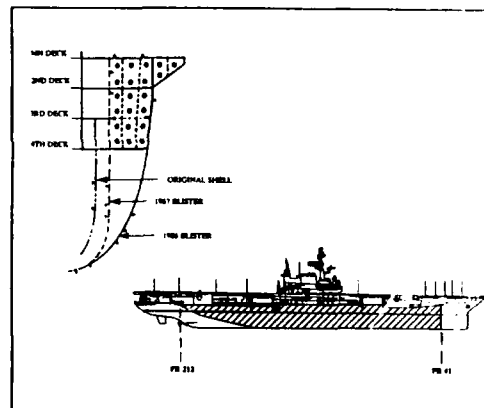


FIGURE 5. 1986 BLISTER CONFIGURATION AND EXTENT

Ricketts and Gale discuss in more detail the greatly accelerated program to design and build the blister to meet a scheduled overhaul period (5). The design goals for strength, draft and directional stability were met by the new blister and fin. But, when USS MIDWAY came out of the yard in late 1986, "it quickly became obvious that the deck motions were often unsatisfactory, as reported almost immediately by the ship, and a totally unexpected phenomenon, excessive flight deck wetness, was experienced. While the deck motions met the existing criteria, they sometimes precluded safe handling of aircraft on the flight deck".(5)

6. APPROACH TO IMPROVING MIDWAY OPERABILITY. The roll motion and deck wetness problem described above for USS MIDWAY was essentially a hull design problem. The program that was planned and executed to solve the problem was named the MIDWAY Motions Improvement Program (MMIP). Many different ideas were explored to modify the blister or add other means for stabilizing the ship. The most promising in terms of performance and cost were taken to the detailed design stage, so that one could be selected and built, given the availability of repair funds. Any ideas that would adversely impact powering, maneuvering, weight or hull strength were eliminated.

The MMIP team recognized that accurate deck motion criteria were essential to determine how much improvement was achievable with each design fix. A criteria working group was formed to plan and execute a program to comprehensively evaluate existing deck motion criteria and recommend improvements.

Besides the authors, the working group included representatives of the Aircraft Carrier Ship Acquisition Program Office at the Naval Sea Systems Command, (NAVSEA) the Surface Ship Dynamics Branch at the David Taylor Research Center and J.J. McMullen, a private Naval Architectural firm. The working group planned and executed a six month program that included the following tasks:

- a. Identify critical motion parameters,
- b. Conduct an air department workshop,
- c. Review the literature on aircraft launch, recovery and handling,
- d. Conduct aircraft recovery simulations,
- e. Assess performance at sea with a ship motion recorder,
- f. Assess motion limits on smaller aviation ships,
- g. Do criteria sensitivity study, and
- h. Assemble improved deck motion criteria

The working group called upon operating personnel in the fleet and engineers at various Navy laboratories to provide technical information and direct support to complete each task. Their contributions are noted in the discussions below. The results of selected tasks are discussed in the sections which follow. The key task was the air department workshop.

6.1 Air Department Workshop. The initial problem faced by the criteria working group was the lack of validated operational limits. The decision to conduct a Air Department Workshop was driven by the requirement to develop a comprehensive set of criteria as quickly as possible. The Air Department Workshop was convened to bring those with a history of hands-on-experience together to discuss ship motion impacts on operations and identify those which were controlling.

The workshop itself was conducted over a two day period. During day one, the participants were segregated by functional specialty (launch, recovery, handling, etc.) and asked to develop consensus values for three criteria:

- a. An optimum level of ship motion - The level at which specified operations can be routinely conducted for an extended period of time. Above this level, ship motion becomes a factor in the decision to undertake an action.
- b. A difficult level of ship motion - The level at which specified operations can be conducted, but ship motion dictates the timing of critical evolutions. Extended operations in this environment are possible, but will degrade the efficiency of the airwing over a long period of time.
- c. A limit case of motion - The level at which operations can be conducted, but only with extraordinary effort. Ship motion is the dominant factor in any evolution. This is the point at which suspension of operations or reduction in operational tempo would be considered under normal circumstances.

On the second day, all attendees met as a group and the individual functional areas compared responses. The intent was to stimulate a dialogue which would serve to validate assumptions, correlate responses and integrate the various disciplines to form a uniform position on limiting values for air operations.

The results of the workshop are presented in Tables II, III and IV. The workshop also identified other limits in the areas of aircraft maintenance (aircraft jacking, system calibration, corrosion control, engine testing), fueling (list/trim control), and ordnance handling (lifting ordnance, dolly control) which tended to correspond to the limits specified for aircraft handling.

The following general observations are relevant:

- a. Roll amplitude and period most significantly impact aircraft handling.

Table II. Workshop Aircraft Launch Limits

	OPTIMUM	DIFFICULT	LIMIT CASE
Roll Period* 1	24 sec	21 sec	20 sec
Roll Amplitude* 1,2,3,4	2 deg	2-3 deg	3 deg
Transverse Acceleration* 2	No Reference - Derive from Motions		
Vertical Acceleration	No Reference - Derive from Motions		
Pitch Period* 8	N/A	N/A	15 sec
Pitch Amplitude* 3,6	N/A	N/A	7.5 m (25 ft)
Trim* 5	1/2 deg Down by the Bow		
Wind Over Deck* 7	Within Bulletin Limits		
Spray Conditions* 6	No Geyser Effect		

*NOTES:

1. Aircraft handling limit. Affects ability to spot aircraft on catapult.
2. No steep rolls.
3. Combination of pitch and roll adds to No. 3 catapult launch restrictions. Impacts ability to conduct flex deck operations.
4. Above 3 degrees, launching while moving aircraft along safe parking line could result in catastrophic accident.
5. Driven by sink off the bow criteria.
6. 7.5 meter limit associated with generation of geysers over the bow on CV 59 and higher hull numbers.
7. Course/speed restrictions imposed.
8. Period must be predictable.

Table III. Workshop Aircraft Recovery Limits

	OPTIMUM	DIFFICULT	LIMIT CASE
Roll Period* 1	20 sec	20 sec	20 sec
Roll Amplitude	1 deg	1-2 deg	2 deg
Transverse Acceleration	No reference - Derive from Motions		
Vertical Acceleration	No reference - Derive from Motions		
Pitch Period* 6	10 sec	10 sec	15 sec
Pitch Amplitude	1m (3.5 ft)	1.5m (5 ft)	3m (10 ft)
Trim* 4	1/4 deg Up by the Stern		
Wind Over Deck* 5	Within Bulletin Limits		
Spray Conditions	Not Controlling		
Sway Amplitude* 2	1.5 m (5 ft)	3.5 m (12 ft)	4.5 m (15 ft)
Heave Period	10 sec	10 sec	15 sec
Ramp Motion* 3,7	1.5 m (5.5 ft)	2.5 m (8 ft)	+3/-4.5 m (10/-15 ft)

*NOTES:

1. Period must be predictable.
2. Increased probability of off center engagements, requiring inspections and maintenance.
3. LSO utilizes displacement of the ramp as governing criteria. Displacements of 1.5, 2.5, and +3/-4.5 meters (5.5, 8, and +10/-15 feet) are absolute limits consisting of pitch and heave components, no matter how achieved.
4. At values above 1 degree, significantly limits less ability to hold stable glide slope (ball brown).
5. Course and speed restrictions.
6. Dictated by LSO reaction/communication/pilot reaction time.
7. Aircraft structural limit.

Table IV. Workshop Aircraft Handling Limits at Flight Deck

	OPTIMUM	DIFFICULT	LIMIT CASE
Roll Period	24 sec	21 sec	20 sec
Roll Amplitude* 4,5	2 deg	2-3 deg	3 deg
Transverse Acceleration	No Reference - Derive from Motions		
Vertical Acceleration	No Reference - Derive from Motions		
Pitch Period	Not a Significant Concern		
Trim	Not a Significant Concern		
Wind Over Deck* 1,3	35 kts any Direction		
Spray Conditions* 2	Avoid Wet Deck		

*NOTES:

1. Wind over deck limit decreases rapidly with wet deck.
2. Deck wetness rapidly degrades handling conditions. Design non-skid condition is 4000-5000 landings (mid cruise), certain amount of petroleum, oils, lubricant (POL) and salt buildup. Wet deck will float POL, reducing coefficient of friction.
3. E-2/C-2 worst case.
4. All course/speed/maneuvering combinations.
5. Roll limits decreased 1/2 degree on elevators and hangar deck due to increased wetness and tighter maneuvering.

In general roll was not a major concern in the launch and recovery evolution except as it impacted the ability to spot aircraft on the catapult and remove aircraft from the landing area.

b. Because of the size of an aircraft carrier, limits may be location specific. Conditions which preclude evolutions on number four elevator may have no impact on launch.

c. Motions combine with environmental factors to limit specific phases of the operational scenario - and ultimately the operational capability. Spray, and the resulting wet deck, rapidly degrades handling conditions.

d. Pitch amplitude and period most significantly impact launch and recovery. In the launch case, the period must be predictable and long enough to insure that the aircraft leaves the flight deck during the upward swing of the bow in order to avoid excessive sink. The amplitude is constrained by the resultant spray. In the recovery scenario, pitch amplitude is limited by the mechanical stops in the Fresnel lens. Pitch period is constrained by the Landing Signal Officer (LSO) reaction/communication/pilot reaction time.

e. Wind over deck significantly impacts handling limits. Traditionally, wind over deck has been a controlled variable in launch and recovery, i.e. allowable envelopes have been published. This tends to constrain course and speed to head winds and seas and low periods of encounter - both of which tend to minimize ship motion. In the handling case, course and speed tend to be driven by transit requirements, which can result in wind loadings, both on the ship and the aircraft, which significantly impact the ability to move aircraft. The limit decreases rapidly with wet decks

f. Heave and sway uniquely impact recovery. Sway will tend to increase the tendency for off center engagements, resulting in more inspections and maintenance of the arresting gear. Heave, in combination with pitch and the other motions, results in ramp displacement. Ramp displacement, no matter how achieved, is the governing criteria utilized by the LSO in recovering aircraft. Ramp displacement and velocity can, in extreme cases, generate aircraft landing loads approaching landing gear limits.

The results of the workshop were submitted to five post command carrier (CV) captains for review. The command screen agreed that the numbers were "about right." They felt that roll and trim control were important and that aircraft handling was most often the controlling process. List above 1/2 degree tended to cause drift port or starboard during run out on recovery. This could be used to the ships advantage if necessary. They recommended that the ship be designed to operate in a moderate sea (SS-4) with an accurate method of predicting ship motion in higher sea states.

Upon completion of the command screen, an initial set of proposed design criteria, shown in Table V, was developed. The design criteria are specified for mod-

Table V. Workshop Design Criteria

	OPERATION SS 4	LIMIT CASE
Roll	< 2 deg	< 3 deg
Roll Period	> 20 sec	> 20 sec
Pitch Amplitude	< 1 deg	< 2 deg
Pitch Period	> 10 sec	> 15 sec
Trim	< 0.25 deg	< 0.50 deg
List	< 0.5 deg	< 1.0 deg
Wind Over Deck	< 35 kts/Bulletin	< 35 kts/Bulletin
Spray	Minimum	Minimum
Horizontal Ramp Displacement	< 1.5 m (5 ft)	< 4.5 m (15 ft)
Vertical Ramp Displacement	< 1.5 m (5.5 ft)	< +3/-4.5 m (+10/-15 ft)

erate (sea state 4, 4 to 8 feet significant wave height) seas with a limit value applicable to the maximum operable sea state (design criteria are synonymous with

the optimum level of motion). Pitch, roll, and ramp displacement are defined in terms of significant single amplitude values to support the design process.

It should be noted that the workshop specified roll periods in the 20 to 24 second range. Their frame of reference was a list of inclining experiment roll periods provided by the Naval Sea Systems Command. Data collected by the Naval Air Test Center (NATC) during Precision Approach Landing System trials indicated that these values were typically two seconds longer than experienced in the open ocean. Roll periods were adjusted to reflect the NATC data.

6.2 Literature Search on Aircraft Launch, Recovery and Handling. In the search for historic data on the effects of deck motion on aircraft operations, little was found on aircraft launch. No data were found for aircraft maneuvering on deck. With regard to vehicle operation, material available included specification data (6,7) and operating criteria (8) for several items of deck handling equipment, test results for the inception of skidding or tipover from dynamic tilt table experiments on weapons handling gear (9), specification data for non skid deck coating systems (10), and additional data on existing and proposed tractor capabilities. Deck inclination and acceleration limits found in these data varied, but were generally above those indicated by the fleet operators for roll and pitch amplitude and period effects on aircraft handling. However, the data did not address the effects of wet or oily decks.

The only significant study on aircraft recovery was the Naval Warfare Analysis Group (NAVWAG) Study (11). Referring to Figure 6, aircraft recovery factors considered in the NAVWAG Study included hook-ramp clearance, touchdown vertical velocity, arresting gear engagement speed, and touchdown lateral offset. Of these, ramp clearance and touchdown vertical velocity were found to be most directly influenced by ship vertical motions; and the NAVWAG study developed equations to relate these motions to flight deck dimensions in the landing area and expected statistical variances in the aircraft flight path and landing velocity.

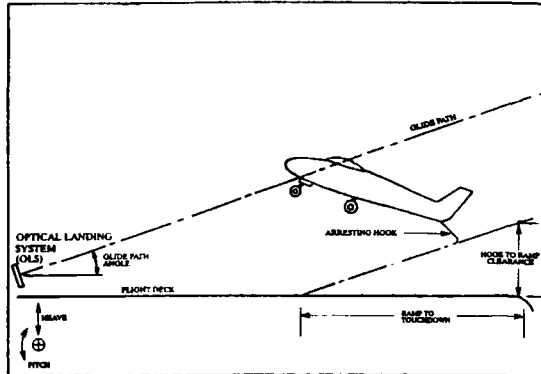


FIGURE 6. GLIDE PATH GEOMETRY

Substituting landing survey data taken aboard ship by test personnel from the Naval Air Development Center between 1968 and 1982 into the NAVWAG equations lead to a ramp vertical displacement limit of 1.7 meters (5.5 feet) significant single amplitude. Similarly, the touchdown vertical velocity limit for the deck was determined to be 1.4 meters/second (4.7 feet/second) significant single amplitude. The vertical velocity limit was initially considered to apply at the center of the cross deck pendant array. However, in response to the need to limit vertical velocities even in the event of low approach, this criteria is applied at the ramp.

6.3 Aircraft Recovery Simulations. The objective of this task was to assess roll, pitch and deck edge displacement limits using carrier landings in a flight simulator.

The Visual Technology Research Simulator (VTRS) at the Naval Training Systems Center (NTSC) in Orlando, Florida was chosen to gather initial data on any difficulties introduced by flight deck motions on aircraft recovery. VTRS includes a Conventional Takeoff and Landing (CTOL) simulator that makes use of a fully instrumented T-2C Trainer cockpit inside a sphere. An image of the USS FORRESTAL which is typical of a large deck carrier, is projected in a rectangular area of the sphere in front of the pilot, as shown in Figure 7.

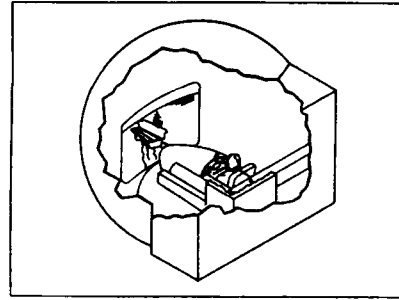


FIGURE 7. CONVENTIONAL TAKEOFF AND LANDING SIMULATOR

Experience was the key to making the simulated T-2C aircraft fly like a fighter and the motions of the USS FORRESTAL flight deck look like those of USS MIDWAY. The Naval Air Test Center (NATC) in Lexington Park, Maryland provided two test pilots to fly in the simulator and two engineers to evaluate the pilots' performance. Both pilots had tours as fighter pilots on USS MIDWAY before the blisters were installed. One was a test pilot on the NATC test team that conducted deck qualifications on USS MIDWAY when she left the yard with blisters installed. His experience made a realistic simulation of USS MIDWAY deck motions possible.

For the simulated aircraft recoveries, deck motions were simulated as combinations of roll, pitch, yaw and heave motions. Each motion component was represented as a simple sinusoid with its own amplitude and period. Amplitudes and periods were selected from U.S. Navy Standard Ship Motion Program (SMP) predictions for the pre-blistered MIDWAY (Hull O), post-blistered (Hull X), and a concept which involved notching the hull at the waterline (Hull A) that was being considered to fix the MIDWAY roll problem. A ship speed of ten knots and heading relative to the waves of 45 degrees were selected as typical for the worst roll motions encountered during aircraft recoveries in the Northwest Pacific Ocean. For sea conditions, 2.5 meters (8.2 feet) (high Sea State 4) and 4.0 meters (13 feet) (high Sea State 5) wave heights and 11 second wave modal period were selected as typical of the swell-corrupted seas in this area. It was reasoned that these ship and

sea conditions would serve to emphasize the effects of varying roll amplitude and period between the different USS MIDWAY hulls.

To measure the effect of deck motions on each pilot's ability to land, each pilot was asked to score each landing attempt according to the Handling Qualities Rating (HQR) Scale listed in Table VI. For each landing attempt, the wire engaged or bolter (missed wire and fly off) or missed deck was recorded.

Table VI. Handling Quality Ratings for Aircraft in Flight

10	Not controllable will loose control during evolution	Improvement Mandatory
9	Not controllable without excessive pilot compensation	Improvement Required
8		
7		
6*	Adequate performance with excessive pilot compensation	Warranting Improvement
5	Adequate performance with little pilot compensation	Fair
4		
3		
2		
1		Good Excellent

*Note: A rating of 6 is very objectionable to pilot. His workload to control the aircraft is high.

The results of the simulated landings included the pilots' handling quality ratings which are plotted in Figure 8 as a function of roll period and roll amplitude. Hull X was rated worst. Hulls A and O were rated nearly the same. Wire engagements, bolters and missed decks occurred on Hull X, but the pilots were still able to land some of the time. Landings on Hull O came closest to the ideal of wire number 3 engagements. These data are too limited to put numbers on roll (or any other motion) criteria, but tend to support the criteria the fleet operators recommended above.

6.4 At Sea Measurements. Within one month after reports came in that USS MIDWAY had roll motion problems, the David Taylor Research Center (DTRC) in Bethesda, Maryland installed a ship motion recorder (SMR). Roll, pitch, speed and course signals were brought in from the ship's own sensors. In addition, triaxial accelerometers (that measure longitudinal, lateral and vertical acceleration) were mounted in three locations as shown in Figure 9.

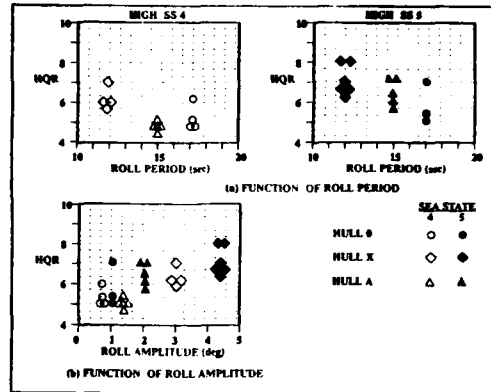


FIGURE 8. ROLL MOTION EFFECTS ON HANDLING QUALITY RATINGS FOR AIRCRAFT RECOVERY

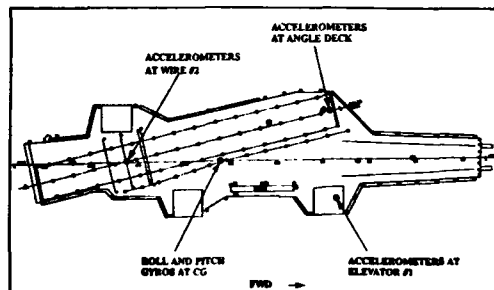


FIGURE 9. USS MIDWAY CV 41 - MOTION SENSOR LOCATIONS

During the course of the MIDWAY Motion Improvement Program, interest in verifying the criteria at more points on the flight deck lead to repositioning accelerometers. Measured longitudinal accelerations had been very small, so the longitudinal accelerometers from all three triaxials were moved. One was relocated to the centerline of the ramp and reoriented to measure ramp vertical motion. The other two were relocated at the port catapult and reoriented to measure lateral and vertical acceleration. In addition, the opportunity presented itself in April 1987 to measure motions on another, larger, carrier, USS CONSTELLATION (CV 64), which was operating in company with USS MIDWAY. The ship's own sensors were

tapped to measure roll, pitch, ship's course and ship's speed. A triaxial accelerometer was provided to measure accelerations in the forward Internal Communications (IC) room where the computer was located. The data obtained allowed some conclusions to be made on the effects of roll motion on aircraft handling.

Deck inclination results from static trim or heel and dynamic pitch or roll. Transverse accelerations are the result of roll amplitude and period; with higher accelerations resulting when roll periods are shorter. Vertical accelerations are the result of heave and pitch amplitudes and periods. The combined effect of deck inclination and transverse acceleration is to put a lateral force on the aircraft or handling equipment, and in the limit cause the aircraft or equipment will skid or tip. The effect of vertical acceleration is to make the equipment effectively lighter (or heavier) and change its adhesion to the deck. From several measurements, movement of aircraft was accomplished to above 0.1 g lateral acceleration, but was suspended when these accelerations reached 0.15 g. If we apply these acceleration levels at the outside forward corner of the angled deck, the corresponding roll angles are 3.5 and 5.25 degrees, respectively. Statistical equations allow us to relate these maximum values, that occurred during periods of a few minutes of exposure in beam quartering seas during turns, to corresponding significant values (averages of the one third highest amplitudes) that would occur when the ship is on a straight course at constant speed, where we would normally apply our design criteria. Thereby, the range of 0.1 to 0.15 g maximum lateral acceleration, would lead to roll criteria in the range of 1.8 to 2.6 degrees significant single amplitude. This tends to support our chosen criteria of 2.0 degrees for aircraft handling on an aircraft carrier with the shorter roll period characteristic of USS MIDWAY.

Aircraft launch and recovery presented no difficulties during the January and April 1987 measurement periods. Pitch motions were well within limits for catapult launches and for stabilizing the optical landing system. Similarly, ramp vertical displacements and touchdown vertical velocities were well within limits for aircraft recovery.

6.5 Criteria Sensitivity Study. Because the criteria evolved during the MIDWAY Motions Improvement Program, there was interest in determining how much changing the criteria effected predicted oper-

ability comparisons between the current MIDWAY, proposed fixes and a larger carrier, USS KITTY HAWK (CV 63). USS KITTY HAWK is in the same ship class as USS CONSTELLATION. Three sets of criteria listed in Table VII were thus evaluated for the preblistered USS MIDWAY (Hull O), postblistered (Hull X for existing), notched (Hull A) and USS KITTY HAWK (CV 63). The roll criteria were picked off curves of roll versus roll period that were developed during early phases of the Motion Improvement Program. As a simple model, it was assumed that a specific ratio of lateral to vertical acceleration would lead to aircraft skidding or tipping. A former aircraft handling officer aboard USS CARL VINSON (CVN 70) had reported that aircraft movement became difficult to dangerous when he read 3 degrees of roll on the clinometer in flight deck control. CVN 70 has a natural roll period of 21 seconds. Taking a constant acceleration ratio down to the 12 second natural roll of USS MIDWAY, yields 2.3 degrees roll which falls in the acceptable range of significant amplitudes reported in measurements discussed above. This curve is shown in Figure 10. In the first set of criteria (Set 1), only this roll curve was introduced to change the criteria from the Sea Based Air Study (6), which also included the generic relative wind envelope shown in Figure 4 for aircraft launch and recovery. In the initial Working Group meetings, numbers were changed to reflect historic data and aircraft launch and recovery bulletins. These are listed in Table VII as Set 2.

Table VII. Criteria Sets for Seasevrey Study

		Set 1 (5 Feb 87)	Set 2 (Working Group)	Set 3 (NAVAIR Workshop)
Both Mission Scenarios				
Roll, deg	CV41 Hull O Hull X Hull A CV 63	2.9 2.3 2.7 3.0	2.9 2.3 2.7 3.0	1.9 1.5 1.8 2.0
Pitch, deg		1.8	2.0	1.8 CV 41 2.0 CV 63
Launch and Recovery				
Vert. Displ.-Ramp, in (ft)		2.2 (7.1)	1.5 CV 41 (5.1) 2.2 CV 63 (7.3)	1.7 (5.5)
Vert. Vel.-Touch Down pt., m/sec (ft/sec)		1.4 (4.7)	1.4 (4.7)	No limit
Relative Wind		Oceanic Envelope	Bulletin Envelope	Bulletin Envelope
Aircraft Handling				
Relative Wind, kn		< 48	< 35	< 35

Criteria Set 3 reflects further refinement from the air department workshop, including the more restrictive curve for roll shown in Figure 10. The computation process described above and illustrated in Figure 3 was used with wave height, wave modal period, and wind occurrence statistics for the North Arabian Sea in June through August (worst season) to produce the operability bar graphs shown in Figure 11 for aircraft handling and launch and recovery.

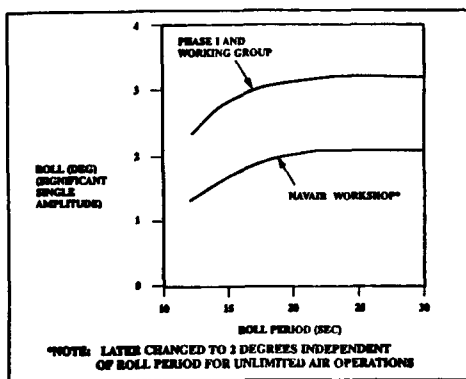


FIGURE 10. LIMITING ROLL CRITERIA

Criteria Set 1 leads to the conclusion that, for all ships except Hull X, pitch limits operability approximately 80-90 percent of the time, with roll limiting the remaining time. For Hull X, the degraded roll performance results in roll limiting 78 percent of the time. The result is significantly lower operability for Hull X relative to all other ships. For Criteria Set 2, the significant change from Criteria Set 1 is the doubling of the pitch limit to 2 degrees. Since all ships but Hull X were limited most of the time by pitch, this results in a significant gain in operability for all but Hull X. Hull X improves very slightly because of the doubled pitch limit gain in those few cases where it is pitch rather than roll limited. For Criteria Set 3, the significant change relative to Set 1 is the reduction in the roll limit. This reduces the operabilities of Hulls O, A and CV 63 some since in those few cases where they were limited by roll, they are now more limited and in some of the cases where they were pitch limited, they are now more limited by the reduced roll limit. Since

Hull X was mainly limited by roll, the reduced roll limit causes a significant decrease in operability.

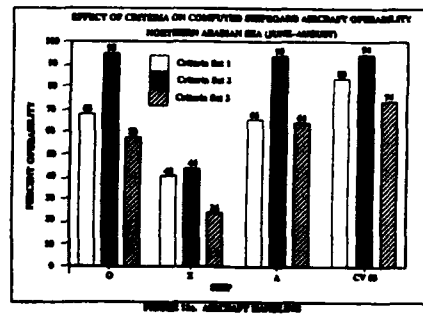


FIGURE 11. AIRCRAFT HANDLING

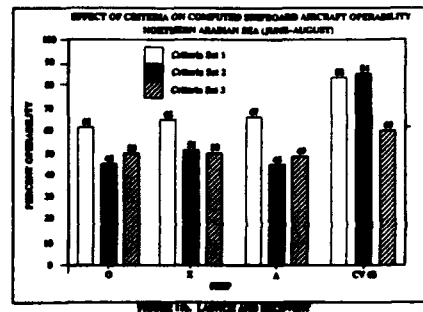


FIGURE 12. LAUNCH AND RECOVERY

It should be noted that the criteria we ultimately adopted were less restrictive in that the lowest roll limit was 2 degrees significant amplitude, independent of roll period.

7. **UPDATED DECK MOTION CRITERIA.** The end results of all the studies discussed above are the criteria for deck motion listed in Table VIII and the criteria for deck attitude listed in Table IX. For wind over deck, a limit of 35 knots applies for aircraft handling; and the limits specified in bulletins for each aircraft and ship combination control for aircraft launch and recovery. These criteria were put forward jointly by the Naval Air Systems Command and the Naval Sea Systems Command (12,13) and were approved by the Office of the Deputy Chief of Naval Operations for Air Warfare (14).

Table VIII. CV/CVN Limiting Deck Motion Criteria

	Values for Unrestricted Air Operations	Limiting Values for Air Operations
Roll Amplitude	< 2 deg	See roll criteria Figure 12
Natural Roll Period of Ship	> 20 sec	See roll criteria Figure 12
Ramp Horizontal Displacement	< 1.5 m (5 ft)	< 4.5 m (15 ft)
Ramp Vertical Displacement	< 1.7 m (5.5 ft)	< 3.0 m (10 ft)
Pitch Amplitude	< 1 deg	See pitch criteria Figure 13
Touchdown Point Vertical Velocity	< 1.4 m/sec (4.7 ft/sec)	< 1.4 m/sec (4.7 ft/sec)

Note: Motion values represent significant single amplitudes.

Table IX. CV/CVN Limiting Attitude Criteria

	Values for Unrestricted Air Operations	Limiting Values for Air Operations
Trim by the Bow	< 0.25 deg	< 0.5 deg
Trim by the Stern	< 0.25 deg	< 0.5 deg
List	< 0.5 deg	< 1.0 deg

The following comments amplifies the criteria listed in Table VIII:

a. Values for unrestricted air operations must be met by any carrier through Sea State 4, 1.2 to 2.5 meters (4 to 8 feet) significant wave height. The levels define motions which permit air operations to be routinely conducted for extended periods of time.

b. The limiting values specified describe the motions during which air operations can be conducted, but with extraordinary effort. Under these conditions, ship motion becomes the dominant factor in any evolution. These criteria will be used to determine carrier operability in higher sea states.

c. Between the two values, performance of air-

craft operations degrades gradually as motions become more influential.

d. Ramp horizontal and vertical displacements and touchdown point vertical velocity limits are specific to aircraft recovery. Roll and pitch limits apply to all aircraft operations (launch, recovery, handling, selected maintenance and weapons handling).

e. Pitch and roll amplitudes, ramp displacements and touchdown point vertical velocities are expressed as significant single amplitude (SSA). It has been found that the observer will characterize ship motion in terms of its significant value. There is greater than 90 percent probability that peak values will not exceed two times the SSA in one hour of operation at constant ship speed and heading.

f. Criteria are met when ship motion significant amplitudes do not exceed the values listed and ship response periods are not less than the values listed.

g. Deck conditions for mid cruise are assumed in applying the criteria. The deck has wet, worn non-skid surface with some imbedded petroleum, oils, lubricants and salt. Worst case combinations of environmental factors (fog, rain, snow, ice, etc.) are not assumed because they do not occur often enough.

h. No distinction is made between daytime and nighttime operations.

i. The criteria are based primarily on aircraft operations at the flight deck level, but recognize the effect of motion on maintenance, weapons handling and aircraft handling on elevators and the hangar deck.

j. It should be noted that ship operators judge roll amplitudes from clinometer readings that are typically higher than true readings from the ship's gyro. The largest clinometer readings are those from the bridge which is several decks above the center of motion of the ship. Readings as high as two times the gyro readings have been observed during high amplitude, short period rolls at this point. Seakeeping operability analysis results reflect true values comparable to the ship's gyro values. Care must be taken when relating clinometer values to true values of roll amplitudes.

Each of the criterion values listed in Table VIII is explained as follows:

a. For natural roll periods down to about 10 seconds, movement of aircraft is possible on a continuous basis if the roll angles are less than 2 degrees SSA. If roll angles exceed 2 degrees, then roll becomes an important factor.

In practical terms, an aircraft move must be completed within 1/4 cycle; thus, a 20-second roll period

affords a 5-second window in which to move aircraft. A 4 1/2-second window is assessed as being limiting, which leads to an 18-second minimum roll period. Figure 12 graphically depicts the criteria. Three degrees of roll amplitude can be accommodated with significant difficulty if the roll period is greater than 20 seconds. Below 18 seconds, 2 degrees is maximum. In the range of 18 to 20 seconds, the ability to work with ship motion is a function of the crew's experience and ability.

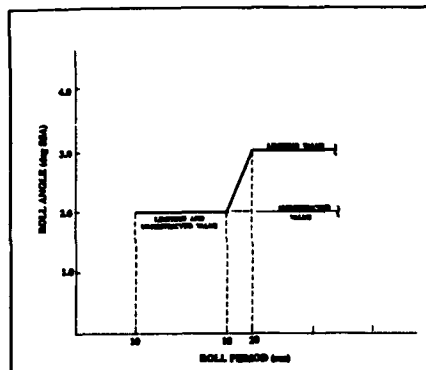


FIGURE 12. LIMITING ROLL CRITERION

b. The landing signal officer can see horizontal displacements of the ramp which result from a combination of sway, roll and yaw. Horizontal displacements less than 1.5 meters (5 feet) do not cause off-center landings.

However, as the horizontal displacement approaches 4.6 meters (15 feet), off center landings become more likely, risking damage to arresting gear and other aircraft. The criteria apply to the total horizontal displacement.

c. Ramp vertical displacement consists of the combined effects of pitch, roll and heave. At the limit value, the motion exceeds the capability of automatically stabilized Fresnel Lens Optical Landing System (FLOLS), increasing the risk of aircraft ramp strikes. For the limiting value, fleet feedback indicates that +3.0 to -4.6 meters (+10 to -15) feet is acceptable. This has been further restricted to ± 3.0 meters (± 10 feet) SSA since ship motion amplitudes are equally distributed about the mean.

d. Pitch affects launch, recovery and handling of aircraft. Figure 13 illustrates the pitch criterion. The apparent pitch period is related to the ship's period of encounter with the dominant waves in the sea-way and is thus dependent on sea state as well as ship

speed and heading. At the 2 degree limit value for pitch amplitude, aircraft must be launched on the up-swing portion of the pitch cycle. Apparent pitch periods of 15 seconds or greater are considered necessary to safely launch aircraft under this condition. In a typical launch scenario in high seas, the ship is slowed down to limit wind over deck. This increases the apparent pitch period and increases the probability of meeting the criterion shown in Figure 13. Below 10 seconds, down to about 7 seconds, 1 degree of pitch is maximum. For aircraft recovery, the limit value of 2 degrees corresponds to the limit on the FLOLS system. Below one degree amplitude, pitch at apparent periods experienced during flight operations is not a problem for either launch or recovery. For large deck carriers, 2 degrees of pitch also corresponds to a bow displacement that is large enough to generate deck wetness and spray. For USS MIDWAY and her sister ship USS CORAL SEA, where the flight deck is significantly closer to the water surface, this limit must be reduced to 1 degree. Thus pitch is also a limit for aircraft handling.

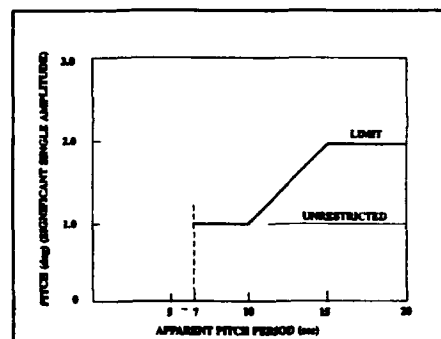


FIGURE 13. LIMITING PITCH CRITERION

e. The maximum allowable relative vertical velocity between the aircraft and the deck is driven by the strength of the aircraft's landing gear. The sink rate of the approaching aircraft uses up part of the allowable velocity. The strength margin remaining sets the maximum allowable deck velocity. Landing survey data indicate that landing points can be described as a distribution, centered within the region of the arresting wires and bracketing the design touchdown point in distance from the ramp. However, since a significant probability exists that aircraft will touch down as far aft as the ramp, to be conservative the criterion is applied at the ramp. The vertical velocity criterion is a single value because, once the landing gear

is fully compressed, the risk of damage is suddenly present.

The following comments apply to the deck attitude limits listed in Table IX:

a. The steady state angles of trim and list will vary with the ship's loading condition and the state of the list compensation system.

b. Trim changes with increasing ship speed (by different amounts for different carriers). The dynamic trim of a ship at a specific speed must be utilized, not the static trim, in assessing operability.

c. Further work is needed to determine the correct way to assess the combined effects of pitch and trim as well as list and roll. A simplified approach would be to add pitch or roll amplitudes to the values of trim or list, and compare the totals to the criteria values in Tables VIII and IX.

d. Aircraft carriers heel during turns. While aircraft launches and recoveries are not done when the carrier is maneuvering, aircraft respotting is necessary at these times to maintain the required operating tempo. Operationally, the ship will often be slowed before it is turned to minimize heel. A computer simulation is being developed to determine the effect of heel and roll in turns. At the present time, if the ability to handle aircraft during a turn needs to be analyzed, the approach outlined above for combining list and roll should be utilized. However, most aircraft handling operability assessment will assume the straight course since turning represents a small percentage of the ship's at-sea time.

Each of the criteria values listed in Table IX is explained by the following notes:

a. The limit value of 0.5 degrees trim by the bow is driven by sink off the bow considerations during aircraft launch. For aircraft recovery, the FLOLS stabilization is unrestricted by trim only up to 0.25 degrees.

The FLOLS has a lower stop that limits the lens' travel to stabilize pitch to 1.25 degrees below the glide slope when the deck is trimmed level. Trim by the bow uses up an equivalent part of the travel. Above 0.25 degrees trim, experience has shown that FLOLS pitch stabilization begins to be restricted too much. Pitch amplitude begins to exceed the remaining lens travel from time to time and the projected ball which the pilot uses to maintain glide slope begins to bounce. Trim by the bow reduces hook-to-ramp clearance and increases bolter rate.

b. Compared with zero trim, the 0.5 degree limit value of trim by the stern increases the minimum wind over deck (WOD) for recoveries by 10 knots to maintain acceptable landing loads. As the minimum

WOD is increased, turbulence increases and adds to the pilot's workload to maintain the proper aircraft attitude. Also, increased WOD is achieved by increasing ship speed, with associated costs. Half a degree of stern trim represents the maximum allowable based on pilot workload. Pilot workload is little changed between 0 and 0.25 degrees of trim. Thus 0.25 degrees is the limit for unrestricted operations.

c. The list limit is driven by the tendency of an aircraft to drift during recovery runout. List in excess of the 1 degree limit will result in unusual catapult wear patterns. Below 0.5 degree, recovery drift is within manageable limits.

For aircraft launch and recovery, wind over deck limits must be within those published in launch and recovery bulletins. Typically, course and speed restrictions are required to achieve 15 to 35 knots wind over deck with 8 knots maximum crosswind relative to either catapult or angle deck centerline for the most sensitive aircraft type. For aircraft handling, a maximum of 35 knots WOD is applied at all headings. In the evaluation of carrier designs, WOD and deck motion limits are applied at the same time.

Salt water spray on the flight deck and wetness and spray on aircraft elevators and in the hangar must be minimized. Green water precludes air operations, and spray can cause serious disruption to both flight deck operations and corrosion control. Wet hangar decks complicate maintenance actions and also add to corrosion problems. Careful design of the carrier hull form and above-water features, such as sponsons, hull flare and elevator guide rail fairings, must be combined with minimizing motions to reduce spray and wetness.

When underway at any speed, most aircraft carriers are directionally stable. However, any directional instabilities that do occur will add to the ship motion, principally yaw. One result is the familiar "dutch rolls" that make it more difficult for pilots to land their aircraft. USS MIDWAY, prior to the 1986 blister, had a significant "dutch roll." This was largely corrected by a stabilizing fin that was added in 1986. The effect of any directional instability must be added to the ship motion induced horizontal ramp displacement and the total compared with the criteria value.

8. SAMPLE DESIGN EVALUATION. To illustrate use of the criteria, a proposed fix for USS MIDWAY was evaluated using the process shown in Figure 3 and discussed above. During the MIDWAY Motion Improvement Program, several concepts

were put forward to fix the roll problem. All concepts were evaluated against a comprehensive set of naval architecture considerations, including hull strength and survivability, weight distribution, resistance and powering, noise, maneuvering, deck wetness and habitability, as well as seakeeping. Details on these concepts and considerations are contained in the paper by Ricketts and Gale (5). Suffice it to say that the chosen concept was to notch the blister at the waterline in as far as structurally feasible to raise the roll period into a range where resonant roll would be excited much less often by the encountered seas. This notch, shown in cross section in Figure 14, would raise the roll period from 12 seconds to 15.7 seconds. By comparison, USS MIDWAY before the blister was installed had a roll period of 18.6 seconds. In this example, all three hulls for USS MIDWAY are compared with a large deck carrier, USS KITTY HAWK (CV 63), which has a roll period of 22.2 seconds.

In the example, aircraft launch and recovery are grouped into one scenario where the ship must be headed into the wind to bring it within the envelope shown in Figure 15. For this example, the predominant direction of the sea is assumed in line with the wind. This will exclude the occasional swell that may come in from a different direction from a distant storm. Aircraft handling is represented by the other scenario where all ship speeds and headings are assumed equally likely.

For the operating environment, we chose the Northwest Pacific operating area in January through March, the three month period with the heaviest weather of the year. For this area and season, the statistical distribution of significant wave heights is shown in Figure 16.

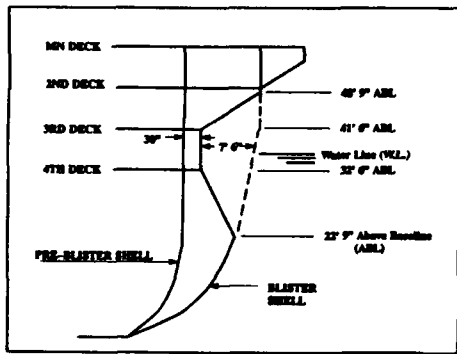


FIGURE 14. MIDWAY NOTCH CONFIGURATION

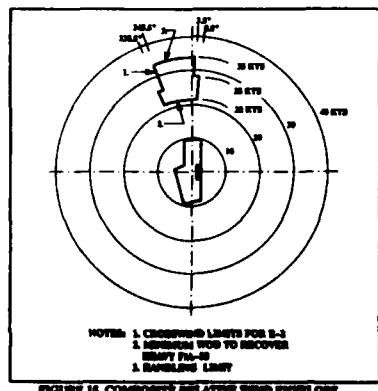


FIGURE 15. COMPOSITE RELATIVE WIND ENVELOPE

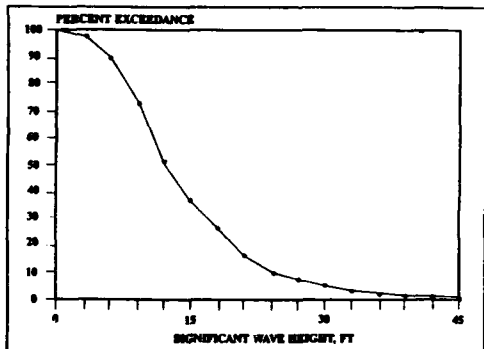


FIGURE 16. SEASONAL WAVE HEIGHT OCCURRENCE NW PACIFIC AREA (JAN-MAR)

Noteworthy is that Sea State 5, which ranges in significant wave height from 4 to 6 meters (12 to 18 feet), is exceeded 35 percent of the time. The distribution of wave modal periods is shown in Figure 17. The most frequent wave modal period is near the 12 second natural period of the blistered USS MIDWAY. For the evaluation, the statistics are assembled into percentages of time that various combinations of discrete wave heights and modal periods occur and that various combinations of wave height and wind speed occur.

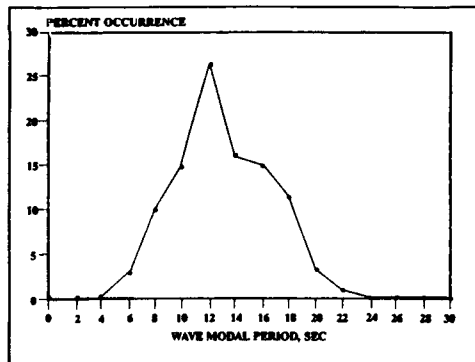
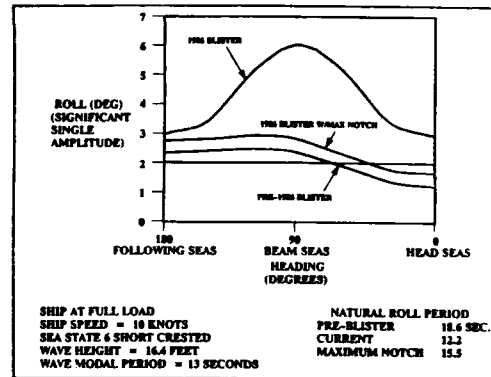


FIGURE 17. SEASONAL WAVE PERIOD OCCURRENCE
NW PACIFIC AREA (JAN-MAR)

The U. S. Navy Standard Ship Motion Program (SMP) (3) is then used to compute ship motions for all four hulls at all headings and speeds into all anticipated combinations of wave height and modal period. For one of these combinations, 5.0 meters (16.4 feet) wave height (Sea State 6) and 13 seconds modal period, and a ship speed of 10 knots, roll motion is plotted versus heading relative to the sea in Figure 18. This case highlights the significantly larger roll response of Hull X in beam seas than that of the other hulls. Also it can be seen that a maximum notched hull (back to the 1967 shell at the waterline) significantly reduces the roll compared to that of Hull X. For reference, the two degree criteria limit line is drawn on the figure. The roll of Hull X exceeds the limit at all headings.



SHIP AT FULL LOAD
SHIP SPEED = 10 KNOTS
SEA STATE 6 SHORT CRESTED
WAVE HEIGHT = 16.4 FEET
WAVE MODAL PERIOD = 13 SECONDS

NATURAL ROLL PERIOD
PRE-BLISTER 11.6 SEC.
CURRENT 12.2
MAXIMUM NOTCH 15.5

FIGURE 18. ROLL MOTION COMPARISONS

With the motion responses calculated for all combinations of wave height and modal period, the limiting values listed in Tables VIII and IX and Figures 12, 13 and 15, and the statistics of wind and wave occurrence from the chosen operating area and season are put into the U. S. Navy Seakeeping Evaluation Program (SEP). For our example, the results are shown in Figure 19. Not surprisingly, the largest differences in operability show up for the aircraft handling scenario where all speeds and headings are equally likely. The roll response of Hull X is the largest contributor to its low operability. On the other hand we assumed head seas for aircraft launch and recovery where roll motions are minimum. If we considered the small percentage of time that seas and winds were not aligned or that we had seas corrupted by swells from other directions, the operability numbers would be somewhat lower and Hull X would appear with the lowest value. In any case, Hull A appears to be a good solution to bring the USS MIDWAY back to performance the ship had before it was blistered.

It should be pointed out that funding limitations in Fiscal Year 1988 precluded fixing USS MIDWAY.

A word of caution here is that the criteria were used as if every operation were carried out 100 percent effectively up to the limiting wind or motion, and zero percent after that. Thus, the percentage values

shown in Figure 19, cannot be considered absolutes for operational planning even though they are good for design comparisons. Additionally, the percentage values assume average statistics for wind and wave occurrence over the season chosen. Separate calculations can be made for the ship's capability to operate in, or at least ride out a specific storm. That these calculations are possible to make on board ship and be displayed to guide the ship operator is the subject of the next section.

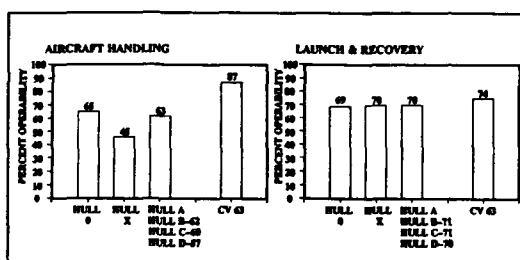


FIGURE 19. SEAKEEPING OPERABILITY ASSESSMENT IN NORTHWEST PACIFIC OCEAN (JAN-MAR)

9. ACTIVE OPERATOR GUIDANCE. Sudden extreme motions, particularly roll motions, have surprised the ship's force on USS MIDWAY during aircraft operations. Most of these surprises have occurred when the ship was maneuvering. Aircraft mishaps (tipping or skidding) resulted from sudden occurrences of extreme rolls when the ship was turned through beam seas. The ship's force may have avoided these mishaps if they had foreknowledge of expected roll amplitudes as functions of ship speed and heading, as shown in Figure 20, which was computed to represent sea conditions USS MIDWAY actually encountered on 12 January 1987. At the time, the ship was steaming due North (001 degree heading) at 30 knots into 2.4 meter (8 foot) seas with 9 second period coming from 255 degrees. The bridge reported reading a sudden 15 degrees of roll on the bridge clinometer. At the same time, the trial team from DTRC read 7.7 degrees from the ship's gyroscope. Noting that maximum roll could be as high as two times the significant, a value of 4 degrees fits

plausibly at point A on the chart, where the significant roll amplitude is predicted to be above 3 degrees. The ship's captain reacted with a "20 degree course change to put seas on the stern," represented by point B on the chart which is in a region of much lower roll. Given the display, the ship's captain may have selected a course which avoided the high roll potential region.

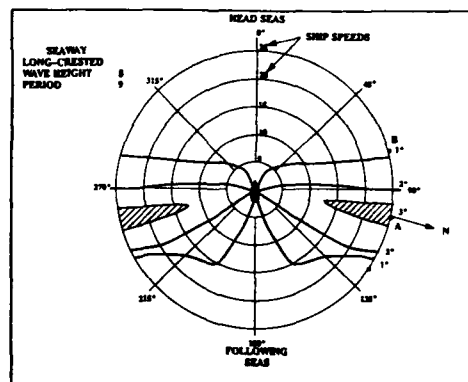


FIGURE 20. COMPUTED ROLL MOTION BLISTERED MIDWAY

DTRC has developed a version of the U. S. Navy Standard Ship Motion Program that runs on a personal computer (PC) and can, therefore, be used with the ship motion recorder on USS MIDWAY, or any other carrier given the funds to install it.

Polar diagrams can be computed and displayed in color for any desired motion response. An initial color code was adopted for easy identification of motion problem areas. Green was selected for regions where the selected motion has little or no effect on operations; yellow for motions up to the limiting value for air operations; red for motions exceeding the limiting value; and brown for motions far exceeding the limiting value. The program is also written to accommodate swell from a different direction than the wind driven sea. Given the true wind speed and direction, polars can also be computed and displayed for ship speeds and headings required to achieve the launch and recovery wind envelopes for various aircraft. An example is shown in Figure 21 for the USS CONSTELLATION (CV 64) in 3.7 meter (12 foot) seas with 11 second modal period coming from 135 degrees. The wind is at 22 knots and is coming from 132

degrees. There is no swell. In addition to roll, pitch, vertical displacement at the ramp, and ship speeds and headings required to put an F-14 aircraft into its wind envelope are also displayed. To achieve the best results for displays like these, the meteorological officer should supply the best information he has on wind and sea conditions, from some combination of weather messages and expert observations.

The active part of this operator guidance system comes in two ways. The measured motions at different headings into adequately defined sea conditions can be used to calibrate the computed polar diagrams. With experience on what motion levels do and do not limit air operations, the ship's force can adjust the criteria. When this is done on enough deployments to get a good statistical sample, our criteria may be further improved.

10. CAUTIONS. The criteria developed reflects the capability to conduct modern "big deck" battle group operations as currently practiced by the U.S. Navy. Acceptable design values are, in the final analysis, a function of the desired operational capability. Any application of these values, or more importantly this methodology, must return to the operational scenario and revalidate the governing assumptions.

The values developed represent design criteria, and are not to be construed as operational limits above which air operations will not be conducted. Operations can, and will, be conducted under more severe conditions if the operational situation dictates. Depending on the levels of training, experience and leadership on the flight deck, the ship may operate routinely in significantly worse environments than specified. It is intended that the design criteria encompass an expanded operational envelope without being overly conservative. The use of any "design" criteria to develop "operator guidance" aids must be approached with the full involvement and concurrence of the operators impacted.

11. ACKNOWLEDGEMENTS. The efforts of many who contributed to the development of the deck motion criteria for aircraft operations are deeply appreciated. It is not possible in this paper to acknowledge everyone by name. So the authors would like to acknowledge a few who made contributions. Erich Baitis, DTRC Code 1561, directed the efforts of several engineers and technicians to instrument two carriers to measure ship motions. He made several visits to the ships, traveling half way around the world each time.

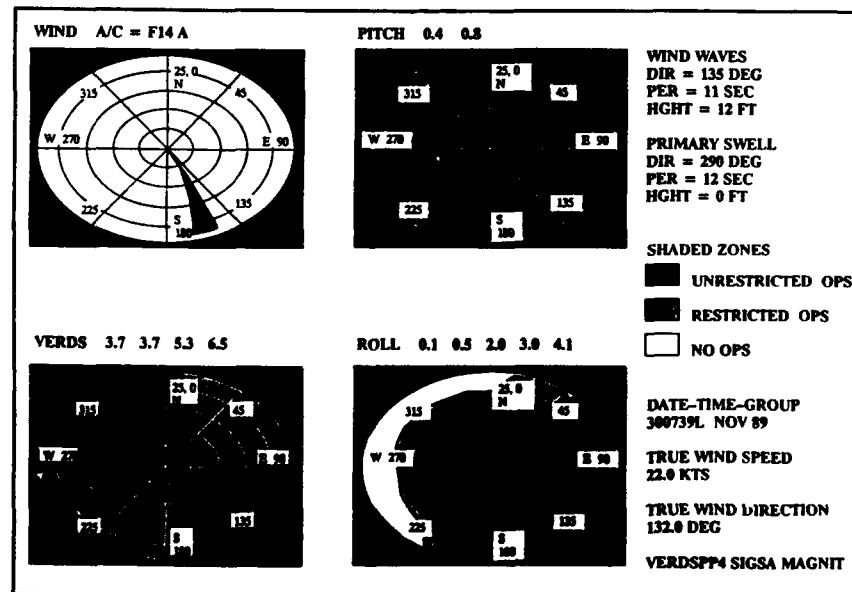


FIGURE 21. ACTIVE OPERATOR GUIDANCE DISPLAY

And he participated in the Criteria Working Group. Dave Walden and Paul Kopp, then both in DTRC Code 1561, did the criteria sensitivity and operability calculations. Lew Motter, DTRC 1561, provided DTRC team leadership during the MIDWAY Motion Improvement Program and directed model tests to verify motion predictions. Alex Smith, then in NATC Code SA70, coordinated variable consultation by engineers in the Carrier Suitability Group and set up the aircraft recovery simulations at NTSC. Then CDR Dave Finney, USN, then also in NATC Code SA70, provided valuable insights as a pilot who had flown to USS MIDWAY both before and after the blister was installed. He also participated in the flight simulations at NTSC. Tom Gallaway, NTSC Code 732, directed the efforts of engineers and technicians to perform the recovery simulations.

Special appreciation goes to many members of the Naval Air Systems Command (NAVAIR), Ship and Shore Installations Division, who coordinated the air department workshop and provide valuable consultation on aircraft operations aboard ship; and to the representatives from U. S. Fleet Air Forces, Atlantic and Pacific, who participated in the workshop.

Helping MMIP Team Leader Pete Gale, with many helpful suggestions and careful review of the criteria were Dave Byers, NAVSEA 55D, Ed Comstock, then NAVSEA 55W3, and Dick Steward, then NAVSEA 503. Ultimately, RADM Myron Ricketts, USN (now retired), then NAVSEA 05 and RADM Wilson, USN, then NAVAIR 05, provided the management atmosphere for the joint effort to succeed, along with their own careful review of the results.

12. REFERENCES.

1. Pierson, W.J., Jr., "The Spectral Ocean Wave Model (SOWM), a Northern Hemisphere Model for Specifying and Forecasting Ocean Wave Spectra," David Taylor Naval Ship Research and Development Center Report DTNSRDC-82/011, July 1982.
2. Comstock, E.N., Bales, S.L. and Gentile, D.M., "Seakeeping Performance Comparison of Air Capable Ships", Naval Engineers Journal, XX, 3, April 1982, pp 101-117.
3. Meyers, W.G., Applebee, T.R. and Baitis, A.E., "User's Manual for the Standard Ship Motion Program, SMP", David Taylor Naval Ship Research and Development Center Report DTNSRDC/SPD-0936-01, September 1981.
4. McCreight, K.K. and Stahl, R.G., "Seakeeping Evaluation Program (SEP) - Revision 1: User's Manual", David Taylor Naval Ship Research and Development Center Report DTNSRDC/SHD-1223-02, August 1987.
5. Ricketts, M.V. and Gale, P.A., "On Motions, Wetness, and Such: The USS MIDWAY Blister Story", The Society of Naval Architects and Marine Engineers, Annual Meeting Paper No. 16, November, 1989.
6. "Truck, Lift, Fork Electric, Solid Tires, 6000 Pound Capacity, 100 Inch Lift, Shipboard Type EE," Military Specification Sheet MIL-T-21869/22E, 17 March 1976.
7. "Truck, Lift, Fork, Diesel, Pneumatic Tires, 6000 Pound Capacity, 130 Inch Lift, Shipboard," Military Specification Sheet MIL-T-21868/4A, 15 March 1976.
8. "Motion Induced Subsystem Performance Degradation", NAVSEA Report 3213-79-24, September 1979.
9. "Mobile Handling Equipment Shipboard Capability Tests, Phase II Report, Roll Table Tests," Report to NSEC Code 6141B, Washington Technological Associates Report 3355.01, June 1970.
10. "Coating System, Nonskid, for Roll or Spray Application," Military Specification DOD-C-24667(NAVY), 11 September 1986.
11. "The Effect of Ship Length, Ship Motions and Landing Geometry upon the Safety of Carrier Operations", Naval Warfare Analysis Group Study No. 20, October 1961.
12. NAVAIR letter 9079 Ser AIR-5512/016 of 21 May 1987.
13. NAVSEA ltr 9079 OPR: 05 Ser 55B/56 of 6 July 1987.
14. OPNAV ltr 9079 Ser 551G/7U404592 of 21 July 1987.

The Aerodynamics of Ship Superstructures

J. Val. Healey,
Department of Aeronautics and Astronautics,
Naval Postgraduate School, Monterey,
California, U.S.A. 93943-5000

Preface

After seventy years of naval aviation, a belated understanding of the aerodynamics of ships is slowly emerging. The essence of the message is that typical superstructure configurations are extremely poor aerodynamically. This means: safe operating envelopes that are severely and unnecessarily limited; exposure of pilots and crew to unnecessary danger and; blade strikes that occasionally result in the complete loss of a helicopter. The airflows around these poor configurations contain many recirculating zones, bounded by shear layers that emanate from the sharp edges of the superstructure. These zones vary enormously in size in an intermittent manner, giving rise to unsteady flows with extreme velocity gradients and turbulence intensity levels that are too high to be measured with hot-wire anemometers.

The only sensible conclusion one can reach after several years of studying the aerodynamics of both non-aviation ships and carriers is that the non-aviation ships are completely unsuited to efficient interfacing with helicopters and carriers could be greatly improved. The very common boxy-hangar/aft-flight-deck combination is an aerodynamic disaster and should be abolished.

A new generation of aerodynamically efficient ships should be designed, which means integrating aerodynamic analyses into the design process. Testing of a prototype in a suitable simulated atmospheric layer should reveal any aerodynamically undesirable features of a design and any addition to the cost would be miniscule. Expected payoffs should include virtually no interface testing, much wider operating envelopes than exist at the present time and the elimination of blade strikes.

Preliminary ideas for new ship superstructures are being developed. It is proposed that flight operations be conducted from a flat expanse of deck, and that landings be made on a platform that can be lowered for storage below deck level. The edges of the deck should be aerodynamically designed - rounded or chamfered to minimize or prevent recirculation zones and relatively low wind velocities over the deck can be obtained by suitable slatted wind-break fences. The effect of helicopter downwash on such fences must be carefully studied.

Ideally, on grounds of cost and convenience, simulation of the interface should be based on numerical predictions of the airwake. However, most practical computational fluid dynamics codes available today are based on the time-averaged Navier-Stokes equations, which cannot predict the spectra of the velocity fluctuations. Without the latter, the response of the helicopter to the turbulent wake cannot be predicted. Spectral and eddy simulation methods hold considerable promise for the future, but today they can be applied to simple geometries only.

It is very likely that, in the near future, a multi-point turbulence model for helicopters will be required. One already exists for airplanes but it based on spatial correlations that are known empirically for flight in the free atmosphere. No such relationships exist for the wake of a ship or structure. Experimental correlation data will then have to be obtained from the wakes of ships or ship models.

Abstract

After seventy years of naval aviation, a belated understanding of the aerodynamics of ships is slowly emerging. The lack of such understanding, and undoubtedly other reasons, has led to superstructure configurations that are unsuited to adjacent helicopter flight. This has resulted in severely limited safe operating envelopes, danger to pilots and ship personnel and blade strikes that occasionally result in the complete loss of a helicopter. The airflows around ships abound with recirculating zones, bounded by shear layers that emanate from the sharp edges of the superstructure. These zones vary enormously in size in an intermittent manner, giving rise to flows with extreme velocity gradients and turbulence intensity levels that are too high to be measured with hot-wire anemometers. This complicates the situation because, at the present time, a database for simulation can be established only via measurement. The essential ingredients for the aerodynamic design of new ships have been proposed and some suggestions for the improvement of the aerodynamics of existing ships have been made. Correcting an aerodynamically poor ship is no substitute for the incorporation of aerodynamics into the ship design process.

1 Introduction

It is an extraordinary fact that, although naval aviation has been with us for over seventy years, there is still a profound ignorance of ship aerodynamics. The reason for this appears to stem from a combination of factors, one of which is a short-sighted view of the problem. Instead of funding fundamental studies of the underlying problems, poorly planned piecemeal approaches have been taken, which have squandered resources and brought the solution no closer. This undoubtedly led to the perception that the problems have no solution and to a reluctance to commit further resources.

A second important factor is that the nature of the problem has its roots in meteorology and in an obscure branch of aerodynamics, known as "bluff-body-aerodynamics", which deals with airflows around blunt bodies that have massive separated regions in their wakes.

Airflows around bluff bodies, such as bridges and similar structures have been studied for over a century, but it was only since the advent of relatively flexible high-rise buildings that extensive studies of the flows around such objects have been conducted. The early to mid 1970's was the most fruitful period and was spurred on by problems with the high-rise buildings and, because of oil scarcity and costs, the need to reduce the drag on ground vehicles. Unfortunately, politics and the return of cheap oil, later in the late 1970's, erased most of the programs.

A further, and perhaps the most significant factor, is that ships are designed by naval architects, whose specialty has little relation to the aerodynamics of helicopters. There is no pressure on them to design the ships with aerodynamics in mind, presumably because those involved in the procurement process have an equal ignorance of the reasons for the problems in the ship/helicopter interface. Undoubtedly, over decades, enormous efforts have been exerted by ship designers and procurement personnel in an attempt to satisfy all the competing interests. It is unlikely that the addition of another element into the competition will be welcome.

Traditional aerodynamics is usually taught in college, with little reference to meteorology, apart from the changes

in atmospheric properties with elevation. To make aerodynamics problems simpler, instead of assuming that the vehicle moves through the atmosphere, it is usually assumed that the vehicle is still and that the air flows past it. Under the usual zero-turbulence assumption and steady flight at some fixed altitude, there is no difference between these flows. Near the ground, however, when the wind speed can be about the same as the vehicle's, the difference can be quite profound, except for the case of a ship steaming in a calm atmosphere.

When a storm rises, winds blow over an initially relatively smooth sea, and the interaction between the two whips the water waves to greater heights, while increasing the turbulence in the air. There is an ultimate equilibrium state between the fully developed water waves and the velocity and turbulence profiles in the air. Apart from contamination of the air by water spray, the wave motion interacts with the air in the same manner as a land surface with an equivalent roughness - approximately a desert.

Wind that blows over such a roughness develops a sheared profile and can have turbulence levels thirty times higher than the level in most wind tunnels, which are usually set up to simulate a uniform velocity profile with the minimum of turbulence. The shear implies a vorticity distribution that decreases with height, whose effect is primarily the generation of a number of "horseshoe", or "necklace", vortices that form around the base of a body immersed in the layer and trail downwind.

Unfortunately, the differences between flows around bluff bodies exposed to uniform and sheared velocity distributions are not well documented. Important studies were made on rectangular blocks by Dianat and Castro [1,2] and showed definite differences. It appears that a body submerged in a thick boundary layer i.e. a simulated atmospheric layer, with one face directed upwind, has a stagnation point very roughly at two thirds of the height. Below this point which, of course is really a zone, because of the unsteadiness, the flow is directed downwards into the vortex and, above the point, the flow goes towards the top.

In a thin boundary layer, i.e. what one obtains in an attempt at a uniform profile, a similar horseshoe vortex exists at the foot of the structure, but it is now only a very small fraction of the height of the body and, on most of the body, the flow stagnates on a vertical line at the mid upwind side and moves horizontally towards the front edges. Near the top front, of course, it will also flow upwards, and in some circumstances the flow there will be somewhat similar to that from the thick boundary layer.

In the thin layer, the freestream turbulence level is almost negligible, but this does not mean a smooth flow in the wake. The shear layers that leave the sharp edges of the body possess an inherent unsteadiness that still generates a highly turbulent wake. In the thick layer case, the flow patterns are somewhat different [1,2] and the shear layers are now buffeted externally by the freestream turbulence which, in general, yields a quite different flowfield. Meroney [3], in a recent review of modeling flows about buildings, suggests that the major influence of the freestream turbulence is on the separating and reattaching shear layers.

As will be reported later, the turbulence levels measured in the wake of a ship model, in a thin layer, maximize close to the ship and die away with distance. The values measured in the wake of the model, in a thick layer, minimize near the model and increase with distance from it. This information alone would appear to be sufficient to establish that a uniform velocity profile does not model the flow around a ship, except for ship-generated winds. Detailed analyses of the modeling of atmospheric boundary layers

are given in References 4 and 5. The former established that the modeling of the layer in a Naval Postgraduate School (NPS) wind tunnel is quite satisfactory.

2 The Wakes of Ship Models

2.1 The Relatively Far Wake

Experience at NPS [4,6,7] indicates that the near wakes of ship models are characterized by steep velocity gradients, unsteady recirculating flows, high turbulence levels and contain significant amounts of low-frequency energy. Preliminary studies [4] were made of the flow around a model of a DD-963, along certain helicopter landing paths, to a point about 2/3 of the hangar height over the touch-down point, in a simulated strong-wind condition. The 3-d hot-wire anemometer measurements were made at 17 points, each 1/16 of a ship length apart, aft of the touch-down point. These points were denoted by 0 over the latter point and 16 at one ship length away. The velocity components were made nondimensional with the along-wind speed u_a recorded at the ship anemometer for each yaw position and the turbulence intensities were formed by dividing the rms values by the same value of u_a . Only the zero yaw results are presented here and more details are given in Reference 4.

In the discussion that follows, it is assumed that the start of a run is one ship-length away from the touch-down point and the "% point" is a percentage of a ship-length aft of the latter point. The along-wind component u/u_a of the mean velocity as a function non-dimensional distance aft of the touch-down point is shown in Figure 1. There is a gradual reduction from about 90% of the ship anemometer reading, at one ship length away, to about 40% of that reading over the touchdown point. As the ship is approached, the gradient becomes steepest between the points 2 and 4 (10-25%). The transverse, v/u_a , and vertical, w/u_a , components are shown in Figure 2; the transverse component is always very small, starts at a few percent of u_a to starboard and gradually declines to zero as the ship is approached. The vertical component, is almost zero from the start (point 17) to about point 12 (75%) and then there is an increasing downflow until the maximum of about 15% of u_a is attained, at about point 2 (15%). The downflow then decreases to zero over the touch-down point.

The corresponding turbulence intensity profiles are shown in Figure 3. All three turbulence intensities lie within a range $6\% < \sigma/u_a < 8\%$ approximately, until point 5 (25%) is reached. Thereafter, all curves decline steeply to zero over the touch-down point. It is interesting, but not too surprising, that Fortenbaugh [8,9] derived an airwake model, for simulation of the flight near a DD-963, from measurements made in a uniform, almost zero-free-stream-turbulence, flow. It indicated that the turbulence intensities increased from almost zero about one ship-length away to a maximum over the flight-deck. This is the exact opposite of the trend indicated above.

It is essential that the turbulence intensities based on the local velocity components be less than about 30%. The results indicate that this is the situation at distances at points 5 through 17. There are considerable deviations from these conditions as the ship is approached, shedding doubt on the accuracy of the measurements.

The spectra for this zero-yaw run is shown in Figure 4 for the along-wind component only. The spectra at five points 0,1,4,8 and 16 are given. It is evident that there is little along-wind turbulent energy at the zero-point i.e. over the

flight-deck. This point is probably located in the slower-moving lower levels of the shear layer that leaves the hangar roof. It is probable that the reading is outside the capacity of the instrument. The general trend is for the turbulent energy to decrease slightly as the ship is approached. The trend for the v -spectra (not shown) is somewhat different, with the zero point having a very energetic flow in a bandwidth near 50 Hz. At this point, however, the energy drops off more rapidly with increasing frequency than for any of the other points. Again this reading could be beyond the range of the instrument. The w -spectra (not shown) look very similar at all five points, there being little more than a factor of two between any of the curves.

The results for all three spectra show that the turbulent energy levels peak somewhere between 10 and 100 Hz. and then decline rapidly to relatively small values at 1 KHz. To transfer this information to the corresponding full size ship, these frequencies should be divided by twelve, which was the Strouhal number, indicating that the energy peaks are roughly in the range of about one to eight Hz. and that there is usually little turbulent energy above about 100 Hz.

The region that includes points 0 through 4 is considered the near-wake and will be discussed further in the next section.

2.2 The Near Wake

The very high levels of turbulence over the flight-deck renders extremely valuable, flowfield information obtained by means of flow-visualization techniques. The most useful of the latter include the use of fluorescent minitufts attached to the body surface and the injection of visualization contaminants such as neutral helium bubbles and smoke. Figure 5 is a good example of the utility of the minitufts attached to a body which is then exposed to the wind tunnel flow and illuminated with ultraviolet light. In this case, the body was a generic destroyer, constructed with blocks and a bow section attached. To apply this technique, the model is first painted a flat black and has a grid of pencil lines drawn on the surface. The tuft threads are then gently stretched along those lines and a very small dab of glue placed at the intersections of the lines. Finally each thread is cut with a very sharp knife to one side of each glue point. The minitufts align themselves with the local flow direction on the surface and, because the photograph exposure was a couple of seconds, a fan shaped blur at the end of a tuft indicates a very turbulent region. In Figure 5 the model was yawed 30° to starboard. The tufts inside the leading edge at the bow show a separated zone that extends about one quarter of the width, where the flow reattaches. Inside the zone, the flow goes aft in a helical motion. The extent of the separated zones are clearly evident in the wakes of the superstructure "blocks".

Helium bubbles are an effective method of illustrating the streaklines in the broader flow. However, photographing them does not reveal any transient nor unsteady phenomena. The principal disadvantage of helium bubbles is that they reflect only about 5% of the incident light and, if injected upstream of the model, they tend to avoid the recirculating regions. Useful information can be obtained from injecting the bubbles into the wake of the model from a point on the floor of the tunnel. Watching them rise along the hull on the lee side of the model and frequently crossing the whole of the deck, in the upwind direction, is an interesting experience.

Figure 6 represents, via helium bubble streaklines, the wake vortex of the generic destroyer yawed slightly to port.

This vortex is relatively small for small yaw angles but becomes quite massive when the yaw reaches about 45° . Figure 7 shows the flow over the aft flight-deck of the U.S.S. Tarawa. The extent of recirculating zones are frequently marked by bubbles that stop in mid-air and reverse their directions. However, this extent varies substantially in time. The out-of-focus bubble traces in the right side of the picture indicate a wake that extends to about double the hangar elevation. Figure 8 illustrates the flow over the bow of the generic model of Figure 5 when yawed to port. The region with many bubble traces, at about one third of the width of the bow from the starboard side, is evidently the boundary of the reattachment zone. The flow in this type of region is discussed later. Figure 9 shows a long exposure photograph of the flow over the flight-deck of the DD-963 at zero yaw. It is clear that there is a recirculating vortical motion that covers the front half of the deck. The bright patch on the left upper side of the picture is the region over the hangar, through which most of the bubbles enter. It is also clear that the flow is very non-uniform well aft of the deck. This recirculating zone is similar to that shown diagrammatically in Figure 10 for the U.S.S. Wabash.

Injection of smoke on the upwind side of the model is a good way to simulate a ship in a fogbank but does not reveal much information. The smoke is best injected into the regions of interest through fine tubes and it reveals the streak-patterns in confined areas better than the helium bubbles. It does scatter fairly rapidly but, nevertheless, the video pictures can give a reasonable picture of the flowfield. Unsteady phenomena, within a certain range of frequencies can be detected by slow-motion and single-frame play.

A recent study [7] was conducted at the NPS, of the flow around the hangar and aft flight deck of a supply ship, in an effort to determine the cause of helicopter blade strikes. It involved extensive flow visualization, and some hot-wire measurements around the locus of the tip of the blade, at a station where most strikes occur. A range of flows, from the port side, were studied for ship yaw angles 0° to 100° and a small-diameter wire was placed around the blade-tip locus.

It was found that the helium bubble flow visualization method can miss important unsteady phenomena occurring over the flight deck. A combination of smoke injection and slow-motion replay of video tape revealed an almost periodic flapping of a shear layer that emanated from the aft vertical corner of the hangar at one yaw angle. At zero yaw, the flow is symmetric about the ship axis as shown in Figure 10. The major recirculating zone covers the aft face of the hangar and there are minor ones, not shown, inside the edges of the deck.

A generic sketch of the flow over the flight deck for non-zero yaw angles, is shown in Figure 11. Three separated regions are identified in the figure. The sizes of the recirculating zones and their intensities vary considerably with ship yaw angle. At small yaw angles, region 1 is by far the largest and most vigorous. It tends to fluctuate, mainly in an unsteady way, but for the 50° case, it was almost periodic. The reattachment point on the hangar face started the cycle about $1/4$ way across and gradually moved to starboard and the zone increases greatly in size. Approaching the edge, it detaches from the hangar and the shear layer swings aft, pivoting at the port edge of the hangar releasing the recirculation in the form of a vortex which then crosses the deck diagonally, aft and starboard. As the vortex moves away, a massive surge of fluid flows in forward of it from the wake of the ship, extending this zone to about two hangar heights. The zone then collapses, and the shear layer at the port edge swings in towards the hangar, reattaches at

the point at which the cycle began and the process starts again. The period for this was $1/5$ of a second approximately, which corresponds to about 2.5 seconds full scale. This period is not related to that due to vortex shedding from a 2-d body with the same section as the hangar.

As the yaw angle increases beyond 50° , this zone reduces in size. At 70° , the flow does not detach from the hangar face, but the stagnation point oscillates, in an intermittent way, between points at about 80% and 90% of the beam from the port edge. At 70° and above, the recirculating zones 2 and 3 play a prominent role, with the port boundary of region 2 intermittently coming upwind to about the ship's axis.

At 90° , region 1 detaches from the hangar face at the starboard edge, as in the 50° case, but is now much smaller and less vigorous. The boundary of region 2 oscillates intermittently about $2/3$ way upwind across the deck, and region 3 reaches about $1/3$ to $1/2$ the hangar height. The region around the blade periphery now becomes strongly influenced by the gyrations of the flow in these two regions and, hardly at all, by region one.

At 110° , at which blade strikes have occurred, region one is confined to the forward 20% or so of the deck, region 3 now dominates the flow around the rotor, and region 2 occasionally pulses onto the deck and retreats again. Region 3 oscillates intermittently back and forth across the deck, varying in size all the while. The flow through the rotor blade is largely the flow exterior to region 3 and obviously fluctuates strongly with the motion of that region.

It is uncertain how much of the intermittent fluctuations that exist over the flight deck are due to the ship itself and how much accrue from intermittency in the artificial atmospheric boundary layer. It is known that these intermittencies occur in the freestream wind tunnel flow more frequently than they do in the atmosphere. Correlation studies could be made to differentiate those due to the freestream flow from ones associated with the separation.

3 Hot-wire Measurements over the Flight Deck

As was mentioned above, it appears that the capacity of the hot-wire anemometer was exceeded near the ship. Even if one uses wind tunnel speeds that are sufficiently high to register on pressure probes, with appropriate resolution and accuracy, such readings are in considerable doubt, if the turbulence intensities, based on the local velocities, are greater than about 30% [11]. To check the previous doubts, further measurements were made over the flight-deck of the AOR at four points around the blade tip locus of the plane of the aft H-46 rotor: forward 1, starboard 2, aft 3 and port 4 for the same range of yaw angles discussed above. The measurements were referenced to the value of the reading taken at the ship anemometer elevation for each yaw angle. The plane of the rotor was about $2/3$ of the hangar height.

The general trends predicted by these measurements were as follows: the along-wind velocity components at all four points generally increase from about 40% of the ship anemometer speed at zero yaw to about 95% at 110° . The transverse components generally decrease slightly to about 40° yaw, increase to a maximum of about 15% of the ship anemometer speed, then drop sharply to 90° and rise again. Generally, the transverse components are never greater than about 20% of the ship anemometer speed. The general trend for the vertical velocity components was to increase from about zero at zero yaw, to a maximum of about

40% of the ship anemometer reading at 110° . This is remarkably high.

The turbulence intensities, which were formed with the rms values of the fluctuations and the ship anemometer speed, behaves more erratically than the velocity components. The alongwind values generally increases to a maximum of about 17%, at about 30° to 50° , and then declines to a value in the 6 to 12% range.

However, it must be stated that, while the above process of forming the turbulence intensities, with the freestream wind speed measured at the ship anemometer, lead to perfectly reasonable turbulence intensity levels, it is also an excellent way of camouflaging hot-wire readings that may be garbage. This is, however, often the "engineering" approach to such problems. Unless the turbulence intensities formed with the local components of the velocity are all less than about 30% [10,11], the readings are questionable. Most of the measurements indicated that the rms values of the fluctuations were a reasonable size and, that the frequently-measured turbulence intensities of several hundred percent were due to very small mean velocity components. A laser doppler anemometer could probably do better here. One far less expensive alternative is a pulsed-wire anemometer, which is well documented by Castro [11] and Bradbury and Castro [12]. This is a time-of-flight device that has no ambiguity in determination of the direction. A thermal pulse is generated at a pair of electrodes and is picked up by a sensor wire. A timing circuit determines the time of flight across the known separation distance.

A flying wire anemometer would resolve the problem of low velocity components. It is essentially a hot-wire anemometer mounted on a sled that flies along a support wire or wires through the region whose velocity field is to be mapped. Melbourne has extensively developed this instrument and it is discussed in a book by Perry [13]. The motion of the probe itself imposes a large mean velocity on the flowfield, rendering possible, the measurements of very low velocities. Although this instrument would be a good choice for measurement of the very low velocities, there would be still be problems of resolution of the low frequency turbulence because of the short sampling times.

4 A new Generation of Aerodynamically Efficient Ships ?

Because of their very poor aerodynamic performance, a new generation of aerodynamically efficient ships should be designed. This means that aerodynamic analyses should be brought into the design process. Testing of a prototype in a suitable simulated atmospheric layer should reveal any aerodynamically undesirable features of a design. Expected payoffs should include far less interface testing, much wider operating envelopes than exist at the present time and the elimination of blade strikes. The following tentative guidelines are proposed for a new generation of ships:

4.1 The Hull Configuration

The ship and the flight deck should be kept as low as possible. Wind velocities decrease as the water surface is approached. The problem, however, is that, to minimize the drag on ships, the length of the ship should be about ten times the beam. Furthermore, the drag on the portion of the ship above the water is far less than that on the submerged part. This means that a large storage region above the water is desirable. Perhaps the SWATH ship

with multi-hulls and with a large storage volume near the water surface is part of the answer. The avoidance of the usual boxy hangar would be a good step in the design process. A flat expanse of deck at a relatively low elevation could have little in the way of separated flows, apart from the edges, which are discussed below. Landing on that deck on a platform that could be lowered below with the helicopter, is a possibility. High wind speeds can be controlled by 50%, or thereabouts, slatted fences, so long as there is no recirculation.

4.2 If a Boxy Hangar must exist

If the current hangar/flight-deck combination is to be retained, the flight deck should be placed, preferably, well forward or well aft of the hangar, which of course increases the problem of storing and retrieving the helicopter. Box-like hangars should not be used without substantial rounding or chamfering of the edges. It probably would be better to place, forward of the hangar, a fairly open flight deck, through which some of the approaching wind could pass. Helicopter pilots are very uncomfortable with a massive structure coming towards them while maneuvering to land. If the landing deck were at or near the hangar roof elevation, the turbulence and recirculation problems would be far less than at the level of the hangar floor and the pilots would feel better because of the absence of the hangar face. The helicopter could then be winched into the hangar or lowered to the level of the hangar floor and rolled into the hangar. The Soviet Kirov class cruisers appear to be the only ships to which aerodynamic design is likely to have been applied. Interesting features of that ship include streamlined superstructural elements placed well forward of the flight-deck which means a minor wake effect at the flight deck position. The flight-deck is placed aft and sunk below the level of the main deck. However, that drop is relatively small and the aft hangar face slopes aft down to the flight-deck. The aerodynamic design could be further improved by increasing the slope, but this introduces new problems.

4.3 The Edge of the Deck

Research is required to determine the optimum shape of the edge of the flight deck. As discussed above, there is a recirculating region inside these edges, whose size and intensity depends on the ship yaw angle. It is likely that these flows can be adequately controlled by rounding of chamfering the edges.

4.4 New Design Procedure

Following the lead of the general aerodynamics field, a combined computational/experimental approach should be made to the design of both aviation and non-aviation ships. The aim would be to determine the configurations that have the lowest levels of velocity and turbulence and the least number of separated flows in the vicinity of the flight deck. These studies, and an experimental validation of the final version, would be a miniscule part of the total cost.

Finally, it is interesting that a streamlined ship also has a smaller radar cross-section, which suggests that stealth and aerodynamic-designs are complementary.

5 Improving Existing Ships

Without a doubt, positioning the flight deck aft of the ill-

shaped hangar is an extremely poor choice. It is important to try to address the question of what steps might be taken to alleviate the problems on the very many existing ships afflicted with this combination.

5.1 Adding a Porous Landing Deck

If sufficient space exists, the relatively open structure, mentioned above in Section 4.2, might be retrofitted forward of the hangar. With small ships, however, care should be taken with the placement of a large mass at high elevations; it could have serious implications for the stability of the ship.

Erecting the open type of structure discussed above over the existing flight-deck, aft of the hangar, would probably improve the current situation but would not be as good as having it forward of the hangar. It was mentioned previously that, at some yaw angles, the wake extends well above the existing hangar of the AOR. Again the helicopter would have to be lowered to the deck for storage or somehow winched into the hangar.

5.2 Separation Control via Deflectors

Some tentative attempts have been made at NPS to control the flow around the edges of the deck and the hangar, using curved deflectors positioned at the edges. It proved a remarkably successful way to control the flow separation at the edges of the deck but only aggravated the flow around the hangar. Further work will have to be done here. It is conceivable that the deflector was too small. Extensive studies have been made of the use of deflectors in an attempt to control the separation on a backward-facing step [14]. The step was intended to represent a simplified model the flow along the axis of a zero yaw ship over the hangar aft-flight deck combination. The aim was to reduce the velocities and turbulence levels in the region where a typical helicopter rotor would operate. These deflectors were flat, or curved and included a range of widths (for the flat ones), radii, turn angles and porosities. Many deflectors aggravated the flow and it has to be concluded that the problem has no simple solution. Reynolds number modeling must be considered in these types of studies, since the flows are no longer those over sharp-edged bluff bodies, for which the flow pattern remains constant for beam-based Reynolds numbers in excess of about 10,000. Retro-fitting ships with separation control devices is likely to be a very laborious process.

5.3 The Shelterbelt Approach

The interface problems are caused by high values of the relative wind speeds. The problems could be alleviated or solved by passing the wind that approaches the ship through a "shelter belt" that would dissipate the kinetic energy of the wind by first forming large turbulent eddies and then smaller ones and finally the destruction via viscosity of the latter. Figure 12 shows the shelterbelt approach. The engineering equivalent would be a "forest" of masts, of various sizes, densely clustered around the hangar roof and along the port and starboard sides.

Since the basic problem arises because of high levels of wind kinetic energy, as the sharp hangar and deck edges are approached, a possible solution is the deployment of a device to reduce that energy. Such a machine is called a

wind turbine. The wake of a wind turbine running in a strong wind is a gentle breeze. A possible configuration, without any protective handrails, is shown in Figure 13. These two figures are provided solely for the entertainment of NAVSEA.

6 Simulation of Flight in the Interface

Ideally, simulation of the wake should be based on numerical predictions. However, most practical computational fluid dynamics codes available today are based on the time-averaged Navier-Stokes equations, which cannot predict the spectra of the velocity fluctuations. Spectral and eddy simulation methods hold considerable promise for the future, but today they can be applied to simple geometries only. This leaves experimental measurements as the only source of complete wake data. Without the spectrum of the velocity fluctuations, the response of the helicopter to the turbulent wake cannot be predicted. Since the wake is everywhere very turbulent, it is very unlikely that the use of mean flow properties alone in a simulator will give any meaningful results. The time averaged codes, however, are adequate for purposes of airwake tailoring or the aerodynamic design of ships.

Existing turbulence models for simulation are based on the assumption that the aircraft is a point mass and that the turbulence acts at the center of gravity only. This is very primitive and whatever success it is likely to have will be in regions where the velocity and turbulence fields change very little across the physical extent of the aircraft. For a helicopter the gradients must be sufficiently small to give small changes only across the rotor disk. It is noted that the Spruance class destroyer is approximately 170 meters in length and, hence, the points 1 through 17 marking data collection sites are roughly 10 meters apart and the point at 10% of a ship-length from touchdown corresponds to about 17 meters away and would be approximately the diameter of a large rotor. The diameters of a number of helicopter rotors are marked on Figure 3 to indicate a scale. The velocities, turbulence intensities and spectra should not change significantly across these diameters. The data referred to are single-point, taken along the line of flight, and steep gradients may exist in the transverse direction. Measurements along adjacent parallel flight paths would be necessary to determine the extent of these variations. For the 30° and 330° yaw positions, the gradients are significantly steeper [4,15] than for the zero yaw results presented here.

A multi-point turbulence model for airplanes already exists [16]. The basis of this study is the assumption that the turbulence acts at five points on the airplane: the nose, center of gravity, two points on the wings and at the tail. However, it is based on spatial correlations that are known for flight in the free atmosphere. No such empirical relationships exist for the wake of a ship or structure. Application to a helicopter will probably involve points at the center of gravity, the tail and some minimum number in the rotor plane. Experimental correlation data will then have to be obtained from the wakes of ships at the corresponding points. It would be instructive to obtain these data from the wake of a model carrier and apply the existing multi-point model to simulating carrier landings. Recent inquiries by the author failed to uncover any evidence that simulations of carrier flight operations have ever been based on airwake data. Alternatively, a multi-point helicopter model

might be developed that is based on some extremes of the existing atmospheric data. These studies would represent an intermediate, confidence building, step between the final stage that involves the multi-point helicopter model and the non-aviation ship airwake.

7 Conclusions

The only sensible conclusion one can reach after several years of studying the aerodynamics of both non-aviation ships and carriers is that the non-aviation ships are completely unsuited to efficient interfacing with helicopters and carriers could be greatly improved. A new generation of aerodynamically efficient ships should be designed, which means integrating aerodynamic analyses into the design process. Testing of a prototype in a suitable simulated atmospheric layer should reveal any aerodynamically undesirable features of a design and any addition to the cost would be miniscule. Expected payoffs should include virtually no interface testing, much wider operating envelopes than exist at the present time and the elimination of blade strikes.

8 References

1. Castro, I. P. and M. Dianat, "Surface Flow Patterns on Rectangular Bodies in Thick Boundary Layers", *Journal of Wind Engineering and Industrial Aerodynamics*, Vol. 11, 1983, pp. 107-119.
2. Dianat, M. and I. P. Castro, "Fluctuating Surface Stresses on Bluff Bodies", *Journal of Wind Engineering and Industrial Aerodynamics*, Vol. 17, 1984, pp. 133-146.
3. Merconey, R. N., "Wind Tunnel Modeling of the Flow about Bluff Bodies", *Journal of Wind Engineering and Industrial Aerodynamics*, Vol. 29, 1988, pp. 203-223.
4. Healey, J. Val. "Establishing a Database for Flight in the Wakes of Structures" To be published.
5. E.J. Plate in "Engineering Meteorology", Elsevier Scientific Publishing Company, Amsterdam, Netherlands (ISBN 0-444-41972-1) 1982.
6. Johns M., and J. Val. Healey, "The Airwake of a DD-963 Class Destroyer", *Naval Engineer's Journal*, May 1989, pp 36-42.
7. Rhoades, M. M. and J. Val. Healey, "The Flight-Deck Aerodynamics of a Non-Aviation ship". To be published.
8. Fortenbaugh, R.L., "Mathematical Models for the Aircraft Operational Environment of DD-963 Class Ships", Vought Corp., Dallas, Texas, Rep. N; 2-55800/8R-3500, 1978, pp 85.
9. Fortenbaugh, R.L., AIAA Paper # 79-1677
10. Lomas, C. G., "Fundamentals of Hot Wire Anemometry", Cambridge University Press, England (ISBN 0-521-30340- 0) 1986.
11. Castro, I. P., "Time domain measurements in separated flows", *Journal of Fluid Mechanics*, Vol. 150, 1985, pp 183-201.
12. Bradbury L. J. S., and Castro, I. P., "A pulsed-wire technique for measurement in highly turbulent flows", *Journal of Fluid Mechanics*, Vol. 49, 1971, p 657.
13. Perry, A. E., "Hot-Wire Anemometry", Oxford University Press, England (ISBN 0-19-856327-2) 1982.
14. Narveson, M. and J. Val. Healey, "Control of Flow over a Backward-facing Step", To be published.
15. Healey, J. Val. "Some Aspects of the Aerodynamics of Spruance and AOR Class Ships", *Proceedings of the Second Ship Aerodynamics Conference*, Washington, D.C., May 1990.
16. Holley, W. E., and A. E. Bryson Jr., "Wind Modeling and Lateral Control for Automatic Landing", *Journal of Spacecraft*, Vol. 14, No. 2, 1977.

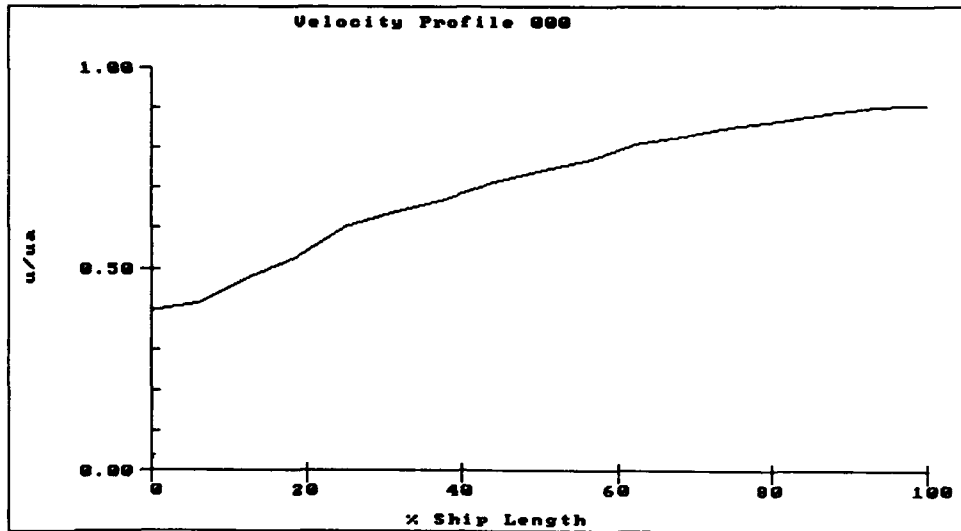


Figure 1 Along-Wind Velocity Profile 000

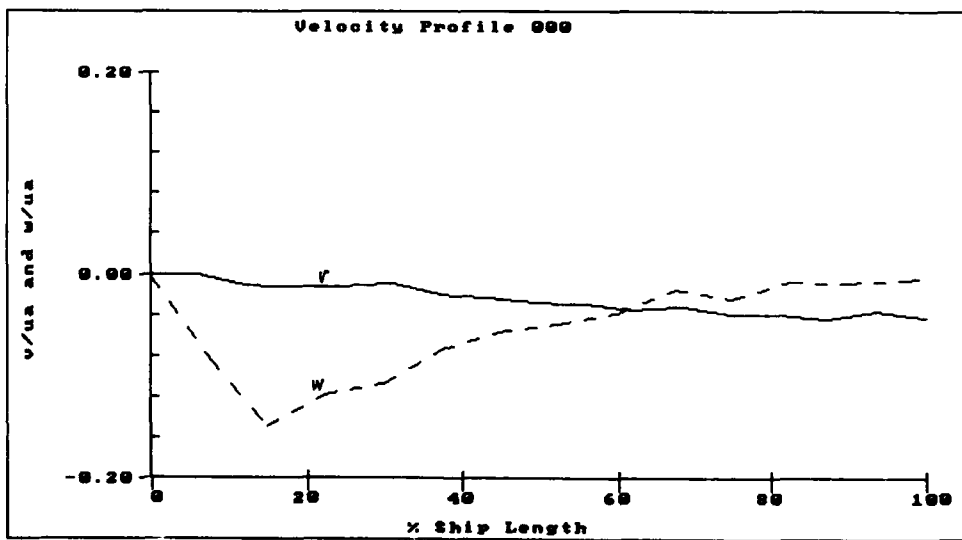


Figure 2 Transverse and Vertical Velocity Profiles 000

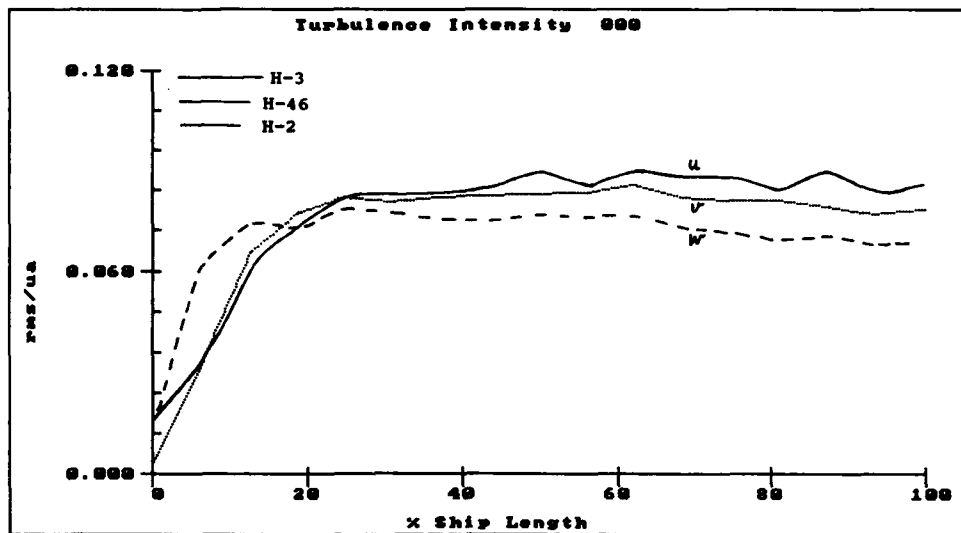


Figure 3 Turbulence Intensities 000

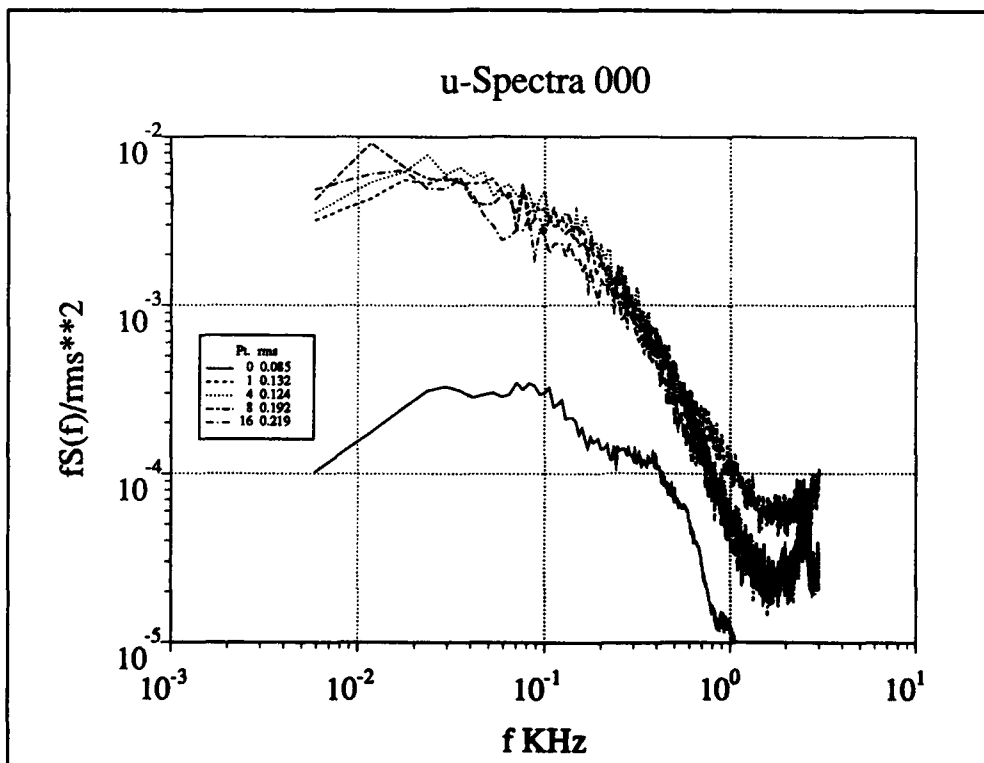


Figure 4. Along-Wind Velocity Spectrum 000

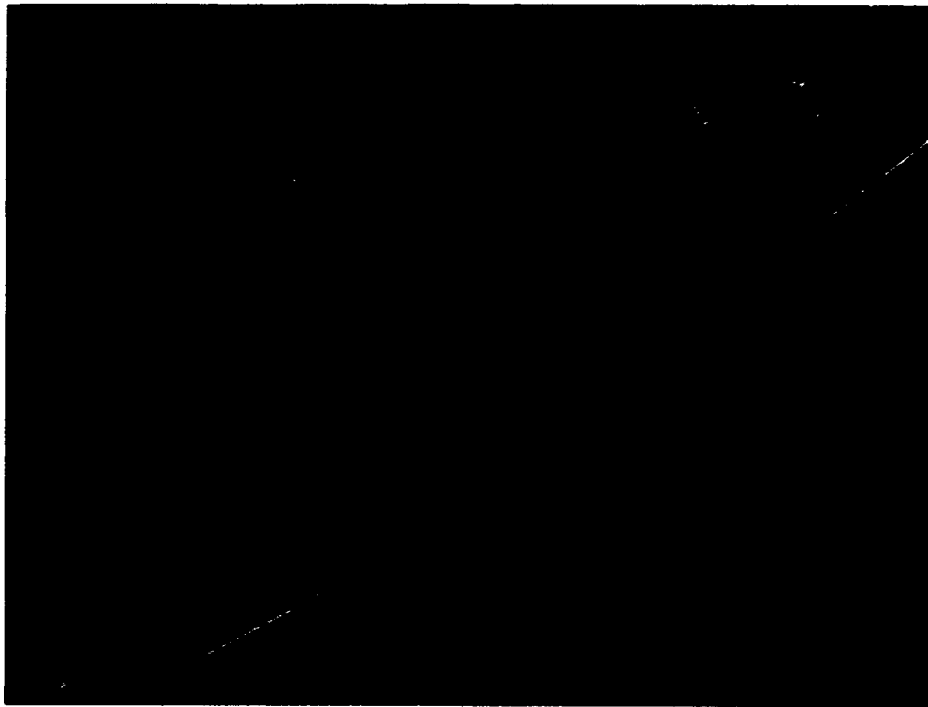


Figure 5 Flow-visualization with Fluorescent Minitufts

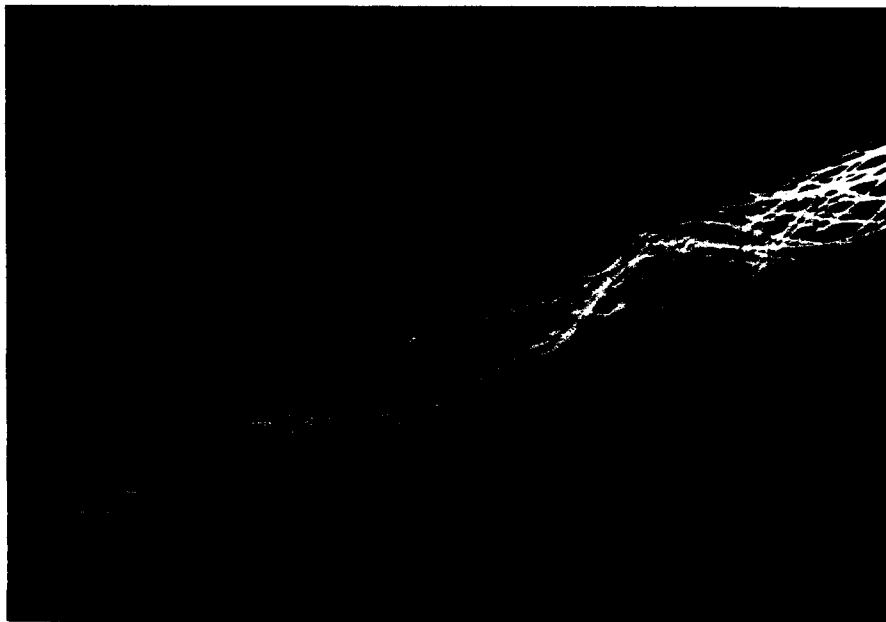


Figure 6 Wake Vortex shown by Helium Bubbles



Figure 7 Helium Bubble Streaklines on U.S.S. Tarawa



Figure 8 Bow Reattachment shown by Helium Bubbles

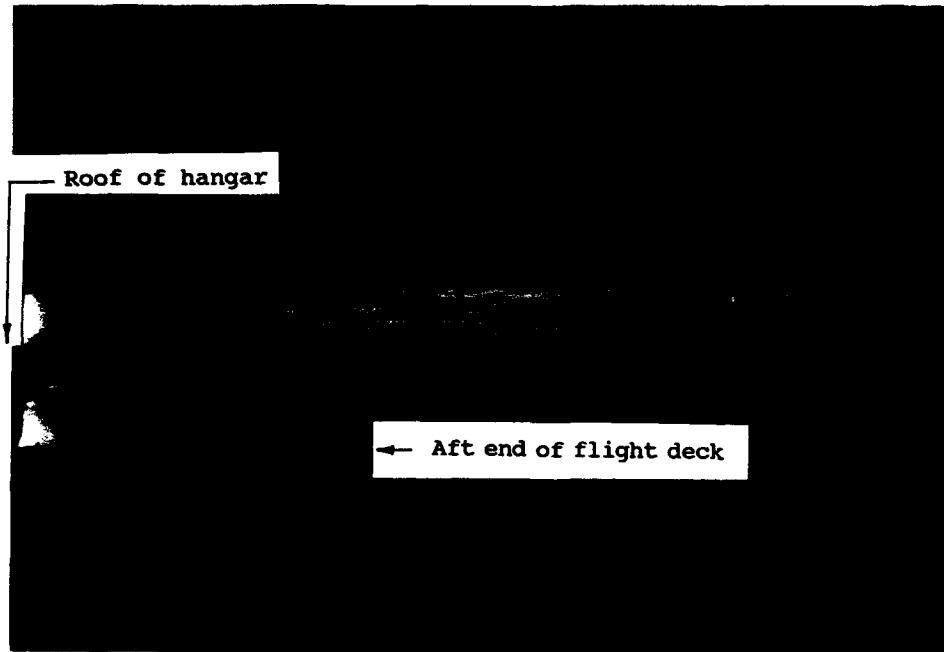


Figure 9 Vortical Flow over the Flight Deck of the DD-963

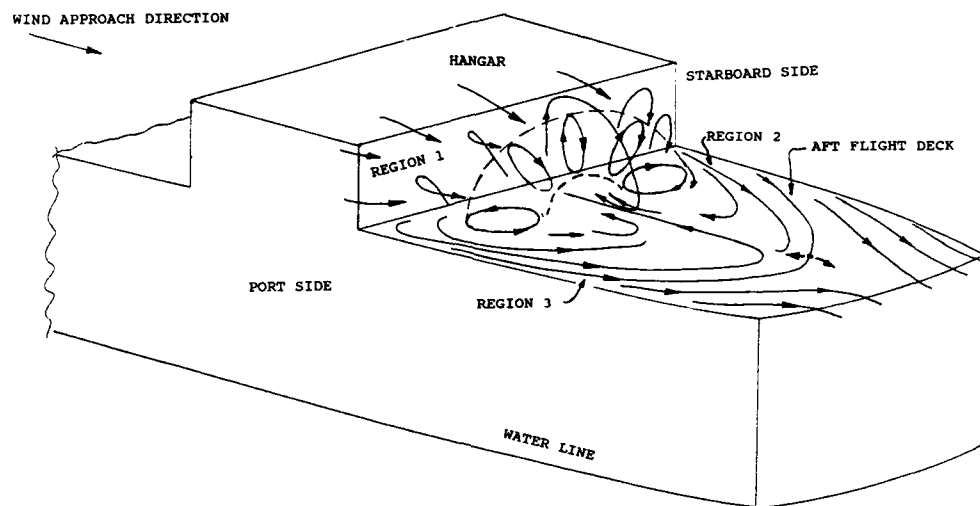


Figure 10 Flow Pattern on U.S.S. Wabash at Zero Yaw

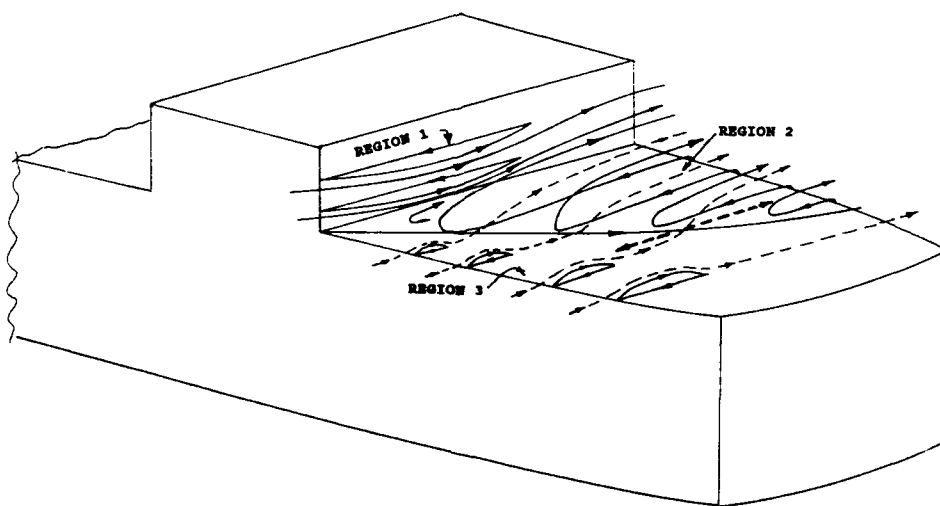


Figure 11 Generic Flow Pattern on U.S.S. Wabash at Nonzero Yaw

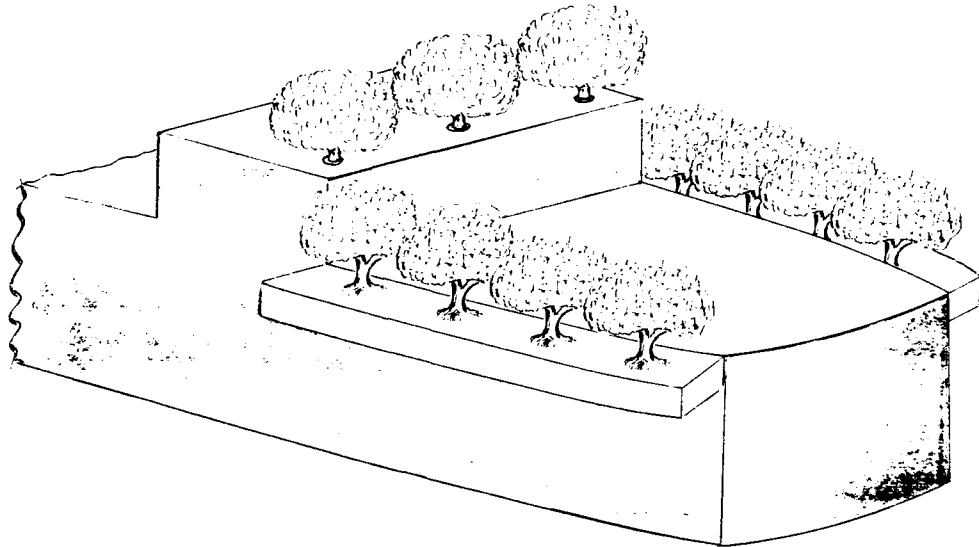


Figure 12 Have Forest Will Travel

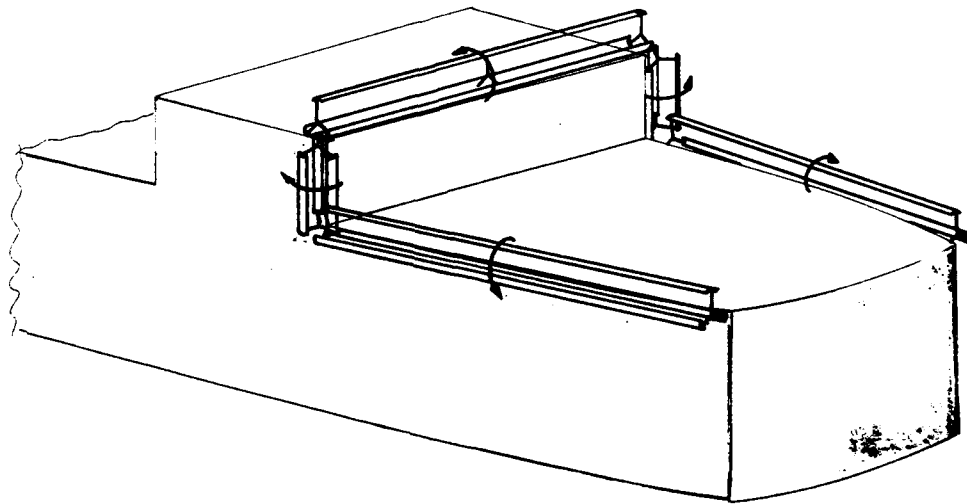


Figure 13 Have Windturbines Will Travel

SHIP AIRWAKE MEASUREMENT AND MODELING OPTIONS FOR ROTORCRAFT APPLICATIONS

Dean Carico, Code RW04B
 Bill Reddy, Code RW40W
 Rotary Wing Aircraft Test Directorate
 Naval Air Test Center
 Patuxent River, MD, USA 20670-5304
 and
 Charles DiMarzio
 Northeastern University
 Center for Electromagnetics Research
 360 Huntington Avenue
 Boston, MA, USA 02115

SUMMARY

Ship airwake is important in defining rotorcraft/ship operational limitations and in predicting those limitations using analysis and simulation. Accurate real-time ship airwake models are required to support pilot shipboard landing training in aviation training devices. Increased emphasis must be placed on obtaining quantitative full scale airwake data and in quantitatively evaluating ship airwake simulation models. Quantitative ship airwake data measurement equipment ranges from hand-held mechanical sensors, to propeller anemometers mounted on a mast, to possible laser velocimeter and other options in the near future. Wind tunnel and computational fluid dynamics options are also possible candidates for ship airwake data generation. It is important to compare the different techniques for obtaining ship airwake data and evaluate the utility and strengths and weaknesses of each technique. Many activities in the U.S.A. and in other countries are involved in rotorcraft shipboard landing flight test, analysis, and simulation. The Naval Air Systems Command (NAVAIRSYSCOM) and Naval Air Test Center (NAVAIRTESTCEN) are sponsoring several FY91 programs which should contribute to the overall rotorcraft/ship modeling database.

INTRODUCTION

Ship airwake is the key parameter in defining rotorcraft/ship operational limitations and in predicting those limitations using analysis and simulation. In this study, the ship airwake is defined as an arbitrary volume surrounding the ship, as shown in figure 1. The airwake volume size is determined by two factors: (1) airflow disturbances caused by the ship that are perceptible to a pilot, and/or (2) approach and landing patterns required for the aircraft to operate aboard the ship. Final approach and landing are the flight phases most influenced by the ship airwake.

The ship wind over deck (WOD) speed and direction are obtained from the ship's anemometers', and are the vector sum of ambient wind and ship speed. Variations in the WOD are often called "gust spread" by the ship crew. The pilot may refer to a turbulence level associated with the freestream air or with airflow over ship superstructure elements. The sharp corners associated with the ship superstructure may produce vorticity of a certain size, strength, frequency, and location.

BACKGROUND

Helicopter/ship operations got started in the U.S. in 1943, but were not formalized until much later. The H-2 Light Airborne

Multipurpose System (LAMPS MK I) started operating aboard the FF-1052 class ship in about 1970. Helicopter/ship or Dynamic Interface (DI) testing was initiated by NAVAIRTESTCEN, during the same timeframe, to define aircraft operational limitations in the shipboard environment. With the advent of the H-60 LAMPS MK III helicopter in the early 1980's, the tempo of aircraft/ship operations increased dramatically. The large number of aircraft types and ship classes requiring testing, combined with difficulty in controlling test conditions at-sea, resulted in the DI program initiating an analytical approach in 1983. The goal was to accelerate conventional DI flight testing, plus use analytics and real-time simulation to supplement the flight test effort, as discussed in reference 1. Although testing was accelerated, instrumentation were not available to measure aircraft flying qualities and performance (FQ&P), or ship airwake and motion parameters. In 1991, renewed program sponsorship spurred on work to develop rotorcraft simulation models for pilot training and for supporting flight testing. The key to the new initiative focused on quantitatively measuring the airwake of selected ships, and on developing real time ship airwake models for piloted simulation.

SHIP AIRWAKE MEASUREMENT OPTIONS

NAVAIRTESTCEN Test Experience

The study of ship airwakes tends to fall into two broad categories: flow visualization and flow measurement. Flow visualization by its very nature provides qualitative information about the flowfield, whereas direct flow measurement gives distinct windspeed/direction data on discrete locations in the flow.

The NAVAIRTESTCEN Rotary Wing Aircraft Test Directorate made an

attempt at ship airwake flow visualization during an H-46 rotor engage/disengage test aboard USS GUADALCANAL (LPH-7) in 1974. The medium used was smoke, generated by Mk 25 smoke grenades. Two grenades were mounted vertically 18 in. apart on a 15 ft pole which was hinged to a 3 ft X 3 ft plywood plank and secured with 3 guy wires. The smoke grenade/pole assembly is illustrated in figure 2.

The grenades produced 2 streamlines at the approximate height of the H-46 rotor. Motion pictures were taken as the streamlines passed through the static rotors, and with the flight deck clear. The smoke tended to dissipate rapidly, especially in gusty conditions. Some drawbacks of the Mk 25 smoke grenade are its short duration of approximately 30 sec and the use of a pyrotechnic device aboard a ship. The grenade/pole assembly was set up in proximity to fueling stations, and some concern was raised about the security of the assembly. At one point during the flight test, one of the grenade canisters detached from the assembly and struck the aircraft. This technique was not employed in subsequent flight tests because of its substantial disadvantages.

Another method for visualizing streamlines in a ship airwake applies "streamers," which are thin ribbons of colorful plastic about 3 in. wide and 30 ft long, attached to the periphery of the hangar face of a single landing spot ship. Figure 3 illustrates the streamer arrangement about the hangar face. As one would presume, turbulence, downdrafts, and reverse flow regions can be depicted clearly, although only specific WOD conditions would produce acceptable results. Winds below 10 kt would tend to make the streamers hang loosely, and winds greater than 35 deg relative to the bow would produce incoherent and nonrepeatable streamer motion. Once again, the

"streamers" technique had more limitations than benefits, and the bubble technique was adopted.

The "soap bubble" technique uses commercially available soap bubble solution and large multi-hole bubble wands to produce countless bubbles averaging 1 in. in diameter. The test engineers' locations depends upon the class of ship and WOD conditions. The most common positions are port/starboard and directly above the hangar face. The general procedure is to produce bubbles for 1/2 to 1 min. for each WOD condition, videotaping from above or abeam depending on the bubble source locations and lighting conditions (figure 4).

The soap bubble technique is superior to other flow visualization techniques in its ability to provide an accurate representation of the airwake far beyond the fantail of the ship, depending on a number of environmental conditions. Another advantage of bubbles is the absence of pyrotechnic and environmental hazards. Minor chemical adjustments to the bubble solution will make the bubbles stronger and able to withstand higher winds without popping.

A fundamental problem with soap bubbles is that they are transparent. Many times, photography cannot provide accurate imaging unless focused upon a particular area, or the day is bright and sunny. Several attempts were made to create more visible bubbles. This effort involved mixing the soap bubble solution with a colored substance, such as fluorescent ink, dye, or luminescent fluid. Everything in this category interfered with the soap solution's ability to produce bubbles. When bubbles were produced successfully, the walls were too thin to create any appreciable color difference. At this point, the focus shifted from trying to dye the soap solution to

trying to fill the bubbles with a colored substance. The outcome was a non-pyrotechnic smoke produced by a smoke machine, although the idea is hard to implement. There is an ongoing effort at NAVAIRTESTCEN to build a bubble machine which is capable of filling the bubbles with smoke. The other attempts involved various photographic techniques including infrared photography and special filters to enhance the background. These techniques are being refined and may be used in conjunction with the smoke bubble machine.

Salt, lack of humidity, and low air temperatures are the Achilles' heel of bubbles. In a shipboard environment filled with salt spray, bubbles tend to break within 10 ft of the source. On very dry days, the air draws the moisture out of the bubbles, causing them to break prematurely. A perfect day for bubble flow visualization is right after a thunderstorm or rainshower. Subfreezing temperatures will cause bubbles to break in the airwake. Nothing has been found that is capable of lowering the freezing point of a soap bubble solution without seriously degrading its ability to form bubbles.

Ship airwake measurements are usually made in conjunction with DI testing. The procedure is quite simple; "airwake mapping" involves one or more test engineers with hand-held mechanical anemometers taking measurements at specific locations on and around the flight deck. A sample grid of flight deck measurement locations is illustrated in figure 5. The engineer waits for a steady reading and then radios the windspeed and direction information to an engineer in the ship Helicopter Control Station (HCS) or debark control where it is recorded. When all of the locations on the flight deck have been measured, a new WOD condition is chosen. A sample computer-drawn vectorial

representation of an AE-26 class ship airwake on the flight deck is presented in figure 6.

Hand-held mechanical anemometers provide a starting point for obtaining quantitative ship airwake data. The next step involves getting an analog or digital signal from a 3-D anemometer to obtain airwake data as a function of time. Several of the 3-D anemometers may be mounted on a mast or other device to obtain 3-D airwake measurements at different heights for a particular location on the ship flight deck. The mast may be designed to be movable to obtain data at different locations on the ship flight deck, as demonstrated by the systems used in Australia and The Netherlands. A final step might involve a non-intrusive sensor that could quantitatively measure the airwake volume surrounding the ship. Some sensors, like lasers, can be used to scan in range, and can be mounted to sweep in azimuth and elevation. The key is to record accurate 3-D, point source data at a frequency high enough to analyze both mean and turbulent WOD components. It is important to review laser and related system programs to determine their application in optimizing ship airwake measurements.

Laser System Test Experience

Previous Work. Carbon dioxide laser components and system functions are summarized in appendix 1. The carbon dioxide laser doppler velocimeter (LDV) or laser doppler anemometer (LDA) has a rich heritage as a research instrument in field tests. In 1980, many of the early results were documented in the reference 2 review article. These programs have considered atmospheric backscatter, attenuation, vibration environments, and operational issues.

Ship Airwake Measurements. A feasibility test demonstration using a mobile Lockheed LDV was conducted

aboard USS NIMITZ in 1975, as discussed in reference 3. The demonstration was conducted in conjunction with NAVAIRTESTCEN Automated Carrier Landing System (ACLS) certifications, and the LDV was configured to scan along glide slope. Fifteen seconds of 1-Hz line-of-sight velocity data were recorded for manually stepped range scan angles of 1.5 to 5.5 deg, in .5 deg increments. Subsequent NAVAIRTESTCEN ACLS testing did not use this LDV.

Wake Vortex. One of the early laser systems was used for detecting the wakes of fixed-wing commercial aircraft landing at Kennedy International Airport. The results of this work are presented in references 4 through 7. During this measurement program, backscatter coefficients greater than 10⁻⁸ per meter per steradian (m-lsr⁻¹) were routinely observed, and some measurements went to 10⁻⁶m-lsr⁻¹. These tests verified that the backscatter was high enough for an LDA to work.

A surface-acoustic-wave delay line spectrum analyzer was used as the signal processor. This device provided detailed spectral information which could be analyzed in detail after the tests. The project also demonstrated that the vortex cores could be located in range with a precision of about one fifth of the range resolution.

Helicopter Remote Wind Sensor (HRWS)

A small laser homodyne system (single laser system) was used for measuring the rotor wash of helicopters in a program at White Sands Missile Range, New Mexico. This program demonstrated the ability of a homodyne system to withstand the vibration environment of a UH-1 helicopter (reference 8). This system introduced a smaller, air-cooled laser to the measurement of atmospheric winds (reference 9).

LDA Testing at NAVAIRTESTCEN

NASA Ames procured a 5 W CO₂ Raytheon laser designed for accurate 3-D true airspeed measurements in a helicopter for flight control systems studies in the early eighties. The unit was never successfully demonstrated on a NASA Ames helicopter. NAVAIRTESTCEN borrowed the unit in 1989 to demonstrate low speed helicopter application and ship airwake measurement application. The application is being developed in conjunction with Northeastern University and the Naval Air Engineering Center. A laser flight test program was scheduled at NAVAIRTESTCEN for the summer of 1990. The test plan provided for a gradual build-up to the helicopter test, beginning with the ground tests, followed by testing aboard a pace vehicle, and finally the helicopter tests.

Ground Tests. The ground tests consisted of setup and measurement of system parameters after transportation of the LDA from Boston to Patuxent River. The signal-to-noise ratio was measured from a spinning sandpaper target, and verified to be 65 dB. This demonstrated that the system had not suffered misalignment in travel.

Pace Vehicle Tests. A pickup truck was used as the pace vehicle. Prime power was provided by a small generator with an 18-amp capacity. The major goals here were to evaluate the performance of the locking system maintaining the two lasers at the desired offset frequency, and to determine the performance of the tracker. Neither of these tests could be completed in a stationary ground test.

System Performance. Three major system performance issues were evaluated during this test: (1) locking performance of the two lasers, (2) strength of the aerosol

return as determined by the spectrum analyzer, and (3) ability of the frequency tracker to track the signal and produce the required output to the computer for processing.

In the early tests at NAVAIRTESTCEN, locking performance was equally good, both in the laboratory and on the pace vehicle. The pace vehicle, at speeds of up to 60 mph, and the generator operating in the back of the truck, a few feet away from the system rack, provided a relatively hostile environment in which to test the system.

In later tests, the performance fell off, and the lasers remained locked less than half of the time. The problem was traced to a beamsplitter in the transmitter path, which apparently had moved slightly. A small change was made in this beamsplitter, and the system then locked as before.

The issue of locking is a major one, since it will determine the viability of a dual-laser system for remote wind measurements. Such measurements have been made in the past from aircraft including helicopters, from fixed ground stations, and from moving ground vehicles, with single-laser systems. The problem with these systems is that they do not determine the sense of the Doppler shift, and the resulting velocity is ambiguous with regard to sign.

Tracking. Initial measurements from the pace vehicle were made using the ground as a target, by raising the back end of the system so that the cone axis was 9 deg below the horizontal. This allowed most of the scan to intersect the ground, although at different ranges. The trees along the runway occasionally provided sufficient target to allow a full scan of ground data to be obtained. Signal-to-noise ratios of up to 40 dB were obtained from

ground returns when the system was focussed at ranges beyond a few meters.

The frequency tracker locked on the desired signal in rooftop tests at Northeastern University, and against sandpaper targets in the laboratory, in addition to a signal generator which was used in the laboratory. In all cases, there was a significant axial velocity component, so that the signal was always far removed from the narcissus return (see appendix I) from the secondary of the telescope. In the tests on the pace vehicle, the system was mounted transverse to the path of the vehicle, so that the Doppler shift passed through zero twice during each scan. This resulted in considerable difficulty in tracking the signal. Two reference notch filters were evaluated. The best one was selected for the tests on the pace vehicle, but it was not good enough to provide reliable tracking. Typical plots of frequency as a function of range show two consistent frequencies at which tracking occurred, one slightly above, and one slightly below 25 MHz. These correspond to the slight sidebands of the narcissus which are visible above the noise.

Alternatives to the tracker include a Surface Acoustic Wave (SAW) delay line spectrum analyzer, a filter bank, and digital signal processing. A SAW line was available for these tests, but was limited in dynamic range, and in any event, could not be used in vehicle tests because of a lack of prime power.

Additional Airwake Measurement Experience

Reference 10 describes the ship airwake measurement experience of Australia and reference 11 describes the experience of The Netherlands. Both countries use Gill UVW 3-D propeller anemometers mounted on a movable mast. NAVAIRTESTCEN is

acquiring a similar system for future ship airwake testing. It is important to maintain airwake test equipment commonality, where feasible, to enhance future international cooperation and data exchange.

The Naval Research Laboratory (NRL) has proposed using a sonic anemometer, and other sensors, suspended approximately 100 ft below an airship flying in formation with a ship. The primary purpose of the experiment, as discussed in reference 12, is to make microwave scatterometer and oceanic surface-flux measurements.

The Georgia Institute of Technology is investigating the use of spatial correlation velocimetry in measuring 2-D unsteady flows, as discussed in reference 13. This technique involves seeding the flow, illuminating the seeded flow with a narrow-width light source, and recording flow movement with video cameras.

A considerable amount of ship airwake data could be obtained, in conjunction with DI testing, if the test helicopter had an accurate 3-D low airspeed sensor. Current helicopter pitot-static systems are not usable below approximately 35-40 kt indicated airspeed. Emphasis should be placed on portable rotorcraft flying and performance data packages, which include the capability to record accurate 3-D airspeed data for speeds down to hover.

SHIP AIRWAKE MEASUREMENT LIMITATIONS

Flight Test Activity Test Equipment

The anemometers used in ship airwake measurements have problems ranging from poor portability to environmental sensitivity and slow frequency response. Limitations of each particular anemometer type will be discussed in detail.

Ship Anemometers: Current ship anemometers are a product of 1940's technology, and are always found in pairs aboard aviation capable ships. The most common location is about 4 ft to 6 ft above the yardarm on the port and starboard sides. The anemometer system is made up of three components: sensor, transmitter, and indicator. Windspeed and direction information is sent to indicators on the bridge, helicopter control station, and debark control station (depending on ship class). Ship anemometer windspeed and direction information is also known as the wind over deck or WOD. WOD speed and direction form the basis for DI launch and recovery flight envelope definition.

The sensor looks like a weathervane, and measures 2.5 ft long. It has a stated accuracy of ± 1.5 kt for winds below 45 kt, ± 2.0 kt for windspeeds between 45 and 60 kt, and a maximum capability of 90 kt. Ship anemometers are usually calibrated once a year to help ensure proper indications and consistency.

Ion Beam. The TSI model 204 ion beam anemometer has two main components: a wind sensor and a processor/display unit. The wind sensor uses the method of ion deflection for measuring ambient windspeed and direction. A finely ground needle, located within the sensor unit, injects ionized molecules into the moving airstream in a direction perpendicular to the flow. The ions then strike an ion collection electrode after being carried downstream and traversing the gap between electrodes. The disk-shaped electrode is made from a carbon coated ceramic substrate and has four connections on the edges of the disk, illustrated in figure 7. The flow of the current from the center of the ion beam will be disproportionate to each of the four contacts. Through a complex mathematical relationship, windspeed and direction can be derived. This

particular sensor unit is usually mounted on an 8 ft pole and moved about the flight deck to get airwake data.

The most prominent problem with the ion beam anemometer is its vulnerability to salt spray. Erroneous output may be produced in as little as an hour when placed in the shipboard environment, depending on the sensor location and sea state. This erroneous output will continue until the sensor needle is rinsed with clear water and adequately dried.

The specifications state the accuracy of the ion beam anemometer as approximately ± 2 kt in the 0-50 kt range, with a frequency response of 2 Hz. In the field, however, coherent data was collected at windspeeds ranging from 10-40 kt. The output is erratic at windspeeds between 5 and 10 kt, and scattered below 5 kt. Questions have been raised as to what frequency response is optimal for ship airwake measurements. An anemometer with a high frequency response (on the order of 100 Hz) will reveal individual velocity fluctuations of shed vortices rather than aggregate values. A limitation of the sensor is its 2-dimensional capability; having the third velocity component would provide a more accurate representation of flow conditions.

Sonic. The Applied Technologies sonic anemometer has two main components: a wind measurement "S" style probe, and a processor/display unit. The probe consists of three pairs of orthogonal transducers, illustrated in figure 8. The probe measures windspeed by sending a sonic pulse across the space between each pair transducers. The speed of sound is then altered by the velocity component of the wind parallel to the transducers. The processing unit then measures the time of the pulse and ambient temperature and calculates

windspeed. The unit is self-calibrating (by electronically measuring the probe transducer distances) and employs an algorithm to take account for the turbulence produced by the probes in the flowfield.

The sonic anemometer has completely sealed transducers and is virtually unaffected by the harsh shipboard environment. It has an excellent low airspeed measurement capability boasting an accuracy of ± 50 cm/s. The sensor measures the flow at a rate of 100 samples per second, with the processor computing the average of every 10 samples, and has an output of 10 Hz.

There are two fundamental problems with the sonic anemometer. The upper limit of measurement is about 40 kt, and the processor and associated hardware are cumbersome. Vibration tends to produce "noise" in the output, but can be easily removed.

Mechanical. The Kahlsico model 03AM120 indicating totalizer cup anemometer, illustrated in figure 9, is hand-held and measures 11 inches high and 3.5 in. at its widest point. Three hemispherical cups are employed, which rotate on a shaft. The rotating cups produce a magnetic field proportional to windspeed, which activates the measuring/indication system. This indicating system has a needle pointer which moves across a cylindrical scale, fully visible through a 180 deg plastic window, with 5 kt and 10 deg divisions. In low winds, 0 - 20 kt, the direction indicator in the anemometer swings sporadically and does not provide a good directional indication.

SHIP AIRWAKE MODELING OPTIONS

Rotorcraft Requirements

Ship airwake measurement and modeling options are directed toward producing real-time, high fidelity

models for rotorcraft/ship analysis and simulation. The goal is to supplement rotorcraft/ship at-sea testing and enhance operational flight trainer capability in training pilots for the shipboard landing task. Rotorcraft simulation limitations are discussed in references 14 and 15. It is important that limitations associated with the rotorcraft math model, simulator cockpit, visual system, motion system, aural system, environmental models, and host computer be evaluated. Environmental models (ship airwake, ship motion, etc.) must be quantitatively evaluated. Airwake model development may be based on full scale data, wind tunnel data, computational fluid dynamic (CFD) data, ship geometric data, or other data source. Full scale airwake data must be used in validating a ship airwake model.

Full Scale Airwake Data

Full scale ship airwake measurements require appropriate airwake measuring equipment, a ship available in an area of high probable ambient winds, plus an engineering test team. As discussed previously, airwake measuring equipment ranges from mechanical hand-held sensors to, perhaps in the near future, lasers that can record accurate, 3D non-obtrusive airwake data. As noted previously, Australia and The Netherlands use Gill UVW propeller anemometers attached to movable masts to get airwake readings at two or three heights above the ship flight deck. NAVAIRTESTCEN has conducted over 140 at-sea DI tests since 1970 (reference 16), but only approximately a half dozen of these tests were primarily oriented toward collecting airwake data. Airwake data were measured, primarily using mechanical hand held anemometers, and presented as shown in reference 17. NAVAIRTESTCEN is acquiring a Gill propeller anemometer system,

similar to that used by the Australians, for FY91. Other ship airwake measuring sensor development, including lasers, will be monitored.

Wind Tunnel Data

Wind tunnels have been used for a long time to support aircraft research and development programs. Wind tunnels can reduce the logistic requirements for obtaining ship airwake data, compared to full scale data. Boundary layer wind tunnels are required for ship airwake data analysis, and the wind tunnel data must be scaled correctly and compared to full scale data. Boeing-Vertol ship airwake data (reference 18) were used as the basis of early simulation airwake models. This data has been criticized because the wind tunnel did not employ an atmospheric boundary layer. References 19 and 20 discuss qualitative smoke tunnel and wind tunnel studies conducted by the Naval Air Engineering Center. Another example of qualitative flow patterns, this time using a watertunnel at David Taylor Research Center, is presented in reference 21. Wind tunnel airwake data obtained by the NRL in the mid 1980's used the British Maritime Tunnel in Teddington, England. This boundary layer tunnel was used to obtain data on LHA, CGN, and CV class ships, as discussed in references 22, 23, and 24. Although over 18,000 LHA airwake data points were recorded, none of these data have been reduced or made available to other organizations. Recent Naval Postgraduate School (NPS) wind tunnel flow patterns for the DD-963 class ship are presented in reference 25. Quantitative DD-963 airwake measurements were reported in reference 26, and reference 27 summarizes the early NPS ship airwake wind tunnel effort. The NPS DD-963 ship airwake data will form one useful source of data for the NAVAIRTESTCEN real time simulation

modeling effort.

Computational Fluid Dynamics

CFD involves nonreal-time numerical solution of partial differential conservation equations to obtain flow and pressure/temperature data. Unlike point source full scale or wind tunnel data, CFD techniques can be used to generate the complete ship airwake for a specified WOD speed and direction. Generating ship airwake data using CFD techniques is computationally intensive, requiring several hours of CPU time (depending on the type of computer) for each WOD speed and direction condition. Determining the effects of ship motion on ship airwake presents unique problems for wind tunnel and CFD approaches.

The Naval Air Development Center initiated a program in 1985 with CHAM of North America, Inc., to generate ship airwake data for scale model DD-963 and LHA-1 class ships using the CHAM PHOENICS CFD code. The unstructured PHOENICS code was set-up using Cartesian (vice body fitted) coordinates with the ship boundaries represented by blocked or partially blocked cells. Reference 28 notes that the CFD DD-963 data compared favorably to 1977 Boeing Vertol wind tunnel data, even indicating the presence of the wind tunnel probe measuring hardware. Full scale cases were executed, using an assumed boundary layer, but the results were not compared to full scale data. This work was repeated in 1987 for the LHA-1 class ship. The goal was to compare the CFD results to NRL BMT LHA wind tunnel data, but the wind tunnel data were never made available (reference 29). NAVAIRTESTCEN is revisiting the previous CFD ship airwake work during FY91 to determine application to ongoing flight test and simulation efforts. A FY91 internal NAVAIRTESTCEN program also focuses on near-term LHA ship airwake definition using

different CFD approaches. An initial comparison between NPS wind tunnel data and CFD data for wind over the bow of the DD-963 ship is presented in figure 10.

Rotorcraft Simulator Ship Airwake Models

Operational Flight Trainers (OFT's) and Weapon System Trainers (WST's) exist for practically all U.S. Navy and Marine Corps rotorcraft. Ship models are included in the trainer visual system data base for helicopter shipboard operations training. Shipboard landing training has been severely limited due to lack of visual system scene detail/resolution and field-of-view, lack of accurate ship airwake models, and air vehicle models incapable of demonstrating the correct response to the airwake. The airwake models included in these trainers have not been quantitatively evaluated and have not been validated using full scale test data. Early flight trainer visual system and air vehicle math model limitations helped to mask ship airwake modeling inadequacies. Simulator visual systems have improved dramatically and helicopter aircraft math model developments are starting to use rotor blade element approaches. An overall increase in trainer model fidelity will require better full scale data for model validation. Specifically, helicopter flight testing should be geared toward collecting individual rotor blade motion and load data during standard FQ&P testing. The DI program should focus on getting full scale ship airwake, ship motion, and aircraft FQ&P data during at-sea testing. A good full-scale test data base will provide more credibility to modeling the rotorcraft shipboard landing scenario.

Future Options

Future program options are focused on supporting NAVAIRTESTCEN

helicopter flight test program and on improving OFT/WST testing techniques. The full effect of the ongoing programs related to ship airwake measuring and/or modeling will not be felt for another 2-5 yr. Near term (FY91) NAVAIRTESTCEN projects include acquiring anemometers to help measure the ship airwake, acquiring limited wind tunnel and CFD airwake data, and sponsoring work to develop a preliminary real-time ship airwake for the DD-963 class ship. At the same time, work is being conducted in conjunction with the Naval Air Development Center to implement an Army/NASA Ames H-60 blade element helicopter model at the NAVAIRTESTCEN Manned Flight Simulator (MFS). Work is also being conducted with the Naval Training System Center to better define existing OFT/WST ship airwake models (reference 15). Work to define the effect of turbulence on rotorcraft handling qualities (such as reference 30) may provide a starting point in developing real-time ship airwake models. Many ongoing U.S. Navy small business programs, including the following:

- a. Helicopter main rotor blade element and disk comparison.
- b. Helicopter tail rotor blade element and interference models.
- c. Portable simulator evaluation package.
- d. Modeling the DI scenario.
- e. Portable helicopter FQ&P data package.
- f. Portable ship motion/airwake measuring package.

These programs should help build the airwake data base and also improve flight test and simulation programs that relate to the airwake problem.

CONCLUSIONS

Ship airwake is the key parameter in defining rotorcraft/ship operational limitations and in predicting those limitations using analysis and simulation.

The soap bubble technique is superior to smoke grenades and streamers in full-scale flow visualization techniques by providing an accurate representation of the airwake far beyond the fantail of the ship.

Nonobtrusive 3-D ship airwake measurements using carbon dioxide lasers or other sources need to be demonstrated.

Analytical tools and data are available to perform a more careful carbon dioxide laser design. More detailed computer codes are available now to evaluate the system design in detail which were not possible in previous years.

Ship airwake anemometer limitations are discussed in terms of portability, environmental sensitivity, and slow frequency response.

RECOMMENDATIONS

Current ship airwake related measuring and modeling programs should be continued to produce both near term and long term quantitative results. Specific recommendations include:

Evaluate existing ship airwake measuring sensors and acquire instrumentation to measure ship airwake data during helicopter/ship DI testing.

Acquire portable aircraft and ship instrumentation systems to assist future DI test and simulation programs.

Review options for using

non-obtrusive ship airwake measuring sensors, including lasers, etc.

Review wind tunnel, CFD, etc., ship airwake data and determine the strengths and weaknesses of each approach and how the results compare to full scale data.

Develop quantitative test techniques and evaluate the ship airwake models on existing rotorcraft simulators.

Work to develop/acquire accurate real-time ship airwake models that can be used to supplement at-sea DI flight testing, and that can be used to enhance rotorcraft flight simulator shipboard landing training.

Work to develop modular, real-time, blade element rotorcraft models that can be used to demonstrate the effect of accurate ship airwake models.

REFERENCES

1. Carico, D. and Madey, CDR S., "Dynamic Interface: Flight Test and New Analytical Approach," AHS Specialist's Meeting, of Oct 1984.
2. Bilbro, James W., "Atmospheric Laser Doppler Velocimetry: An Overview," Optical Engineering 19(4), of Jul/Aug 1980, pp. 533-542.
3. Wilson, D.J. et. al., "Full-Scale Wake Flow Measurements with a Mobile Laser Doppler Velocimeter," Article No. 78-823, Journal of Aircraft, Volume 16, Number 3, pp. 155-161, of Mar 1979.
4. Jeffreys, H. B., J. W. Bilbro, C. A. DiMarzio, C. M. Sonnenschein, and D. W. Toomey, "Laser Doppler Vortex Measurements at John F. Kennedy International Airport," presented at the 17th Conference on Radar Meteorology, American Meteorological Society, Seattle, Washington, of Oct 1976.

5. Bilbro, J. W., G. D. Craig, R. W. George, H. B. Jeffreys, P. J. Marrero, E. A. Weaver, M. C. Krause, T. L. Dunn, C. A. DiMarzio, C. E. Harris, C. M. Sonnenschein, and D. W. Toomey, "Laser Doppler Vortex Measurements at John F. Kennedy International Airport," in J. N. Hallock, ed., Proceedings of the Aircraft Wake Vortices Conference, 15-17 Mar 1977, pp. 81-105.
6. DiMarzio, C. A., H. B. Jeffreys, and C. M. Sonnenschein, "Aircraft Wake Vortex Velocity Measurements Using a Scanning CO₂ Laser Doppler Velocimeter," presented at Electro-Optics '75, and the International Laser Exposition, Anaheim, CA, 11-13 Nov 1975.
7. Sonnenschein, C. M., C. A. DiMarzio, and H. B. Jeffreys, "Performance of CO₂ Laser Vortex Detection System," Presented at 1975 IEEE/OSA Conference on Laser Engineering and Applications, Washington, D.C., 28-30 May 1975.
8. Dickson, David H., "Atmospheric Wind Sensing with CW Lidar Systems," Third Topical Meeting on Coherent Laser Radar - Technology and Applications, at Great Malvern, Worcs., England, on 8 Jul 1985.
9. Dickson, David H., and Charles M. Sonnenschein, "Helicopter Remote Wind Sensor System Design," ASL-CR-79-0008-A, ASL, USA ERADCOM, White Sands Missile Range, NM, 45 pages, 1979.
10. Arney, A.M., et. al., "A Review of Australian Activity on Modeling the Helicopter/Ship Dynamic Interface," Paper No. 20, AGARD FMP Symposium on Aircraft/Ship Operations, Seville, Spain, 20-23 May 1991.
11. Fang, R., "Helicopter/Ship Qualification Testing," Paper No. 18, AGARD FMP Symposium on Aircraft/Ship Operations, Seville, Spain, 20-23 May 1991.
12. Blanc, Theodore V., Plant, William J., and Keller, William C., "The Use of an Airship as a Platform for Conducting Oceanographic Research," AIAA89-3156-CP, 8th Lighter Than Air Technical Conference, Jacksonville, FL, 1989.
13. Fawcett, P.A. and Komerath, N.M., "Spatial Correlation Velocimetry in Unsteady Flows," AIAA91-0271, 29th Aerospace Sciences Meeting, Reno, Nevada, of 7-10 Jan 1991.
14. Carico, D., McCallum, K., CDR, and Higman, J., "Dynamic Interface Flight Test and Analytical Limits," ERF Paper No. 100, of Sep 1985.
15. Galloway, T., Frey, F., and Carico, D., "The Ship Environment Simulation Problem," AIAA90-3171-CP, of Sep 1990.
16. Baty, Roger L., Major USMC, and Long, Kurt, "Dynamic Interface Testing," Naval Helicopter Association Rotor Review, No.22, Winter 1991.
17. Childers, R., CAPT, et. al., Post-Fram WHEC 715 Class Dynamic Interface Testing of SH-2F Aircraft Aboard USCGC MELLON (WHEC 717), NAVAIRTESTCEN Report No. RW-65R-90, of 5 Dec 1990.
18. Garnett, T. S., Jr., Investigation to Study the Aerodynamic Ship Wake Turbulence Generated by a DD-963 Destroyer, Boeing Vertol Report D210-11545-1, of Aug 1979.
19. Perrelli, Richard J., "Smoke Tunnel Study of a 1/200 Scale DD-963 Ship Model," Report NAEC-91-8030, of 19 Jun 1984.
20. Paragiri, S.R., Wind Tunnel Survey of the Flow Characteristics Over the Flight Deck of a 1/100th Scale Model of the USS VINSON (CVN-70), Report NAEC-ENG-91-8081, of 25 Aug 1985.

21. Karafiath, G. and West, E., Diesel Generator Exhaust Gas Dispersion Experiments with Model 5413 Representing an Amphibious Assault Ship, Report DTNSRDC/SPD-231-23, of Jun 1984.
22. Blanc, Theodore V., Superstructure Flow Distortion Correction for Windspeed and Direction Measurements Made from Tarawa Class (LHA-1 through LHA-5) Ships, NRL Report 9005, of 31 Oct 1986.
23. Blanc, Theodore V., Superstructure Flow Distortion Correction for Windspeed and Direction Measurements Made from Virginia Class (CGN38-41) Ships, Naval Research Laboratory Report 9026, of 10 Apr 1987.
24. Blanc, Theodore V. and Larson, Reginald E., Superstructure Flow Distortion Correction for Windspeed and Direction Measurements Made from Nimitz Class (CVN68-CVN73) Ships, Naval Research Laboratory Report 9215, of 19 Oct 1989.
25. Johns, M. K., "Flow Visualization of the Airwake Around a Model of a DD-963 Class Destroyer in a Simulated Atmospheric Boundary Layer," M.S. Thesis, Naval Postgraduate School, Monterey, CA, of Sep 1988.
26. Anderson, Gustav A., "Mapping the Airwake of a Model DD-963 Along Specific Helicopter Flight Paths," M.S. Thesis, Naval Postgraduate School, Monterey, CA, of Dec 1989.
27. Healey, J. Val, "Simulating the Helicopter/Ship Interface as a Alternative to Current Methods of Determining Safe Operating Envelopes," Naval Postgraduate School Report, NPS 67-86-003, Monterey, CA, of Sep 1986.
28. Mahaffey, W. A. and Smith, C. E., Turbulent Ship Airwake Environment Prediction Methodology, Cham of North America, Inc., Interim Report, of Mar 1987.
29. Mahaffey, W. A., Turbulent Ship Airwake Environment Prediction Methodology, CHAM of North America, Inc., Final Report, of Sep 1987.
30. Costello, M., "A Theory for the Analysis of Rotorcraft Operating in Atmospheric Turbulence", AHS 46th Annual Forum Proceedings, Washington D.C., of 21-23 May 1990.

For additional information related to this paper, on the following topics:

1. Rotorcraft simulation or options to improve basic rotorcraft flight testing, contact

Mr. Dean Carico, RW04B
Rotary Wing Aircraft Test Directorate
Naval Air Test Center
Patuxent River, MD, USA 20670-5304

Telephone (301) 863-1382, A/V 326-1382
FAX (301) 863-1753

2. Helicopter/ship Dynamic Interface testing or test equipment, contact

Mr. Bill Reddy, RW40W
Rotary Wing Aircraft Test Directorate
Naval Air Test Center
Patuxent River, MD, USA 20670-5304

Telephone (301) 863-1345, A/V 326-1345
FAX (301) 863-1340

3. LASER system concepts, design, and testing, contact

Mr. Charles DiMarzio
Senior Staff Scientist
Center for Electromagnetics Research
235 Forsyth Building
Northeastern University
Boston, MA 02115

Telephone (617) 437-2034/8570
FAX (617) 437-8627
E-MAIL to CDIMARZIO@lynx.northeastern.edu

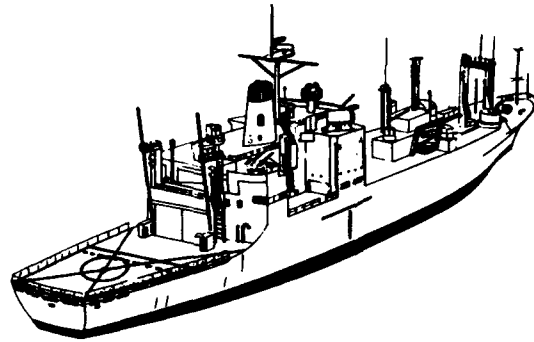


Figure 1 Ship Airwake Illustrated

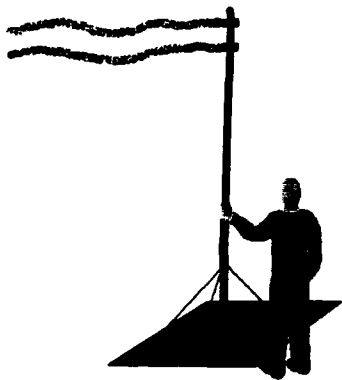


Figure 2 Smoke Grenade/Pole Assembly

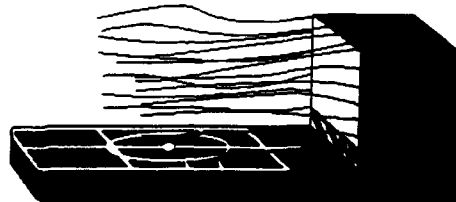
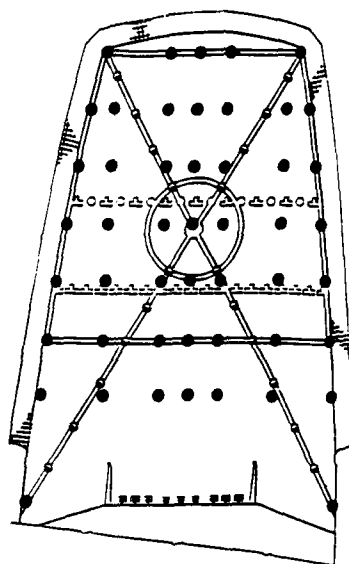


Figure 3 Streamers Illustrating Flow Patterns



Figure 4 Soap Bubble Technique



● WOD Measurement Location

Figure 5 Flight Deck Grid

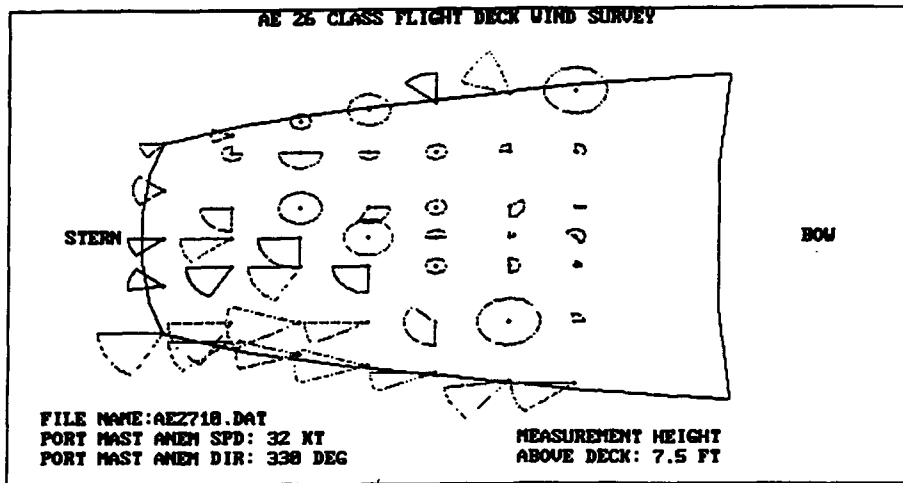


Figure 6 Sample Ship Airwake Data

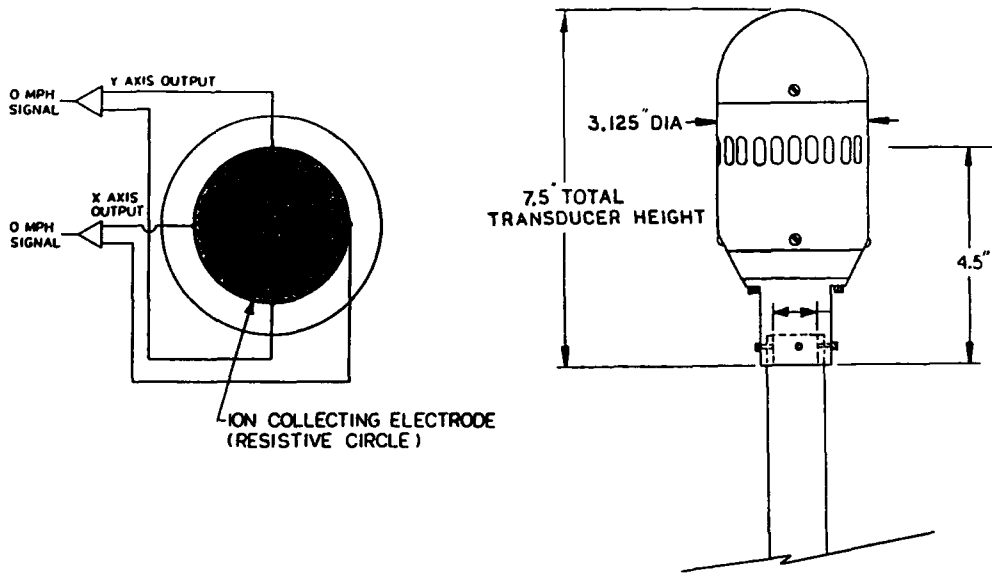


Figure 7 Ion Beam Anemometer

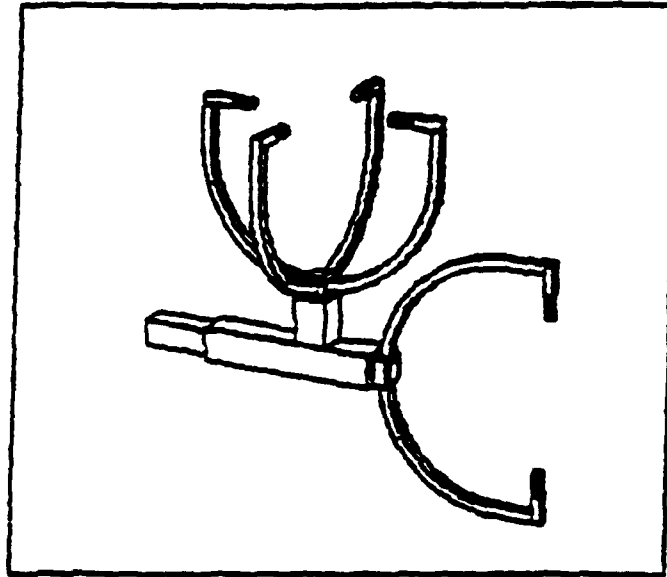


Figure 8 Sonic Anemometer

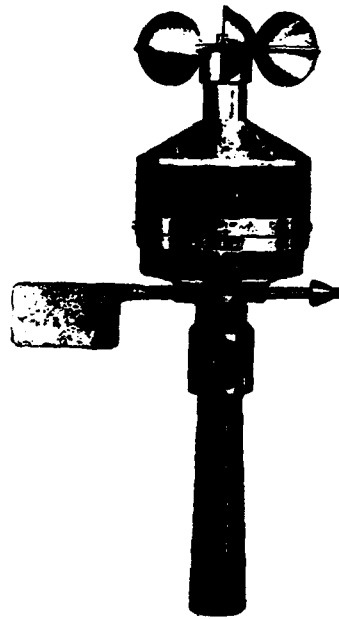


Figure 9 Cup Anemometer

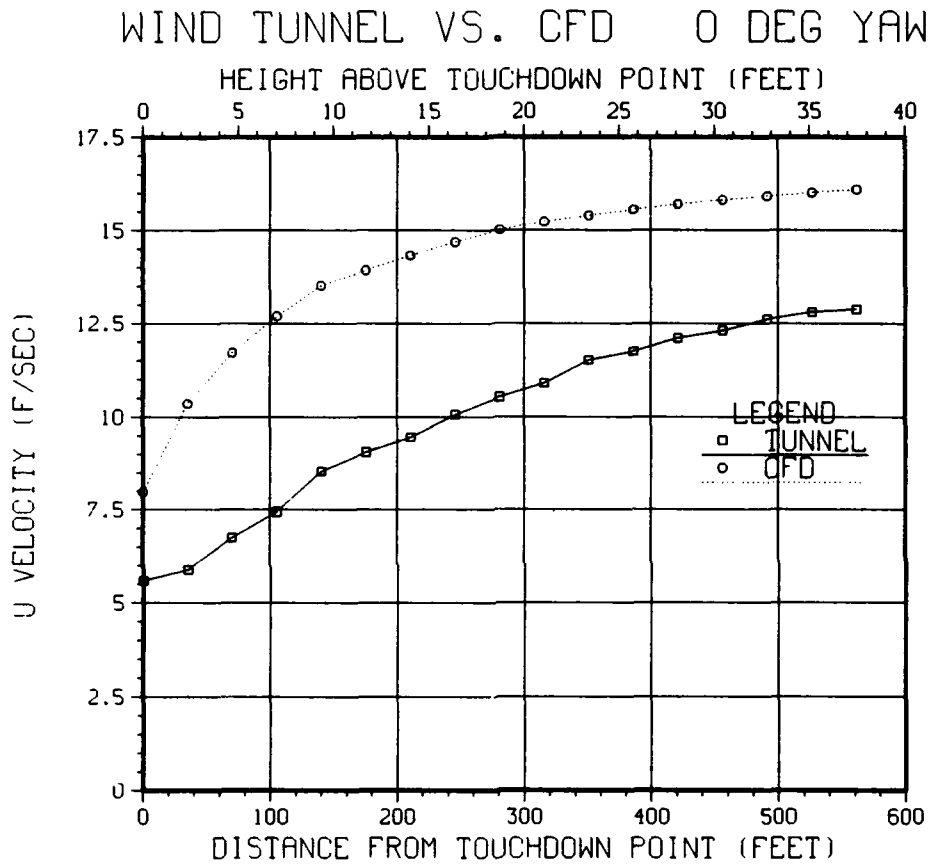


Figure 10 Wind Tunnel and CFD Data Comparison

APPENDIX I

CARBON DIOXIDE (CO₂) LASER REVIEWCO₂ Operating Principles

General LDA Principles. Velocity measurements with a laser Doppler anemometer may be understood with the aid of figure A1-1. This figure shows a typical idealized laser radar. Most of the energy from the laser transmitter is directed to the object being used as a target, which may be either a hard target or the dust particles normally suspended in the atmosphere. A smaller fraction of the transmitter energy is diverted toward the infrared detector and is used as a reference beam. Some of the energy backscattered from the target, which is delayed in time and Doppler shifted according to the line of sight component of the target's velocity, is also incident on the detector. Figure A1-2 illustrates the component of velocity which is actually measured by the LDA. Single velocity measurements yield only that component which is along the line of sight of the laser beam.

As described above, there are two beams incident on the detector. The first is a reference beam of approximately one milliwatt in power at the transmitter frequency. The second is the signal return beam which is offset from the transmitter frequency by the Doppler frequency of the target. This beam is typically at a level of ten femtowatts. These two beams, as shown in figure A1-3, are detected by the square law detector, resulting in a peak at the difference frequency. This corresponds to the Doppler shift generated by the target motion. A typical atmospheric wind return is shown in figure A1-4.

Laser Doppler Anemometer. The laser Doppler anemometer, also known as the Laser Low Airspeed Sensor and Processor (LLASP), is a heterodyne system, which, in contrast to the

idealized system above, contains two lasers, a transmitter and a separate local oscillator. The function of the separate local oscillator is to determine the direction of the velocity. The LDA is one of two modular sensors built in the mid 1970's (reference A1-1). The LDA has the capability of scanning in range and angle to determine the three-dimensional velocity as a function of range from the sensor. A schematic showing the LDA layout is presented in figure A1-5.

The sense can be determined by using an offset local oscillator. In this case, the difference between the local oscillator and the signal is always of the same sign, and the offset frequency corresponds to a stationary target. The offset frequency must be greater than any frequency expected in the signal. However, the lower the offset, the better from the point of view of the hardware implementation.

The offset can be generated in one of two ways. First one may start with a single laser, and shift the frequency of the transmitter or local oscillator with a Bragg Cell. This device uses a travelling acoustic wave, transverse to the light wave, which acts like a moving diffraction grating. A diffraction grating separates light into several diffracted beams representing different orders of diffraction. Each order represents a solution to

$$(n)(\lambda) = (d)(\sin)(\theta)$$

where λ is the wavelength, d is the grating spacing, and θ is the angle of diffraction. The order is defined by the value of integer n . Each order will be located at a different angle. The first order is increased in frequency by the acoustic frequency due to the Doppler shift from the moving acoustic wavefronts. Frequencies of up to 100 MHz are

easily obtained. The requirements for a Bragg cell are a high efficiency of conversion to the first order, and purity of the order. That is, it is desirable to shift most of the beam to the offset frequency, and to ensure that this order is not contaminated by scattered light from other orders.

Initially, Bragg cells were used in the 1970's in the local oscillator beam because of their poor efficiency and power-handling capability. The "feedthrough" problem of unshifted light being scattered along a path coaxial with the first order limited their utility. Successful demonstrations were done only with the highest SNR, under ideal circumstances. Recent advances make it possible to place the Bragg cell in the transmitter path, where the feedthrough problem is less important.

An alternative method of designing a heterodyne system is the use of two lasers. In this case, the lasers must be near enough in frequency for the Doppler shift to lie in the passband of the detector, receiver, and signal processor. Furthermore, the difference frequency must be known to the accuracy required of the Doppler shift. Two lasers can be frequency locked or phase locked using a discriminator-based feedback system or a phase-locked loop. In either case, samples of both beams are combined together on a detector, referred to here as the offset detector. The resulting signal is used to drive the piezoelectric transducer (PZT) on one of the lasers to maintain its frequency with respect to the other.

Signal and Data Processing. The signal frequency is determined by a frequency tracker. This device is a phase-locked loop, which scans in frequency to locate the signal, locks onto it, and tracks it as it varies during the scan. The frequency (velocity) is passed, along with angle data from the scanner, to a microprocessor, controlled by an LSI-11/23 computer. These are used to determine the three components of the vector velocity, and from them, other relevant parameters.

Telescope and Scanners. The telescope is used to expand the laser beam and focus it at the desired location. The signal return will be strongest from the range at which the beam is focussed. Diffraction effects cause larger beams to diverge less, leading to better focussing, and better range resolution.

If the transmitter and receiver share a common aperture, the optical elements will unavoidably reflect some of the transmitted light into the receiver. If the transmitter power is of the order of watts and the received signal is of the order of femtowatts this so-called narcissus will certainly be much larger than the signal. A wire in front of the secondary blocks some of the returning power reflected from the secondary. In spite of the anti-reflection coating, a small amount of power (perhaps a milliwatt) is reflected. This power, called narcissus, is at the transmitter frequency, corresponding to zero velocity, and will usually be stronger than the desired signal.

The range scanner consists of a stepper motor and a belt drive, moving the secondary of the telescope to focus from 1 to 32 meters. The telescope has a refractive primary made from germanium with a focal length of about 15 centimeters, and an aperture of 10 centimeters. This is controlled by a microprocessor, connected to the same LSI-11/23 computer.

REFERENCES

- A1-1. Krause, M. G., R. L. Chandler, C. A. DiMarzio, D. Dickson, and R. Donaldson, "Modular CO₂ Laser Radars for Atmospheric Sensing," Presented at Second Coherent Laser Radar Conference, Aspen, CO, of Jul 1983.
- A2-2 DiMarzio, C., Zaniboni, P., and Simsek, C., Jr., "LDA Tests at NATC," Contract Report CD:485, Northeastern University, Boston, MA, of May 1990.

LASER DOPPLER ANEMOMETER SCHEMATIC

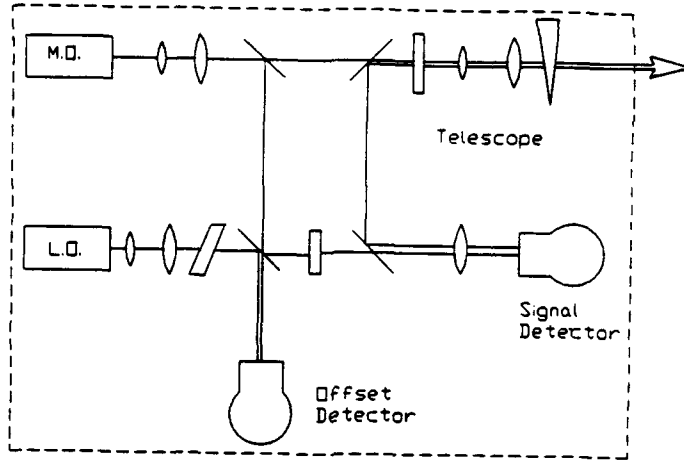


Figure A1-1
LDA Operating Principles

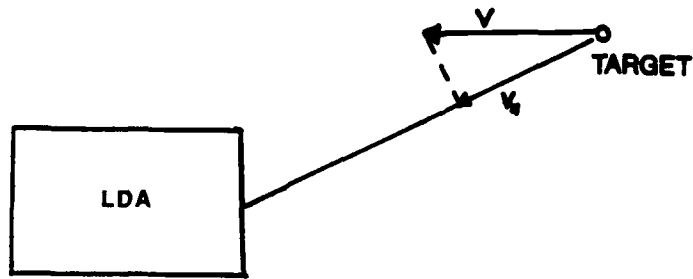
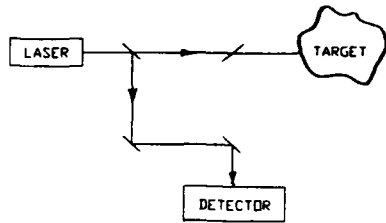
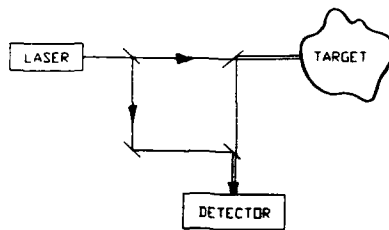


Figure A1-2
Parallel Velocity Component



PATHS OF TRANSMITTED BEAM



PATHS OF TRANSMITTED AND RECEIVED BEAMS

Figure A1-3
Beams Incident on Detector

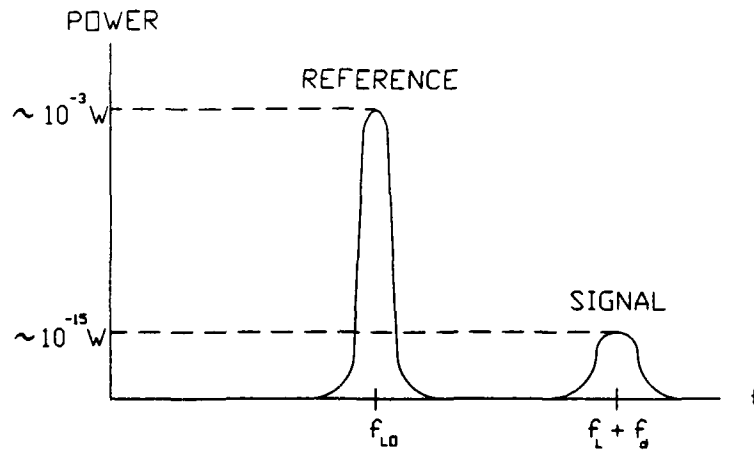
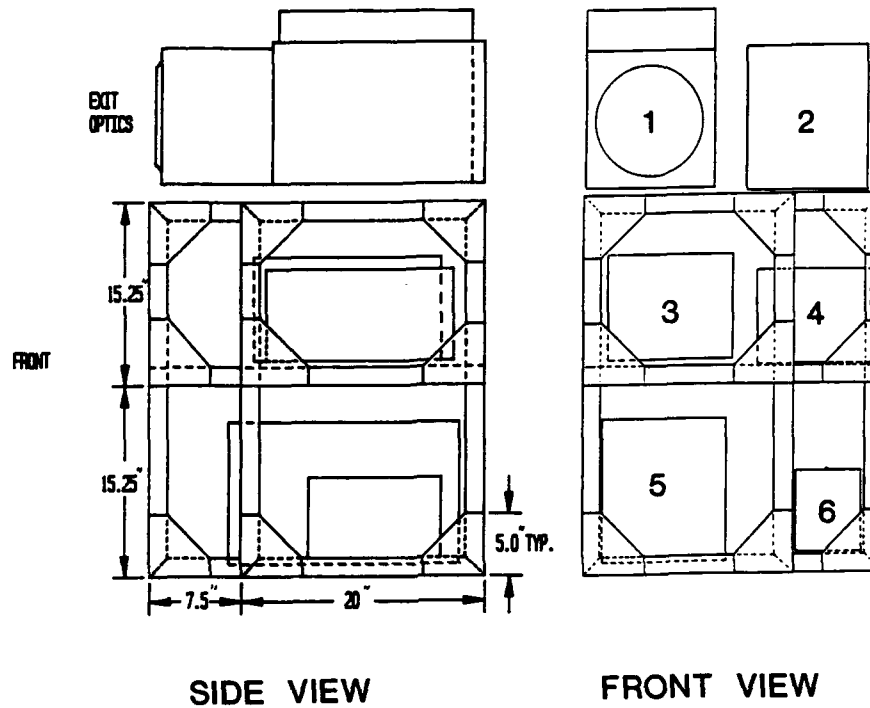


Figure A1-4
Typical LDA Beat Signal

LDA RACK ASSEMBLY



SIDE VIEW

FRONT VIEW

UNIT NO.	NAME
1	TRANCEIVER
2	INPUT/OUTPUT MODULE
3	LOW VOLTAGE POWER
4	LASER COOLING
5	SENSING PROCESSOR
6	TEMPERATURE COMPENSATOR

Figure A1-5 LDA System Layout

**MEASUREMENT OF THE FLOW DISTRIBUTION OVER THE FLIGHT
DECK OF AN AIRCRAFT CARRIER**

M.Mulero
F.Gomez Portabella
Instituto Nacional de Tecnica Aeroespacial
28850 Torrejon de Ardoz, Madrid

SUMMARY

A study was conducted, under requirement of the Logistic Support Directorate of the Spanish Navy, on the general configuration of the air flow over the flight deck of the Spanish Aircraft Carrier " Principe de Asturias ".

The study was aimed at determining the level of fluctuations of the wind vector in certain points of the deck where operations of VSTOL planes and helicopters take place.

It was decided to investigate the possibility of making wind tunnel testing over a reduced scale model of the ship and, later on, taking some limited data over the actual ship, due to availability of dates and cost reasons.

Preliminary tests, to asses the validity of the simulation of the main flow features in the wind tunnel, were performed over a simple geometrical obstacle (square cube) and they showed a systematic constancy in the shape of the cavity and the wake as a function of the Reynolds numbers investigated (from 2×10^4 to 5×10^5). Tests were then performed on a reduced scale model (1:100) of the ship and data were gathered by means of hot-film probes and by photographing wool tufts attached to the surface of the model.

Results show separation past the leading edge of the ramp, which produces vortices that trail along and over the deck to distances that depend on the direction of the approaching wind.

Limited data of local velocities and direction in the horizontal plane were obtained over the real ship, which show the highly disturbed flow in these points due to the effect of the ramp and the island of the ship.

1. - PRELIMINARY WIND-TUNNEL TESTS.

The peculiar configuration of the ship, with a prominent ramp in the bow, with a 12 degrees slope extending to approximately 150 ft, produces a strong effect on the air flow over the flight deck, varying its influence as a function of the bearing of the relative wind to the ship.

In order to asses the validity of a simulation in the wind tunnel on a reduced scale model, it was decided to perform a series of tests on a more simple geometrical model, such as a cube, tridimensional object with sharp edges as the vessel has. Obviously, it was impossible to reproduce the Reynolds numbers of the real case, of the order of 10^8 , but, as the main important feature expected was the separation of the flow past the ramp for relative bearings of the wind from 20 degrees port to 10 degrees starboard, it was decided that a good proof of the sensitivity of the simulation with respect to the Reynolds number, could be the length and shape of the separated zone past the cube. If these do not vary as a function of the wind speed, that means that the reproduction of the flow configuration will not differ much from the real one in that range of speeds and bearings of the relative wind.

The cube was 300 mm in side, and it was tested from 1 to 23 m/sec (Re from 2×10^4 to 5×10^5). Wool tufts were attached to the faces of the cube and also to vertical wires on a frame placed in the vertical plane of symmetry which extended $2H$ upstream and $4H$ downstream of the cube (H is the cube side). Pictures were taken at exposures of 4 seconds to visualize the amplitude of the oscillations at each point. Some results are presented in Fig.1-1.

Also, hot-film anemometry data were obtained along vertical lines in the same plane of symmetry, from $-3H$ to $8H$ approximately from the cube centre base point and up to approx. $2H$ in height from this point. Although the probes used were not able to discriminate reversed flow, its indications were sufficiently indicative of the configuration of the overall flow and the extent of the separated bubble, as depicted in Figs. 1-2 to 1-4.

The values shown in Fig. 1-2, are normalized to the free flow velocity, corresponding the length of the triangles to the local normalized velocity, their orientation to the mean Beta and their aperture to twice the standard deviation of Beta. Fig. 1-3 shows the non-dimensional standard deviation normalized by the local mean velocity and Fig. 1-4 shows the vertical profiles for the standard deviation of the angle.

Both sets of tests showed that the separated zone extended to approximately $2.95H$ downstream from the center base point, starting at the upper leading edge of the cube and reaching a maximum height of $1.24H$ at a distance of $0.5H$ from the base point, being this configuration independent of the free flow velocity from approximately 3 m/sec up to the maximum investigated of 23 m/sec. Based on these results, the simulation was conducted on the reduced scale model of the ship in a environmental wind tunnel of rectangular test section, at a free stream velocity of the order of 5 m/sec.

2. - WIND TUNNEL RESULTS.

Data was, as in the previous tests, both photographic and hot-film signals. The results of the visual tests are qualitative, but very instructive in respect to the overall configuration. The hot-film data are more difficult to interpret but give quantitative results in the points of interest. The tests on the model of the ship were done therefore at a single free-flow velocity, varying the relative bearing to this flow from -20 degrees (20 deg. port) to $+10$ degrees (10 deg. starboard). Data was

taken in vertical profiles at locations 1 to 6 (see Fig. 2-1) and along the take-off strip.

A fixed hot-film probe was attached to the model, on the same position that the actual anemometers should be located in the mast, and was always kept facing the incoming free flow.

A tridimensional hot-film probe was attached to a traversing system running along rails in the top wall of the tunnel, which permitted to position the probe at any point X, Y, Z in space with accuracies of millimeters in each axis, being the overall dimensions of the sampled zone of 4000 mm (X) by 2000 mm (Y) by 900 mm (Z).

Data were taken at every point every 2 seconds, sampling 20 times before moving to next position, sampling all channels at the same time through a sample and hold circuitry and then, digitized and stored via a 20 channel data logger. These data were then transferred to hard disk in a PC, previously transformed to physical units by means of appropriated software and manipulated to obtain mean values and standard deviations. Final data for each point consisted of: Local mean velocity and standard deviation normalized by the mean free-flow velocity; Mean and s.d of the horizontal and vertical angle (Alfa and Beta) of the velocity vector, plus the coordinates x, y, z of each point.

An extract of the results are given in Figs. 2-2 to 2-5, grouped by points, showing the evolution with the relative wind. In Fig. 2-6 it is shown, as an example, the situation in these four points for a bearing of 20 degrees port. In these graphs, port side wind is denoted by B_r and starboard by B_s .

The variability of the horizontal angle of the velocity vector with height, denotes the presence of the trailing vortices originated in the ramp. This is shown too in the results for the vertical angle, Beta, and the normalized velocity in Figs. 2-7 and 2-8, where it is presented, as an example, the situation in the Point number 3.

3. - MEASUREMENTS ON BOARD.

Data were gathered on board the actual ship during a 24 hour period. The ship maneuvered so as to acquire the relative intensities and bearings to the wind that were required, typically 25 and 40 knots at 20 and 10 degrees port, 0 degrees and 10 degrees starboard. Each condition was maintained for approximately 45 minutes.

The necessity of carrying out other type of tests simultaneously, obliged to withdraw the sensor mounts and cabling often, to clear the flight deck for these aircraft operations, with the result of a malfunctioning of three of the anemometers, which couldn't be replaced in time and, consequently, it resulted in a loss of data on wind speed at these points.

The sensors consisted of anemometers and wind vanes, mounted on top of a telescopic mast (see Fig.3-1), able to position the sensors at 7 and 12 feet above the deck. Signals were directed to a datalogger, digitized and stored on hard disk of a Compaq portable computer.

Data on speed and horizontal direction of the local wind in the six points specified were taken every 2 seconds. Another sensor system was moved along the take-off strip, stopping at regular intervals and storing data in these points for 10 minutes at each position.

As said, data on wind speed was lost for points 1, 2 and 6 and for the case of 0 degrees wind, for the take-off strip. Due to proximity of points 3 and 4, a single set of sensors was installed in between both (called here point 34).

Data on the free wind velocity and bearing were supplied by the ship's sensors every minute, as well as ship's velocity and absolute course.

Results for points 1 to 6 for the horizontal angle of the local velocity, as a function of the relative course of the free wind, are given in Fig.3-2 for the two velocities achieved: 25 and 40 knots and the Fig.3-3 reflects the standard deviation of this angle for the two cases. We can see there the similarity between both cases, in mean and s.d., denoting, as previously assumed, a relative independence of the configuration of the local flow with the velocity of

the approaching wind for each relative course.

Due to the short time available for testing on board the ship, it was not possible to measure the vertical profiles in the points selected, which would have allowed to compare the results with the wind tunnel data. It is to notice from the wind tunnel results, the high variability of the local wind vector in angle, both horizontal and vertical, with strong gradients in the lower layers and only reaching free wind conditions at 30 or 40 feet above the deck in most of the cases. This renders direct comparison a very uncertain task, lacking more information on the flow structure above the deck.

4. - CONCLUSIONS

A fairly comprehensive set of data has been obtained in wind tunnel tests on a reduced scale model of the Aircraft Carrier "Principe de Asturias". A limited amount of data was gathered on board the ship.

The effect of the frontal "ski-jump" of the ship has been shown to propagate downstream, affecting the flow conditions in the locations of operations of aircrafts.

These effects are different at each point, depending on the relative bearing of the free wind, but remain similar with different wind velocities for the same bearing.

The data taken on board the ship, confirm these observations, although data is too scarce to permit a direct comparison.

The "cleanest" situation for the point 3, where VSTOL aircrafts do their final hovering till touch-down, seems to be for 10 degrees starboard, when the gradients, as well as the fluctuations in direction are minimum.

For point 5, where helicopters operate, there is no much difference for any of the cases investigated, while for the point 6, also an helicopter area, the worst cases, in which data were obtained, are for 20 degrees port and 10 degrees starboard.

Point 1, being much more close to the ramp, is quite sensitive to the relative course of the wind, as can be seen in Fig.2-2.

ACKNOWLEDGEMENTS.

The authors wish to acknowledge the Junta de Apoyo Logístico (JAL) for their permission to publish part of the extense work performed under funding of the Spanish Navy.

BIBLIOGRAPHY.

1. Wind Tunnel Modelling of Heated Stack Effluents in Disturbed Flows. James Haliksky. Atmospheric Environment. Vol 13 (1979). pp. 449-452.
2. Physical Modeling of the Atmospheric Boundary Layer (ABL) in Long-Boundary-Layer Wind Tunnels (BLWT). J.E. Cermak. Wind Tunnel Modeling for Civil Engineering Applications. Ed. Timothy A. Reinhold. N.B.S. U.S. Dept. of Commerce. Cambridge University Press. pp. 97-125.
3. Wind-Tunnel Measurements in the Wakes of Structures. H.G.C. Woo, J.A. Peterka and J.E. Cermak. NASA CR-2806. March 1977.

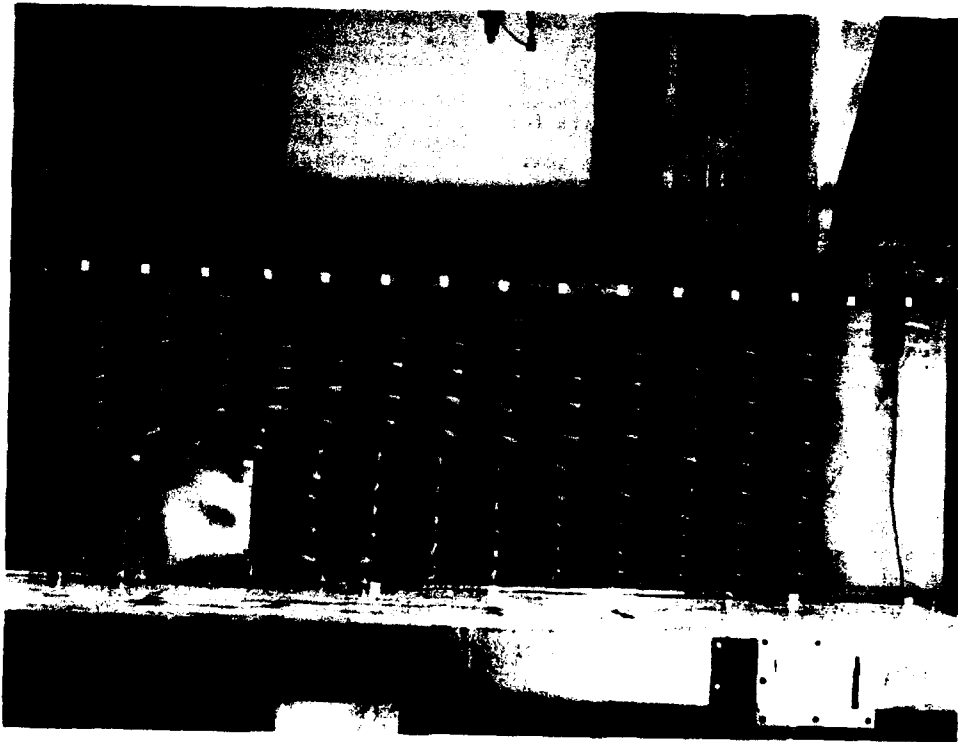


Figure 1-1

FLOW FIELD. 14.47 M/SEC

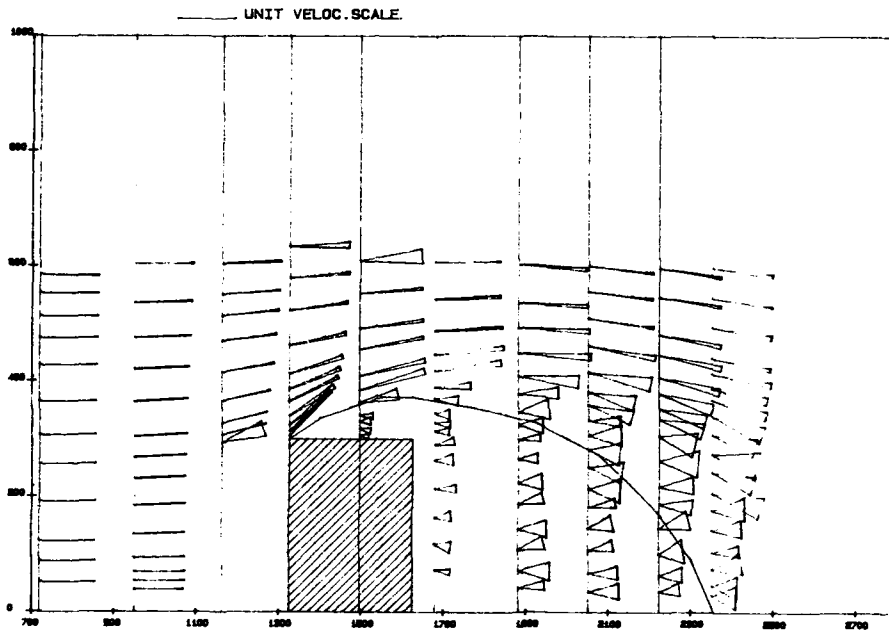


Figure 1-2

$(SD(V)/V)_{local}$

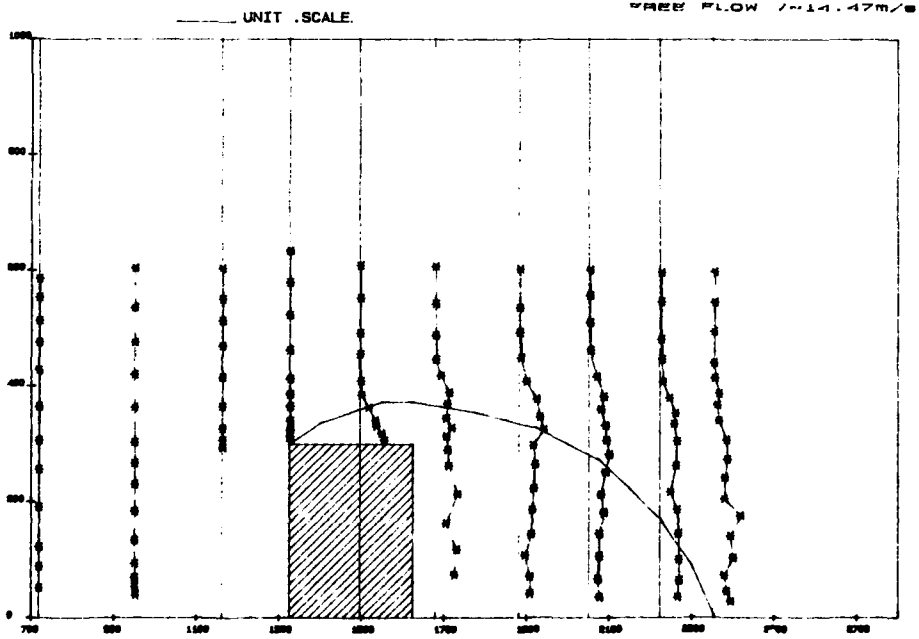


Figure 1-3

STANDARD DEVIATION OF ANGLE

UNIT SCALE

FREE FLOW $V=14.47m/s$

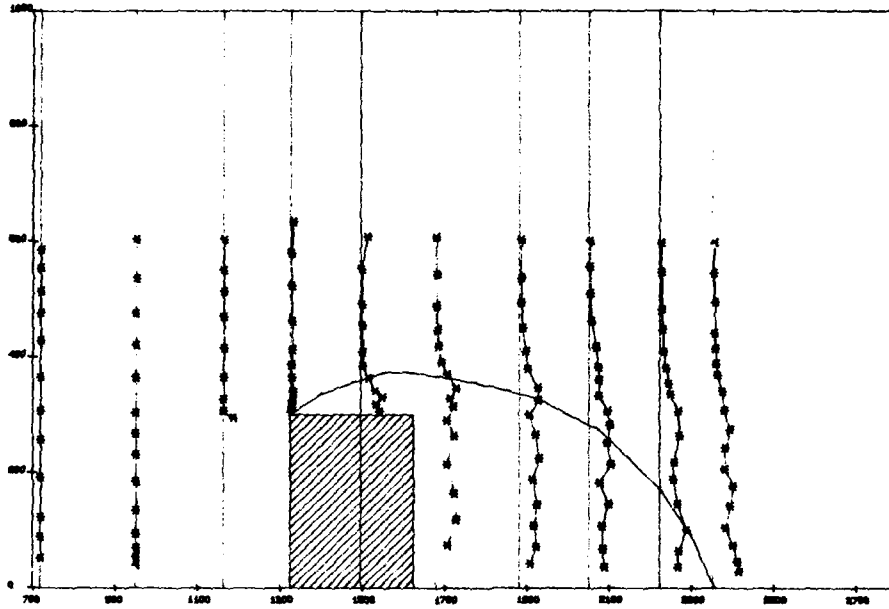
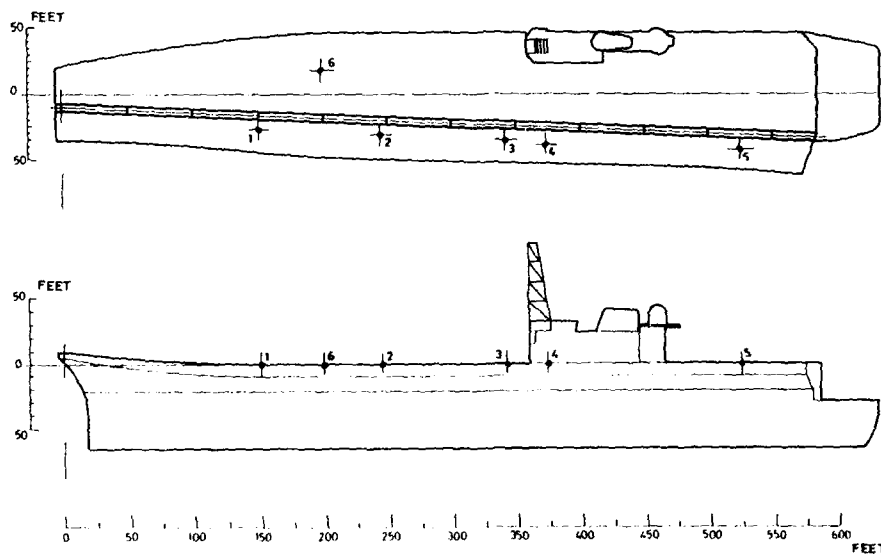


Figure 1-4



AIRCRAFT CARRIER "PRINCIPE DE ASTURIAS"

Figure 2-1

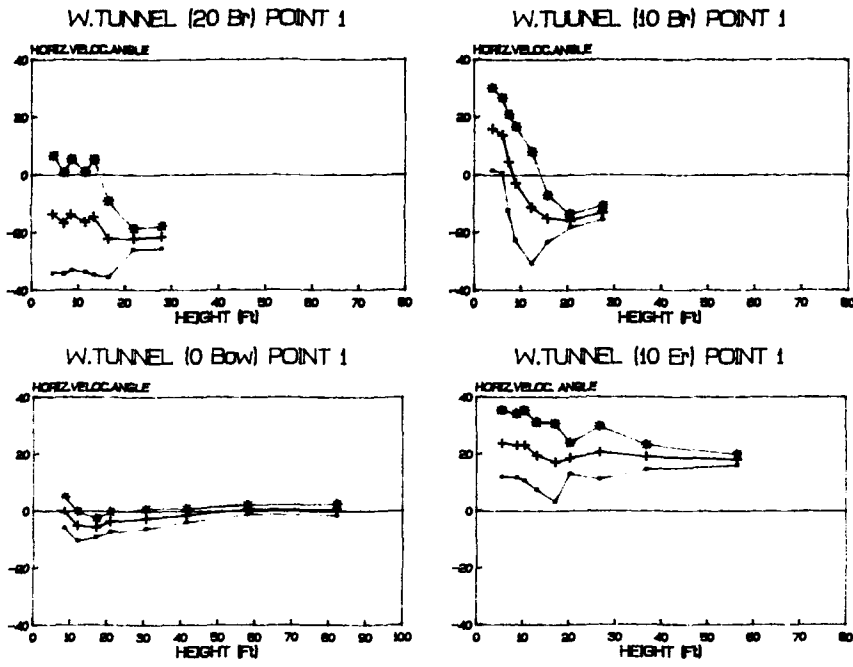


Figure 2-2

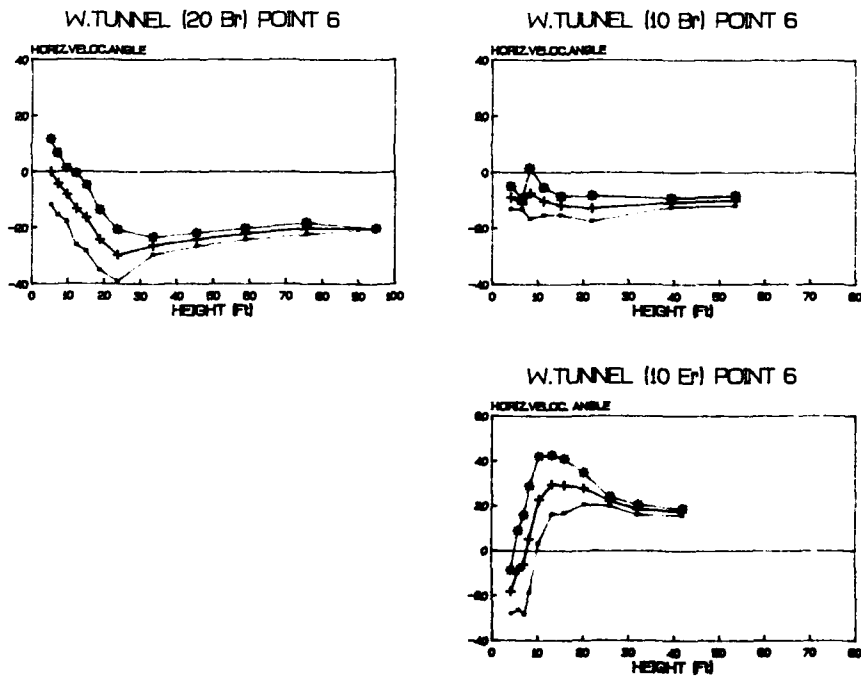


Figure 2-3

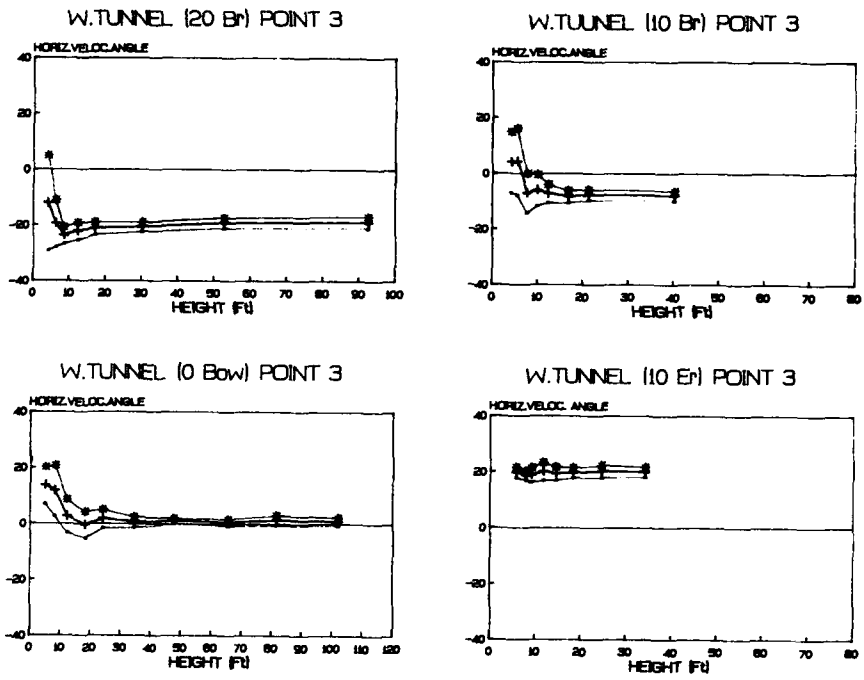


Figure 2-4

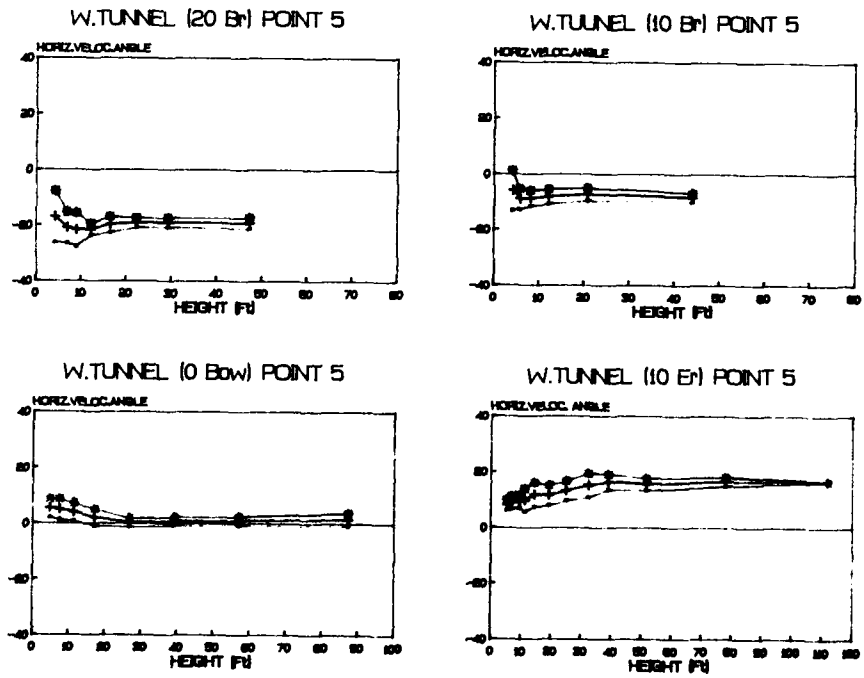


Figure 2-5

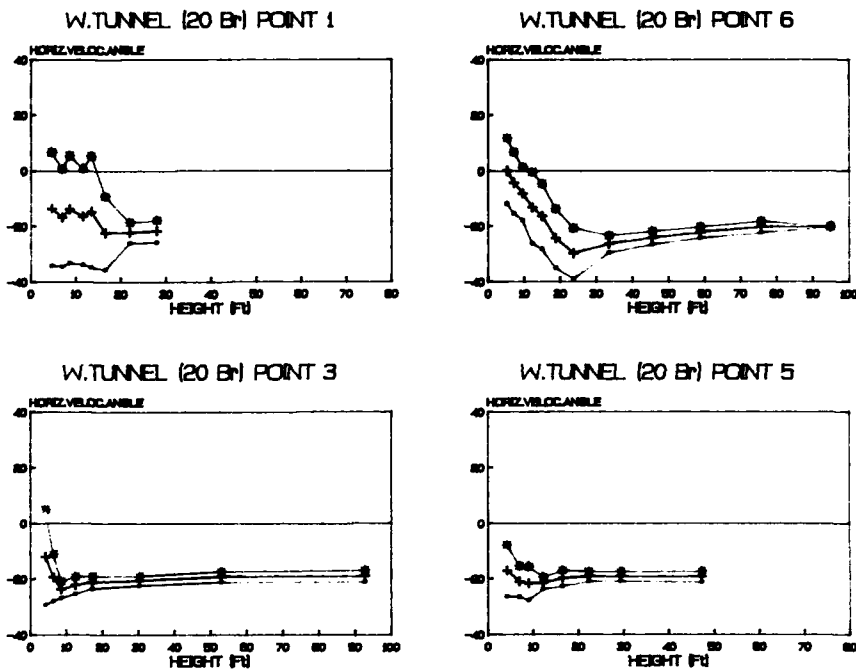


Figure 2-6

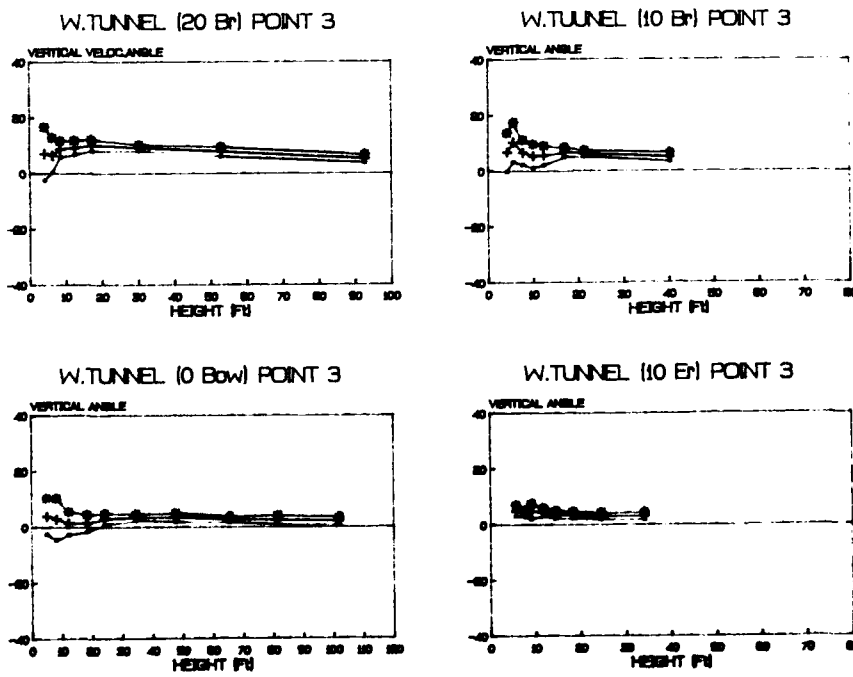


Figure 2-7

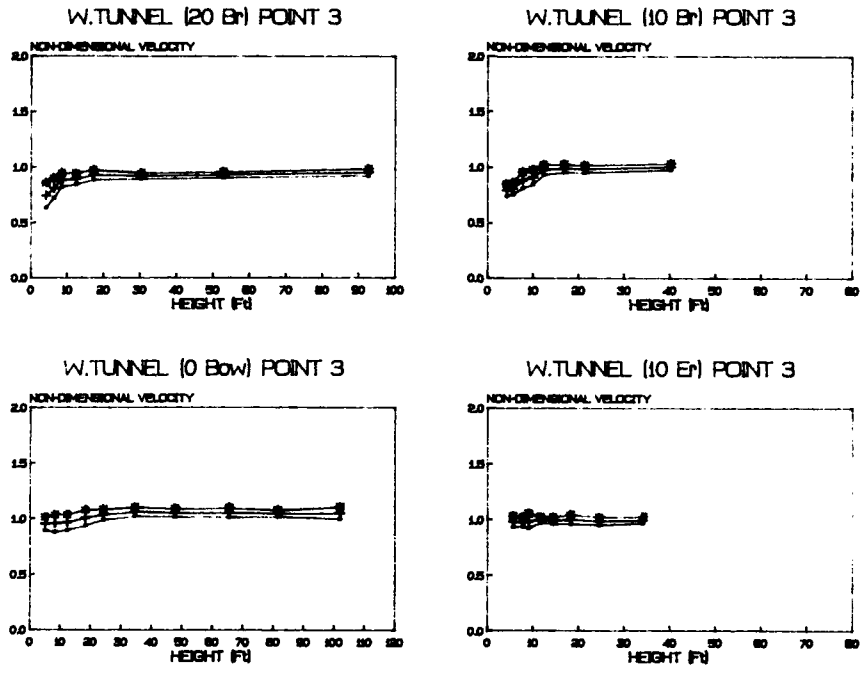


Figure 2-8

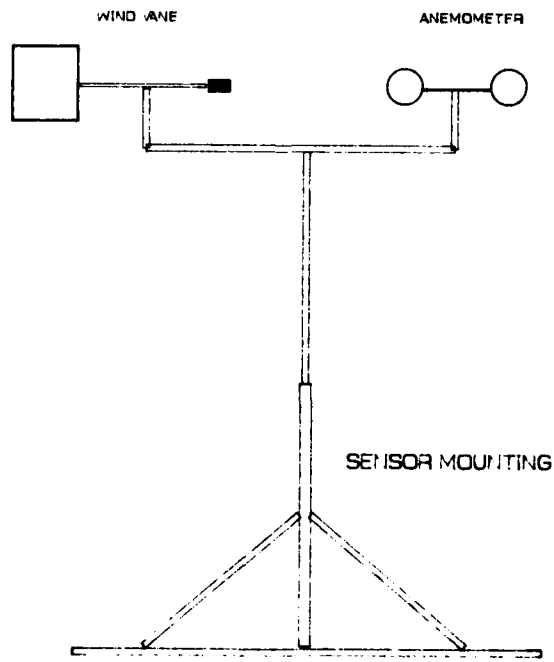
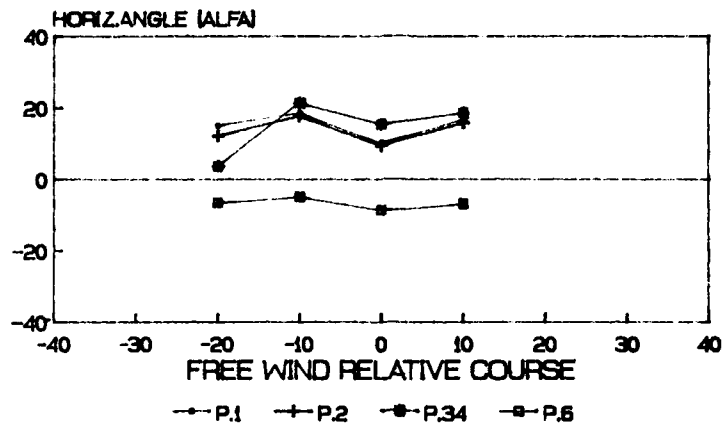


Figure 3-1

MEAN VALUES (25 KNOTS)



MEAN VALUES (40 KNOTS)

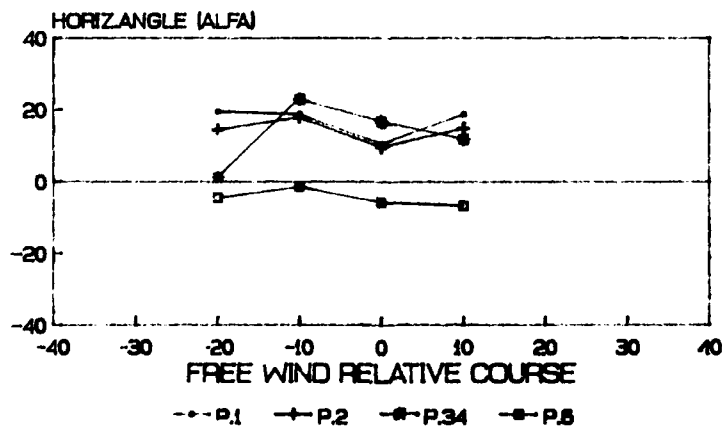
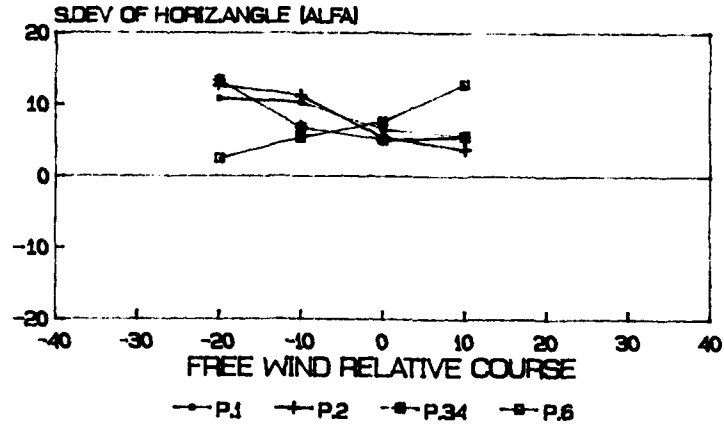


Figure 3-2

STANDARD DEVIATIONS (25 KNOTS)



STANDARD DEVIATIONS (40 KNOTS)

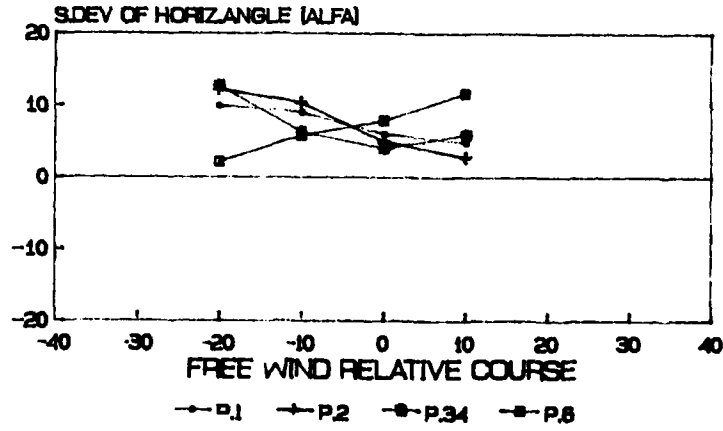


Figure 3-3

A NEW METHOD FOR SIMULATING ATMOSPHERIC TURBULENCE FOR ROTORCRAFT APPLICATIONS

J. Riaz*, J. V. R. Prasad**, D. P. Schrage+
School of Aerospace Engineering
Georgia Institute of Technology
Atlanta, Georgia 30332

and
G. H. Gaonkar+
Department of Mechanical Engineering
Florida Atlantic University
Boca Raton, FL 33431

ABSTRACT

Simulation of atmospheric turbulence as seen by a rotating blade element involves treatment of cyclostationary processes. Conventional filtering techniques do not lend themselves well to the generation of such turbulence sample functions as are required in rotorcraft flight dynamics simulation codes. A method to generate sample functions containing second-order statistics of mean and covariance is presented. Compared to ensemble averaging involving excessive computer time, the novelty is to exploit cycloergodicity and thereby, replace ensemble averaging by averaging over a single-path sample function of long duration. The method is validated by comparing its covariance results with the analytical and ensemble-averaged results for a widely used one-dimensional turbulence approximation.

BACKGROUND

Turbulence experienced by a helicopter rotor blade station can differ appreciably from that experienced by nonrotating stations such as the hub center (Refs. 1 and 2). This is because of the rotational motion of the blade; the sinusoids of turbulence waves that a translating and rotating blade cuts through are different from the sinusoids of turbulence waves that a translating hub center cuts through. This difference translates into basic changes in the stochastic structure of turbulence excitations. For example, the vertical turbulence at the hub center is stationary; energy is concentrated in the low-frequency ($<1/2P$ or $1/2$ per rev) region with rapid attenuation with increasing frequency (Refs. 1 and 2). In contrast, the turbulence at a blade station, or blade-fixed turbulence is cyclostationary; its frequency-time spectral density shows transfer of energy from the low-frequency region to the high-frequency region with occurrence of peaks at $1/2P$, $1P$, $3/2P$, etc. (Refs. 1 and 2). This transfer of energy has appreciable

bearing on vehicle response. In fact, for conventional helicopters (advance ratio $\mu < 0.4$), neglect of rotational velocity effects on turbulence modeling can lead to erroneous prediction of turbulence and blade response statistics (Ref. 2).

To determine the response of rotorcraft to atmospheric turbulence in flight dynamics investigations, a "Monte Carlo" type of approach is used to generate turbulence sample functions. This is a routine approach of passing white noise through constant-coefficient shaping filters (Refs. 3 and 4). However, for simulating cyclostationary processes it is not practical because of the necessity of numerically constructing periodic-coefficient filter systems. An alternate approach is to represent the turbulence sample function as a series of cosine functions with weighted amplitudes, almost evenly spaced frequencies and random phase angles (Ref. 5). The novelty of the new method is the adaptation of the alternate approach for the generation of sample functions to represent cyclostationary turbulence process as seen by a rotating blade element. By exploiting the cycloergodicity (Ref. 6), it is verified that ensemble averaging over a large number of sample functions can be replaced by temporal averaging of a single-path sample function of long duration.

To facilitate an appreciation of this investigation, we mention that little information is available on the generation of sample functions of cyclostationary turbulence as required in the rotorcraft flight dynamics simulation studies. One exception is Ref. 7, in which a combination of digital-cum-analog or hybrid computer approach is used to generate sample functions of cyclostationary flapping response to stationary turbulence excitation. This contrasts with a fairly intensive coverage of methods devoted to the prediction of response statistics of rotorcraft idealized as linear systems; such methods are not applicable to nonlinear problems typical of flight dynamics codes. Thus, the proposed method offers promise in finding applications to flight dynamics problems and in complementing

* Graduate student
** Assistant Professor
+ Professor

development of analytical methods to predict response statistics of rotorcraft using nonlinear model representation.

CORRELATION FUNCTION AND DISTANCE METRIC

We follow the widely-used theory of isotropic, homogeneous atmospheric turbulence and the Taylor's frozen field approximation (Refs. 7 and 8). The modeling parameters are the turbulence intensity, σ , the turbulence scale length, L , and the distance metric, ξ . Meteorological conditions dictate the values of the turbulence intensity and the scale length. The distance metric is defined as the relative distance between the two points of interest on the lifting surfaces at two points in time with respect to the atmospheric frame as shown in Fig. 1 (Refs. 7 and 8). Turbulence models are obtained by calculating the distance metric and then using it in a fundamental correlation function, R_0 . For this purpose a number of fundamental correlation functions of the form

$$R_0 = f(\sigma, L, \xi) \quad (1)$$

are available for use, e.g., von Karman, Dryden, etc (Refs. 1,2,7,8).

The most general representation comprises a three-dimensional turbulence field; vertical, lateral (side-to-side) and longitudinal (fore-to-aft) velocities and the distance metric that accounts for spatial changes in all three directions. The present investigation, following earlier studies (Refs. 1-3) considers only the vertical turbulence velocities in level flight, heading into the mean wind direction as sketched in Fig. 1. For simulation purposes, the concept of time lag between the hub center and a typical blade station in experiencing turbulence is important. Preparatory to illustrating that concept in the next section, we use a simplified picture of spatial variation of ξ only in the flight direction.

As seen from Fig. 2, the distance along the x-axis covered by a point of interest between times t_1 and t_2 is

$$\xi = V(t_2 - t_1) - r(\cos \psi_2 - \cos \psi_1) \quad (2)$$

Here, ψ_1 and ψ_2 represent the azimuthal angle of the blade at times t_1 and t_2 , r is the distance of the element under consideration from the center of rotation, and V is the relative wind velocity. If this value of ξ is substituted in the fundamental correlation function, we obtain the temporal correlation of blade-fixed turbulence (Refs. 2 and 3).

SIMULATION METHODOLOGY

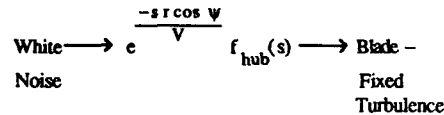
Compared to the hub, an element located at radius r and azimuthal angle ψ will experience turbulence velocity with a time lag, Δt , given by

$$\Delta t = \frac{r \cos \psi}{V} \quad (3)$$

where V is the relative wind speed. The turbulence experienced by the hub can easily be simulated by exciting a time-invariant filter driven by white noise. If the frequency response of such a filter is given by $f_{\text{hub}}(s)$, then the frequency response of a filter generating turbulence seen by the blade element, $f_{\text{blade}}(s)$, is

$$f_{\text{blade}}(s) = e^{-\frac{sr \cos \psi}{V}} f_{\text{hub}}(s) \quad (4)$$

We observe that $e^{-sr \cos \psi / V}$ distributes turbulence over the rotor disk when ξ is given by Eq. (2), which will be referred to as the Rotational Sampling Operator (RSO). Schematically,



From the expression for RSO we notice that the rotational velocity effects increase with increasing radial distance and decreasing relative wind speed. Thus, the rotational velocity effects will be dominant at the blade tip for low relative wind speeds. Sample function for the vertical turbulence at the hub center can be expressed as a sum of cosine series which is given by (Ref. 5)

$$w_{\text{hub}}(t) = 2 \sum_{i=1}^N \sqrt{S_0(\omega_i) \Delta \omega} \cos(\omega_i t + \Phi_i) \quad (5)$$

where $S_0(\omega_i)$ is the value of the two-sided, power spectral density or PSD (corresponding to the fundamental correlation function) of the stationary turbulence process at the temporal frequency $\omega_i = (i-1)\Delta\omega/2$, $i = 1, 2, \dots, N$. In Eq.(5), the frequency band of interest of the power spectral density curve has been divided into equal subdivisions, $\Delta\omega$, and Φ_i is the phase of the i th spectral component. If Φ_i is treated as a random variable with uniformly distributed probability

density between 0 and 2π , this is equivalent to exciting the system with a band-limited white noise (Ref. 5). Transformation of Eq.(4) in time domain is

$$w_{\text{blade}}(r,t) = w_{\text{hub}}\left(t - \frac{r \cos \psi}{V}\right) \quad (6)$$

Combining Eqs. (5) and (6), we get

$$w_{\text{blade}}(r,t) = 2 \sum_{i=1}^N \sqrt{S_0(\omega_i) \Delta \omega} \cos \left[\omega_i \left(t - \frac{r \cos \psi}{V} \right) + \Phi_i \right] \quad (7)$$

The above equation in terms of positive spatial frequencies ω_k and $\Delta \omega$ can be expressed as

$$w(r,t) = 2 \sum_{k=1}^N \sqrt{S_0(\omega_k) \Delta \omega} \cos \left[\omega_k \left(Vt - r \cos \psi \right) + \Phi_k \right] \quad (8)$$

which gives an expression for sample function for the vertical turbulence as seen by a rotating blade element. The ensemble autocorrelation, $R(r,t_1,t_2)$, for an element of blade located at radius r is

$$R(r,t_1,t_2) = E\{w(r,t_1)w(r,t_2)\} \quad (9)$$

where $E\{\cdot\}$ is the expectation operator. After substituting for $w(r,t)$ in the above expression and simplifying, we get

$$R(r,t_1,t_2) = \int_{-\infty}^{+\infty} S_0(\omega) \cos(\omega \xi) d\omega, \quad (10)$$

where ξ is given by Eq. (2).

NUMERICAL RESULTS

We now present numerical results of correlation at the 0.75R blade station computed from Eq. (9) using ensemble averaging of a "large number" of sample functions and temporal averaging of a single-path sample function of "long duration." (The terms in quotes are quantified subsequently.) These two sets of results are compared with those from an analytical expression of correlation function with distance metric ξ given by Eq. (2). We use the following exponential

form of the fundamental correlation function

$$R_0 = \sigma^2 e^{-\frac{|\xi|}{L/2}} \quad (11)$$

for which the spectral density is

$$S_0 = \sigma^2 \frac{2}{\pi} \frac{L}{4 + \omega^2 L^2} \quad (12)$$

The following numerical values of parameters are used:

Relative wind velocity (V) = 40 ft/sec
 Turbulence Intensity (σ) = 5 ft/sec
 Rotor Radius (R) = 28 ft
 Rotor Angular Velocity = 27.0 rad/sec
 Advance ratio (μ) = 0.1
 Turbulence Scale Length (L) = 56 ft

Only 20 terms in Eq.(8) are used to generate the sample functions. While Fig. 3a shows the analytical correlation function, Fig. 3b shows the results of the ensemble average of the correlation over 1200 samples; each sample is of length of 4 rotor revolutions. Figure 3c presents the same results obtained from a single-path sample function of 400 rotor-revolution duration. In both the ensemble and temporal averaging cases, it is seen that all the essential features such as rms values, periodicity along the t -axis and decay along the τ -axis, where t is the average time and τ is the elapsed time, are predicted. Figure 4, a section of the correlation perspective at $t=0.4375$ sec from Fig. 3 shows that the sample functions generated using the new method contain the correct correlation statistics.

CONCLUSIONS

A new method for simulating turbulence sample functions suitable for rotorcraft dynamics applications is presented. It is numerically shown that the method takes into account appropriate second-order statistics of turbulence as seen by a translating and rotating blade. It can easily be integrated with any rotorcraft flight simulation codes.

ACKNOWLEDGEMENTS

This work was done under the NASA-University Consortium grant No. NCA2-512 from the Aeroflightdynamics Directorate, NASA Ames Research Center.

REFERENCES

1. Gaonkar, G. H., "A Perspective on Modeling Rotorcraft in Turbulence," *Probabilistic Engineering Mechanics*, Vol. 3, (1), 1988.
2. George, V.V., Gaonkar, G.H., Prasad, J.V.R. and Schrage, D.P., "On the Adequacy of Modeling Turbulence and Related Effects on Helicopter Response," International Technical Specialists' Meeting on Rotorcraft Basic Research, Atlanta, GA, March 25-27, 1991.
3. Gaonkar, G.H. and Hohenemser, K.H., "Stochastic Properties of Turbulence Excited Rotor Blade Vibrations," *AIAA Journal*, Vol. 9, (3), 1971.
4. Dahl, H.J. and Faulkner, A.J., "Helicopter Simulation in Atmospheric Turbulence," *Vertica*, Vol. 3, 65-78, 1979.
5. Shinozuka, M. and Jan, C.-M., "Digital Simulation of Random Processes and its Applications," *Journal of Sound and Vibration*, Vol. 25, (1), 111-128, 1972.
6. Gardner, W. A., *Statistical Spectral Analysis: A Non-Probabilistic Theory*, Prentice Hall, New York, 1988, Chapter 10.
7. Gaonkar, G.H., and Hohenemser, K.H., "Comparison of Two Stochastic Models for Threshold Crossing Studies of Rotor Blade Flapping Vibrations," AIAA-ASME 12th Structural Dynamics and Materials Conference, Anaheim, CA, April 19-21, 1971, AIAA paper No. 71-389.
8. Costello, M. F., "A Theory for the Analysis of Rotorcraft Operating in Atmospheric Turbulence," Proceedings of the 46th Annual National Forum of the American Helicopter Society, Washington, D.C., May 1990.

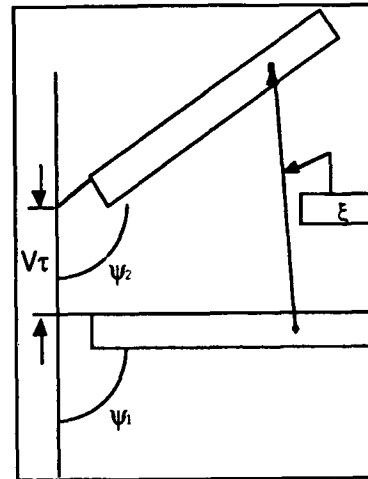


Figure 1. Distance Metric in Level Flight.

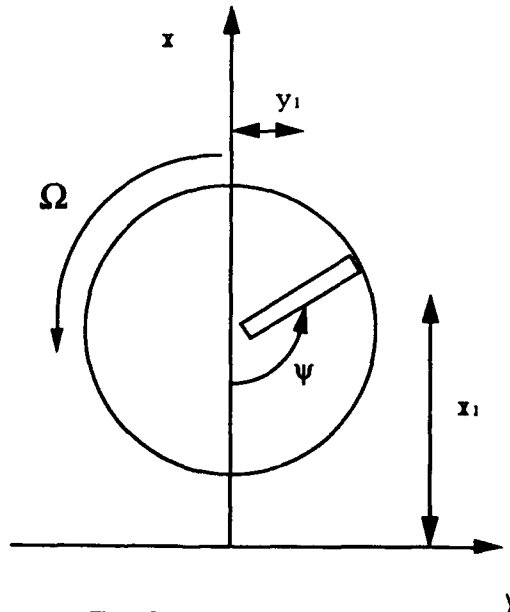
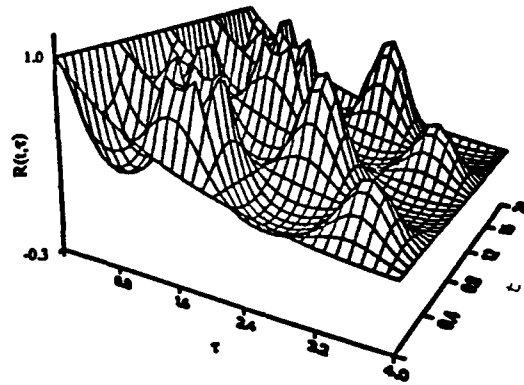
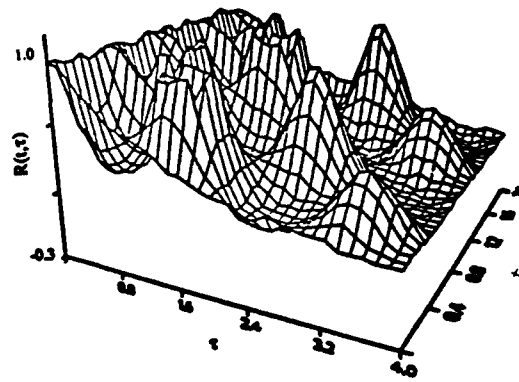


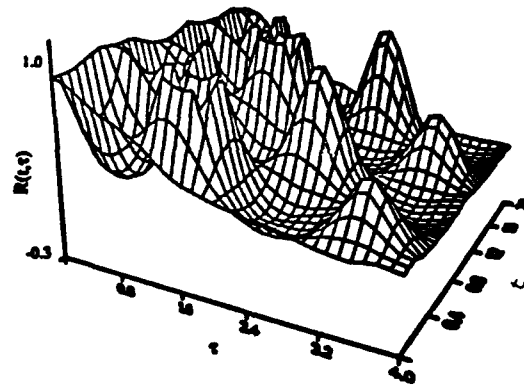
Figure 2. A Simplified Rotor Model.



3a. Analytical



3b. Ensemble Averaging



3c. Temporal Averaging

Figure 3. Correlation Function of Vertical Turbulence.
($\mu = 0.1$, $L/R = 2$)

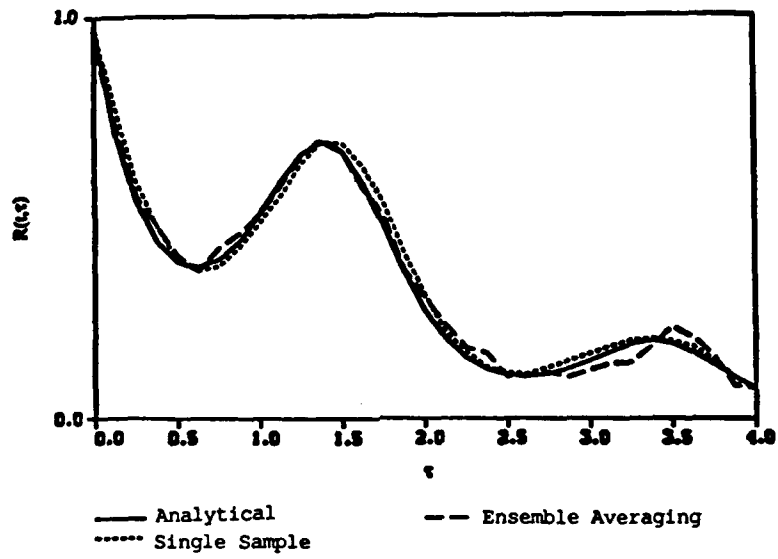


Figure 4. Correlation Function at $t = 0.4375$ sec
from Analytical, Ensemble-Averaging
and Temporal-Averaging Techniques.
($\mu = 0.1, L/R = 2$)

Enhanced Displays, Flight Controls, and Guidance Systems for Approach and Landing

R. W. Huff
G. K. Kessler
Naval Air Test Center
Panuxent River, Maryland USA

SUMMARY

The United States Navy has had an ongoing objective to provide a safe and reliable approach and landing capability with minimum interference from severe weather and sea state, and no limitation due to low ceiling and visibility. In the past, efforts to achieve these objectives in the past have not been as successful as desired due to the lack of integrated development of landing guidance systems, aircraft flight controls (automatic and manual modes), aircraft displays (flight director and situation displays), data link (capacity), and aircraft and shipboard sensors. The Naval Air Test Center (NATC) has been involved with the development, test and evaluation of U.S. Navy landing systems for over 25 years. In addition, we are the flight certification activity for landing guidance systems aboard aircraft carriers and amphibious ships.

This paper will present NATC's overview of the present and future U.S. Navy displays, flight controls, and guidance systems for approach and landing. The results of simulation studies and flight tests concerning enhancements to aircraft displays and flight controls are discussed. The various tradeoffs and issues that must be considered are also discussed. Tradeoffs in landing system accuracy requirements versus integration of aircraft and shipboard data are explored.

NOMENCLATURE

ACLS	Automatic Carrier Landing System
AOA	Angle of Attack
APCS	Approach Power Compensator System
DMC	Deck Motion Compensation
FLOLS	Fresnel Lens Optical Landing System
FPM	Flightpath Marker
HUD	Heads-Up Display
ICLS	Instrument Carrier Landing System
INS	Inertial Navigation System
MLS	Microwave Landing System
NATC	Naval Air Test Center
nmi	nautical mile
PFPM	Potential Flightpath Marker
SAS	Stability Augmentation System
TACAN	Tactical Air Control and Navigation System
VLA	Visual Landing Aid

INTRODUCTION

There are many issues that must be addressed in developing an approach and landing capability such as desired visibility minimums, vehicle stability, space available for shipboard and airborne equipment, communication requirements, shipboard and airborne sensors, displays, multipath environment, ship motion, accuracy requirements, and monitoring. For instance, blending of aircraft inertial data with the shipboard data reduces the accuracy requirements of the landing guidance data. In addition, the visual landing aids should be aligned with the other landing guidance systems and should have stabilization modes identical to the landing guidance systems.

NATC has conducted many simulation studies over the last few years to determine what command control laws (flight director and autoland modes), aircraft flight control laws (for

manual and autoland modes), aircraft display formats, data link formats, and landing system accuracies are required to meet the Navy's approach and landing objectives. These studies have included aircraft such as the F/A-18, F-14, and A-6. Aircraft display studies and developments have primarily consisted of flight directors, situation displays, flightpath marker (FPM) lead compensation (for aircraft dynamics), potential FPM, and range displays. The F-14D has incorporated the FPM lead compensation and potential FPM and will incorporate the flight director. Manual control modes which have been studied include flightpath control modes which optimize the aircraft flightpath response to the stick inputs and approach power compensator modes which command the engine power setting. Automatic control modes for the landing guidance systems which have been studied include replacement of the older aircraft autopilot pitch command mode with a vertical rate command mode, state estimator control laws, and data fusion (blend or Kalman) filter control laws.

In addition to aircraft displays and flight controls, monitoring of landing guidance data and integration of aircraft and shipboard data are two areas which significantly affect approach and landing capabilities. Both require substantial upgrades to the current data link formats. Integration (data fusion) of aircraft sensor data with ships inertial data provides the best estimate of aircraft position and reduces the accuracy requirements of the landing guidance data. Implementation of an automatic monitor function comparing aircraft position data from all landing guidance systems and aircraft sensors would increase safety, reduce pilot workload, and increase pilot confidence.

LANDING GUIDANCE SYSTEMS

General

The approaches to meeting the U.S. Navy landing guidance system objectives can be grouped into several categories. Primary guidance systems are those systems with the capability to meet all the approach and landing guidance objectives. Secondary guidance systems are those systems with the capability to meet some of the approach and landing guidance objectives or that complement the capabilities provided by the primary systems. The secondary guidance systems include the Tactical Air Control and Navigation (TACAN), Global Positioning System (GPS), aircraft radars, Inertial Navigation System (INS), and any aircraft tracking components associated with other systems. Visual landing aid systems are those shipboard systems which provide the pilot visual cues of the aircraft position.

The above systems also can be categorized as air derived or ground derived systems. Air derived systems are those that derive the aircraft position in the aircraft. Ground derived systems are those that derive the aircraft position on the ground or ship. As discussed in the following paragraphs, both types of systems have components on the aircraft and ship. Air derived systems have generally unlimited capacity while ground derived systems are generally limited to one or two aircraft at a time (unless a phased array radar is utilized). Ground derived systems have demonstrated guidance accuracies sufficient to meet the Navy objectives while air derived systems need more development to meet all the Navy objectives (particularly

Distance Measuring Equipment (DME) and multipath rejection). Some of the other characteristics of the two systems that have been viewed as advantages and disadvantages can be equalized with adequate communications. Phased array antenna systems could be developed that are capable of radar tracking (ground derived) and generating air derived signals simultaneously. This would allow either a reduction in the amount of shipboard equipment or an increase in redundancy.

The components required for air derived systems are divided between the aircraft and ship as follows. The ship components are the landing guidance transmitter, DME transponder, stabilization platform, inertial sensors, displays and controls, computer, and data link. The aircraft components are the landing guidance receiver, DME transponder, data link, displays and controls, inertial sensor, computer, and autopilot.

The components required for ground derived systems are divided between the aircraft and ship as follows. The ship components are the radar, inertial sensor, displays and controls, computer, and data link. The aircraft systems are the point tracking source (corner reflector or radar beacon), data link, displays and controls, inertial sensor, computer, and autopilot.

The components required for Visual Landing Aid (VLA) systems are the visual display, stabilization platform, inertial sensor, controls, and computer. The VLA must be integrated and fully compatible with the other landing guidance systems.

Current Landing Guidance Systems

The primary current U.S. Navy landing systems aboard the large carriers are the AN/SPN-42/46 Automatic Carrier Landing System (ACLS), the AN/SPN-41 Instrument Carrier Landing System (ICLS), and the Fresnel Lens Optical Landing System (FLOLS).

The ACLS uses data from a Ka band conical scan tracking radar and ship motion sensors and performs the following functions:

- a. Derives stabilized aircraft position data.
- b. Computes angular glidepath errors and autoland or flight director commands to null the errors.
- c. Transmits the errors, commands, and control discretures to the aircraft via a UHF data link.

The glidepath errors are sent to the cockpit displays and the autoland commands are sent to the automatic flight control system. A radar beacon system on the aircraft provides a point source for the radar. The data flow is shown in figure 1. A more complete description is given in reference 1.

The ICLS is a split site Ku band scanning beam system. An elevation antenna (stabilized for ship's pitch and roll) is located at the side of the landing area and the azimuth antenna (stabilized for ship's yaw and roll) is located at the stern of the ship under the landing centerline. No data link or ranging systems are used. The aircraft decodes the angle data encoded on the scanning beam and the resulting glidepath errors are sent to the cockpit displays. A more complete description is given in reference 2.

The FLOLS consists of a set of five vertically mounted Fresnel lenses ("cells") with integral source lights located between two sets of horizontal datum lights. The Fresnel lenses and source lights result in a light bar image ("meatball") which moves above or below the datum lights by an amount proportional to the angular error of the aircraft from the glide slope setting. The meatball is normally amber except at the lowest angles where it transitions to red. The Fresnel cells are stabilized for ship's pitch, roll, and vertical heave of the

intended touchdown point relative to the ship's center of motion. A more complete description is given in reference 3.

Other optical landing systems include:

- a. Close-in Approach Indicator (CAI) MOD 2 - The CAI MOD 2 is an Optical Landing System (OLS) consisting of two vertically stacked light boxes located between two sets of horizontal datum lights. Each source light box contains ten vertically mounted light cells consisting of source lights, dichroic filter, fiber optic coupler, and lens. The two stacked light boxes provide a 20 cell "meatball" display similar to the FLOLS meatball display. The CAI MOD 2 provides 2.4 deg elevation coverage. The meatball operates similar to the FLOLS except that it has higher sensitivity in the middle 1.6 deg of coverage, it flashes in the top and bottom 0.2 deg of coverage, and it is red in the bottom 0.4 deg of coverage. The CAI MOD 2 is stabilized for ship's pitch and roll and has the potential to be stabilized for vertical heave. A more complete description is given in references 4 and 5.
- b. Horizontal Approach Path Indicator (HAPI) - The HAPI is a derivative of a British system which is designed to provide long range glide slope and lineup information to the pilot. The HAPI consists of two individual light source units positioned on the port side of the ship slightly higher than the deck edge. Each unit contains a red over white filter and each unit is stabilized for ship's pitch and roll. The forward and aft light source units are aligned to allow the pilot to fly a glide slope corridor of about 3.0 deg. The forward light source is aligned to 3.5 deg and the aft to 2.5 deg. If the pilot maintains a red over white presentation, he is within the glide slope corridor. If he transitions above the glide slope corridor, he sees a white over white presentation. If he transitions below the glide slope corridor, he sees a red over red presentation. The positioning of the HAPI light source units also allows the pilot to use the HAPI for course lineup information outside 1/2 nmi (0.93 km). When the two light source units appear in line with each other, the pilot is lined up on the ship's port edge. A more complete description is given in reference 4.
- c. Hover Position Indicator (HPI) - The HPI is a derivative of a British system which provides hover height and longitudinal position information for vertical landings. The HPI is located to the side of the landing area centerline and forward of the landing spot so that the azimuth angle from the landing spot to the HPI is approximately 30 deg from forward down the centerline. The HPI consists of horizontal (green) and vertical (white over green over amber) datum lights and a red reference light mounted in front (towards the direction of the landing spot) of the datum lights. The horizontal and vertical datum lights intersect at the starboard light of the horizontal datum and the middle light of the vertical datum. The horizontal datum lights are angled perpendicular to the line of sight to the landing spot. As the aircraft moves down the deck and descends, the red reference light appears to move starboard and up relative to the datum lights. The height above deck of the datum lights and the location of the red reference light relative to the datum lights are such that, assuming that the pilot has aligned the aircraft with the landing area centerline, the aircraft is at the proper hover height and over his landing spot when the red reference light is in line with the intersection of the vertical and horizontal datum lights. A more complete description is given in reference 4.

These other OLS's are primarily installed aboard amphibious assault ships.

Future Electronic Landing Systems

The Signature Managed Air Traffic Control, Approach, and Landing System (SMATCALS) program was initiated by the USN to address and solve the operational and system problems in the current air traffic control, approach, and landing systems. The technical objectives of this program are to develop systems which:

- Provide all weather capability, from acquisition to touchdown, and allow ships and aircraft to operate safely and efficiently.
- Reduce the vulnerability of aircraft carriers and amphibious assault ships and their associated task group/task force to detection and localization.
- Reduce the vulnerability of aircraft carriers and amphibious assault ships to anti-radiation missiles.
- Allow ships and aircraft to be electromagnetically compatible with other United States and allied forces.

For the last several years, system concept studies and experiments have been conducted to examine advanced technologies and designs to meet the SMATCALS program objectives. Contracts will likely be let in 1992 to build SMATCALS technology demonstrators for tests in 1994-1995.

Future Optical Landing Systems

Concepts for future OLS's are being developed and evaluated by the Naval Air Engineering Center and NATC in the Improved Carrier Optical Landing System (ICOLS) program. The primary goals have been to improve the long range capabilities over current optical landing systems with a secondary goal to improve the glide slope indications in close to touchdown. ICOLS concepts which have shown promise include the following:

- Modifying the standard FLOLS by adding additional Fresnel lens cells to provide increased glide slope sensitivity and coverage.
- Adding a Laser Glide Slope Indicator (LGI) near or abeam the FLOLS location to provide an amber light indication when close to the glide slope, a green light indication when high (flashing green when excessively high), and a red indication when low (flashing red when excessively low).
- Adding a Laser Centerline Localizer (LCL) on the centerline under the aft landing area deck edge to provide precise centerline lineup cues at ranges of up to 10 nmi (18.5 km). This system provides an indication whether the aircraft is on centerline (amber light), to the right (red light), or to the left (green light). The lights flash to indicate the aircraft distance from centerline (steady near centerline, increasing flash rate with distance off centerline).

Control Laws

Three principal control law types have been explored in various U.S. Navy landing system programs to generate commands to null glidepath errors:

- Conventional control law. In the current AN/SPN-42/46 system, the pitch (or vertical rate) and bank commands are computed by processing the vertical and lateral errors through conventional digital shaping filters. The standard pitch command control law is of the following form:

$$\frac{\theta_c}{Z_e} = \left(\frac{K_c K_x}{K_p s + 1} \right) \left(\frac{1}{1 + \frac{s}{3.5} + \frac{s^2}{25}} \right) + \left(\left(1 + \frac{s}{3.9} \right) \left(1 + \frac{T_I K_x}{s} \right) + R_O s \left(T_I + \frac{T_D s - 2}{K_e s + 1} \right) \right)$$

Where s is the Laplace transform operator, θ_c is the pitch command, Z_e is the vertical error, and all the gains and time constants are constant except for K_x and R_O which are range scheduled. The gains and time constants are normally different for each aircraft type.

The vertical rate and bank command control laws are similar.

- State estimator control law. Simulator studies of various state estimator control laws have been conducted. Figure 2 shows a simplified version (the tested version combined the centerline range and lateral position axis) of the lateral control law implementations. A conventional ACLS aircraft autopilot was used. The expected aircraft lateral acceleration response was modeled with a second order filter for the bank command lateral axis. The expected aircraft vertical rate response was modeled with a third order filter for the pitch command vertical axis. Compared to a well optimized conventional control law, no significant improvements were obtained in the tradeoff between aircraft glidepath deviations due to turbulence and command perturbations due to landing system tracking errors (noise). However, significant improvements were obtained in the initial capture of glidepath. This is particularly important in the lateral axis where stability problems prevent the roll command control law gains from being lowered below a certain point. This can result in an unacceptable tradeoff between centerline capture performance and perturbations in roll command for landing system with large tracking errors. Figure 3 shows a large reduction in roll command perturbations with a state estimator control law which also has far superior centerline capture performance. Limited flight tests have been conducted with a state estimator control law in the Marine Air Traffic Control, Approach, and Landing System with promising results.
- Data fusion (blend or Kalman filters) control laws: As discussed in the following paragraph, significant control law advantages are obtained when additional sensors are used to measure aircraft and ship states (parameters). An INS is a highly desirable sensor due to its accuracy and the number of aircraft states measured. Various U.S. Navy programs have studied and utilized data fusion control laws. Figure 4 shows a generic data fusion control law. A flight test program conducted in the early 1970's with the Hovering Vehicle, Versatile, Automatic Control (HOVVAC) system in a UH-1N helicopter used blend filters in the aircraft autopilot for approaches with TACAN, prototype Microwave Landing Systems (MLS), and ACLS (reference 6). An ACLS vertical rate autopilot development program with F-4J and F-4S airplanes in the late 1970's (reference 7) used a blend filter in the autopilot for ACLS approaches and landings. An MLS development program in the late 1970's with an F-4J airplane (reference 8) used a blend filter in the autopilot for approaches with a prototype MLS. A blend filter was used in a ground control computer for automatic approaches with the Pioneer

Unmanned Air Vehicle in the late 1980's. A program underway with the Multi-Mode Receiver system in a F/A-18 airplane is designed to use blend filters in the aircraft autopilot for approaches with commercial Instrument Landing System (ILS), MLS, and ICLS.

Aircraft/Shipboard Landing System Integration

A variety of items need to be considered when implementing the data fusion blend (or Kalman) filters and control laws. How will the data fusion filters be reconfigured in the event of data dropouts? What sensors are available? How reliable are the sensors? How accurate are the sensors? How much data link capacity is required (number of parameters, resolution, update rate)? What are the transport delays?

As indicated in figure 5, utilizing sensor data in addition to the landing guidance data in a blend filter (data fusion) to provide a better estimate of the aircraft state has many advantages. Higher frequency error components of the landing system data can be greatly reduced in the blended data. However, low frequency or bias errors cannot always be eliminated. The improved blended data quality (reduced errors and time delays) sent to the cockpit displays will provide the pilot with better situational awareness. The pilot or automatic control gains can be increased to take advantage of the reduced errors and time delays in the blended data. Control law integrator terms can sometimes be reduced in gain or eliminated by utilizing the bias estimates from the blend filter. The improved control laws will result in better performance for either automatic or flight director approach. The improved pilot situational awareness and control performance should enable improved operational capabilities such as being able to operate with higher levels of turbulence, increased ship motion, or reduced visibility minimums. The data blend filter incorporated in the HOVVAC, F-4S ACLS vertical rate autopilot, and Pioneer Unmanned Air Vehicle (see above paragraph) all demonstrated greatly improved performance in turbulence.

As shown in figure 5, other issues besides data fusion need to be considered when attempting to obtain the most operational capability. More integrated displays of key monitor data and automated comparisons of related data will improve the pilot situational awareness. Flight director displays and more advanced flight control laws (and more responsive and stable aircraft responses) will improve the autopilot's or pilot's ability to follow the commanded flightpath over what can be achieved with basic situation displays and control laws. The ability to operate with higher ship motions and reduced visibility minimums are currently hampered by poor integration of the various landing systems and cockpit displays. One problem in this area is the differences in heave stabilization between the FLOLS and ACLS glide slopes. The FLOLS glide slope is stabilized for heave (except for the heave motion of the ship's center of motion). The ACLS glide slope is completely inertially stabilized until the final 12 sec of the approach where the autoland deck motion compensation (DMC) mode commands the aircraft to fly in phase with the heave of the touchdown point. Another problem is the inability of the ICLS to provide a monitor capability to touchdown due to misalignment with the ACLS commanded glide slope and differences in stabilization. The misalignment results because the ICLS glideslope cannot be corrected for the antenna to touchdown offset due to lack of DME and offset data in the airplane.

Monitoring of Approach and Landing Guidance Data

Monitoring of approach and landing guidance data is currently done by the pilot. He utilizes the heads-up display (HUD) and other cockpit displays to monitor the approach. The ACLS situation data (tadpole) and the ICLS situation data

(needles) are currently displayed simultaneously on the F/A-18 and F-14D HUD's; however, all other aircraft must switch between the two sources of landing guidance data. The pilot also monitors other guidance data such as range to touchdown, altitude, and rate of descent during the approach. Monitoring all of this data takes time and increases pilot workload.

Automating the monitoring of the landing guidance data would increase safety, reduce pilot workload, and increase pilot confidence. Implementation of an automatic monitor function requires changes in the uplink and downlink of the current data link system. If the comparisons of the various landing guidance data were done in the aircraft, an uplink data link change is required. If the comparisons of the various landing guidance data were done on the ship, a downlink data link change is required. The optimum solution would be to do the comparisons in both places to increase the redundancy. The comparison of the air-derived and ground-derived landing guidance data along with the other aircraft sensors would be done in a computer and alert both the pilot and the ground controller if errors got outside of specified limits.

Deck Motion Compensation versus Deck Motion Prediction versus Stabilization

As mentioned above, one current problem is that the FLOLS glide slope is stabilized for heave (except for the heave motion of the ship's center of motion), while the ACLS autoland DMC mode commands the aircraft to fly in phase with the ship's heave. The autoland DMC mode works very well and is able to minimize variations in touchdown position and vertical velocity relative to the moving flight deck. The FLOLS does not minimize variations in either of these parameters. However, although limited manned flight simulation efforts have been promising, there is some concern that a manual flight director DMC mode may not work as well or be acceptable to pilots. An alternative being considered is to continuously predict what the flight deck height will be when the aircraft arrives at touchdown. The commanded glide slope would be translated vertically starting at about 10 sec to terminate at the predicted touchdown point height. The accuracy of the predicted touchdown height would improve as the aircraft nears touchdown. However, a problem with this alternative is that the FLOLS would require the time to touchdown which requires that the range to touchdown be measured.

Alignment Between VLA and Electronic Landing Systems

Pilots have expressed a strong desire to have the FLOLS and electronic landing systems (ACLS and ICLS) aligned to within 0.15 deg (1/2 of a FLOLS "meatball") in order to maintain confidence in the various landing systems. The primary problem with maintaining this alignment accuracy aboard ship has been the utilization of various independent stabilization gyro systems for the different landing systems. The obvious solution (besides using more accurate gyro's) is to provide a central processor which takes inputs from all the gyro sources, compares them, and outputs the "best" gyro source to all the landing systems. Another problem is that the FLOLS is aligned to a deck reference plane while the electronic systems are aligned to the reference plane of the gyro systems.

FLIGHT CONTROLS

Automatic Flight Controls

The automatic flight control laws used in all of the current ACLS capable aircraft, except for the F/A-18, are pitch and bank command control laws similar to the one shown in figure 6. These control laws utilize aircraft attitude and attitude rate feedback terms summed with the data link commands to fly the aircraft to the commanded glide slope and centerline. This type

of control system is very susceptible to air turbulence and ship's burble. Typical shipboard longitudinal touchdown dispersions (1 sigma) range from 40 to 60 ft (12 to 18 m) and glide slope dispersions range from 3 to 6 ft (1 to 2 m) in moderate turbulence. These dispersions result in a significant number of approaches which are unacceptable to the pilot.

The F/A-18 incorporates the vertical rate (H-Dot) automatic flight control law shown in figure 7, which utilizes pitch rate and inertial vertical rate and acceleration feedback terms summed with the data link command to fly the aircraft to the commanded glide slope. This type of system performs very well in wind gusts, turbulence and burble due to the inertial feedbacks. Typical shipboard touchdown dispersions average 25 ft (7.5 m) for the F/A-18 and glidepath dispersions are minimal (1-2 ft (0.3-0.6 m)) in moderate turbulence. Simulations of other aircraft with this type of system have predicted performance equal to or better than the F/A-18 performance. Figure 8 shows A-6E simulation time histories of glidepath dispersions during step gusts with the pitch command autopilot and the H-Dot autopilot. As can be seen, the H-Dot autopilot nulls out the error much quicker than the pitch command autopilot.

Manual Flight Controls

The older manual flight control systems normally utilize a Stability Augmentation System (SAS) with attitude rate feedbacks in the various axes to augment the aircraft short period damping. These control systems typically result in high pilot workload and degraded glidepath performance in turbulence. Over the last 15 years, enhancements in the manual flight controls for approach and landing have been investigated and sometimes implemented in fleet airplanes.

The current F/A-18 airplane utilizes a Command Augmentation System with the following features:

- a. A longitudinal control law with angle of attack (AOA) and pitch rate feedbacks to help the pilot maintain the reference trim AOA through the pitch axis and to provide pitch damping.
- b. A lateral control law with roll rate feedback and a rudder to roll interconnect to provide roll damping and turn coordination.
- c. A directional control law with lateral acceleration and estimated sideslip rate (based on roll rate, yaw rate, lateral acceleration, and dynamic pressure) feedbacks to provide directional damping.

These control laws provide a substantial improvement in power approach flying qualities over previous Navy airplanes. Further information is contained in reference 10.

In the longitudinal axis, the two modes that have been evaluated in A-6 and F-14, simulations are a Pitch Command Augmentation System (PCAS) mode and a Precision Flightpath Control (PFPC) mode. In the lateral axis, a Roll Command Augmentation System (RCAS) mode has been evaluated.

The PCAS mode, shown in figure 9, consists of a blend of aircraft motion feedback terms which are compared to an augmented stick command term. The combination of the integrator in the stick command term with the pitch attitude term results in a pitch rate response proportional to stick displacement. The proportional part of the stick command term together with the mechanical path provide lead in the pitch rate response to stick displacement. The pitch rate term provides damping. The roll compensation term minimizes pitch attitude variations during turns. The RCAS mode, shown in figure 10,

is similar to the PCAS. The RCAS provides a roll rate response proportional to stick displacement.

The PFPC mode, shown in figure 11, consists of a blend of aircraft motion feedback terms which are compared to an augmented stick command term. The combination of the integrator in the stick command term with the flightpath term results in a flightpath rate response to stick displacement. The proportional part of the stick command term together with the mechanical path provide lead in the flightpath rate response to stick displacement. The pitch rate and either vertical or normal acceleration provide damping. The roll compensation term minimizes flightpath variations during turns. A more complete description of these enhanced flight control modes is contained in reference 11.

Pilot evaluations during the simulations have indicated significant preferences for these enhanced modes over the SAS currently flown in these aircraft. The combination of PFPC with RCAS has been the most preferred mode. Using the Cooper Harper Handling Qualities Rating Scale (HQR), pilots, on the average, rate this mode 2.0 points better than the current SAS. The HQR improvement is even more with higher turbulence levels.

Approach Power Compensator System

The Approach Power Compensator System (APCS) installed in U.S. Navy aircraft is designed to control airplane AOA and augment vertical flightpath control during all phases of the approach and landing by commanding the engine power setting. Typical current APCS control law designs include the following input terms:

- a. AOA for the primary feedback.
- b. Integral AOA to eliminate biases and to insure that the AOA will return to the commanded reference AOA.
- c. Normal acceleration to augment the flightpath damping.
- d. Elevator/stabilator position and pitch rate to provide a lead term for aircraft pitch maneuvers.
- e. Bank angle to provide a feed forward term to provide the steady state thrust required for aircraft bank maneuvers.

Separate APCS control laws are generally needed for pilot controlled and automatic approaches. Figure 12 shows a block diagram of the APCS used in the F/A-18 airplane.

A properly designed APCS will reduce pilot workload by enabling him to concentrate on making pitch corrections to control vertical flightpath instead of having to control both flightpath and AOA/airspeed. However, this pilot technique is different from the standard U.S. Navy pilot technique of making throttle corrections to control vertical flightpath and pitch corrections to control AOA/airspeed. Therefore, some pilot retraining is required to adapt to the technique required for APCS approaches. The best APCS is not necessarily the one with the tightest AOA control, but is the one with which the pilot has the best glide slope control while maintaining other parameters within an acceptable tolerance.

Simulation studies of various APCS control law improvements have been conducted in recent years with promising results. The main thrust of these studies has been to try to eliminate some of the compromises between performance in turbulence and performance during aircraft maneuvers. The following design approaches appear optimum:

- a. Design the APCS and longitudinal axis augmentation control laws to work together. A design which provides a linear flightpath or flightpath rate response to longitudinal stick inputs is probably the best.

- b. Design the longitudinal axis control laws to minimize flightpath deviations in turbulence by utilizing flightpath and vertical acceleration feedbacks.
- c. Optimize the APCS control law feedback terms to minimize flightpath deviations in turbulence. These terms include AOA, integral AOA, and normal or vertical acceleration.
- d. Optimize the APCS control law feed forward terms to provide the desired aircraft response to pilot commands. The APCS feed forward terms include those terms which can be used to calculate the thrust required during maneuvers and to compensate for the feedback terms. These terms might include pitch attitude, pitch rate, roll attitude, roll rate, vertical rate, airspeed, longitudinal control stick position, control surface positions, etc. The expected aircraft responses can be combined with the feedback terms to prevent the feedback terms from degrading the aircraft response to pilot commands.

AIRCRAFT DISPLAYS

Current aircraft approach and landing displays are normally presented to the pilot on the HUD, although some older aircraft still utilize mechanical displays. These displays generally consist of landing guidance situation data (displayed as needles), AOA data (indexer or "E" bracket), and other pertinent aircraft data such as attitudes, airspeed, altitude, and rate of descent. These displays have not been well optimized or integrated to reduce pilot workload or enhance pilot performance during approach and landing. The following paragraphs will discuss the development of integrated aircraft displays which reduce pilot workload and enhance performance. Additional information is contained in reference 11.

Situation Data

Figure 13 shows a generic HUD for approach and landing. The primary focal point on the HUD is the FPM, which shows the flightpath of the aircraft. The most used symbology on the HUD (situation symbol, AOA indexer, and flight director symbol) moves with respect to the FPM. The landing guidance situation data is currently displayed on the HUD as needles for the ICLS data and as a tadpole for the ACLS data. Both sets of data are required for monitor purposes for low visibility conditions. Both are currently displayed as angular data to touchdown with the display limits of ± 1.4 deg vertical and ± 6.0 deg lateral. The situation displays are very difficult to fly at ranges inside 1 nmi (1.85 km) when used as the primary source of guidance during precision approaches. This is primarily due to the fact that the sensitivity of the display continuously increases until it reaches infinity at touchdown. To the pilot, a certain correction at 1/2 nmi (.93 km) does not result in the same display change at 1/4 nmi (0.46 km). Figure 14 shows an approach, called course softening, to eliminate this display sensitivity problem. Course softening basically changes the display of the situation data from angular error to error in feet at some given range from touchdown. This display does two things: (1) the display sensitivity does not change during the last 4,000 ft (1,200 m) of the approach, and (2) the display immediately tells the pilot the glidepath error, in feet, during the last 4,000 ft (1,200 m) of the approach. Limited shorebased and shipboard flight tests have indicated that pilots prefer the course softened display; however, no extensive tests have been done to collect quantitative data.

A limited simulation evaluation has been conducted of the box symbol shown in figure 13 as an alternative to the current horizontal and vertical needles for the landing guidance situation data. The box symbol was implemented for two reasons: (1) it

was noted that, on the HUD, the pilot had to look at one needle with respect to the other needle to determine the magnitude of the error, and (2) when properly scaled, the box would immediately indicate to the pilot an unsafe condition. The current scaling of the box is half of the full scale deflection of the course softened display during the last 4,000 ft (1,200 m) of the approach. Preliminary evaluations indicate that most pilots prefer the box display to the needle display. The course softened box symbol shows great potential for providing the situation data required for approaches in 0/0 ceiling/visibility conditions.

Flightpath Marker Dynamics

The dynamics of the HUD FPM is critical in enabling the pilot to make aggressive corrections during approach and landing with minimal overshoots. Lead compensation or "quicken" of the FPM has been used to augment the FPM display. Without this augmentation, the pilot must compensate for the lags in the aircraft flightpath response, which results in increased pilot workload and degraded approach performance. In addition, during aggressive maneuvers, the display will leave the HUD field of view. The F/A-18 FPM display incorporates a pitch rate lead term as shown in figure 15. This lead term is not optimum for approach and landing and will have lags in it during maneuvers.

A much better lead compensation for the FPM during approach and landing is a washed-out pitch attitude lead term as shown in figure 15. This lead term should be optimized dependent on the type of control law augmentation as follows:

- a. For aircraft with a relatively weak level of flight control law augmentation (such as a pitch SAS) which requires the pilot to actively damp the pitch axis, the time constant of the wash-out filter should be made equal to the time it takes the aircraft AOA to settle back to the approach AOA. This relationship between AOA, pitch attitude and flightpath angle is derived in figure 16. In the short term, the "quicken" FPM moves like pitch and can be used by the pilot like a waterline symbol to damp pitch motions. During aggressive pitch maneuvers, the "quicken" FPM stays approximately stationary on the HUD and is less likely to leave the HUD field of view. The "quicken" FPM indicates where the aircraft flightpath will go once the short term AOA perturbation caused by a pitch maneuver is eliminated. The F-14D has this FPM washed-out pitch attitude lead compensation implemented during all flight regimes. For up and away flight, the wash-out filter time constant is scheduled with airspeed. Pilot comments during the flight test program indicate that the pilots significantly prefer the "quicken" FPM. The British have implemented a similar FPM lead term in the AV-8 Fast Jet HUD.
- b. For aircraft with a relatively strong level of flight control law augmentation (such as a flightpath control mode), the FPM lead term should be optimized to indicate where the flightpath angle would stabilize when the stick is returned to the detent. Figure 17 shows a time history, from an A-6 simulation, of a FPM lead display optimized with a flightpath control mode. As can be seen in figure 17, the FPM lead makes the FPM respond with an accurate rate response to stick inputs while the true flightpath angle takes about a second to start and stop in response to stick movements. When using the FPM with lead, the pilot doesn't have to compensate for the lag in the flightpath response; he can take his stick correction out when the FPM reaches the desired true flightpath angle.

Flight Director

The flight director, shown in figure 13 as a box with three dots, is a symbol on the HUD which "directs" the pilot to fly the aircraft so that the FPM symbol moves inside the flight director symbol. This will result in the aircraft capturing and following the landing system commanded glide slope and centerline. The horizontal deviation of the flight director symbol from the FPM represents the error between the commanded and actual bank angle and the vertical deviation represents the error between the commanded vertical rate and the actual vertical rate. The flight director symbol also rotates an amount corresponding to the error between the bank command and bank attitude to give an indication of the size of the bank correction required (primarily useful for following large bank commands during centerline captures). The vertical deviation is scaled on the HUD so that it gives an indication of the vertical flightpath angle correction required.

Various simulation studies have been conducted over the last 7 years utilizing A-6, F-14, and F/A-18 aircraft. Results of these studies show that pilot workload is drastically reduced and glidepath performance is significantly improved when using the flight director display. Figure 18 shows a comparison of typical simulation approaches in 1/2 nmi (0.93 km) visibility with and without the flight director when the final bearing is only known within 15 deg. As seen by the lateral traces, the pilot had a very hard time capturing the final bearing without having the flight director. Also, the glide slope control was not very good because more effort was required for capturing the final bearing. Pilots have commented that the flight director is by far the most impressive item that they have evaluated, even when compared to advanced flight control law modes.

The flight director implementation shown in figure 19 utilizes vertical rate and bank commands from the ACLS via the digital outputs of the Data Link and aircraft state parameters from the INS. Blend filters use aircraft vertical rate data from the ACLS (when available) and aircraft heading to eliminate the affect of biases by modifying the INS vertical rate and bank feedbacks respectively. This flight director scheme, without the vertical rate blend, is being implemented in the F-14D and will be flight tested in the April - May 1991 timeframe. Without the vertical rate data to eliminate biases in the INS, this implementation will probably only enable approaches to 100 ft/1/4 nmi (30 m/0.46 km). Another version of the flight director control algorithms which utilizes landing guidance data along with aircraft INS data has been evaluated in the F/A-18 simulation. This air-derived scheme requires auxiliary data from the ship, such as ship's heading and heave, and more accurate range data to enable approaches to touchdown. Implementation of a flight director scheme using the current AN/SPN-41 ICLS (no auxiliary data) along with TACAN range information is predicted to allow approaches to 200 ft/1/2 nmi (60 m/0.93 km). We are attempting to keep the integrators in the control laws set to zero. This is because the pilot may not aggressively try to keep the flight director centered until the final portion of the approach. When this is the case, the integrator can build up a large bias and cause a flightpath error when the pilot finally tries to aggressively capture the flight director. Figure 20 shows simulation approaches made with and without the integrator set to zero in the control laws when the pilot did not keep the flight director centered at range. As seen by the lateral traces, the integrator built up an error that drove the aircraft off of the centerline near touchdown.

Potential Flightpath Marker

The potential flightpath marker (PFFM) symbol is a cart to the right of the FPM on the HUD shown in figure 13. The vertical displacement of the PFFM from the FPM indicates the

aircraft's acceleration along the flightpath angle. The PFFM shows the flightpath angle at which steady state velocity could be achieved if the current thrust and drag are maintained. In the approach configuration, pilots can use the display as an early indication of the AOA bracket movement. Pilots have found the display very useful during manual throttle approaches and have commented that "the PFFM is a backup APCS". This display has been evaluated in the A-6 and F-14 simulations and flight tested in the F-14D. The PFFM is used by the F-14D pilots in all flight regimes. The PFFM is used by the pilot as an indication of required changes in engine power setting. Since the APCS commands the engine power setting, the PFFM is not displayed during approaches made with the APCS.

In-Close Range Information

The remaining area which requires further development is the presentation of range to touchdown. Currently, TACAN range to touchdown is displayed digitally in the lower right corner of the HUD as shown in figure 13. Since it is TACAN data, it is only accurate to within 1/2 nmi (0.93 km). This obviously is not good enough to support a QVO approach capability. The ACLS range data is accurate to within 3 m (10 ft), but is not currently uplinked to the aircraft. Some limited simulation work has been done to develop an in-close range display when more accurate range information is available in the aircraft, but more work is required. Another approach being looked at is displaying either forward looking infrared sensor or Millimeter-wave Radar images on the HUD along with the display data. This would give the pilot an actual outside-the-world presentation for low visibility conditions. This requires both the sensors and a Raster-scan HUD in the aircraft. It is unlikely that these sensors will be installed if they are dedicated solely to landing because of the limited space available for airborne equipment. Therefore, it is not envisioned that all the airwing aircraft will have these capabilities.

CONCLUDING REMARKS

All of the technology required to provide a safe and reliable all weather (severe weather and sea state, QVO ceiling/visibility) approach and landing capability (automatic and, possibly, manual) have been available for some time. This capability requires the integrated development of landing guidance systems, aircraft flight controls and displays, and higher capacity data links. Simulation studies over the last 15 years have proven the effectiveness of enhanced flight controls and displays in reducing pilot workload, improving glidepath performance, and enhancing situational awareness. The F/A-18 has proven the significant improvements in automatic approach capabilities with the H-Dot system. The equipment required are a landing guidance system accurate to touchdown with range data, and a high capacity data link with uplink and downlink capabilities to automatically monitor the landing guidance data.

REFERENCES

1. NAVELEX-0967-LP-304-4300, Operational Logistics Summary for AN/SPN-42A and AN/SPN-42-T4 Landing Control Central, of Jun 1979.
2. SHIPS-T-5368, AN/SPN-41 Specification, of Mar 1968.
3. NAVAIR 51-40ABA-8, Technical Manual - Installation, Service, Operation and Maintenance Instructions, Fresnel Lens Optical Landing System Mk 6, Mod 3.
4. NATC SA-61R-87, AV-8B Visual Landing Aid/Deck Lighting Shipboard Installation Evaluation; Varner, E., of Jul 1987.

5. NAEC Misc-51-OR723, Operation and Maintenance Instructions with Illustrated Parts Breakdown for Close In Approach Indicator 9CAI) Mod 2 Feasibility and Preproduction Models, of 10 Oct 1989.
6. NATC RW-48R-76, National Microwave Landing System (MLS) Supporting Development; Huff, R.W., Russell, R.A. and Zalesak, T.W., of Dec 1976.
7. NATC SA-30R-81, F-4S Airplane H-Dot Automatic Carrier Landing System Development and Evaluation; Huff, R.W. and Benjes, C. Lcdr, of Aug 1981.
8. NATC SA-59R-79, Navy High Performance Tactical Aircraft Compatibility with the National Microwave Landing System (MLS); Schust, Jr., A.P. and Miyashiro, S. K., of Dec 1979.
9. NATC SA-11R-75, "Investigation of Automatic Coupled Approaches; Guyther, J.R., Huff, R. W., Russell, R.A., and Zalesak, T. W., of Jun 1975.
10. McDonnell Douglas Corporation, F/A-18A Flight Control System Design Report, MDC A7813, of Dec 1982.
11. NATC SA-118R-66, A-6F Airplane Power Approach Systems Development and Analysis; Kessler, G. K. and Huff, R. W., of Apr 1987.

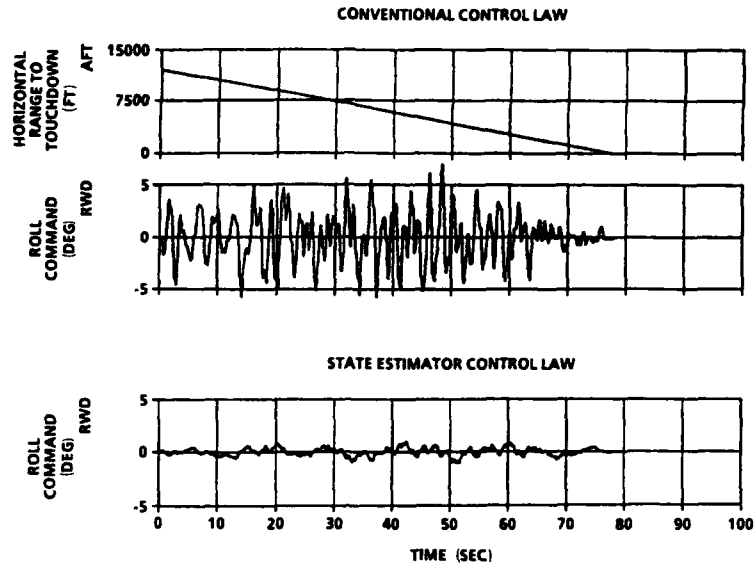


Figure 3
COMPARISON OF ROLL COMMAND PERTURBATIONS WITH CONVENTIONAL AND STATE ESTIMATOR CONTROL LAWS (A-6E AIRCRAFT SIMULATION)

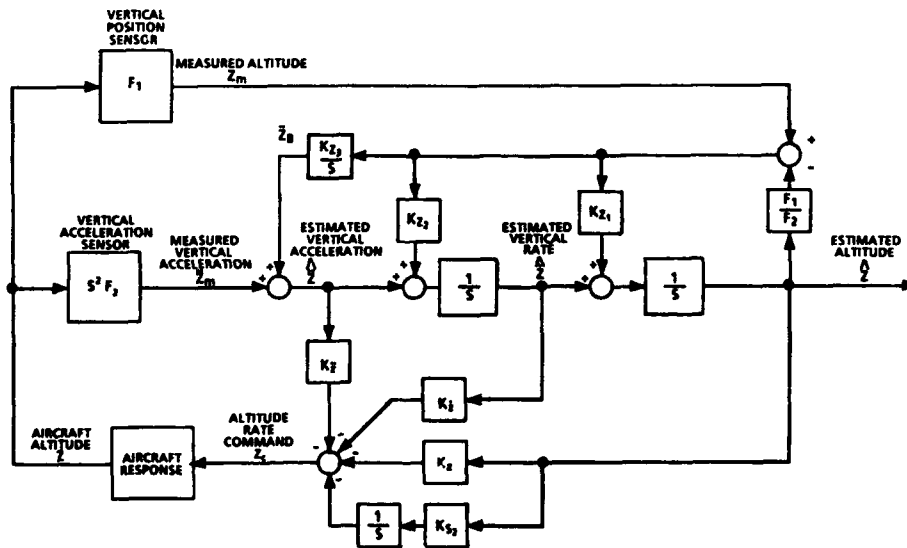


Figure 4
DATA FUSION CONTROL LAW BLOCK DIAGRAM

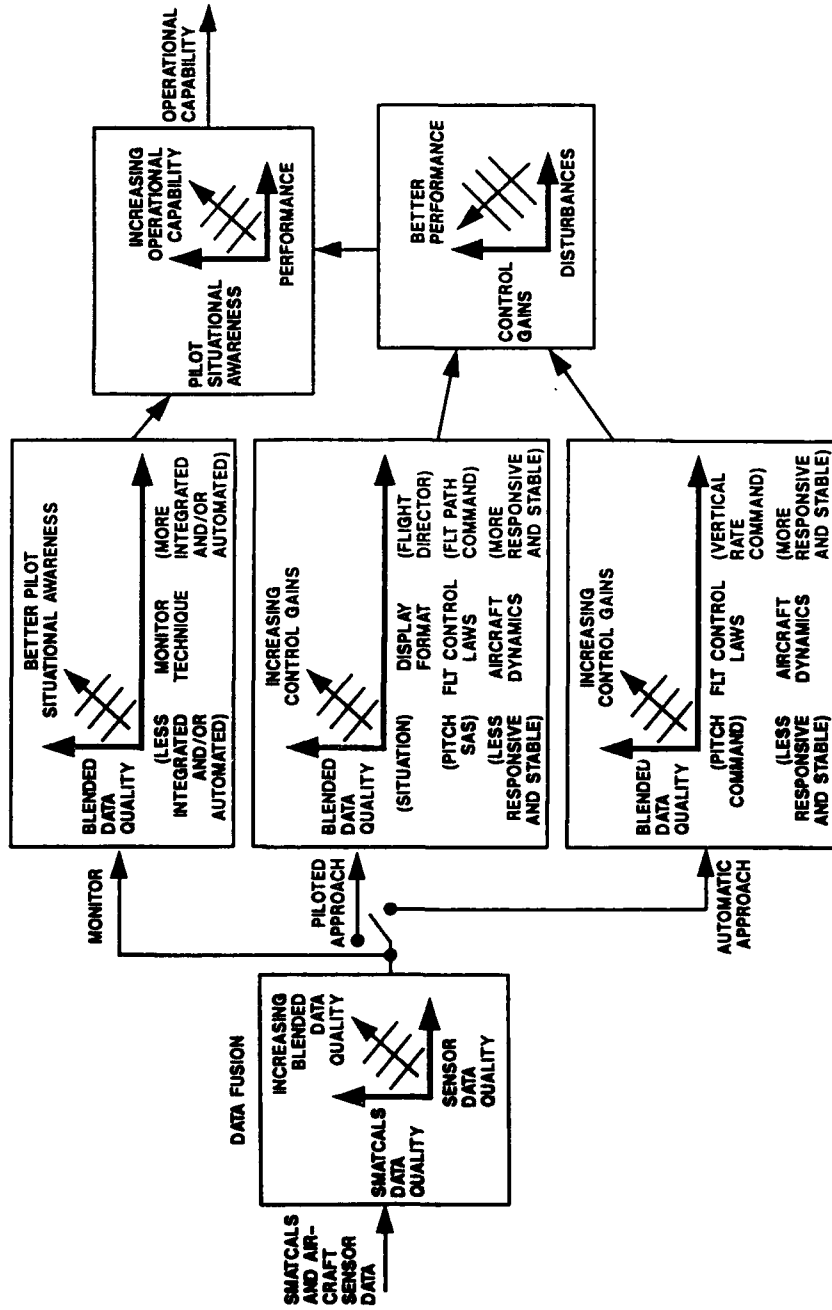


Figure 5
APPROACH AND LANDING TRADE-OFFS

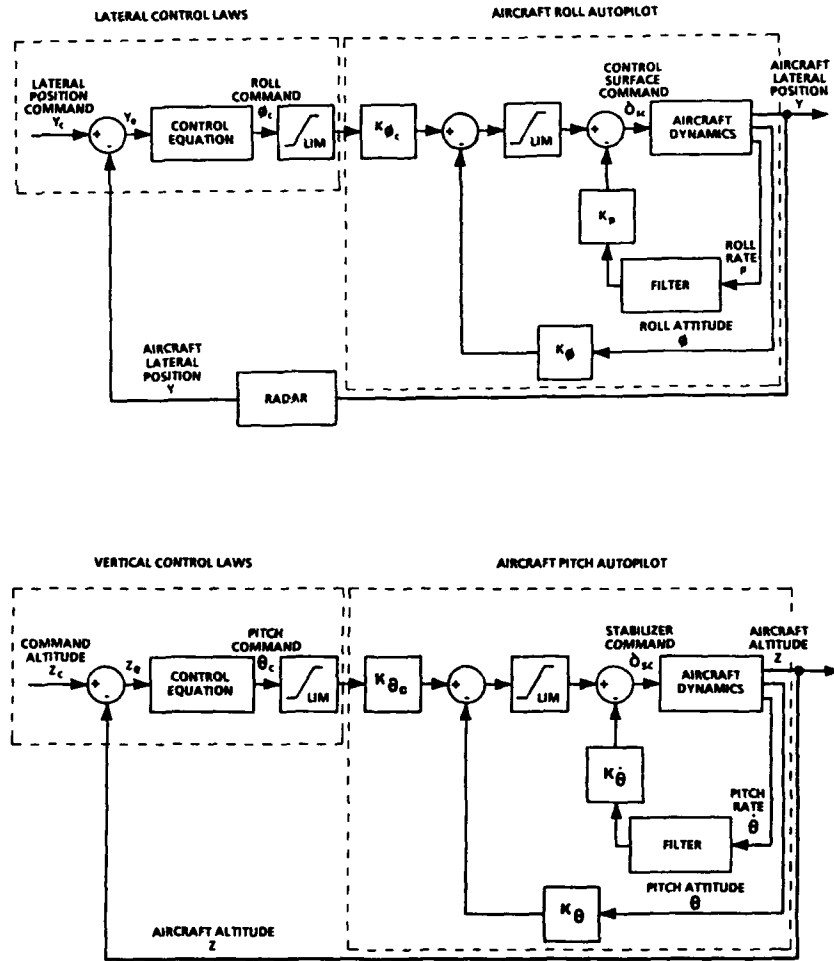


Figure 6
ACLS PITCH AND ROLL COMMAND AUTOPILOTS

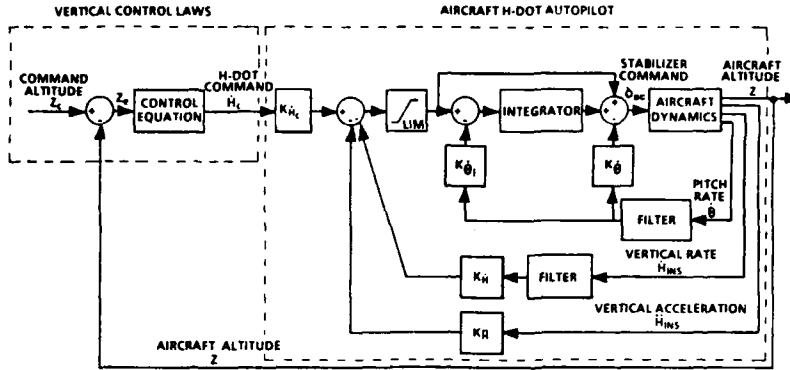


Figure 7
ACLS H-DOT AUTOPILOT

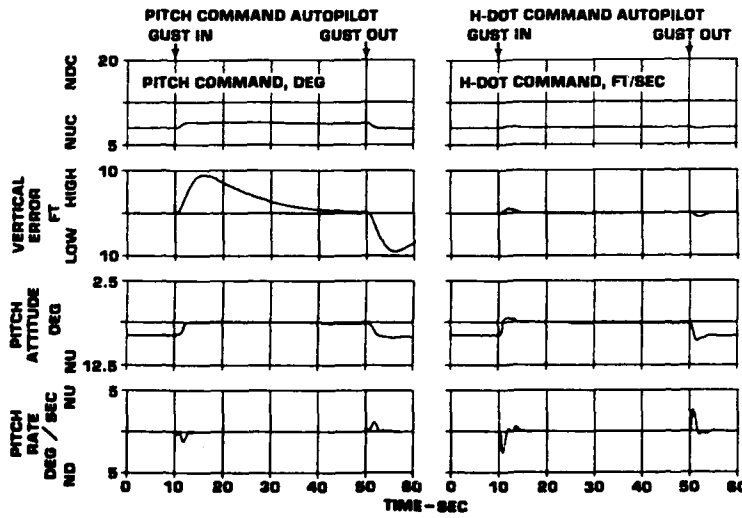


Figure 8
COMPARISON OF PITCH COMMAND AND H-DOT AUTOPILOT RESPONSE
TO 5 FT/SEC STEP UP GUST
(A-6E SIMULATION)

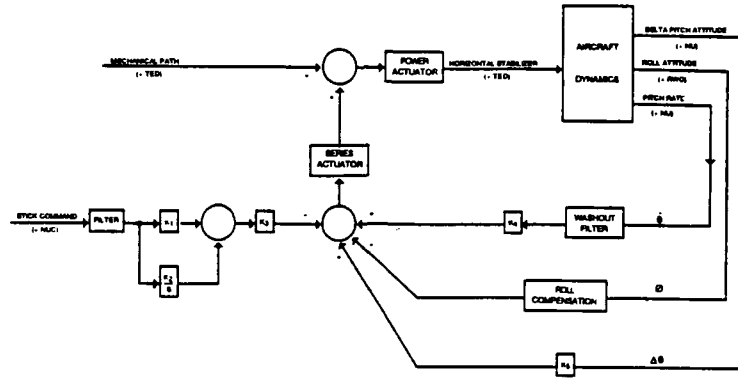


Figure 9
BLOCK DIAGRAM OF A-6F PCAS

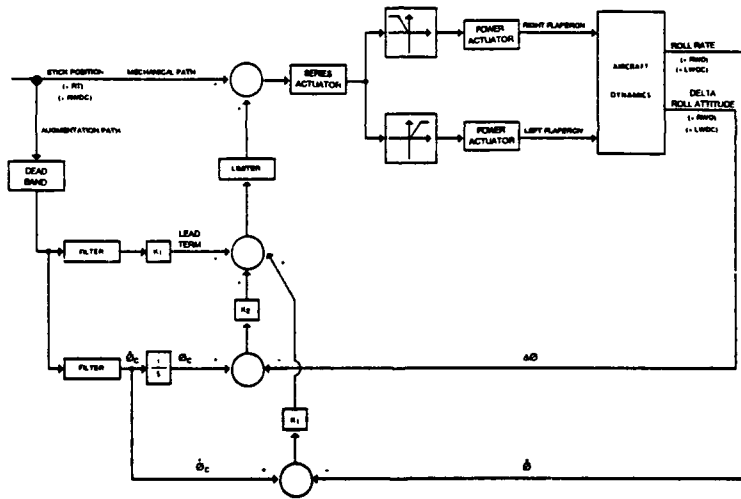


Figure 10
BLOCK DIAGRAM OF A-6F RCAS

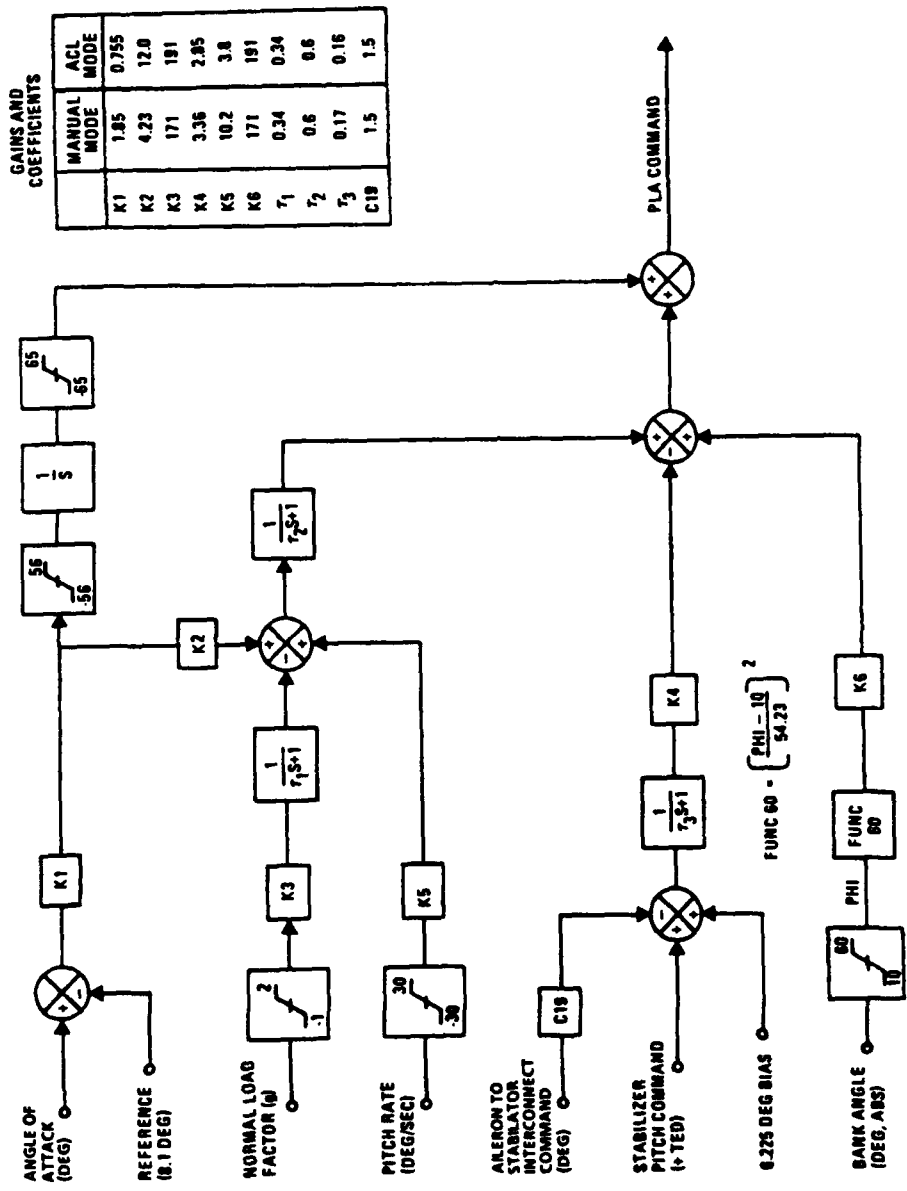
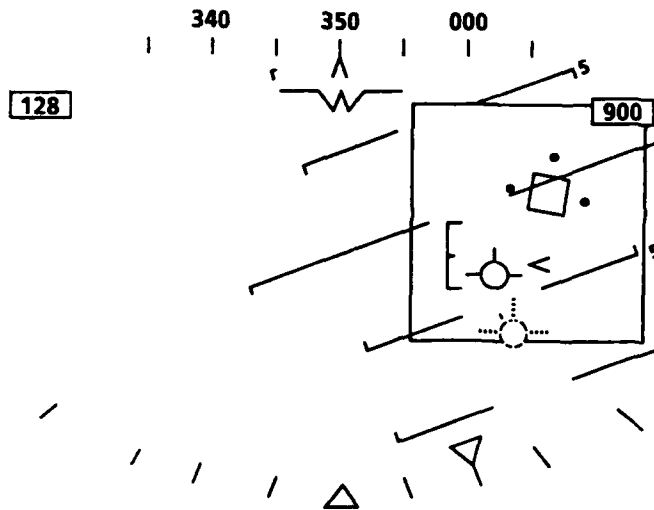


Figure 12
F/TF/A-18A AIRPLANE APCS CONTROL LAW DIAGRAM
(FUNCTIONAL EQUIVALENT)



**FLIGHT DIRECTOR
SYMBOL (FD)**



**FLIGHT PATH MARKER
(FPM)**



**LANDING SYSTEM
SITUATION DATA
NEEDLES**



**TRUE FLIGHT PATH
POSITION**



**LANDING SYSTEM
SITUATION DATA
BOX**



**POTENTIAL FLIGHT PATH
MARKER (PFPM)**



**LANDING SYSTEM
SITUATION DATA
TADPOLE**



AOA BRACKET



Figure 13
HUD

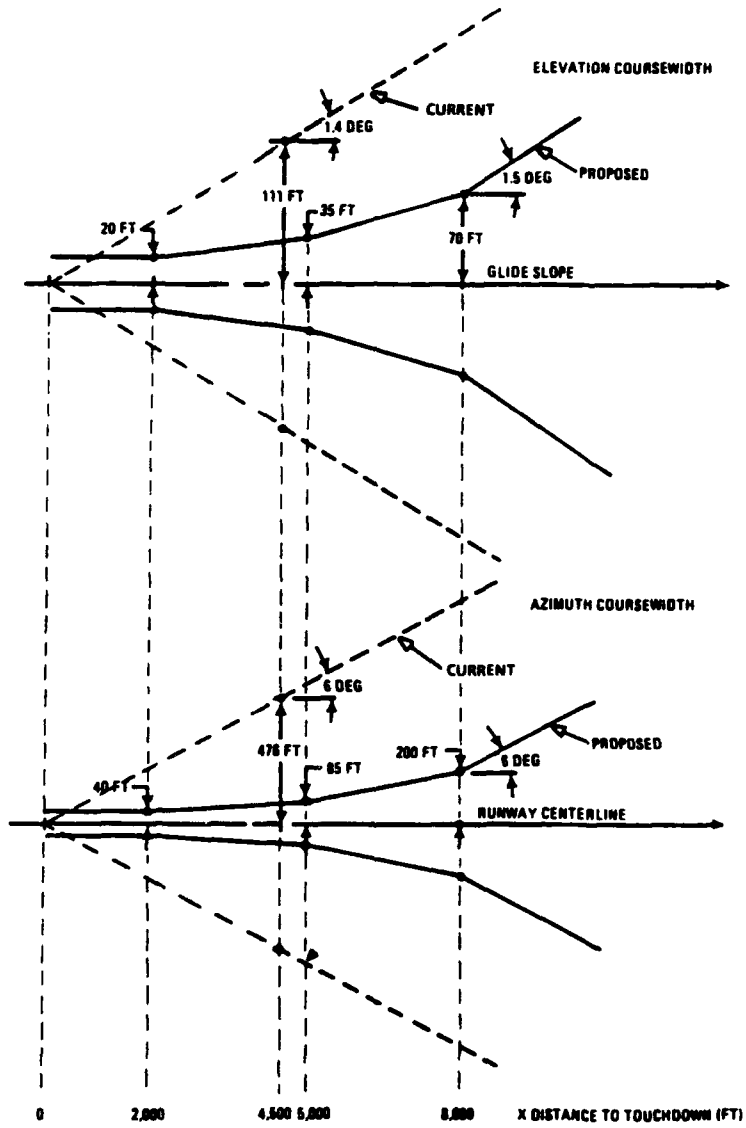


Figure 14
COURSE SOFTENING

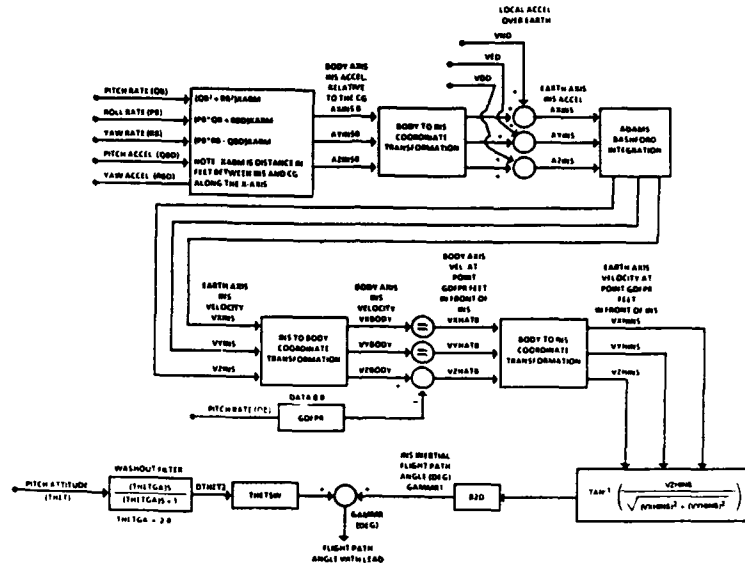


Figure 15
BLOCK DIAGRAM OF INS AND FLIGHT PATH ANGLE
WITH LEAD CALCULATIONS

θ : PITCH ANGLE

γ : FLIGHT PATH ANGLE

$\hat{\gamma}$: γ THAT AIRCRAFT WOULD ATTAIN AT CURRENT θ IF AOA REACHES AOA_{TRIM}

WASHOUT

$$AOA = \left(\frac{KB}{KB+1} \right) \theta + AOA_{TRIM} \quad \left\{ \text{WHEN AOA IS BEING CONTROL TO } AOA_{TRIM} \right.$$

$$\theta = \gamma + AOA = \gamma + \left[\left(\frac{KB}{KB+1} \right) \theta + AOA_{TRIM} \right]$$

$$\gamma = \theta - AOA \Rightarrow \hat{\gamma} = \theta - AOA_{TRIM}$$

$$\hat{\gamma} = \gamma + \left(\frac{KB}{KB+1} \right) \theta$$

Figure 16
PITCH ATTITUDE LEAD DERIVATION

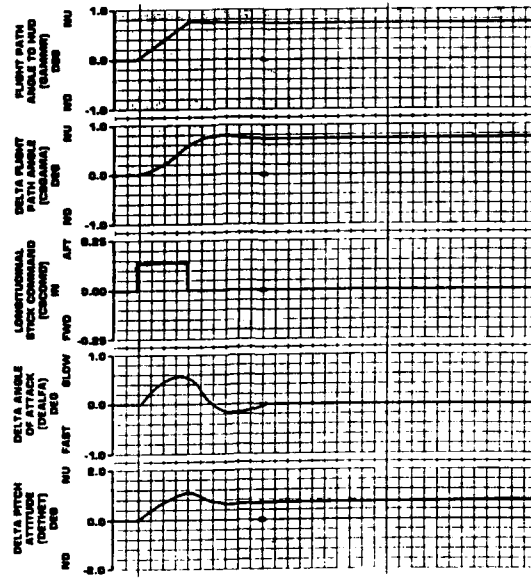


Figure 17
TIME HISTORY SHOWING LEAD COMPENSATION

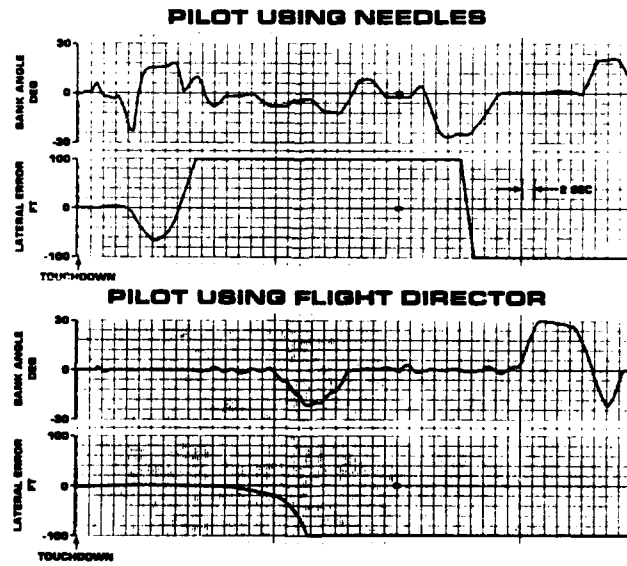


Figure 18
TIME HISTORY OF APPROACHES WITH AND WITHOUT FLIGHT DIRECTOR
(FINAL BEARING KNOWN WITHIN 15 DEG)

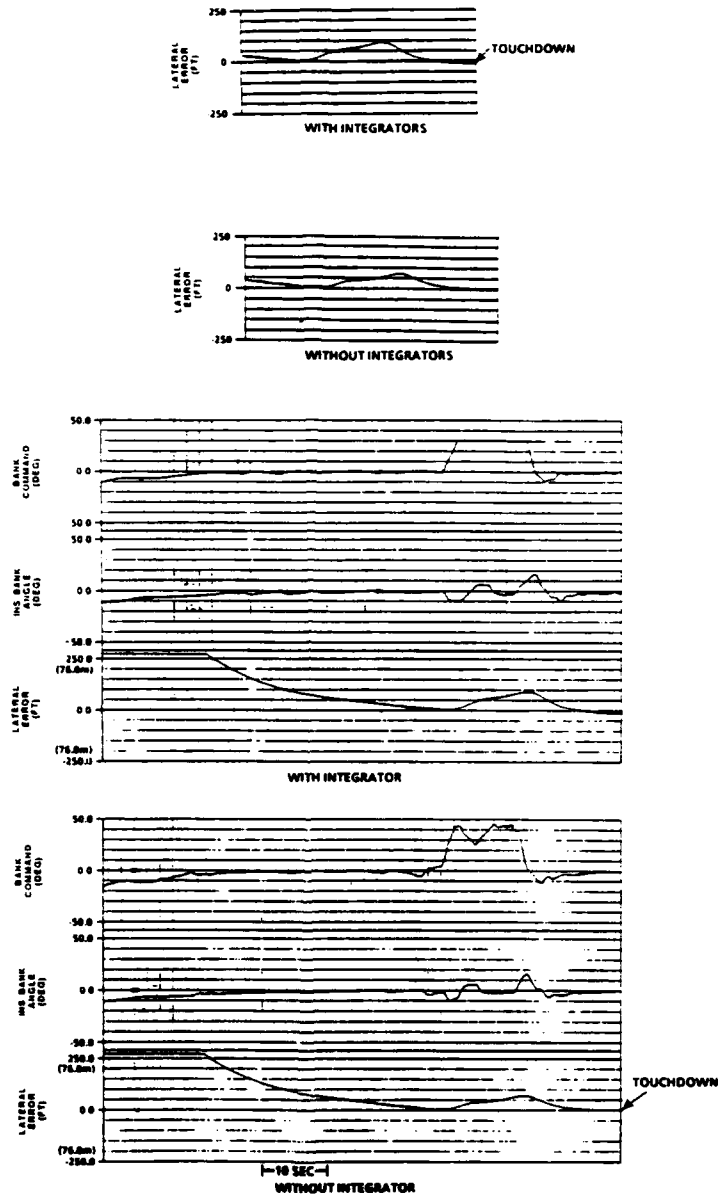


Figure 20
 COMPARISON OF FLIGHT DIRECTOR APPROACHES WITH
 AND WITHOUT THE INTEGRATORS IN THE CONTROL LAWS

INTEGRATION DU PILOTAGE ET DES SYSTEMES D'AIDE A L'APPONTAGE POUR LES OPERATIONS EMBARQUEES

par

B. Dang Vu, T. Le Moing et P. Costes*
Office National d'Etudes et de Recherches Aéronautiques
29 Avenue de la Division Leclerc
92322 Châtillon Cedex
France

RESUME

La disponibilité opérationnelle d'un porte-avions tient pour une grande part à l'aptitude de ses équipements et de son aviation embarquée à opérer dans un vaste domaine de conditions météorologiques et d'états de la mer. Pour repousser les limites d'emploi du futur porte-avions français pour l'appontage des avions, divers équipements ont été réalisés ou sont en cours de développement : système de tranquillisation des mouvements de plate-forme, système de prédiction des mouvements de plate-forme, système de mesure tous temps de la position relative de l'avion...

L'impact des progrès apportés par ces nouveaux systèmes sur les procédures d'appontage et sur le pilotage des avions embarqués futurs est présenté ici. Une nouvelle trajectoire d'appontage prenant en compte la prédiction du mouvement du porte-avions est proposée. La consigne de pente de descente constante actuellement appliquée est remplacée par une consigne de guidage où la pente de la trajectoire et la vitesse de l'avion sont modifiées en fonction de l'état de la plate-forme prévu à l'instant d'impact, de sorte à respecter les contraintes de l'appontage (garde à l'arrondi, vitesse à l'impact...). L'intégration des systèmes d'aide à l'appontage avec le système de commandes de vol de l'avion permet d'envisager, soit un mode d'appontage automatique, soit un mode de pilotage manuel avancé de type pilotage par objectifs. Les premiers résultats de simulation numérique donnent un aperçu de l'amélioration des performances de l'appontage en fonction de la précision de la prédiction du mouvement du porte-avions.

1. INTRODUCTION

La phase de vol correspondant à l'approche et à l'appontage sur un porte-avions est particulièrement critique. Elle exige de la part du pilote un pilotage très précis pour arriver à poser l'avion dans de bonnes conditions en un point situé à l'intérieur d'une zone très réduite et bien délimitée sur le pont du porte-avions, et ceci en dépit de perturbations diverses : mouvements de la plate-forme, sillage aérodynamique...

Pour permettre au pilote de réaliser l'approche, un certain nombre d'indications lui sont fournies à partir du porte-avions concernant la position de son avion par rapport à la trajectoire nominale de descente. En ce qui concerne la phase finale d'approche, ces indications sont à l'heure actuelle fournies principalement au travers d'un système optique d'aide à l'appontage composé d'un miroir et de signaux lumineux que le pilote doit maintenir alignés tout au long de l'approche. Le pilote est également aidé dans sa tâche par l'officier d'appontage qui peut lui dicter, le cas échéant, des consignes de pilotage depuis le pont du porte-avions.

Les techniques d'appontage actuelles sont bien éprouvées mais présentent toutefois encore des lacunes, notamment par mauvaise visibilité et par fort mouvement de plate-forme. Pour repousser les limites d'emploi du porte-avions pour l'appontage des avions, divers systèmes ont été réalisés ou sont en cours de développement pour le futur porte-avions français : système de tranquillisation des mouvements de plate-forme, système de prédiction des mouvements de plate-forme, systèmes de mesure tous temps de la position relative de l'avion... Par ailleurs, des progrès sont attendus dans les domaines de l'instrumentation et des commandes de vol des avions embarqués futurs (commandes de vol électriques).

L'impact des progrès apportés par ces nouveaux systèmes sur les procédures d'appontage et sur le pilotage de l'avion est présenté ici. Grâce à la prédiction du mouvement du porte-avions, de nouvelles trajectoires d'approche pourront être envisagées pour permettre aux avions d'apponter par fort mouvement de plate-forme. L'appontage automatique pourra être également envisagé grâce aux moyens de mesure tous temps de la position de l'avion par rapport au porte-avions. Les commandes de vol électriques des avions embarqués futurs autoriseront une mise en oeuvre plus aisée des modes de pilotage optimisés pour l'appontage. Ces nouvelles possibilités sont regroupées dans un concept intitulé "Intégration du Pilotage et des Aides à l'Appontage" (IPAP).

Cette communication est organisée en trois parties. La première présente une brève revue de l'état de l'art dans le domaine de l'appontage. Dans la deuxième partie on présente les problèmes spécifiques liés à la trajectoire de l'avion en phase d'approche. On propose ensuite une nouvelle procédure permettant aux avions d'apponter en cas de mer forte. La troisième partie présente un outil de simulation développé pour évaluer l'intérêt de cette procédure. On décrit les modèles retenus pour le mouvement du porte-avions, les perturbations associées, le mouvement de l'avion et le système intégré IPAP. A partir des résultats de simulation numérique, on analyse l'influence de la précision de la prédiction du mouvement du porte-avions sur les performances de l'appontage.

* Actuellement à l'Aéronautique-Divisions Hélicoptères, Marignane, France.

2. BREVE REVUE DE L'ETAT DE L'ART DE L'APPONTAGE

On décrit ci-après succinctement les systèmes d'aide à l'appontage actuellement en service, la procédure d'appontage actuelle, les systèmes IPAP existants et les équipements en cours de développement.

2.1 Systèmes d'aide à l'appontage sur les porte-avions français

Les aides à l'appontage sont constituées d'équipements embarqués sur le porte-avions d'une part, sur l'avion d'autre part [1].

A bord du porte-avions, quatre moyens sont actuellement utilisés : le radar d'appontage, l'optique, le système DALAS et la mire d'appontage.

- Le radar est utilisé par l'opérateur radar à bord du porte-avions pour guider l'avion en approche jusqu'à l'acquisition visuelle de l'optique, de nuit ou par mauvais temps.

- L'optique fournit au pilote la position relative de son avion par rapport à la pente idéale de descente. Le signal optique apparaît au pilote sous la forme d'une tâche lumineuse qu'il doit aligner avec des feux de référence (figure 1). Le réglage du plan de descente est obtenu en agissant sur l'inclinaison de l'optique et sur sa position en hauteur. Il existe une optique de secours commandée manuellement par l'officier d'appontage et utilisée dans certaines circonstances : panne de l'optique normale, mer forte, silence radio ...

- Le système DALAS (dispositif d'aide à l'appontage par laser) fournit à l'officier d'appontage la position de l'avion et sa tendance par rapport à l'axe idéal de descente, grâce à trois capteurs télémètre écartomètre laser, caméra IR et caméra TV (figure 2 [2]). Le rayon laser émis par l'émetteur récepteur laser est dirigé vers l'avion, qui le réfléchit vers le récepteur au moyen d'un rétro-rélecteur monté sur le train avant de l'avion.

- La mire d'appontage est un triangle isocèle peint sur l'extrémité avant de la piste oblique. Elle est utilisée par les pilotes d'appareils tels les Super-Etendard pour effectuer un appontage au viseur.

A bord de l'avion :

- Un indicateur d'incidence du type BIP (Badin Idrac-Perineau) fournit l'incidence de manière qualitative. C'est une boîte à trois lampes, rouge, vert et ambre ; le vert correspond à l'incidence optimale d'appontage, le rouge à une incidence plus forte et l'ambre à une incidence plus faible. Cet indicateur est également reproduit à l'extérieur de l'avion par une série de lampes montées sur le bras du train avant, de façon qu'il soit visible du porte-avions par l'officier d'appontage.

- Un viseur tête-haute fournit au pilote, sous la forme de réticules projetés à l'infini, les informations d'aide à l'appontage suivantes (figure 3) : horizon artificiel, repère de pente réglable, vecteur vitesse-air, repère d'incidence, échelle de cap, hauteur radio-sonde. Le pilote doit maintenir le repère de pente sur la base de la mire peinte sur le pont du porte-avions. Les réticules ayant une faible épaisseur, le moindre écart est détecté, la tenue de pente est plus précise.

2.2 Procédure d'appontage actuelle

Le circuit d'appontage à vue comporte un passage à tribord du porte-avions, un virage au vent, une phase avec vent arrière dont l'écartement par rapport au porte-avions dépend du type d'avion, puis un virage à partir du point 180° jusqu'à l'acquisition visuelle de l'optique, et enfin une phase d'approche proprement dite comportant elle-même une partie en virage et une ligne droite (figure 4). Il existe un autre type d'approche dite "CCA" (Centre de Contrôle d'Approche) où l'approche s'effectue dans l'axe de la piste d'appontage. Dans ce cas, l'avion est guidé par l'opérateur radar à bord du porte-avions jusqu'à l'acquisition visuelle de l'optique ; la cadence d'appontage des avions est alors plus lente. La phase finale s'effectue de façon identique au cas de l'appontage avec circuit.

L'approche finale s'effectue à taux de descente constant et à incidence constante. L'inclinaison de l'optique et la pente affichée au viseur doivent donc être réglées en fonction du vent mesuré sur le pont du porte-avions et en fonction de la vitesse d'approche de l'avion (figure 5).

Les techniques de pilotage de l'avion dépendent du système d'aide à l'appontage utilisé (optique ou viseur). Dans les deux cas, la tenue de pente est assurée par un pilotage coordonné au moteur et au manche. Le tableau 1, extrait de [1], résume les corrections à effectuer par le pilote appontant à l'optique, suivant les différents cas de présentation de l'avion en approche. Le tableau 2, également extrait de [1], montre une technique de pilotage au viseur assez empirique qui permet de corriger une trajectoire basse. L'officier d'appontage peut aussi intervenir par voie radio pour aider le pilote à recalculer l'avion sur la ligne d'approche, en lui dictant directement des consignes de pilotage. S'il juge que l'approche ne peut être rattrapée, l'officier d'appontage envoie l'ordre de remise des gaz. Par fort mouvement de plate-forme, la référence optique est donnée par l'optique de secours dont l'inclinaison est commandée manuellement par l'officier d'appontage. Celui-ci peut ainsi ajuster le plan de descente que doit suivre l'avion en fonction d'une certaine anticipation du mouvement du porte-avions.

2.3 Intégration du pilotage et des aides à l'appontage

Aucun système d'appontage intégré n'existe encore à l'heure actuelle sur les porte-avions français. Aux Etats-Unis, les porte-avions ont été équipés au début des années 70 d'un système d'appontage automatique comme le SPN-42. A partir des mesures de mouvement de la plate-forme, de mesures de direction et de vitesse du vent et de mesures radar du mouvement relatif de l'avion, le système génère puis transmet par voie UHF des ordres de tangage et de roulis à l'avion afin de le maintenir sur la trajectoire idéale d'approche. Ces ordres sont reçus par le système de liaison de données (data link) de l'avion puis exécutés au travers du système de pilotage automatique. Sur le plan opérationnel, l'appontage automatique a été utilisé par les pilotes essentiellement pour l'acquisition du système optique. Il n'a pas été utilisé pour la phase finale d'approche à cause de son manque de précision.

2.4 Systèmes en cours de développement

Un système de tranquillisation et de prédiction des mouvements de plate-forme (SATRAP) est en cours de développement pour le futur porte-avions français (PAN). Pour la fonction tranquillisation, le système utilise deux paires d'ailerons latéraux et une paire de gouvernails de direction pour réduire les mouvements d'embarquée, de roulis et de lacet. Le système utilise aussi un dispositif de transfert de masses pour réduire la gîte due au vent, aux déplacements de poids sur le pont et à la giration. Des essais à la mer sur une maquette à l'échelle 1/12 du PAN ont permis d'évaluer les performances obtenues [3]. Les mouvements de tangage et de pilonnement font intervenir des efforts considérables et leurs amplitudes ne peuvent pas être diminuées de manière significative. Des techniques de prédiction de ces mouvements ont été développées par l'ONERA/CERT [4,5] et le CAPCA [6]. Des essais à la mer sur une maquette de prédicteur installée sur le porte-avions FOCH ont permis d'évaluer les performances obtenues avec les deux méthodes.

En ce qui concerne les systèmes de poursuite et de mesure du mouvement relatif de l'avion, les informations élaborées par le système DALAS pourront être remontées vers l'avion par une liaison montante (datalink) pour permettre l'appontage automatique. Par ailleurs, des travaux sont en cours à la SAGEM pour la réalisation d'un système aéroporté permettant, grâce un traitement numérique de l'image du porte-avions, de déterminer la position relative de l'avion par rapport au porte-avions [7]. Dans ce cas, l'élaboration des ordres de guidage pour l'appontage automatique ne nécessitera pas de liaison montante. D'autre part, le mouvement absolu du porte-avions pourra être connu en combinant le mouvement relatif de l'avion avec le mouvement absolu donné par le système inertiel; ceci donnera la possibilité d'implanter sur l'avion les algorithmes de prédiction des mouvements du porte-avions.

Conclusion : Les techniques d'appontage actuelles sont bien éprouvées bien que des lacunes subsistent encore et que des progrès peuvent être réalisés :

- La procédure actuelle (plan de descente fixe) peut conduire, par mer forte, à des hauteurs de passage à l'arrondi dangereusement réduites; pour 1° de tangage, l'arrière du pont peut s'élever de 2 mètres, alors que la garde normale à l'arrondi est de 3 mètres. L'utilisation de la prédiction des mouvements de la plate-forme devrait permettre d'étendre les limites opérationnelles.

- Les corrections de trajectoire sont actuellement effectuées par le pilote à partir de références essentiellement visuelles. La mise au point de systèmes précis de mesure de position pouvant opérer dans des conditions météorologiques difficiles devrait permettre également d'étendre les limites opérationnelles avec l'appontage automatique.

- Le pilotage des avions embarqués actuels s'avère assez difficile car il nécessite une action coordonnée au moteur et à la profondeur. Les commandes de vol électriques des avions embarqués futurs autoriseront une implantation plus aisée des modes de pilotage optimisés pour l'appontage.

3. ETUDE PRELIMINAIRE DE L'APPONTAGE

On considère ici uniquement la phase finale de l'appontage (10 - 15 dernières secondes). Les contraintes spécifiques à l'appontage sont d'abord exprimées sous forme de relations mathématiques, puis appliquées sur un cas simplifié de mouvement du porte-avions limité au tangage pur. A partir d'une certaine amplitude du mouvement de la plate-forme, la procédure d'appontage actuelle ne permet plus de respecter les contraintes précédentes. Une nouvelle procédure utilisant la prédiction du mouvement du porte-avions est alors proposée.

3.1 Contraintes spécifiques de l'appontage

Elles peuvent se résumer ainsi : l'avion doit survoler la poupe du porte-avions à une hauteur de garde suffisante, toucher le pont en un point précis, avec une vitesse verticale à l'impact compatible avec la limite de structure du train d'atterrissage, et avec une vitesse d'entrée dans les brins compatible avec la résistance de la crosse et la capacité de dissipation d'énergie du système d'appontage.

La contrainte de garde à l'arrondi peut être exprimée par l'inégalité suivante sur la pente de la trajectoire (figure 6) :

$$\gamma_f < \gamma_{\text{garde}} = - (H_{\text{min}} + H_A \cdot H_B) / L_{AB}$$

- où : γ_f : pente relative de la trajectoire par rapport au porte-avions
 L_{AB} : distance arrondi-point d'impact visé (brin)
 H_{min} : hauteur de garde minimale de sécurité
 H_A : hauteur de l'arrondi à l'instant de passage de l'avion au droit de la poupe
 H_B : hauteur du brin à l'instant d'impact.

Rappelons que la pente relative γ_f est donnée par l'expression suivante :

$$\gamma_f = V_z / (V - V_{SP})$$

- où : V_z : vitesse verticale de l'avion
 V : vitesse aérodynamique de l'avion
 V_{SP} : vitesse du vent sur le pont du porte-avions.

La contrainte de vitesse verticale à l'impact peut être exprimée par l'inégalité suivante sur la pente de la trajectoire (figure 7) :

$$\gamma_f > \gamma_{\text{impact}} = - (V_{z\text{max}} + V_{zB}) / (V - V_{SP})$$

- où : $V_{z\text{max}}$: vitesse verticale relative maximale admissible
 V_{zB} : vitesse verticale du brin à l'instant d'impact.

Les contraintes de vitesse d'entrée dans les brins d'une part, de limite de décrochage de l'avion d'autre part peuvent être exprimées par les inégalités suivantes : $V_{\text{min}} < V < V_{\text{max}}$.

3.2 Exemple simplifié

L'exemple numérique présenté ci-après permet d'examiner l'évolution des contraintes précédentes en fonction de l'état de la mer. Le pont du porte-avions est supposé animé d'un mouvement de tangage sinusoïdal :

$$\theta = \theta_0 \sin \Omega t$$

- où : θ : assiette du porte-avions.

L'instant courant t est repéré par rapport à un instant origine $t=0$ pour lequel l'angle d'assiette est nul. Par la suite, t désignera plus particulièrement l'instant d'arrondi défini par le passage de l'avion au droit de la poupe du navire. La hauteur de l'arrondi H_A à l'instant d'arrondi et la hauteur du brin H_B à l'instant d'impact sont données par les expressions suivantes :

$$H_A = (L_{AB} + L_{BC}) \theta_0 \sin \Omega t$$

$$H_B = L_{BC} \theta_0 \sin \Omega (t + L_{AB} / (V - V_{SP}))$$

où : L_{AB} : distance arrondi-brin

L_{BC} : distance brin-centre de rotation du porte-avions.

Le déphasage entre H_A et H_B provient du temps mis par l'avion pour parcourir la distance séparant l'arrondi du brin.

La figure 8 présente l'évolution de la hauteur de l'arrondi H_A en fonction de l'instant d'arrondi pour une amplitude de tangage de $0,5^\circ$ (mer moyennement agitée). Les variations de la hauteur du brin H_B et de la vitesse verticale du brin V_{zB} sont également tracées. On en déduit les variations des pentes γ_{garde} et γ_{impact} correspondant respectivement aux contraintes de garde à l'arrondi et de vitesse verticale à l'impact. On constate que la pente de descente nominale de $-3,5^\circ$ satisfait les contraintes de l'appontage, quel que soit l'instant d'arrondi lorsque cet instant varie. Il existe cependant une dispersion du point d'impact égale à (voir figure 10) :

$$\Delta x = H_B / (\theta + \gamma_r)$$

Les valeurs maximales de la dispersion sont toutefois limitées pour une amplitude de tangage de $0,5^\circ$:

- appontage court : 2,53 m sur l'arrière brin 1,

- appontage long : 1,08 m sur l'arrière brin 2.

Pour une amplitude de tangage de 1° (mer agitée), on constate sur la figure 9 que le maintien de la pente de descente nominale de $-3,5^\circ$ ne permet plus de satisfaire la contrainte de garde à l'arrondi à certains intervalles de temps. Par ailleurs, les valeurs maximales de la dispersion du point d'impact sont :

- appontage court : 10,70 m sur l'arrière brin 1,

- appontage long : 3,52 m sur l'arrière brin 3.

La première valeur est trop importante et est le résultat d'une garde à l'arrondi insuffisante.

3.3 Etude de trajectoires respectant les contraintes

Pour satisfaire les contraintes de garde à l'arrondi et de précision de l'impact, il faut théoriquement rectifier la trajectoire de descente de l'avion en fonction de la position du porte-avions à l'instant d'arrondi. On admettra que les commandes de l'avion sur lesquelles on peut agir sont le facteur de charge longitudinal n_x et le facteur de charge normal n_z , ce qui suppose que les braquages des gouvernes sont pourvus de retours appropriés. L'efficacité de ces commandes est discutée ci-après.

Effet du facteur de charge longitudinal

En supposant que les positions du pont du porte-avions aux instants d'arrondi et d'impact puissent être prédites avec une bonne précision, on peut envisager de retarder ou d'avancer l'instant d'arrondi pour que l'appontage ait lieu lorsque toutes les contraintes de l'appontage sont satisfaites, en particulier la contrainte de garde à l'arrondi (figure 9). En supposant très grossièrement qu'une variation de vitesse ΔV puisse être appliquée instantanément à l'avion, la variation de l'instant d'arrondi qui en résulte est :

$$\Delta t_{go} = -t_{go} \Delta V / V_r$$

où : t_{go} : temps restant avant l'arrondi

$V_r = V - V_{SP}$: vitesse relative de l'avion par rapport au porte-avions.

Pour $t_{go}=10$ secondes, durée maximale supposée en-dessous de laquelle une bonne prédiction du mouvement du porte-avions peut être obtenue, et pour $\Delta V = \pm 5$ m/s, on trouve $\Delta t_{go} = \mp 1$ s. Ces valeurs sont évidemment théoriques car il faut tenir compte du temps de réponse de l'avion à une sollicitation de variation de poussée. Par ailleurs, compte tenu des contraintes sur l'incidence de l'avion et sur les conditions d'impact, les écarts tolérés sur la vitesse ΔV sont nettement plus faibles dans la réalité ; il en est de même pour la durée maximale de prédiction. L'effet d'une commande de facteur de charge longitudinal appliquée dans le but de satisfaire les contraintes de l'appontage est donc négligeable.

Effet du facteur de charge normal

Une action sur le facteur de charge normal permet de modifier la pente de l'avion. Or, l'examen de la figure 9 montre que pour satisfaire la contrainte de garde à l'arrondi, il suffit d'augmenter la pente de descente, dans les limites imposées par la contrainte de vitesse verticale à l'impact bien entendu. Le plan de descente doit, en outre, passer par le point visé sur le pont afin que la contrainte de précision à l'impact soit satisfaite. En supposant qu'une variation de facteur de charge normal puisse être appliquée instantanément à l'avion, on peut exprimer la durée minimale de la manoeuvre de changement de plan de descente en fonction de la variation de pente requise, de la dispersion du point d'impact à rattraper et du facteur de charge maximal dont est capable l'avion. On peut montrer que la commande de facteur de charge optimale est du type "bang-bang" et elle comporte une commutation comme indiquée sur la figure 11. La durée t_1 de la manoeuvre est exprimée ci-après dans le cas limite où l'instant d'arrondi coïncide avec l'instant où l'avion atteint le nouveau plan de descente [8] :

$$t_1 = 2z - \frac{(\gamma_{t1} - \gamma_{t0})V_t}{g\Delta n_{max}}$$

L'instant de commutation est donné par l'expression :

$$\tau = \sqrt{\frac{l}{g\Delta n_{zmax}} \left[\frac{V_r^2}{2g\Delta n_{zmax}} (\gamma_{r1} - \gamma_{r0})^2 - L_{AB}(\gamma_{r1} - \gamma_{r0}) + \gamma_{r0}\Delta x + L_{BC}\theta \right]}$$

où :

- θ : assiette du porte-avions à l'instant d'impact
- $\gamma_{r1} - \gamma_{r0}$: variation de pente requise
- Δx : dispersion du point d'impact à rattraper
- V_r : vitesse relative de l'avion
- L_{AB} : distance arrondi-brin
- L_{BC} : distance brin-centre de rotation
- Δn_{zmax} : facteur de charge maximal de l'avion.

La durée minimale de prédiction nécessaire pour le mouvement du porte-avions est alors donnée par :

$$t_{impact} = t_1 + L_{AB} / V_r$$

Pour une amplitude de tangage de 1° , une variation de pente requise de -1° et une dispersion d'impact à rattraper de -14 m, on trouve $t_1 = 2,80$ s et $t_{impact} = 3,86$ s en prenant $\Delta n_{zmax} = 0,2$. Ces valeurs ne sont qu'approchées car elles ne tiennent pas compte du temps de réponse du facteur de charge. En supposant qu'il est de l'ordre de la seconde, la valeur de t_{impact} reste toutefois dans les limites actuellement envisageables pour la durée de prédiction du mouvement du porte-avions.

3.4 Proposition d'une nouvelle procédure d'appontage

L'étude préliminaire précédente montre que la prédiction du mouvement du porte-avions permet théoriquement d'espérer d'étendre les limites d'emploi du porte-avions pour l'appontage par mer forte. On propose ci-après une nouvelle procédure d'appontage tenant compte de cette prédiction.

- Au début de la phase d'approche, la procédure actuelle est maintenue : pente de descente et vitesse constantes, réglées pour un vent sur le pont donné et une position moyenne nulle du pont.

- Quand l'avion se trouve à une distance à partir de laquelle la position et la vitesse du pont peuvent être prédites avec une bonne précision, la pente et la vitesse de l'avion sont modifiées de façon à satisfaire simultanément les quatre conditions suivantes :

- i) la hauteur de passage à l'arrondi doit être supérieure à une valeur minimale de sécurité,
- ii) la vitesse verticale à l'impact doit être inférieure à une valeur compatible avec la limite de structure du train d'atterrissage,
- iii) il doit y avoir impact effectif au point visé du pont,
- iv) la vitesse d'entrée dans les brins et l'incidence sont limitées.

- Au fur et à mesure que l'avion se rapproche du porte-avions, le plan de descente est réajusté en fonction d'une meilleure connaissance du mouvement du pont (prédiction sur un horizon de temps de plus en plus court).

La figure 12 présente dans le plan (V , γ) (vitesse aérodynamique, pente relative) la contrainte de garde à l'arrondi i) prédite à l'instant d'arrondi et la contrainte de vitesse verticale ii) prédite à l'instant d'impact. Les instants d'arrondi et d'impact dépendant de la distance et de la vitesse de l'avion, ces contraintes sont établies en tenant compte du temps mis par l'avion pour passer de la vitesse actuelle à une nouvelle vitesse désirée comprise entre les valeurs limites V_{min} et V_{max} (contraintes iv)). Le choix de la pente et de la vitesse "optimales" est obtenu en prenant à chaque instant les valeurs équidistantes aux limites correspondant aux trois contraintes i), ii) et iv) définies précédemment. Cette valeur centrale permet d'assurer une bonne robustesse vis-à-vis des erreurs : erreurs de prédiction du mouvement du porte-avions, erreur sur le temps restant avant l'arrondi, erreur de modèle de réponse en vitesse de l'avion...

Pour permettre la mise en oeuvre de cette nouvelle procédure avec les systèmes d'aide à l'appontage actuellement en service, il est nécessaire de régler l'optique en inclinaison pour chaque appontage, ce qui n'est pas réalisé à l'heure actuelle. Une autre solution envisageable est la présentation dans le viseur tête-haute d'une mire calculée prédite sur laquelle le pilote doit maintenir aligné un repère de pente mobile matérialisant la pente "optimale" γ^* comme le montre la figure 13.

4. OUTIL DE SIMULATION DEVELOPPE POUR L'ETUDE DE L'APPONTAGE

La nouvelle procédure d'appontage proposée se résume en une consigne de guidage dans laquelle la pente et la vitesse de l'avion sont modifiées en fonction du mouvement futur prédit du porte-avions. Cette consigne est appliquée à partir d'un instant en-dessous duquel on estime que la prédiction du mouvement du porte-avions est suffisamment fiable. On peut être tenté de choisir cet instant le plus tard possible car plus le temps restant est court, meilleure est la prédiction. Il faut cependant s'assurer que l'avion possède les capacités de manoeuvre suffisantes pour effectuer les ultimes corrections de trajectoire. Un outil de simulation a été développé pour permettre d'étudier ce compromis, grâce à des modèles plus affinés que ceux utilisés dans l'étude préliminaire précédente. Le programme est constitué de modules modélisant la dynamique des différents mobiles (porte-avions, avion), l'environnement (houle, sillage aérodynamique), le fonctionnement du système d'aide à l'appontage et son interface avec le système de commandes de vol de l'avion. Une première version simplifiée de ces modules est décrite ci-après.

4.1 Mouvement du porte-avions et perturbations associées

Modélisation du mouvement

La figure 14 présente la structure générale de la modélisation retenue pour le mouvement du porte-avions. On se limite pour l'instant aux mouvements de tangage et de pilonnement qui sont les plus importants. Le modèle est constitué d'un filtre houle et d'un filtre navire. Le filtre houle, excité par un bruit blanc gaussien fictif, permet de donner un spectre convenable au processus aléatoire que représente la hauteur d'eau. Le filtre navire permet de reproduire la dynamique du porte-avions en réponse à l'excitation que constitue la hauteur d'eau. Une représentation d'état du modèle est donnée par :

$$\begin{array}{ll} \text{Houle : } \dot{x}_h = A_h x_h + B_h \eta & x_h : \text{états de la houle} \\ h = C_h x_h & \eta : \text{bruit blanc} \\ & h : \text{hauteur d'eau} \\ \text{Navire : } \dot{x}_n = A_n x_n + B_n h & x_n : \text{états du navire} \\ y_n = C_n x_n & y_n : \text{sorties du navire (tangage et pilonnement)} \end{array}$$

Prédiction des mouvements de tangage et de pilonnement

Dans l'étude réalisée par l'ONERA/CERT [4], la méthode utilisée pour la prédiction comporte les étapes suivantes :

- Les paramètres du modèle, c'est-à-dire les coefficients des fonctions de transfert, sont d'abord identifiés à partir d'enregistrements de la hauteur d'eau et des variables du mouvement du porte-avions sur une certaine durée.

- La prédiction proprement dite est ensuite obtenue par intégration des équations du mouvement sans bruit de l'ensemble houle-porte-avions, à partir d'un état estimé initial. La qualité de la prédiction de l'état du porte-avions à l'instant d'appontage est améliorée au fur et à mesure du rapprochement de l'avion grâce à une réactualisation de l'instant initial et de l'état initial intervenant dans le modèle. L'instant initial est remplacé par l'instant courant et l'état du porte-avions est estimé par un filtre de Kalman utilisant les informations provenant de divers capteurs disponibles à bord.

Ces algorithmes de prédiction, qui ont été validés par des essais à la mer, seront implantés dans le programme de simulation dans une étape ultérieure. Il est retenu ici pour l'instant un modèle très simplifié de prédiction, défini de la manière suivante :

- Les modèles de houle et de porte-avions sont supposés parfaitement connus ; la prédiction est obtenue simplement en intégrant le modèle dynamique utilisé pour la simulation mais avec un bruit d'entrée nul.

- Les sorties des modèles de houle et de porte-avions sont supposées parfaitement connues également, ce qui permet une réactualisation parfaite du modèle de prédiction sans recourir à un filtre de Kalman (figure 15).

Avec ce modèle simplifié de prédicteur, la précision de prédiction à un instant final t_f est donnée par la variance des variables de sortie du navire :

$$\begin{array}{l} P = C Q(t_f) C^T \\ \text{avec } \dot{Q} = A Q + Q A^T + B B^T \\ A = \begin{bmatrix} A_h & 0 \\ B_n C_h & A_n \end{bmatrix} \quad B = [B_h \ 0]^T \quad C = [0 \ C_n] \end{array}$$

et $Q(t_0) = 0$ à chaque réactualisation du prédicteur.

Modélisation des perturbations atmosphériques

Les perturbations atmosphériques sont constituées essentiellement du sillage c'est-à-dire l'environnement modifié par la présence du porte-avions et ses superstructures. Le modèle de sillage retenu pour l'instant est celui de la norme américaine MIL-F-8785 C [9]. Des essais en soufflerie ont été réalisés récemment sur la maquette du futur porte-avions dans la soufflerie F1 de l'ONERA [10]. Les essais ont permis de déterminer le champ aérodynamique autour du porte-avions, notamment sur l'axe d'appontage, grâce à des sondages anémométriques et diverses techniques de visualisation. Ces résultats d'essai seront incorporés ultérieurement dans le modèle de sillage du programme de simulation.

4.2 Mouvement de l'avion et appontage intégré

Structure du guidage-pilotage

La figure 16 présente l'architecture proposée pour un système intégré de pilotage IPAP dont toutes les fonctions sont réalisées à bord de l'avion : mesure de la position relative de l'avion, calcul de la position absolue du porte-avions et prédiction de ses mouvements, élaboration des ordres de pilotage pour le système de commandes de vol soit par un pilote automatique, soit par un système de pilotage par objectifs. Il est à noter que le couplage du système d'aide à l'appontage avec le système de commandes de vol ne modifie pas la structure de ce dernier, ceci pour des raisons de stabilité et de sécurité du vol de l'avion. On considérera seulement le mode automatique car il se prête plus facilement aux études de simulation sur ordinateur ; l'étude des modes manuels nécessiterait l'emploi d'un simulateur de vol. On présente ci-après le système de pilotage de l'avion et le système de guidage en approche.

Pilotage et modèle de comportement

Pour les études d'intégration du guidage-pilotage concernant les phases spécifiques de vol d'un avion comme c'est le cas ici, il n'est souvent pas nécessaire de simuler un modèle complet de l'avion avec son aérodynamique, sa motorisation, ses capteurs, ses gouvernes et ses lois de commandes. Au stade d'une étude de faisabilité, il suffit d'un modèle dit de "comportement" ; l'avion naturel est supposé muni de retours appropriés de sorte que l'ensemble avion-capteurs-estimateur-système de commandes de vol possède une certaine dynamique proche de celle du modèle complet. On présente ci-après la démarche utilisée pour obtenir un modèle de comportement dont la dynamique peut être réglée par un nombre restreint de paramètres.

Les équations du mouvement de l'avion et les variables de sortie à contrôler peuvent être exprimées sous forme d'un système linéaire suivant :

$$\Delta \dot{x} = A \Delta x + B \Delta u$$

$$\Delta y = C \Delta x$$

avec x : vecteur d'état de l'avion
 u : vecteur de commande
 y : vecteur de sortie à contrôler.

Les composantes des vecteurs x et y sont :

$$x = (V \ \eta_k \ \alpha \ q \ p \ \beta \ r)^T$$

$$y = (V \ q^* \ p_a \ \beta)^T$$

où : V : vitesse aérodynamique

η_k : pente-sol

α : incidence

q : vitesse de tangage

p : vitesse de roulis

β : dérapage

r : vitesse de lacet

q^* : combinaison linéaire du facteur de charge normal et de la vitesse de tangage

p_a : vitesse de roulis aérodynamique.

Pour une loi de commande proportionnelle et intégrale de la forme :

$$\Delta u = K_1 \Delta x + K_2 \int_0^t (\Delta y - \Delta y_c) d\tau$$

où Δy_c représente les ordres du pilote, le mouvement de l'avion est régi par le système en boucle fermé suivant :

$$\frac{d}{dt} \begin{bmatrix} \Delta x \\ \int (\Delta y - \Delta y_c) \end{bmatrix} = \begin{bmatrix} A + BK_1 & BK_2 \\ C & 0 \end{bmatrix} \begin{bmatrix} \Delta x \\ \int (\Delta y - \Delta y_c) \end{bmatrix} + \begin{bmatrix} 0 \\ -1 \end{bmatrix} \Delta y_c$$

et les modes sont déterminés par les valeurs propres et les vecteurs propres du système. Par un choix approprié des matrices de gains K_1 et K_2 , il est possible de régler ces modes en limitant en même temps le nombre de paramètres du modèle. Ces paramètres sont les suivants :

- mode phyoïde : pulsation ω_{PH} et amortissement ζ_{PH}
- mode oscillation d'incidence : pulsation ω_{SP} et amortissement ζ_{SP}
- constante de temps τ_q du terme intégral $\int (q^* - q_c)$
- constante de temps en roulis τ_p
- mode roulis hollandais : pulsation ω_{DR} et amortissement ζ_{DR}
- constante de temps τ_β du terme intégral $\int (\beta - \beta_c)$

Les coefficients aérodynamiques nécessaires pour compléter le modèle sont $C_{x\alpha}$, $C_{z\alpha}$ et $C_{y\beta}$.

Guidage en approche

Les objectifs du guidage durant la phase d'approche sont la tenue de la vitesse aérodynamique affichée, la tenue de la pente désirée et le maintien de la position de la crosse d'appontage suivant une trajectoire passant par le brin visé. Les valeurs désirées sont constantes dans le cas d'une procédure classique d'appontage ; elles dépendent du mouvement prédit du porte-avions dans le cas de la nouvelle procédure proposée (cf. 3.4). Pour formuler la loi de pilotage, on utilise un vecteur d'état augmenté ΔX composé des variables d'état Δx du modèle de comportement de l'avion et des variables de position de l'avion par rapport au porte-avions. Le système linéarisé augmenté s'écrit :

$$\Delta \dot{X} = F \Delta X + G \Delta y_c$$

$$\Delta z = H \Delta X$$

avec $\Delta X = (\Delta x^T \ \Delta z_{cg} \ \Delta y_{cg})^T$

$$\Delta z = (\Delta V \ \Delta z_{crosse} \ \Delta \Phi \ \Delta y_{crosse})^T$$

où z_{cg} : altitude du centre de gravité de l'avion

y_{cg} : écart latéral du centre de gravité de l'avion par rapport à l'axe de la piste

V : vitesse aérodynamique

Φ : angle de roulis

z_{crosse} : altitude de la crosse

y_{crosse} : écart latéral de la crosse par rapport à l'axe de la piste.

L'objectif est de faire tendre le vecteur Δz vers une valeur désirée Δz_d correspondant à la trajectoire idéale d'approche. Il est à noter que le terme de pente désirée est contenu implicitement dans la composante Δz_{crosse} du vecteur Δz_d . On veut par ailleurs obtenir une erreur de régulation nulle en régime permanent sur la consigne Δz_d . Pour obtenir la commande optimale Δy_c^* , on utilise la méthode classique linéaire quadratique. On considère le système augmenté suivant :

$$\frac{d}{dt} \begin{bmatrix} \Delta \dot{X} \\ \Delta z - \Delta z_d \end{bmatrix} = \begin{bmatrix} F & 0 \\ H & 0 \end{bmatrix} \begin{bmatrix} \Delta \dot{X} \\ \Delta z - \Delta z_d \end{bmatrix} + \begin{bmatrix} G \\ 0 \end{bmatrix} \Delta y_c$$

La minimisation de l'indice de coût quadratique :

$$J = \int_0^{\infty} \left(\Delta \dot{X}^T \Delta z^T - \Delta z_d^T \right) Q \begin{bmatrix} \Delta \dot{X} \\ \Delta z - \Delta z_d \end{bmatrix} + \Delta y_c^T R \Delta y_c dt$$

donne la commande optimale :

$$\Delta y_c^* = G_1 \Delta \dot{X} + G_2 (\Delta z - \Delta z_d) .$$

Les matrices de gains G_1 et G_2 sont obtenues à partir de la résolution d'une équation algébrique de Riccati. L'expression de la commande s'écrit aussi sous forme intégrale :

$$\Delta y_c^* = \Delta y_c^*(0) + G_1 \Delta \dot{X} + G_2 \int_0^t (\Delta z - \Delta z_d) dt$$

4.3 Résultats de simulation

Données

Un modèle d'avion fictif a été utilisé ; les paramètres permettant de régler la dynamique du modèle (cf 4.2) sont fixés aux valeurs suivantes :

$$\omega_{PH} = \pi/3 \text{ rd/s} \quad \omega_{SP} = 2\pi \text{ rd/s} \quad \omega_{DR} = \pi \text{ rd/s} \quad \tau_q = 1,5 \text{ s} \quad \tau_\beta = 1,5 \text{ s} \quad \tau_p = 0,6 \text{ s}$$

$$\zeta_{PH} = 1 \quad \zeta_{SP} = 1 \quad \zeta_{DR} = 1$$

$$C_{x\alpha} = 0,5 \quad C_{z\alpha} = 3 \quad C_{y\beta} = -0,6 .$$

La vitesse aérodynamique nominale est égale à 70 m/s. Le vent sur le pont est égal à 15 m/s. Les valeurs limites de garde à l'arrondi et de vitesse verticale à l'impact sont respectivement $H_{\min} = 2,5$ m et $V_{z\max} = 5$ m/s. Les simulations sont effectuées pour des conditions de mer moyennement agitée.

Résultats

Les résultats temporels suivants sont présentés sur les figures 17 et 18 :

- les mouvements du porte-avions (traits pleins) et leur prédiction (traits pointillés). La hauteur de l'arrondi est prédite à l'instant de passage de l'avion au droit de la poupe. La hauteur du brin d'arrêt est prédite à l'instant d'impact prédit. La prédiction est réactualisée toutes les secondes.

- la pente désirée γ_f^* (trait plein) et les pentes γ_{garde} et γ_{impact} (traits mixtes) correspondant aux contraintes de garde à l'arrondi et de vitesse verticale à l'impact.

- l'écart d'altitude de la crosse par rapport à la consigne de pente désirée et par rapport au brin prédit à l'instant d'impact.

- la trajectoire de la crosse par rapport à la position du brin réel à l'instant d'impact (trait plein), la pente désirée γ_f^* issue du brin prédit (trait mixte) et les deux pentes γ_{garde} et γ_{impact} issues du brin réel (traits pointillés).

La figure 17 présente le cas où l'appontage est effectué avec la procédure actuelle c'est-à-dire avec une pente constante réglée pour la valeur du vent mesurée sur le pont. La figure 18 présente le cas où l'appontage est effectué en tenant compte de la prédiction du mouvement du porte-avions qui débute à 5 secondes avant l'impact. Dans le cas sans prédiction, la crosse de l'avion passe en-dessous de la hauteur minimale de sécurité à l'arrondi. Dans le cas avec prédiction, la crosse passe au-dessus de cette hauteur tandis que la vitesse verticale à l'impact reste dans les limites autorisées.

Afin d'obtenir des statistiques sur les performances de l'appontage en fonction du temps de prédiction, 100 simulations ont été effectuées pour des durées de prédiction variables de 0 à 10 secondes. Les tirages aléatoires ont porté sur les variables suivantes : états initiaux de l'avion, états initiaux du porte-avions, hauteur de la houle, turbulence atmosphérique. Les mesures de localisation sont supposées sans erreur.

La figure 19 présente l'évolution de la moyenne et de l'écart type des variables de performance suivantes, en fonction du temps de prédiction : hauteur à l'arrondi, vitesse verticale à l'impact, écart longitudinal du point d'impact par rapport au brin visé. La procédure d'appontage actuelle correspond sur la figure au temps de prédiction nul. Les moyennes semblent indépendantes du temps de prédiction; en effet le modèle de houle est excité par un bruit blanc gaussien de moyenne nulle. En revanche l'écart type sur la hauteur d'arrondi diminue à partir d'un temps de prédiction supérieur à 3 secondes et se stabilise à partir de 6 secondes. L'écart type de la vitesse verticale décroît dès que la prédiction est effective, et à partir d'une durée de prédiction supérieure à 2 secondes l'écart type se stabilise. L'écart type sur la position du point d'impact décroît jusqu'à un temps de prédiction voisin de 5 secondes, puis se stabilise pour des horizons de prédiction de plus longue durée.

La figure 20 présente les fonctions de répartition des variables précédentes, pour deux valeurs du temps de prédiction : 0 seconde (trait pointillé) et 5 secondes (trait plein). Pour la garde à l'arrondi, la fonction de répartition indique le nombre de simulations pour lesquelles la hauteur à l'arrondi est supérieure à une valeur donnée. Pour la vitesse verticale et l'écart longitudinal du point d'impact, les fonctions indiquent le nombre de simulations pour lesquelles ces variables sont inférieures à une valeur donnée. On constate que la prédiction permet de respecter dans la quasi-totalité des cas les contraintes de garde à l'arrondi et de vitesse verticale à l'impact. Le gain est très important dans les cas limites.

5. CONCLUSION

Les techniques d'appontage actuelles sont bien éprouvées bien que des lacunes subsistent encore et que des progrès peuvent être réalisés. Ainsi la procédure actuelle (plan de descente fixe) peut conduire, par mer forte, à des hauteurs de passage à l'arrondi dangereusement réduites; pour 1° de tangage, l'arrière du pont peut s'élever de 2 mètres alors que la garde normale à l'arrondi est de 3 mètres. Les travaux effectués sur la prédiction du mouvement du porte-avions suggèrent une procédure d'appontage qui permettrait d'espérer élargir les conditions d'emploi des avions embarqués. Il est proposé une nouvelle procédure consistant à élaborer en temps réel une consigne de guidage où la pente et la vitesse de l'avion sont modifiées en fonction du mouvement prédit du porte-avions aux instants d'arrondi et d'impact, afin de satisfaire à ces instants les contraintes de garde minimale à l'arrondi et de vitesse verticale maximale à l'impact. La consigne est réactualisée en fonction d'une prédiction qui s'améliore au fur et à mesure que l'avion se rapproche du porte-avions. Les toutes premières simulations simplifiées qui sont présentées ici confirment l'intérêt de la procédure proposée. En particulier, elles semblent indiquer que la durée minimale de prédiction nécessaire se situe dans les limites actuellement envisageables avec les méthodes de prédiction existantes. Cette nouvelle procédure d'appontage s'inscrit dans la perspective d'un nouveau concept de pilotage qui pourrait intégrer le système de commandes de vol avec les systèmes futurs d'aide à l'appontage. L'étude se poursuit actuellement avec la prise en compte de modèles plus réalistes dans le programme de simulation développé à cet effet.

REFERENCES

- (1) "Règlement d'appontage. Instruction permanente", Marine Nationale, Commandement de l'Aviation Embarquée et du Groupe des Porte-Avions, Juillet 1981.
- (2) "Dispositif d'aide à l'appontage par laser. Principes généraux", CSEE, Novembre 1987.
- (3) J.P. Jung, G. Hardier, "Stabilisation des mouvements de plate-forme et techniques de ralliement de cap à gîte minimum pour le futur porte-avions nucléaire", Mémoire ATMA, Session 1991.
- (4) J.P. Jung, G. Hardier, "Modélisation et prédiction des mouvements de tangage et de pilonnement d'un porte-avions nucléaire", rapport technique ONERA/CERT n°317390, Décembre 1984.
- (5) J.P. Jung, G. Hardier, "Prédiction des mouvements de plate-forme d'un porte-avions. Premiers résultats d'essais", note technique ONERA/CERT n°142190, Septembre 1990.
- (6) S. Sifredi, M.A. Grandclement, J.P. Puy, "Prédiction de mouvements de plate-forme à l'aide d'algorithmes ayant une structure de treillis", mémoire ATMA, Session 1987.
- (7) M.Y. Le Guilloux, R. Feuilloy, "Guidage automatique lors de l'appontage par traitement d'image embarqué", AGARD FMP, Aircraft/Ship Operations, 20-23 Mai 1991, Seville.
- (8) B. Dang Vu, P. Costes, "Etude préliminaire de l'intégration du pilotage et des aides à l'appontage", rapport technique ONERA n°13/5158SY, Juin 1990.
- (9) "Military Specifications, Flying Qualities of Piloted Airplanes", MIL-F-8785C, November 1980.
- (10) C. Chatelard, J.C. Raynal, "Essai à F1/CFM de la maquette au 1/100^e du PAN", procès verbal ONERA n°118394, Novembre 1988.

Tableau 1

CORRECTIONS DE PILOTAGE
APPONTAGE A L'OPTIQUE

MIROIR	R V A	DO NUT (Sens de l'écart à droite)	1ère CORRECTION	2ème CORRECTION
—●—	○ ● ○	○	Diminuer le régime	Reprendre l'assiette
—●—	○ ● ○	○	Augmenter le régime	Reprendre l'assiette
—●—	○ ● ○	○	Diminuer le régime	Prendre l'assiette
—●—	○ ● ○	○	Augmenter le régime	Prendre l'assiette
—●—	○ ● ○	○	Réduire franchement le régime	Augmenter légèrement l'assiette en rajustant le régime
—●—	○ ● ○	○	Diminuer l'assiette	Augmenter le régime
—●—	○ ● ○	○	Augmenter l'assiette	Ajouter un peu de moteur
—●—	○ ● ○	○	Mettre beaucoup de moteur	Diminuer l'assiette

Tableau 2

CORRECTIONS DE PILOTAGE
APPONTAGE AU VISEUR



Écart détecté



Par une correction au manche et au moteur, l'ensemble vecteur vitesse et parenthèse est ramené du double de l'écart détecté.



Le repère de pente remonte doucement vers le bas de la mire



Quand le repère de pente est revenu à la bonne hauteur, réduire la correction de moteur, ce qui doit constituer une nouvelle position moyenne.

Figure 1

APPONTAGE
Optique

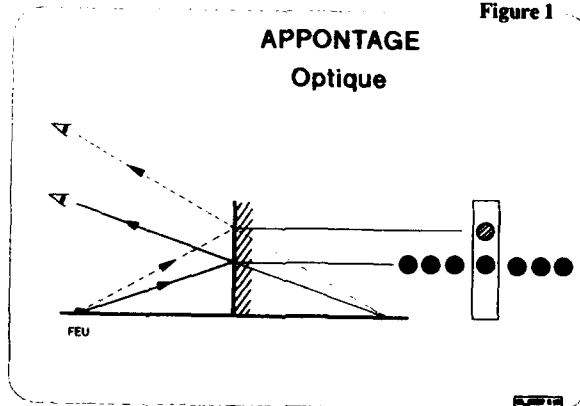


Figure 2

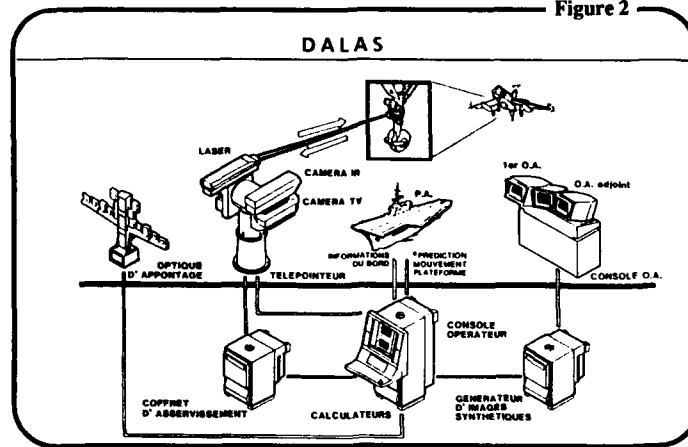


Figure 3

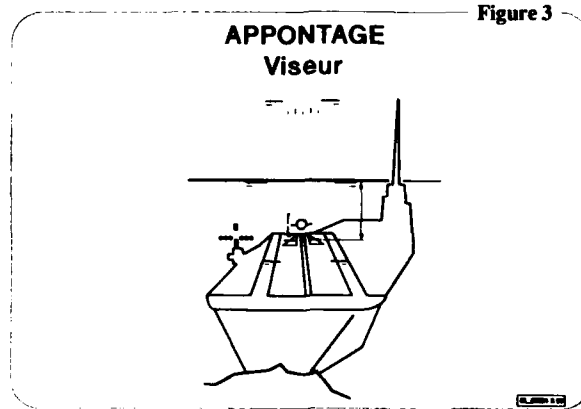


Figure 4

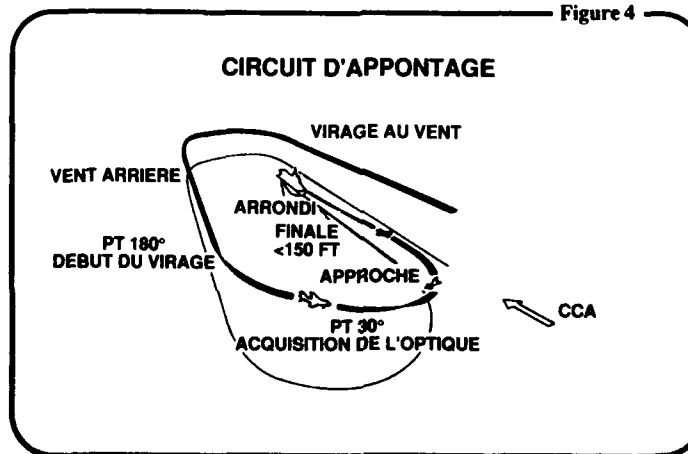


Figure 5

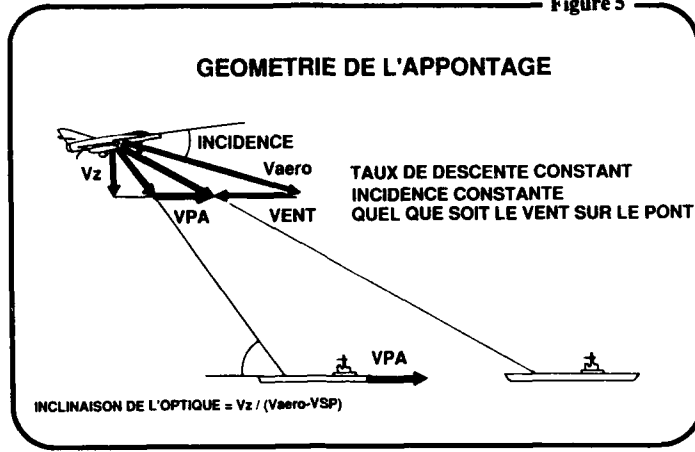


Figure 6

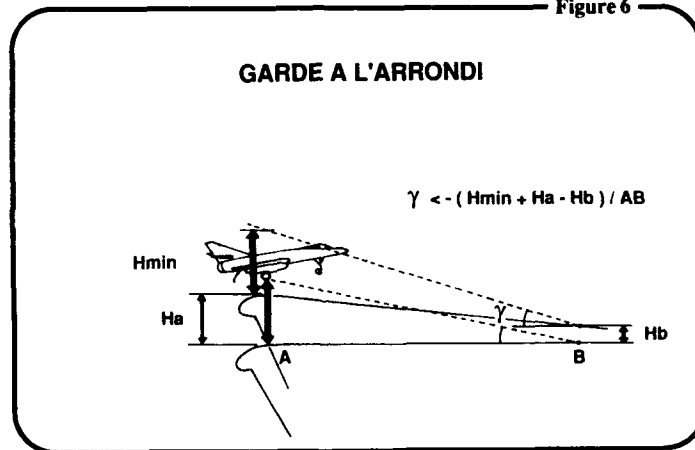


Figure 7

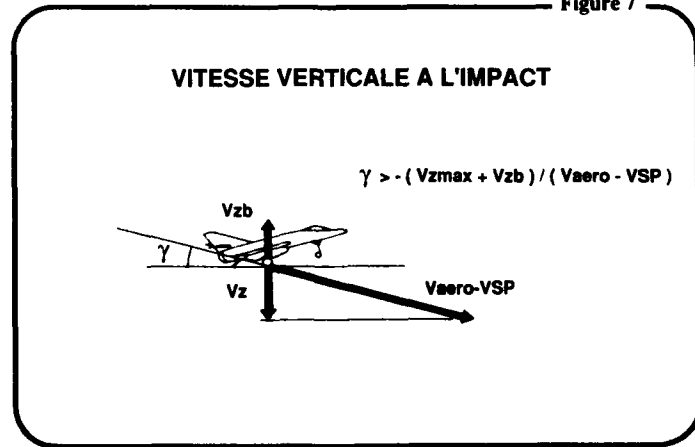


Figure 8

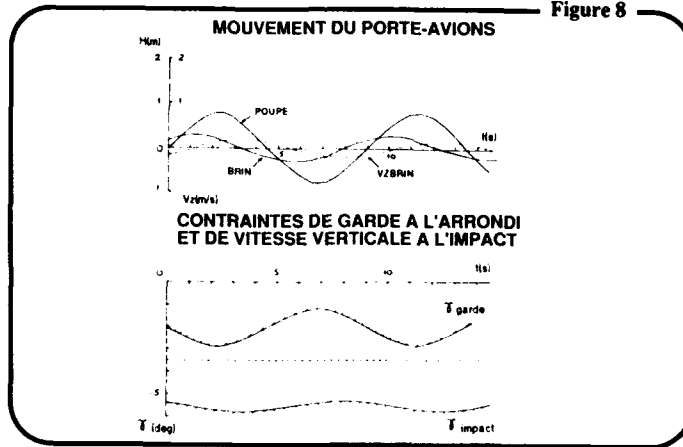


Figure 9

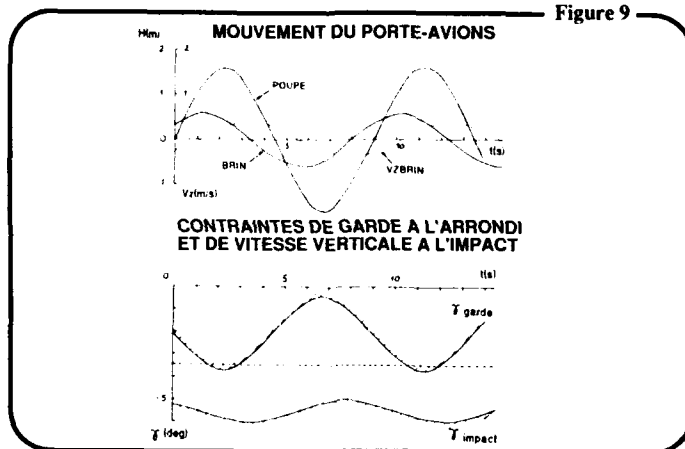


Figure 10

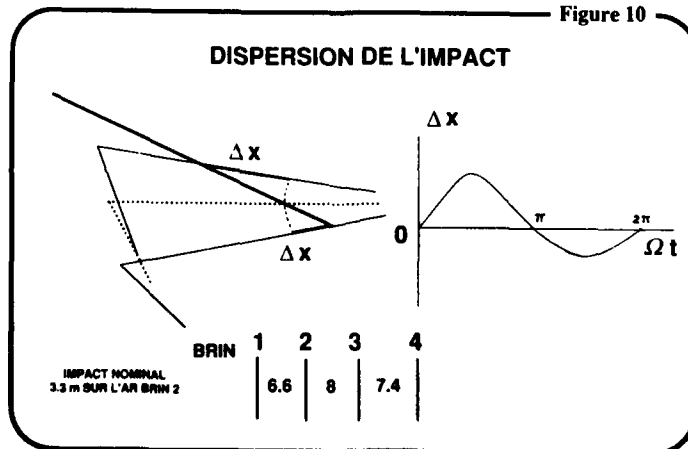


Figure 11

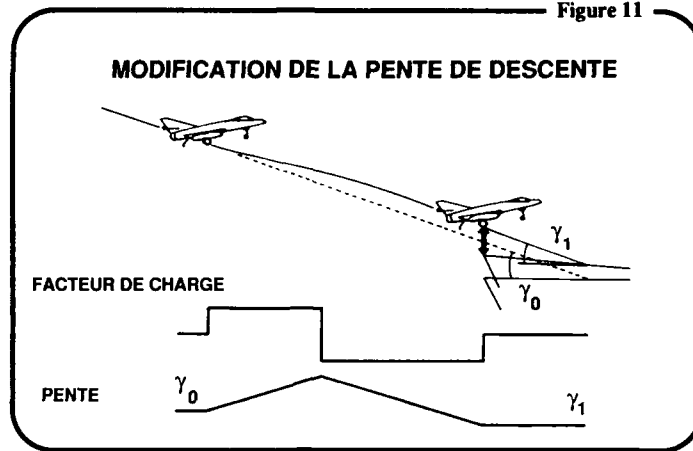


Figure 12

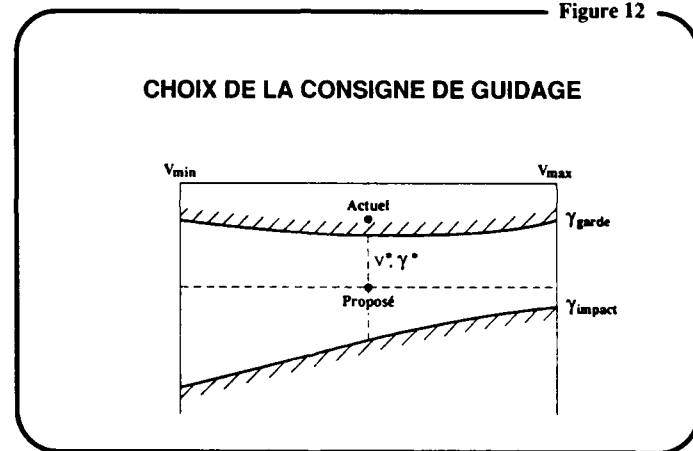


Figure 13

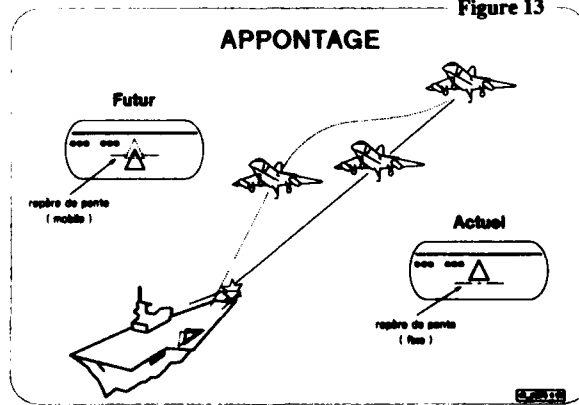


Figure 14

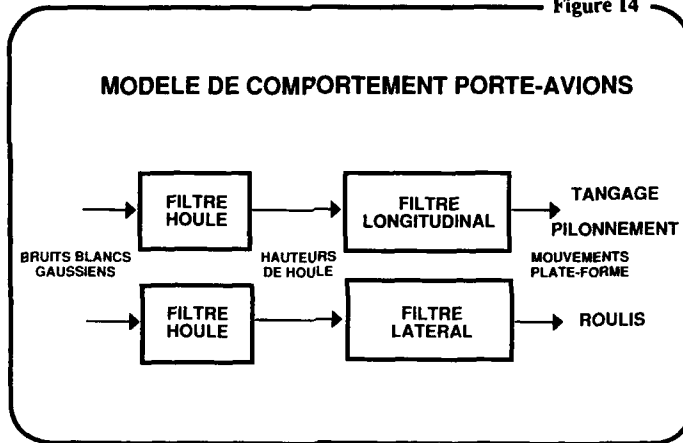


Figure 15

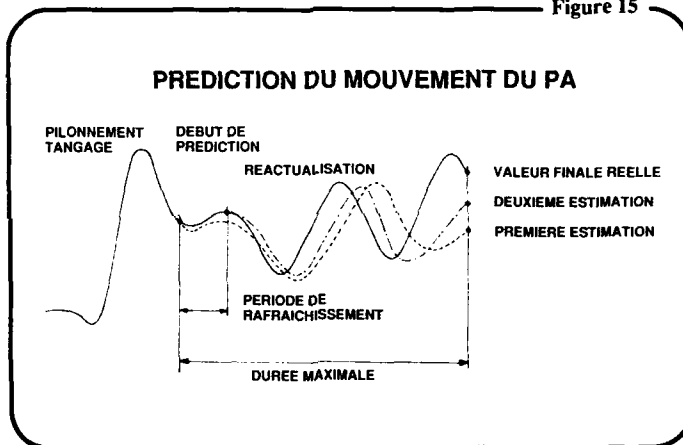
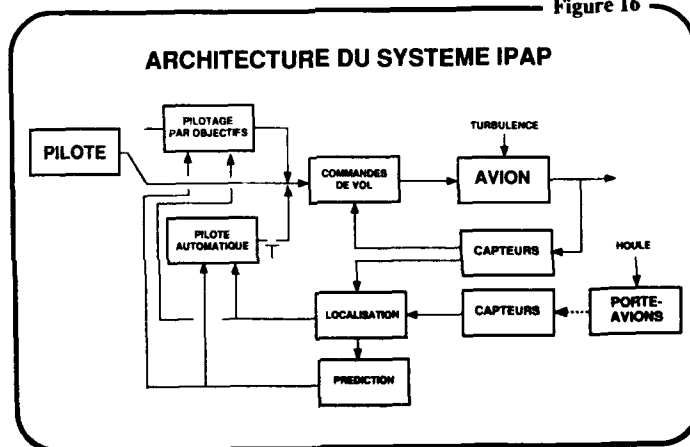


Figure 16



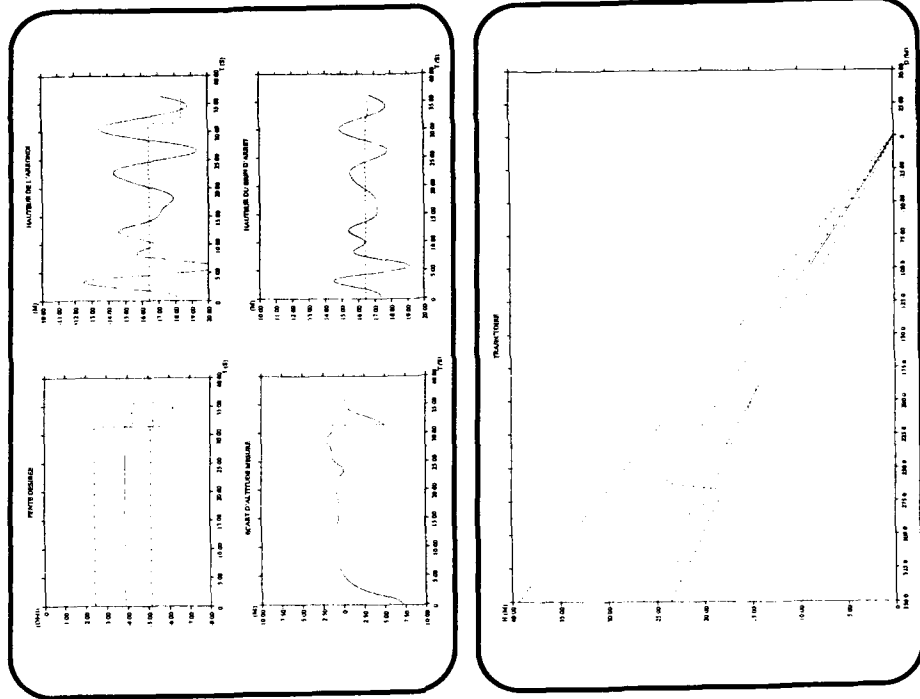


Figure 17 Sans prédiction du mouvement

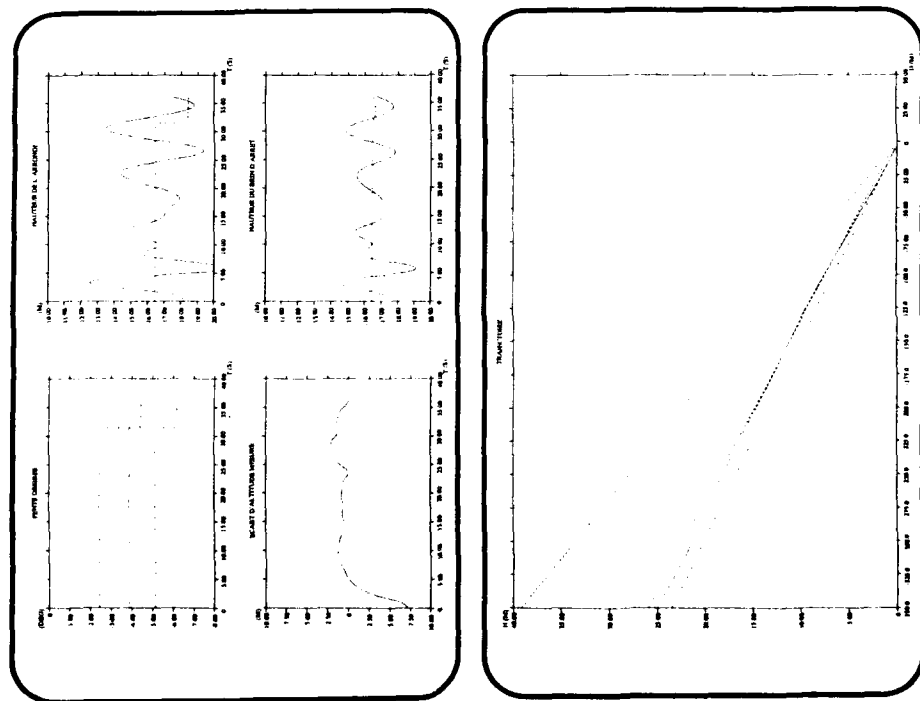


Figure 18 Avec prédiction du mouvement

Figure 19

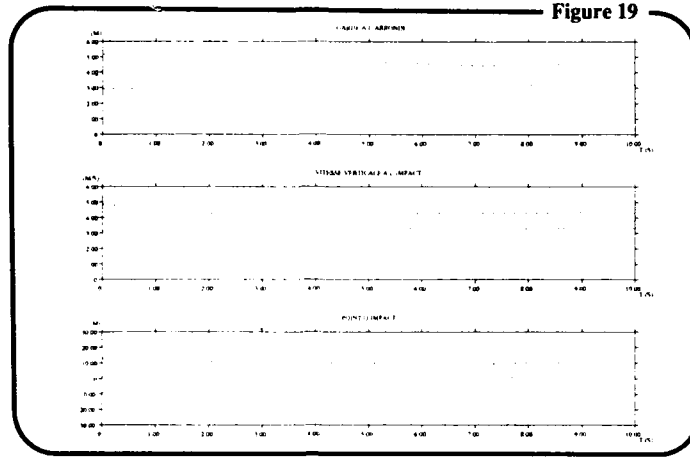
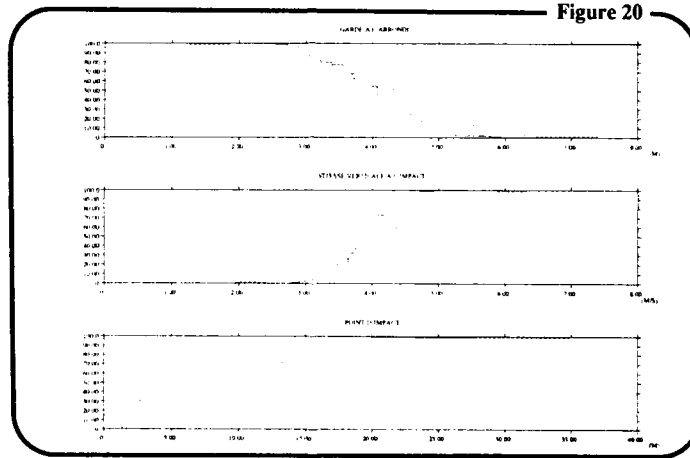


Figure 20



INTEGRATION OF FLIGHT AND CARRIER LANDING AID SYSTEMS FOR SHIPBOARD OPERATIONS

by

B. Dang Vu, T. Le Moing et P. Costes*
Office National d'Etudes et de Recherches Aérospatiales
29 Avenue de la Division Leclerc
92322 Châtillon Cedex
France

ABSTRACT

The operational availability of a carrier depends to a large extent on the capacity of its equipment and its aviation to operate in a wide domain of meteorological conditions and sea states. Some equipments are under development for the French future Nuclear Carrier in order to extend its operational limits for aircraft: launch and recovery ; a deck motion tranquillization system, a deck motion prediction system and an all-weather aircraft localization system.

The impact on deck landing procedures for future carrier-based fighter aircraft is presented here. An improved terminal guidance landing strategy making use of the prediction of the carrier motion is proposed. The actual glide path with fixed slope is replaced by a flight path along which the aircraft airspeed and flight path angle are updated in accordance with the predicted deck motion at touchdown, such that all the landing constraints are respected : minimum hook-to-ramp clearance, maximum touchdown sink rate... The integration of the landing aid systems with the aircraft flight control system will allow the implementation of an automatic landing mode or advanced manual task-tailored control modes. Preliminary simulation results give a general idea on the improvement of deck landing performances with respect to the accuracy of the prediction of the carrier motion.

1. INTRODUCTION

Landing an aircraft on the deck of a carrier in adverse weather and sea state is a demanding task. The aircraft must be precisely controlled to a relatively small area of the carrier deck despite not only the wind disturbances caused by the ship airwake, but also the large motion of the impact point.

A certain number of guidance informations are generated on board the carrier and provided to the pilot. Concerning the final phase of the approach, these informations are actually mainly provided by the Fresnel Lens Optical Landing System (FLOLS) which requires visual acquisition by the pilot. The pilot is also assisted by the Landing Signal Officer (LSO) who can dictate if necessary control orders from the deck of the carrier.

The actual landing procedures are well proven although some deficiencies still remain, especially when the carrier operates under adverse weather and sea conditions. Some equipments are currently being developed for the French future Nuclear Carrier to extend the operational limits for aircraft recovery ; a deck motion tranquillization system, a deck motion prediction system and an all-weather aircraft localization system. The impact on deck landing procedures of future shipborne aircraft is presented here. As carrier motion can be predicted, improved terminal guidance landing strategies can be defined. Automatic Carrier Landing Systems (ACLS) can also be developed using all-weather localization systems which provide an accurate determination of the aircraft position relative to the carrier. Fly-by-wire flight control systems (FCS) of future carrier-based fighter aircraft will make possible the implementation of advanced task-tailored control modes which are optimized specifically for the landing phase.

This paper is divided into three parts 1) a brief review of the state-of-the-art of landing aid systems and landing procedures 2) a preliminary analysis of the constraints related to the aircraft flight path during the terminal phase, leading to the proposition of a new landing procedure making use of the prediction of the carrier motion 3) a description of a simulation code developed in order to evaluate the new landing procedure, and discussion of some preliminary results.

2. BRIEF REVIEW OF THE STATE-OF-THE-ART

We describe hereafter the landing aid systems which are actually operational on French carriers, the usual landing procedure and equipments under development.

2.1 Carrier landing aid systems

Landing aid systems consist of shipborne and airborne equipments [1].

* Now with Aérospatiale-Helicopter Division, Marignane, France.

Aboard the carrier, four systems are used :

- The radar is used at night or in adverse weather to guide the aircraft within visual range of the FLOLS.
- The FLOLS system provides glide slope information to the pilot. A stand-by FLOLS system can be manually operated by the LSO in certain circumstances : failure of the main FLOLS, rough sea, silence radio operations...
- The Deck Approach and Landing Laser System (DALLAS) provides to the LSO informations on the aircraft position and motion relative to the carrier by means of three sensors : laser telemeter and deviation sensor, IR camera and TV camera (Figure 1 [2]). The laser beam emitted by the transmitter is directed towards the aircraft which reflects the beam to the receiver by means of a reflector mounted on the nose landing gear.
- The aiming marker is an isosceles triangle painted on the fore end of the runway. It is used by Super-Etendard pilots to make a HUD approach and landing.

Aboard the aircraft :

- Angle of attack (AOA) indication is provided to the pilot by means of three lamps red, green and amber : the green colour corresponds to the optimal AOA, the red to a higher AOA and the amber to a lower AOA. For LSO information purposes, these lamps are produced outside the aircraft on the nose landing gear.
- The HUD provides the following informations (Figure 2) : horizon, glide slope reference, airspeed vector, AOA reference, heading and radio-altitude. The pilot has to align the glide slope reference reticle on the base of the triangular aiming marker. The thickness of the reticles is relatively small which allows a more accurate flight path control than in the case of an approach using the FLOLS system.

2.2 Actual deck landing procedure

A typical carrier landing pattern is shown in Figure 3. Our interest lies in what happens during the last 10-15 seconds before touchdown. During this terminal phase, the actual procedure consists of a guidance strategy in which the aircraft vertical speed and AOA are kept constant, resulting in a fixed glide slope. Therefore the inclination of the FLOLS system and the glide slope reference reticle on the HUD have to be theoretically adjusted with respect to the meteorological wind magnitude and the carrier speed. In fact a fixed glide slope is provided by the FLOLS system using a measurement of the wind over deck (WOD) (Figure 4).

Piloting techniques to keep the aircraft on the ideal flight path depend on the type of landing aid system used (FLOLS or HUD) and require a coordinated action on the thrust and pitch commands (control in the vertical plane). Although most of actual shipborne aircraft are equipped with an autothrottle, handling characteristics still remain relatively poor. The safety of the terminal phase rests on the LSO who can dictate if necessary control orders to the pilot from the deck of the carrier. In case of large deck motion magnitude, the glide slope reference is provided by the stand-by FLOLS system whose inclination is manually commanded by the LSO with respect to a certain estimation and prediction of the deck motion.

2.3 Integration of flight and carrier landing aid systems

Actually no integrated carrier landing system exists on French carriers. US carriers have been equipped since the late 60's with ACLS systems like the SPN-42. The SPN-42 system senses ship motions, wind direction and speed, and aircraft motion relative to the ship ; develops reference approach trajectories and produces pitch and roll commands for UHF transmission to the approaching aircraft. These commands are intended to maintain the aircraft on the ideal approach trajectory. The aircraft receives the SPN-42 pitch and roll guidance commands via its data link system and executes these commands with the aid of its Automatic Flight Control System (AFCS). No information related to the deck motion prediction is used by the ACLS system, but the motion of the deck is calculated in the SPN-42 computer, and a Deck Motion Compensation (DMC) is used to filter the calculated deck position to provide the proper shaping to bring the vertical motion of the aircraft flight path in phase with the deck motion. This mode, called "deck chasing" is activated during the final one-half mile of the approach [3].

2.4 Systems under development

A deck motion tranquillization system and a deck motion prediction system are currently being developed for the French future carrier. The tranquillization system uses two pairs of lateral fins and one pair of steering rudders to reduce the sway, roll and yaw motions. A mass transfer system is also used to reduce the heel due to winds or load displacements on the deck, or during gyration manoeuvres. The sea tests on a free scale model have permitted the evaluation of the performance [4]. Pitch and heave motions develop considerable forces and their magnitudes cannot be reduced significantly. Concerning these motions, prediction techniques have been developed in France by ONERA/CERT [5,6] and CAPCA [7]. The sea tests performed with a predictor mock-up implemented on the carrier FOCH have permitted the evaluation of the performances obtained with the two methods.

Concerning aircraft tracking and localization, the DALLAS system can be further developed to become an ACLS system which needs in this case a data link between the ship and the aircraft. Another system under development is an airborne localization system using image processing of the carrier to calculate the position of the aircraft relative to the carrier [8]. In this case, the generation of guidance orders for automatic landing will not need any data link between the aircraft and the ship. As the ship motion can be determined by combining the relative motion of the aircraft and the absolute motion measured by the inertial system, the algorithms of the deck motion predictor can be implemented aboard the aircraft.

Conclusion : The present deck landing procedures are well proven although some deficiencies still exist and improvements can be realized :

- The actual flight path with fixed glide slope can bring the aircraft to cross the deck edge with very low height margins, especially in adverse sea conditions : for 1° of ship pitch, the stern can rise up to 2 meters while the nominal hook-to-ramp clearance is only 3 meters. The use of a deck motion prediction would extend the operational limits in aircraft recovery. This problem is mainly treated in this paper.
- Flight path controlling is actually performed from references which are essentially visual. The development of accurate localization systems with all-weather operating capability would also extend the operational limits of the carrier with the implementation of an automatic landing mode.
- Handling qualities of actual shipborne aircraft are relatively poor. Fly-by-wire FCS of future aircraft will allow a much easier implementation of task-tailored control modes which are optimized for the landing phase.

3. PRELIMINARY ANALYSIS OF THE DECK LANDING PROBLEM

We consider hereafter only the final phase of the approach (last 10-15 seconds before touchdown). The specific constraints related to the aircraft trajectory are first determined. An application to a simple case of carrier deck motion limited to the pitch motion is then presented. When the deck motion reaches a certain magnitude, the actual landing procedure (fixed glide slope) leads to a violation of the above constraints. A new landing procedure making use of the predicted motion of the ship is then proposed.

3.1 Specific deck landing constraints

These constraints can be summarized as follows : the aircraft must cross the stern or ramp at a minimum safety height, touchdown the deck at a defined point with a sink rate compatible with the structure limit of the main landing gear, and with a longitudinal speed compatible with the structure limit of the hook and with the capability of the arrestment cables system to dissipate accumulated energy.

The hook-to-ramp clearance constraint can be expressed by the following relation (Figure 5) :

$$\gamma_f < \gamma_{\text{clear}} = -(H_{\text{min}} + H_A - H_B) / L_{AB}$$

where : γ_f : relative flight path angle
 L_{AB} : distance from ramp to ideal touchdown point
 H_{min} : minimum hook-to-ramp clearance
 H_A : ramp height at ramp crossing instant
 H_B : arrestment wire height at touchdown instant.

We remind that the relative flight path γ_f is given by :

$$\gamma_f = V_z / (V - W_{OD})$$

where : V_z : aircraft vertical speed
 V : aircraft airspeed
 W_{OD} : wind-over-deck.

The constraint relative to the touchdown sink rate can be expressed as follows (Figure 6) :

$$\gamma_f > \gamma_{\text{impact}} = -(V_{z\text{max}} + V_{zB}) / (V - W_{OD})$$

where : $V_{z\text{max}}$: maximum relative vertical speed allowable
 V_{zB} : vertical speed of arrestment wire at touchdown instant.

The constraints on the airspeed are :

$$V_{\text{min}} < V < V_{\text{max}}$$

the low value of airspeed corresponding to the stall limitation.

3.2 Application to a ship pitch motion

With the following simplified example, we examine the evolution of the previous constraints with respect to the sea state. The deck motion is limited to the pitch component and assumed sinusoidal :

$$\theta = \theta_0 \sin \Omega t$$

where : θ : pitch angle.

The current instant is referred to an initial instant $t=0$ for which the pitch angle is zero. Afterwards t will designate the ramp crossing instant. The ramp height H_A at ramp crossing instant and the wire height H_B at touchdown instant are respectively given by :

$$H_A = (L_{AB} + L_{BC}) \theta_0 \sin \Omega t$$

$$H_B = L_{BC} \theta_0 \sin \Omega (t + L_{AB} / (V - W_{OD}))$$

where : L_{AB} : distance from ramp to wire
 L_{BC} : distance from wire to center of rotation.

The phase between H_A and H_B comes from the time of flight between ramp crossing and touchdown.

Figure 7 shows time histories of stern or ramp height, arrestment wire height and vertical speed for a ship pitch magnitude of 0.5° . Time histories of the constraints related to hook-to-ramp clearance and touchdown sink rate are also plotted for an aircraft speed of 128 knots and a WOD of 25 knots. We can see that the -3.5° nominal glide slope satisfies the two constraints for any ramp crossing instant when this instant varies. The touchdown dispersion is equal to :

$$\Delta x = H_B / (\theta + \gamma_f)$$

The dispersion is relatively low for a ship pitch magnitude of 0.5° :

- short : 2,53 m behind wire n°1,
- long : 1,08 m behind wire n°2.

For a larger ship pitch magnitude (1°), we can see on Figure 8 that a fixed glide slope of -3.5° leads to a violation of the hook-to-ramp clearance constraint at certain time intervals and therefore to high touchdown dispersions :

- short : 10,70 m behind wire n°1,
- long : 3,52 m behind wire n°3.

3.3 Flight paths respecting the landing constraints

To satisfy the constraints of ramp clearance and touchdown sink rate, the aircraft flight path has to be adjusted and updated with respect to the predicted motion of the carrier at touchdown instant. We assume afterwards that the aircraft commands consist of a longitudinal load factor and a normal load factor. The effectiveness of these commands is discussed hereafter.

Longitudinal load factor effectiveness

If we assume that the deck motions at ramp crossing and touchdown instants are exactly predicted, the landing could be delayed or made earlier by changing the approaching speed such to satisfy the ramp clearance constraint (Figure 8). By assuming roughly that a speed increment ΔV can be applied instantaneously, the resulting variation of the time-to-go before the aircraft crosses the ramp is given by :

$$\Delta t_{go} = -t_{go} \Delta V / V_r$$

where :

- t_{go} : time-to-go before ramp crossing
- $V_r = V - W_{OD}$: aircraft speed relative to the carrier.

For $t_{go}=10$ seconds and $\Delta V=\pm 5$ m/s we find $\Delta t_{go} = \mp 1$ s which is not very significant. These values will be more lower if the time response of the aircraft to a thrust command is taken into account. Furthermore the allowable deviations on airspeed ΔV are much lower in reality and the time interval within which a good prediction of the deck motion can be obtained is smaller. Therefore the effectiveness of a longitudinal load factor command in changing the instant of landing is negligible.

Normal load factor effectiveness

The response of the aircraft to a normal load factor input is a change of the flight path angle. Now from Figure 8 we see that increasing the glide slope within the bounds of the touchdown sink rate constraint is another solution to satisfy the ramp clearance constraint. Assuming an instantaneous response of the aircraft to a command of normal load factor, we calculate the minimum time of the manoeuvre bringing the aircraft from an initial glide slope to a final glide slope which verify the constraints. This will give an approximation of the minimum time interval required to predict the motion of the carrier (assuming the prediction perfect). The optimal load factor command is a bang-bang law with one switch (Figure 9). The time of the manoeuvre is calculated hereafter in the limit case where the ramp crossing instant coincides with the instant the final glide slope is reached [9] :

$$t_1 = 2x - \frac{(\gamma_{f1} - \gamma_{r0})V_r}{g\Delta n_{zmax}}$$

The switching instant is given by the relation :

$$\tau = \sqrt{\frac{1}{g\Delta n_{zmax}} \left[\frac{V_r^2}{2g\Delta n_{zmax}} (\gamma_{f1} - \gamma_{r0})^2 - L_{AB}(\gamma_{f1} - \gamma_{r0}) + \gamma_{r0}\Delta x + L_{BC}\theta \right]}$$

where :

- θ : ship pitch attitude at touchdown instant
- $\gamma_{f1} - \gamma_{r0}$: required glide slope variation
- Δx : touchdown dispersion to recover
- V_r : aircraft relative speed
- L_{AB} : distance from ramp to wire
- L_{BC} : distance from wire to center of rotation
- Δn_{zmax} : maximum increment of normal load factor.

The minimum time interval required to predict the deck motion is therefore :

$$t_{impact} = t_1 + L_{AB} / V_r$$

where the time of the manoeuvre t_1 is calculated for a maximum ship pitch attitude. Figure 10 shows the variation of the minimum time to predicted touchdown point with respect to the maximum load factor increment, in the limit case where the final glide slope satisfies just the ramp clearance constraint i.e $\gamma_{f1} = \gamma_{clear}$. For a ship pitch magnitude of 1° which is the actual operational limit, and for an aircraft manoeuvrability $\Delta n_{zmax}=0.2$ we find $t_{impact}=3.9$ seconds. This value is only approximated as the response to a load factor input is assumed instantaneous. As this time response is of the order of the second, the value of t_{impact} still remains within the limits actually realizable for the prediction of the carrier motion.

3.4 Proposition of a new deck landing procedure

From the preliminary analysis performed in the previous paragraph, we define the new landing procedure as follows :

- At the beginning of the approach phase, the actual procedure is maintained i.e fixed glide slope and fixed airspeed, the glide slope being determined for a given WOD and for a zero mean position of the deck.
- As soon as the time-to-go reaches a value below which an accurate prediction of the deck motion can be made, the glide slope and the aircraft airspeed are updated to satisfy simultaneously the four following constraints :
 - i) the aircraft must cross the ramp above a minimum safety height,
 - ii) the vertical speed at touchdown must be lesser than a maximum value compatible with the structure limit of the landing gear,
 - iii) touchdown must occur at the ideal touchdown point,
 - iv) the longitudinal speed and the AOA are limited.
- The guidance law is updated with respect to a deck motion prediction which becomes more and more accurate as the aircraft approaches the carrier.

Figure 11 presents in the plane (V, γ) (airspeed, relative flight path angle) the hook-to-ramp clearance constraint i) predicted at ramp crossing instant, and the touchdown sink rate constraint ii) predicted at touchdown instant, for aircraft speeds ranging from V_{\min} to V_{\max} (constraints iv)). These constraints are established while taking into account the time response of the aircraft to a thrust command. The optimal glide slope and optimal approach airspeed chosen for the new procedure are represented by the point on Figure 11 which is equidistant to the limits corresponding to the three constraints i) ii) and iv) defined above. This central position is chosen to assure a good robustness with respect to errors: error of prediction of the deck motion, error on the time-to-go, error on the aircraft time response to thrust command...

The proposed landing procedure requires an adjustment of the FLOLS system in inclination for each approach, which is not the case at present. One solution consists to display in the HUD a predicted aiming marker on which the pilot has to maintain aligned a glide slope reference reticle materializing the optimal glide slope γ^* as shown in Figure 12.

4. DESCRIPTION OF THE DECK LANDING SIMULATION CODE

The new landing procedure consists of a terminal guidance strategy in which the aircraft airspeed and flight path angle are updated with respect to the predicted motion of the carrier at the touchdown instant. The procedure is applied when time-to-go is within a time interval where an accurate prediction of the deck motion can be obtained. As the shorter the time-to-go the better the prediction, we can be tempted to choose this time interval as small as possible but we must make sure that the aircraft has enough manoeuvrability to perform the ultimate flight path corrections. A simulation software has been developed to evaluate this trade-off. The software is composed of modules modeling the carrier dynamics, the aircraft dynamics, the environment (wave and airwake), the landing aid systems (aircraft localization and deck motion prediction) and their interfaces with the aircraft FCS (Figure 13). A simplified version of these modules is described hereafter.

4.1 Ship motion and related disturbances

Wave model and ship motion model

We are interested only in the most important motions of the carrier which are the pitch and heave motions, as the roll and yaw motions can be significantly reduced by means of a tranquillization system. A large amount of data exist describing the motion of carrier at sea. Experiments have been conducted both at sea and in basin establishing frequency response curves and power spectral density functions as a means of representing ship pitch and heave motion characteristics. Figure 14 shows the functional diagram retained for the ship motion model. The purpose of the wave model is to generate the stochastic variation of sea surface height at some point along the ship length. This is used as the disturbance driving the ship motion model. The Pierson-Moskowitz power spectral density is chosen as the starting point for the wave modeling. When travelling on the ship through the waves, a disturbed spectrum called spectrum of encounter depending on ship velocity and heading is observed. For estimation design and systems analysis, it is convenient to represent the wave model by a linear time invariant dynamic system driven by a gaussian white noise and written in state space form. A 6th-order system has been retained for the wave model and an 8th-order system has been retained for the ship motion model. The parameters of both models have been identified with data derived from the SMP program [5]:

$$\begin{array}{ll} \text{Wave : } \dot{x}_h = A_h x_h + B_h \eta & x_h : \text{wave states} \\ h = C_h x_h & \eta : \text{white noise} \\ \text{Ship : } \dot{x}_n = A_n x_n + B_n h & h : \text{sea surface height} \\ y_n = C_n x_n & x_n : \text{ship states} \\ & y_n : \text{ship outputs (pitch and heave)} \end{array}$$

Prediction of pitch and heave motions

The prediction technique adopted by ONERA/CERT [5] comprises the following steps:

- The parameters of the model are first identified from measurements of the sea surface height (optional) and the ship motion variables during a certain time interval.
- The prediction is then made by integrating the equations of the noise-free identified model, the initial state being estimated by a Kalman filter. The prediction is updated in order to improve the precision.

The prediction algorithms developed by ONERA/CERT which have been validated by sea tests, will be incorporated later in the simulation code. At present, a simplified prediction model has been retained:

- The wave and ship dynamic models are assumed perfectly known; the predicted motion is simply derived by integrating the equations of the simulated model with no input noise.
- The outputs of the wave and ship models are also assumed exactly known which allows a perfect update of the predictor without having recourse to a Kalman filter (Figure 15 with $Q_0 = 0$).

With this simple predictor, the precision of prediction at a final instant t_f is given by the variance of the output variables of the ship

$$\begin{aligned} P &= C Q(t_f) C^T \\ \text{with } \dot{Q} &= A Q + Q A^T + B B^T \\ A &= \begin{bmatrix} A_s & 0 \\ B_s C_s & A_s \end{bmatrix} \quad B = [B_h \ 0]^T \quad C = [0 \ C_n] \end{aligned}$$

and $Q(t_0) = 0$ at each update of the predictor.

Atmospheric disturbances modeling

The atmospheric disturbances consist essentially of the ship airwake or burble. At present we use the carrier landing disturbance model included in MIL-8785C [10]. Flow field data have been obtained recently at the ONERA Fauga wind-tunnel on a 1/100 scale model of the French Nuclear Carrier [11]. These data will be incorporated later in the simulation code.

4.2 Aircraft model and integrated landing system

Figure 13 presents the block diagram of a fully airborne integrated system which integrates the aircraft FCS and the landing aid systems. All the functions are performed aboard the aircraft: measurement of the aircraft motion relative to the carrier, calculation of the carrier absolute position and prediction of its motions, generation of control orders for the FCS, automatically by an autopilot coupler, or manually by the pilot through a shaping filter. We consider afterwards only the automatic mode as it is more suitable for computer simulation.

Aircraft model and FCS

For control and guidance studies concerning specific flight phases as it is the case here, it is not often necessary to simulate an aircraft model with its complete and complex aerodynamics, engines, sensors and FCS. At a stage of feasibility, it is enough to simulate a "model of behaviour" of the aircraft; the aircraft is assumed augmented by appropriate feedback control laws so that its dynamics are close to the real aircraft. We describe hereafter the method adopted to derive an aircraft model of behaviour whose dynamics can be adjusted by a limited number of parameters.

The linearized equations of the aircraft dynamics and outputs are:

$$\Delta \dot{x} = A \Delta x + B \Delta u$$

$$\Delta y = C \Delta x$$

with x : state vector
 u : input vector
 y : output vector.

The components of x and y are:

$$x = (V \quad \gamma_k \quad \alpha \quad q \quad p \quad \beta \quad r)^T$$

$$y = (V \quad q^* \quad p_a \quad \beta)^T$$

where: V : airspeed
 γ_k : ground flight path angle
 α : angle of attack
 q : pitch rate
 p : roll rate
 β : sideslip angle
 r : yaw rate
 q^* : combination of normal load factor and pitch rate
 p_a : aerodynamic roll rate.

With a proportional integral control law of the form:

$$\Delta u = K_1 \Delta x + K_2 \int_0^t (\Delta y - \Delta y_c) dt$$

where Δy_c represents the pilot inputs, the aircraft dynamics are governed by the following close-loop system:

$$\frac{d}{dt} \begin{bmatrix} \Delta x \\ \int (\Delta y - \Delta y_c) \end{bmatrix} = \begin{bmatrix} A + BK_1 & BK_2 \\ C & 0 \end{bmatrix} \begin{bmatrix} \Delta x \\ \int (\Delta y - \Delta y_c) \end{bmatrix} + \begin{bmatrix} 0 \\ -1 \end{bmatrix} \Delta y_c$$

and the modes are determined by the eigenvalues and eigenvectors of the system. By choosing appropriately the gain matrices K_1 and K_2 , it is possible to set these modes while limiting the number of parameters of the system. These parameters are:

- phugoid mode : pulsation ω_{PH} and damping ζ_{PH}
- short period mode : pulsation ω_{SP} and damping ζ_{SP}
- time constant τ_q of the integral term $\int (q^* - q_c)$
- roll time constant τ_p
- Dutch-roll mode : pulsation ω_{DR} and damping ζ_{DR}
- time constant τ_β of the integral term $\int (\beta - \beta_c)$

The only aerodynamic coefficients necessary to complete the model are $C_{x\alpha}$, $C_{z\alpha}$ et $C_{y\beta}$.

Approach and landing guidance

Guidance objectives during landing approach are airspeed control, flight path control and hook position control about desired values. Concerning airspeed and flight path angle, the desired values are constant in the conventional landing procedure; in the new landing procedure, these values depend on the predicted motion of the carrier (cf. 3.4). To formulate the control law, we define an augmented state vector ΔX composed of aircraft state variables Δx used in the "model of behaviour", and variables of position relative to the carrier. The augmented linearized system is then :

$$\dot{\Delta X} = F \Delta X + G \Delta y_c$$

$$\Delta z = H \Delta X$$

$$\text{with } \Delta X = (\Delta x^T \Delta z_{cg} \Delta y_{cg})^T$$

$$\Delta z = (\Delta V \Delta z_{hook} \Delta \Phi \Delta y_{hook})^T$$

where z_{cg} : altitude of aircraft center of gravity
 y_{cg} : lateral deviation of aircraft center of gravity from runway axis
 V : airspeed
 Φ : roll angle
 z_{hook} : hook altitude
 y_{hook} : hook lateral deviation from runway axis.

The objective is to make Δz tend to a desired value Δz_d corresponding to the ideal approach trajectory. Note that the term of desired glide slope is implicitly contained in the component Δz_{hook} of the vector Δz_d . A classical linear quadratic method is used to derive the optimal control law Δy_c^* . We consider the augmented system :

$$\frac{d}{dt} \begin{bmatrix} \Delta X \\ \Delta z - \Delta z_d \end{bmatrix} = \begin{bmatrix} F & 0 \\ H & 0 \end{bmatrix} \begin{bmatrix} \Delta X \\ \Delta z - \Delta z_d \end{bmatrix} + \begin{bmatrix} G \\ 0 \end{bmatrix} \Delta y_c$$

The minimization of the cost function :

$$J = \int_0^{\infty} \left(\begin{bmatrix} \Delta X^T & \Delta z^T - \Delta z_d^T \end{bmatrix} Q \begin{bmatrix} \Delta X \\ \Delta z - \Delta z_d \end{bmatrix} + \Delta y_c^T R \Delta y_c \right) dt$$

gives the optimal control law :

$$\Delta y_c^* = G_1 \Delta X + G_2 (\Delta z - \Delta z_d)$$

The gain matrices G_1 and G_2 are obtained from the resolution of an algebraic Riccati equation. The control law can also be expressed in the integral form :

$$\Delta y_c^* = \Delta y_c^*(0) + G_1 \Delta X + G_2 \int_0^t (\Delta z - \Delta z_d) dt$$

4.3 Simulation results

Data

A fictitious aircraft model is used ; the parameters which characterize the model dynamics are fixed to the following values :

$$\omega_{PH} = \pi/3 \text{ rd/s} \quad \omega_{SP} = 2\pi \text{ rd/s} \quad \omega_{DR} = \pi \text{ rd/s} \quad \tau_q = 1,5 \text{ s} \quad \tau_\beta = 1,5 \text{ s} \quad \tau_p = 0,6 \text{ s}$$

$$\zeta_{PH} = 1 \quad \zeta_{SP} = 1 \quad \zeta_{DR} = 1$$

$$C_{x\alpha} = 0,5 \quad C_{z\alpha} = 3 \quad C_{y\beta} = -0,6$$

The nominal airspeed is 70 m/s. The WOD is 15 m/s. The limit values of hook-to-ramp clearance and touchdown sink rate are respectively $H_{min} = 2,5$ m and $V_{zmax} = 5$ m/s. Simulations are made with a moderate rough sea condition.

Results

The following time histories are presented in Figures 16 and 17 :

- Deck motion (solid line) and deck predicted motion (dotted line). The ramp height is predicted at ramp crossing instant. The arrestment wire height is predicted at touchdown instant. The prediction is updated every seconds.
- Desired glide slope γ_f^* (solid line) and the slopes γ_{clear} and γ_{impact} (mixed lines) corresponding to the ramp clearance and touchdown sink rate constraints.
- Vertical deviation of the hook from the desired flight path.
- Hook trajectory with respect to the wire position at touchdown instant (solid line), desired glide slope γ_f^* plotted from the predicted wire position (mixed line) and the slopes γ_{clear} and γ_{impact} plotted from the real wire position (dotted lines).

Figure 16 presents the results obtained with the conventional landing procedure. Figure 17 presents the results obtained with the new landing procedure with a deck motion prediction starting 5 seconds before touchdown. We can see that with no prediction, the hook crosses the ramp under the minimum safety height. With prediction, the hook crosses the ramp above the safety height while the vertical speed at touchdown remains within the admissible limits.

In order to obtain statistic results on landing performances with respect to the prediction time, a number of 100 simulations has been made for prediction times varying from 0 second to 10 seconds.

Figure 18 shows the evolution of the mean values and the standard deviations of the hook-to-ramp clearance, the touchdown sink rate and the touchdown error. The conventional landing procedure is represented on the figure by the zero prediction time. We can see that the mean values are independent of the prediction time as the wave model is driven by a gaussian white noise with zero mean. The standard deviation of the hook-to-ramp height decreases from a prediction time of 3 seconds and becomes constant beyond 6 seconds. The standard deviation of the touchdown vertical speed decreases as soon as the prediction is effective, then becomes constant beyond 2 seconds of prediction time. The standard deviation of the touchdown error decreases until the prediction time reaches 5 seconds, then becomes constant for longer prediction times.

Figure 19 shows the distribution functions of the previous performance characteristics for two values of the prediction time: 0 second (dotted line) and 5 seconds (solid line). The functions indicate the number of simulations for which

- the hook-to-ramp clearance is greater than a given value
- the vertical speed is lesser than a given value
- the touchdown error is lesser than a given value.

We can see that in almost all simulations, the ramp clearance and touchdown sink rate constraints are respected when the prediction is effective. The improvement with respect to the no prediction case is especially important in limit landing conditions.

5. CONCLUSION

The present deck landing procedures are well proven although some deficiencies still exist and improvements can be realized. In adverse sea conditions, an approach with fixed glide slope can lead to a ramp crossing with very low height margins; for 1° of ship pitch, the stern can rise up to 2 meters while the nominal hook-to-ramp clearance is only 3 meters. Research works on carrier motion prediction suggest a landing procedure which would extend the operational limits of the carrier. It is proposed a new landing procedure consisting of generating in real-time a guidance law in which the aircraft flight path angle and airspeed are changed with respect to the predicted motions of the carrier at ramp crossing and touchdown instants, in order to satisfy the constraints of hook-to-ramp clearance and touchdown sink rate. The guidance law is updated with respect to a motion prediction which becomes more and more accurate as the aircraft approaches the carrier. Preliminary simulation results with simplified models show an improvement of the landing performances, in particular, they seem to indicate that the minimum prediction time necessary is inside the limits actually reachable with present prediction techniques. This will be further confirmed or infirmed with the introduction of more realistic models in the simulation code developed for this matter.

REFERENCES

- (1) "Règlement d'appontage. Instruction permanente", Marine Nationale, Commandement de l'Aviation Embarquée et du Groupe des Porte-Avions, Juillet 1981.
- (2) "Dispositif d'aide à l'appontage par laser. Principes généraux", CSEE, Novembre 1987.
- (3) J.M. Ufford, K. Hess, R.F. Moomaw, R.W. Huff, "Development of the Navy H-Dot Automatic Carrier Landing System Designed to Give Improved Approach Control in Air Turbulence", AIAA paper 79-1772, 1979.
- (4) J.P. Jung, G. Hardier, "Stabilisation des mouvements de plate-forme et techniques de ralliement de cap à gîte minimum pour le futur porte-avions nucléaire", Mémoire ATMA, Session 1991.
- (5) J.P. Jung, G. Hardier, "Modélisation et prédiction des mouvements de tangage et de pilonnement d'un porte-avions nucléaire", rapport technique ONERA/CERT n°3/7390, Décembre 1984.
- (6) J.P. Jung, G. Hardier, "Prédiction des mouvements de plate-forme d'un porte-avions. Premiers résultats d'essais", note technique ONERA/CERT n°142/90, Septembre 1990.
- (7) S. Sifredi, M.A. Grandclement, J.P. Puy, "Prédiction de mouvements de plate-forme à l'aide d'algorithmes ayant une structure de treillis", mémoire ATMA, Session 1987.
- (8) M.Y. Le Guilloux, R. Feuillo, "Guidage automatique lors de l'appontage par traitement d'image embarqué", AGARD FMP, Aircraft/Ship Operations, 20-23 Mai 1991, Seville.
- (9) B. Dang Vu, P. Costes, "Etude préliminaire de l'intégration du pilotage et des aides à l'appontage", rapport technique ONERA n°13/5158SY, Juin 1990.
- (10) "Military Specifications, Flying Qualities of Piloted Airplanes", MIL-F-8785C, November 1980.
- (11) C. Chatelard, J.C. Raynal, "Essai à F11CFM de la maquette au 1/100^e du PAN", procès verbal ONERA n°118394, Novembre 1988.

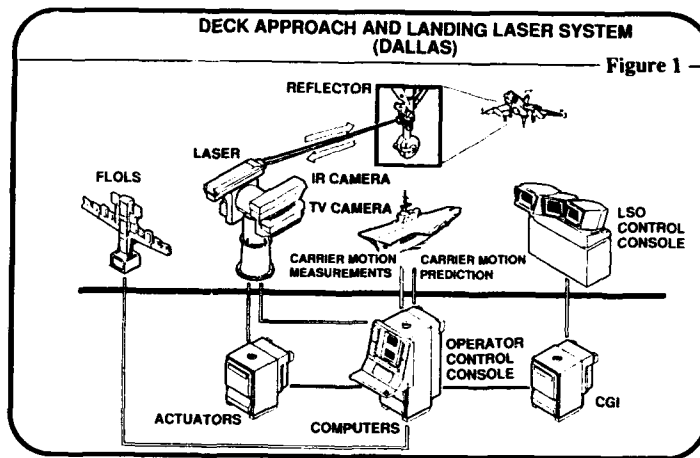


Figure 2

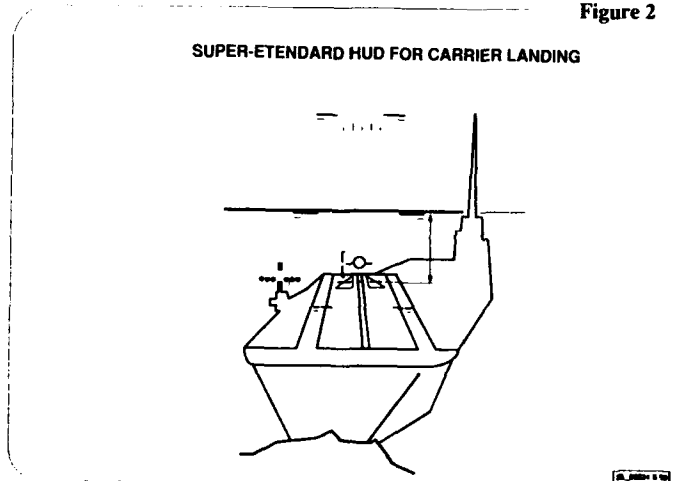


Figure 3

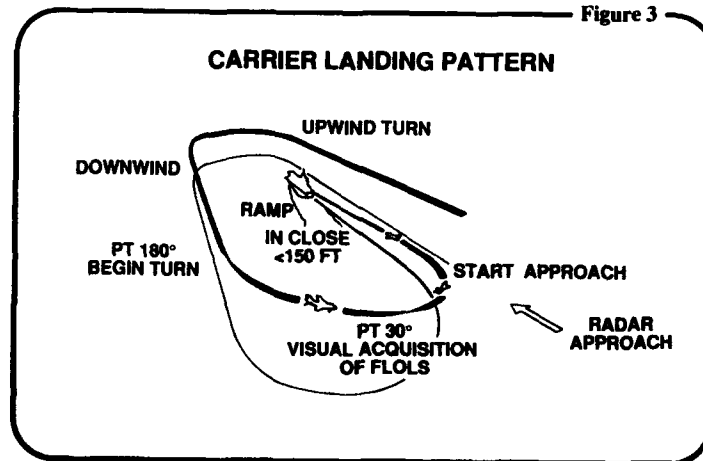


Figure 4

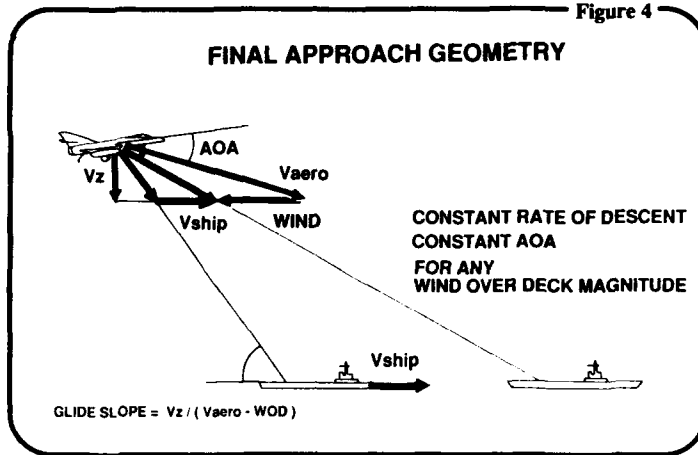


Figure 5

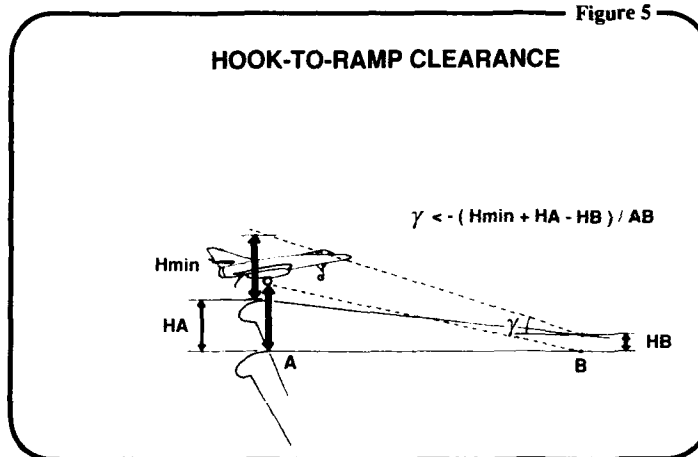


Figure 6

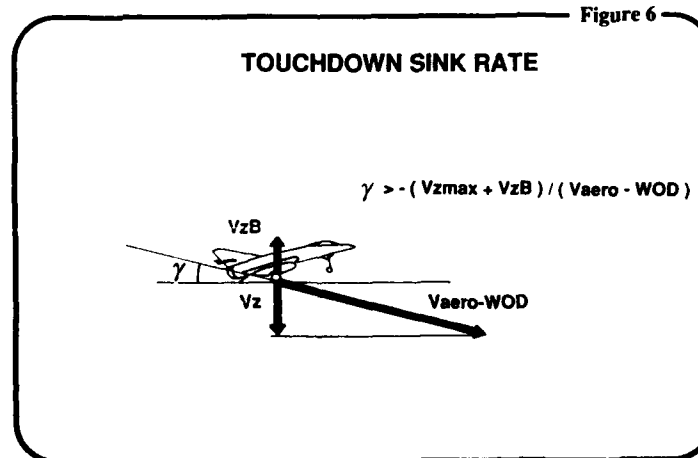


Figure 7

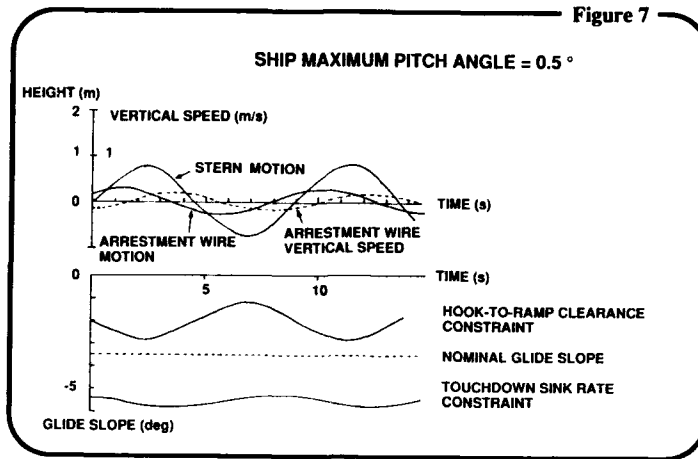


Figure 8

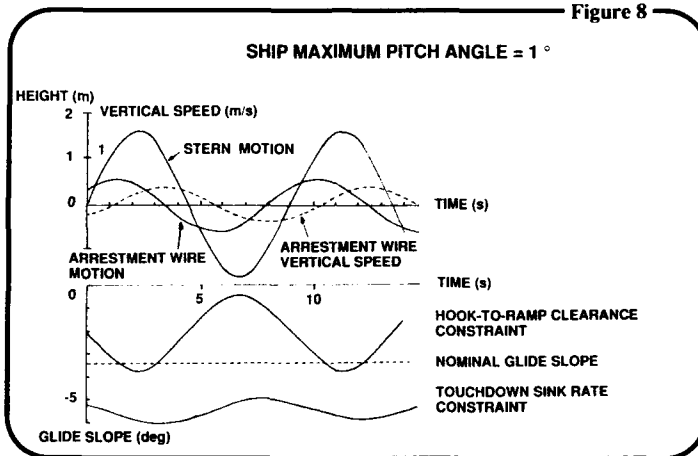


Figure 9

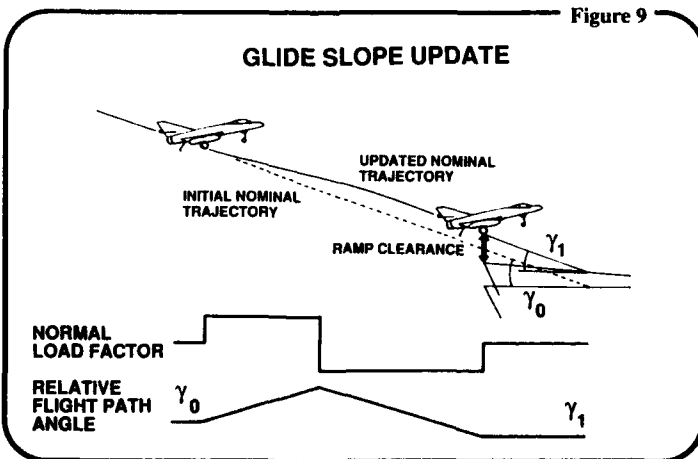


Figure 10

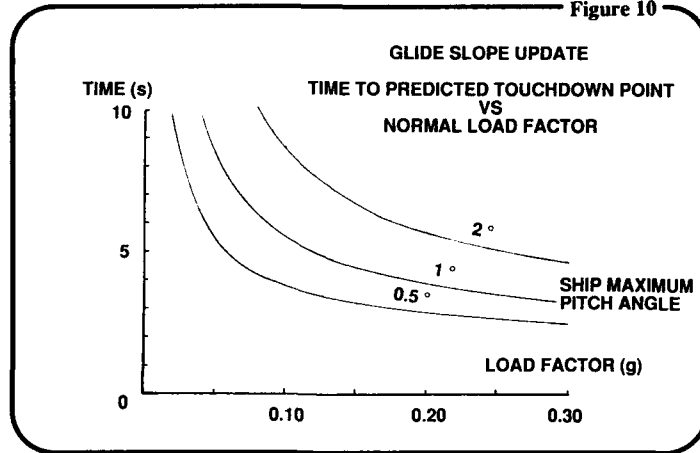


Figure 11

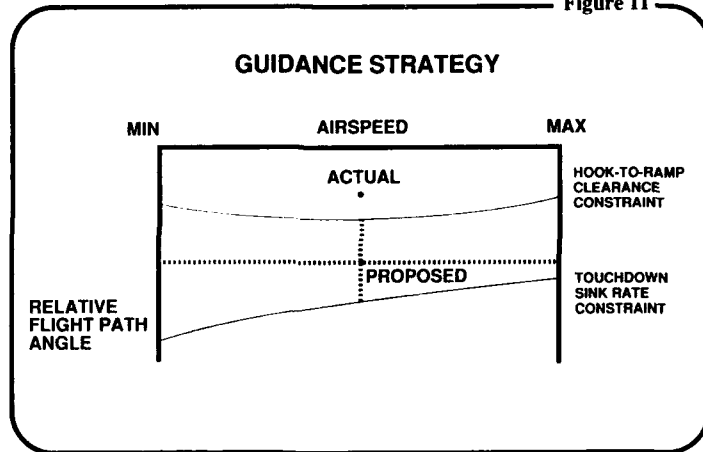


Figure 12

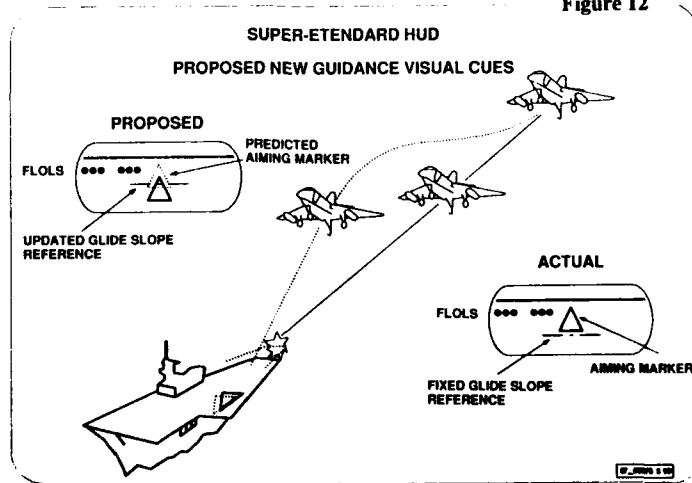


Figure 13

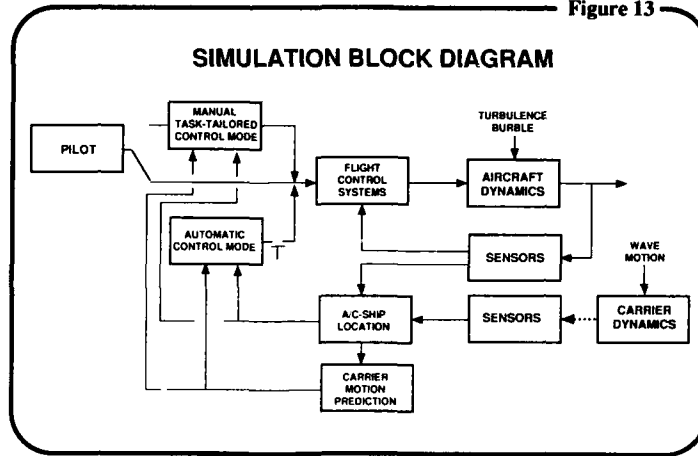


Figure 14

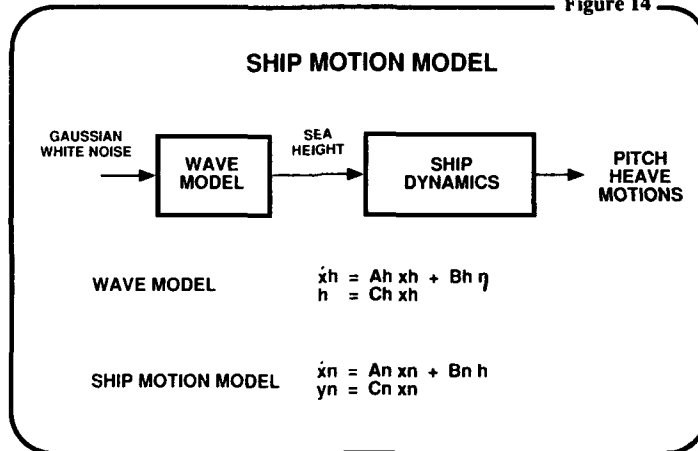
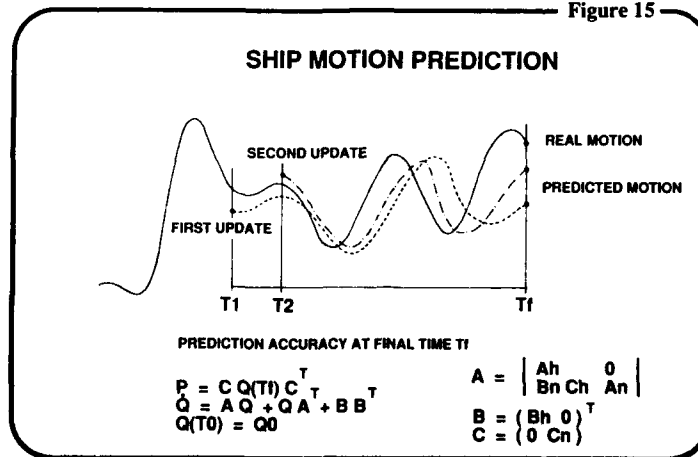


Figure 15



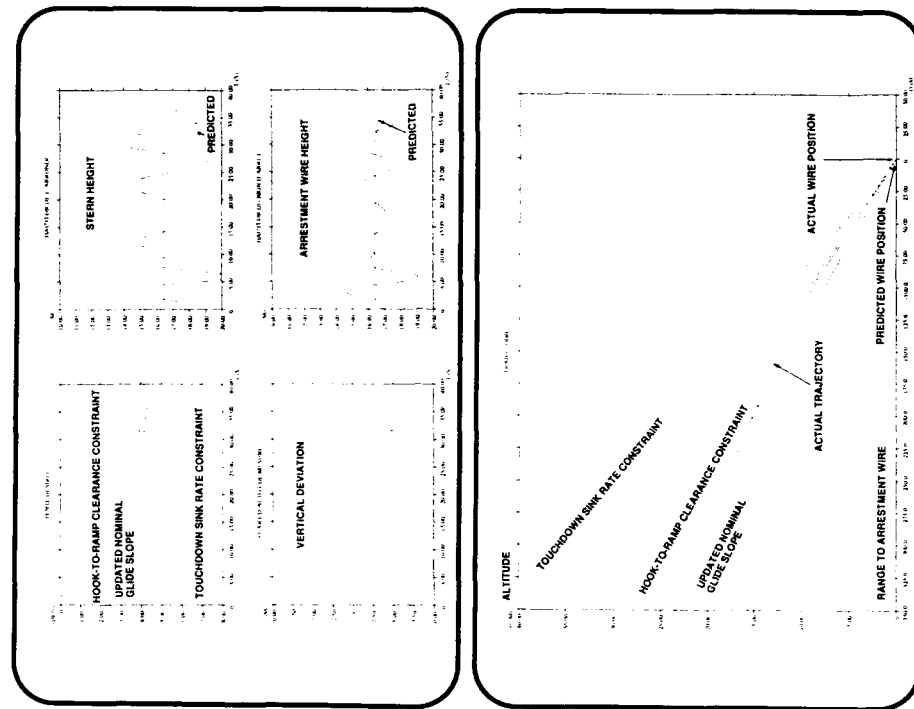


Figure 16. Without deck motion prediction

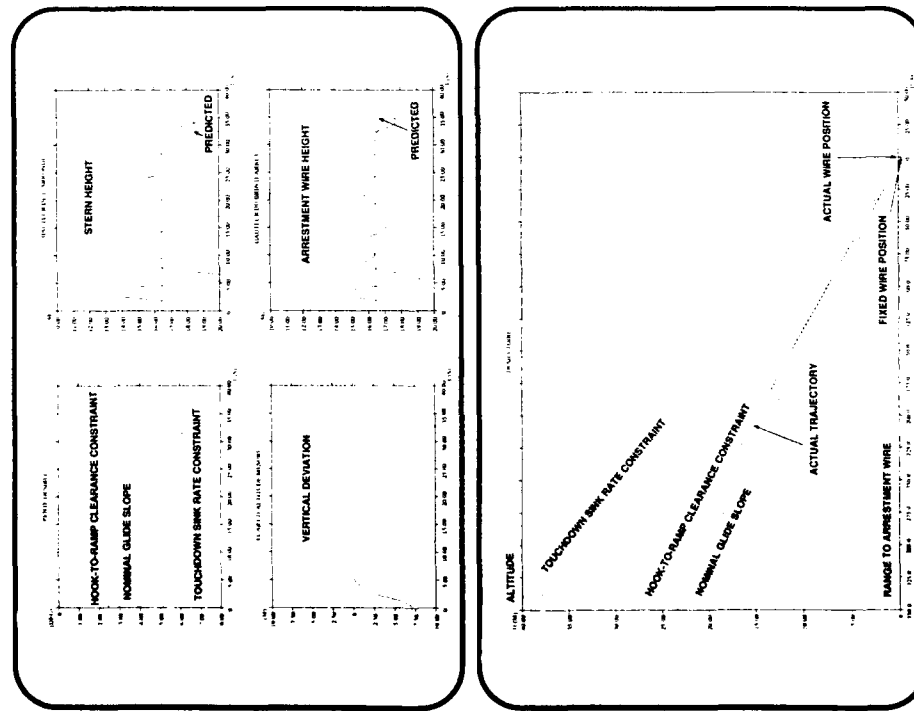


Figure 17. With deck motion prediction

Figure 18

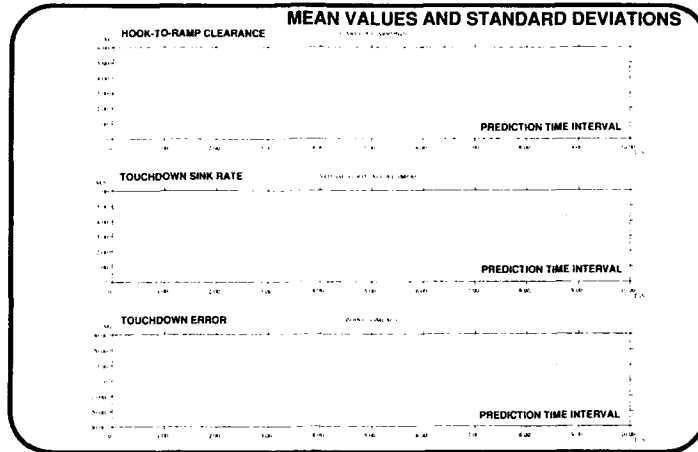
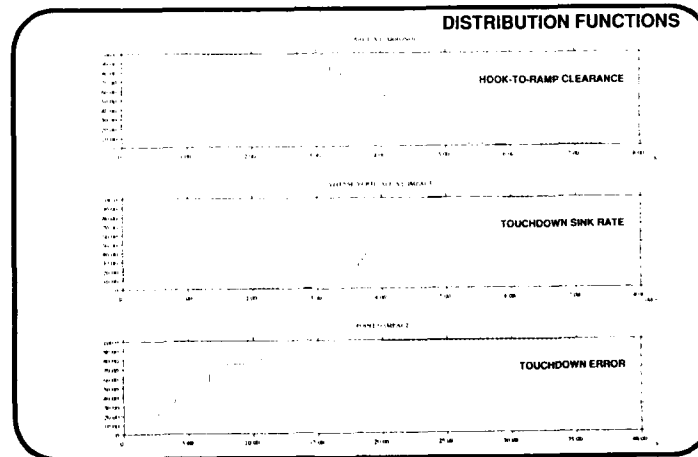


Figure 19



APPROCHE ET APPONTAGE ASSISTES PAR TRAITEMENT D'IMAGE EMBARQUE SUR AERONEF

Y. Le Guilloux
R. Feuilloley

SAGEM
27, rue Leblanc
75512 PARIS CEDEX 15
FRANCE

RESUME

On étudie l'automatisation du contrôle visuel effectué par le pilote d'un aéronef lors de la phase d'appontage. Le système envisagé, qui comprend une caméra (infrarouge) et l'électronique de traitement d'image temps réel associée, fournit en continu la position tridimensionnelle de l'avion par rapport au porte-avions. Pour ce faire, les caractéristiques principales du porte-avions sont d'abord localisées dans l'image, puis appariées avec leurs équivalents dans le modèle tridimensionnel du porte-avions connu a priori. Cette correspondance permet, par transformation perspective inverse, de retrouver la position du porte-avions par rapport à l'avion, d'où l'on déduit la position et le mouvement relatifs de l'avion par rapport au porte-avions. Ainsi, le système est capable de mesurer l'écart à une cinématique idéale d'appontage, d'où l'on déduit les actions compensatrices appropriées. En outre, le mouvement absolu de l'avion, donné par le système inertiel, peut être combiné avec le mouvement relatif pour donner le mouvement absolu du porte-avions.

1 INTRODUCTION

Nous commencerons par évoquer les grands principes inhérents aux trajectoires de recueil des aéronefs sur les portes-avions, puis nous ferons le point du matériel et des procédures actuellement en service sur les portes-avions français. Après en avoir noté les avantages et les limites d'utilisation, nous aborderons la façon d'utiliser l'image (thermique ou visible) du porte-avions vue de l'avion en finale d'approche, pour ramener l'avion sur la trajectoire idéale grâce à l'élaboration d'une consigne de pilotage.

2 EXPOSE DU PROBLEME DE L'APPONTAGE

Nous parlerons surtout des trajectoires d'approche et d'appontage d'avions conventionnels sur porte-avions, par commodité et simplification, mais le raisonnement autour du couple avion/porte-avions est bien souvent transposable au couple hélicoptère/porte aéronefs.

Notre exposé se basera plus précisément sur l'expérience acquise sur les deux porte-avions français CLEMENCEAU et FOCH, tous les deux semblables de la classe des 22000 tonnes Washington.

Ils sont entrés en service actif respectivement en 1961 et 1963 et mettent en oeuvre un groupe aérien d'environ quarante appareils.

Avant d'encren dans le vif du sujet, on rappelle quelques faits de base sur la vie du couple avion/porte-avions.

Le porte-avions est d'abord un navire et il est normalement intégré au sein d'une force navale qui a une route et une vitesse moyenne à tenir. Le porte-avions est donc une piste d'aviation mobile dans un environnement variable au fil des minutes.

Pour lancer les avions et les ramasser, le porte-avions manoeuvre pour se placer face au vent. Lorsque la route aviation est à l'inverse de la route moyenne de la force navale, le porte-avions doit donc effectuer en temps utile le demi-tour nécessaire, ce qui peut prendre cinq minutes et peut jeter la stupefaction dans la cohorte d'avions empilés sur une mauvaise radiale. Le trafic aérien est souvent dense au moment des lancements et ramassages. Il faut donc non seulement naviguer pour rejoindre le porte-avions, mais aussi éviter la trajectoire des autres appareils.

Il faut éviter les autres appareils qui tentent de se poser simultanément, mais il faut aussi s'insérer en bon ordre et avec le bon intervalle dans la séquence de présentation à l'appontage.

Le météorologie joue un rôle essentiel. Une mauvaise visibilité imposera des trajec-

toires longues et coûteuses en pétrole, la houle fera tanguer et rouler le porte-avions, la pluie gênera l'acquisition visuelle du bateau par le pilote en finale, le vent ne doit être ni trop fort, ni trop faible. Pour se poser sur un porte-avions, il faut donc dans l'ordre, naviguer vers lui, s'intégrer dans la chronologie d'appontage, rejoindre le trajectoire finale d'approche, voir le bâtiment, et enfin piloter l'avion jusqu'à l'impact en suivant les aides optiques.

3 ETAT DE L'ART EN 1991 SUR LES PORTE-AVIONS FRANCAIS

Un exemple d'appontage consiste à amener un aéronef de la classe du Super-Etendard, volant à 125 noeuds, sur la piste oblique, qui est un rectangle de 168 x 20 mètres. La crose doit accrocher un des 4 brins d'arrêts, situés dans un zone allant de 46 m à 68 m depuis l'arrondi. La pente idéale est de 3,5° et le vent optimal sur le pont est de 30 noeuds.

De jour, et par beau temps, les avions se présentent par patrouilles au break, prennent un espace entre eux de 45 secondes et effectuent un tour de piste à vue, vent arrière à 600 pieds d'altitude. Les références sont visuelles, les aides à l'appontage aussi.

De nuit et de jour par mauvais temps, les avions se présentent en ligne droite tout sorti à 1 500 pieds, par guidage radar et commencent leur descente à 4,3 Nq sur l'arrière du bâtiment, sous guidage radar jusqu'à la prise de vue par le pilote de l'optique d'appontage à 1 Nq et 350 pieds. Pour une description précise des circuits d'appontage, on se référera à [6]. Nous pouvons dénombrer les différentes aides à l'appontage disponibles sur les porte-avions du type FOCH.

Les aides du bateau vers le pilote sont :

- 1) Le Radar d'appontage DRBA 51 dont la portée pratique sur l'arrière du porte-avions est de 15 Nq à 1 Nq. Le contrôleur fournit par radio au pilote le guidage en cap et la distance restante. Ce radar ne donne pas d'indication de site.
- 2) Le Système DALAS (Dispositif d'Aide à l'appontage utilisant le LASer). Ce système, réalisé par la C.S.E.E. en 1988 utilise trois senseurs - télémètre laser, caméra infrarouge et caméra lumière visible - groupés sur une tourelle installée en abord de la piste oblique. L'avion en finale est repéré par un opérateur situé devant une console d'exploitation, qui observe les deux caméras. Il désigne la cible au télémètre Laser. Celui-ci émet alors un rayon qui, réfléchi par un rétroreflécteur situé

sur l'avion, revient vers l'émetteur-récepteur. L'exploitation continue de ces mesures permet d'élaborer les écarts de l'avion par rapport à la trajectoire idéale mais aussi de prédire la tendance de l'avion avec 2 à 3 secondes d'avance. Ces informations sont présentées sur des consoles à l'officier d'appontage, qui peut s'il l'estime nécessaire conseiller par radio le pilote. La portée du système est de 1 à 2 Nq.

- 3) L'optique d'appontage OP 3 réalisée par la SAGEM. Elle est utilisée obligatoirement dans la finale, à partir de 1 Nq. Elle donne au pilote sa position relative en pente par rapport à la pente idéale.

L'officier d'appontage peut actionner les feux "appel moteur" et "wave off". Cette optique est réglée en fonction du vent sur le pont (donc de la vitesse relative d'approche) et du type d'appareil. Elle est stabilisée en tangage.

Il existe une optique de secours dite "optique manuelle", située plus avant sur le côté bâbord de la piste oblique et qui sert par fort tangage; la position du faisceau est commandée par l'officier d'appontage.

- 4) Le Balisage de la piste oblique :

- un rectangle de peinture jaune avec des feux de contour la nuit,
- un triangle blanc dont la base sert de cible de visée, pour le viseur tête haute des Super-Etendard.

En effet, le viseur du Super-Etendard en mode approche permet de se passer du "miroir", en superposant un repère de pente calé dans le viseur à 3,5°, sur la base du Triangle Blanc. L'inconvénient est que le pilote appontant au viseur ne voit plus les éventuels signaux de remise des gaz que l'O.A. peut lui envoyer par le miroir.

On constate que le radar termine son aide à 1 Nq et que le miroir guide ensuite le pilote en pente.

Le DALAS, qui n'a pas de remontée directe vers le pilote, aide l'O.A. à conseiller par radio le pilote.

4 PRESENTATION DU SYSTEME

Le système à base d'imagerie que l'on propose ci-après, peut permettre de guider le pilote de 2 Nq jusqu'à l'arrondi. Il vient donc en complément d'installations actuelles et a la particularité d'être porté par l'avion et non par le navire. Il donne donc une certaine souplesse d'emploi sur d'autres navires et des pistes à terre dès lors que l'on a numérisé leurs caractéristiques.

Il est entièrement lié à l'avion. Ce choix est imposé par la nécessité d'informer en temps réel le pilote. Les éléments constitutifs comprennent donc une caméra sous l'aéronef et un système de traitement d'image et de calcul. Il présente une consigne de pilotage en viseur tête haute permettant de suivre avec précision le profil de descente idéal. On décrit successivement la caméra et son positionnement et les traitements mis en œuvre à partir de l'image numérique qu'elle produit.

5 CAMERA ET GEOMETRIE DE L'IMAGE

On suppose la caméra placée sous l'aéronef, son axe optique étant orienté sur l'axe de descente idéale afin de centrer la piste dans l'image.

La piste se présente donc comme un trapèze (Figure 1)

En supposant par exemple que la caméra couvre un champ de $15^\circ \times 15^\circ$, représenté par une image numérique de 512×512 pixels, on peut donc, par un calcul trigonométrique simple, estimer les dimensions de ce trapèze dans l'image numérique vue depuis de la trajectoire idéale en fonction de la distance au porte-aéronefs (Figure 2).

La précision absolue de localisation de l'aéronef, qui dépend fortement de ces dimensions, et notamment de la plus petite d'entre elles, se dégrade naturellement à grande distance. Toutefois, il faut également remarquer que la précision absolue requise à grande distance est moins importante, en raison du temps de correction possible.

6 ALGORITHMES DE VISION PAR ORDINATEUR

6.1 Description

Ces traitements permettent, à partir de l'image observée par la caméra, de calculer l'écart de l'aéronef à la trajectoire de descente idéale. Cet écart consiste en une valeur d'écart latéral (par rapport à l'alignement de la ligne médiane de la piste) et une valeur d'écart vertical par rapport au profil visé.

Pour ce faire, on extrait de l'image les segments rectilignes, et l'on déplace un modèle connu a priori pour le faire correspondre aux segments de l'image. Le déplacement nécessaire permet de localiser l'aéronef relativement au porte-aéronefs, ce qui suffit à mesurer l'écart à la trajectoire souhaitée. L'extraction des segments comprend trois étapes :

Extraction des contours,
Seuillage des gradients,

Chainage des contours et approximation polygonale.

A l'issue de cette extraction, on doit identifier les segments du modèle par mise en correspondance, puis effectuer les calculs géométriques précis permettant de déterminer la position de l'aéronef par rapport au porte-aéronefs.

6.2 Extraction des contours

On trouve dans la littérature de nombreux détecteurs de contours dont le principe est toujours de mesurer les transitions locales de niveau de gris. On s'appuie ici sur l'opérateur bien connu de Sobel, et sur le détecteur de Deriche[1]. Le premier demande assez peu de calculs par point, mais le second produit généralement des résultats de meilleure qualité. En effet, le détecteur de Sobel effectue de simples convolutions sur des voisinages limités. Le détecteur de Deriche, qui possède une réponse impulsionnelle infinie, requiert des calculs récursifs, ce qui interdit une mise en œuvre parallèle. Toutefois, une approximation parallélisable de ce dernier opérateur peut offrir un bon compromis.

A l'heure actuelle, il est prématuré d'arrêter un choix définitif car on devra prendre en compte la qualité des résultats obtenus sur de nombreuses images et d'éventuelles contraintes de volume d'électronique.

A l'issue du calcul du gradient effectué par l'une ou l'autre méthode, on supprime tous les points dont le gradient n'a pas un module extrême dans la direction du gradient, afin d'amincir les contours et de ne garder que des lignes d'épaisseur unitaire.

6.3 Seuillage des gradients

Il subsiste dans l'image des gradients après la suppression des non-maxima, de nombreux contours d'intensité faible, bien que localement maximale. Généralement, on prend la décision de retenir ou d'écarter définitivement des points de contours par comparaison du module du gradient à un seuil. Cette procédure soulève quelques difficultés.

Le premier problème consiste à choisir le seuil. Certaines méthodes consistent à analyser l'histogramme de gradients sur toute l'image, afin de ne retenir qu'une tranche supérieure prédéterminée ($n\%$). Une telle démarche pose quelques difficultés lorsque l'image ne présente pas un éclaircissement uniforme. Des seuillages locaux (basés sur des histogrammes de voisinages) contournent cette difficulté.

Enfin, on constate que le calcul des gradients tend parfois à introduire des discontinuités dans les lignes de contours, ce qui est pénalisant pour la représentation

par segments de droite visée ici. Une technique de seuillage à deux seuils (seuil d'acceptation inconditionnelle, seuil de rejet inconditionnel) permet de définir un intervalle de doute dans lequel la décision locale nécessite l'observation de pixels voisins qui peuvent confirmer ou invalider la présence de contour. On peut ainsi combler certaines discontinuités. On obtient donc, à ce stade, une image binaire, dans laquelle chaque point est soit un point de contour, soit un "non-contour".

6.4 Chainage des contours et approximation polygonale

Cette étape vise à dégager les segments rectilignes parmi les contours détectés dans l'image. Pour ce faire, on approxime les lignes de contours obtenues par suivi dans l'image, par des segments de droites. On trouve dans la littérature plusieurs procédés d'approximation polygonale. On utilise ici la méthode décrite dans [2] et [3]. Le principe consiste à ne chaîner les points de contours que sous la condition de "cône admissible", c'est-à-dire dans la direction approximative du contour (orthogonale au gradient). Les sous-chaînes ainsi délimitées sont alors simplement approximées par autant de segments de droites. Naturellement, tous les segments de petite taille (correspondant à des chaînes courtes) sont éliminés, afin de ne conserver qu'un nombre restreint de segments nettement visibles, comparables à ceux du modèle à localiser.

6.5 Mise en correspondance des segments

On dispose, à ce niveau, d'une part des segments rectilignes de contours extraits de l'image, d'autre part du modèle géométrique tridimensionnel du porte-aéronefs, connu a priori, et décrit par un ensemble de segments dans l'espace. Le but de cette étape est d'identifier, lorsque cela est possible, les segments du modèle présent dans l'image un à un. Naturellement, tous les segments du modèle ne sont pas toujours visibles depuis le point d'observation ; ils peuvent aussi ne pas avoir été détectés (ou pas sur toute leur longueur), ce qui explique la latitude laissée à l'algorithme. Cette étape ingrate est, en général, très difficile dans le cas d'objets complexes dont la position et l'attitude sont a priori totalement inconnues. On utilise une technique assez générale issue d'une étude précédente - surdimensionnée pour le problème posé. Elle s'adapte, en effet, à des modèles d'objets variés, ce qui dépasse le cadre de l'application visée. On envisage

donc des simplifications basées sur la simplicité du modèle.

Par ailleurs, on a vu plus haut que le fait de restreindre la position de l'objet à une portion de l'espace (aéronef aux environs du profil de descente) pouvait simplifier les traitements en proposant une configuration a priori du modèle proche de celle effectivement vue.

6.6 Calcul de la position de l'aéronef

Il s'agit maintenant, connaissant la correspondance précise entre les segments du modèle et leurs contreparties dans l'image, de calculer la position du point d'observation. Cela n'est possible naturellement que par la connaissance de modèle tridimensionnel précis du porte-aéronefs, et suppose également que la caméra est calibrée, c'est-à-dire que l'on connaît les éventuelles distorsions qu'elle introduit. Le problème de localisation de l'observateur équivaut à celui de localisation tridimensionnelle d'un objet mobile par rapport à un observateur fixe, qui a fait l'objet de nombreuses études dans le domaine de la vision robotique.

On utilise ici une méthode comparable à [4]. En effet, cette méthode s'applique aux modèles décrits par des segments de droites. De plus, elle permet une simplification sensible des calculs lorsque les segments du modèle sont coplanaires, ce qui est le cas des marquages vus sur la piste. Pratiquement, on estime d'abord la rotation du modèle, puis sa translation. On obtient alors huit solutions dites "admissibles". Le choix de la bonne solution parmi ces huit se résout aisément dans le cas de l'appontage, car on connaît, a priori, l'aspect approximatif du porte-aéronefs dans l'image, vu depuis l'aéronef. La méthode itérative décrite dans [5] permet d'affiner la solution ainsi obtenue. Le résultat final produit par l'algorithme est donc la position du modèle par rapport à l'observateur. On doit en déduire, par simple inversion, la position de l'aéronef par rapport au porte-aéronefs. Le profil de descente souhaité étant lui-même lié au porte-aéronefs, on est donc capable de mesurer l'écart de l'aéronef au profil idéal (figure 3).

On remarque que les écarts transversaux et verticaux permettent d'évaluer l'erreur à corriger. La distance au porte-aéronefs, également estimée, n'est pas utilisée.

7 CONSIGNE DE PILOTAGE

7.1 Calcul de la consigne de pilotage

Il s'agit d'évaluer la consigne à présenter au pilote en fonction des écarts mesurés par la vision. Cette consigne doit être

stable, c'est-à-dire qu'elle ne doit pas sauter ou trembler au rythme des mesures. On doit donc filtrer les informations fournies par la vision afin de stabiliser la consigne, sans toutefois exagérer l'inertie de la réaction. En tout état de cause, le réglage des gains de ce calcul passe par une expérimentation dans les conditions réalistes, et doit recueillir l'agrément des utilisateurs en termes de stabilité et de souplesse.

7.2 Visualisation de la consigne de pilotage

Pour présenter au pilote la consigne permettant de s'approcher au mieux du profil théorique de descente, on envisage d'une façon classique de visualiser en viseur tête haute l'objectif de direction à rejoindre comme le suggère la figure 4.

8 EXPERIMENTATION ET RESULTATS

On illustre ici la validité de l'approche en effectuant les traitements décrits plus haut sur une image de porte-avions prise dans le spectre visible (figure 5). Cette image est prise depuis une position grossièrement assez voisine de la trajectoire d'appontage, bien que décalée vers la gauche. Les conditions de prises de vue ne posent pas de problème particulier. Le modèle des marquages de la piste est par ailleurs illustré par la figure 6. On se limite volontairement aux grands traits du marquage. En effet, ceux-ci présentent la propriété de grande probabilité de détection en raison de leur contraste. De plus, leur linéarité correspond à la modélisation adoptée. Enfin, leurs grandes dimensions permettent une grande précision de localisation. Les dimensions réelles de ces marquages sont bien évidemment connues avec exactitude.

Le calcul des gradients seuillés permet de retenir les points de contours de l'image d'origine (figure 7). Les contours détectés représentent des lignes minces et continues, en accord avec le principe de l'algorithme de suppression des non-maxima utilisé. Il subsiste naturellement de nombreux éléments de contours non significatifs dans les zones perturbées de l'image.

Les points de contours sont alors chaînés et représentés par un ensemble de segments rectilignes (figure 8). Bien que l'aspect graphique de la figure ne diffère pas fondamentalement de la précédente, chaque élément de l'image est ici un segment de droite, et non un simple point de contour. La numérotation reflète les appariements avec les segments du modèle. On identifie ici la quasi totalité des segments du modèle du marquage, et ce pratiquement sur l'intégralité de leur longueur. Le segment

n° 11 n'est pas identifié car une rampe de catapultage le traverse, ce qui provoque son morcellement et empêche sa détection. On remarque également que certains segments ne sont pas détectés d'une extrémité à l'autre, ce qui survient souvent, quelles que soient les techniques utilisées. Cependant, les algorithmes de localisation utilisant ces segments sont insensibles à ce problème, puisqu'ils n'exploitent que l'axe des segments.

Cette coïncidence permet de calculer la position de l'aéronef par rapport au porte-avions. La figure 9 illustre les conventions utilisées. Les traitements permettent de situer l'aéronef dans un repère lié au porte-aéronefs.

$$\begin{pmatrix} X_c \\ Y_c \\ Z_c \end{pmatrix} = \begin{pmatrix} -11,9 \text{ m.} \\ -20,6 \text{ m.} \\ -146,2 \text{ m.} \end{pmatrix}$$

Ils permettent également de connaître l'orientation de l'aéronef (ici, en fait, de la caméra) relativement au même repère.

$$\begin{pmatrix} \Phi_x \\ \Phi_y \\ \Phi_z \end{pmatrix} = \begin{pmatrix} 6^\circ 18' \\ 4^\circ 1' \\ 0^\circ 7' \end{pmatrix}$$

Si l'on compare cette position à la trajectoire théorique idéale, on relève donc un écart transversal de 11,9 mètres puisque l'origine est située dans le plan vertical contenant l'axe de la piste. Pour l'écart vertical, on trouve une différence à la rampe de descente idéale de 11,3 mètres (figure 10).

Le filtrage de cette mesure effectuée en continu permet de calculer une consigne de pilotage appropriée, présentée au pilote en viseur tête haute.

9 CONCLUSION

L'étude permet de valider le concept d'appontage aidé par traitement d'images embarqué sur l'aéronef.

Les techniques employées, adaptées de techniques récentes générales en vision par ordinateur, permettent effectivement de localiser l'aéronef dans les trois dimensions, condition nécessaires au contrôle de la trajectoire et au calcul d'une consigne correctrice de pilotage.

La suite des travaux comprend la validation quantitative des calculs effectués sur un grand nombre de situations réelles et l'intégration électronique des traitements permettant l'exécution des algorithmes en temps réel.

Par ailleurs, le recours à l'imagerie thermique permet naturellement d'étendre le domaine d'utilisation à une obscurité et une passivité totales.

10 BIBLIOGRAPHIE

- [1] "Optimal Edge Detection using Recursive Filtering", R. Deriche, 1st Int. Conf. on Computer Vision, London, 8-12 June 1987.
- [2] "Chainage efficace de contour", G. Giraudon, Rapport de recherche 605, I.N.R.I.A., février 1987.
- [3] "Vision stéréoscopique et perception du mouvement en vision artificielle", F. Lustman, Thèse de l'université de Paris-Sud, Orsay, 1987
- [4] "Determination of the attitude of 3-D Objects from a Single Perspective View", M. Dhôme, M. Richetiq, J.-T. Lapresté and G. Rives, I.E.E.E. Trans. on P.A.M.I., December 1989, Vol 11 Number 12, p. 1265-1278.
- [5] "Three-Dimensional Object Recognition from Single Two-Dimensional Images", D. Lowe, Artificial Intelligence, Vol 31, 1985, p. 355-395.
- [6] "Intégration du pilotage et des systèmes d'aide à l'appontage pour les opérations embarquées", B. Dang Vu et P. Costes, Proc. of the 78th AGARD Symposium in the Flight Mechanics Panel on Aircraft Ship Operations, Seville , May 1991.

11 COLLABORATION

Les expérimentations informatiques sont dûes à R. Goulette.

12 FIGURES

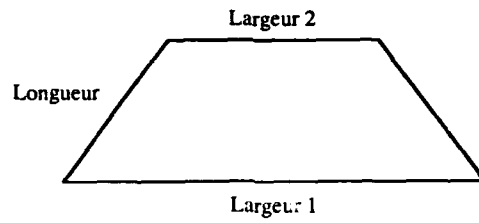


Figure 1

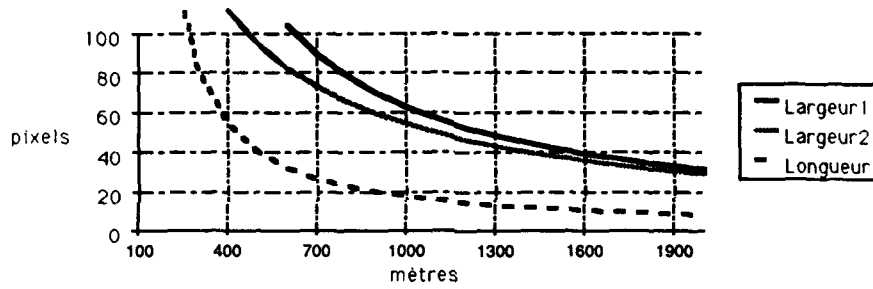


Figure 2

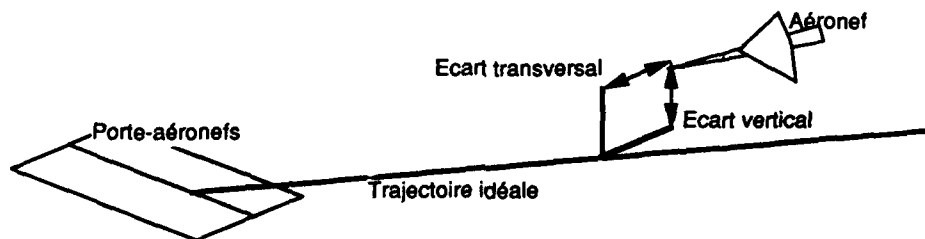


Figure 3

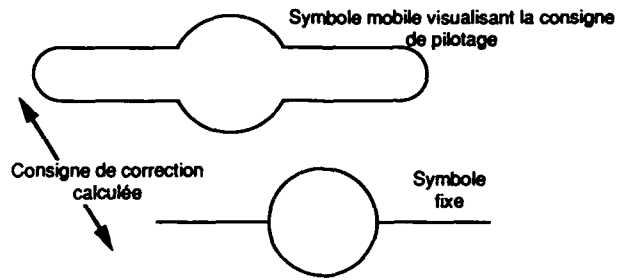


Figure 4

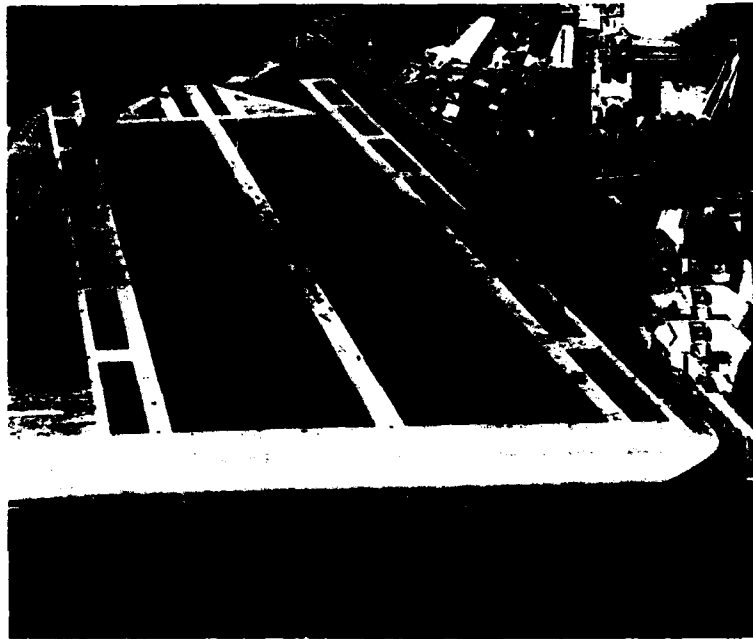


Figure 5

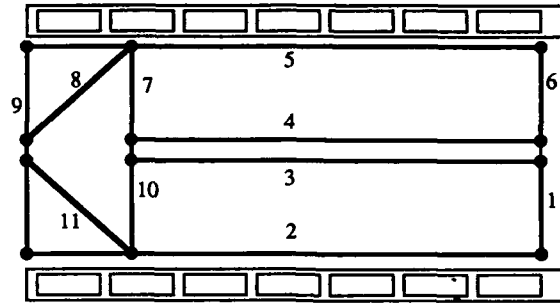


Figure 6

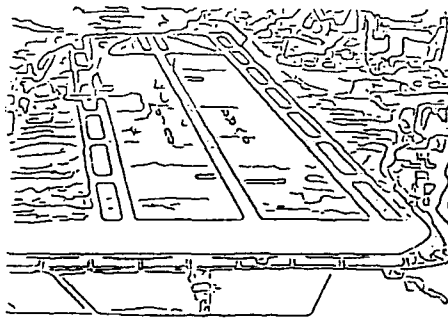


Figure 7

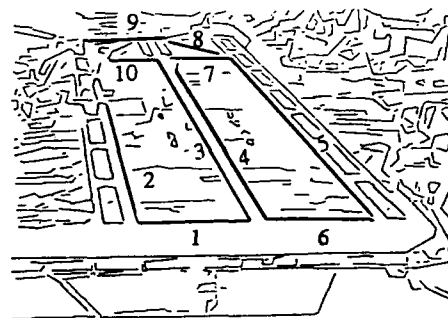


Figure 8

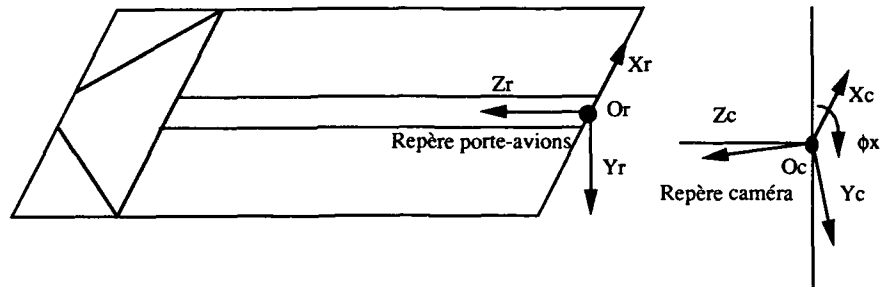


Figure 9

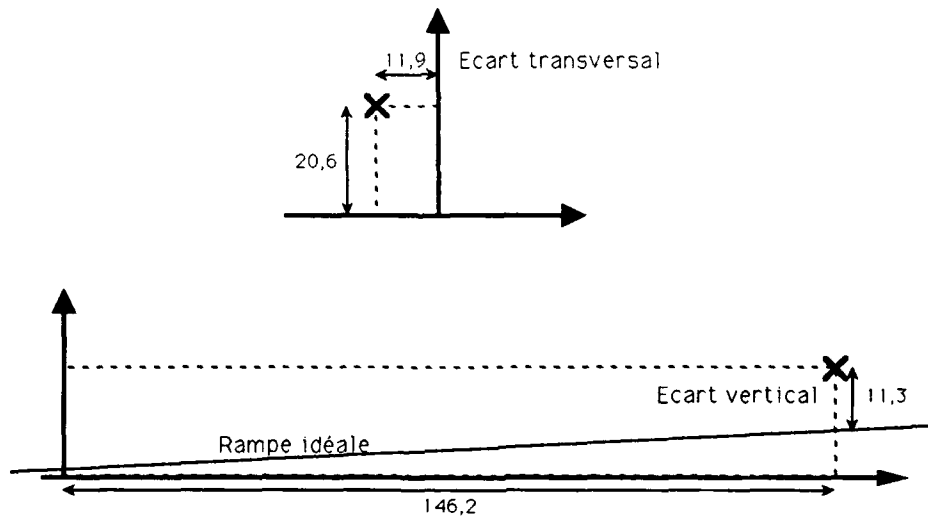


Figure 10

APPROACH AND LANDING GUIDANCE

A. J. Smith
 E. J. Guiver
 Flight System 2
 Royal Aerospace Establishment
 Bedford MK41 6AE
 England

SUMMARY

The final approach and landing of any aircraft operating from a ship is always a difficult task, even in benign conditions. Ship motion, adverse winds and atmospheric attenuation compound the problems. High levels of integrity and reliability are an essential feature of any guidance aid in the ship environment since diversion facilities are often not available. Issues related to costs, maintainability, levels of training and covertness further constrain the choice of guidance aid. The handling characteristics of the user aircraft and operational procedures also influence the choice of aid.

To achieve the objective of regular and safe operations in all weather conditions, some form of guidance must be provided. The options range from painted markings and lighting systems that are used by the pilot to augment naturally occurring visual cues to precision radio or radar systems that are integrated into cockpit displays and flight control systems. In military operations there is a perceived need for passive or covert forms of guidance. The development of electro-optical sensors in recent years has increased the number of options and the availability of GPS will provide even more potential solutions to the design problem of providing precision guidance.

The topic of approach and landing guidance has encouraged a large amount of research and development over the years, with many special-to-type solutions being devised. Except for the helicopter landing case, where relatively little research and development effort has been expended, the system designer is confronted with a large number of potential solutions.

1 INTRODUCTION

Throughout the history of naval aviation the landing of aircraft on the flight deck of ships has been identified as a hazardous activity; one in which pilot workload and anxiety levels are frequently above desired levels. The operational effectiveness of the aircraft as a primary weapons system is however crucially dependent on the ability to recover it after a sortie. Deck landings are difficult for several reasons:

- the deck area is very small
- significant obstacles are located close to the landing deck
- the view of the deck available to the pilot is often restricted by aircraft structural members and

- the visual cues available to the pilot are significantly less than those available on shore, both in content and extent.

Ship motion and ship manoeuvring, variations in relative wind speed and direction resulting from ambient conditions and the operational necessities of pre-set ship courses, wind turbulence caused by the ship superstructure, night operations and reductions in visibility caused by atmospheric attenuation all increase the level of difficulty. Because the individual and compounded effects of these various parameters are not easy to quantify precisely in operational conditions, significant penalties are imposed on tactical planners who have to make conservative decisions as to when to launch and recover aircraft.

Approach and landing guidance systems can make a major contribution to the amelioration of these problems by enhancing the precision and repeatability of the operation and by overcoming or reducing the effects of various environmental conditions. A well designed guidance system increases the operational availability of the aircraft and reduces pilot work-load.

2 A TOTAL-SYSTEMS APPROACH

The achievement of safe landing operations at a consistently high level of availability is dependent on the provision of a comprehensive recovery system that takes account of several inter-related factors including:

- (i) Physical characteristics of the aircraft and ship deck.
- (ii) Environmental conditions.
- (iii) Aircraft handling and performance.
- (iv) Pilot performance.
- (v) Aircraft displays and controls.
- (vi) Guidance aids, performance and characteristics.

The designer of approach and landing guidance systems must take account of the impact of all these factors during research and development work. Guidance aids are best developed in an environment where the total recovery problem is addressed by the various specialists working in an interactive environment.

The approach and landing guidance system that is chosen for a given aircraft/ship combination will generally consist of more

than one aid. System integration is therefore also of paramount importance at this level.

The successful development of any approach and landing guidance system involves several phases - definition of operational requirement, performance specification, technology definition, prototype build and test and a total recovery system trial evaluation.

Procurement of a satisfactory guidance system depends on good quality work in all of these phases. This paper considers the first 3 phases, with particular emphasis on operational requirements and the technology choices available for systems currently under development.

3 OPERATIONAL REQUIREMENTS

The operational requirements documentation should describe what the system is required to do: not what the equipment should be. Broadly the operational requirement for any approach and landing guidance system will state that a certain type of fixed wing aircraft or helicopter is to be operated from the deck of a certain class of ship. This statement defines the physical dimensions of the problem.

However, a far more explicit document is essential. Major features of the requirements should include:

- (i) A description of the functions of the ship/aircraft combination as a weapons system.
- (ii) Acceptable limiting environmental conditions such as minimum visibility, maximum precipitation rates, wind speeds and sea states.
- (iii) An indication of the level of operational readiness required from the system.
- (iv) The frequency of landing required, especially in multi-aircraft scenarios.
- (v) The overall ATC environment including clear EMCON policy guidelines.

At this stage of the process it is important that the user produce a clear and well-founded set of requirements that describe what the system is required to do and that the research team understand that the document as written is their brief describing the task that the system should perform. The importance of this stage cannot be over-emphasised. If there is indecision and imprecision in the operational requirement then the likelihood of a system being developed that 'does the job' is not very great. Furthermore, cost over-runs will probably be induced.

4 PERFORMANCE SPECIFICATION

The performance specification is based on the operational requirement. It translates what the user wants into a technical specification that defines the performance characteristics of the total approach and landing guidance system. From this is deduced the apportionment of the total

specification limits to the individual system modules. The performance specification should also define any practical constraints on system design.

The specification should be developed by a multi-discipline team that appreciates both the requirements of the user and the impact on the total recovery system, of those elements such as aircraft handling and performance, discussed in paragraph 2.

The performance specification must address the following areas:

- Accuracy
- Data rate
- Range and (angular) coverage
- Approach and landing profiles
- Signal formats
- Field-of-view
- Stabilisation
- Atmospheric attenuation
- Signal covertness
- Electrical power requirements

4.1 BASIC CONCEPTS

The operation of both fixed and rotary wing aircraft from ships is increasingly an all weather task. To achieve these objectives it is necessary to identify a system or combination of systems that will enable a combat aircraft to locate, approach and land on a specified ship by day or night, irrespective of the weather conditions, or within limits agreed at the operational specification stage of the project.

Although operationally attractive the cost and complexity of a fully automatic landing system continues to be too high. It is therefore assumed in this paper that what is required is a system that allows the approach to the ship to be flown on instruments to a minimum safe decision range or height after which the final approach and landing will be flown by the pilot using outside visual references, as his primary guidance.

In determining the specification for the performance requirement it is essential that the time critical nature of operations to a ship and the lack, in many circumstances of a diversion facility be recognised.

The operational effectiveness of a large decision range against the increasing complexity and hence cost when this is reduced must be balanced. In determining this figure it is instructive to consider Fig 1.

This figure illustrates the occurrence of various meteorological visibility in hours per year. Visibilities below 100 m have a low significance because of their limited occurrence level. The range of interest for precision guidance systems lies on the plateau between 100 and 2000 m.

The Royal Navy currently looks for operational visibility limits of 800 m for fixed wing aircraft and 400 m for rotary wing aircraft, together with 200 ft and 100 ft cloud bases respectively. However, operational studies have suggested a minima of 100 m visibility and 100 ft cloud base as a design goal for helicopter recoveries under strict emission control (EMCON) conditions.

It is relevant to note that for specified areas in the North Atlantic the adverse effects, in terms of probability of occurrence place visibility behind high-winds and significant sea states, see Fig 2.

Radio communications between the ship and aircraft is liable to suffer deterioration of its basic systematic performance due to multipath signals reflected from the sea surface. The magnitude of the problem will be a function of the system and the variation in the ship-sea-aircraft geometry. Initially the effect will be observed as an increase in system noise but could be so great as to cause the system to fail in a cyclic manner. Optical guidance will be adversely effected by ship motion, most significantly by pitch roll and heave.

Stabilisation of radio systems can be produced to deal with such problems although their reliability will depend on high levels of processing in order to ensure that only soft and predictable failures occur. Extensive built-in self test is also essential. Visual aids can be stabilised to combat the effects of pitch and roll when the aid is essentially a point source. It is not possible to stabilise systems that rely on patterns of lights and markings.

Ship motion therefore makes the hover and land-on manoeuvres difficult particularly at night. This is an area of the recovery operation that has been neglected in research programmes in the past, but must be addressed now if the demanding operations conditions to be encountered in the future are to be met.

It has been normal practice for all aircraft landings on ships to try to reduce the effects on these operations of cross-winds and ship induced turbulence by choosing a ship course for the land-on such that the final approach is made in-to-wind. Operational constraints, which preclude such flexibility are expected to apply in the future, particularly for helicopter operations. Thus future guidance systems must be developed that support adequately this new and significant requirement.

It should also be noted that in addition to the problems caused by the operational environment there are a number of fundamental constraints that apply to any guidance aid. These are discussed in the following paragraphs.

4.2 VISUAL AIDS

Visual aids conventionally consist of deck markings and lights that augment the visual cues that are available from the pilot's view of the outside world scene.

Visual aids offer the great advantage of being essentially simple low cost, low technology, using highly reliable and easily maintained equipment. They require no aircraft equipment. In a wide range of conditions day and night they can provide adequate cues for the task. However, for current and future needs they have limitations which prevent any further significant fundamental developments. These limitations include:

- Range limitations in low visibility conditions (Fig 3). There are practical limits to the levels of intensity that can be produced from practical sized light fittings. Furthermore, intense light sources produce disabling glare at close ranges. This latter problem is more acute on ships than at airfields because the distances that the aircraft is from the lights when it is close to the landing are much reduced due to the small size of the deck.
- Angular discrimination limitations. Where a visual aid consists of a pattern of lights a pilot can only receive guidance out to the range at which the individual lights can be discriminated. In practical terms the minimum usable separation is 3 min arc, equivalent to 1 metre between lights for every kilometre of required range, ie for two lights to be discriminated at a range of 10 km they must be mounted at least 10 m apart.
- Colour, intensity and frequency discrimination limitations. Pilots are able to discriminate subtle changes in colour, intensity or frequency of a light signal if there is a reference source for comparison. Where single source aids are provided, the number of readily identifiable colours, intensities and frequencies are therefore very limited and signal coding to indicate position or rate is therefore also very limited. For long range signalling only red and green lights provide unambiguous signals under all conditions. Pilots can just discriminate a 2:1 change in intensity, 5:1 is a more practical value. A similar ratio is required for frequency coding. With this latter method of coding it is found that if the frequency is below 2 Hz, the data rate is too low to meet the pilot's need for guidance and frequencies above 5 Hz are found to be discomforting for constant viewing.
- Eye illumination threshold limitations. Unless the level of illumination is above a minimum value the eye will not detect the presence of a light source. In addition, if the received energy level is above a certain value the light is perceived as a glare source. The difference between these 2 boundary conditions is typically 1000:1 in illuminance levels. However, this operational range of 3 orders of illuminance is related to an absolute scale of background luminance spanning at least 11 orders (10^{11}) (ie the eye adapts to ambient light levels). Thus at any instant, depending on the adaptation state of the eye, the required level of luminance for visual aids to work effectively can be anywhere in the range 10^{-8} to 10^3 lux. The intensity of the light must be chosen to provide the

required performance in terms of maximum and minimum viewing ranges for the aid.

Other considerations when deciding on the application of visual aids to a guidance problem include:

- All visual cues rely on there being a contrast between the light or marking and the background. The presence of surface water or shallow fog, particularly when the sun is at a low elevation angle can so modify the background luminance that an aid becomes un-usable. Under such circumstances a light that is generally prominently displayed may not be seen from a range as large as the range at which the ship that it is mounted on can be seen.
- Flashing lights are not infallible attention getters. There are practical circumstances where the ship will be detected before the flashing light that is mounted on it. The location of a flashing light can also be difficult to determine, when it is the only visual cue in the field-of-view. In these situations a pilot may see occasional flashes and therefore conclude that the aid is malfunctioning when in fact his eye-point-of regard is drifting during the period when the light signal is not displayed, thus causing him to miss seeing subsequent flashes.

4.3 NON-VISUAL GUIDANCE

Recent major advances in sensors and signal processing have impinged beneficially on the utility of the whole radio frequency band thereby offering the possibility of a significant increased capability for military applications. These advances have resulted in improvements to existing equipment performance. The potential for new adaptive systems also exists. These advances are timely in that there is an increasing need for the system flexibility that comes from the combining of sensors. There is also an increasing realisation of the potential and need for covert operations.

However, as with visual aids there are some fundamental limitations:

- Atmospheric transmission losses
Although the technological advances in sensors and signal processing are applicable across the spectrum the increased bandwidth available in the millimetric and visible fields is where the most benefit will be gained in future systems. It is unfortunate that it is at these higher frequencies that atmospheric transmission losses are not only high but variable, as shown in Fig 4.
- Aperture size
The size of aperture required for the transmission and reception of radio signals is directly dependant on the operating frequency. For

example to produce a 1° guidance beam the following dimensions are required:

Frequency	Aperture dimension	Practicality on a ship
200 MHz	100 m	Impossible
4 GHz	5 m	Difficult
60 GHz	300 mm	Easy

These factors are shown in more detail in Fig 5. From this figure it can be seen that whilst recognising the limitations imposed by atmospheric attenuation frequencies above the UHF band are the most suitable for the guidance task. At these frequencies aperture sizes for transmitter and receiver arrays are correspondingly small and are therefore more physically compatible with the limitations imposed by ship environments.

- Multipath signals

The problem caused by multipath signals can be illustrated by considering a likely elevation profile for helicopter recovery consisting of an initial long range horizontal element, the height being between 400 and 800 ft, followed by a descent down a 3° glide slope and terminating in a plateau starting at 1.5 n miles, 70 ft above sea level. At the start of this plateau the aircraft-sea-ship geometry is as shown in Fig 6.

At these very low angles the sea reflection coefficient is very nearly unity and hence periodic cancellation of the guidance signal is highly likely. The geometry of the situation is illustrated in Fig 7 together with the received signal strength. The high integrity required of non-visual guidance compels us to address this problem.

5 TECHNOLOGY

5.1 Visual aids

The suites of visual aids that have been developed to support aircraft operations are shown for fixed wing aircraft in Fig 8 and for helicopters in Fig 9.

In general, ship-borne visual aids only give meaningful approach alignment and glideslope guidance from ranges below 2 km. The fundamental limitations discussed in section 4.2 impose these practical limitations on the current systems. However, research and development is producing new aids that enhance the guidance significantly. For fixed wing aircraft long range approach guidance in both axes has always been a goal, since good landings are based on long stable approaches. High intensity lighting aids, stabilised against pitch and roll motions and having signal formats

based on a combination of colour and frequency coding are being developed. These aids are intended to augment the existing facilities.

An example of this new type of guidance is shown in Fig 10. Being essentially digital in nature and being limited to a small number of sectors it results in guidance that is limited in sensitivity but which is useful as an aid to deliver the aircraft into the more detailed guidance at close range where the greatest precision is required.

For helicopter operations research is largely focussed on short range visual signalling. Recent research by the RAE (Bedford UK) has produced an improved form of glideslope indicator. The signal format is shown in Fig 11 and the light output characteristics are shown in Fig 12. The improvements that this new aid offers include:

- (i) a usable range that is twice that of earlier systems. The aid can also be used in day time.
- (ii) wider azimuth coverage, to make acquisition and use easier, particularly in crosswind conditions.
- (iii) unambiguous signals in all conditions, by avoiding the use of white or yellow as a signal colour, since most ambiguous colour signals are perceived as white or yellow in this type of projection system.
- (iv) improved stabilisation, so that in roll and pitch the guidance is maintained within 2 min arc of the datum position

Textural cues obtained from the deck markings, which are floodlit at night are an essential feature of the hover and landing manoeuvres. Considerations of covertness cause concern when flood lighting is used. One possible solution to this problem is to use electro-luminescent panels to produce internally lit markings. Such a system emits usable light levels in the directions required by pilots whilst emitting very little light close to the horizontal, thus making it difficult to see from surface vessels. Choice of appropriate phosphors can give an NVG compatible option.

The potentially most significant area for research for helicopter visual aids is related to the cues required for the hover over the deck and the subsequent landing manoeuvre. This is a difficult area that has not been researched in the past although it profoundly and adversely affects the ship/helicopter operational envelope, especially at night. Research at RAE (Bedford) is currently addressing this issue in a novel manner.

The prototype of a ship based sensor system that detects the position of the helicopter over the deck in 3 axis to accuracy better than 0.5 M at a data rate of 10 Hz has been developed and built. Flight and simulator trials will be the basis of a development programme to devise a display of hover and landing guidance that will be located on the ship superstructure immediately in

front of the pilot. The novel features of this development include the concept of an active visual display of optimum format and symbology to indicate the necessary information rather than a passive fixed lighting pattern or format. Since helicopter position signals are generated by the sensor it is possible to use software to remove all rotation and translational motion from the guidance and to compute rate aided guidance to augment the basic positional information. Fig 13 illustrates the concept.

5.2 NON-VISUAL AIDS

In low visibility conditions the aircraft has to be flown close to the sea and the ship before visual contact is achieved. Therefore any non-visual guidance aid must provide accurate position information at an adequate data rate with very high integrity.

Typical guidance accuracy requirements at the visual transition are illustrated in Fig 14.

The achievement of regular and safe approaches in all weather conditions is critically dependant upon the provision of low noise, reliable and accurate elevation guidance, range information and azimuth guidance.

The following systems are currently candidates to provide the necessary guidance in the next generation of equipment:

- a. Inertial navigation system (IN)
- b. Global positioning system (GPS)
- c. Airborne radar (AR)
- d. Ship-based infra-red trackers (IRT)

INERTIAL NAVIGATION SYSTEM (IN)

The performance of IN systems has improved considerably in recent years through developments in gyroscope technology and computing capability. Simple systems typically have a velocity error of up to 5 knots whilst for modern precision systems this is reduced to 0.1 knots. At normal approach speeds the precision system velocity error would result in approximately 1 m/km drift in position indicated. IN by itself is not able to meet the recovery guidance need, since accuracies of the order of 2 m in elevation guidance datum are required. See Fig 14. However the short term accuracy capability could be significant in a multi-sensor system.

GLOBAL POSITIONING SYSTEM (GPS)

It seems likely that GPS will be fitted to many aircraft. It will be fitted to the Merlin but other helicopters may not warrant the weight or cost penalty of a 5-channel receiver. However lower cost/performance receivers could be developed in the future thereby broadening the fitting of GPS.

Performance measurements of a GPS (P-code) receiver indicate that height information has a potential datum error of up to 10 m. The plan position performance is

significantly better. A height error of this magnitude is too large for the system to be used for approaches to low heights.

Any GPS employed for approach guidance to a ship will be operated in a relative position mode. This will reduce some of the errors. Nevertheless GPS alone will not meet the guidance accuracy needs for guidance to low heights and short ranges.

AIRBORNE RADAR (AR)

A conventional airborne radar with frequency agility, antenna design to reduce side lobes and controlled sector scan will still be detected by electronic intelligence (ELINT) systems at a very long range. Consequently use of AR will probably have to be restricted to essential activities in an attempt to reduce the exposure to anti-radiation missile response. However assuming it will be operationally acceptable to occasionally illuminate the ship down to ranges of 5 km, the question arises; would the ship position deduced from this scan provide sufficient information to enable a precision approach to be made? Existing airborne radar angle accuracies are no better than 1.5 mR. Ignoring ship lateral motion during the approach this angular accuracy would result in an error due to the radar fix of the order of 7.5 m. Such an error is unacceptable in the elevation guidance. To achieve a level of performance commensurate with a precision approach with such a system would require nearly an order improvement in the angular resolution. This would only be achieved at considerable cost. It must also be noted that the provision of the essential approach path datum relative to the ship would require continuous knowledge in the aircraft of the ship range, speed and direction after radar switch-off.

SHIP BASED INFRA RED (IR) TRACKER

A stabilised IR tracker on the ship could provide azimuth and elevation angular approach guidance and range information with an accuracy of 3 percent in all axes. The system is shown in Fig 15. As with GPS and AR a ship-aircraft data-link would be needed.

It is likely that with continuing development of IR systems their resolution capability will improve and possibly equal that of the eye.

One major disadvantage of any IR system is that it is prone to limitations caused by atmospheric attenuation. With a visibility of 400 m an IR operating range of 1600 m in wet fogs can be achieved. This limitation necessitates the use during an approach of a suitable alternative guidance aid having adequate performance down to a range of 1300 m. An IR tracker cannot, by itself, satisfy the all-weather requirement although it may form a component of a total system. For example, if on-board sensors could be used to guide the aircraft to a range of 1300 m, then those sensors plus the IR tracker could provide a complete covert guidance system.

5.3 DISCUSSION

It is clear that no single equipment visual or non-visual is capable of fulfilling all

the approach and landing guidance needs. Consequently some fusing of appropriate systems is needed. At the basic level it is envisaged that the use of complimentary and consistent visual and non-visual aids will continue. An important consideration must be the increasing awareness by the military of the need for Low Probability of Intercept (LPI) or covert operations. Receive-only systems such as IR and GPS integrated with the stand alone IN system are attractive. IR has severe limitations due to its poor wet fog performance. It could however, be of assistance on the ship in monitoring aircraft on the approach to provide warning of deviations from the optimum elevation profile. Prior to landing, visual aids have the advantages that by control of the lamp power the usable range can be readily adjusted. The intensity setting being determined by ambient viewing conditions.

It can be concluded that although individual aircraft and their proposed equipment fit will probably drive the choice of integrated systems the best performance is likely to be achieved using a relative GPS and an IN system, together with a radio altimeter and a two way ranging ship to aircraft data-link for the initial approach phase, blending in visual aids for the final approach and landing. The two way data link is necessary for relative GPS operations but it would also provide accurate range between aircraft and ship which together with radio height could be employed to generate accurate elevation guidance. If such a recovery package is to be provided then there are two elements which require attention to satisfy the LPI/covert requirements; the radio altimeter and the two-way data link.

Where the peak of the transmitting antenna polar diagram is directed at the sea, eg for a radio altimeter, the horizontal power level is likely to be low. It can be further reduced by adaptive systems which adjust the beam pointing angle to accommodate aircraft manoeuvres on the approach whilst constantly adjusting the transmitted power level to a minimum compatible with satisfactory system performance. The beam width of the transmitter array could also be reduced for such a stabilised system further reducing the radiated power. An LPI system therefore appears to be easily achievable. However, the LPI/covert data-link between the aircraft and ship is much more difficult to achieve. Operationally it may be essential that the covert option be provided.

Intercept susceptibility is a function of many variables such as transmitter power, bandwidth, polar diagrams, signal/noise ratio, spreading function, system operating range and detection range all of which can be massaged to reduce the likelihood of detection. For a selected set of conditions the chance of detection of an LPI system would be extremely low but still result, by chance, in the system being detected at switch-on.

COVERT GUIDANCE

By covert or secret is meant a system where no perceptible emissions occur. This is a very difficult objective but the operative word is 'perceptible'. We will need to

first define our operating range and then the perceptible range. This latter range is that at which an enemy could detect the transmission. Advances in navigation equipment accuracies have allowed the operating range of the approach and landing guidance to be reduced and currently we can consider 2.5-3 n miles to be adequate. The visual detection of a ship by an observer will clearly depend upon the visibility. In clear weather due to earth curvature it will also depend upon the observers height and mast head height for the observed ship. Ranges of 10-20 n miles are a practical maximum. The perceptible range will ideally equate with this visual detection range.

We can assume therefore that the relevant design ranges are 2.5 n miles for the user and 10 n miles for the enemy observer. The ratio of ranges is only 4 which gives the operator an advantage over the enemy, due to geometric dispersion of only 6 dB. This is not significant and means must be introduced to improve this figure. Although spread spectrum, frequency hopping and/or pencil beams can effectively reduce power levels, they are all basically LPI methods and not covert. The suggested alternative is to operate the guidance system at an atmospheric stop band frequency of which there are a number, the lowest frequency one being centred on 60 GHz, see Fig 16. At this frequency, at sea level, due to oxygen absorption there is an additional propagation loss of 15 dB/km above the 6 dB from geometric losses. This would result in an extra 112.5 dB for the 2.5-10 n miles operating to detection range previously considered. This would increase to 255 dB if the higher range figures are assumed. Such attenuations effectively build a natural wall around the transmitter. Nevertheless, spatial power management is still important and consequently both transmitter power and multipath effects must be addressed. However, operating in a stop band does bring with it a need to produce considerable millimetric power levels to balance the power budget at the operating range needed. The current millimetric solid state power generation capabilities do not satisfy the perceived operational specification. Consequently it will be necessary to move the operating frequency away from the peak attenuation at 60 GHz to balance the system power budget. Fortunately, such a system having achieved a significant degree of covertness by operating in a stop band can then benefit from what previously were referred to as LPI method. The two-way ranging facility needed can achieve higher accuracy by employing a spread spectrum modulation which with a readily achievable processing gain of 100 would reduce the peak power level by a further 20 dB. Transmitter power management to ensure an acceptable bit error rate together with acceptable data integrity are also straight forward with a two-way system. Clearly, although the operating frequency employed is paramount in the covert debate, the management of transmitted power is equally important.

As explained earlier multipath signals reflected from the sea surface combine with the direct signal and cause cyclic variations to the received signal strength. If a robust link is to be provided, essential in the non-visual guidance application then

adequate power budget margin must be provided for the whole of the approach. This specifically applies during the low signal periods when the direct signal and multipath are in anti-phase. The consequence of this would be that excessive power would be propagated at those elevation angles when the direct signal and multipath combine. This would clearly jeopardise the covertness of the system and in any case is inefficient in the use of expensive millimetric power. It would therefore be prudent to introduce on the ship a suitable adaptive data-link array. The aperture would only need to be 300 mm high and with current printed circuit techniques and parallel processing a tracking, high gain beam could be generated. Such an adaptive array would be able to both deal with the multipath problem and stabilise the spatial beam against the effect of ship pitch.

The technologies developed to meet the covert task set out above are equally applicable to a radio altimeter, although the complexity of active power management may not be operational needed for a 60 GHz system.

6 CONCLUSIONS

- 1 Future guidance will be a mix of visual and non-visual elements.
- 2 New visual aids will involve the provisions of long range guidance for fixed wing aircraft operating in reasonable visibilities particularly at night. However, the major development in helicopter operations is expected to be a visual aid that uses a ship-mounted display driven by an accurate position sensor. This aid will provide hover and landing cues and in high sea states will significantly extend the operational envelope.
- 3 It can be concluded that although any new non-visual guidance system will, on economic grounds, be biased towards using the equipment fit needed for other tasks, the best performance will be achieved with the system previously described. This requires a GPS, IN and radio altimeter in the aircraft with a two-way ranging data-link to the ship on which is conveyed the ship's GPS location. The perception of our military customers to the need and hence form of this link has still to be defined.

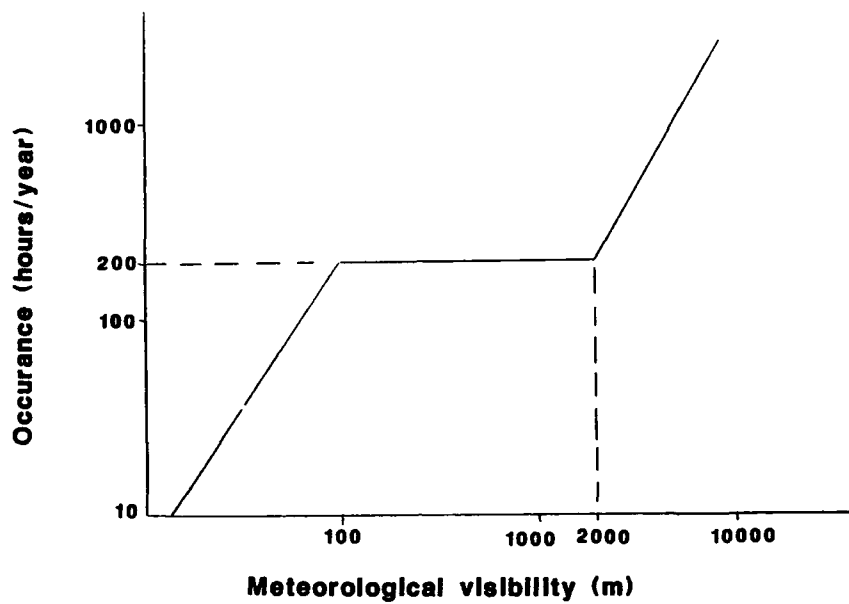


Fig 1 Typical annual occurrence of given visibilities

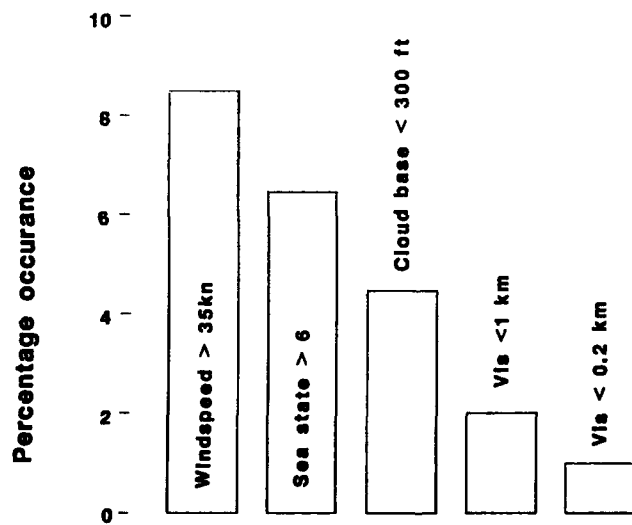


Fig 2 Relative frequency of occurrence

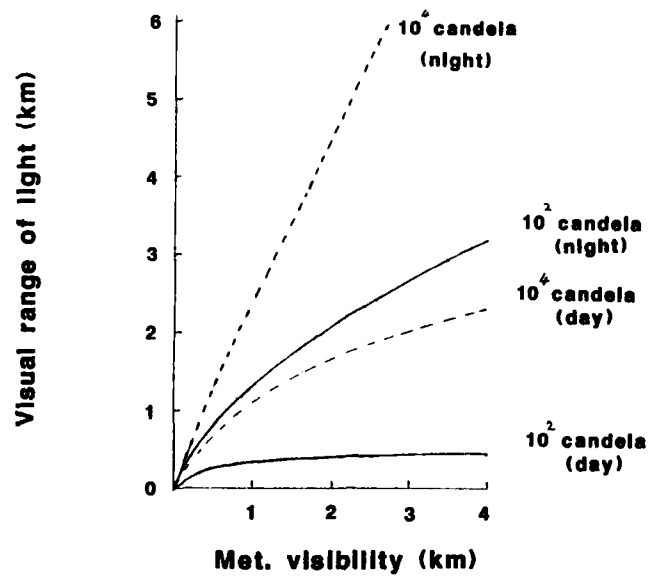


Fig 3 Relationship between VR, MV and light intensity

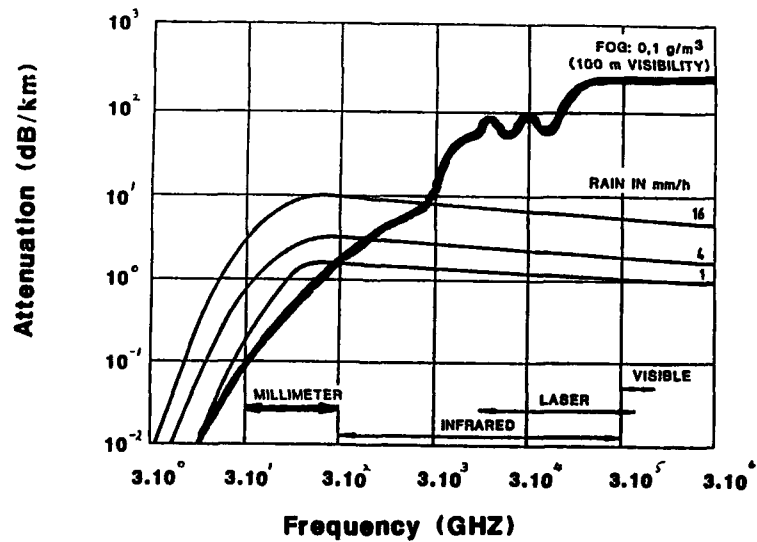


Fig 4 Atmospheric attenuation due to fog and rain

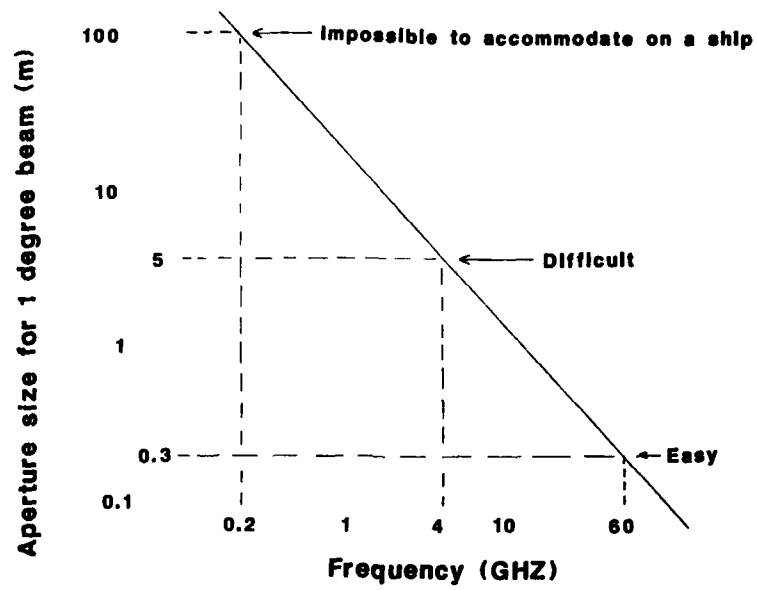


Fig 5 Relationship between frequency/aperture size

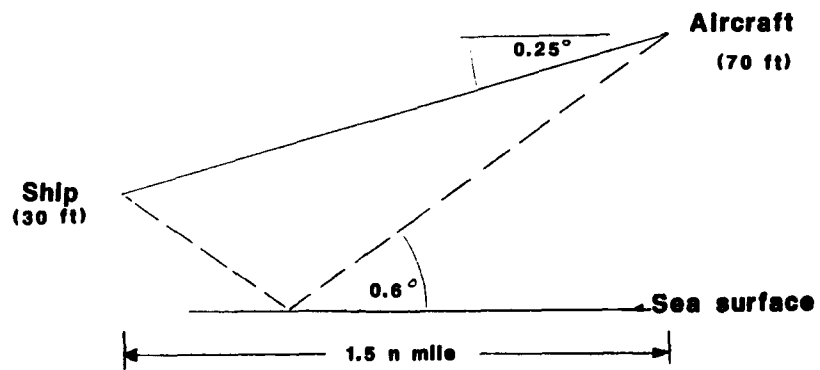


Fig 6 Multipath geometry

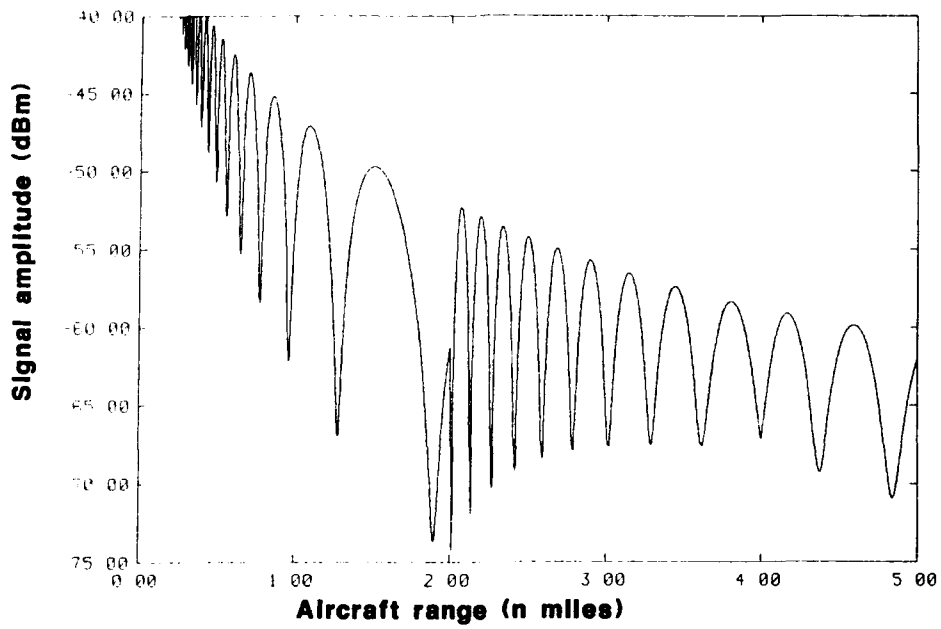


Fig 7 Typical effect of multipath on received signal

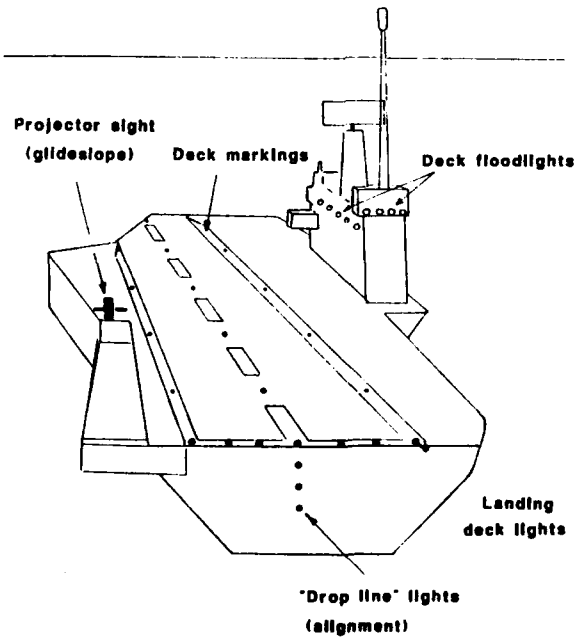


Fig 8 Fixed wing visual aids

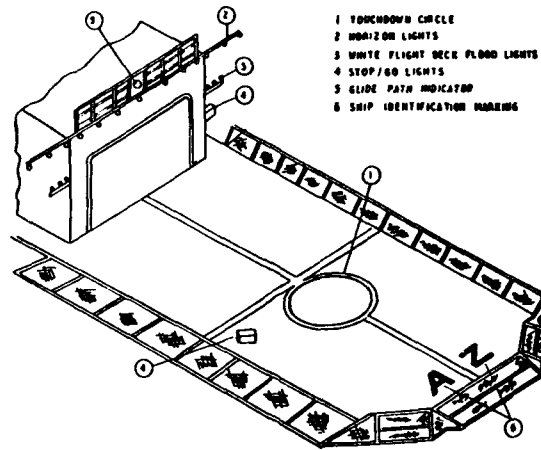


Fig 9 Typical rotary wing visual aids

$L @ L_2$ emit sharp transition red/white beams

Divergence of red/white interfaces $\approx \pm 0.5 \text{ deg.}$

Beam Intensity 30,000cd (white)

Beam spread $\approx 15 \text{ deg.}$

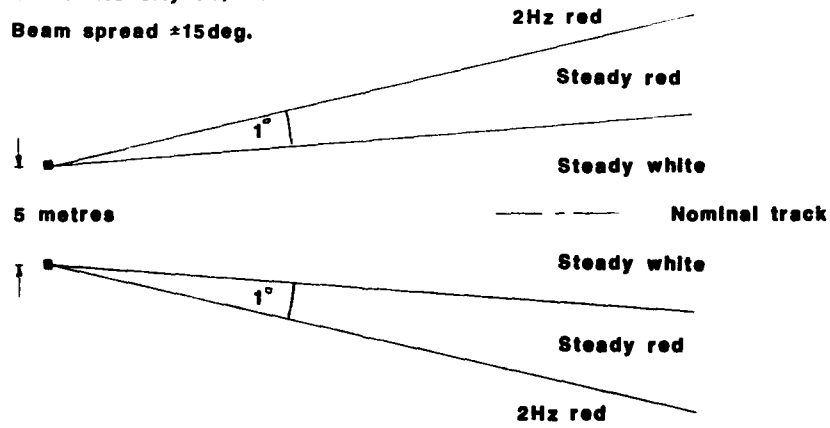


Fig 10 Long range azimuth guidance

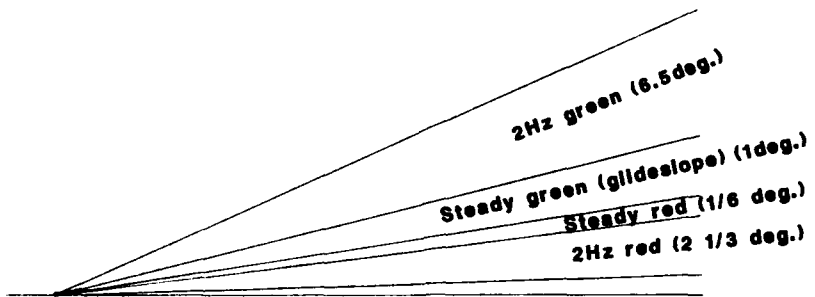


Fig 11 HAPI signal

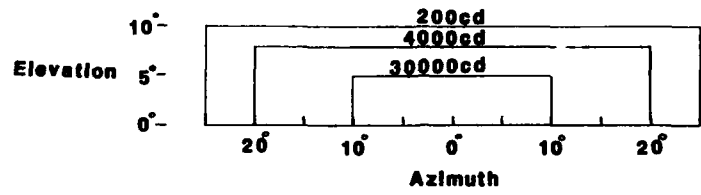


Fig 12 HAPI beamspread

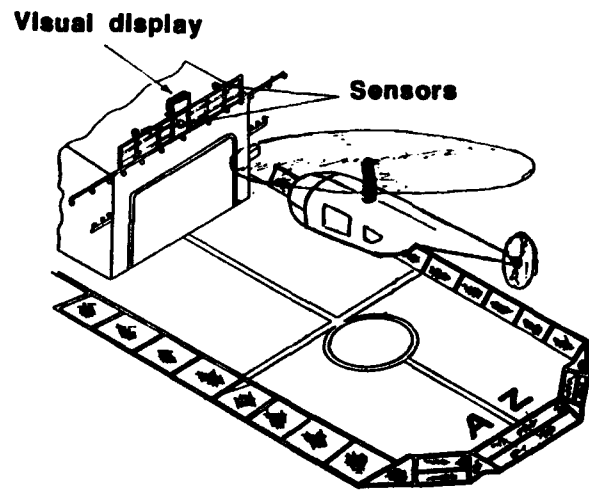


Fig 13 Hover Q concept

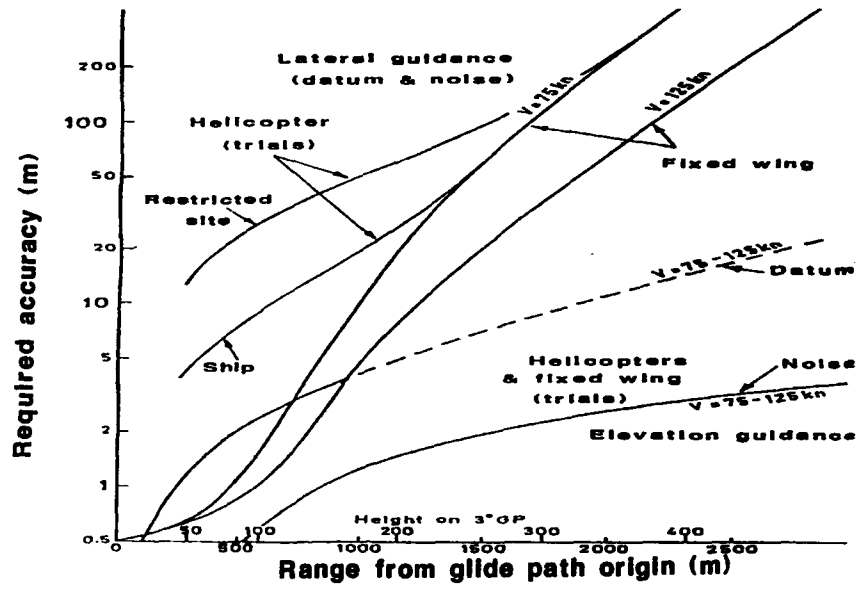


Fig 14 Required guidance accuracy at visual transition

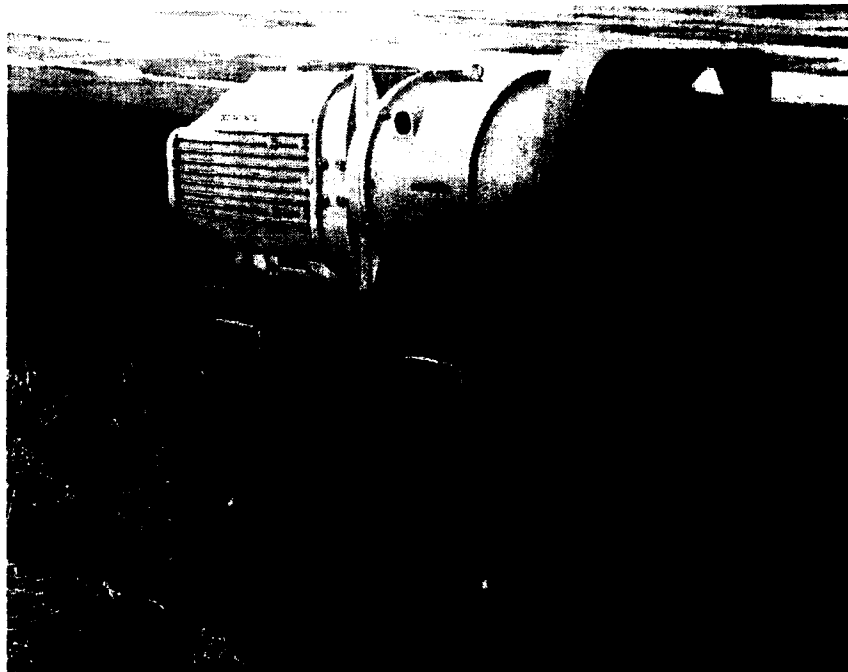


Fig 15 IR tracker-sensor unit

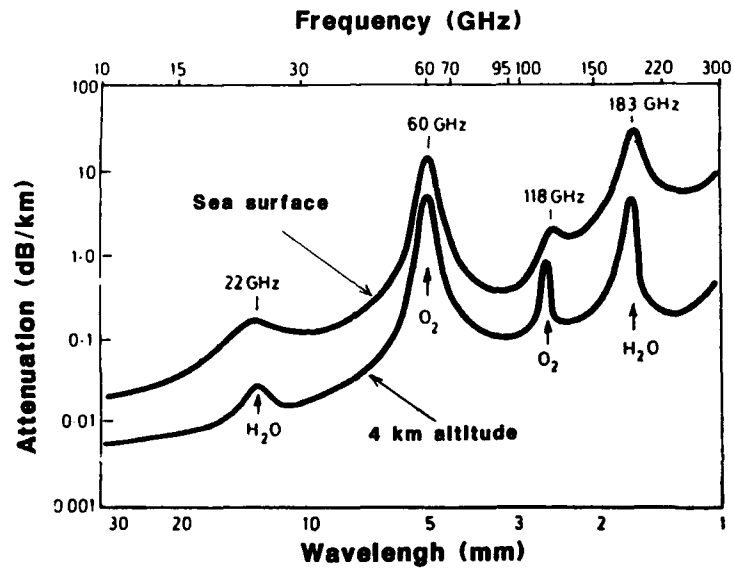


Fig 16 Attenuation around 60 GHz

**ANALYTICAL MODELING OF SH-2F
HELICOPTER SHIPBOARD OPERATION**

Fu-Shang Wei
Kaman Aerospace Corporation
Old Windsor Road, P. O. Box 2
Bloomfield, Connecticut 06002-0002

Erich Baitis
William Myers
David Taylor Research Center
Bethesda, Maryland 20084

SUMMARY

An analysis of the shipboard characteristics of the SH-2F helicopter in response to prescribed deck motion, deck friction, and steady wind conditions has been developed. The objective of deriving the SH-2F shipboard dynamic model is to define the safe conditions for launching and recovering the helicopter from the flight deck of Navy frigates and destroyers. Operational conditions of interest include helicopter and ship deck dynamic interactions which would potentially cause dangerous interference between the helicopter and the ship such as sliding or tipping of the helicopter. The wind condition, ship deck motion, helicopter rotor thrust, and friction coefficients between helicopter tires and flight deck surfaces are found to be important parameters which affect the helicopter shipboard operations. Four sets of aerodynamic characteristics are modeled in the analysis: one with the rotor operating at very low thrust; one for the rotor stopped and inoperative; one for rotor folded; and one for the fuselage. The ship motion data, including three linear translation and two angular rotation degrees-of freedom (roll and pitch) are described in the time domain. The equations of motion of the shipboard dynamic model are derived using the energy method. These equations are solved in the quasi-steady fashion within one-third of a second refresher rate to the prescribed deck motion time histories and steady wind conditions.

INTRODUCTION

An analysis of the shipboard characteristics of the SH-2F helicopter (shown in Figure 1) in response to prescribed deck motion, deck friction, and steady wind conditions has been developed and analyzed. Over 200 SH-2F helicopters have been deployed aboard US Navy frigates and destroyers. Having a shipboard dynamic analytical model on-board the ships to obtain a safe flight envelope under adverse sea conditions is essential because SH-2F helicopters will remain in combat missions until the year 2010.

A sea trial involving an SH-2F helicopter and a DE-1052-class ship was conducted in 1974 and reported in Reference 1. The report concerns two different types of analyses of ship motion, including the standard power spectrum analysis of ship motions and the aircraft event analysis of ship motions during the specific time interval of an aircraft event. Both types of analyses are required in order to relate ship motions to the degree of difficulty encountered in such events.

Sea trial results which deal with the direct operation of the aircraft have been documented in Reference 2. The rationale for relating ship motions to degree of difficulty in aircraft events for predicting operations on ships other than the 1052 class was reported in References 3 and 4.

The operation of the SH-2F helicopter from the decks of small ships was also simulated using a large amplitude motion simulator reported in Reference 5. It describes the simulation facility

and the mathematical programs. The results show the simulator to be a useful tool in simulating the ship-landing problem.

In Reference 6, a computer program was developed to predict helicopter landing and arresting system loads and deflections for the SH-60B operating on ships equipped with the Recovery Assist, Securing and Traversing (RAST) system. The computational capability is restricted to on-deck operations where the loading environment is associated with the dynamic responses of the ship in a given sea state. The helicopter rotor aerodynamic forces and moments do not include steady wind effect. The main rotor lift generated by the rotor is assumed to be 25% of helicopter total gross weight. A static solution is obtained based on an iteration procedure.

In Reference 7, the mathematical models were presented for a baseline visual landing aids suite, two versions of the airwake and the ship motions. Existing operational procedures for launch and recovery of helicopters on small aviation facility ships were used as a baseline for quantifying the models. The baseline visual landing aids suite is the current DD 963 visual landing aids complement, plus the mini optical landing system.

For SH-2F helicopters flown with -101 Rotors or Composite Main Rotor Blades (CMRB), the correlation between test data and analyses are shown in References 8 and 9. Vibration reduction analyses on the SH-2F helicopter equipped with a -101 Rotor using higher harmonic control inputs are also presented in Reference 10.

For this paper, the QuickBasic language developed by Microsoft Company was used on an IBM personal computer to solve the equations that predict the SH-2F helicopter c.g. responses due to ship deck motion. The SH-2F helicopter is represented with the rotor turning, stopped, and folded in order to simulate all possible combinations of the helicopter operation on the flight deck as shown in References 11 and 12. Operational conditions of interest include helicopter and ship deck dynamic interactions which would cause helicopter sliding or lifting one main wheel off the ship deck. Three translational and three rotational degrees-of-freedom of the helicopter c.g. motions are modeled to predict the helicopter responses due to the excitation. All coordinate systems defined on the helicopter and the ship locations are using right hand rule which has longitudinal axis positive forward, lateral axis positive to the left, and vertical axis positive upward.

The aerodynamic forces and moments generated by the SH-2F helicopter rotor and fuselage due to wind speeds are also computed. For rotor operating cases, a set of equations in the wind axis system is used to determine the proper aerodynamics. The orientation of the wind axis system with respect to the ship is accomplished by axes transformations. Three sets of aerodynamic characteristics other than the operating rotor cases are utilized as the ratios of the forces and moments to the dynamic pressure.

These ratios are given as functions of the wind azimuth angles with respect to the helicopter longitudinal axis.

The equations of motion are solved in the quasi-steady fashion in less than one-third of a second refresher rate to the prescribed deck motion time histories. This quick response solution characteristic can be used to run the program in a real time manner to obtain the safe flight envelope when interfaced with the ship motion data.

TECHNICAL ANALYSIS

A. ANALYTICAL ASSUMPTIONS

There are several assumptions used in the analysis to obtain the equations of motion of the ship and aircraft interaction due to ship deck motion and steady wind conditions. These assumptions should be carefully considered when interpreting and determining the helicopter reaction loads and motions. The assumptions are as follows:

1. A rigid body helicopter fuselage is assumed in the analysis.
2. The equations of motion of the helicopter with respect to the ship are linearized based on small angle assumptions. Ship motion, helicopter orientation on the flight deck, and wind direction are considered large angles.
3. The helicopter landing gear spring rates and damping are assumed linear.
4. All aerodynamic tables are determined as a function of the steady wind angle with respect to the longitudinal axis of the helicopter when the ship is at the level position.
5. The natural frequencies introduced by the helicopter landing gear spring rates are assumed much higher than the ship motion natural frequencies; therefore, the helicopter natural frequencies will not be affected by the ship deck motion.
6. The steady wind speed and direction and ship motion data are assumed unchanged for every one-third second time interval.

B. SHIP MOTION DATA

Ship motion data due to the sea wave and the steady wind conditions are defined in the ship coordinate system (Figure 2). These data include relative speed and direction, and also include 3 linear accelerations (X, Y, Z), 2 angular displacements (q, p), 2 angular velocities (\dot{q} , \dot{p}), and 2 angular accelerations (\ddot{q} , \ddot{p}) of the ship motions. All the data are given in the time domain. Ship motions are measured on the centerline of the ship deck directly under the landing platform. The instrumentation station is equipped to measure pitch, roll, yaw of ship course, and accelerations in the vertical, lateral, and longitudinal directions. Yaw degree of freedom of the ship motion is not used in the analysis. Ship speed and course are taken by means of repeaters from the ship's own sensors. Ship angular velocities and accelerations are obtained by differentiating the angular displacement with respect to time once and twice, respectively. Every one-third second new wind condition and ship motion data will be given as the inputs to the computer program. Inputs of ship motion data to the analysis must be consistent with the sign convention, units, and the coordinate system described in this analysis.

C. HELICOPTER AERODYNAMIC CHARACTERISTICS

1. Aerodynamic Tables Setup - The aerodynamic forces and moments on the helicopter rotor and fuselage due to steady wind conditions are determined. The rotor operating is given as a series of equations in the wind axis system shown in Reference 11. The three forces and moments are given as derivatives with respect to rotor angle of attack and pitch rate.

Three different aerodynamic tables for fuselage and nonoperating rotor conditions are used for tables look up as a function of wind azimuth angles. These aerodynamic tables are: (a) one table for the rotor stopped, but extended; (b) one table for the rotor folded; and (c) one table for the fuselage. Three sets of aerodynamic characteristics are utilized as the ratios of the three forces and three moments to the dynamic pressure. These ratios are given as functions of the wind azimuth angles with respect to the helicopter longitudinal axis.

2. Relative Wind Angle - The relationship between relative ship and helicopter wind angles is shown in Figures 3 and 4. The relative ship wind angle (θ_{WS}) with respect to ship longitudinal axis is obtained from ship motion data. The helicopter operating onboard the ship flight deck is not coincident with the ship axes. In normal operation on the landing platform, there is an angle between the helicopter and the ship longitudinal axes (θ_{AS}). Therefore, the relative wind angle (θ_{WA}) with respect to helicopter longitudinal axis is the difference between the relative wind angle with respect to ship axis minus the helicopter longitudinal axis with respect to ship axis as shown in Figure 3. θ_{WA} is the angle used to compute or to look up the aerodynamic characteristics for (a) rotor turning in operation, (b) rotor folded, and (c) helicopter fuselage aerodynamics. The procedure to obtain the wind angle with respect to the ship is as follows:

- a. Wind angle (θ_{WS}) with respect to ship axis is obtained from ship motion data.
- b. Helicopter has angle (θ_{AS}) with respect to the ship longitudinal axis.
- c. Wind angle (θ_{WA}) with respect to the helicopter longitudinal axis is:

$$\theta_{WA} = \theta_{WS} - \theta_{AS}$$
- d. θ_{WA} is used to find helicopter aerodynamics.

For rotor extended, inoperative, additional information is required to fully define the relative wind angle between the wind axis and the pitch axis of the rotor blades, shown in Figure 4. The blade angle with respect to helicopter longitudinal axis θ_{BA} is needed when the blades are stopped at any angle other than straight into the helicopter longitudinal axis. The wind angle with respect to helicopter rotor blade no. 1 is defined as follows:

$$\theta_{WB} = \theta_{WA} - \theta_{BA}$$

θ_{WB} is used to find the rotor aerodynamics from the aerodynamic table when the rotor is extended at any azimuth without turning.

3. Helicopter Relative Location - The relationship between helicopter and ship angular motions is shown in Figure 5. The helicopter has roll (ϕ), pitch (θ), and yaw (ψ) angular motions about its own c.g. axes and the ship also has roll (q) and pitch (p) angular motions about the ship coordinate axes. Because the helicopter c.g. axes has an angle with respect to the ship longitudinal axis, the total helicopter angular motion roll (ϕ'_n) and pitch (θ'_n) about the helicopter c.g. system due to ship motion are given as follows:

$$\phi'_n = \phi + q \cos \theta_{AS} + p \sin \theta_{AS}$$

$$\theta'_n = \theta - q \sin \theta_{AS} + p \cos \theta_{AS}$$

SH-2F LANDING GEAR

The SH-2F helicopter has two retractable main landing gears, each with dual wheels, located in the forward fuselage and one, full-swivel, non-retractable tail gear located in the aft fuselage. The tail wheel can be swiveled through 360° and locked in the fore and aft positions. The main landing gears are designed to have relatively larger left and right wheel span suitable for operating from smaller classes of Navy ships. The spring rates and damping characteristics of the landing gear are obtained from various tests conducted in the development of the high energy absorption landing gear. Non-linear landing gear spring rate effects are neglected in the first phase of the analysis.

EQUATIONS OF MOTION

The equations of motion of the shipboard dynamic model are derived about the helicopter c.g. using the energy method. The position vectors of the points of interest on the helicopter are first defined with respect to helicopter c.g. without the ship motion. Then, the ship motion effects are added in the kinetic energy terms of the equations to represent the actual responses of the system. The helicopter landing gear spring terms are not changed by the ship motions because the landing gear spring deflections are defined with respect to the ship deck. All the aerodynamics generated by the rotor and fuselage due to steady wind conditions are transformed into the helicopter c.g. location. Also, the helicopter gravitational force effects are added on the right hand side of the equations due to ship deck motion. Quasi-steady solution technique is used to find the response of the system due to ship motion. The computational time used to find the solution is within one-third of a second using the QuickBasic language.

Numerical Results

The friction coefficients between the SH-2F helicopter and the ship flight deck surfaces are important parameters which affect the helicopter shipboard operation. The variation of friction coefficients between wet, oily, and worn deck conditions changes up to a factor of 5 from the dry deck condition. Table 1 presents the numerical results for SH-2F helicopter and ship flight deck surface friction coefficient effects due to ship rolling motion. Ship rolling angles which would cause a helicopter to dangerously slide or tip-off on the flight deck are presented. Helicopter c.g. rolling angle and landing gear reaction forces are also listed at the helicopter sliding on or tipping-off the flight deck condition.

In the no wind situation and no relative ship speed, the helicopter starts to slide on the dry deck ($\mu = 0.7$) when the ship rolls more than 26°,

with typical helicopter mission gross weight at 12,800 lbs and with both helicopter and ship coordinate axes coincident. The helicopter also lifts one main wheel off the flight deck when the ship rolls more than 31°. In the worst condition, when the ship flight deck becomes wet and oily ($\mu = 0.15$), the helicopter starts sliding when the ship rolls more than 6.0°. Numerical results indicate that good and well-maintained ship flight decks can have 20° more roll angle before causing the helicopter to slide on the deck, as compared to wet and oily deck.

Table 2 presents the numerical results of crosswind effects on helicopter shipboard operation when the helicopter rotor is turning, sitting on an old and worn flight deck ($\mu = 0.5$), with longitudinal axis straight into the ship axis. Under 45 kts crosswind condition, the helicopter starts to slide on the flight deck when the ship rolls more than 13°, 6° sooner than the no wind situation. Also, under 45kts crosswind condition, the helicopter starts to tip one wheel off the deck when the ship rolls more than 24° which is 7° sooner than the no wind condition. Because the helicopter rotor blades generate lift under the crosswind condition when the ship rolls about its longitudinal axis, this lift force will reduce total helicopter weight exerted on the flight deck and cause the helicopter landing gear to slide or tip-off sooner than in the no wind condition. Also, the drag force generated by the fuselage will push the helicopter into sliding along the wind direction due to the crosswind. For a 30 kt crosswind condition, the helicopter slides when the ship's rolling angle is more than 17.5°, 1.5° sooner than the no wind situation, and lifts one main wheel off the deck when the ship rolls more than 25°, 6° sooner than the no wind condition.

Table 3 presents the numerical results for wind angle effects on SH-2F helicopter shipboard operation with both helicopter and ship longitudinal axes coincident with each other. The wind direction is measured with respect to the ship coordinate system. For a wind speed of 30 kts and a flight deck friction coefficient of $\mu = 0.5$, the helicopter starts to slide when the ship's rolling angle reaches 19° under the head wind condition. This roll angle gives 1.5° more than the value obtained from the crosswind condition. Under the head wind condition, the helicopter starts to lift one main wheel off the deck when the ship's rolling angle reaches 27°, 2° higher than the crosswind condition.

For a 30 kt wind with a 45° wind angle condition, analysis indicates that the helicopter slides on the deck above an 18° ship roll angle. This roll angle gives 0.5° higher than the crosswind condition. Similarly, the helicopter lifts one main wheel off the deck above a 26° ship roll angle which is 1° higher than the baseline crosswind value.

Table 4 presents the numerical results of the helicopter and ship relative angle effects on the SH-2F helicopter shipboard operation when the helicopter rotor is turning at the 30 kt crosswind condition. The helicopter operating onboard the ship flight deck is not necessarily coincident with the ship axes. In normal operation on the landing platform, there is an angle between helicopter and ship longitudinal axes.

For the helicopter longitudinal axis having 45° with respect to the ship longitudinal axis, the helicopter slides on the flight deck as the ship angle rolls above 22°, 4.5° higher than the value obtained at 0° between the helicopter and ship axes. This is because the cosine effect of the

ship roll angle applied on the helicopter longitudinal axis has a stabilizing effect on the helicopter shipboard operation.

Also for the 45° helicopter and ship angle condition, the helicopter starts to tip-off on the flight deck as the ship roll angle reaches 31°, 6° higher than 0° helicopter and ship relative angle condition.

With this information, the shipboard officer can give the best order for ship speed and course to avoid dangerous shipboard operation under adverse sea conditions.

Table 5 presents the numerical results of ship lateral acceleration effects on helicopter operation on ships. Ship lateral acceleration, obtained from ship motion data, was treated as a forcing function in the analysis applied on the right hand side of the equations of motion and can be a very important factor for helicopter on-deck operations. Ship motion data obtained from Reference 1 during a 4-day sea trial indicated that the maximum range of the ship lateral acceleration, 0.3g, is enough to simulate most of the sea-states encountered.

For a ship having 0.2g lateral acceleration, the helicopter starts to slide on the flight deck as the ship's angle rolls more than 7°, 10.5° less than no lateral acceleration condition. Numerical results also indicate that ship lateral acceleration has little effect on helicopter tip-off one main wheel on the flight deck condition.

For a ship having 0.3g lateral acceleration, the helicopter starts to slide on the flight deck when the ship's angle rolls more than 3°, 14.5° less than no lateral acceleration condition. Analysis proves that ship lateral acceleration is an extremely critical parameter for helicopter shipboard operation. Extra care must be implemented to operate a helicopter on the flight deck if the ship has lateral acceleration more than 0.3g.

The numerical results for ship vertical acceleration effects on helicopter on-deck operation are presented in Table 6, with both helicopter and ship longitudinal axes coincident. Under 30 kts crosswind and ship flight deck friction coefficient of $\mu = 0.5$ condition, the helicopter starts to slide on the flight deck as the ship angle rolls more than 13° with -0.1g ship vertical acceleration and 12° with -0.2g ship vertical acceleration, respectively. These ship roll angles have at least 4.5° less than the value obtained from no ship vertical acceleration condition. For a ship having -0.2g vertical acceleration, the helicopter starts to tip-off the flight deck as the ship attains a roll angle more than 19°, 6° less than zero ship vertical acceleration condition.

Table 7 presents the numerical results of SH-2F helicopter landing gear friction coefficient effects with the rotor blades inoperative and folded under no wind and no relative ship speed condition. The helicopter c.g. moves aft 8 in. at the rotor folded, 12,800 lbs mission gross weight configuration. This c.g. shift will slightly destabilize the helicopter operation on ships because the reaction force on the tail gear increases as helicopter c.g. moves aft. No significant numerical result differences are noticed compared to Table 1.

Table 8 presents the numerical results of crosswind effects on SH-2F helicopter operation on the flight deck with helicopter rotor blades folded. Analysis indicates that there is a slight variation on ship roll angle before causing helicopter sliding on the flight deck for crosswind speed up to 30 kts.

Under a 30 kt crosswind condition, the helicopter lifts one main wheel off the flight deck as the ship rolls more than 25°, 6° less than the no wind condition.

Table 9 presents the numerical results of ship lateral acceleration effects on helicopter shipboard operation, with rotor folded under 30 kts crosswind condition. Numerical results indicate that the degree of difficulty to operate a helicopter on the flight deck is higher with the helicopter rotor folded as compared to the rotor in operation.

For a ship having 0.2g lateral acceleration, the helicopter starts to slide on the flight deck as the ship's angle rolls more than 6° which is 12° less than the no lateral acceleration condition. For 0.3g ship lateral acceleration condition, the helicopter slides on the deck as the ship rolls more than 1°.

CONCLUSIONS

Based on technical analysis and numerical results, the analytical modeling of SH-2F helicopter shipboard operation has been successfully developed. The conclusions obtained from these numeric results are as follows:

1. The friction coefficients between SH-2F helicopter and ship flight deck changed up to a factor of 5 from the dry deck to wet and oily deck conditions are found to be important parameters which would cause helicopter slide on or tip-off the flight deck.
2. The helicopter rotor lift will reduce total weight on the landing gear, therefore, causing the helicopter slide on or tip-off the flight deck sooner than the no lift condition.
3. Best ship speed, relative wind angle, and helicopter and ship angle can stabilize helicopter shipboard operation under adverse sea conditions.
4. Ship lateral acceleration is the most important factor to cause helicopter slide on the flight deck. For a ship having 0.3g or more lateral acceleration, the helicopter will slide on the flight deck as the ship rolls more than 3°.
5. For a ship having more than -0.1g vertical acceleration, there is an increasing trend of difficulty to operate a helicopter on board a ship.
6. With the helicopter rotor blades folded, the degree of difficulty on helicopter shipboard operation is higher than the rotor turning condition.
7. Further study and test are required to verify the analytical model.

REFERENCES

1. Baitis, A.E., "The Influence of Ship Motions on Operations of SH-2F Helicopters From DE-1052-Class Ships: Sea Trial with USS Bowen (DE-1079)," DTNSRDC Ship Performance Dept., Report SPD-556-01, July 1975.
2. Comatos, M.J. et al. "Second Interim Report: SH-2F Helicopter/DE-1052 Class Destroyer Dynamic Interface Evaluation," NATC Report FT-20R-74, March 1974.

3. Baitis, A.E., Meyers, W.G., and Applebee, T.R., "A Non-Aviation Ship Motion Database for the DD 963, CG 26, FF 1052, FFG 7, and the FF 1040 Ship Classes," DTNSRDC Report STD-738-01, December 1976.
4. Bales, S.L. et al. "Response Predictions of Helicopter Landing Platform for USS BELKNAP (DLG-26) and USS GARCIA (DE-1040) Class Destroyers," NSRDC Report 3868, July 1973.
5. Paulk, C.H., Astill, D.L., and Donley, S.T., "Simulation and Evaluation of the SH-2F Helicopter in a Shipboard Environment Using the Interchangeable CAB System," NASA TM 84387, August 1983.
6. Pape, G., "Shipboard Loads Computer Program for SH-608 Helicopter," Sikorsky Aircraft, Report No. SER-520234, December 1981.
7. Fortenbaugh, R.L., "Progress in Mathematical Modeling of the Aircraft Operational Environment of DD-963 Class Ships," AIAA Paper 79-1677, Boulder, Colorado, 1979.
8. Wei, F.S., and Jones, R., "Dynamic Tuning of the SH-2F Composite Blade," American Helicopter Society 43rd Annual Forum, St. Louis, Missouri, May 1987.
9. Wei, F.S. and Jones, R., "Correlation and Analysis for the SH-2F 101 Rotor," Journal of Aircraft, 25, July 1988, pp. 647 - 652.
10. Wei, F.S., Basile, J.P., and Jones, R., "Vibration Reduction on Servo Flap Controlled Rotor Using HHC," American Helicopter Society National Specialists Meeting on Rotorcraft Dynamics, Arlington, Texas, November 1989.
11. Wei, F.S., "SH-2F Helicopter Shipboard Motion Analysis," Kaman Aerospace Corporation, Report No. R-1872, April 1988.
12. Fitzpatrick, J.E., "Mechanical Instability Analysis of the SH-2F Helicopter with DAF Recovery Assist System," Kaman Aerospace Corporation, Report No. G-209, 1976.

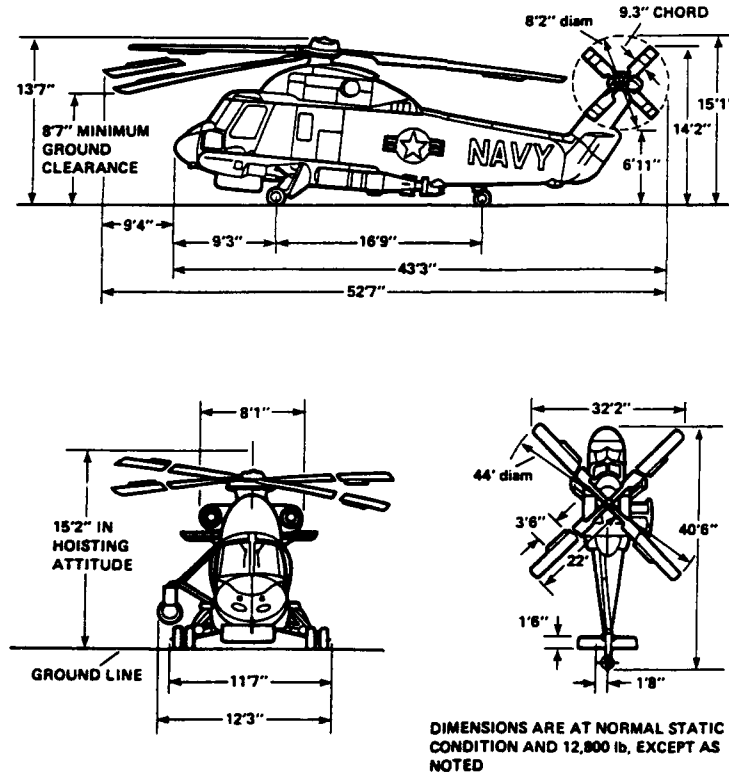


Figure 1. Kaman SH-2F Helicopter.

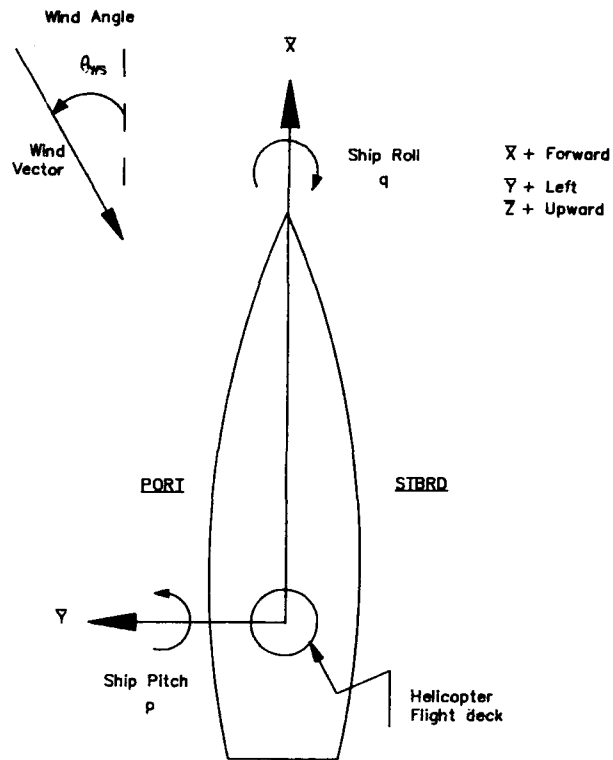


Figure 2. Ship Coordinate System for Ship Motion Parameters and Relative Wind Angle.

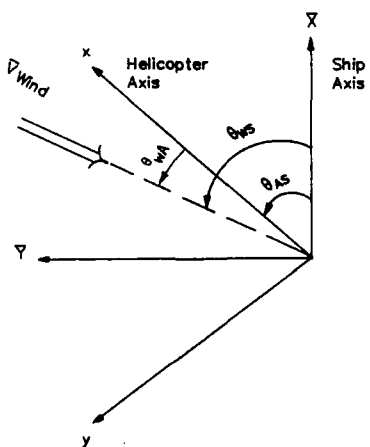


Figure 3. Wind Angle Relationship Between Ship and Helicopter.

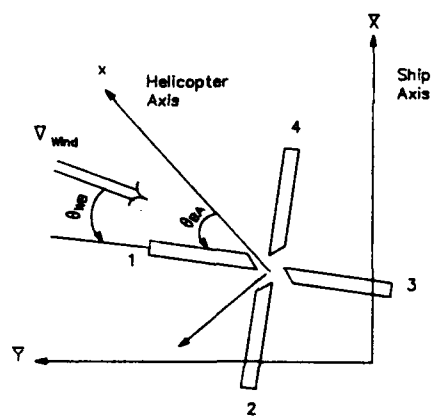


Figure 4. Relationship Between Ship and Helicopter Wind Angle for Rotor Inoperative.

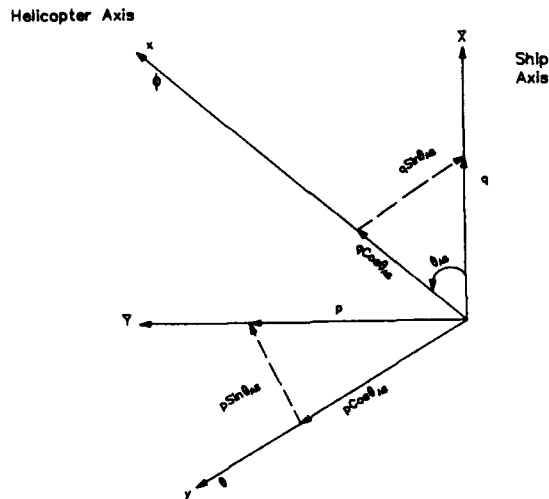


Figure 5. Relationship Between Helicopter and Ship Angular Motions.

TABLE 1. HELO LANDING GEAR FRICTION COEFFICIENT EFFECT NO WIND, $\theta_{AS} = 0$, 12,800 LB GM					
FRICTION COEFFICIENT BETWEEN HELO LANDING GEAR AND SHIP DECK		0.7 ⁽¹⁾	0.5 ⁽²⁾	0.3 ⁽³⁾	0.15 ⁽⁴⁾
HELO SLIDES ON SHIP DECK	SHIP ROLL ANGLE (DEG)	26°	19°	12°	6.0°
	HELO ROLL ANGLE (DEG)	4.8°	3.8°	2.4°	1.2°
	RIGHT WHEEL FORCE (LB)	8157	7862	7009	6075
	LEFT WHEEL FORCE (LB)	326	1641	3149	4086
	TAIL WHEEL FORCE (LB)	2207	2473	2644	2645
HELO WHEEL LIFTS OFF SHIP DECK	SHIP ROLL ANGLE (DEG)	31°	31°	31°	31°
	HELO ROLL ANGLE (DEG)	5.9°	5.9°	5.9°	5.9°
	RIGHT WHEEL FORCE (LB)	9412	9412	9412	9412
	LEFT WHEEL FORCE (LB)	0	0	0	0
	TAIL WHEEL FORCE (LB)	2376	2376	2376	2376

- (1) Dry Flight Deck
 (2) Worn Flight Deck
 (3) Wet Flight Deck
 (4) Oily Flight Deck

TABLE 2. CROSSWIND SPEED EFFECT					
$\theta_{AS} = 0$; 12,800 LB GW; ROTOR TURNING; WIND ANGLE = 90°; $\mu = 0.5$					
WIND SPEED WITH RESPECT TO SHIP (KTS)		0	15	30	45
HELO SLIDES ON SHIP DECK	SHIP ROLL ANGLE (DEG)	19°	18.5°	17.5°	13°
	HELO ROLL ANGLE (DEG)	3.8°	3.5°	2.7°	2.5°
	RIGHT WHEEL FORCE (LB)	7862	7156	6066	5586
	LEFT WHEEL FORCE (LB)	1641	1496	1690	1454
	TAIL WHEEL FORCE (LB)	2473	2337	2286	2322
HELO WHEEL LIFTS OFF SHIP DECK	SHIP ROLL ANGLE (DEG)	31°	26°	25°	24°
	HELO ROLL ANGLE (DEG)	5.9°	4.4°	4.0°	2.8°
	RIGHT WHEEL FORCE (LB)	9412	6991	6084	4342
	LEFT WHEEL FORCE (LB)	0	0	0	0
	TAIL WHEEL FORCE (LB)	2376	1865	1799	1744

TABLE 3. WIND ANGLE EFFECT						
$\theta_{AS} = 0$; 12,800 LB GW; ROTOR TURNING; WIND SPEED = 30KTS; $\mu = 0.5$						
WIND ANGLE WITH RESPECT TO SHIP (DEG)		0°	30°	45°	60°	90°
HELO SLIDES ON SHIP DECK	SHIP ROLL ANGLE (DEG)	19°	19°	18°	18°	17.5°
	HELO ROLL ANGLE (DEG)	3.7°	3.5°	3.0°	2.9°	2.7°
	RIGHT WHEEL FORCE (LB)	7909	7043	6649	6345	6066
	LEFT WHEEL FORCE (LB)	1798	1324	1796	1644	1690
	TAIL WHEEL FORCE (LB)	2591	2317	2382	2301	2286
HELO WHEEL LIFTS OFF SHIP DECK	SHIP ROLL ANGLE (DEG)	27°	26°	26°	25°	25°
	HELO ROLL ANGLE (DEG)	4.5°	4.3°	4.0°	3.9°	4.0°
	RIGHT WHEEL FORCE (LB)	7671	6959	6331	6368	6084
	LEFT WHEEL FORCE (LB)	0	0	0	0	0
	TAIL WHEEL FORCE (LB)	2089	1851	1689	1813	1799

TABLE 4. ANGLE BETWEEN HELO AND SHIP EFFECT				
12,800 LB GW; ROTOR TURNING; WIND SPEED = 30 KTS; WIND ANGLE = 90°; $\mu = 0.5$				
ANGLE BETWEEN HELO AND SHIP (DEG)		0	30	45
HELO SLIDES ON SHIP DECK	SHIP ROLL ANGLE (DEG)	17.5°	18°	22°
	HELO ROLL ANGLE (DEG)	2.7°	2.3°	1.9°
	RIGHT WHEEL FORCE (LB)	6066	5265	4224
	LEFT WHEEL FORCE (LB)	1690	1475	1181
	TAIL WHEEL FORCE (LB)	2286	2754	2893
HELO WHEEL LIFTS OFF SHIP DECK	SHIP ROLL ANGLE (DEG)	25°	27°	31°
	HELO ROLL ANGLE (DEG)	4.0°	2.7°	2.2°
	RIGHT WHEEL FORCE (LB)	6084	4429	3250
	LEFT WHEEL FORCE (LB)	0	0	0
	TAIL WHEEL FORCE (LB)	1799	2781	2717

TABLE 5. SHIP LATERAL ACCELERATION EFFECT					
$\theta_{AS} = 0$; 12,800 LB GW; ROTOR TURNING; WIND SPEED = 30 KTS; WIND ANGLE = 90°; $\mu = 0.5$					
SHIP LATERAL ACCELERATION (g)		0	0.1	0.2	0.3
HELO SLIDES ON SHIP DECK	SHIP ROLL ANGLE (DEG)	17.5°	12.0°	7.0°	3°
	HELO ROLL ANGLE (DEG)	2.7°	2.1°	1.2°	0.3°
	RIGHT WHEEL FORCE (LB)	6066	6029	5611	5336
	LEFT WHEEL FORCE (LB)	1690	2629	3694	4827
	TAIL WHEEL FORCE (LB)	2286	2477	2605	2797
HELO WHEEL LIFTS OFF SHIP DECK	SHIP ROLL ANGLE (DEG)	25°	25°	25°	26°
	HELO ROLL ANGLE (DEG)	4.0°	3.7°	3.5°	3.1°
	RIGHT WHEEL FORCE (LB)	6084	5864	5643	4972
	LEFT WHEEL FORCE (LB)	0	0	0	0
	TAIL WHEEL FORCE (LB)	1799	1797	1796	1611

TABLE 6. SHIP VERTICAL ACCELERATION EFFECT					
$\theta_{AS} = 0$; 12,800 LB GM; ROTOR TURNING; WIND SPEED = 30 KTS; WIND ANGLE = 90°; $\mu = 0.5$					
SHIP VERTICAL ACCELERATION (g)		0	-0.1	-0.2	-0.3
HELO SLIDES ON SHIP DECK	SHIP ROLL ANGLE (DEG)	17.5°	13.0°	12.0°	12.0°
	HELO ROLL ANGLE (DEG)	2.7°	2.5°	2.3°	2.3°
	RIGHT WHEEL FORCE (LB)	6066	5565	5236	4729
	LEFT WHEEL FORCE (LB)	1690	1490	1416	908
	TAIL WHEEL FORCE (LB)	2286	2067	1954	1689
HELO WHEEL LIFTS OFF SHIP DECK	SHIP ROLL ANGLE (DEG)	25°	24°	19°	18°
	HELO ROLL ANGLE (DEG)	4.0°	3.5°	3.3°	3.0°
	RIGHT WHEEL FORCE (LB)	6084	5507	5102	4684
	LEFT WHEEL FORCE (LB)	0	0	0	0
	TAIL WHEEL FORCE (LB)	1799	1709	1539	1449

TABLE 7. HELO LANDING GEAR FRICTION COEFFICIENT EFFECT					
NO WIND, $\theta_{AS} = 0$, 12,800 LB GM, ROTOR FOLDED					
FRICTION COEFFICIENT BETWEEN HELO LANDING GEAR AND SHIP DECK		0.7	0.5	0.3	0.15
HELO SLIDES ON SHIP DECK	SHIP ROLL ANGLE (DEG)	25°	19°	12°	6.0°
	HELO ROLL ANGLE (DEG)	4.9°	3.8°	2.3°	1.2°
	RIGHT WHEEL FORCE (LB)	8432	7595	6730	5800
	LEFT WHEEL FORCE (LB)	395	1406	2891	3824
	TAIL WHEEL FORCE (LB)	2918	2976	3181	3180
HELO WHEEL LIFTS OFF SHIP DECK	SHIP ROLL ANGLE (DEG)	31°	31°	31°	31°
	HELO ROLL ANGLE (DEG)	5.9°	5.9°	5.9°	5.9°
	RIGHT WHEEL FORCE (LB)	9145	9145	9145	9145
	LEFT WHEEL FORCE (LB)	0	0	0	0
	TAIL WHEEL FORCE (LB)	2858	2858	2858	2858

TABLE 8. CROSSWIND SPEED EFFECT				
$\theta_{AS} = 0$; 12,800 LB GM; ROTOR FOLDED; WIND ANGLE = 90°; $\mu = 0.5$				
WIND SPEED WITH RESPECT TO SHIP (KTS)		0	15	30
HELO SLIDES ON SHIP DECK	SHIP ROLL ANGLE (DEG)	19°	19°	18°
	HELO ROLL ANGLE (DEG)	3.8°	4.0°	4.0°
	RIGHT WHEEL FORCE (LB)	7595	7728	8089
	LEFT WHEEL FORCE (LB)	1406	1247	1483
	TAIL WHEEL FORCE (LB)	2976	2999	3292
HELO WHEEL LIFTS OFF SHIP DECK	SHIP ROLL ANGLE (DEG)	31°	26°	25°
	HELO ROLL ANGLE (DEG)	5.9°	4.9°	5.6°
	RIGHT WHEEL FORCE (LB)	9145	8031	8984
	LEFT WHEEL FORCE (LB)	0	0	0
	TAIL WHEEL FORCE (LB)	2858	2675	3023

TABLE 9. SHIP LATERAL ACCELERATION EFFECT					
$\theta_{AS} = 0$; 12,800 LB GM; ROTOR FOLDED; WIND SPEED = 30 KTS; WIND ANGLE = 90°; $\mu = 0.5$					
SHIP LATERAL ACCELERATION (g)		0	0.1	0.2	0.3
HELO SLIDES ON SHIP DECK	SHIP ROLL ANGLE (DEG)	18°	12°	6°	1°
	HELO ROLL ANGLE (DEG)	4.0°	2.8°	1.4°	0.1°
	RIGHT WHEEL FORCE (LB)	8089	7062	5905	4842
	LEFT WHEEL FORCE (LB)	1483	2512	3641	4676
	TAIL WHEEL FORCE (LB)	3292	3293	3284	3274
HELO WHEEL LIFTS OFF SHIP DECK	SHIP ROLL ANGLE (DEG)	25°	25°	26°	26°
	HELO ROLL ANGLE (DEG)	5.6°	5.4°	5.1°	4.7°
	RIGHT WHEEL FORCE (LB)	8984	8760	8537	7807
	LEFT WHEEL FORCE (LB)	0	0	0	0
	TAIL WHEEL FORCE (LB)	3023	3021	3019	2760

HELICOPTER/SHIP ANALYTIC DYNAMIC INTERFACE

Bernard Ferrier*
Bombardier Inc
Canadair, Surveillance Systems Division
Dynamic Interface Analysis Program
Case Postale 6087, Succ. A.
Montréal (Québec) H3C 3G9 Canada

Lt(N) Henry Potvi
DGMEM/DME 5-5-2
National Defence Headquarters
Maj General George R. Pearkes Bldg.
OTTAWA (ONT) K1A 0K2 Canada

François A. Thibodeau
Bombardier Inc
Canadair, Surveillance Systems Division
Landing Period Designator Project
Case Postale 6087, Succ. A.
Montréal (Québec) H3C 3G9 Canada

Abstract

An analytic approach to helicopter/ship dynamic interface testing is introduced. The development of dynamic interface from Ship Motion Simulation is presented, discussing operational simulation applications. A demonstration of a Deck Handling Clearance Study is performed for a EH101 helicopter and CPF ship model. Preliminary results of the Landing Period Designator development project are provided.

Sommaire

Il existe plusieurs applications possibles pour les programmes de simulation du mouvement des navires (SMS). Cet article présente une approche analytique pour étudier des problèmes reliés à l'interface dynamique aéronef/navire basée sur la simulation d'activités opérationnelles. Un exemple d'étude est présenté concernant le couple aéronef/navire (EH101/CPF). Cette étude établit des enveloppes opérationnelles pour la manutention de l'hélicoptère sur le pont du navire en utilisant un modèle analytique. Une seconde application des programmes de simulation est aussi présentée, il s'agit du développement de l'algorithme d'un indicateur de périodes d'atterrissage. Quelques résultats préliminaires sont inclus dans ce rapport.

1.0- Introduction

Maritime helicopters operating from aircapable warships are limited mainly by high winds and rough seas. These factors result in irregular six degrees-of-freedom motion coupled with extreme levels of wind-over-deck velocity gradients and turbulence. Healey [1] has noted that helicopter operations are limited to only ten per cent availability for a 122 m (400 ft) frigate in the wintertime North Sea environment. Dynamic Interface (DI), defined as the study of the relationship between an air vehicle and a moving platform, is therefore performed to reduce the risks and maximize operational flexibility [2].

* Ferrier is a graduate student in the Département de Génie civil, École Polytechnique de Montréal.

Experience with DI testing in countries, such as the U.S.A, is an on-going necessity. The American Navy matrix alone accounts for over a dozen VTOL/VSTOL manned and unmanned vehicles and more than 20 classes of aviation capable ships [3]. In Canada, the Aerospace Engineering Test Establishment (AETE) is responsible for the Department of National Defence (DND) interface flight deck certification testing. However, in-house practical experience in interface testing is minimal [4] since there has not been a large testing requirement. This is primarily owing to few new acquisitions leaving a small interface matrix.

Recent capital acquisition and R & D programs have renewed DND's interest in DI. Through a Memorandum of Understanding (MOU) between the United States and Canada the means for participation in DI analysis became available. The purpose of this paper is to present highlights of the aircraft/ship interface simulation programs, the DND supported deck clearance study, and the Landing Period Designator application.

1.1- Experimental vs Analytical DI

Dynamic Interface is divided into two broad categories: the *experimental* or at-sea measurement of limitations; and *analytical* which centres on computerized simulation studies [5]. The two methods are not mutually exclusive. Neither method alone can synthesize an effective, comprehensive and timely solution of the complete DI problem.

Experimental DI is the traditional approach. Helicopter DI experimentation investigates operational launch and recovery, engage/disengage of rotors, vertical replenishment and helicopter in-flight refueling envelopes. "Shipboard suitability testing" assesses the adequacy, effectiveness, and safety of shipboard aviation.

Experimental DI has evolved into a science. Testing methodologies and procedures have been standardized by laboratories, such as, NATC (USA) and NRL (the Netherlands). These establishments integrate various testing approaches, such as wind tunnel analysis, with at-sea experimentation. Typically, air vehicles are instrumented to record many aspects of the interface [6]. While the testing has numerous objectives, the concentration is on launch and recovery envelope development and expansion. The procedure requires a helicopter launch or recovery in a specific prevailing environmental and ship condition. The launch or recovery is rated by the pilot on a scale termed the Pilot Rating Scale (PRS), based on an assessment of pilot workload resulting from aircraft control margins, aircraft flying qualities, and performance in the shipboard environment [7]. Envelopes are developed for various environmental conditions in day and night operations. Other DI ship tests, such as aviation facilities evaluations and deck handling, investigate specific support issues [8].

Deck handling studies investigate problems associated with the movement of air vehicles on the flight deck and in the hangar. The air vehicle conditions with respect to the ship (restrained or unrestrained) and air vehicle configuration (fuselage or rotor fold position) are individually investigated. Clearance measurements are recorded during static (dockside) and dynamic (at-sea) test phases with the test aircraft fueled or empty and the main rotor blades spread and folded [9]. Engage and disengage studies and deck airwake surveys are also components of a complete DI test.

DI analytics emphasize mathematical modeling and simulation to support flight testing. Analytics can be used to help define the safe operational limitations of any ship/helicopter combination by:

- i)- simulating ship motion in space and time.
- ii)- simulating helicopter on deck.
- iii)- simulating degraded operational conditions.

Analytics were created as a data handling tool to treat the enormous bulk of data which was accumulating at increasing rates [10]. Initial breakthroughs revolved about ship definition

and motion, such as the Standard Ship Motion Program or SMP series [11]. This genre of simulation attempts to describe the responses of marine vehicles and structures in a seaway [12]. Products of the analysis predict vehicle/structure motions, accelerations under wave induced forces and moments. Shortly after the initial SMP series publication, O'Reilly [13] published the first air vehicle/ship frequency analysis program using the theories of Korvin-Kroukovsky [14], Michael St.Denis [15], and Willard Pierson [16]. A joint experimental and analytical DI approach was proposed by NATC in 1983 [17]. SMS notwithstanding, computer analysis was still generally limited and required further development. Presently, development is limited only by computer availability and time (table 1.1).

Table 1.1
Experimental Limitations and
Analytic Advantages

Experimental DI Limitations	Analytic DI Limitations
Availability of test assets (ship/a.c.)	Availability of computer system
Availability of desired maritime environmental climate	Not applicable, programmable condition
Logistics required manpower, equipment	Not applicable perform study in laboratory
Large costs for assets & manpower	Smaller costs for computer & manpower
Time required to complete envelope	Batch computer simulations, multiple runs
May entail physical danger	No risk to the researcher

While analytics may seem less taxing to the DI system, *it cannot, nevertheless, replace experimentation.* Envelope studies will always require physical verification. Analytics may provide a means of controlling the DI test environment and, thus, a short-cut mechanism to test more efficiently [18].

1.2- DND Activity and Program Interest

The Canadian Department of National Defence's (DND) interest in Analytical Dynamic Interface increased during the preliminary studies involved with the New Shipborne

Aircraft (NSA) project in the mid-1980's. It was realized that a complete analytical capability was unavailable within DND and that such a tool could be useful for streamlining flight tests and in determining the limitations of operating relatively large and heavy aircraft from Canadian warships.

Concurrently, CANADAIR obtained the ability to develop DI through the Tripartate Technical Cooperation Program (TTCP) Memorandum of Understanding (MOU) and subsequently submitted an Unsolicited Proposal to DND to conduct a Deck Motion Study and develop a "Landing Period Designator" (LPD). A contract was eventually awarded to CANADAIR in November 1989 to modify existing software to provide a dedicated VAX data base, develop an analytical clearance envelope addressing an unsecured air vehicle, and to provide fundamental arguments for follow-on work. The LPD concept was not supported by DND and is being developed solely by Canadair.

The Canadian Navy has developed helicopter operations from small warships since 1957 [19]. Now, the Canadian Navy faces several challenges in the near future, with a fleet in transition and a requirement to undertake Flight Deck Certification Trials for the new Canadian Patrol Frigate (CPF) and Tribal-class Update and Modernization Project (TRUMP) ships. The CH-124 SEAKING helicopter will be operated from these ships and an NSA replacement project is in progress. The NSA choice includes a variant of the Westland/Agusta European Helicopter EH101, which is significantly larger than the current CH-124 SEAKING. Finally, other Canadian ship-classes such as the Auxiliary Oiler Replenishment (AOR) ships and "ISL/ANS" DDHs are operating helicopters in a variety of environments on assorted missions, including R&D. After a lapse of several years, Canada will once again conduct flight deck clearances.

With the flexible roles and varied environments all maritime forces are involved with worldwide, an accurate and verified helo/ship modelling resource should be available to test for safe yet aggressive operational limits. An economical method combining analytics and experimentation to streamline the flight testing, determine clearance envelopes and examine helo traversing stability would thus be extremely useful.

Within DND, it is envisaged that DI has potential to provide a starting point for actual flight testing. The helo/ship interface software as transferred under TTCP would complement the existing ship motion analytic capability, following validation. The initial step would be to use analytics to identify the appropriate ship motion conditions necessary to test various launch and recovery envelopes. The challenge is to confirm the veracity of the analytic method in order to provide confidence to all concerned with Naval helicopter/ship operations.

2.0- Ship Motion Simulation

The Ship Motion Simulation (SMS) part of the analytic DI program, was developed by Peter J.F. O'Reilly at Bell Helicopter Textron for the USN (NAEC) between 1973 to 1984. The SMS mathematical model, which utilizes synthetic time history traces, was adopted by Hughes Helicopters, Inc. (now McDonnell Douglas Helicopter Company) from NATC in 1984 for the experimental AH-64 Apache marinization program. In 1987, NAVAIR transferred, under the auspices of the TTCP MOU, the simulation to the Canadian DND for further study and development. As a result, SMS has many homes under TTCP with one centre of excellence, currently at Bombardier Inc, Canadair Surveillance Systems Division in Montréal.

2.1- SMS Theoretical Synopsis

The O'Reilly Ship Motion Simulation Model is derived from the relationship between the wave and ship motion spectrum [20]. It incorporates seakeeping philosophy and applies various definitions of seaway spectral formulation, such as, Pierson-Moskowitz [21], and Bretschneider [22].

SMS defines a seaway, computes the hydrodynamic and hydrostatic forces imposed on a ship and calculates the resulting ship motions. The simulation is an extensive treatment of a floating object's response to the dynamic loads on its structure.

SMS is divided into two basic themes, *spectral analysis* of a desired seaway/ship condition and calculation of *synthetic time histories* representing plausible ship motion.

The SMS fundamental relationship is:

$$S_r = S_\omega(\omega) \times \text{RAO} \times f(V, \mu) \quad (2.1)$$

where;

S_r = Ship Response Spectrum
 $S_\omega(\omega)$ = Seaway Spectrum
 RAO = Response Amplitude Operator
 $f(V, \mu)$ = frequency mapping
 (encountered spectrum)

At the conception of SMS, *Pierson-Moskowitz* was used as a standard for comparison. This may no longer be true, but its simplicity is still appealing. In SMS, the sea spectrum defined by *Pierson-Moskowitz* is given by:

$$S_\omega(\omega) = \frac{a g^2}{\omega^5} e^{\left(\frac{4ag^2}{H_s^2 \omega^4}\right)} \quad (2.2)$$

where,

a = constant
 g = acceleration due to gravity
 ω = wave circular frequency
 $S_\omega(\omega)$ = spectral density

SMS can also apply the *Bretschneider* sea spectrum which is adaptable for both fully and partially developed seaways. *Bretschneider* is given by:

$$S_\omega(\omega) = \frac{483.5}{\omega^5 T_0^4} * H_s^2 e^{\left(\frac{-1944.5}{(T_0 \omega)^4}\right)} \quad (2.3)$$

Other spectral formulations available in SMS include the International Towing Tank Conference (*ITTC*, which resembles the *Bretschneider*) and the Joint North Sea Wave Project (*JONSWAP*). *JONSWAP* is a two parameter formulation using fetch length and wind speed as the variables.

The spectral characteristic of a vessel is defined in the SMS by experimental or computationally developed transfer functions termed Response Amplitude Operators (RAO). The response amplitude operators are transfer functions which define the dynamic responses of the ships for a specified load/operating condition [23].

The *ship response spectrum* is created as the product of the RAO and the driving sea

spectrum (figure 2.1) over the entire range of frequencies.

The procedure is conducted simultaneously for all degrees-of-freedom and reduced to corresponding *harmonic components*. The sets of harmonic components form the basis on which synthetic time histories of ship motion are developed. Synthetic time histories are created *stochastically* in the SMS. Each component is defined by an amplitude, A , a circular frequency, ω , and a phase angle, ϵ [24]. A typical *time history* equation is as follows (here in the vertical direction):

$$A_z = \sum_{n=1}^k (A_{zn} \cos(\omega_n t - \epsilon_{zn})) \quad (2.4)$$

The various time history samples created by a harmonic component and seaway calculation are combined, in the case of SMS, as a sum of 48 synthetic functions ($k=48$). Figure 2.2 displays typical time history traces using the SMS program.

2.2- SMS Program Description

Throughout the evolution of the SMS and related subject routine programs, "user-friendliness" and versatility have been priorities. Software development that requires "User-friendliness" generally cannot be too complex, while complexity usually occurs at the expense of User-friendliness. There are more than 150 subject routines developed over the years related to SMS for both the IBM and VAX environments.

Figure 2.3 is a flowchart of the VAX core subject routines in SMS. The simulation core may be attached to either the Ship Motion Program (David Taylor Research Center) or SHIPMO (Defence Research Establishment Atlantic) RAO master files. The subject routine NAV2 selects the appropriate master file and scans for the selected ship/sea condition. NAV3 (ahead seas) and NAV4 (following seas) read the RAO tables, create the encountered seaway in the frequency domain and generate harmonic component sets for the centre of motion six degrees-of-freedom. These motions are resolved to the point of interest (nominally the landing deck bullseye). and are termed, "Vertical, Lateral and Longitudinal".

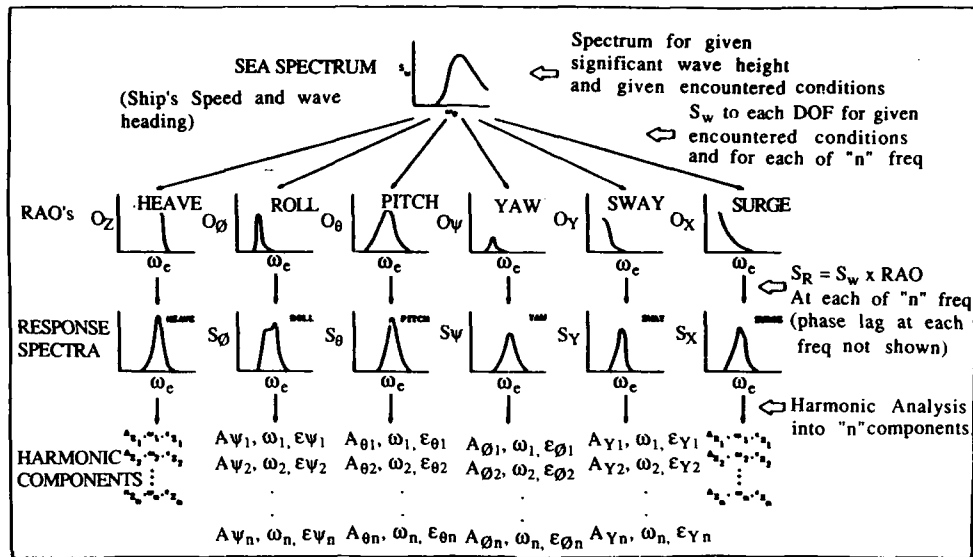


Figure 2.1-SMS Computational Summary

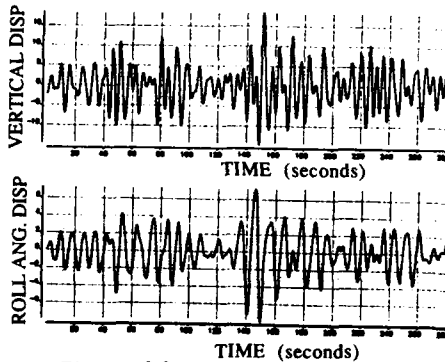


Figure 2.2-Typical SMS Time History Traces

Thus, in summary, the Ship Motion Simulation program, as developed by O'Reilly, applies deterministic measurement to a probabilistic spectrum. Deterministic synthetic time histories are derived from the probabilistic spectrum.

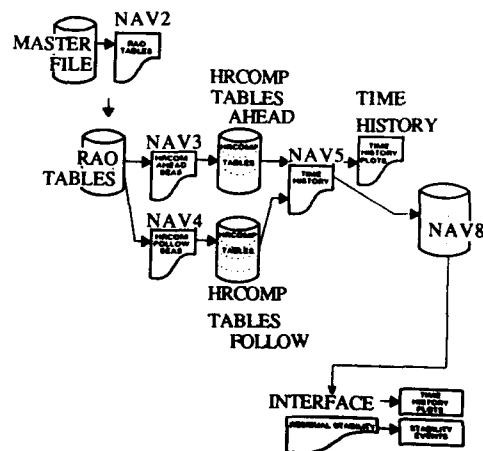


Figure 2.3-SMS System Flowchart

The harmonic component tables are used create synthetic time history reports. NAV5, the ship response time history trace subject routine, contains numerous menu selections of studies, motion statistics and traces. The purpose of the routine is to create a series of synthetic time history traces resolving ship motion in any of the six DOF at the C.G and at any point of interest on the ship.

3.0- Aircraft/Ship Interface Simulation

The most important applications of SMS are in direct operational simulation such as aircraft launch and recovery; deck handling; and general flight readiness (or availability). These applications use the core programs and another subject routine termed NAV8 (FLYNAVCDN), the interface program.

NAV8CDN.VAX is a mathematical *description of conditions limiting the on-deck availability of an air device*. Factors affecting an air vehicle on a moving platform are primarily ship motion; Wind Over Deck/ship airwake turbulence; and deck conditions (eg: wet, dry, oily, obstructed).

Launch and recovery studies can be developed to determine impact dispersion, landing aids, hauldown system effectiveness, and ship stabilization system effectiveness.

Deck handling clearance or safety, is a study of the motion sensitive activities involved in handling a vehicle in the marine environment. This is usually directed at the handling of an air vehicle on small air capable ships. In SMS, the limitations can be defined as the point at which an aircraft/ship incident occurs. Incident means an occurrence of aircraft turnover, pitchback or on-deck slide at any point from the on-deck recovery to hangar stowage and back to launch.

Availability involves maintenance concepts, reliability impacts and human factor limitations. Deck handling or clearance studies determine turnover limits, sliding freedom, tiedown forces, traversing factors, and pitch back limitations (Results of a deck clearance option are presented in section 4.2).

3.1- Theoretical Synopsis

Aircraft movement on the flight deck can be defined by its landing gear footprint; deck location and orientation; aircraft weight and inertias, centre of gravity, lateral drag area and centre of pressure. The aircraft on the deck experiences ship forces and moments which create rectilinear and angular accelerations on the air vehicle. The accelerations can be integrated numerically to determine the position and attitude of the helicopter relative to the ship as a function of time, for various ship motions [25]. With the air vehicle and ship deck defined and the ship

motion characteristics transmitted by SMS, the only remaining environmental condition requiring definition is the on-deck air flow. The model addresses the issue simply by a unidirectional wind-over-deck model. This is represented as a force in the same direction as the prevailing wave front and remains constant for the duration of the simulation run.

Ship deck accelerations are resolved for the helicopter. The inertial loads at the helicopter center of gravity (F_{ix} , F_{iy} and F_{iz}) are determined as follows:

$$\begin{aligned} F_{ix} &= W * AX_{CG} \\ F_{iy} &= W * AY_{CG} \\ F_{iz} &= W * AZ_{CG} \end{aligned} \quad (3.1)$$

where;

$$\begin{bmatrix} F_{ix} \\ F_{iy} \\ F_{iz} \end{bmatrix} = \text{Inertial Forces due to ship motion}$$

$$W = \text{Aircraft Weight}$$

In the longitudinal, lateral and vertical directions, these inertial loads become:

$$\begin{bmatrix} X \\ Y \\ Z \end{bmatrix} = \begin{bmatrix} T_{11} & T_{12} & T_{13} \\ T_{21} & T_{22} & T_{23} \\ T_{31} & T_{32} & T_{33} \end{bmatrix} \begin{bmatrix} F_{ix} \\ F_{iy} \\ (F_{iz} + W) \end{bmatrix} \quad (3.2)$$

where;

$$T_{ij} = T(\phi, \theta, \psi) \text{ (transformation matrix from ship's axis system to horizontal level/vertical axis system)}$$

where;

$$\begin{aligned} \phi &= \text{Roll} \\ \theta &= \text{Pitch} \\ \psi &= \text{Yaw} \end{aligned}$$

The Wind Over Deck (V_{WOD}) and ψ_{WOD} define the magnitude and direction of the wind with respect to the ship's longitudinal axis. To compute the lateral force applied at the aircraft Centre of Pressure due to the wind,

the V_{WOD} is resolved along and normal to the aircraft centre line (V_{Wlong} and V_{Wlat}). The lateral component is used to compute the lateral force per MIL-T-81259 (U.S. military standard) as follows:

$$F_{wy} = 35 * A_y * \left(\frac{V_{Wlat}}{100} \right)^2 \quad (3.3)$$

where;

- A_y = Aircraft Projected Area Normal to the V_{Wlat} Component
 F_{wy} = Lateral force applied at the aircraft Centre of Pressure due to wind

The axial forces on the main landing gears due to wind force F_{wy} is given by:

$$F_{RMGwind} = \frac{(F_{wy})(WL_{CP} - WL_G)}{(L_{BL} + R_{BL})} \quad (3.4)$$

where;

- $F_{RMG(wind)}$ = Right Main Gear Axial force
 F_{wy} = Wind Force Lateral Component
 WL_{CP} = Centre of Pressure Waterline
 WL_G = Ground Waterline
 L_{BL} = Left Wheel Butteline
 R_{BL} = Right Wheel Butteline

The incremental aircraft roll due to the wind is determined by:

$$\Delta\phi_{(wind)} = \tan^{-1} \left(\frac{F_{RMG(wind)}}{K * L_{BL}} \right) \quad (3.5)$$

where;

- K = Aircraft Spring Constant

The axial forces on the main landing gears due to aircraft inertial forces in the plane of the main gear, is given by:

$$F_{RMG(inertia)} = Y * \left(\frac{WL_{CG} - WL_G}{L_{BL} + R_{BL}} \right) \quad (3.6)$$

where;

- WL_{CG} = Centre of Gravity Waterline
 $F_{RMG(inertia)}$ = Right Main Gear Axial Force due to the lateral inertia force Y defined in equation (3.2).

Assuming perfect rocking, the axial force on the left main gear is vectorially opposite to the force acting on the right main gear:

$$F_{LMG(inertia)} = -F_{RMG(inertia)} \quad (3.7)$$

where;

- $F_{LMG(inertia)}$ = Left Main Gear Axial Force

The incremental aircraft roll due to inertial loads is determined as follows:

$$\Delta\phi_{(inertia)} = \tan^{-1} \left(\frac{F_{RMG(inertia)}}{K * L_{BL}} \right) \quad (3.8)$$

The model assumes the wind is constant, therefore the $\Delta\phi_{(wind)}$ is constant throughout the simulation run. However, $\Delta\phi_{(inertia)}$ is continuously changing with ship motion. The total incremental change in aircraft roll with respect to the ship (absorbed by the landing gears) is then determined by:

$$\Delta\phi_{(total)} = \Delta\phi_{(wind)} + \Delta\phi_{(inertia)} \quad (3.9)$$

Deck condition, eg: dry or with substances on the deck, such as water or oil, is a variable in the program. This affects the stability of the air vehicle through the landing gear friction. Air vehicle slide may be detected with the deck condition set for oil or water while the same sea condition/environment on a dry deck may show the air vehicle as stable.

The aircraft is modelled for "worst case" scenarios. For the greatest landing gear deflection, nose gears are modelled unlocked and castored for turnover. The model is lined up with the ship centreline and is rotated on the deck to find the least stable, but realistic, orientation (figure 3.1).

As an input to the model, the aircraft centre line direction with respect to the ship lateral axis (y) is given as (μ) along with the polar coordinates of the right main gear R and (θ) on the flight deck plane. These parameters together with the aircraft center of gravity coordinates, nose gear, main gears (right and left) and nose gear pivot, are geometrically adequate to compute the following aircraft/ship interface critical boundaries:

- a) The 'worst case' hinge line on the flight deck about which the aircraft will turnover (right or left). Two lines are defined, R_{TO} and L_{TO} . Each line is computed from its relevant main gear position to the nose gear swivelled for worst case right or left turnover.
- b) The azimuth of these two lines are then determined with respect to the ship's longitudinal axis, AZ_{RTO} and AZ_{LTO} .
- c) The distance from the aircraft C. of G. to each line is computed, TODR and TODL. They define the distance that the Center of Gravity (in virtual condition) should move to the right or to the left for a turnover to occur.
- d) Two more angles are then defined. These are TOR and TOL. They are Turn Over Right or Left angles, expressed as follows:

$$TOR = \tan^{-1} \left(\frac{TODR}{WL_W - WL_G} \right) \quad (3.10)$$

$$TOL = \tan^{-1} \left(\frac{TODL}{WL_W - WL_G} \right) \quad (3.11)$$

They describe the angle between a vector from the C.G. normal to the R_{TO} or the L_{TO} and the vertical.

- e) For the pitchback condition, similar boundaries are computed. These are as follows:

- The hinge line about which the aircraft is likely to pitchback is the line which joins the right to left main gear.

- The distance from the Centre of Gravity to the hinge line is defined as PBD (Pitch Back Distance) and expressed as:

$$PBD = (STAW - STAM) \quad (3.12)$$

- The Pitch Back Angle (PBA) is expressed as follows:

$$PBA = \tan^{-1} \left(\frac{STAM - STAW}{WL_W - WL_G} \right) \quad (3.13)$$

where;

WL_W = Water Line to the aircraft C.G.
 WL_G = Water Line to the the deck
 $STAW$ = Station of aircraft C.G.
 $STAM$ = Station of aircraft main gears

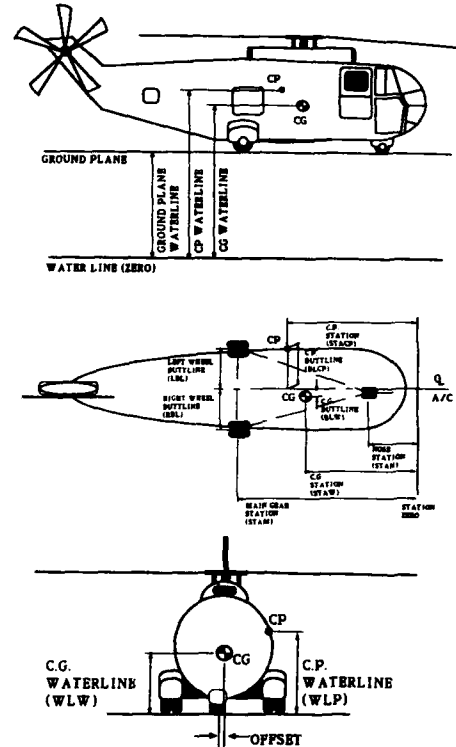


Figure 3.1a- Aircraft Model Definitions

Turnover incidents can be static or dynamic. The static turnover condition is the same as on shore. The resolved weight vector as a result of the wind force goes beyond either the friction forces causing the aircraft to displace (figure 3.2) or the reaction forces causing the aircraft to turnover.

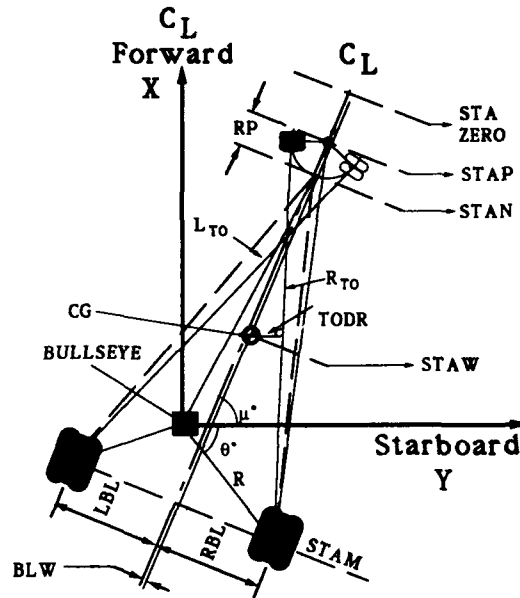


Figure 3.1b- A/C On Deck Definitions

In dynamic turnover, with rotors not turning, the aircraft centre of gravity is in motion induced by the ship in addition to the wind forces.

Descriptively, as the centre of gravity translates, the weight vector is modified by inertial forces and the TODR/TODL and TOR/TOL traces reflect the corresponding 'stability' conditions. At the point at which both TOR and TODR are equal to zero, the aircraft is in its 'metastable' state. Going beyond this point will cause an aircraft incident. Similarly, when the landing gear/ship deck friction values are exceeded by the aircraft weight and inertial forces, slippage is indicated. When the vertical inertial force equals and opposes the aircraft weight, the deck friction goes to zero and an unintentional liftoff is indicated.

With the above aircraft/ship interface boundaries established, the aircraft centre of gravity position time history is monitored and compared against these boundaries to detect turnover and pitchback incidents. In addition the aircraft resultant vertical forces are monitored to detect the unintentional liftoff incident.

3.2- NAV8 Program Description

The Naval Dynamic Interface subject routine also known as FLYNAV or Flying Carpet, was created by P.J.F.O'Reilly in 1977. It has been modified, revised and improved since 1977 under various projects at numerous installations in the United States and Canada. The program calculates *system stability* and indicates detection of static or dynamic on-deck turnover; pitchback, sliding or

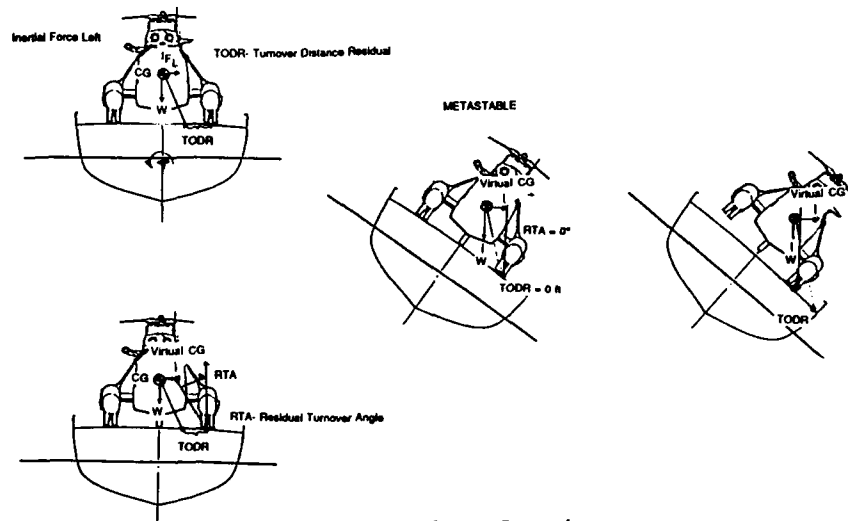


Figure 3.2- Rotor Static Dynamic Turnover

unintentional liftoff incidents. NAV8, like the SMS, was originally developed for the USN on an IBM system computer and in PL1. The program was converted to VAX PL1 and improved with simple menus for easy application.

Referring back to figure (2.3), NAV8 uses ship time history data created in NAV5. Using Command files it is possible to fully automate SMS. Executing NAV8 interactively can be done with ease. The User is asked to enter data representing the helicopter model, including the free stream wind forces and select the type of output reports.

The aircraft is defined by entering details about various aspects of its construction such as the landing gear configuration (single, double nose wheel, tail dragger, or quad gear configuration), centre of gravity, location of the vehicle geometrically on the deck, and air vehicle weight, moments and inertia products. In NAV8, the aircraft model is programmed with rotors spread and free, but not rotating.

The program requests the deck coefficient of friction is (usually 0.8 for dry deck and 0.5 for water wet deck), information on the wind component and the definition of the aircraft's centre of pressure. There are currently 17 options for report outputs including stability

traces, inertial/frictional force diagrams and motion data.

4.0- Deck Clearance Option EH101 vs CPF Example

Deck handling safety analysis was conducted using models representing the Canadian Patrol Frigate (CPF) and what was known about the EH101 helicopter. The purpose of the analysis was to demonstrate the DI software capabilities by assisting in the development, in this case, of unsecured deck handling safety envelopes.

4.1- Interface Description

The CPF is Canada's newest warship, designated FFH-330. The particulars of the first-of-class, HMCS HALIFAX, are tabulated on Table 4.1 in comparison with the other Canadian DDHs [26].

The flight deck is 16.5 m. wide by 23.6 m. long. A RAST-track runs lengthwise along the centerline of the flight deck and hangar for the Canadian-designed "Beartrap" rapid securing and traversing device. The "Beartrap" ensures safe operations in conditions up to Sea State 5. A Landing Safety Officer (LSO) compartment is inset in the forward starboard corner of the flight deck with a Flight Deck Control Room (FDCR)

compartment overlooking the flight deck high on the port side of the hangar face. The hangar is large enough for one SEAKING CH124 ASW helicopter with sufficient clearance to conduct routine maintenance as sea.

Table 4.1
Comparison of Dimensions

CLASS	DISPLACEMENT	LENGTH (m)
CPF	4750 tonnes	134.1
TRUMP	4700 tonnes	121.4
ISL/ANS	3000 tonnes	113.1

A variant of the European Helicopters Inc, EH101 is under consideration as Canada's NSA (New Shipborne Aircraft). In table 4.2, the dimensions of the Royal Navy "Merlin" EH101 prototype [27] are compared to the CH-124 SEAKING. The introduction into service of the EH101 will demand significant changes to current operating procedures and limits. Notwithstanding the large size difference, the "nose-wheel" EH101 will require substantially different deck-straightening procedures from those used with the "tail-wheel" CH-124. Straightening must be conducted quickly with a minimum of personnel involved.

Table 4.2
CH124 vs EH101 Attributes

HELICOP- TER	Max.Wt (kg)	Length folded	Width folded
EH101 NSA	14, 300	15.86 m	5.49 m
CH-124	9, 500	14.40 m	4.96 m

The Canadian and European versions of the EH101 may vary substantially, thus it was difficult to precisely define the EH101 for the DI analysis and simulation conducted. Figures 4.1 and 4.2 depict the CH-124 and EH101 on a CPF flight deck [Note: Detailed compatibility studies have been completed for the EH101 and CPF, TRUMP, and AOR classes by the Prime Mission Vehicle Contractor, the results of which will not be discussed here]. It must be stressed that a Canadian variant NSA is still not fully defined nor is the EH101 accepted as the NSA. The Canadair studies were only a demonstration of DI application to a hypothetical problem using available data. The studies conducted also facilitated the software development.

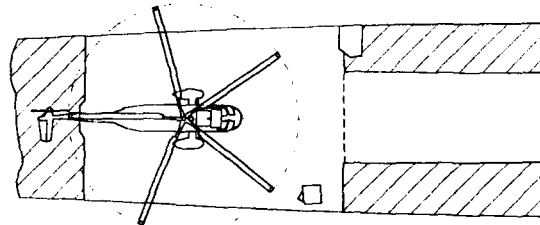


Fig. 4.1- SEAKING/CPF Flight Deck Interface

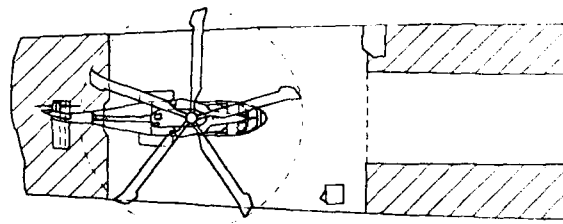


Fig. 4.2- EH101/CPF Flight Deck Interface

4.2- Deck Safety Clearance Results

The contracted study analysed the CPF versus EH101 stability combination. Although Canadian Naval practice is to limit helicopter movements while unsecured, the study conducted provides guidance into free-deck operations should an aircraft the size of the EH101 become the NSA.

The objective of the exercise was to identify envelopes of activity for deck handling and general flight readiness or availability. The testing was conducted using the Ship Motion Simulation (SMS) program. SMS was applied to develop the flight deck motion information. Ship speed, relative wave heading, significant wave height and modal period are the primary ship motion markers. The relative motions are calculated at the point of interest (bullseye or spot of the landing deck). The test matrix using the CPF model reduces to table 4.3.

Table 4.3
CPF Model Test Matrix

Ship Velocities:	05, 10, 15, 20 knots	
Wave Angles:	0 - 180°, every 15 degrees	
Sig. Wave Height: (Equivalent Sea State ~)	1, 3, 6, 9 metres	3, 5, 6, 7)
Modal Period:	5, 9, 11, 15 seconds	
<i>NAV8 additional matrix attributes</i>		
Deck Condition: (Coefficients)	DRY and 0.8	WET (water) 0.5
Wind-Over-Deck:	0 - 50 knots	

Important ship based assumptions are:

- 1)- Physical characteristics described by the RAOs
- 2)- Ship hull is symmetric
- 3)- By symmetry, the vessel would respond identically (quadrants 1 and 4) with motions in quadrants 2 and 3.

A unidirectional Wind-Over-Deck model was introduced in NAV8. In this study, all cases were exposed to a maximum 50 knot wind on both wet and dry decks. Standard NAVAIR

definitions for the coefficients of deck friction were used (0.8 for dry deck and 0.5 for sea water wet deck) [28].

As indicated earlier, the aircraft is defined by its landing gear footprint; deck location and orientation; aircraft weight and inertias; its centres of gravity and pressure, and the lateral drag area.

In this study, the aircraft was modelled with a high centre of gravity and corresponding minimum mission weight. This is generally the worst case weight scenario. The air vehicle was modelled unsecured on the deck as in a free deck operation, with rotors spread but not rotating, and the vehicle fuselage unfolded and locked. The helicopter was modelled centered at the bullseye/bellmouth. The landing gear deflection and forward gears were modelled unlocked and castored for turnover. The aircraft was set on the ship's centreline and rotated to -20 degrees to provide the least stable orientation.

Envelopes were based on limitations defined by the point at which an aircraft/ship incident occurs. Thus, *incident means occurrence of aircraft turnover, pitchback, ondeck slide or uncontrolled liftoff*. The ground rules imposed demanded that if at any point during the simulation analysis an incident was identified, the entire data point was declared out-of-limit. This approach was taken initially without regard to the plausibility of the environmental condition under study (eg: 1 m seas and 50 knot winds). In a second pass, implausible environmental conditions were eliminated.

Interface testing was performed according to the test matrix in table 4.3. In order to graphically describe the results, various methods were considered including the traditional launch and recovery flight envelopes. The final presentation borrowed heavily from the traditional envelopes, with some obvious variations.

Deck Safety Envelopes were created as a function of ship velocity (for every 5 knots of speed) and deck condition (dry and wet). All cases were tested in seas ranging from 1 to 9 metres, 180 degrees in bearing (and by symmetry 360 degrees) and a maximum of 50 knots wind-over-deck.

As an example, only 5 knot and 15 knot ship speed deck safety envelopes are reproduced here (figures 4.3 - 4.6). Comparison between figures 4.3 and 4.4 clearly display the impact that deck conditions may have on aircraft on-deck stability. The envelope is 'tight' on the wet deck diagram with about 50 % less room for error than for the same sea condition dry deck. With increasing speed, this seems to be less evident (figures 4.5 and 4.6) particularly in following seas. Indeed, deck safety in general seems to be less restrictive in following seas. In all cases, beam sea conditions are the most restrictive. When coupled with a wet deck, operations in a three meter beam sea are questionable for an unsecured helicopter.

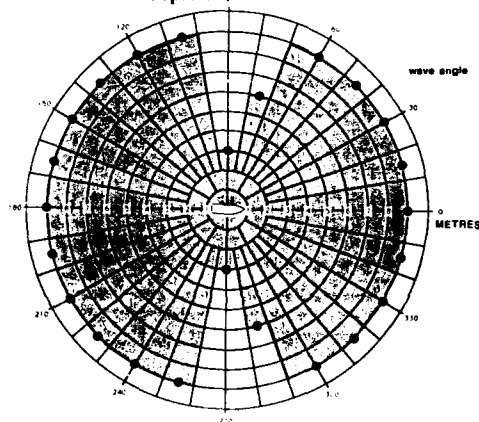


Fig. 4.3- EH101/CPF 5 knots, dry deck

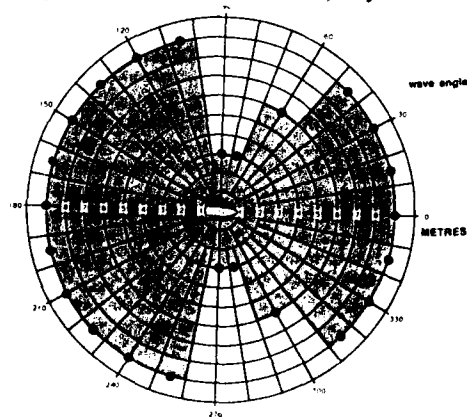


Fig. 4.5- EH101/CPF 15 knots, dry deck

From the results, it may be generally stated that deck clearance for the EH101 is physically very tight, but should not be so limiting as to infringe on launch and recovery envelopes in 'normal operating conditions'. As conditions become degraded or abnormal, the impact on launch and recovery envelopes by deck clearance may become more significant.

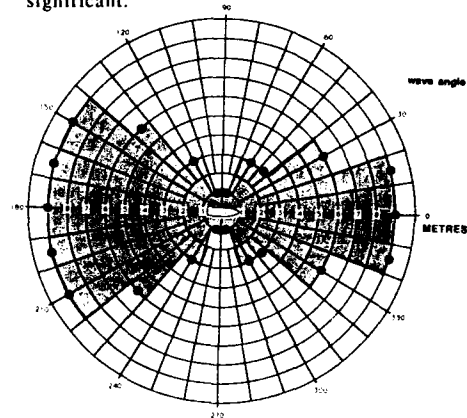


Fig. 4.4- EH101/CPF 5 knots, wet deck

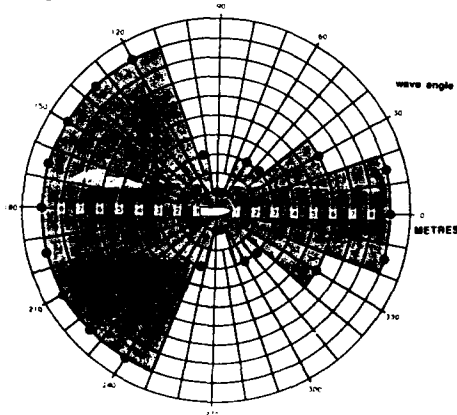


Fig. 4.6- EH101/CPF 15 knots, wet deck

5.0- SMS APPLICATION - Landing Period Designator

5.1- System Definition and Purpose

The landing period designator (LPD) is a system developed to aid helicopter pilots to land or take-off on small vessels in moderate and heavy seas. It reduces the pilot workload

by evaluating ship motions and by determining the proper times to initiate safe landings or take-off. It is an economical system designed to increase the safety of aircraft/ship operations.

The LPD determines the quiescent periods of motion of the ship's landing platform using an energy index (EI) calibrated for a specific aircraft/ship combination. The EI equation consists of eight motion terms calibrated by coefficients which are adjusted in time according to the particular situation. The program allows for a continuous calculation of the index coefficients at sea, providing an operational LPD in all conditions. A threshold standard is applied to the EI value to qualitatively judge the deck activity for a given aircraft/ship combination. The result is then disseminated to the pilot/operator user.

THE THRESHOLD CRITERIA

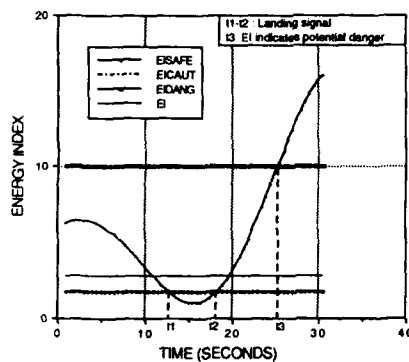


Figure 5.1
Energy index threshold criteria

This section focuses on the methodology used to test the theoretical structure of the Landing Period Designator algorithm using SMS. The preliminary results are discussed.

5.2- Background

The LPD MK I development began in 1974 by Bell Helicopter Textron (J.Love BHT) funded by the USN. The Energy Index (EI) concept was tested at sea in November 1975 aboard the *USS Koelsch*. The EI concept showed promise but deficiencies were identified. Many were addressed in the subsequent LPD MK II work at BHT under the supervision of Peter J.F. O'Reilly. The first EI equation was modified and re-evaluated using ship motion

synthetic time histories. The new equation was calibrated using eight fixed coefficients adjusted for a specific ship/aircraft combination. The fixed coefficients approach for the energy index calibration yielded good results in specific situations but overall optimization was a major problem. It was concluded that several sets of coefficients were needed to cover a single ship/aircraft combination. In 1987, LPD MK III was begun at Canadair as an internal R & D program. The primary objective (LPD MK III) was to resolve the coefficient issue in real-time.

5.3 Theory Synopsis

The landing period designator development is based on a simple formulation called the Energy Index. The Energy Index formulation is as follows:

$$\begin{aligned}
 EI = & A_1 * \Phi^2 & + & A_2 * \dot{\Phi}^2 \\
 & + A_3 * \Theta^2 & + & A_4 * \dot{\Theta}^2 \\
 & + A_5 * \dot{VT}^2 & + & A_6 * \ddot{VT}^2 \\
 & + A_7 * \dot{LT}^2 & + & A_8 * \ddot{LT}^2
 \end{aligned}$$

Where Φ is the Roll angle, Θ is the Pitch angle, VT is the vertical motion of the landing deck and LT is the lateral motion of the landing deck. The lateral motion and the vertical motion of the helicopter landing platform are expressed in the ship's equilibrium frame of reference.

For each air vehicle, deck motion safety limits must be established (also called aircraft limitations). These limits may be measured experimentally on board ships or calculated analytically. The aircraft structural integrity and its maneuverability are the major factors that determine the acceptable limits of motion. The landing impact may be unacceptable for the aircraft structure or the the landing dispersion may be incompatible with the size of the landing deck or the proximity of the ship's superstructure. When aircraft performances are not well known, low motion limitations are chosen to test the LPD performance. This conservative approach ensures the required landing objective is respected, since aircraft limitation data are part of the coefficient calculations.

The energy index formulation uses eight terms to represent the motion in four degrees of freedom (DOF). The four DOF selected are

the most significant in landing period detection [29] [30] and thus, aircraft recovery. Over the previous LPD generations, it was determined that yaw and surge were the least important motions in determining deck quiescent periods. The acceleration and velocity terms in the EI equation give indications of the motion the vessel could travel in the near future [31].

The LPD algorithm continuously optimizes the coefficients A_1 to A_8 . The eight coefficients modify each motion term in such a way that the calibrated EI value correlates the level of deck activity at all times. Pilots or landing safety officers (LSO) can be constantly informed of the deck situation by the depiction of the EI value through a color coding device. Different colors correspond to a separate Energy Index level, determined by threshold values. A color code is proposed as follows:

Flashing Green: Immediate landing signal, with a minimum recovery window of 3 to 5 seconds.

Green: Safe landing deck with low deck motion activity

Yellow: Caution landing deck with medium deck motion activity

Red: Unsafe landing deck with high deck motion activity

When the motion of the landing deck exceeds the aircraft limitations, the coefficient calculation ensures that the LPD displays a red signal. A green or a yellow signal ensures that the deck is safe. These conditions are always verified by the coefficient calculation. The flashing green signal indicates an adequate time to initiate a landing.

When the index is low the ship is stable and the deck displacements and accelerations are benign. For a ship to move from a stable situation to a dangerous situation, the sea must transfer a quantity of energy to the ship's structure. Safe landing windows can thus be identified owing to the limited energy available in a seaway.

In the case of an unmanned air vehicle (UAV), the EI value or the landing signal would be transmitted directly to the control station

The concept can be applied to even the

smallest air capable ships, as shown in the preliminary results. For larger ships, the approach provides longer landing windows: the LPD performance increases with increasing ship inertia.

5.3.1 Coefficient Calculation

Coefficient optimization is performed in three distinct steps. The three steps are executed simultaneously. First, relative coefficients are established between each of the four degrees of freedom and their derivatives. The second step analyzes the relationship between coupled degrees-of-freedom. The third step introduces the aircraft limitations and threshold standards. From the three steps the final coefficients for a given sea condition and air vehicle/ship combination are derived [32]. A flow diagram which summarizes the LPD calculations is presented in figure 5.2.

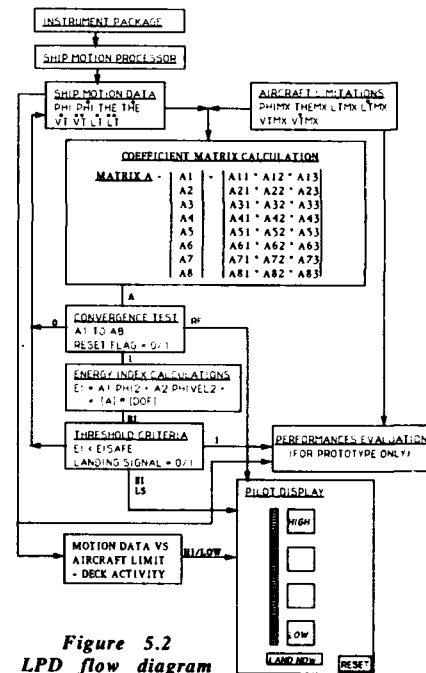


Figure 5.2
LPD flow diagram

5.3.2 Convergence Criterion

The coefficients are adjusted in time and driven by ship behavior. For a significant change in ship's speed or heading,

readjustment of the coefficients will be necessary. During the readjustment a delay may occur until the coefficients are optimized. A signal would be transmitted to the operator indicating the setting period. When the environmental conditions develop gradually, such as a change in wave height or modal period, the LPD system remains operational. However, the coefficients will continue to evolve consistent with the evolving environment.

Preliminary results indicate that the convergence times, in the rapid change ship condition case, are below five minutes. This is considered acceptable in terms of the operational system.

5.4- LPD Development Testing Program

A test model of the LPD has been programmed on the Canadair IBM mainframe. The LPD model was fed with ship motion synthetic time histories provided by the O'Reilly ship motion simulation (SMS). The RAO's were obtained from the NAVSEA SMP87 program (a DTRC derivative). The objective was to demonstrate the EI concept using an empirical approach and to test the performance of the optimization algorithm.

Worst case scenarios were chosen in which the deck motion exceeded the aircraft landing limitations 50% to 90% of the time. The LPD ability to determine safe landing windows was evaluated for each programmed ship condition.

The testing program features a self-verifying capability which indicates any malfunction of the index. Each landing window designated by the LPD is verified retroactively to be sufficiently long to allow the air-vehicle to land safely. The landing window is defined as the period of time, measured after the landing signal, in which the deck remains safe to land a specific air vehicle. Should the LPD indicate safe landing conditions, the pilot/operator could expect a non-incident recovery with some reserve seconds assured [33].

5.4.1- PRELIMINARY SIMULATION RESULTS

A summary table of the first set of LPD tests is presented in table 5.1. The aircraft/ship combination used is the CL-227/FFG8 combination. The coefficients have been calculated in a continuous automatic manner using the LPD MKIII algorithm. Each simulation represents nine thousand data points over a period of thirty minutes with a time step of 0.2 seconds (5 Hz). For each simulation the number of landing periods detected is indicated by category.

The categories are: a) *unacceptable* (less than 3 sec of safe deck following the end of the landing signal), b) *acceptable* (between 3 and 5 sec) and c) *good or very good* (over 5 seconds). The second to last column gives the percentage of time the deck motion does not exceed the aircraft landing limitations. The last column indicates the number of safe landing windows actually present in the data

Table 5.1
Preliminary simulation results

REFERENCE NUMBER OF RUN	SHIP VELOCITY (Knots)	SHIP HEADING (Degrees)	WAVE HEIGHT (Feet)	WAVE PERIOD (Sec)	ENERGY INDEX COEFFICIENTS								UNACCEPT LANDINGS (Below 3 SEC)	ACCEPTABLE LANDINGS (Between 3 & 5 sec)	GOOD LANDINGS (Greater than 5 sec)	SAFE DECK (% of time)	No. safe landing windows
					A1	A2	A3	A4	A5	A6	A7	A8					
NB047	15	15	7.4	9	2.503	2.636	7.070	6.703	0.408	0.364	3.607	2.319	0	2	28	47.16	53
NB049	15	30	7.4	9	2.593	2.796	6.947	6.428	0.408	0.353	3.607	3.524	0	1	21	47.87	54
NB050	15	45	7.4	9	2.965	3.235	7.286	6.827	0.408	0.352	3.607	3.470	0	0	17	45.93	57
NB051	15	80	7.4	9	3.264	3.679	7.835	7.051	0.408	0.342	3.607	3.502	0	0	6	44.80	59
NB052	15	75	7.4	9	4.184	5.109	9.485	8.243	0.408	0.324	3.607	3.293	0	0	3	47.93	73
NB053	15	90	7.4	9	3.888	5.828	6.655	3.773	0.408	0.395	3.607	3.842	0	0	8	52.67	76
NB035	15	15	13	9	1.298	1.656	5.995	5.977	0.408	0.356	3.607	2.482	0	1	15	31.56	45
NB022	15	30	13	9	1.800	1.860	6.746	5.322	0.408	0.355	3.607	3.758	0	1	3	30.42	87
NB017	15	45	13	9	2.255	2.255	6.621	5.533	0.408	0.310	3.607	3.382	0	0	2	26.67	95
NB028	15	60	13	9	2.840	3.408	7.337	6.887	0.408	0.298	3.607	3.417	0	0	1	20.02	39
NB043	15	75	13	9	4.132	4.843	11.71	9.723	0.408	0.310	3.607	3.178	0	0	0	12.53	38

areas of real concern for further detailed consideration during flight testing. The report also confirmed that a restraint device, such as RAST, is required to achieve the broadest possible operating envelope.

While encouraging, the analytic DI method cannot address all the problems or variables associated with Naval helicopter operations. Depending on the level of confidence in the analytic results, considerable time and effort may be required to define operational envelopes experimentally. The developments undertaken through TTCP and the subsequent Canadian DND contract, provide a strong basis for an eventual DI analytic method accepted by all concerned. It is apparent that, with interoperability requirements and multinational procurement projects, a high level of co-operation among all Naval helicopter operators is necessary to refine and improve the DI discipline.

Figure 6.1 illustrates various analytic DI study possibilities, indicating the subject matter is sufficiently varied to occupy any technical interest. The Canadian analytic DI project is an evolving program. New helicopter models, on-going ship studies, exploration of turbulence and wind-over-deck modelling, are some of the directions being taken. The Canadian Maritime Air community has indicated a requirement for an advanced aid to predict quiescent periods in six degrees-of-freedom motion. The device should be designed to complement the pilot's and Landing Safety Officer's (LSO) subjective impressions. As with DI analytics; however, an LPD device would require a significant level of confidence to be a useful tool.

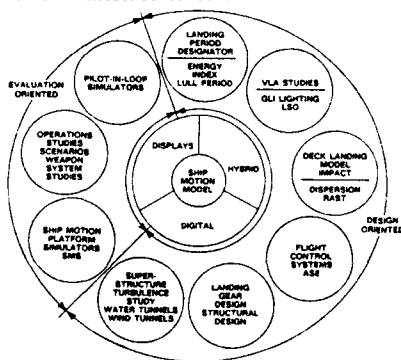


Figure 6.1- DI Analytic Studies

To this end, validation and verification is invaluable in building confidence within the DI community and with system User's. The National Research Council Institute for Marine Dynamics has proposed to undertake in house SMS/LPD investigation, with results to be widely circulated. The CL227 Sea Sentinel (USN) MAVUS demonstration will offer another arena for validation and verification. The requirement for the development of an AUTOLAND tool is driving the proposed incorporation of the LPD into that system. Another step in this direction is the programming of the LPD algorithm into the CL227 ship motion simulator (SMS ship motion has already been successfully programmed in simulators at NATC & CL227). These actions are being advanced in order to build confidence in the user community.

The programs discussed above were the product of intense interdisciplinary efforts by numerous participants, some pillars in their fields (gendre: Bales, Baitis, Carico, O'Reilly). It is hoped that the discussion above may stimulate additional activity throughout the aircraft/ship community in efforts to improve the safety of maritime aviation.

ACKNOWLEDGEMENT

The Authors wish to dedicate this paper to Peter J F O'Reilly, mentor, confidant, and father of the SMS, and to Maj Dave Church (Retired), for his endorsement of the Canadian DI program and unfailing support of the LPD concept. Gratitude is expressed to many members of the DI community, in particular: Readers- Terry Applebee (DTRC), Dean Carico (NATC), Dr. Indra Datta (NRC-IMD), Dr. Neil Gilbert (ARL), Dr. J.Val Healey (NPS), Dr. René Kahawita (POLY), Jim Colwell (DREA), Capt. Bernard LeTourneau (DMAEM), Samy Nasry, ing (CI). In addition, DI Analytics appreciates the dedication of Dale Hutchins (NAVAIR), LCDr Nick Leak (HMCS Protector), Major Alan MacDonald (DND), Claude March (POLY), Ashley Arney (ARL) and Jeff Semenza (NATC).

REFERENCES

- [1] Istchenko, Maj W.O and Bossé, Capt. J.M (1989). Ship-Helicopter Interface Testing for the Canadian Forces in the 1990's. CASI Flight Test Symposium. CFB Cold Lake. Medley.
- [2] Healey, J.Val (86). Simulating the Helicopter-Ship Interface As An Alternative to Current Methods. NPS67-86-003. Naval Postgraduate School Monterey.

- [3] Carico, D (1988). Proceedings of the First DI Working Group Meeting. DI-RWD. NAVAIR-TESTCEN. Patuxent River.
- [4] Istchenko and Bossé (1989).
- [5] Ferrier, B & Semenza, J (1990). NATC Manned Flight Simulator VTOL Ship Motion Simulation and Application. *Proceedings of the AHS*. Washington.
- [6] Hoekstra, T; Fang, R; Leijnse, G; Renirie L (1978). Qualification Tests with helicopters for use on board ships. Nationaal Lucht-en Ruimtevaartlaboratorium(NRL).NLR NP78032U. Amsterdam.
- [7] Ferrier & Semenza (1990).
- [8] Curtis, LCdr J.T, Lescher, Lt(N) W.K, Smith, Lt(N) P, Long, K R (1988). SH-60B Dynamic Interface Test Aboard USS Cushing (DD985). RW-15R-88 (FOUO). NATC. Patuxent River.
- [9] Hammond, Lt(N) A & Dubois, J (1986). SH-60B Manual Deck Handling Tests. Quick Response Report. RW-79R-86. NATC. Patuxent River.
- [10] O'Reilly, P.J.F (1985). Aircraft/Deck Interface Dynamics for Destroyers. *Marine Technology*. Vol.24, No:1. SNAME. New York.
- [11] Meyers, W; Applebee, T; Baitis, A E (1981). "User's Manual to Standard Ship Motion Program, SMP81". DTNSRDC/SPD-0936-01. Washington.
- [12] Ochi, M & Bales, S (1977). Effect of Various Spectral Formulations in Predicting Responses of Marine Vehicles and Ocean Structures. *Proceedings of the 9th Offshore Technology Conference*. OTC 2743. Houston.
- [13] O'Reilly, P.J.F (1974). Destroyer Motion Simulation Study. BHTI 299-010-923. Ft.Worth.
- [14] Korvin-Kroukovsky, B.V (1961). Theory of Seakeeping. *Monograph of the Society of Naval Architects and Marine Engineers*. SNAME. New York.
- [15] St.Denis and Pierson, W (1953). On the Motions of Ships in Confused Seas. *Transactions of SNAME*. Vol.61. New York.
- [16] *ibid*
- [17] Carico, D and Madey, Cdr S (1984). Dynamic Interface Flight Test and New Analytical Approach. AHS Specialist Meeting. Williamsburg.
- [18] *ibid*
- [19] Brown, Maj N. Brown (1977). Canadian Navy Experience With Small Ship Helicopter Operations. CP-233 AGARD Flight Mech.Panel Symp. NASA/AMES (May 16-17).
- [20] St.Denis and Pierson, W (1953)
- [21] Pierson, W and Moskowitz, L (1964). A Proposed Spectral Form for Fully Developed Wind Seas Based on the Similarity Theory of S.A. Kitaigorodsky. *Journal of Geophysical Research*. Vol. 69, No:24.
- [22] Bretschneider, C. L (1959). "Wave Variability and Wave Spectra for Wind-Generated Gravity Waves". Beach Erosion Board. U.S.Army Corps of Engineers. Technical Memo No: 118.Washington.
- [23] Baitis, A.E; Meyers, W.G; Applebee, T R (1976). "A Non-Aviation Ship Motion Data base for the DD963, CG26, FF1052, FFG7 and the FF1040 Ship Classes". DTNSRDC Report. SPD-738-01. Washington.
- [24] O'Reilly, Peter J.F (1978). Ship Motion Analysis. BHTI. 699-099-087. Ft. Worth.
- [25] Blackwell, J and Feik, R.A (1988). "A Mathematical Model of the On-Deck Helicopter/Ship Dynamic Interface (U)". Aerodynamics Technical Memorandum 405. Aeronautical Research Laboratory Melbourne.
- [26] Sharpe, Capt (N) R (1990). Jane's Fighting Ships. Janes Information Group. Surrey.
- [27] EHI (1988). Response to NSA RFP. EH101 Dimensions. Yeovil.
- [28] Ferrier, B and Semenza J (1990)
- [29] Love, J (1976). "Evaluation of a helicopter landing period designator aboard the USS Koelsh". Volume 1. BHTI. Ft.Worth.
- [30] O'Reilly, P J. F (1980). "Landing Period Designator Mk II". BHTI. Ft. Worth.

[31] Thibodeau, F (1989). "Projet d'interface dynamique aéronef VTOL/bateau. Etude du Mouvement des océans et de la réponse des bateaux". *Projet de fin d'étude*. Département mécanique. Ecole Polytechnique de Montréal.

[32] Thibodeau, F (1990). "Energy Index Formulation for Canadair LPD Mk III". CI SYS. Montréal.

[33] Ferrier, B and Semenza J (1990)

BIBLIOGRAPHY

Quellet, Y (1973). "Analyse spectrale de la houle". *Cours GCI-60-333*. Université Laval. Québec.

Brown, R & Camaratta, F (1978). "Ship Motion Computer Program" (SMS). NAVAIRENGCEN. NAEC. MISC-903.8 . Lakehurst.

Neumann, Gerhard (1952). Über die komplexe Natur des Seeganges- Zweiten Teil- Das Anwaschen der Wellen unter dem Einfluss des Wind. *Deutsch Hydr. Zeit.* BAND 5, 1952. Bonn.

Bonnefille, R (1976). "Cours d'Hydraulique Maritime". école Nationale Supérieure de Techniques Avancées. Paris.

EVALUATING FIXED WING AIRCRAFT
IN THE AIRCRAFT CARRIER ENVIRONMENT

by

Mr. C. P. Senn

STRIKE AIRCRAFT TEST DIRECTORATE
NAVAL AIR TEST CENTER
PATUXENT RIVER, MARYLAND 20670-5304
UNITED STATES OF AMERICA

Summary

Operating fixed wing aircraft from today's modern aircraft carrier is a demanding task. Evaluation of aircraft/ship compatibility, both during the concept development phase and Full Scale Development (FSD) ground and flight tests presents the evaluation team with unique challenges. The capabilities and characteristics of high performance carrier based tactical aircraft must be quantified for the catapult launch and subsequent flyaway, and the carrier approach and arrested landing tasks. Catapult launching involves determining the minimum safe launch airspeeds while maintaining acceptable flight characteristics in this low altitude, high angle of attack (AOA) regime. Approach and landing requires the slowest possible approach airspeeds while retaining the performance and handling qualities needed for precision glide slope control. Defining the lowest catapult launch and landing airspeeds reduces wind over deck (WOD) requirements, resulting in reduced ship's operating speed and increased operational flexibility. The tight operating confines of the flight and hangar decks, in conjunction with the large number of other aircraft, support equipment, and personnel dictate unique design requirements which must be considered in the earliest design stages of a new airplane. This paper addresses the shore based and shipboard ground and flight tests which are conducted to assess the flying qualities, performance, and structural suitability of an airplane in the aircraft carrier environment.

The Aircraft Carrier Flight Deck Layout

The flight deck layout of today's modern aircraft carrier is shown in figure 1. Two steam powered catapults are located forward (bow catapults) and two catapults are located amidships on the port side (waist catapults). Retractable Jet Blast Deflector (JBD) panels are located aft of each catapult. The centerline of the landing area is angled relative to the ship's centerline, permitting simultaneous catapult launch operations from the bow catapults and arrested landing operations. Four arresting gear cables, connected to arresting engines are located in the landing area. The first is approximately 170 ft (51.8 m) from the stern with approximately 50 ft (15.2 m) between each arresting gear cable. Visual glide slope information is provided to the pilot by a Fresnel Lens Optical Landing System (FLOLS). Aircraft are moved between the flight deck and the hangar deck by four elevators.

Catapult Launch

Evaluation of the catapult launch environment of an airplane covers many disciplines. These areas include:

- a) Compatibility with the catapult accessories.

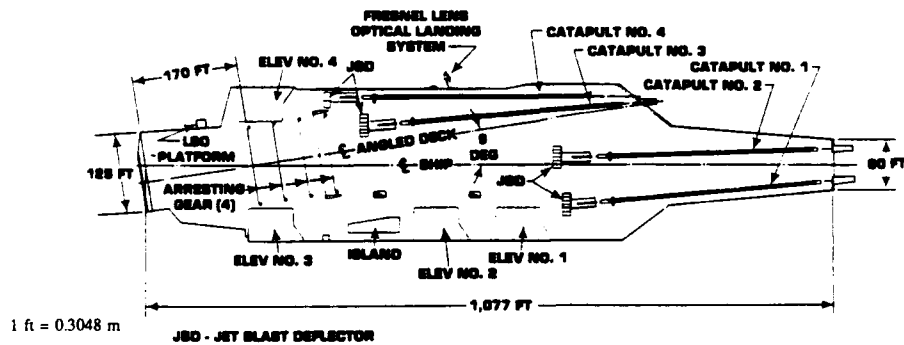


Figure 1
Plan View of Flight Deck
NIMITZ Class Aircraft Carrier

- b) Exhaust gas recirculation/reingestion and the thermal/acoustic environment when operating at maximum power in front of the JBD's.
- c) Tolerance of the engines to ingestion of steam emitted from the catapult during the power stroke.
- d) Structural integrity during the catapult power stroke.
- e) Minimum catapult launch airspeeds and characteristics during the rotation and flyaway phases.
- f) Shipboard catapult launch operations such as waist catapult operations, lateral/directional trim requirements for asymmetric external stores and crosswinds, etc.

Catapult Accessories

Catapult accessories are the items of hardware necessary to attach the airplane to the catapult. Items considered are:

- a) Ease of installation of the repeatable release holdback bar on the nose gear.
- b) Tracking of the launch bar tee head and holdback bar in the catapult nose gear launch guide rails.
- c) Mating of the launch bar tee head with the catapult spreader.
- d) Clearance between the airframe and external stores and above deck obstructions such as the catapult shuttle, catapult control station, etc.
- e) Holdback bar dynamics following release due to the sudden release of high strain energy.

Jet Blast Deflectors

Exhaust gas recirculation and reingestion can occur when an airplane is operating at maximum power levels when positioned in front of the JBD. Reingestion of exhaust gas can cause an excessive temperature rise in both the compressor and turbine sections, resulting in damage to the engine. Ingestion of exhaust gas by the airplane positioned behind the JBD can also result in damage to its engine. Impingement of the exhaust plume on the JBD panels can result in local hot spots which can cause premature warping and cracking. JBD operations can also result in a severe acoustic and thermal environment. Shore based tests are conducted using a shipboard representative JBD installation. Testing consists of placing one airplane forward of the JBD panels and a second airplane aft of the panels as shown in figure 2. The position of the airplane in front of the JBD is varied from the minimum to the maximum engine tailpipe to JBD distances representative of shipboard JBD/catapult combinations. Military and afterburner thrust (if available) runs are conducted for approximately 30 seconds. Both airplanes monitor engine inlet and exhaust gas temperatures and other critical parameters. The acoustic and thermal environment is monitored using microphones and thermocouples mounted on the airframe and in the vicinity of the JBD. Pole mounted instrumentation provides jet blast velocities and temperatures in the flow field beside and behind the JBD. Generally, the wind over deck during shipboard operations tends to alleviate any recirculation, reingestion, or thermal problems. However, if an airplane has demonstrated a tendency to have excessive exhaust gas ingestion, a shipboard test program may be

warranted to define a wind over deck envelope which reduces the ingestion to acceptable levels.

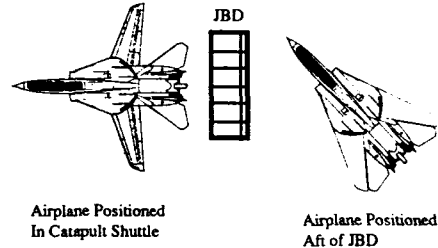


Figure 2
Airplane Locations
During JBD Testing

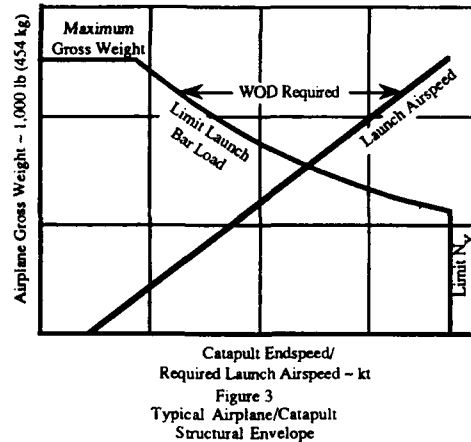
Steam Ingestion

Steam catapults typically emit launch steam above the deck during the launching operation. The design of the engine inlets and the proximity of these inlets to the catapult shuttle frequently cause this above deck steam to be ingested through the engine(s) of the airplane being launched. The result is that the engine is forced to operate at off-design conditions and instabilities can occur. These instabilities can take the form of minor pressure fluctuations within the compressor or the afterburner and could result in blowout, compressor stall, or engine flameout.

The primary method of determining susceptibility to stall is to conduct shore based catapult launches from a degraded catapult. The catapult is intentionally degraded by removing plugs in the aftermost plate of each piston assembly. This allows steam in the cylinders to travel forward of the aft face of the piston, bypass the catapult cylinder sealing strip as the shuttle assembly lifts the sealing strip during the power stroke, thus allowing the steam to exit above deck around the catapult spreader. This steam leakage produces conditions that are more severe than those encountered in the actual shipboard environment. The airplane is launched a sufficient number of times (about 30 launches) to reasonably ensure that no instabilities are encountered. An appropriate number of additional launches will also be required if the engine is equipped with an afterburner. Testing is confined to those days when the surface winds are less than 10 knots and ± 20 deg relative to the catapult centerline. Telemetered engine performance parameters are monitored to ensure continued satisfactory engine performance.

Structural Requirements

A typical catapult launch structural envelope is shown in figure 3. This figure shows the longitudinal acceleration (N_x)/launch bar load/maximum gross weight boundaries.



The N_X and limit launch bar load limits are design numbers which are defined by the mission requirements and maximum performance capabilities of the catapult types from which the airplane is to operate. The maximum gross weight is an airplane design factor based on a 10% growth factor of the basic operating weight of the design. Shore based structural testing consists of increasing the catapult end speed until either the limit N_X or launch bar load is reached. Catapult tests involving a new airframe are initially conducted with full internal fuel loads only. As testing proceeds, additional external and internal stores are carried until all weapon stations have demonstrated adequate strength for catapult launch to the limits of the basic airframe. Most launches are conducted with the airplane oncenter; however, offcenter launches with the main landing gear up to 24 inches (0.61 m) offset from the centerline position are performed to evaluate structural loads resulting from yaw accelerations and airplane directional characteristics during and following launch. The airplane and suspended stores are extensively instrumented to monitor strains and accelerations for all critical structural areas. A new airplane catapult launch structural demonstration program may require up to ten loading configurations to adequately test the structure/functional integrity during catapult launch.

Catapult Launch Minimum End Airspeeds

The most extensive test program relating to catapult launch is the determination of the minimum catapult launch airspeeds. From an operational point of view it is desirable that a minimum catapult launch end airspeed be defined. This minimum airspeed is the slowest equivalent airspeed achieved at the end of the catapult power at which the airplane can safely fly. Establishing the lowest possible launch airspeed has the following advantages:

- a) Decreases the wind over deck required for launch, thus decreasing the ship's speed and increasing the operational flexibility of the aircraft carrier.
- b) Decreases the loads imposed on the airframe increasing service life.

c) Decreases the amount of energy imparted to the airplane resulting in conservation of water and fossil fuel/core life.

The catapult launch minimum end airspeed is defined by a set of related criteria. Although these criteria generally have interrelated effects, the following addresses each factor separately:

a) Proximity to or warning of stall: The stall airspeed/angle of attack defines an absolute minimum. The required safety margin is dependent upon the characteristics of the airplane under consideration. If stall warning (generally in the form of artificial stick/rudder shaker and/or airframe buffet) occurs at some AOA below stall and the warning does not increase in intensity as the airspeed is decreased to the stall, then the angle of attack (AOA) corresponding to stall warning will likely define the minimum end airspeed.

b) Flying qualities/characteristics at high AOA: Frequently an airplane may exhibit adverse flying qualities or characteristics at high AOA, yet at airspeeds well in excess of the stall airspeed. The pilot must then determine the minimum airspeed/maximum AOA at which the airplane characteristics/flying qualities remain acceptable. Examples of limiting characteristics include: buffet, wing rock, wing drop, pitch up tendency, nonlinear stick force gradient, and unacceptable lateral/directional characteristics.

c) Proximity to the airspeed at which thrust available equals thrust required or "lockpoint": For practical purposes, the minimum launch airspeed should be at least 8 kt above the lockpoint. Pilots have indicated that the minimum level of longitudinal acceleration at which he has the sensation of accelerating is approximately 1 kt/sec. This level of acceleration must be available even though this airspeed may be more than 8 kt above the lockpoint. This acceleration capability must be available at the minimum end airspeed. This minimum launch airspeed may become the dominant factor at higher ambient temperatures due to the decreased thrust available with increased temperature. The maximum catapult launch gross of an airplane may be limited as a function of ambient temperature or the minimum launch airspeed may be increased to put the airplane on a more favorable position on the thrust required curve. Longitudinal acceleration characteristics can also be improved by reducing drag, such as using half flaps instead of full flaps or by the use of afterburner on airplanes so equipped. However, the use of reduced flap settings will increase the minimum launch airspeed and the use of afterburner greatly increases fuel usage during takeoff.

d) Airplane rotation requirements and subsequent sink off the bow: The postlaunch rotation requirement to achieve the flyaway attitude will frequently cause the minimum obtained to be higher than that predicted exclusively from proximity to stall or adverse flight characteristics. If the airplane attitude during the catapult launch differs significantly from the desired flyaway attitude, a lift deficiency exists during the period of time required to rotate the airplane. This causes the airplane to generate a sink rate and results in sink off the bow until airplane performance/aerodynamics provides sufficient vertical acceleration to establish level flight and subsequent flyaway. For a given airplane end airspeed, sink off the bow will vary with time required to rotate, average lift deficiency during rotation, and excess lift and thrust at the flyaway airplane attitude. Airplane CG sink off the bow of 20 ft (6.1 m), as measured from the static position on the deck (CG vertical height), is considered the maximum acceptable.

e) Failure of one engine on a twin engine aircraft during launch: Two factors must be considered if an effort is to be made to establish a minimum end airspeed at which an airplane can remain airborne after losing one engine during launch. Foremost of these is the single engine minimum control airspeed (V_{MC}) at which sufficient control authority is available to counter the yawing forces. Secondly, is whether the single engine rate of climb performance of the airplane is sufficient to permit safe flyaway. The single engine minimum control airspeed will establish an absolute minimum launch airspeed. If only a small increase in minimum end airspeed is required to improve single engine rate of climb performance enabling single engine flyaway, it should be a consideration in establishing the minimum end airspeed. The use of afterburner, if available, should significantly improve single engine performance, but will necessitate an increase in the minimum launch airspeed to provide single engine control.

f) Automatic flight control response: The incorporation of digital, fly-by-wire flight control systems into more recent aircraft models has eliminated the need for pilot programmed flight control inputs to attain a predetermined rotation and flyaway response. Current systems are implemented such as to achieve a desired flyaway trim AOA. However, flight control response due to pitch rate feedback during the highly dynamic conditions during the first several seconds following catapult shuttle release may result in flight control surfaces reaching their physical limits. If any of the primary flight control surfaces reach full deflection during the rotation or initial flyaway phases, the minimum end airspeed is then limited by this criterion.

Test Procedures

A considerable amount of time and effort is expended during shore based build-up to generate prerequisite data prior to tests aboard ship. Careful consideration is given to all the factors governing the minimum end airspeeds so that the results are applicable to the entire range of Fleet operating conditions. These factors include the high lift configuration (half or full flaps), external store loadings, CG positions, longitudinal trim requirements, and thrust (Military or afterburner).

Since the intent of determining the minimum airspeed is to define the lowest launch airspeed, the highest lift configuration is tested. With airplanes having more than one flap setting, the maximum flap deflection is suggested. However, this decision has to be tempered with the possibility of reduced nose up pitch authority which could result in increased time to rotate to the flyaway attitude, thus reducing sink off the bow. Additionally, there is an increased chance of reaching control surface limit deflections. The higher flap setting also results in more drag, thus decreasing longitudinal acceleration. External stores are selected to cover the range of anticipated gross weight, CG, and drag conditions expected during operational use. Forward and aft CG positions are tested to evaluate rotation characteristics and to define longitudinal trim requirements to be set prior to launch.

Shore based build-up flight tests are conducted in each of the high lift, external store, and CG position conditions. Classical flight test techniques are used to define the longitudinal/lateral/directional characteristics at high AOA up to stall, static/dynamic single engine control airspeeds, and thrust available and required. Shore based catapult launches are conducted at the predicted minimum end airspeed to investigate trim requirements, flyaway characteristics, and pilot technique. Shore based catapult launches are preliminary in nature because the airplane remains in ground effect and, of course, there is sink off the bow. All of these shore

based tests enable prediction of the catapult launch minimum end airspeeds. The final judgement comes aboard ship.

Testing at Sea

The shipboard tests are conducted in a tightly controlled environment. Tests are conducted in steady winds from dead ahead and minimal deck motion. The catapult is maintained at a constant thermal state to ensure repeatability of catapult end speeds during subsequent launches. A calibrated boom anemometer is installed on the bow to provide accurate wind speed and direction. Noncritical external store loadings and CG's are tested initially. Initial launches are conducted well in excess of the predicted minimum airspeed (approximately 25 knots). Upon recovery following the launch the airplane is refueled and external stores expended prior to recovery are reloaded to re-establish the desired gross weight and CG. The catapult end airspeed is reduced in suitable decrements; initially 5 knots and then 3 knots as the predicted minimum end airspeed is approached. The initial reductions in catapult end airspeed are achieved by reducing the catapult end speed and as the predicted minimum end airspeed is approached, the catapult end speed is maintained constant and the wind over deck is lowered by reducing ship's speed. Airplane performance parameters; such as sink off the bow, rotation characteristics, flight control response, longitudinal acceleration, etc. are monitored and analyzed by the engineering test team via telemetered instrumentation. Catapult launch end airspeed is thereby reduced until one of the previously mentioned criterion are reached. This sequence of catapult launch tests are repeated for each critical gross weight, CG position, and external/internal store loading until the operational envelope has been defined.

In general, no minimum end airspeed criterion is the determining factor throughout the operational gross weight range of an airplane. An airplane may be V_{MC} limited at lighter gross weights, sink off the bow limited at medium gross weights, and longitudinal acceleration limited at high gross weights and ambient temperatures. Figure 4 represents these three different criteria.

It is important to note that the minimum catapult launch end airspeeds are the lowest airspeeds that an airplane can be safely launched. However, these airspeeds are determined under optimum conditions. These conditions include day VMC, a nonpitching deck, steady winds monitored by a calibrated anemometer, skilled aircrew trained in the optimum technique, gross weight and CG accurately known, catapult performance closely monitored, and end speed corrections made for ambient temperature and barometric pressure. In view of this, operational catapult launch operations are conducted at a recommended airspeed 15 knots above the minimum launch airspeed.

b) **Rolled and yawed attitude at touchdown:** This type of landing represents a last second lineup correction. The target attitude for both roll and yaw at touchdown is 5 deg. Landings are conducted with the roll and yaw in the same direction and also in the opposite direction.

c) **Free flight arrestment:** Occasionally an arresting hook will engage the arresting gear cable prior to main landing gear touchdown. This could happen with an inclose pitchup attitude change or during a waveoff. This type of arrestment is called a free flight. High nose gear landing loads are obtained upon touchdown. Free flight arrestments are intentionally conducted during the shore based test program.

d) **Offcenter:** All landings don't always occur in the center of the targeted landing area. Offcenter arrestments, up to 20 ft (6.1 m) left and right of the centerline are conducted to investigate the high side loads imposed on the arresting hook and airframe structure during this type of landing. The wing rock dynamics induced during this type of arrestment are monitored to determine any potential for contact of the wingtip or wing mounted external stores with the runway or arresting gear cables.

e) **High sinking speed:** To meet the design requirements for shipboard landings, U. S. Navy airplanes are designed for touchdown sinking speeds up to 26 fps (7.9 m/s). High sinking speed tests are the most critical of all the arrested landing structural tests. In the interest of safety, actual flight tests are conducted to 80% of the design limit. During testing, the targeted sinking speed is increased by slowly increasing the angle of the optical glide slope until the targeted sinking speeds achieved. In addition, this sinking speed is required to be tested at three different airplane pitch attitudes; 1) the normal landing attitude, 2) nose down (three point landing or nose gear first), and 3) a taildown attitude 3 degrees higher than the normal landing attitude.

The above five landing conditions are repeated in each of the critical loading combinations that the airplane will experience operationally.

Approach AOA and Airspeeds

Many factors must be considered relating to the determination of the recommended approach AOA and the associated airspeeds for the range of recovery gross weights. It is desired that the slowest possible approach AOA and airspeed be defined in order to minimize recovery WOD requirements. However, the need to establish the slowest AOA must be weighed against the requirement to ensure adequate flying qualities and performance to safely perform the carrier landing task. To this end, a number of criteria, mainly quantitative, have been developed to enable evaluation of the approach AOA and airspeeds. These criteria are part of the performance guarantees specified in the requirements for new aircraft. Attaining these criteria "should" ensure satisfactory carrier approach flying qualities and performance characteristics. For an airplane in the landing configuration on a 4 deg glide slope on a 89.8°F (32.1°C) day and at the carrier landing gross weight, the minimum useable approach airspeed (V_{PA}) should be the highest of the airspeeds required to meet the criteria detailed in the following paragraphs.

Acceleration Response to Large Throttle Inputs: For a large throttle input, such as a waveoff, the slowest airspeed will be that airspeed at which it is possible to achieve a level flight longitudinal acceleration of 5 fps^2 (1.5 m/s^2) within 2.5 seconds after throttle movement. If any flight control effectors or speed brakes are automatically scheduled with throttle movement, then these

surfaces may be moved. It is important to note that this requirement does not imply that the airplane must be in level flight with an acceleration of 5 fps^2 (1.5 m/s^2), rather that, during the approach, the engine(s) be operating in a region such that the acceleration characteristics would enable the engine to accelerate from the thrust required on glide slope to that thrust level equalling 5 fps^2 (1.5 m/s^2) acceleration at the same airspeed in level flight.

Acceleration Response to Small Throttle Inputs: The second approach airspeed criterion relating to acceleration capability is rapid engine response to small throttle movement. At the approach airspeed, step throttle inputs corresponding to a 3.86 fps^2 (1.18 m/s^2) longitudinal acceleration command will result in achieving 90% of the commanded acceleration within 1.2 seconds. This requirement applies both to acceleration and deceleration. This requirement applies throughout the weight range and anticipated drag levels of the airplane. Figure 6 shows this requirement.

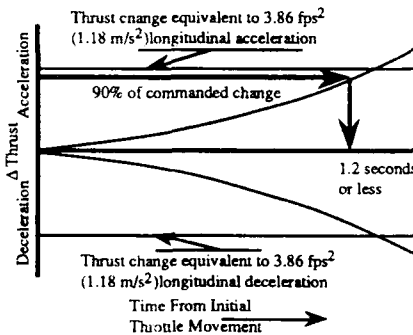


Figure 6
Acceleration Response
to Small Throttle Inputs

Over The Nose Field of View: The slowest acceptable approach AOA must provide adequate over the nose field of view. With the airplane at an altitude of 600 ft (182.9 m) above the water in level flight and with the pilot's eye at the design eye position, the waterline at the stern of the ship must be visible when intersecting a 4 degree optical glide slope. The source of the optical glide slope is 500 ft (152.4 m) forward of the ramp of the ship and 65 ft (19.8 m) above the water.

Margin Over Stall: The slowest airspeed equating to $1.1 V_{SPA}$, where V_{SPA} is the power-on stall airspeed using the power required for level flight at $1.15 V_{SL}$, which is the power-off stall airspeed. The determination of this airspeed is to first calculate V_{SL} , calculate the power required to maintain unaccelerated level flight at $1.15 V_{SL}$, determine the power-on stall airspeed at this power level, then calculate $1.1 V_{SPA}$.

Flying Qualities: The slowest approach airspeed shall provide Level I stability and flying qualities.

Glide Slope Transfer Maneuver: This requirement is often referred to as the 50 ft (15.2 m) pop-up maneuver. The airplane is to perform a glide slope maneuver so as to transfer from one glide slope to another glide slope which is 50 ft (15.2 m) above and parallel to the first glide slope. The 50 ft (15.2 m) transfer is referenced to the CG of the airplane. The maneuver must be completed within 5.0 seconds. Longitudinal control can be inputted as necessary with the constraint that the maximum incremental load factor cannot be greater than 50% of that available at the start of the maneuver. The throttle setting cannot be changed during the maneuver. This maneuver is often misunderstood to mean that the altitude of the airplane is increased. In fact, the altitude at the end of the maneuver can be somewhat below that when initiated. For example, if the sink speed of the airplane is 15 fps (4.6 m/s) at the start, the airplane will intercept the new glide slope 25 ft (7.6 m) lower in altitude than when the glide slope transfer was started [$15 \text{ fps (4.6 m/s)} \times 5 \text{ sec} - 50 \text{ ft (15.2 m)} = 25 \text{ ft (7.6 m)}$]. Once the new glide slope has been intercepted, longitudinal control and throttle inputs can be made to establish a new glide slope parallel to and at least 50 ft (15.2 m) above the initial glide slope. Figure 7 presents this maneuver.

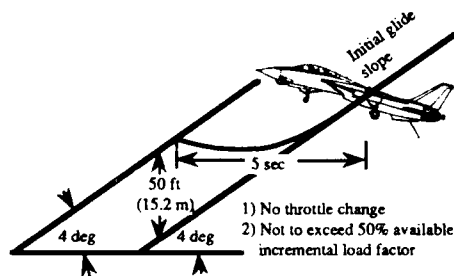


Figure 7
Glide Slope Transfer Maneuver

Additional Considerations:

Single Engine Control Airspeed: For a multi-engine airplane the slowest approach airspeed will not be less than the single engine control airspeed (V_{MC}). This will ensure adequate control in the event of a total engine failure during a waveoff when performed at the approach airspeed.

Touchdown Attitude: Touchdown attitude considerations have on occasion dictated the selection of an approach airspeed/AOA. The pitch attitude must be such that a tail down, free flight, or nose down arrested landing with resultant airframe damage be only remotely possible.

Glide Slope Tracking: The combination of airframe/engine performance is of prime importance in evaluating the handling characteristics of an airplane on the glide slope. The speed/power (or flight path) stability characteristics of an airplane have a great deal of influence on the ability of the pilot to make corrections in airspeed and rate of descent.

The following glide path correction capabilities are considered over the approach airspeed/AOA range:

- a. The ability to make glide path corrections by changing the rate of descent at a constant thrust setting.
- b. The ability to make glide path corrections by varying the thrust while maintaining a constant airplane AOA.

In making glide path corrections, the pilot instinctively attempts to do so initially with longitudinal control. Effective control of airplane pitch attitude necessitates that the longitudinal control power, damping, and mechanical characteristics be such as to permit small, precise pitch attitude corrections. It is extremely desirable that the airplane have maneuvering capability at a constant thrust setting for small changes in AOA on the order of one or two degrees. For making large corrections to the glide path which are sometimes necessary early in the approach, it is necessary to determine the change in thrust required for changes in AOA. An airplane that possesses this characteristic is easier to fly on the glide slope by correcting to glide slope with longitudinal control, returning to the proper approach angle of attack, and then adjusting thrust to correct for the original erroneous setting. Using this method, rapid glide path corrections are possible and thrust corrections in only one direction are required for each evolution.

If an airplane does not respond satisfactorily to longitudinal control, an alternate technique is evaluated. The airplane is maintained at the desired AOA and thrust corrections are used exclusively to make glide path corrections. With this technique, the airplane response as a function of the excess thrust available for maneuvering ($\Delta T/W$), the increase in thrust for small throttle movements, the engine acceleration characteristics, and the contribution of thrust to lift are all evaluated. Because of the lag in engine and airplane response to throttle movement and because of the tendency to "overcorrect" in order to establish vertical acceleration, it is difficult to determine the proper thrust setting required to hold the glide path. As a result, the pilot gets "behind" the airplane and the airplane follows a mild oscillatory path in the vertical plane of the glide slope. Therefore a procedure in which thrust and longitudinal control are initiated simultaneously is necessary for rapid corrections even though it requires precise coordination and increases pilot workload. The use of speed brakes may lessen the aircraft perturbations since increased power setting may provide better engine acceleration and the addition of any parasite drag device such as speed brakes contribute to speed stability by reducing the airspeed for minimum drag.

A combination of the numerous approach airspeed/AOA criteria dictates that the approach be made on the unstable portion (back side) of the thrust required curve. If an approach is made in this area, the use of the throttles is mandatory for making corrections in airspeed and rate of descent and thereby increases the difficulty of executing a precision approach. Further, if the approach must be made on the unstable portion, it is desirable that the thrust changes required are not large for small excursions from the approach airspeed. In terms of flight path stability, the change in flight path angle with airspeed should not be greater than 0.06 deg/kt. A rapidly increasing slope of the curve means that the airplane may decelerate rapidly and require the pilot to add much more thrust to stop a deceleration when compared to the thrust reduction necessary to stop an acceleration. It is also desirable that the approach be made where the curve has a gradient and not on the flat or neutral flight path stability portion where a range of airspeeds are possible for approximately the same thrust setting.

Lineup Control: Effective control of airplane heading is mandatory for carrier deck lineup control. Lateral control power, damping, and mechanical characteristics (trimmability, stick breakout forces, stick gradients, stick deadbands) should be such

that the pilot can effect small, precise line up corrections during the approach. The use of lateral control should not cause distracting pitching or yawing moments.

The previous discussions have highlighted in general terms the numerous items which have a bearing on the selection of the approach airspeed/AOA and an optimum pilot technique. Frequently, several flying qualities and performance characteristics become marginal at the same airspeed/AOA and one may mask another. It is important to recognize all of the factors involved since improvements of one may render another more acceptable or unacceptable.

Qualitative Evaluation Tasks: In addition to the quantitative and qualitative evaluation techniques which are used in defining the approach AOA and associated airspeeds, it is possible to evaluate the approach and landing by defining the tasks the pilot must accomplish for each phase of the landing. Table 1 specifies the distinct phases during landing and lists suggested tolerance bands for the required performance. These levels of performance should be attainable with an HQR - 3 or better.

Table 1
Approach and Landing
Qualitative Evaluation Tasks

Phase	Task	Tolerance Band
Downwind	Airspeed Control	± 2 kt
	Heading Control	± 2 deg
	Trimmability	---
Base Leg	AOA Control	± 1/2 deg
	Roll Attitude Control	± 1 deg
	Heading Capture	± 2 deg
Final	AOA Control	± 1/2 deg
	Lineup Control	± 1 deg
	Glide Slope Control	± 1/2 "ball" (see note)
Touchdown	Runway Centerline	± 5 ft (± 1.5 m)
	Longitudinal Dispersion	± 20 ft (± 6.1 m)
	Waveoff or Bolter	Attitude Capture AOA Control

Note: A "ball" is equivalent to one cell on the Fresnel Lens Optical Landing System. One cell equals 0.34 degrees of arc.

Waveoff Performance and Characteristics. A waveoff is a frequent occurrence in the shipboard environment and one which may be required due to the landing area going "foul" or not being ready to recover aircraft, unacceptable pilot technique, or conditions outside safe recovery parameters, such as excessive deck motion. A late waveoff is extremely demanding on airplane performance because of airplane sink rate and proximity of the ship. Flight tests are conducted to quantify airplane performance and determine the optimum pilot technique. This information is generated for both the normal recovery configuration(s) and all potential emergency modes, either airframe or engine related, for which shipboard recovery is possible.

Waveoffs are initially conducted at a safe altitude to assess airframe and engine response. The airplane is stabilized onspeed on a -3.0 deg flight path angle. Pitch tendency with power is noted. The landing configuration(s) and emergency conditions should be investigated. Simulated single engine characteristics and

airspeeds, both static and dynamic, must be investigated prior to approaches at the field.

Two basic types of approaches terminating in a waveoff are investigated. They are:

a) **Stabilized, on glide slope condition:** This simulates a stabilized approach condition where a waveoff is required in response to an unsafe condition such as the deck going "foul". The airplane should be in a relatively stabilized condition at the approach AOA with the throttles at the approximate approach setting. To evaluate the variation of waveoff altitude lost and time required to achieve a positive rate of climb with sinking speed, the FLOLS basic glide slope angle is varied. In addition to onspeed conditions, AOA's as slow as 2 degrees higher than the approach AOA should be tested.

b) **A high comedown condition:** This condition represents a large throttle input by the pilot attempting to correct from a high (above glide slope) condition. The use of this "gross" correction technique will usually result in an immediate waveoff by the LSO. The test procedure should be to stabilize on glide slope, but holding a "one ball high" condition. At the desired time, the pilot retards the throttles to IDLE. From 1.0 to 2.0 seconds later, the waveoff signal should be given. This test technique has limited applicability within 1,000 ft of touchdown (a point approximately 500 ft (152.4 m) past the ramp) as this type of throttle "play" would result in an immediate waveoff being commanded by the LSO; however, this technique will identify unacceptable waveoff performance and excessive altitude loss due to adverse engine response characteristics.

Two pilot techniques for MIL thrust waveoffs are investigated. The first technique involves maintaining the approach AOA throughout the waveoff maneuver. The second technique involves rotation to higher values of AOA. *Level I flying qualities* must be retained at all times during the waveoff. Airplane pitch response to MIL thrust application and/or automatic configuration changes, such as speed brakes, may result in a slight uncommanded AOA rotation during the waveoff. This can be a favorable response in the noseup direction; however, is unacceptable in the nose down direction. Although rotation may minimize altitude loss, a point is reached near the ramp where rotation is undesirable due to reduction in hook/ramp clearance and the probability of a free flight engagement outside of the airplane design envelope. This undesirable characteristic is most noticeable for aircraft with large linear distance from the pilot's eye to the hook, such as the F-14A, where the vertical hook-to-eye distance increases approximately 1 ft (0.3 m) for each degree increase in pitch attitude.

The use of afterburner, if available, should also be investigated. Frequently, the time required to obtain MAX A/B thrust obviates its use to lessen the altitude loss during the waveoff maneuver. However, Max A/B thrust does provide an increase in acceleration once a positive rate of climb has been established and can avert a ramp strike for an airplane which has developed a high sinking speed prior to reaching the critical distance from the ramp. Average altitude loss determination for the various loadings and approach conditions should be based on at least twelve data samples because of differences in pilot techniques.

Fleet experience has shown that waveoff performance will be satisfactory if the following criteria is met from waveoff initiation during an approach on glide slope with the proper AOA and 0.7 sec pilot reaction time:

- a) An hook point altitude loss not greater than 30 ft (9.1 m).
- b) A time to zero sink speed not greater than 3 sec with a corresponding level flight longitudinal acceleration of 3 kt/sec on a 90°F (32.2°C) ambient temperature day.
- c) A controllable aircraft pitch attitude change not greater than 5 deg airplane nose up or an AOA increase not more than 3 deg.

Bolter Performance and Characteristics. A bolter is an unintentional touch and go landing on the ship. A bolter can occur due to:

- a) Improper in-close thrust or pitch attitude inputs or an excessively high glide slope position which result in the arresting hook point passing over the top of all the arresting gear cables. This is the more critical condition in that the minimum flight deck is remaining to execute the bolter maneuver.
- b) The arresting gear hook point landing in the desired position, but the hook point failing to engage a cross deck pendant (CDP) due to: 1) hook point dynamics resulting in excessive hook bounce or lateral swing of the arresting hook shank preventing the hook point from engaging a CDP, or 2) improper tension on the CDP from the arresting engine allowing the CDP to be closer to the deck than desired limiting the ability of the hook point to engage the CDP. In either case this is commonly referred to as a "hook skip bolter".

The distance from the last arresting gear cable to the angled deck round down varies from a minimum of 427 ft (130.1 m) on KITTY HAWK class ships to a maximum of 495 ft (150.9 m) on NIMITZ class ships.

Shore based touch and go landings are conducted to determine bolter performance, characteristics, and desired pilot technique. Landing sinking speeds at touchdown should be at least the mean carrier landing sinking speed to ensure that the airplane's pitch dynamics during the bolter, due to compression/extension dynamics of the main and nose landing gear, are representative of a shipboard landing. Flared landings will not produce realistic test conditions! All normal and emergency configurations should be tested. The forward and aft CG positions can be critical because of the potential effect on nosewheel liftoff airspeeds at forward CG's and adverse longitudinal characteristics at aft CG's.

The preferred method of obtaining bolter performance is to use LASER tracking data. The data is used for ground speed and ground roll only. Desired airborne instrumentation, in addition to the standard suite, includes nose and main landing gear weight on wheels (WOW) discretes which can be used to "time tag" their respective touchdown and liftoff times. The ground roll distances from main landing gear touchdown until nose landing touchdown, nose landing gear liftoff, and main landing gear liftoff are calculated from the LASER data. The calculated bolter distances are corrected for test day surface winds and then recomputed for anticipated recovery WOD in the shipboard environment.

The recommended pilot technique during these tests should be application of MIL power at touchdown and longitudinal control input as necessary to achieve the desired flyaway attitude. However, the use of full aft control can produce undesirable over-rotation tendencies. Other techniques should be considered if the characteristics of the airplane warrant.

It is desired that the airplane achieve both nose and main gear liftoff prior to rolling off the end of the angled deck round-down. However, if this condition is not achievable, it is still acceptable if there is no aircraft sink following rolling off the angled deck. Any CG sink is unacceptable. This requirement for no CG sink is based on a "normal" bolter. Situations will occur that will result in some CG sink. Delayed pilot response to the proper bolter technique of throttle and longitudinal control or initial landing gear touchdown well beyond the last CDP are examples.

The airplane pitch characteristics during the shore based bolter tests should be monitored. Landing gear dynamics can cause pitch oscillations (rocking) during the bolter. In an extreme situation, the airplane could be in a nose down pitch cycle when the nose gear rolls off the angled deck, resulting in unacceptable airplane characteristics and excessive sink following rolling off the angled deck.

Testing at Sea

Final determination as to the suitability of an approach airspeed/AOA, pilot technique, and bolter and waveoff performance and characteristics can only be obtained from actual tests aboard the carrier because of airflow disturbances over the landing area and aft of the carrier. Turbulence in the form of sudden updrafts and downdrafts which occur aft of a carrier cannot be duplicated ashore. The range of WOD's to be used should be from the minimum recovery headwind up to 40 knots, if achievable. Crosswinds components, both port and starboard, up to ship's limit (7 knots) should be investigated to evaluate the ship's island structure.

Initial approaches are terminated in waveoffs at approximately 1/2 nautical mile (1.9 km); the waveoff point is moved closer to the ship as test results merit. The first landings are "hook-up" touch and goes, finally with hook down to achieve the first arrested landing.

Intentional landings beyond the CDP's should be conducted to minimize deck remaining and time available to initiate bolter inputs, and also to evaluate rocking characteristics due to landing gear dynamics.

EH 101 SHIP INTERFACE TRIALS - FLIGHT TEST PROGRAMME AND PRELIMINARY RESULTS

R. LONGOBARDI - Chief Test Pilot
G. VISMARA - Chief Flight Test Department
B. PAGGI - EH 101 Flight Test Engineer
AGUSTA S.p.A.
21017 Cascina Costa di Samarate (VA)
Italy

ABSTRACT

The development programme of the EH 101 includes, for its naval variant, the investigation of the ship-helicopter interface characteristics to grant a preliminary release of the helicopter operations on board of both Italian and British Navy units. We intend to approach the programme using the following scheme:

- 1 - EH 101 handling qualities assessment while operating in proximity of a ship, during the final approach phase.
- 2 - Deck landings and take-offs for a preliminary identification of deck motion limits and wind envelope.
- 3 - Assessment of the deck landing technique with the use of landing aids.
- 4 - Assessment of the aircraft landing on the deck, rotors folding, refueling, armament loading, taxiing, tie downs, etc.
- 5 - Assessment of helicopter operations in a heavy electromagnetic environment.
- 6 - Assessment of the maintainability characteristics of the EH 101 in limited spaces (engine and gear boxes change).

Furthermore this paper will present the initial results of the preliminary sea trials carried out with the EH 101 prototypes in cooperation with Italian and British Navy vessels.

LIST OF CONTENTS

1	<u>INTRODUCTION</u>	1
2	<u>STATUS OF THE DEVELOPMENT PROGRAMME</u>	1
	2.1 Achievements	1
	2.2 Future Plan	2
3	<u>ON SHORE ACTIVITY</u>	2
	3.1 Aircraft basic characteristics investigation	2
	3.2 Activity done	2
	3.3 Correction of the pitch up	2
	3.4 Tail rotor configuration and tail stroke	4
4	<u>PREPARING FOR THE SHIP TRIAL</u>	4
5	<u>SHIP TRIAL PROGRAMME</u>	4
	5.1 The plan	4
	5.2 The object of the test	4
	5.3 The methodology	5
	5.4 The instrumentation	6
	5.5 Ground resonance stability	6
6	<u>PRELIMINAR SEA TRIALS</u>	6

1 INTRODUCTION

This paper presents the type of tests we have so far carried out and those we are planning, to investigate the EH 101 ship interface.

The EH 101, for those we are not totally familiar with it, has been designed to operate continuously from the type 23 Frigate of the Royal Navy, from the light carrier Garibaldi of the Italian Navy and occasionally from other smaller ships of the Italian fleet.

The programmes we have proposed to the two Navies describe all the operations and the related systems that we deem necessary to obtain an initial clearance.

The actual deck qualification of the EH 101 on the various host ships is and remain a responsibility of the Navies. This paper will start with a description of the extensive on shore activity that has been completed before undertaking any over water operation.

Since the first flights of the EH 101, more than 120 flights were carried out with the purpose of investigating, characterizing and optimizing the aircraft configuration for its major role.

Having to operate on board of relative smaller ships, in heavy sea states and strong winds, much efforts was dedicated to obtain the best handling qualities and performance to cope with this task.

Areas of particular concern were pitch attitude, hover performance, control response, field of view. In addition to the above subject this paper will briefly present the results of the activity carried out in cooperation with Italian and UK navy war-ships during last year.

2 STATUS OF THE DEVELOPMENT PROGRAMME

Before proceeding to describe the activity that we intend to conduct during the ship trials, we consider important to report briefly on the development programme of the EH 101, the results achieved and the future plan.

2.1 Achievements

The fleet of the preproduction (PP) aircraft is now completed.

Last January, in fact, PP9, the civil-utility variant, took off, for its maiden flight at Agusta in Cascina Costa.

This was the last of the nine aircraft foreseen by EHI master plan for the development of the four variants of the EH 101: naval, civil passenger, civil and military utility.

Five aircrafts are currently flying in UK, under Westland responsibility, with the main purpose of developing the basic naval vehicle, avionics (PP1, PP4, PP5) and the passengers variant (PP3, PP8).

Four PP's are flying in Italy, at Agusta test center, for the naval (PP2, PP6), utility civil and military (PP7, PP9) variant development.

In Italy is also located a GTV for the testing of the drive system.

The total flight hours achieved by the fleet at the end of February were 1050 in 1200 flights: plus 740

hours of ground run on GTV.

The development of the basic vehicle was concentrated, from the beginning, on PP1 and PP2, flying in their own countries.

But after one year EHI decided, to enhance progress of the programme, to collocate the two PP's at Agusta flight test center with a joint integrated team of pilots, flight test engineers and specialists of the different branches.

This new phase, named Single Site Operation, began on November 1988 and was concluded last March after the second OTC's preview.

During this period proper solutions have been found for all the critical areas, reaching a satisfactory level of development.

This is well demonstrated by the fact that in 1988 PP1 arrived in Italy from UK in the hold of merchant ship while last March it went back flying on its own. In detail the nose-up tendency at low airspeed was eliminated by the low asymmetric tailplane; the tail rotor strength and performance have been improved by the double teetering tail rotor and rear fuselage strakes; the hover and level flight performance have been enhanced by modifying the main rotor blades and reducing the fuselage drag.

Furthermore a very noticeable tail-shake has been cured with aerodynamic features: a beanie on the main rotor head and the so called horse-collar around the engine cowlings.

Also the flight controls have been modified introducing different gearing to reduce the roll sensitivity, the collective to longitudinal cyclic coupling and extending the range of collective and yaw control.

But the most significant improvement was obtained in reducing the vibration level caused by the main rotor.

The problem was tackled in two different ways: preventing the vibration to reach the cabin and modifying the cabin natural frequencies.

The first approach gave the best results with both the system tested: a passive one, installed on the rotor head and a active system, called ACSR (Active Control of Structural Response).

The latter that will be incorporated into the production configuration, has been tested at Westland test center in Yeovil on PP3.

In the mean time many modification have been designed and tested with the purpose of extending the life of the critical dynamic components.

In parallel the avionic system were developed on the remaining PP's: AFCS on PP3, common avionic on PP4, the mission system for Royal Navy and Marina Militare Italiana (MMI) on PP5 and PP6 while PP7 was developing both the basic utility configuration and the military avionic.

2.2 Future Plan

Two major changes are still to be tested before the development programme of the EH 101 can be concluded: the updated main gear box and the RTM 322 installation.

The 5200 HP gearbox, the current one is limited to 4640 HP, will be common to all the EH 101 variants. It has been fitted for the first time last March on the GTV for an initial endurance test of 300 hours that will be concluded by the end of July. At that time PP2 will receive a similar box and we will start flying for the extension of the flight envelope.

The integration tests of the RTM 322 will initiate in the middle of 1992 on PP4 and will continue for two years.

This engine will be installed on the helicopters of the Royal Navy while the civil and the MMI variants will maintain the G.E. engines.

At the end of 1992, having all the PP's the proper configuration, the qualification phase will start. It will lead to the civil certification by September

1993 for both the civil variants.

According to our plane the certification will be obtained simultaneously by the CAA, the FAA and the RAI.

One year later the industry qualification for the naval variant will also be concluded.

3 ON SHORE ACTIVITY

3.1 Aircraft basic characteristics investigation

Ship trials are a very expensive, time consuming and, in some way, a risky exercise.

Therefore it is of paramount importance to investigate and understand all possible aspects of the helicopter handling and performance in the low speed regime before attempting any activity over the water.

As previously stated this has been one of our major task during the last two years.

Various option of tailplane, tail rotor and tail cone strake have been evaluated in order to achieve the highest performance and the minimum pilot workload when the aircraft operates in the very unsteady condition typical of approach and landing on a small deck in adverse weather.

The relative wind envelope requirements stated that the helicopter should be safe to operate up to 50 Kts from 0° to 45° left or right, 35 Kts from 45° to 135° and 20 Kts rearward.

We tested the aircraft up to 55 Kts, with additional attention on the "sensitive" sector wich, as for most helicopters, are the left or right 45° to 70°, where the airflow around the tail rotor is highly disturbed by the main rotor downwash and tail unit masking. The results obtained were eventually considered acceptable to proceed with the ship trials.

3.2 Activity done

The activity done for the above purpose amount at:

120 hrs	Total flight time
90	Flights
3	Tailplane configuration change
4	Tail rotor configuration change
5	Tail strake configuration change

These figures can give an idea of how extenuating can be trying to achieve low workload flying characteristics in gusty wind up to 50 Kts from any direction.

However, obtaining this level of results was considered essential to proceed with adequate margins to the actual investigation of the EH 101 ship interface.

The tailplane configuration, in particular, raised much concern as we wanted to provide on almost constant pitch attitude approach capability to minimize the typical reduction of vertical field of view during the flare.

3.3 Correction of the pitch up

It has been widely publicized that the original symmetric low set tailplane caused a distinct pitch up when it moved in the main rotor downwash.

To correct this undesirable characteristic we explored the following main options: a reduction of the tailplane effective surface and the relocation of it to a totally different position, where it could not be affected by the rotor downwash.

After various attempt of reducing the tailplane effective surface by reducing either the chord or the span, the choice was restricted to the following configurations:

- 1) Asymmetric tailplane attached to the top of the

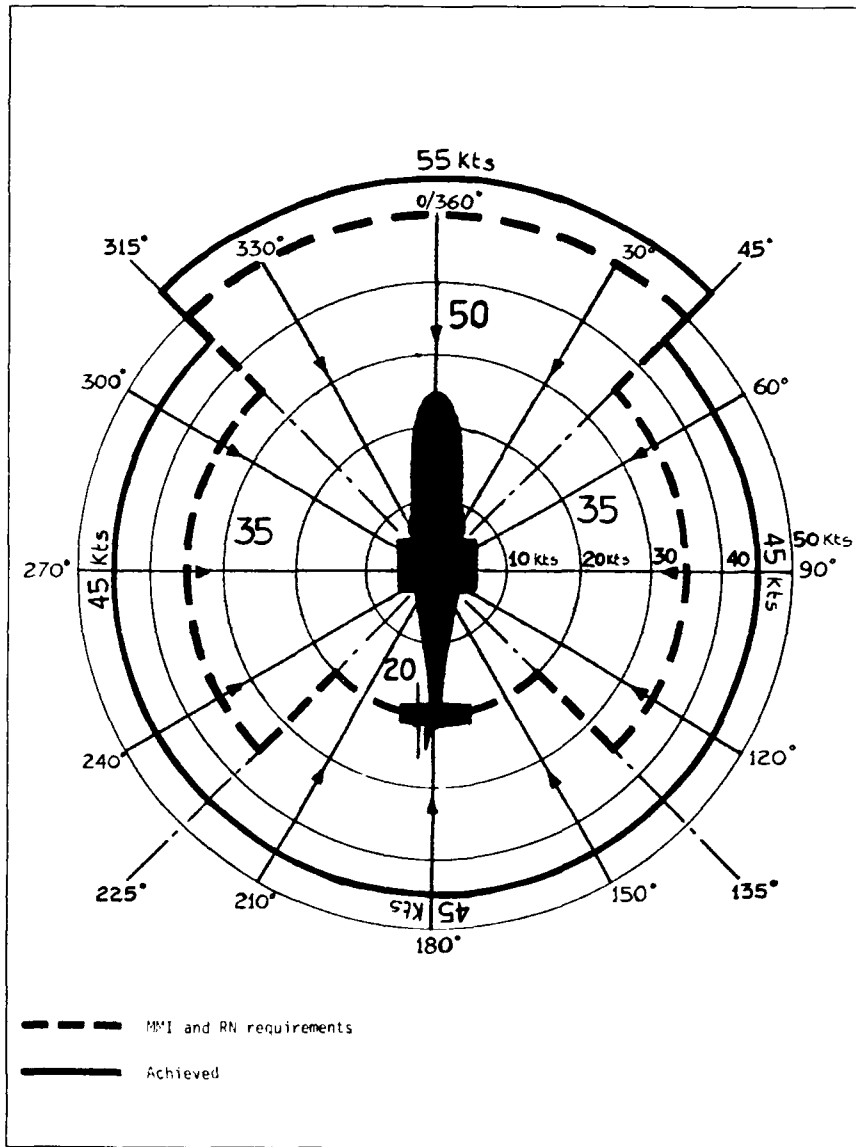


Figure 1 - EH 101 Relative Wind Envelope

tail fin on the opposite side of the rotor.

2) Asymmetric tailplane set in the same position than the original one but limited to the right portion.

The first configuration appeared immediately the most effective in eliminating the pitch up, as one can expect, but had the following disadvantages:

- 1) It was not compatible with the tail unit folding geometry.
- 2) It required a major redesign of the tail unit as its load distribution would have been different.
- 3) It would have had a remarkable effect on the programme in terms of cost and scheduling.

The second configuration was tested after the analysis of load distribution on the standard tailplane.

It was found that in forward flight more than 75% of total downlift required to maintain a proper relationship between airspeed and attitude was generated by the right portion of the surface. Choosing a different profile we could improve the effectiveness of the remain section losing only a negligible contribution to pitch damping. This small reduction of the dynamic stability could be easily accounted for by the Automatic Flight Control System.

For what pitch up at low speed was concerned the residual effect of the main rotor downwash created a very small reaction that could be detected only conducting accurate testing.

We concluded that, as the asymmetric low set tailplane was much easier and cheaper to install, this configuration might be preferred.

However a doubt remained in the test pilot department that in less than favourable conditions the operational pilot could suffer from the less than perfect helicopter behaviour.

Therefore it was considered necessary, to carry out proper testing in a more realistic conditions. This was the reason for asking to the programme leaders the clearance to set up a short trial to investigate the helicopter behaviour when operating in proximity of a moving deck, activity that will be described later and that led to the selection of the low set asymmetric tailplane as a viable tail configuration change.

3.4 Tail rotor configuration and tail strake

Since the early flying in the low speed regime it was evident that tail rotor power available was not sufficient to produce the required thrust to meet 50 Kts relative wind velocity from all directions.

To improve this performance we followed two lines of action.

- 1 - Increase the tail rotor thrust.
- 2 - Decrease the tail rotor power required by generating additional contribution to the antitorque moment.

The increase of the tail rotor thrust was obtained by selecting a different concept of rotor hub that was modified to allow each pair of opposite blades to flap independently.

This modification reduced the related loads and allowed to reach higher blade angles of attack, hence more thrust.

The additional contribution to the thrust was obtained by applying a strake, along the stringers of the left hand side of the rear fuselage, which, by disrupting the airflow around it reduced the force

generated by the airflow on the left side of rear fuselage.

The combination of higher thrust capability of the tail rotor and the thrust contribution generated by the strake, various size and locations of which were tested, made possible to meet the tail rotor performance requirements and reduced to acceptable level the pedal activity within entire relative envelope.

4 PREPARING FOR THE SHIP TRIAL

Encouraged by the good results of the basic development, the good performance and excellent control response, we are now working for the preparation of PP6 in Italy and PP5 in UK with the aim to carry out our tests in early autumn. A lot is still to be done, on our PP6, to make it usable for extensive flying over water and autonomous operation over the deck:

- The management system, although not completely necessary for the handling tests, must be on board and perfectly tuned at least in its AFCS, communication and navigation sub system.
- The APU, necessary to start the engines without an external airstarter, must be installed.
- The emergency flotation gear are essential.
- All the mooring points must be verified.
- Landing gear brake system, sprague and castoring system must be fully operational.
- The main rotor and tail unit folding system must be thoroughly tested.

PP5 is already in proper configuration.

5 SHIP TRIAL PROGRAMME

Preliminary Ship Interface Trial (PSIT) will be conducted with the naval variant of the EH 101 in conjunction with RN and MMI ships.

The aim of the trial is to verify all the interface aspects with the class of ships the EH 101 has to cooperate and to define a limited flight envelope in term of wind speed, sea state and deck motion. The operational trial will be conducted by the two navies with production aircrafts.

5.1 The plan

According to the existing plan the PSIT's should be undertaken by Agusta, in autumn 1991 with the MMI EH 101 (PP6), and by Westland with the RN EH 101 (PP5) in the spring 1991 (harbour trial) and in the spring 1992 (sea trial).

Each trial will require approximately 10 flight hours shared between harbour and over sea activity. The MMI trial will assess the EH 101 compatibility with the Caribaldi light carrier, the Duilio class cruiser and the Arditio class Destroyer while the RN trial will be limited to the Type 23 Frigate.

5.2 The object of the test

The following aspects will be evaluated during the trial:

1) Ship/helicopter clearances

The aim of the test is to verify that no physical interferences exist between the ship structure and the helicopter, in all the possible situations such as during the approach, on the deck with the rotors turning, during the main rotor blades and tail folding, during the deck handling, on the elevators,

in the hangar, during weapons loading and servicing activities.

2) Deck operation

An hydraulic deck lock is fitted on the RN helicopter to improve safety, during take-off and landing from/on the ship, providing a short term method of securing the helicopter to the deck. The system will be evaluated with a large number of engagement and release sequences, in normal and emergency mode.

The capability of the helicopter to turn in either direction about the engagements point will also be assessed.

After any operation the locking parts will be inspected to determine any damage and the manoeuvre that might have caused it.

3) Deck handling

The Type 23 Frigate are equipped with a system which provides helicopter handling from the deck to the hangar and viceversa, in high sea states, with no men on the ship's deck and with the helicopter misaligned after landing.

This system has to be operated in conjunction with the deck lock.

The deck handling system may also be used to transport weapons to the aircraft once it has been aligned at the datum position.

The behaviour of the system will be assessed with as many as possible combinations of deck engagements points/aircraft headings.

A limited assessment of the weapons loading procedure will also be done using the deck handling system to verify the weapon trolleys are properly operated and aligned with the aircraft.

On the Italian navy ships deck handling presents less problems than on the Type 23 Frigate.

In fact no special equipment is envisaged to assist the manoeuvring and positioning of the helicopter on the deck.

On the Garibaldi deck the EH 101 will be towed and positioned using similar, if not the same, equipment currently used for the SH 3D.

Rather normal tractors will move the helicopter in the hangar and on the deck.

Therefore we do not expect to spend too many energies for this phase of the trial.

For what the other ship are concerned, the helicopter has not to be moved from its landing spot therefore the handling will be minimal.

4) Ship helicopter physical interface

All the necessary interface between the ship and the helicopter will be checked.

This activity will consist in verifying the proper positioning and functioning on the deck and in the hangar for:

- electrical ground supply
- pressure refuel and defuel hoses
- nitrogen charging
- external hydraulic power supply
- telebrief system (only cable position)
- lashing points

Engines starting will be evaluated using the APU and external power supply

5) EMC tests

Because many of the helicopter system are not fully representative of the production standard, the aim of these tests is essentially to define any potential EMI that could jeopardize the flight safety during the trial.

For this reason the initial landings will be done

with all the ship system, involving radio frequency emission, turned off.

Once on the ship deck, tests will be conducted to determine the influence of the ship radios and radar equipment on the helicopter systems, particularly on AFCS, cockpit instruments, communication system and experimental instrumentation.

Having cleared the EMC aspects on the deck the activity will be repeated in flight.

6) Dynamic interface

The dynamic interface is, obviously, the haviest part of this set of trial.

The time available is limited and the conditions to investigate could be numerous.

We will use all our experience to identify the most relevant ones it is our intention to reach the operating envelope limits with a reasonable graduality.

There are some information available that will greatly help us in reducing the number of condition to test, especially for the Italian part of the programme, as the Italian Navy ships are currently conducting similar operation with the Sea King and AB 212 ASW.

The wind over the deck data and the experience accumulated by the current helicopters will direct our investigation toward the most critical areas. The dynamic trials for the Royal Navy are further limited in scope therefore what is said in this paper is more related to the Italian Navy trials.

The operating envelope is defined as function of the helicopter weight, c.g. position, ship motion, and environmental condition such as visibility, day or night.

We will restrict our investigation to day time, and to the maximum ship motion we can obtain during the week, or so, that our programme will last.

As the aircraft relative wind envelope is rather wide we will progress by 10 Kts increments to maximum speeds obtainable by the combination of ship and natural wind speeds available.

During the test both quantitative and qualitative data will be gathered using on board recorder.

The Cooper Harper scale will be used by the pilots to express their qualitative assessment of the ease with which each manoeuvre can be carried out using average pilot skill.

The evaluating crew will be totally formed by company personnel, however some participation of Italian Navy Pilot is planned mainly to familiarize them with standing procedures.

Before each sortie a conference will be held with the relevant ship's personnel to discuss all the details of each test and how to match the test requirements with other possible ship constraint.

The sequence of the conditions will be agreed in order to minimize ship manoeuvring.

During the tests a flight test engineer will be on the deck all the time to verify the test conditions.

Each condition will provide a test point that will be used to build the diagrams that eventually will indicate the flight envelope.

Some rotor engagements and stopping will be conducted in various position on the deck of the Garibaldi to evaluate the effect of the possible unusual turbulence.

Landings and take offs will be conducted from and to all approved directions.

Extensive manoeuvring over the deck will be necessary to identify any possible handling deficiency.

5.3 The methodology

To enhance the safety the tests will be initially conducted with the ship moored to quayside or to a buoy.

Being this assessment completed all the tests will be repeated with the ship sailing in order to evaluate the influence of wind, deck motion, deck turbulence on the aircraft operation.

As stated before the sea trial will be conducted with the wind speed and the sea state available during the tests.

5.4 The instrumentation

The helicopter will have an experimental instrumentation system installed.

The relevant parameters to be required are:

- loads on main/tail rotor blades, hubs, airframe and undercarriage.
- Undercarriage vertical velocity, vertical, lateral and longitudinal acceleration.
- Aircraft control position, attitude, angular rates, rotor speed, and 3 axis load factor.
- Engines control parameter i.e. torque, gas generator and power turbine speed, turbine temperature.

In addition to the aircraft parameters also ship parameters will be recorded using portable instrumentation package in order to correlate the phenomenon seen on the aircraft with the external conditions.

In particular will be recorded:

- wind speed and direction relative to the ship
- ship attitudes

5.5 Ground resonance stability

The EH 101 has been thoroughly tested in all combination of C.G. position, weight, NR and airborne percentage and found totally free of any tendency to enter in ground resonance by large margins. Nevertheless we consider necessary to conduct further investigation of this aspects of the helicopter characteristics in consideration of the possible effect that the ship deck motion and the deck handling system motion, installed on the Type 23 Frigate, might have on landing gears and main rotor damper response.

During the test the relative wind will be maintained within the hover envelope to allow prompt take-off. A select combinations of RPM, C.G. position and collective pitch will be explored using the standard method of applying cyclic pulses to the cyclic of about 2 inch diameter and 2/3 of 1/R frequency. Keeping in mind the limited scope of our tests we intend to carry out our resonance investigation not up to the extremes of the ship motions operational values but just to 5° degrees of roll and 1.5 degrees of pitch.

6 PRELIMINARY SEA TRIALS

It has been mentioned previously of a short activity done with the EH 101 during last year in cooperation with Italian Navy vessels.

The Purpose of that activity was to confirm the results, of the optimization of the tailplane configuration.

Unfortunately at that time the state of the programme did not allow unlimited over water operations as we lacked all the necessary auxiliary system such as the definitive flotation gears, the proper AFCS the APU and so on.

Nevertheless a decision had to be taken in a short time so we were forced to take acceptable shortcuts, and set up a limited sea trial programme.

The Italian navy very willingly provided ground

support, at the helicopter base in La Spezia, and made available suitable warships to use as reference. The ship belonged to the Maestrale class equipped with a helideck 24 meters long and 14 meters wide.

The initial intention were to carry out, during a maximum of 3 ship's sorties, various type of approach and over the deck manoeuvres with the two selected configurations of tailplane.

We did not plan actual landings, as the time available was short and we wanted to concentrate on the main purpose of the trials in order to get the most valuable results.

The handling of an aircraft is essentially a matter of opinion.

In other words, there was the possibility that what was considered easy by one pilot might be evaluated less optimistically by another one.

For this reason we decided to involve in the trials a good number of company and military test pilots in order to obtain the broadest possible range of comments.

The initial trials, which included approaches to the ship steaming up to 20 Kts were carried out using the Italian and Royal Navy procedure and it was easy to conclude that, in the condition tested, the differences in the handling between the two configurations were minimal, thus confirming that the low set asymmetric tailplane was a suitable solution. In fact everything was going so smoothly that, having cleared the main purpose of the flight, we proposed to the Italian Navy representatives to carry out deck landings.

The size of the deck was barely sufficient but the flight conditions were excellent and we could not envisage any problem.

As previously stated this additional activity had not the aim to get any form of qualification for deck operation, but just to verify the ease of the manoeuvre from the approach to touchdown.

Landings were easy to do as expected.

The only criticism we raised were related to the over the nose visibility that was considered poor and the excessive spray caused by the downwash.

The first item was known, as the aircraft tends to stay in hover with a nose up attitude.

The excessive spray was due to the low height of the deck and was minimized using the Italian type of approach along the ship centerline while was remarkable when moving over the deck from along the side hover.

Nevertheless the whole exercise was a success both for the good serviceability record of the helicopter in such an early stage of development and for the encouraging results of the handling assessment.

A further proof of the ease of the approach and landing manoeuvre was given by this fact.

The Italian military test pilot involved in the assessment happened to be a young major of the Italian Air Force assigned to the official test center team.

This pilot had no a previous experience of landing or even approaching to a ship deck.

Nevertheless he controlled the helicopter easily and accurately to the narrow deck as the other more experienced test pilots.

In November 1990 a similar but shorter activity was carried out in UK when PP5 was landed on the deck of HMS Norfolk cruising off Portland.

The purpose of what was mainly promotional however some additional valuable indications were obtained. Manoeuvring over the larger and higher deck of the Norfolk was found easier than over the Maestrale, as one could expect and without the annoying effect of the sea spray.

We believe these two occasions although very limited in purpose and in the conditions tested, have provided us valuable indications for a more effective planning of the future and more exhaustive sea trials.



Figure 4 - EH 101 Deck Landing on Frigate " MAESTRALE " Class

DETERMINATION OF LIMITATIONS FOR HELICOPTER SHIP-BORNE OPERATIONS

by

R. Fang
National Aerospace Laboratory NLR
P.O. Box 90502
1006 BM Amsterdam
The Netherlands

SUMMARY

A brief outline of helicopter-ship qualification programmes as carried out by NLR is given in this paper. It describes how detailed information about the helicopter capabilities, ship's motion characteristics and the wind-climate above the ship's flight deck, is used to set up and to execute a safe and efficient helicopter flight test programme. The programme leads to a safe and maximum operational availability of the helicopter on board the ship in terms of take-off and landing capabilities as function of relative wind and sea-state.

1 INTRODUCTION

In recent years operations of a large variety of helicopter types from various classes of navy ships have steadily increased worldwide. The improved capabilities of present-generation helicopters offer a wide range of possibilities for attractive ship-helicopter combinations to cope with the growing demand being put on modern navies. Therefore, many even relatively small vessels are being equipped with a helicopter flight deck. Sometimes an almost marginal facility is provided for take-off, landing and deck handling. Yet, helicopter operations are required in a rough environment (Fig. 1) by day and at night.



Fig. 1 Helicopter operations on board ships; a rough environment

Of course one wants to operate the helicopter in as many operational conditions (day, night, sea-state, wind, visibility etc) with as high a payload as possible. Nowadays, in line with the increasing importance of helicopter/ship operations the helicopter manufacturer sometimes provides, in addition to limitations for shore-based take-off and landing (Fig. 2), limitations of a general nature for helicopter-ship operations.

The difference between the two sets of limitations is explained by the fact that for shore-based operations the limitations (determined after extensive factory testing) are based a.o. on a rigid and unobstructed landing site whereas the limitations for ship-borne operations are to be based on an obstructed landing site (flight deck) which shows oscillatory movement and where a.o. extremely turbulent conditions can prevail.

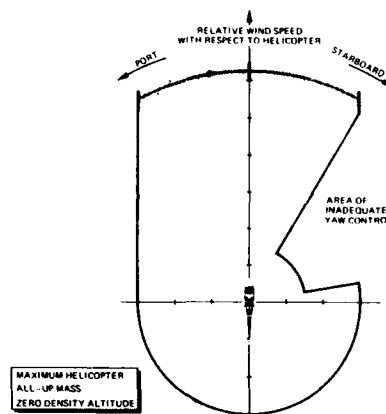


Fig. 2 Relative wind- and mass limitations for helicopter take-off and landing for shore-based operations, as provided by the manufacturer

Because of the unique characteristics of each helicopter type/class of ship combination and the innumerable combinations possible it is understandable that usually no (extensive) testing has been carried out by the manufacturer for the combination that is of interest. It follows that the limitations given, if any must be considered as general guidelines, with large safety margins with respect to the helicopter capabilities and pilot ability to control the helicopter, and thus do not provide a maximum availability of the helicopter on board the ship. It is expected that the actual limitations, i.e. those that allow maximum availability of the helicopter within the constraints of safety, are lying somewhere between the limitations for shore-based and those for ship-borne operations as given by the manufacturer. To determine these limitations a dedicated helicopter-ship qualification programme is needed. During about 20 years NLR has carried out successfully 12 test programmes (for Dutch as

well as foreign contractors) in which 9 classes of ships and 6 types of helicopters were involved.

In this paper an overview is given about the factors influencing the helicopter-ship operations, the way they are determined in various qualification programme elements and how they are used to set up a flight test programme on board the ship. Furthermore it is described how the ship-borne flight tests, within the constraints of safety and efficiency, are carried out and in what way, during the tests, again use is made of the data obtained in the previous programme elements, as well as the experience of the test team, resulting in an as small as possible number of flying hours without affecting the quality of the results. The attention is focussed on helicopter take-off and landing which in fact constitutes the main part of the tests. Finally some results are given.

2 ESTIMATION OF THE OPERATIONAL ENVELOPE FOR HELICOPTER-SHIP OPERATIONS

2.1 General

An important aspect of helicopter-ship qualification testing is safety. The problem is to define this in quantitative terms, taking into account the limitations imposed by the environment, the capabilities of the helicopter and the abilities of the pilot. In order to

The nature of the problems that may be encountered, and the preparatory measurements and analyses that can be carried out to estimate the operational envelope for helicopter-ship operations are discussed in this chapter. The additional flight tests, that are required because some aspects cannot be evaluated analytically, are discussed in the next chapter.

2.2 The effect of the ship on the environment for helicopter operations

The basic factor, limiting the helicopter operations from ships, in comparison to shore-based operations is the small flight deck for take-off and landing, which is:

- oscillating (pitch, roll)
- surrounded by obstacles (mainly the hangar in front of the flight deck) which, apart from collision risk, generate
 - . distorted air flow
 - . a complicated turbulence field (in addition to natural turbulence)
- and were also present
- exhaust gas, which may cause
 - . additional turbulence
 - . an increase of the outside air temperature above the flight deck (increase of density altitude)
 - . a reduced view over the flight deck
- spray also causing a reduced view over the flight deck.

Although the ship's speed and course as such do not constitute limiting factors for helicopter-ship operations, yet they may create, in combination with sea-state, wave/swell direction and natural wind a limiting condition.

To determine the environment of the flight deck quantitatively, the following measurements are carried out:

Wind-tunnel tests on a scale model of the ship
These tests are carried out to determine the air flow characteristics (air flow deviations, turbulence) above the flight deck and at the possible approach paths of the helicopter to the ship as function of true wind and ship's course and speed (relative wind condition). Furthermore the ship's exhaust plume paths and prediction of plume temperature (by plume dispersion measurement) as a function of ship's power settings and relative wind conditions are determined. Finally the position error of the ship's anemometer is determined which is, apart from the instrumentation error of the anemometer, needed to establish the relation between the undisturbed relative wind conditions and those prevailing above the flight deck and at the helicopter approach paths.

Note: If these tests are carried out in the design stage of the ship and if it is determined e.g. that with a small change to the super structure the wind climate above the flight deck can be improved and the exhaust gas nuisance can be decreased, costly modifications of the existing ship may be prevented. The same holds for the position of the ship's anemometer.

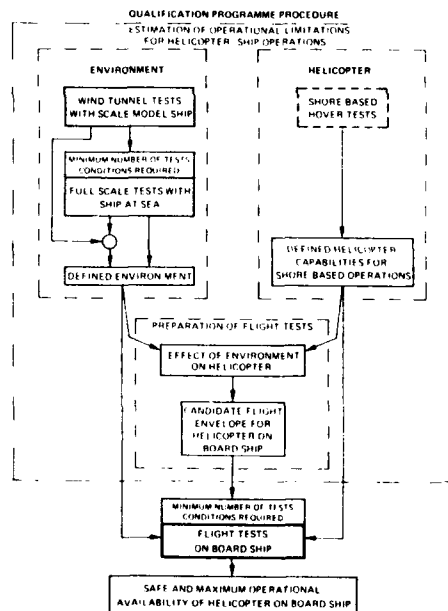


Fig. 3 Set-up of helicopter-ship qualification programme as carried out by NLR

obtain the required data in a safe and efficient way a mix of preparatory measurements, analysis and flight testing is executed. The scheme, presently in use, is depicted in figure 3.

Full-scale ship's wind climate and motion tests
The wind climate tests on board the ship are carried out to verify the wind-tunnel test results concerning the air flow characteristics above the flight deck. With the established relation between both types of results the real wind climate at the various helicopter approach paths is predicted. Furthermore the instrumentation error of the ship anemometer is determined and the position error, established during the wind-tunnel tests, is verified. With the information obtained an unambiguous relation between the anemometer readings, the air flow conditions above the flight deck and at the helicopter approach paths and the undisturbed relative wind condition is determined. Ship motion characteristics (pitching, rolling) are determined as a function of sea-state, wave/swell direction and ship's speed. Examples of results concerning ship motion, turbulence, exhaust gas and spray above the flight deck are shown in the figures 4, 5 and 6.

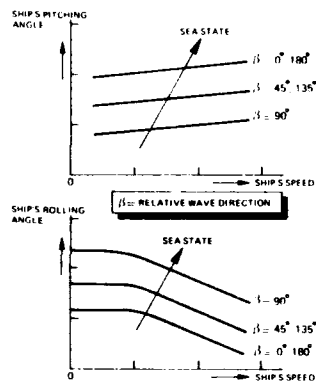


Fig. 4 Ship's pitching- and rolling angle as function of ship's speed, relative wave direction and sea-state

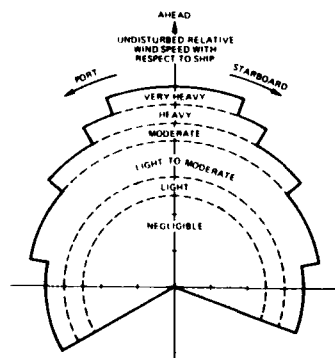


Fig. 5 Turbulence levels above the flight deck as function of relative wind

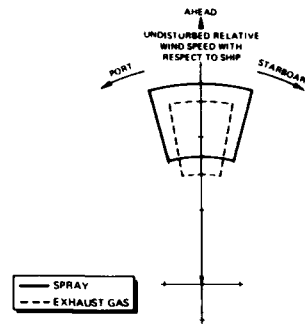


Fig. 6 Relative wind conditions during which spray- and exhaust gas nuisance above the flight deck are present

2.3 The effect of the ship environment on the helicopter performance

Since the operational environment on a ship is much more complex than for shore-based operations it should be determined in what way the take-off and landing envelope as provided in the flight manual for shore-based operations (Fig. 2) is affected.

To evaluate the effect of the ship environment on the helicopter performance, detailed data of the helicopter capabilities are needed. If not available in advance, these are obtained during shore-based hover tests. These tests are used to evaluate yaw control performance in cross wind conditions and also at high torque values needed in the low speed region. Furthermore helicopter pitch- and bank angles needed for hover at high wind speeds are determined. Finally tests are carried out in those wind conditions where main-/tail rotor interference might exist, causing helicopter yaw oscillations.

It is understood that these tests are executed within the limitations for shore-based operations as given by the helicopter manufacturer (Fig. 2). The data obtained should indicate where, within the shore-based envelope, regions exist where the margin between available and required helicopter performance is small. An example of torque- and yaw control performance obtained from such tests is given in figure 7.

Knowing the operational environment created by the ship, and the relevant properties of the helicopter, the effects on helicopter performance can be estimated, if not quantitatively, then at least qualitatively.

Such effects can be grouped into two classes:

- effects that may result in hazardous flight conditions, which will have to be prohibited
- effects which will create a difficult and demanding situation for the pilot. These situations should be evaluated carefully and the operational applicability should be evaluated by means of flight testing.

In most cases the operational envelope for shipborne operations will be reduced with respect to the shore-based envelope under the following conditions.

Hazardous conditions

Inadequate yaw control

Conditions where inadequate yaw control exists (areas B and E in Figure 7) must be avoided. Furthermore when performing a decelerating flight from approach speed to hover, while the relative wind above the flight deck is situated in one of the shaded areas (Fig. 7), the relative wind condition of the area B or E will be traversed.

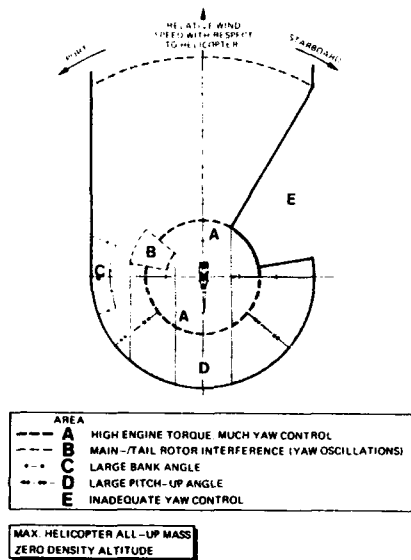


Fig. 7 Some detailed results of shore-based helicopter hover tests

Such an approach to an obstructed flight deck with inadequate yaw control is hazardous and has to be avoided. Relative wind conditions with large cross wind components where large helicopter bank angles are needed to hover above small flight decks must also be avoided (area C in Figure 7). This large bank angle reduces the pilot's view over the flight deck.

High wind speed from ahead

Relative wind conditions where very heavy turbulence exists (Fig. 5; high wind speed from ahead), in combination with rather large ship's oscillations especially in pitch (Fig. 4; inherent to the accompanying large sea-state), and spray nuisance (Fig. 6; reducing pilot's view over the flight deck), have to be avoided. In such cases the control inputs required to counteract the helicopter response to turbulence in combination with manoeuvring, necessary to avoid collision with the oscillating obstructions may be too large (overtorquing, pedal stop), and create a hazardous condition.

Strong tail-wind

Taking into consideration the presence of obstacles near the flight deck, strong tail-wind conditions (area D in Figure 7) can create a hazardous situation in case of an engine failure. Such wind conditions further result in large helicopter pitch-up angles reducing pilots view over the flight deck. For these reasons strong tail-winds have to be avoided.

When areas of the shore-based relative-wind diagram in which either of the hazardous conditions may occur are left out, a candidate ship-operation-relative-wind diagram results of which an example is shown in figure 8.

It should be noted that this diagram results from measurement of the ship's environment, helicopter performance measurements and analyses. Whether or not the diagram can be used operationally has to be determined by means of dedicated flight tests. To determine those areas, in which testing has to be carried out an evaluation (also based on the measurement and analysis mentioned before) of the following conditions, where difficult and demanding situations will occur for the pilot, has to be made.

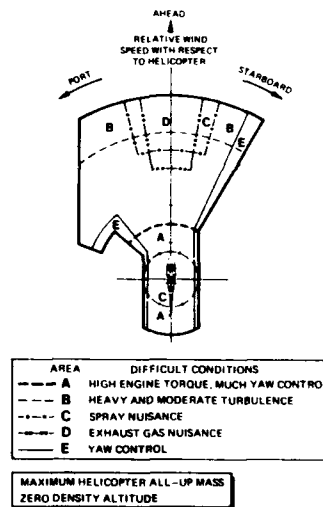


Fig. 8 Relative-wind envelope to be tested during helicopter flight tests on board the ship

"Difficult" conditions

Low relative wind speed

Because much engine torque is needed at low relative wind speed and at high helicopter mass (area A in Figure 8), the power- and yaw control margins might be too small in that condition to counteract adequately a certain amount of ship's oscillation to avoid collision with the obstacles.

Therefore helicopter mass and density altitude should be watched very carefully. Furthermore at low relative wind speed spray is generated by the downwash of the rotor which is most bothersome when the helicopter hovers alongside the flight deck.

High relative wind speed from ahead

At high relative wind speed from ahead, the accompanying turbulence (heavy and moderate; area B, Fig. 8) and especially the large pitch oscillations of the ship (Fig. 4) need much control effort of the pilot which might result in such large torque variations that the maximum allowable torque is often exceeded. Besides, the presence of spray and exhaust gas (Fig. 6; Fig. 8, areas C, D), reducing the pilot's view over the flight deck, increases his workload even more. Furthermore the hot exhaust gas, increasing the density altitude above the flight deck and possibly at the helicopter approach path, affects rotor- and engine performance.

Helicopter yaw control

Wind conditions bordering on those areas where inadequate yaw control exists (hazardous conditions B and E (in Figure 7) must be approached very carefully because of yaw control variations needed to counteract turbulence and ship's oscillations adequately. These are shown in figure 8 area E.

The relative-wind envelope (Fig. 8) in which the "difficult" conditions are indicated, is the basis for the flight test programme to be carried out on board the ship.

2.4 Take-off and landing procedures

In general take-off and landing with a helicopter are easiest into the wind. However, on ships this procedure is not always applicable and furthermore does not always provide optimal results because of the presence of obstacles. Because of that other take-off and landing procedures are applied, thus increasing the operational availability of the helicopter on board the ship enormously, as will be seen in the following. The procedures given hereafter are visualized in figure 9.

Fore-aft procedure (FA)

A fore-aft take-off is performed as follows:

- the helicopter is aligned with the ship's centerline, with its nose in the sailing direction;
- hover above the flight deck with initial heading;
- fly sideways to hover position alongside the ship either to port or starboard (windward side);
- turn away 30° from ship's heading;
- climb out.

A fore-aft landing is performed as follows:

- approach the ship to a hover position alongside the ship (preferably to port because of pilot's view over the flight deck). The helicopter's longitudinal axis is parallel to the ship's centerline;

- fly sideways to the hover position over the landing spot;
- land.

Relative-wind procedure (RW)

The relative-wind take-off is performed as follows:

- swivel (if possible) the helicopter with its nose into the relative wind direction;
- hover with this heading above the flight deck;
- if necessary to avoid obstacles (e.g. the hangar), fly sideways to a hover position alongside the ship;
- climb out.

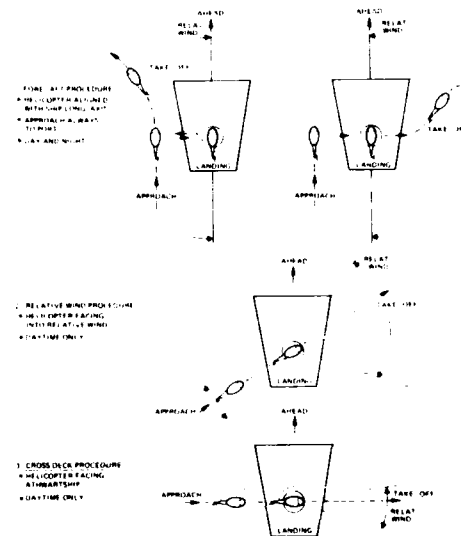


Fig. 9 Take-off and landing procedures on board the ship

The relative-wind landing is performed as follows:

- approach the ship from the leeward side;
- continue flight up to the hover position above the landing spot (helicopter nose into the relative wind);
- land.

Cross-deck procedure (XD)

The cross-deck take-off is performed as follows:

- swivel (if possible) the helicopter until its longitudinal axis is perpendicular to the ship's centerline;
- Lift off and climb out at this heading

The cross-deck landing is performed as follows:

- approach the ship from abeam either from port or starboard (leeward side);
- continue flight up to the hover position above the landing spot;
- land.

Comparing the take-off and landing procedures, the following remarks can be made:

- The FA procedure has the advantage that pilot's view over the flight deck is rather good, especially during the approach (to the port side of the ship) and sideways flight before landing. For that reason this procedure can also be carried out at night. However, this procedure is only applicable if the cross-wind component with respect to the helicopter (and thus also to the ship) does not exceed the helicopter limitations (Fig. 3).
- During the RW procedure where no or only small cross-wind components are present, yaw control is not a factor. However, during this procedure pilot's view over the flight deck is rather poor especially during the approach from port. In spite of the fact that wind is from ahead it is expected that a lower wind speed limit will apply compared to the FA procedure. The same holds for ship's oscillations. The RW procedure is only carried out by day.
- During the XD procedure cross-wind components can be encountered. Therefore yaw control has to be watched very carefully. Besides, the pilot's view over the flight deck is, compared to that during the RW procedure, rather restricted, especially during the approach from port. Because of this, the wind speed- and ship's oscillation limits are expected to be even lower than those for the RW procedure. The XD procedure is only carried out by day.

2.5 The pilot

Controlling the helicopter in the conditions encountered during ship operations is a demanding job. The workload depends a.o. on the amount of ship (flight deck) motion, the turbulence level encountered, the view over the flight deck, visibility and lighting conditions (day or night). In this highly dynamic environment the workload of the pilot may become too high, and conflict with the safety of operation. Thus additional operational limitations may result due to excessive workload situations. While at the present time no analytical or experimental means other than flight tests are available to evaluate the dynamic behaviour of the helicopter/pilot combination in the complex turbulent environment of the moving flight deck of a ship the use of skilled test pilots is crucial in the process of establishing operational limitations for operations from ships. Apart from flight-technical skills that are required a good knowledge of the skill level that can be expected from normal operational pilots is mandatory. Although during the qualification flight tests the pilot is backed up by recordings of the helicopter performance and behaviour, his opinion remains one of the most important contributions to the process of determining operational limitations due to high workload and dynamic response effects. Furthermore the safety of the flight testing ultimately rests on his ability to properly judge the severity of the actual conditions in which the testing takes place.

3 HELICOPTER FLIGHT TESTS ON BOARD SHIPS

3.1 Preparations

From the analyses described in the previous chapters a number of take-off and landing procedures result, with for each of these a candidate wind diagram. (Example in Fig. 10).

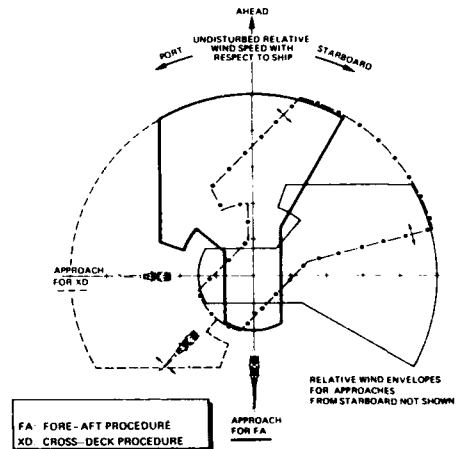


Fig. 10 Relative-wind envelopes for various helicopter approach headings with respect to the ship

These diagrams then are combined to a candidate helicopter-ship operations envelope. Since overlaps of the relative-wind diagrams for the various procedures will occur a choice is made, taking into account the relative size of each of the overlapping sectors (maximizing the ship-based operations envelope) and the expected ease of operating the helicopter. The trade-off is made, using operator requirements, engineering- and pilot judgement. An example of a candidate helicopter-ship operations diagram is shown in

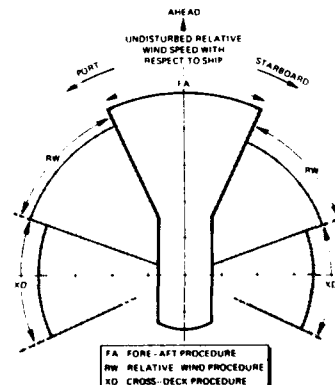


Fig. 11 Total relative-wind envelope for take-off and landing to be tested during helicopter flight tests on board the ship

figure 11. Using ship anemometer calibration data, obtained during the wind climate measurements that have been carried out, this operational envelope is related to relative-wind indications available on the ship in relation to actual wind conditions above the flight deck. An example of such an envelope (valid for the fore-aft procedure) is shown in figure 12.

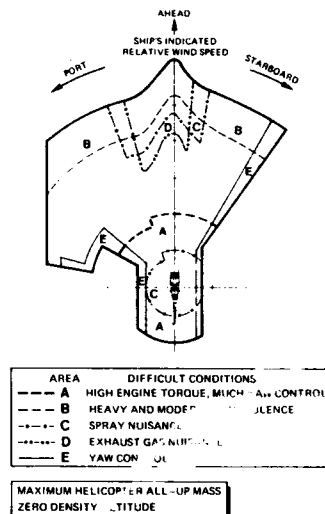


Fig. 12 Relative-wind envelope for fore-aft take-off and landing to be tested on board the ship

In this candidate operational envelope there will be a number of areas for which the analyses indicate a requirement for testing. The problems that may occur are identified and the test procedure and instrumentation, required to investigate these areas safely, are determined.

Since the flight testing is to be carried out on board a ship in a limited period of time, the exact conditions at which tests have to take place cannot be determined beforehand. Conditions that will be tested depend on the sea-state and wind conditions that will become available in the area in which the tests are going to take place. Of course, selection of the area and time of the year so as to maximize the probable occurrence of the desired test conditions is possible, but this still does not provide the experimenter with a free hand to vary his environment at will.

3.2 Flight testing

As evident from the previous paragraph, the flight-test programme has to be defined in an interactive way during the testing period. The actual execution of the flight-test programme is governed by two main aspects:

- safety
- efficiency.

Safety is principally obtained by starting the flight tests at easy conditions for pilot and

test team familiarization:

- . low helicopter mass
- . relative-wind conditions, far within the boundaries of the relative-wind envelope (no "difficult" conditions; e.g. Fig. 12)
- . fore-aft procedure (easiest)
- . fair weather
- . first by day, later on at night.

After a thorough familiarization, efficiency is obtained by making adequate use of the information that becomes available during the flight tests and by analyzing, on board the ship, that information in conjunction with the data base obtained prior to the tests. Thus maximum use is made of the information obtained from the tests, and the number of test flights required can be minimized.

During the test period the selection of test conditions is a major task. Based on the interpreted results of tests that have already been carried out, a number of alternatives for the next test point is defined. This exercise is carried out in parallel for test points related to each of the potential problem areas of the candidate operational envelope, thus yielding a large selection of usable test conditions. The choice of the next test point then depends on the available forecast wind/sea-state conditions in the area within reach of the ship. Problems like judging the reliability of weather forecast versus time of the ship to travel to the area of interest are to be solved.

Given certain environmental conditions (wind, sea state, temperature) a number of conditions can be created by changing ship speed and heading relative to the wind (relative wind conditions) and waves (flight deck motion), although these cannot be changed always independently. The only parameter that can be changed independently appears to be helicopter mass.

Clever use of information obtained on board, in conjunction with thorough knowledge of the factors that limit operations will have to offset the problems created by the difficulty to establish the most desirable test conditions. Thus often it is not a question of demonstrating the capability to operate the helicopter at the point specified, but to obtain data at differing conditions and interpolating or extrapolating the results to the conditions required.

To aid this process, the following data are normally acquired during the tests:

Information becoming available during the flight tests is:

- actual data of helicopter parameters such as:
 - . engine torque
 - . pedal deflection
 - . pitch- and bank angles;
- actual data of ship parameters such as:
 - . speed
 - . course with respect to wave/swell direction
 - . pitching- and rolling angles
 - . anemometer readings (relative wind condition);
- pilot's comment on workload, influenced by:
 - . take-off and landing procedure
 - . ship's oscillation
 - . turbulence
 - . view over the flight deck

. spray and exhaust gas nuisance.
Pilot's workload is expressed with the following adjectival rating scale:

- . minimal
- . moderate
- . considerable
- . unacceptable

Note that two types of data become available. Quantitative data on helicopter performance and ship state and qualitative data on pilot workload and helicopter controllability. The latter should be referenced to the normal operational pilot skill level.

Within the constraints imposed by the environment in which the tests have to be carried out, all effort is made to carry out the testing as efficient as possible. To this end the nominal procedure as depicted in figure 13 is used. For each condition tested the results are evaluated and subsequently the required increase in severity-of the conditions of the next test point is determined. Of course in this process both engineering and flight technical skill (the pilot) is involved.

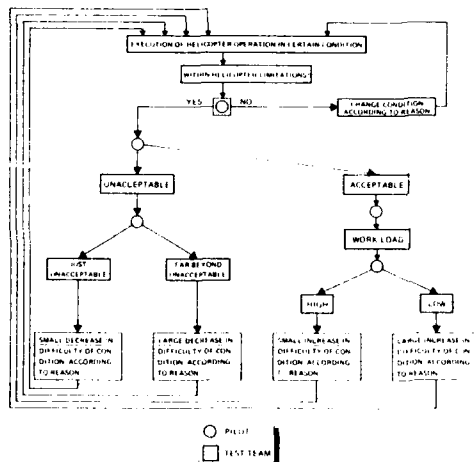


Fig. 13 Flight-test procedure on board the ship

The influence of a certain increase in difficulty on the helicopter can, with the knowledge available in advance and the data obtained during the previous test flight, be predicted rather well.

A prediction of the increase in pilot workload, for a certain increase in the difficulty of a condition, is only possible to a certain extent. If for example the workload in a certain condition is "low", the permitted increase in difficulty of the condition will be more than in case the workload would have been "high". The same is applied (in reverse) in case a condition is considered "unacceptable". If it is "far beyond unacceptable" (occurring sporadically) a large decrease in difficulty is applied whereas if the condition is considered "just unacceptable" a small decrease in difficulty is applied. With the application of these simple prediction methods, good engineering judgement

and the experience of pilot and test team the number of flying hours can be reduced to a minimum, and a maximum of results will be obtained in a as short as possible time period.

4 RESULTS

At the completion of the flight tests on board the ship, a fair idea about the operational limitations has usually been obtained. For final results, measured data (helicopter, ship) together with pilot's comment are analyzed in detail.

The operational limitations are presented in the form of graphs. Examples of these graphs are given in the figures 14 and 15.

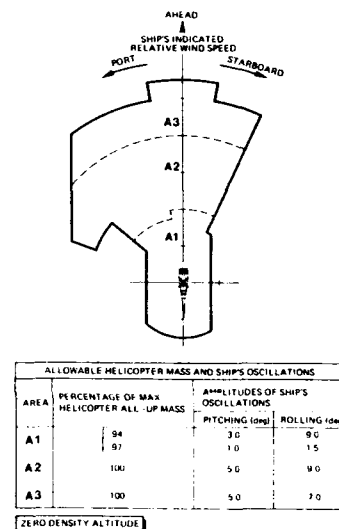
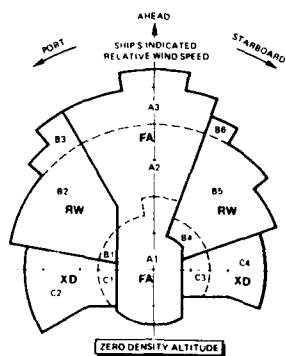


Fig. 14 Take-off and landing limitations for fore-aft procedure; daytime

In figure 14 limitations are given for the fore-aft take-off and landing procedure while in figure 15 the result is shown for the total relative-wind envelope optimized within the constraints of safety and maximum availability of the helicopter.

During the last decade the four step programme has been applied for nine qualification programmes for agencies at home and abroad. Three types of helicopters and six classes of ships were involved. Helicopter maximum take-off mass ranged from 4040 kg (8900 lbs) to 9715 kg (21400 lbs). Ship's maximum water displacement ranged from 485 tons to 16800 tons. For three classes of ship the operational envelopes had to be adjusted due to modifications built in deemed necessary to perform some additional wind-tunnel testing. Thereafter it was possible to estimate new operational envelopes. Those results were finally validated with flight testing on board and showed that the applied methodology leads to desired results.



ALLOWABLE HELICOPTER MASS AND SHIP'S OSCILLATIONS			
AREA	PERCENTAGE OF MAX HELICOPTER ALL-UP MASS	AMPLITUDES OF SHIP'S OSCILLATIONS	
		PITCHING (deg)	ROLLING (deg)
A1	94	3.0	9.0
	97	1.0	1.5
A2	100	5.0	9.0
A3	100	5.0	7.0
B1	94	2.0	8.0
	97	1.0	1.5
B2	100	5.0	9.0
B3	100	4.0	9.0
B4	94	1.5	6.0
	97	1.0	1.5
B5	100	3.5	8.0
B6	100	2.0	6.0
C1	94	2.0	7.0
	97	1.0	1.5
C2	100	5.0	8.0
C3	94	1.5	5.0
	97	1.0	1.5
C4	100	3.0	6.0

Fig. 15 Limitations for take-off and landing procedures (by day) optimized within the constraints of safety and helicopter availability

5 CONCLUDING REMARKS

In conclusion it may be stated that the qualification of helicopters for use on board ships can be carried out safely and efficiently when applying the methodology as described in this report. The effort to be invested in the helicopter flight programme on board the ship is minimized by a thorough preparation, which

consists of obtaining detailed information about the helicopter capabilities, ship's motion characteristics and the wind-climate above the ship's flight deck, by means of experimental tests to an optimum operational availability of the helicopter on board the ship.

UNITED KINGDOM APPROACH TO DERIVING
MILITARY SHIP HELICOPTER OPERATING LIMITS

B. A. FINLAY
ROTARY WING PERFORMANCE SECTION
AEROPLANE AND ARMAMENT EXPERIMENTAL ESTABLISHMENT
BOSCOMBE DOWN
SALISBURY SP4 OJF, UK

SUMMARY

In the United Kingdom the Aeroplane and Armament Experimental Establishment (A&AEE) is responsible for conducting trials to determine the limitations appropriate to military Ship Helicopter Operations. This paper describes the philosophy behind these trials and gives details of the many considerations which play a part in their successful outcome. The tests which are carried out before trials at sea are described together with details of how trials are conducted with a helicopter and a ship to determine the widest possible operating envelopes. The paper concludes that the methods used by the A&AEE establish envelopes for any particular combination of aircraft and ship that are both operationally valuable and safe.

LIST OF SYMBOLS

P Power in kW or SHP
M Mass
 M_t Test Mass
 M_o Operational Mass
 δ Air Pressure Ratio
 θ Air Temperature Ratio
 σ Air Density Ratio
 σ_t Test Density Ratio
 σ_o Operational Density Ratio
 ω Rotor Speed Ratio
 ΔM Mass Correction

1 INTRODUCTION

The aim of this paper is to describe the approach to deriving clearances for helicopters on ships for use by the United Kingdom armed forces. This normally involves the clearance of Royal Navy (RN) aircraft on Royal Navy or Royal Fleet Auxiliary (RFA) ships. However, the same approach

has been used for clearances of Army and Royal Air Force (RAF) helicopters on these ships, clearance of UK military helicopters on the ships of other countries and military helicopters from other nations on their own ships.

The paper will describe the philosophy that has been evolved for such clearances and how this is put into practice during trials at sea. The techniques used have been developed since the late 1960s and although refinements have been made, the same basic techniques have been used for nearly 25 years by the Aeroplane and Armament Experimental Establishment (A&AEE) at Boscombe Down.

The whole process starts with an Operational Requirement to employ a particular helicopter on a particular ship. This requirement is raised by the appropriate Service Department; be it RN, RAF or Army, but the Royal Navy are responsible for issuing any clearance and it is they who call upon the services of the A&AEE for advice concerning the need for and extent of any trials. Should trials be necessary, they are conducted using the techniques described here. However, it is necessary to understand the basic philosophy which dictates the way that these are conducted.

It should be pointed out that all the data presented in this paper is idealised and not real aircraft data. This enables the various tests and results to be understood without presenting the actual capabilities of UK military helicopters and ship combinations which are obviously more highly classified than this paper.

2 UK CLEARANCE PHILOSOPHY

The philosophy behind the clearances is simple, the aim is to provide the widest possible envelope in terms of wind speed and direction relative to the ship and maximum deck motion limits. This requirement is interpreted to mean that the helicopter should be cleared to take-off and land with relative winds up to the limits of the low speed envelope of the helicopter in deck motion conditions which are either specified by the aircraft design authority or determined by some other criteria.

The take-off and landing envelopes are for use during visual take-offs, approaches and landings - we are not yet in the business of considering any sort of automatic or assisted approach and landing. Thus we are concerned with assessing the last $\frac{1}{4}$ mile of the approach to a ship on a nominal 3° glideslope and the 3 landing techniques used by the RN. These techniques are:

- a. An approach to arrive in the hover alongside the port side of the ship's flight deck with the helicopter facing forward and aligned along the fore/aft axis of the ship. The aircraft is then transitioned sideways to hover over the landing spot before executing a vertical landing on the spot. The hover height above the deck is normally of the order of 15 to 20 feet. This sort of landing is termed a "port forward facing landing".
- b. As above but arriving alongside the starboard side of the ship's flight deck. This is termed a "starboard forward facing landing".
- c. An approach along the relative wind vector to hover alongside the deck facing into wind before transitioning forward over the spot followed by a vertical landing. The aircraft may land facing in any direction through 360° . This is termed an "into wind landing".

These 3 landing techniques are shown at Figure 1.

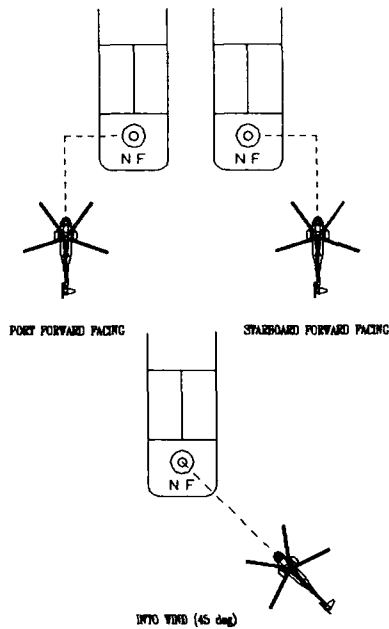


FIGURE 1. RN LANDING TECHNIQUES

It should be noted that the ability of an aircraft to execute each type of landing is determined by the physical clearances available on the deck. Not all ship/aircraft combinations permit 360° operations.

In describing the above, although the emphasis is placed on approach and landing, the take-off phase also needs to be considered. For each wind condition a take-off must also be performed. Generally if an aircraft can land in a particular condition it can also take-off; thus take-offs are assessed to ensure that this is a correct assumption. The take-off is performed with either the aircraft facing forward or into wind. A forward facing take-off involves lifting to the hover, turning the aircraft to windward and transitioning to forward flight in one smooth motion. An into wind take-off is basically the same but there is no need to turn to windward.

The operational envelopes are divided into various mass bands as generally an aircraft can have a wider operating envelope at light all up mass (AUM) than at heavy AUM due to reducing control and power margins as mass increases. The bands are decided upon before any trials take place and depend upon the particular aircraft. It is aimed to produce about 4 or 5 bands covering the range of masses at which the aircraft will be required to operate. This range normally extends some way beyond the maximum permitted AUM of the aircraft to account for non standard atmospheric conditions. The test mass, calculated in terms of M/ω^2 , is referred to as CORRECTED MASS. The trials are conducted at various values of M/ω^2 , and used to produce the "corrected envelopes" which are issued to the users. The process used to determine corrected mass will be described later, at this stage it is only necessary to realise that tests are conducted at a nominally constant M/ω^2 . This means that in order to test at the desired M/ω^2 it is necessary to fly at a mass which straddles this value by plus or minus X kg and frequent fuelling is needed to maintain the desired test AUM. X is chosen so that the aircraft can fly for a sufficient period of time to gain useful data and yet be close enough to the desired value to permit small corrections to be made when the aircraft is either too heavy or too light. Thus there is a need for correction to be applied to each landing to account for this. Tests on land are needed to determine these corrections and these land based tests are described later.

EXAMPLE: Target = 5000 kg M/ω^2
 OAT = +14°C
 Sea Level Pressure = 1005 mb
 $\delta = 0.9919$
 $\theta = 0.9965$
 $\sigma = 0.9954$
 $\omega = 1.0$

Test at $5000 \times (0.9954 \times 1^2) = 4977$ kg
 let X = 100 kg

Then aircraft refuels to 5077 kg and refuels at 4877 kg.

During the trial it is necessary to have a means of assessing the acceptability of each landing and at A&AEE this is achieved using rating scales. Each landing is assessed for control and power margins and a pilot handling qualities rating is applied. The assessment of control usually means assessment of tail rotor pitch or rudder pedal margins where it has been assessed that cyclic and collective margins are adequate. Power is assessed using torque thus the rating scales are based on indicated torque values in relation to transmission or engine limits. Torque and tail rotor considerations are not adequate on their own to cover all eventualities and it is necessary for the pilots flying trials landings to assess the handling difficulty or workload associated with a landing. Typical rating scales for pedal, torque and handling qualities are shown at Figures 2 and 3.

RATING	MEAN TORQUE % DURING LANDING	PEAK TORQUE % DURING LANDING	
1 or 2	<95	<105	Acceptable
3	95 to 98	105 to 110	
4	98 to 100	110 to 115	
5	>100	>115	Unaccept.
RATING	MEAN TAIL ROTOR PITCH MARGIN %	PEAK TAIL ROTOR PITCH MARGIN %	
1 or 2	>12	>10	Acceptable
3	12 to 10	10 to 7.5	
4	10 to 8	7.5 to 5	
5	<8	5 to 0	Unaccept.

FIGURE 2. TORQUE AND PEDAL RATING SCALES

SCALE No.	REMARKS
1	NO PROBLEM Minimal pilot effort required, resulting in an easy task.
2	SATISFACTORY Landing carried out with low pilot workload.
3	LIMIT(S) APPROACHED OR REACHED Safe landings can be carried out, but limits of power etc approached or reached, or moderate pilot workload. Situation becoming difficult due to one or more factors.
4	These points define the fleet limits recommended by the A&AEE.
5	UNACCEPTABLE Test pilot able to land helicopter under controlled conditions but limits of power etc are exceeded. High pilot workload.
6	DANGEROUS Test pilot attempting the landing causes aircraft limitations to be exceeded. Excessive pilot workload.

FIGURE 3. PILOT HANDLING RATING SCALE

It can be seen that for the first 2 performance assessments a 5 point scale is used but for handling a 6 point scale is used. It can also be seen that both mean and maximum torque and pedal values are rated and the more limiting value is used to assess the landing.

To attempt to assess all wind conditions at all masses would be a very large if not untenable task. The philosophy therefore allows for this by permitting landings at different masses to be read-across to others. However, there are rules for this and not all landings can be read-across. In essence landings which are rated as unacceptable at low mass (>4 on the rating scale) are also read up to higher masses as unacceptable. Landings which are rated as easy (1 or 2 on the rating scale) at high mass are read down to lower masses. The reasoning behind this is perhaps obvious; an easy landing at high mass is also likely to be easy (if not easier) at a lower mass. Equally a landing which is rated as unacceptable at low mass because of lack of power or control margins will not be any better at a higher mass and the same is considered to be true of handling

issues. This provided a rational basis for expanding the evidence available at any one mass without conducting a particular test point at that mass.

Different envelopes are produced for use by day and by night. The night envelopes are similar to those used by day but all winds abaft the beam are removed. This is because it is much more difficult to judge closing speed at night due to the absence of suitable cues. In order to ensure that closing speed is not too high all stern winds are excluded from the night envelopes. In general this is the only difference between day and night wind envelopes but this is assessed during tests at sea to ensure that other areas can be included at night. The deck motion limits applied at night might also be somewhat less than those permitted by day. Before conducting tests at sea it is necessary to conduct land based tests to establish a number of fundamental characteristics of the aircraft and obtain data which can be used to correct to the ideal test mass.

3 AIRFIELD TESTS

Airfield tests are required to establish the following:

- a. The aircraft's low speed envelope with adequate control and power margins.
- b. The hover performance at operational masses and in appropriate atmospheric conditions.
- c. The relationship between pedal position/tail rotor pitch and relative wind speed and direction.
- d. The adequacy of other control margins with varying CG.
- e. The relationship between pedal position/tail rotor pitch and aircraft mass for specific wind conditions.

In order to obtain the results for tests a, c and d it is necessary to

fly the aircraft with a pace vehicle and assess the pedal or tail rotor pitch requirements. This is done through 360° in 15° and 5 knot increments up to the maximum permitted side and tail wind limits and at values of M/ω^2 which have been chosen as the mass bands for use on board ship. The results of this testing would look something similar to Figure 4.

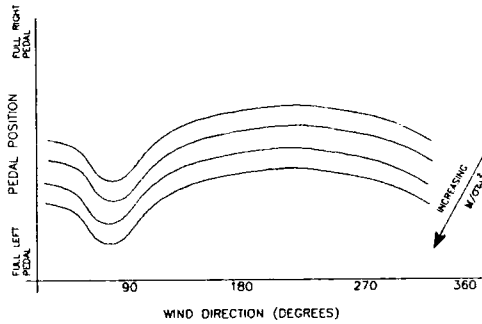


FIGURE 4. PEDAL REQUIREMENTS DURING LOW SPEED FLIGHT

Analysis of this would allow the relationship between pedal and mass to be plotted for constant wind conditions. By plotting pedal against mass we obtain Figure 5. The pedal correction for mass is then the tangent to the slope at the maximum value of M/ω^2 at which the aircraft will be cleared.

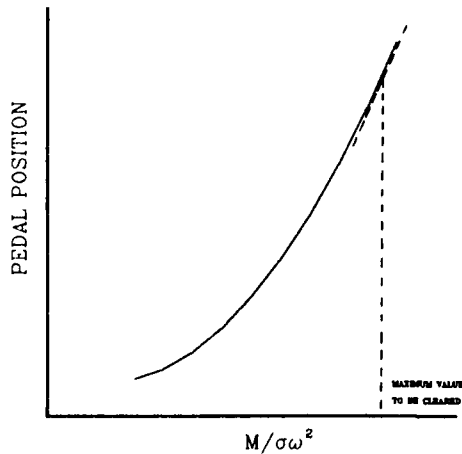


FIGURE 5. RELATIONSHIP BETWEEN PEDAL AND MASS

In order to establish the relationship between power and mass it is necessary to establish the hover performance for the helicopter. The method used at A&AEE is tethered hovering as shown in Figure 6.

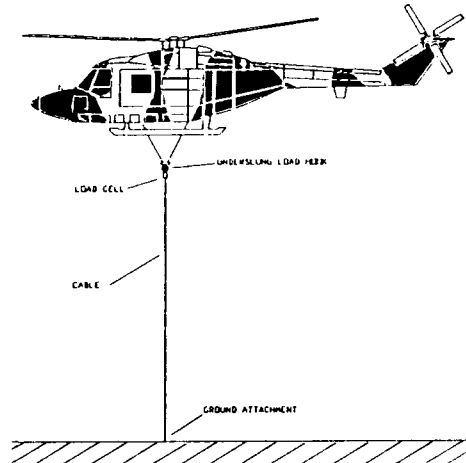


FIGURE 6. TETHERED HOVERING TESTS

The aircraft is tethered to a hard point on the ground using a cable. The cable is attached to the aircraft using its underslung load hook via a load cell. This enables the helicopter to apply different amounts of thrust, measured as load in the cable, and the torque required can be read from the aircraft system. The results would be plotted as shown in Figure 7.

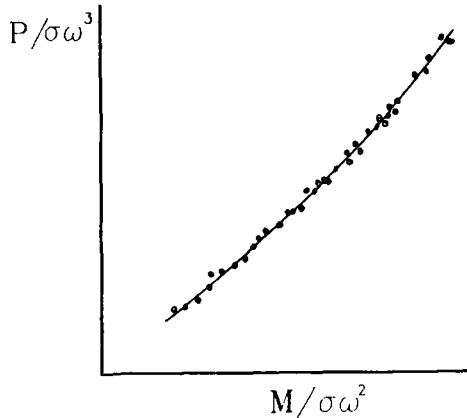


FIGURE 7. HOVER TEST RESULTS

From these it is possible to derive the torque correction for hover OGE, again at the highest value of $M/\sigma\omega^2$ to be cleared. The hover performance results are also used in deriving the operational mass correction which is applied to the actual aircraft AUM to determine which of the envelopes is used. The way in which this is done will be explained later in this paper.

These tests are only conducted on new aircraft or following significant changes to an old aircraft which might affect hover performance or tail rotor control. Once established the information then exists for future ship trials and so it is not necessary to conduct these land based tests prior to tests with a known helicopter.

4 OTHER TESTS CONDUCTED PRIOR TO TESTS AT SEA

Apart from the tests that are conducted by A&AE prior to tests with an aircraft and ship, other trials are conducted by other agencies which provide data to assist in pre-trial planning. The requirement for these tests vary depending upon the type of ship being considered and some or all of the following may be available prior to helicopter tests.

Airflow trials are conducted on every ship prior to helicopter tests. The aim of this test is to establish the magnitude of errors in the ship's anemometer system. Such information is vital since unless the system is to a required accuracy, helicopter operations from that ship will not be recommended.

Air pattern trials are normally only conducted on multi-spot ships ie those with more than one landing spot such as a CVS(G). These trials, which would be conducted at the same time as Airflow tests, map the variation in wind speed and direction compared to free stream, along and across the flight deck at the various landing points. The results of these can be plotted as shown in Figure 8. This can give an indication of areas where there may be difficulty in operating but more importantly it can show the variation between landing spots and thus determine the degree of read-across between spots. This would reduce the amount of separate testing required on each landing spot during subsequent tests with a helicopter.

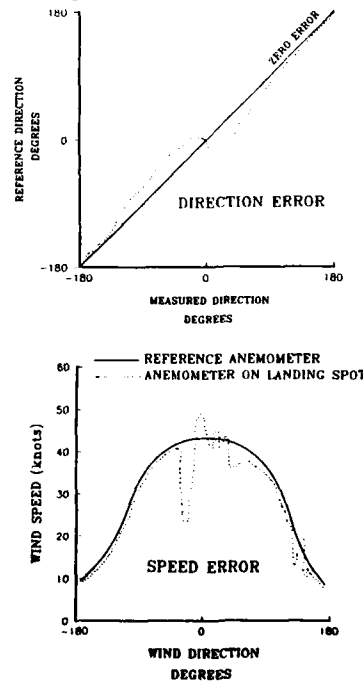


FIGURE 8. AIR PATTERN RESULTS

Wind tunnel test results of ship models can be used in a similar way to Air pattern results. Flow visualisation across the flight deck can show areas of turbulence and down draughting air which may create problems for an aircraft. Such results are useful but are treated with caution by A&AEE as evidence to show a correlation with the real ship is not usually available. Consequently any areas or conditions of likely turbulence would not be excluded from testing but these test points would be approached in an extremely cautious and progressive way. The tunnel test results may also explain unusual results obtained with the aircraft during trials at sea.

One such case involved tests on a ship with a large superstructure in front of the flight deck. Model tests showed that vortices tended to build around the superstructure and shed in a random fashion. During helicopter tests it was found that when landing with particular relative winds the turbulence over flight deck varied with time. Conducting the same landing more than once gave different handling ratings for apparently identical conditions. The explanation for this was attributed to the periodic shedding of vortices from the superstructure indicated by the model tests.

5 SHOL TRIAL PLANNING

Having conducted the land based tests and obtained all the necessary corrections, Ship Helicopter Operating Limit (SHOL) trials can proceed. However, considerable planning is required to ensure that the testing goes smoothly and valuable time with the ship is used as efficiently as possible. The aim of the trial must be established in consultation with the operators and any priorities must be set to ensure that the Services get what they need.

Aircraft and ship instrumentation requirements need to be established with sufficient time available to install such equipment. The degree of sophistication of the

instrumentation needs to be considered and at A&AEE a comprehensive suite of aircraft parameters are normally recorded using a digital system for subsequent analysis and also presented in the aircraft in either analogue or digital form for manual recording during trials. The following aircraft parameters are mandatory during any trial:

- Torque for each engine - visual and recorded
- Tail rotor pitch and/or pedal position (whichever is the more limiting) - visual and recorded
- Fuel state (to determine aircraft mass) - visual
- OAT - visual
- Pressure altitude - visual and recorded
- Rotor speed - visual and recorded

The following additional parameters would also normally be recorded on instrumentation except when suitable data dictated otherwise:

- Engine temperature and Compressor speed
- Radar altimeter height
- Rate of descent on landing
- Undercarriage oleo position
- Aircraft pitch, roll and heading
- Pitch, roll and yaw rate
- Cyclic and collective control positions

The recording system installed in the aircraft is usually a digital system and so it is necessary to have a replay facility to produce output. This places a constraint upon the trial location. The replay station used at the moment occupies a cabin some 8x3x3 metres in dimension. Few ships are large enough to take this on board and the size of the replay station is one of the reasons why A&AEE ship trials are normally land based with the aircraft setting off in the morning to conduct tests with the ship at sea but returning to land at night. Future development of our instrumentation facilities is seeking to provide a more compact system which will eliminate the requirement for the cabin and speed up analysis of data.

A similar digital recording system is positioned on the ship to record relevant deck motion parameters. These are currently:

Ship pitch and roll attitude
Vertical and lateral acceleration at the flight deck

A reference anemometer is installed on the ship, the output of which is recorded using the deck motion instrumentation package. A visual relative wind indicator for this anemometer is also used to enable real time comparison with the ship's indicated wind. Although this involves repeating the work done during the airflow trial, in practice this is a more economical way of obtaining the result in a form which is of use during post trials analysis. Airflow results are presented in a particular way to demonstrate that the magnitude of any errors in the anemometers are within acceptable limits. This presentation is not easily used during SHOL trials. Although it would be possible to present the data in a different form, this would require about the same amount of effort as it does to simply record the values indicated during a trial. By recording the results at the time of the trial, a better impression is gained of the magnitude of any errors and their significance, since a SHOL trial covers a wider range of wind speeds than those used during airflow trials.

As mentioned above, given the constraints upon instrumentation replay facilities it is sometimes necessary to base the trials on land; indeed this has become the preferred method for A&AEE. Apart from the considerations of the physical size of the replay facility there are a number of other considerations which have lead to this conclusion. First there is a need for extensive ongoing analysis during the trial. This ensures that the results upon which daily plans are made are up-to-date, as landing ratings can change following analysis. This analysis takes place after the day's flying and it is preferable to work in the

generally more pleasant surroundings of land-based accommodation than the usually cramped accommodation of warships in perpetual motion. Secondly, the aircraft will require maintenance each day and this is more easily undertaken ashore where specialist facilities and better spares support are available. Thirdly, few modern warships have spare accommodation for a team of personnel, 12 or more in number.

In addition to instrumentation, other provisions must be made to ensure that testing can be conducted at the desired AUM and CG. This is normally achieved by ballasting an aircraft either internally, externally or both. The ballast schemes must allow the basic AUM of the aircraft to be high enough to cover a number of operating masses by altering fuel state and allow for variation due to different ambient conditions on any one day. External ballast is useful as it can be jettisoned should the aircraft encounter a problem which threatens the safety of the aircraft such as an engine failure in the hover. This, in combination with internal ballast to alter CG position, and fuel state to alter AUM, offers the most flexible scheme to cover all the trials requirements. One further consideration on the ballasting of the aircraft occurs when the trials aircraft is also used to ferry personnel to and from the ship on a daily basis. When this is the case, the ballast scheme must allow for passengers yet still observe AUM and CG limits. This could involve the need to pressure defuel the aircraft on completion of trials flying. Such considerations complicate the trial planners life but in our experience, they do not present serious problems.

In the past when the trials team was embarked the ship was able to sail in search of stronger winds. Although this apparent advantage is denied to a shore based trial, experience has shown that chasing the weather can be a fruitless activity as it is rarely where it is

predicted to be. By using the areas of the UK during the winter months the results of shore based trials have been equally as wide as those from earlier ship based exercises.

The business of exploring low speed envelopes in a ship environment is potentially hazardous as even cautious exploration cannot always guarantee that the aircraft will not encounter severe turbulence or, perhaps more significantly, down draughting air. These can result in high torque being used to hover, and occasionally these values exceed normal permitted limits. To offset any lengthy servicing or inspections which would normally be required following an over-torque, A&AEE applies to the aircraft Design Authority for extended limits; these exist for both Sea King and Lynx helicopters, the 2 most common types used on ship trials. Of course such extensions are only granted by the Design Authority provided accurate records of exceedence of normal limits are available and time spent above specified values must be logged on a time and peak torque basis. This information is sent to the Design Authority following the trial and may result in a reduction in life for certain dynamic components.

6 CONDUCT OF THE TRIALS

The daily routine of a ship trial is essentially the same for the duration of the trial which is usually 2 to 3 weeks. Overnight, the servicing team check the aircraft and prepare it for the next day's flying by altering ballast or fuel load to suit the requirement of the trials officer in scientific control. The scientific trials officers and pilots will spend the evening considering the day's results to ensure all the results have been accurately recorded and instrumentation output is ordered for the day's flying. A check of the weather forecast is made to determine the tests that can be conducted the following day.

The aircraft will take off early in the morning with the trials team onboard to join the ship at sea. On arrival the ship's officer of the watch is briefed on the details of the day's flying programme and positions the ship for the first test points. A&AEE always rely upon the skill of ship's personnel to provide the required wind conditions. An experienced seaman knows the best way to provide what we as aircraft testers want; they manoeuvre the ship to give very precise conditions thus enabling the trials team to achieve their goals in the quickest time possible. It is appropriate to pay tribute to the seamanship of such people, without whom the aircraft trials team would undoubtedly not achieve the same degree of success.

The wind speed and direction are varied during the trials by the ship altering direction and speed to give the required relative wind over the deck. Direction is normally altered in 15° increments; wind speed is more difficult to control as it depends upon the natural wind but as a guide 5 or 10 knot increments are common. The natural wind has a major influence on the success of any trial as it is necessary to obtain a wide range of conditions to cover the whole low speed envelope. It is necessary to experience wind speeds in the range 5 to 35 knots to allow side wind components of up to 30 knots. For this reason A&AEE normally conducts tests between October and March in the coastal waters around the UK. This gives the best statistical probability of achieving the necessary wind.

Deck motion is another factor which is assessed during these trials and this tends to be a function of sea state and swell. By using the sea areas close to the South West Approaches to the UK, it is possible to use areas close to land where the sea state is less to carry out initial tests and then to expose the ship and aircraft to the Atlantic swell to look at deck motion in higher sea states.

The starting point of any trial is usually with winds close to ahead at about 20 knots with the aircraft at light mass. The subsequent test points then move around the azimuth to about Red 45° and then Green 45° before continuing around to winds on the beam. As the ship manoeuvres the side wind component will invariably reduce to perhaps 10 to 15 knots depending upon the natural wind speed. Subject to satisfactory results the next points would continue to vary the direction of the wind until stern winds were achieved. At this point the trials officer must decide whether to increase the aircraft AUM or explore higher wind speed values. This decision is governed by the prevailing conditions, we aim to have the aircraft at its maximum permitted operating mass as soon as possible; safety permitting. As explained earlier, these points will read down to lower masses and once limits have been established at the higher mass the aircraft can be made lighter to further explore the envelope until new limits are reached.

During a day's flying we would hope to fly 3 hours in the morning and 3 hours in the afternoon. The rate at which landings are achieved varies but in the initial stages of a trial we would expect to carry out about 12 landings an hour. Over the trial period we would do some 60 hours flying and perhaps 300 to 400 landings.

The trials team would position the officer controlling the tests on the bridge of the ship to liaise directly with the captain or officer of the watch. Another trials officer would be on the bridge to record wind conditions and test results; he would be in constant contact with the aircraft by radio. The aircraft would normally be crewed by one test pilot and a trials officer who records visual data in the aircraft and rates torque and pedal values. The pilot assesses handling qualities and these ratings are passed to the trials officer on the bridge who can

then plot the progress of the trial and review the results to determine whether the flying plan needs to be amended in the light of the results.

Each landing is rated against the appropriate scale and these are plotted using different colours on the blank polar diagram which, as the trial progresses rapidly becomes covered in many different coloured crosses as shown in Figure 9. The highest rating is plotted and marked to denote whether a handling, torque or pedal point is the critical parameter. At the end of the day the team returns ashore to review the tests carried out and decide upon the next days programme.

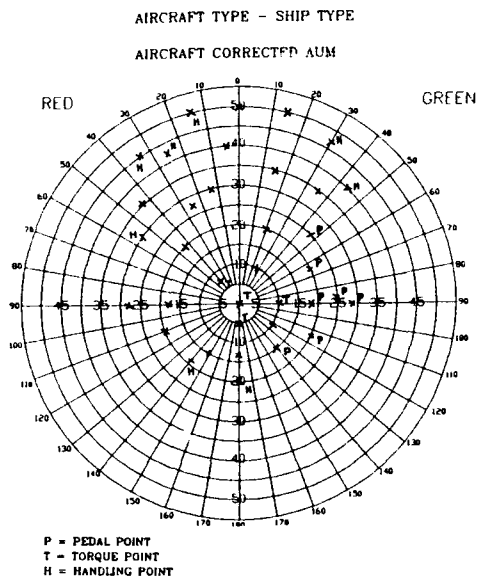


FIGURE 9. TRIAL RESULTS PLOT

At night all the SHOL plots for the different bands are updated and limiting points are read up to higher SHOLs and satisfactory points at high mass are read down to lower SHOLs. Thus as time progresses the plots are filled and areas which need to be explored at lower mass become apparent when these were not attainable at high AUM.

Towards the middle of the second week of the trial the SHOLs will hopefully be taking shape and it can be seen at that stage what will be the likely envelopes. It is at this stage that a night assessment is carried out. This seeks to explore the day SHOLs but with winds abaft the beam removed, to determine whether they are suitable for use at night. Also deck motion limits need to be considered and any reduction at night compared with the day limits needs to be determined. The other aspects of night assessments concern the adequacy of flight deck lighting and markings. Any comments upon deficiencies are passed to the operators to consider ways in which these might be modified to improve cues.

7 TRIALS ANALYSIS

At the end of the trial there is usually little analysis of the wind and envelopes left to be done. The ongoing analysis at the end of each day's flying has corrected each point for being slightly over or under the target mass and all the plots have been adjusted accordingly. The one significant area of analysis that is carried out post the trial is that of deck motion. During the trial the rate of descent on landing is either measured using Doppler radars mounted on the undercarriage or high speed video is used to film the aircraft as it lands. These values are then correlated against the ship motion that was present at the time and the subjective assessment of deck motion given by the test pilot.

Up until the mid 1980s the Royal Aerospace Establishment at Bedford (RAE(B)) were responsible for determining deck motion limits. The work carried out by RAE(B) determined limits and correlated rate of descent (and thereby undercarriage structural limits) with deck motion. This data was passed to aircraft manufacturers to enable fatigue spectra to be established. Since assuming responsibility for this aspect of deck trials A&EE has determined deck

motion limits based on a subjective assessment of the pilots. Limits have been set at the point where deck motion significantly affects pilot workload. We record rates of descent on landing and can supply this data to manufacturers.

The wind envelopes are drawn up around the acceptable test points attained during the trial and these are promulgated to the users. However, it occasionally happens that due to the prevailing weather the limits of the aircraft capability have not been encountered in some areas or at some masses. When this occurs we consider whether the results are sufficiently similar to those from other similar ships in which limits were obtained. If such data exist and they indicated similar results we would consider using that to expand the SHOLs and provide the widest possible envelopes that we can reasonably recommend.

8 CLEARANCE RECOMMENDATIONS

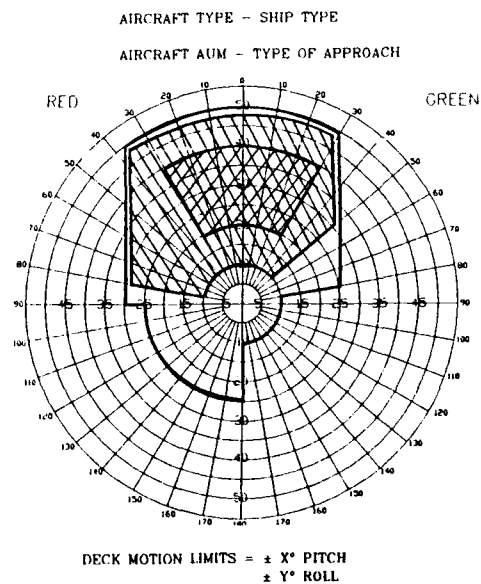


FIGURE 10. FINAL SHOL PLOT

The envelopes and deck motion limits are then issued to the operators together with advice concerning modifications to the ship such as improved deck markings or lighting and any warnings about turbulence. Should any aircraft deficiencies have come to light during the trials then these would also be brought to the attention of the appropriate authority. The only other area that needs to be addressed is that of Mass Correction. This is the process by which the operators determine which of the SHOLs they should use for a given combination of ambient conditions. The aim of this process is to retain the same power and pedal margins seen during the trials in other conditions and give a simple means of working out the appropriate equivalence.

9 OPERATIONAL USE OF SHOLS

The SHOLs that are produced from the trials cover mass bands which are in terms of M/σ^2 and are derived in conditions where σ is close to one and then corrected to equal one. ω is always equal to one during our trials and can be ignored here. In order to provide the users with a simple means of converting from non-unity values of sigma a process known as Mass Correction is used. However, simply converting the operational AUM to M/σ would not retain the power margins seen during the trials as engine power available is not a simple function of σ . Therefore A&AEE developed the Mass Correction diagram as a simple graph which operators can use to derive their correction. This is added to or subtracted from the actual aircraft mass to give a corrected mass. The SHOLs are presented in terms of corrected mass and so by simply consulting one graph and adding or subtracting one number the operators can decide in which band their aircraft falls and use the appropriate SHOL for that mass.

The Mass Correction diagram is made up of 3 elements. These are:

PEDAL LINES

TRANSMISSION LINES

ENGINE LINES

The pedal lines are simply lines of constant M/σ and are aimed at maintaining the pedal or tail rotor pitch margins seen during the trial as these are a function of M/σ .

Thus:

$$\begin{aligned} M_t/\sigma_t &= M_o/\sigma_o \text{ and} \\ M_t/1 &= M_o/\sigma_o \text{ } (\sigma_t = 1) \\ \therefore M_o &= M_t \times \sigma_o \text{ and} \\ \Delta M &= M_t - M_o \\ \Delta M &= M_t - (M_t \times \sigma_o) \\ \Delta M &= M_t (1 - \sigma_o) \end{aligned}$$

To calculate the values of ΔM , M_t is chosen as the highest corrected for which the operators require SHOLs. This is obviously restrictive as it gives a larger correction for pedal than would be the case for each lower band. However, to produce separate diagrams for each band would complicate the process unacceptably and so a single value is chosen which is conservative and therefore safe to be used at all masses.

The pedal lines are plotted as shown at Figure 11. The X axis is correction and the Y axis is OAT in ° Celsius. Lines of constant pressure (in millibar) enable the OAT and mean sea level pressure to be used to determine the correction for any ambient conditions.

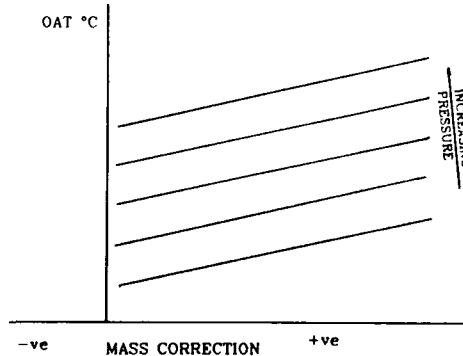


FIGURE 11. EXAMPLE OF PEDAL CORRECTION LINES

TRANSMISSION LINES are determined by comparing the maximum transmission power available (usually the gearbox continuous limit) with the power required during the tests as shown at Figure 12. This is the hover power required graph and the mass correction is determined as follows:

During the tests the aircraft hovered at a mass M_t using power P_t . The test density ratio was $\sigma_t = 1$. The maximum M/σ at which the aircraft can hover in other conditions is dictated by P/σ . If the limit set for operational use is P , then P/σ_0 gives a mass of M_0/σ_0 . By multiplying this by σ_0 we get the maximum mass at which the operators can hover in operational conditions, M_0 . As test mass was M_t , $M_t - M_0$ is the difference in mass which will give the same power margin as the test conditions. This is then the mass correction. By calculating M_t for different combinations of temperature and pressure (ie values of sigma) and subtracting these from the maximum corrected mass for which SHOLs are required we get lines as shown in Figure 13. Once again the maximum value of corrected mass is chosen as opposed to several lower test masses and although this is restrictive, this avoids the complication of having different corrections for different bands.

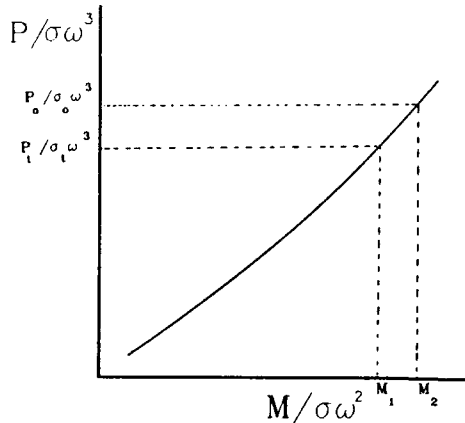


FIGURE 12. HOVER PERFORMANCE CURVE

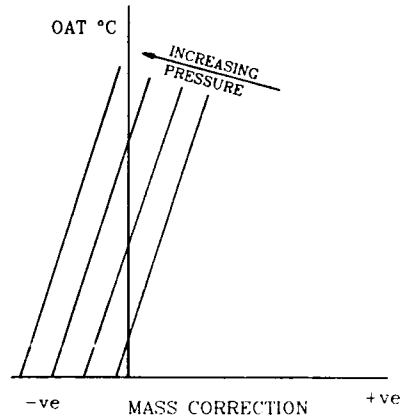


FIGURE 13. EXAMPLE OF TRANSMISSION LINES

ENGINE LINES are derived in exactly the same way as transmission lines except the limiting value of P varies with ambient conditions and whether the engines are Gas generator speed (N_g) of Turbine inlet temperature (PTIT) limited in the ambient conditions. These values are determined from the engine manufacture's data sheets with due allowance for installation losses. The lines so derived are shown at Figure 14 and these may have a gradient change if there is a point at which the engine is limited by one or other of N_g or PTIT.

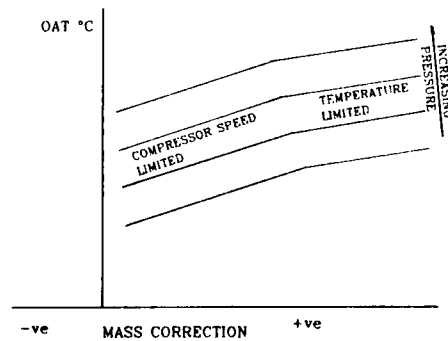


FIGURE 14. EXAMPLE OF ENGINE LINES

The 3 elements of the correction diagram have now been derived and they are combined using the most conservative line of each element as the final value. This is shown at Figure 15 for one value of pressure. Figure 16 shows a typical final correction diagram.

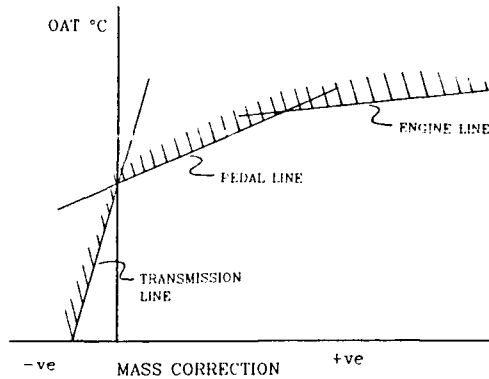


FIGURE 15. COMBINATION OF 3 TYPES OF LINE

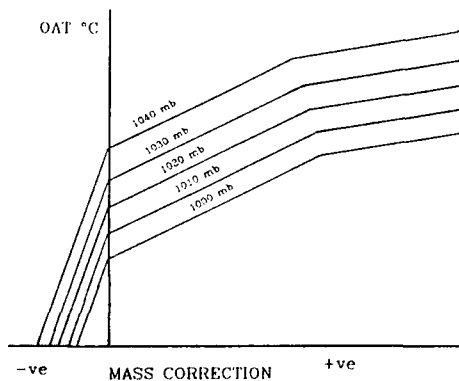


FIGURE 16. FINAL CORRECTION DIAGRAM

It is recognised that by determining the graph as shown, this is restrictive in many cases. For instance if the ambient conditions dictate use of a pedal line but the aircraft is operating in a relative wind in which pedal margins are

large, the correction that needs to be applied could be less using the transmission line. By using the value of maximum SHOL to drive the correction imposes larger corrections on lighter SHOLs than might otherwise be the case. However, to attempt to produce a correction diagram which accounts for different masses and different wind speeds and directions would complicate the process unnecessarily and would not produce a corresponding increase in operational capability. The essence of this process is simplicity.

10 CONCLUSIONS

This paper has described the UK philosophy for deriving military ship helicopter operating limits and presented detail of the many facets that go into a successful trial. The resulting envelopes represent the widest possible that an aircraft is capable of for a given mass and these are achieved at relatively little cost in terms of ship and aircraft time. The correction process gives a quick and simple method of converting the aircraft to a corrected mass equivalent to the test conditions and aims to preserve the same margins seen during tests. Years of operational use by the Royal Navy has testified to the fact that the SHOLs produced by A&AEE are both operationally acceptable and most importantly safe.

ACKNOWLEDGEMENTS

The author wishes to express his gratitude to Mr P A Knowles (S/L RWPS A&AEE) and Cdr M R Swales RN (OC RWTS A&AEE) for their help in preparation of this paper.

This work has been carried out with the support of Procurement Executive Ministry of Defence.

A REVIEW OF AUSTRALIAN ACTIVITY ON MODELLING THE HELICOPTER/SHIP DYNAMIC INTERFACE

A.M. Arney
J. Blackwell
L.P. Erm
N.E. Gilbert

*Flight Mechanics and Propulsion Division
Aeronautical Research Laboratory - Melbourne
506 Lorimer Street, Fishermens Bend, Victoria 3207, Australia*

SUMMARY

The Aeronautical Research Laboratory (ARL) has been tasked by the Royal Australian Navy (RAN) to develop a computer model of the S-70B-2 Seahawk/FFG-7 dynamic interface and to use this to investigate operational problems and limitations. An overview of the status of this task is presented, with particular emphasis on undercarriage dynamics and studies of the airwake in the region of the flight deck. For the undercarriage model, modifications resulting from static trials, as well as plans for dynamic trials, are given. For the airwake studies, only preliminary results are available. These relate to full-scale airwake and ship motion trials aboard the FFG-7 class frigate HMAS Darwin, and 'mean flow' airwake studies in the low-speed wind tunnel at ARL using a 1/64 th size model of an FFG-7.

LIST OF SYMBOLS

F	Oleo load
F_{stat}, F_{dyn}	Static and dynamic components of oleo load
G	Oleo damping coefficient
G_1, G_2	First and second stage oleo damping coefficients (original model)
K_1, K_2	Oleo spring coefficients (original model)
K_3, K_5	Oleo spring coefficients (improved model)
P	Fraction of normal oleo pressure
P_t	Fraction of normal tyre pressure
a_x, a_y, a_z	Ship longitudinal, lateral, and vertical acceleration components
g	Acceleration due to gravity
p, q, r	Ship roll, pitch, and yaw rates
u, v, w	Ship longitudinal, lateral, and vertical velocity components
z	Oleo compression
z_1, z_2	Oleo break points
Ψ	Ship wind-over-deck direction
ϕ, θ, ψ	Ship roll, pitch, and yaw Euler angles
<i>Subscripts</i>	
b	Bias error
m	Measurement

1. INTRODUCTION

The RAN has operated the Aérospatiale Squirrel (~ 4000 lb maximum gross weight) aboard the FFG-7 class of guided-missile frigates for several years, and is currently augmenting these with the much larger Sikorsky S-70B-2 Seahawk (~ 21000 lb maximum gross weight). A new light frigate, known as the ANZAC frigate and based on the Meko 200, is to replace the present River class of destroyer escorts, and is also expected to operate the Sikorsky aircraft.

A computer simulation model was obtained from the US Naval Air Test Center (NATC) through The Technical Cooperation Program (TTCP), Technical Panel HTP-6. This model includes helicopter (Seahawk) flight dynamics and engine dynamics, undercarriage dynamics, ship motion, and a representation of the airwake. Also included is the RAST (Recovery Assist, Secure, and Traverse) system. The code is capable of modelling the complex interactions in the dynamic interface between ship and helicopter, in particular between the FFG-7 and the SH-60B Seahawk, as used by the US Navy. Although current interest is on the Seahawk/FFG-7 combination, the general approach should be applicable to other combinations such as the Seahawk and the ANZAC frigate.

The simulation program has been modified significantly from its original state, and has been used to investigate a number of potential operational problems affecting helicopter radome clearance. This is a primary concern since the radome on the Australian Seahawk (S-70B-2) is deeper and mounted further forward than its US counterpart (SH-60B), and is therefore more likely to make contact during landing. The problems investigated include the effect of a delayed pilot control input while landing, a comparison between landing on ground (full ground effect) and landing on a frigate flight deck (partial ground effect), and the effect of ship motion on an aircraft sitting on the flight deck (Ref. 1).

In Section 2, a brief outline of the simulation code and planned future improvements are given, followed in Section 3 by a description of the experimental programs devised to gather necessary data. Section 4 discusses the data processing, as well as the application of results obtained from these experimental programs to the development of the code as part of the validation process.

Throughout most of this paper, imperial units are used since these units are used in the available documentation for the US designed Seahawk and FFG-7. The wind tunnel measurements are given in metric units as these are the

prime units used in the ARL wind tunnels; however, full-scale equivalent dimensions are expressed in imperial units.

2. STATUS OF SIMULATION CODE

The primary tool to be employed in examining the helicopter/ship dynamic interface is the SH-60B/FFG-7 simulation code obtained from NATC. Figure 1 is a block diagram showing the various modules of the simulation code, and how they interact with each other. A brief description of each of the modules is given in Reference 1.

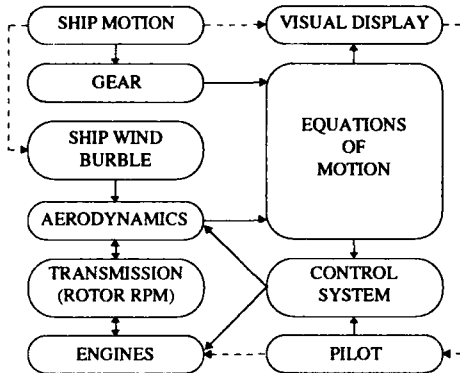


Figure 1. Simulation Code Modules

Initial modifications to the simulation were first required to adapt the program to the Elxsi 6400 mainframe computer in use at ARL, and then to make the program more user-friendly in the time history environment, since it is no longer used in conjunction with a real-time moving base simulator. Because the study of radome clearances was of primary concern, the existing undercarriage model was replaced with one developed at ARL (Ref. 2), and the code was modified to allow radome clearance to be given as an output. The new undercarriage model, which has been further developed since Reference 2, will be discussed in detail in Section 4.1.

As part of an exchange with the US through TTCP HTP-6, ARL will be provided with the NASA Ames version of the Black Hawk simulation model that uses the Sikorsky generic simulation code GENHEL (Ref. 3). It is planned to replace the aerodynamic model (actuator disc) in the Seahawk/FFG-7 simulation code with the blade-element representation of rotor aerodynamics found in the GENHEL model. This should allow more realistic modelling of airwake effects due to the presence of the superstructure of an FFG-7.

3. EXPERIMENTAL PROGRAMS

To establish and then validate an adequate model of the helicopter/ship dynamic interface, comprehensive data bases are required for the various component models shown in Figure 1. This section describes the various experimental programs devised to gather the requisite data. With the exception of the wind tunnel tests, all the

experimental data were gathered using a PC based data acquisition system designed and built by the Instrumentation and Trials Group at ARL. A description of the data acquisition system is given in Reference 4.

3.1 Aircraft Performance and Flight Dynamics

In order to validate the aircraft representation, it was planned to measure all pertinent variables on a RAN Seahawk during a number of steady-state (performance) and dynamic manoeuvres (see Table 1). Since the Navy require an instrumented aircraft to carry out First of Class Flight Trials (FOCFT), it was intended to perform model validation trials at the same time. This meant that the aircraft would be out of squadron service for a minimum time (the RAN has only 16 Seahawks). FOCFT are designed to determine the operating limits of a particular aircraft/ship combination. These trials are performed by the Aircraft Maintenance and Flight Trials Unit (AMAFTU), based at the Naval Air Station at Nowra on the New South Wales coast.

Table 1
Steady State and Dynamic Manoeuvres Required for Model Validation

Steady State	
Hover Out of Ground Effect	
Hover In Ground Effect	i) 20 ft above water ii) 20 ft above flight deck
Trim from -20 to +120 kn (positive fwd) every 10 kn	
Trim from -20 to +20 kn (positive to stbd) every 10 kn	
Dynamic	
Pulse, step, and doubiet inputs of collective, cyclic, and pedals at hover, 40, 80, and 120 kn	
Single engine cut	
Twin engine cut	
Pedal turns	

Table 2 lists the variables necessary for validation of the aircraft dynamics, with channels 1 to 14 required by the RAN for FOCFT purposes.

Because of anticipated problems with radome clearances during landing, AMAFTU attached a dummy radome to a Seahawk. Four Ultrasonic Transducers (USTs) were also attached to the aircraft fuselage, around the circumference of the radome, in order to measure the proximity of the deck. The Rotary Wing Group at ARL developed a computer program, which ran on a portable Compaq 286 computer, the same PC used by the data acquisition system, to find the point on the radome surface with minimum clearance. Two programs were provided, one which gives the pilot an idea of radome clearance after each landing (simplified so as to speed up execution time for use on the aircraft), and the other which does a more extensive computation of the radome surface (for use at the data processing stage). The method chosen was to first deduce the relative Euler angles between ship deck and aircraft from the UST measurements (so as not to require separate processing of both shipborne and aircraft data acquisition systems, since relative angles are required), and then to transform the equations

Table 2
Aircraft Parameters Required for FOCFT and Aircraft Model Validation

Channel Number	Description
1	Longitudinal cyclic stick position
2	Lateral cyclic stick position
3	Collective stick position
4	Pedal position
5	Tail rotor position
6	Event marker
7	Radome forward UST
8	Radome starboard UST
9	Radome aft UST
10	Radome port UST
11	Torque port engine
12	Torque starboard engine
13	Radar altitude
14	Vertical doppler
15	Longitudinal cyclic mixer input
16	Lateral cyclic mixer input
17	Collective mixer input
18	Pedal mixer input
19	Stabilator angle*
20	Airspeed
21	Pitch attitude
22	Roll attitude
23	Yaw attitude (heading)*
24	Pitch rate
25	Roll rate
26	Yaw rate
27	Longitudinal acceleration
28	Lateral acceleration
29	Vertical acceleration
30	Longitudinal doppler
31	Lateral doppler
32	Rotor RPM*

representing the radome surface from radome body axes to ship axes in order to find the point of minimum clearance. During a short trial prior to the FOCFT, AMAFTU determined, from data obtained from the USTs, that radome strikes could occur under certain conditions during shipboard operations.

For approximately 20% of the time allocated for the FOCFT, channels 15 to 20 were substituted with channels shown in Table 3 in order to obtain oleo compressions using Linear Variable Differential Transformers (LVDTs), and tyre compressions using USTs. This was done during a series of landings to provide additional data to complement the ground-based aircraft undercarriage trials (discussed in Section 3.2).

* Channels which, for various reasons, were not actually measured.

Table 3
Undercarriage Validation Channels

Channel Number	Description
15	Starboard main LVDT
16	Port main LVDT
17	Starboard main UST*
18	Port main UST*
19	Tail wheel UST*
20	Tail fuselage UST

A number of parameters aboard ship were also measured (Table 4) using a separate data acquisition system to determine ship motion during landings.

The FOCFT were planned to be done on the FFG-7 class frigate HMAS Adelaide during 1990 while en route from Australia to Hawaii, where the ship was scheduled to take part in a major naval exercise. Unfortunately, because of damage sustained during a heavy landing at the end of the first two days of flying, the flight tests were cancelled so that the aircraft damage could be properly assessed ashore. Due to some problems with the aircraft instrumentation and the limited amount of flying, none of the manoeuvres required for validating the model were completed, although limited data are available for a number of landings. With the RAN commitment to the Gulf crisis, future trials have been delayed, and it is now hoped to obtain the requisite data when the aborted FOCFT are resumed.

Table 4
Ship Motion Channels

Channel Number	Description
1	Longitudinal acceleration
2	Lateral acceleration
3	Vertical acceleration
4	Pitch attitude
5	Roll attitude
6	Heading
7	Pitch rate*
8	Roll rate*
9	Yaw rate*
10	Ship speed
11	Relative Wind speed
12	Relative Wind direction
13	Ambient temperature

3.2 Undercarriage Dynamics

The undercarriage model developed at ARL contains static and dynamic components for both oleos and tyres. A series of static and dynamic trials was proposed involving a complete helicopter. The use of an isolated oleo strut or wheel was considered unacceptable since it was not expected to yield similar results to an oleo or wheel that is part of a complete helicopter. In particular, an isolated oleo/wheel fails to take account of the flexibility of the helicopter fuselage (quite considerable in a Seahawk),

which is believed to contribute significantly to the effective spring and damping characteristics of the fuselage/undercarriage combination. Static trials have already taken place (Ref. 5), and dynamic trials are expected to be undertaken during 1991. Once these dynamic trials are completed and a validated undercarriage model is obtained, it is proposed to use the code to determine the changing loads on the aircraft tie-down points for a Seahawk secured in a ship hangar.

The aim of the static trials was to obtain load and compression data for tyres and oleos both at normal and reduced (nominally 85% of normal) operating pressures. Using interpolation, results could then be estimated at intermediate pressures, thus enabling a model representation which allowed for underserviced tyres and/or oleos. An underserviced landing gear is potentially dangerous, since fuselage/deck clearances are likely to be reduced in such circumstances. The original undercarriage model had no representation of underserviced tyres and/or oleos. The static trials involved sitting the helicopter on three load cells (one for each wheel), and then jacking up the helicopter so that the aircraft weight was gradually transferred from the undercarriage to the jacks. At various intermediate points, the load on each gear, as well as the gear compressions/extensions, were recorded. Results were taken for both increasing load (lowering helicopter) and decreasing load (raising helicopter) to take account of any possible hysteresis. As a result of the trials, major changes were subsequently made to the static oleo equations. The static tyre equations retained their form, but were modified to allow for reduced tyre pressures. These changes are discussed in Section 4.

The aim of the dynamic trials is to obtain load and compression rate data for tyres and oleos both at normal operating pressure and at 85% of normal pressure. Due to difficulties in recording the dynamic load directly on each gear, it has been decided to record helicopter accelerations, rates, and attitudes during the trial, and determine time-varying gear loads from the deduced motion of the helicopter. Flight trials in which a helicopter lands were therefore considered inadequate, since aerodynamic loads would need to be measured accurately so they can be removed when calculating gear loads. It was therefore decided that the trials will be ground-based, requiring the helicopter to be raised by either a collapsible jack or crane with quick-release hook attached to the helicopter tie-down points. In either case, the helicopter will be subsequently released from its raised position and allowed to settle on the ground.

Time-varying oleo and tyre compressions will be recorded during the dynamic trial using a combination of USTs and LVDTs. The gear compressions and helicopter motion will be recorded simultaneously using the previously mentioned PC based data acquisition system. Gear compression rates will be determined from the time-varying gear compressions. Redundancy is built into the trial in the sense that gear compressions and rates can also be deduced from the helicopter motion given the gear moment arms, and vice versa. Since blade flexing is expected to be quite considerable in the unloaded state, the main rotor blades will need to be removed. Results from these trials will be

complemented by data obtained during the RAN FOCFT (see Section 3.1).

3.3 Ship Motion and Airwake

3.3.1 Full-Scale Trial

While en route from Sydney to New Zealand, from 18 to 21 September 1989, a trial was undertaken aboard HMAS Darwin, an FFG-7 class frigate, fitted with stabilisers and RAST equipment. The objective of the trial was to measure the ship motion and airwake over the flight deck for a variety of wind-over-deck velocities (the trials instructions are detailed in Ref. 4).

This section gives both a brief description of the scope of the trial and details of the data gathering aboard ship. The preliminary results of the data processing techniques involved with obtaining the ship motion and airwake velocity components in Earth axes are described in Section 4.2.

A comprehensive envelope of relative wind speed and direction was required in order to establish a data base for the airwake model in the Seahawk/FFG-7 simulation code. Due to the uncharacteristically benign conditions encountered during the voyage to New Zealand, a somewhat limited envelope was achieved. Figure 2 details the required and measured relative wind envelopes.

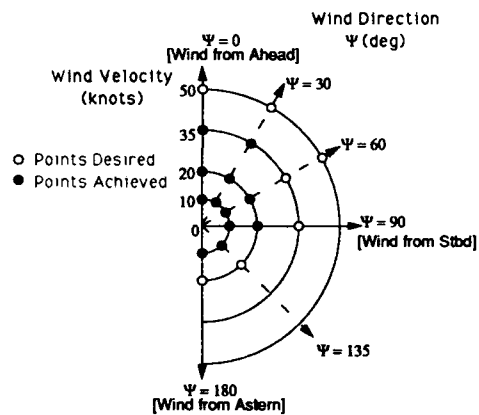


Figure 2. Relative Wind Envelope

To record the ship motion and airwake about the flight deck, the previously mentioned PC based data acquisition system was used (Ref. 4 gives more detail). A ship motion platform was assembled comprising a three-axis accelerometer; pitch, roll, and yaw rate gyros; and pendulum attitude sensing devices. Additional ship motion parameters such as ship speed and heading were obtained from standard ship instruments. Measurements of the airwake were obtained using a specially designed and built collapsible, mobile, anemometer mast. When erected, the mast stood 33 ft high and was fitted with three sets of tri-axial Gill anemometers, three temperature probes at each anemometer set, and an accelerometer based attitude sensor

Table 5
Ship Motion/Airwake Analogue Channels

Channel Number	PC Channel	Description
1	A01	Mast direction (Low 9)
5	A05	Ship pitch attitude
6	A06	Ship roll attitude
7	A07	Ship pitch rate
8	A08	Ship roll rate
9	A09	Ship yaw rate
10	A10	Ship vertical accel'n
11	A11	Ship lateral accel'n
12	A12	Ship longitudinal accel'n
13	A13	Mast temperature (Top)
14	A14	Mast temperature (Mid)
15	A15	Mast temperature (Low)
16	A16	Cup anem. port speed
17	A17	Cup anem. port direction
18	A18	Cup anem. stbd speed
19	A19	Cup anem. stbd direction
20	A20	Mast speed (Top 1)
21	A21	Mast speed (Top 2)
22	A22	Mast speed (Top 3)
23	A23	Mast speed (Mid 4)
24	A24	Mast speed (Mid 5)
25	A25	Mast speed (Mid 6)
26	A26	Mast speed (Low 7)
27	A27	Mast speed (Low 8)
28	A28	Mast speed (Low 9)
29	A29	Mast longitudinal slant
30	A30	Mast lateral slant
31	A31	Aerovane speed
32	A32	Aerovane direction

Table 6
Ship Motion/Airwake Digital Channels
(0 ⇒ wind into propeller, 1 ⇒ wind out of propeller)

Channel Number	PC Channel	Description
33	DI1	Mast direction (Top 1)
34	DI2	Mast direction (Top 2)
35	DI3	Mast direction (Top 3)
36	DI4	Mast direction (Mid 4)
37	DI5	Mast direction (Mid 5)
38	DI6	Mast direction (Mid 6)
39	DI7	Mast direction (Low 7)
40	DI8	Mast direction (Low 8)

Prior to sailing, a number of procedures were followed while the ship was 'stationary' at the pier. To ensure the mobile mast position at each grid point was identical for each data run, the flight deck was marked with yellow adhesive tape. Due to the sloping flight deck, the mast was found to be at significantly different attitudes, with respect to the ship

Table 7
Ship Motion/Airwake Synchro Channels

Channel Number	PC Channel	Description	Comments
51	SY1	Ship heading	0° ⇒ North 90° ⇒ East
52	SY2	Ship speed	0° ⇒ 0 kn 360° ⇒ 40 kn
53	SY3	Ship anemometer speed	0° ⇒ 0 kn 360° ⇒ 100 kn
54	SY4	Ship anemometer direction	0° ⇒ from bow 90° ⇒ from stbd

datum, for each of the grid points. At each grid point, the height of the mobile mast stabilising legs was adjusted and recorded so that the mast was nominally vertical (indicated by spirit levels). This ensured that the measured airwake velocities could be related to the ship datum while the ship was in motion at sea.

3.3.2 Wind-Tunnel Tests

Wind-tunnel measurements are currently being taken in the 2.74 m by 2.13 m (9 ft by 7 ft) low-speed wind tunnel at ARL using a 1/64 th size model of an FFG-7 class frigate. Measurements are for a nominal freestream velocity of 50 m/s and for seven angles of yaw of the ship, namely 0, 15, 30, 60, 90, 135, and 180 deg, for zero pitch and roll angles of the ship.

A rake of yaw probes is being used to measure three-dimensional mean-flow velocities at various locations around the ship model. The rake contains eight similar probes spaced at intervals of 50 mm, with five orifices on each probe tip. Details of the probe and calibration procedure are described in Reference 6.

All measurements are based on a rectangular cartesian coordinate system that is fixed with respect to the wind tunnel. The flowfield affected by the presence of the ship is referred to as the 'burble'. The extent of the burble will vary depending on the particular angle of yaw of the ship. The extremities of the measurements in the three directions in the different cases have been chosen to include parts of the burble likely to be encountered by the helicopter during approach and landing. For an angle of yaw of 30 deg, Figure 6 shows a plan view of the overall grid pattern, as well as the grid points at which measurements are to be taken (shaded). For this angle of yaw, the measurements on the model will extend 300 mm forward and 1400 mm aft of the grid origin, from the flight deck to 350 mm above it (at 50 mm intervals), and 800 mm to the port side and 400 mm to the starboard side of the grid origin. The full-scale distances on the ship corresponding to the above model distances are 63 ft forward and 294 ft aft of the grid origin, 73.5 ft vertically (at 10.5 ft intervals), and 168 ft to the port side and 84 ft to the starboard side of the grid origin.

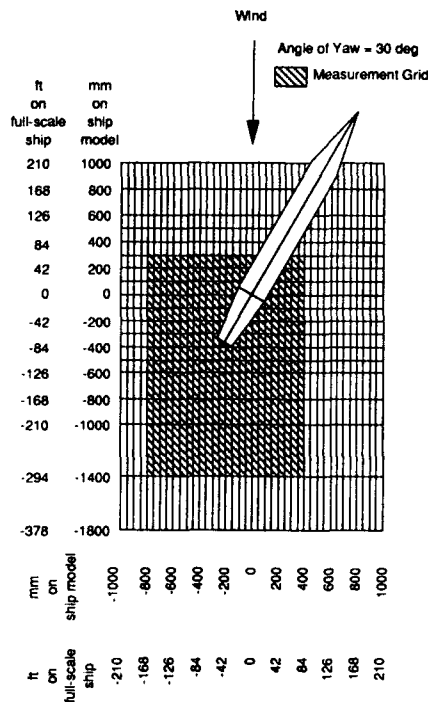


Figure 6. Measurement Grid for FFG-7 Wind Tunnel Tests

Preliminary results of the wind tunnel test are given in Section 4.2.2.

4. STATUS OF DATA PROCESSING

Both the undercarriage model calculations and the determination of ship motion from data have involved the use of a generalised non-linear maximum likelihood parameter estimation program developed at ARL. The standard maximum likelihood procedure for estimation of unknown parameters in a model is normally applied to linear systems and is well documented (e.g. Ref. 7). In its early stages, the ARL maximum likelihood code COMPAT (named because of its application in the area of compatibility checking) was able to estimate parameters from non-linear systems; however, the amount of user input required was fairly extensive. In particular, a large number of sensitivity matrix elements, representing the partial derivative of a given output with respect to a particular parameter, had to be determined by the user, thus making the program highly problem specific. A small alteration to the model structure could require significant modifications to the program. However, the program was used successfully to determine parameters from flight data (Ref. 8).

Further modifications to COMPAT involved the numerical determination of sensitivity matrix elements using a

forward difference technique, and resulted in a generalised program which was able to be used on a wide variety of systems, both linear and non-linear (Ref. 9). User input was much reduced and unknown quantities such as initial conditions, break points (where discontinuities occur), and time delays could be determined, in addition to the usual parameters.

4.1 Undercarriage Trial

As a result of static trials completed in 1990 (Ref. 5), the form of the static oleo equations in the undercarriage model was significantly altered, while the static tyre equations retained their form, but were modified to allow for reduced tyre pressures. The original ARL oleo model (Ref. 2) was of a two-stage type and expressed oleo load, F , as a function of static load, F_{stat} , and dynamic load, F_{dyn} , in the form

$$\begin{aligned} F &= F_{stat} + F_{dyn} \\ &= K_1 z^2 + G \dot{z} \quad z < z_1 \\ &= K_1 z_1^2 + K_2 (z - z_1)^2 + G \dot{z} \quad z \geq z_1 \end{aligned}$$

where K_1 and K_2 are first and second stage oleo spring coefficients respectively, z is the oleo compression, z_1 is the oleo break point, and G is a damping coefficient whose value depends on whether the oleo is in the first stage of compression ($G = G_1$ for $z < z_1$) or second stage ($G = G_2$ for $z \geq z_1$). The model structure was similar to that used in the original NATC undercarriage code, with coefficients being modified using parameter estimation techniques applied to limited isolated oleo drop test data.

As a result of the static undercarriage trials, the oleo model was modified to the form

$$\begin{aligned} F &= F_{stat} + F_{dyn} \\ &= K_3 + K_4 z + K_5 z^2 + G \dot{z} \end{aligned}$$

where K_3 to K_5 are oleo spring coefficients. In the absence of new dynamic undercarriage data, the form of the dynamic part was left unchanged except that only a single damping coefficient was retained. Its value was determined using parameter estimation techniques applied to the same drop test data referred to above, using the modified undercarriage model with K_3 to K_5 held fixed. For the tail oleo, three distinct stages were observed during the trial so that parameters K_3 to K_5 are assigned different values in the ranges $z < z_1$, $z_1 \leq z < z_2$, and $z \geq z_2$, where z_1 and z_2 are oleo break points. The main oleo showed one stage only. The tail oleo also showed hysteresis effects, with different parameters for the upstroke and downstroke. No hysteresis was observed for the main oleo.

Figure 7 shows the main oleo load-compression results for both normal oleo pressure and 85% pressure. The principal difference is a vertical translation indicating that parameter K_3 is highly dependent on oleo pressure. Parameters K_4 and K_5 only vary slightly with pressure. If P is the fraction of normal oleo pressure, then for $0.85 \leq P \leq 1$, and assuming linear variation, the main oleo parameters are given by

$$\begin{aligned} K_3 &= (5920 P - 3365) \text{ lbf} \\ K_4 &= (-513 P + 99) \text{ lbf/ft} \\ K_5 &= (1287 P - 5746) \text{ lbf/ft}^2 \end{aligned}$$

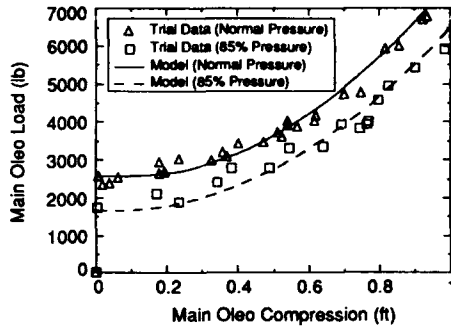


Figure 7. Main Oleo Load-Compression Results for Normal Oleo Pressure and 85% Pressure

Similar effects were observed with the tail oleo.

Figure 8 shows a comparison between the original ARL model results and the modified model results, determined using the recent trial data, for the main oleos. The inadequacies of the original model are clearly demonstrated.

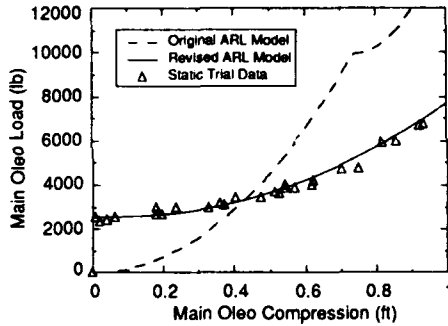


Figure 8. Comparison of Original ARL Model with Modified Model for Main Oleo

The static tyre model was left unchanged as a result of the trial, but was extended to take account of reduced tyre pressure. Figure 9 shows the trial results at both normal and 85% pressure for the twin tail tyres. Since a constant scale factor of 0.82 links the two curves to a reasonable degree of accuracy, the static load at any intermediate pressure can be readily determined from the normal pressure data base, assuming linear interpolation, by scaling using a factor of $(1.2 P_t - 0.2)$, where P_t is the fraction of normal operating tyre pressure. The main tyres exhibit similar behaviour, but with a scale factor of 0.74.

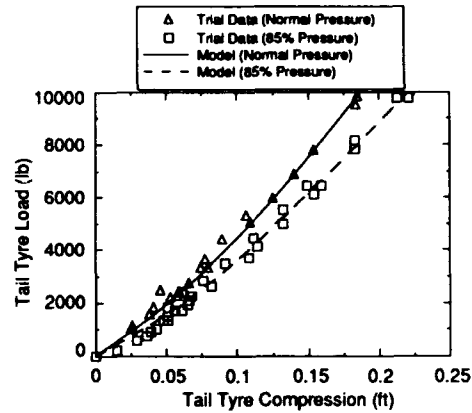


Figure 9. Twin Tail Tyres Load-Compression Results for Normal Pressure and 85% Pressure

4.2 Full-Scale Ship Motion and Airwake Trial

Data reduction of the measurements obtained from the full-scale ship motion airwake trial is taking place in two distinct phases. Phase 1 involves obtaining the ship velocity components and attitudes from the ship motion platform instrumentation, and Phase 2 involves correction of the anemometer measurements and removal of the ship motion components from the measured airwake velocities. A process is being developed whereby the ship attitudes and velocities, including initial conditions, may be determined through parameter estimation. The software necessary to remove the resulting ship motion from the airwake measurements, as well as the computer programs to present this data graphically in three-dimensional form, will soon be developed.

4.2.1 Deriving Ship Motion

The parameters measured by the ship motion platform included the three acceleration components (a_x, a_y, a_z); roll, pitch, and yaw rates (p, q, r); and pitch and roll 'attitudes'. Two additional parameters recorded from the ship instrumentation were ship heading (yaw attitude) and ship speed. It should be noted that the ship speed is measured using a device which would tend to average the actual longitudinal velocity component. After the trial was completed, it was determined that the pendulum devices, designed to measure pitch and roll attitudes in the static case, actually measure accelerations in the dynamic case, with the overall effect of duplicating the accelerometer measurements. This is illustrated in Figure 10, which shows a comparison of the longitudinal and lateral acceleration components (measured by the accelerometer) with the respective pitch and roll 'attitudes' (measured by the pendulum devices), dimensionalized appropriately. The duplication is evident, with the offsets attributed to measurement bias errors that have yet to be removed.

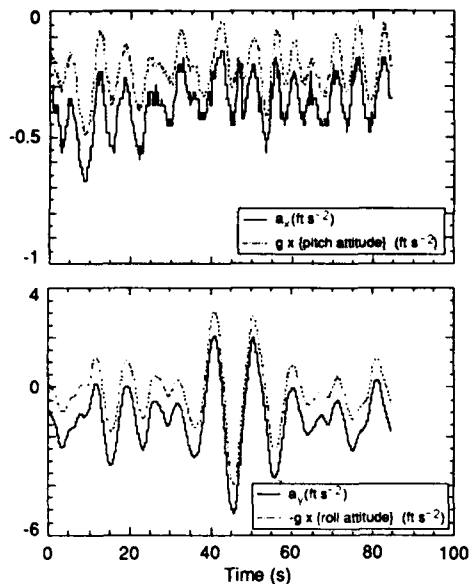


Figure 10. Equivalence of Ship Acceleration and Pendulum 'Attitude' Measurements

Thus to determine the ship velocity components, the measurements available are

- three acceleration components
- pitch, roll, and yaw rates
- average longitudinal velocity
- yaw attitude

Since the ship is not at a known trimmed condition when recording of data commences, initial conditions are unknown. By using parameter estimation techniques, the ship attitudes and velocity components, including the initial conditions, may be determined after first making a few reasonable assumptions given below.

The standard rigid body equations of motion (Ref. 10) are

$$\begin{aligned}\dot{\phi} &= p + q \sin\phi \tan\theta + r \cos\phi \tan\theta \\ \dot{\theta} &= q \cos\phi - r \sin\phi \\ \dot{\psi} &= (q \sin\phi + r \cos\phi) \sec\theta \\ \dot{u} &= -qw + rv + a_x - g \sin\theta \\ \dot{v} &= -ru + pw + a_y + g \cos\theta \sin\phi \\ \dot{w} &= -pv + qu + a_z + g \cos\theta \cos\phi\end{aligned}$$

Examination of these equations shows that the Euler rate equations are decoupled from the velocity rate equations. In order to reduce the number of unknown parameters to be estimated, the Euler angles are first determined.

The parameter estimation program COMPAT may also be used to check measured data against expected values (as determined from the equations of motion) to determine drift or biases in instrumentation, and may be useful in

determining incorrect signs in the calibrated data. An error model for p , q , and r is assumed to be of the form

$$p = p_m + p_b$$

$$q = q_m + q_b$$

$$r = r_m + r_b$$

where p , q , and r are the actual rates; p_m , q_m , and r_m are the measurements; and p_b , q_b , and r_b are constant bias errors to be determined.

As previously discussed, the pendulum devices do not give accurate representation of the variation of pitch or roll attitude, but instead measure accelerations about some mean. Since the ship is maintaining a steady forward velocity, it may be assumed that the average acceleration components are zero. Thus the mean values given by the pendulum devices are assumed equal to the average Euler angles, as determined by COMPAT, and so provide additional information necessary for the parameter estimation process to succeed. COMPAT was used with the above constraint to determine initial Euler angles as well as errors in rates p , q , and r . Typical results are shown in Figures 11 and 12 for the case of a wind-over-deck velocity of 10 kn, at a yaw angle of 180 deg.

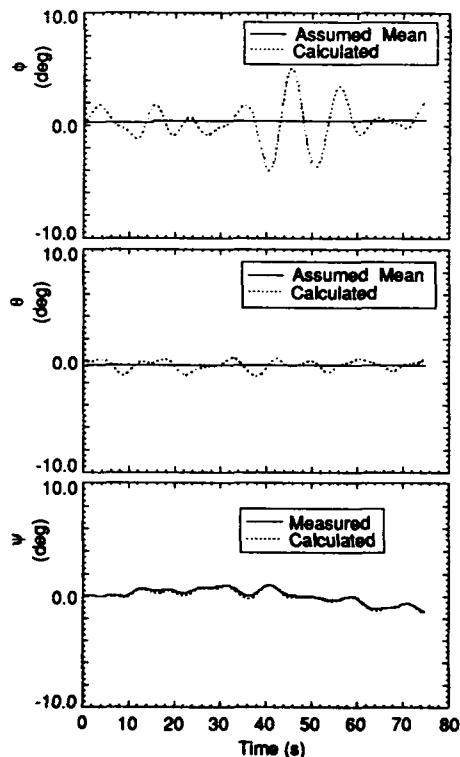


Figure 11. Estimated Euler Angles

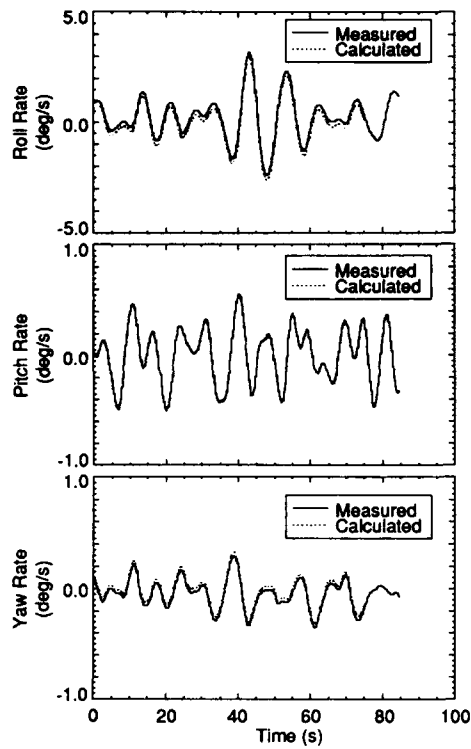


Figure 12. Corrected Rates

Now that the Euler angles and rate errors have been determined, the velocity components may be found by making certain assumptions. For a long, slender ship, maintaining forward velocity, it is reasonable to assume that the average vertical and lateral velocity components are zero. The average longitudinal velocity is measured by the standard ship instruments. An error model for the accelerometers is assumed to be of the form

$$\begin{aligned} a_x &= a_{xm} + a_{xb} \\ a_y &= a_{ym} + a_{yb} \\ a_z &= a_{zm} + a_{zb} \end{aligned}$$

where a_x , a_y , and a_z are the actual accelerations; a_{xm} , a_{ym} , and a_{zm} are the measured accelerations; and a_{xb} , a_{yb} , and a_{zb} are the instrument bias errors.

COMPAT may now be used to estimate the initial velocity components and the accelerometer bias errors. Typical results are shown in Figure 13.

Having determined the ship motion referenced to the centre of ship motion (see Fig. 14), the apparent velocity due to ship motion, as measured by the airwake anemometer mast, may then be found.

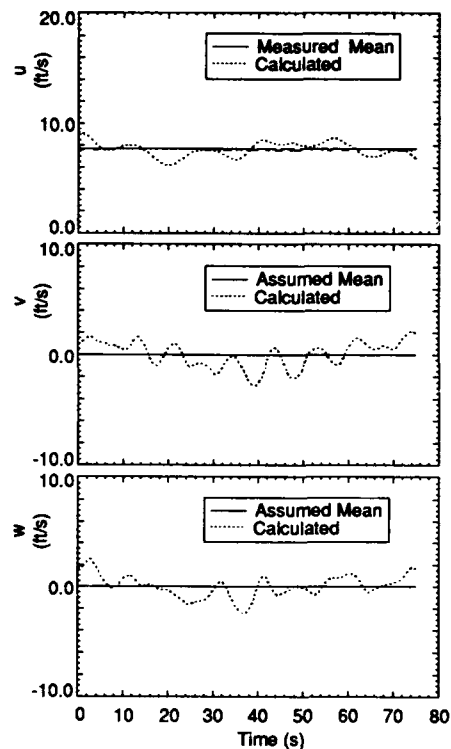


Figure 13. Ship Velocity Components

4.2.2 Preliminary Airwake Results

A preliminary study was made of the data obtained from the airwake trial in order to ensure that useful data had been recorded for the full range of data points for each of the combinations of wind-over-deck velocities. This preliminary examination involved the application of calibration factors and offsets to obtain engineering units from the raw data. It should be noted that the velocity components presented here, measured by the three-axes Gill anemometers, have not yet been corrected for known errors due to non-axial flows (Ref. 11; up to 5% error in direction and 10% error in magnitude) and that the ship motion components have not yet been removed to obtain the airwake in Earth axes.

Examination of the time histories shows that the majority of the data were of good quality (i.e. channels were functioning consistently), but there were some exceptions. Very early in the trial it was apparent that the mid-level temperature probe on the mobile mast was faulty and that the data from this particular channel were unsalvageable. It is also apparent that, for some of the data runs, high frequency interference occurred, possibly from the HF radio of the ship, or the radar. This affected mainly the digital

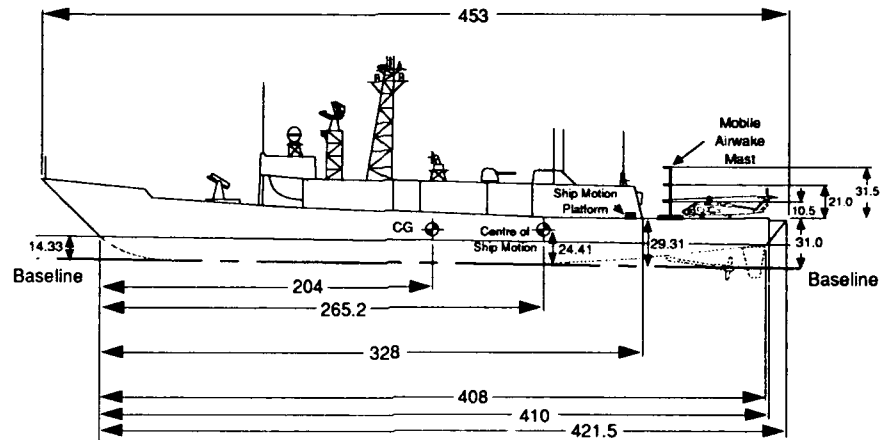


Figure 14. Elevation of FFG-7 Showing Key Elements of the Ship (dimensions in feet)

channels which indicated airwake flow direction. Unfortunately, this interference occurred for the entire 20 kn, 90 deg wind-over-deck case, but since the flow is expected to be fairly steady at 90 deg, it may be possible to salvage these results.

At the higher ship speeds, the stabilisers damp out the motion, and as a first approximation the anemometer data may be assumed to contain small components due to ship motion. The full-scale velocities and those predicted by the simulation code are shown superimposed in Figure 15. The full-scale velocities are preliminary only and have yet to be corrected for non-linear angular response of the Gill anemometers and also for the effects of ship motion.

The comparison between predicted velocities and those measured from full-scale trials was made for a 35 kn relative wind at 30 deg off the starboard bow and for a height of 21.0 ft (6.4 m) above the bullseye. This height corresponds to the mid-location of Gill anemometers. These conditions were set precisely in the simulation code, but for the full-scale trials some variations in the magnitude and direction of the relative wind inevitably occurred.

A meaningful comparison of velocity components containing turbulence would normally be done statistically. However, the objective here in showing a comparison of time histories is to observe the overall mean values and trends. For the velocities shown in Figure 15, it is apparent that the mean values of corresponding velocities in the longitudinal and lateral directions are significantly different. Mean values of corresponding velocities in the vertical direction show reasonable agreement, but the full-scale velocity shows far more variation about its mean value than the predicted velocity. The large differences between predicted and full-scale velocities indicates that there are serious deficiencies within the simulation program, which is not unexpected since the model was based, using geometric scaling, on experimental results obtained from a Knox class frigate.

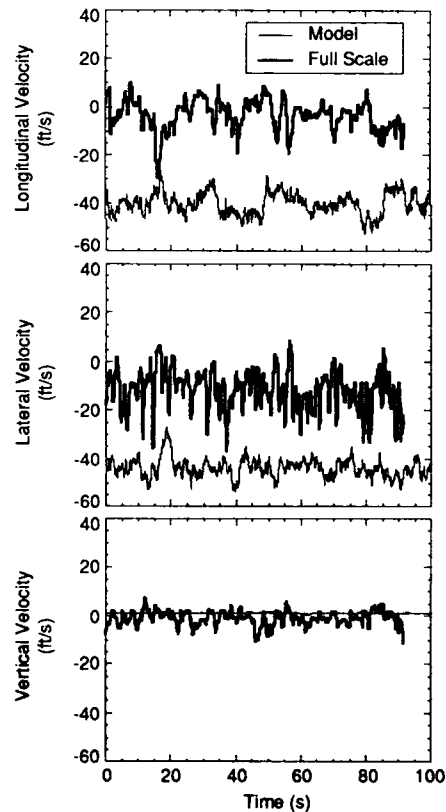


Figure 15. Comparison of Full-Scale with Predicted Airwake Velocities

To determine the dominant energy-containing frequencies of fluctuating velocities, it is necessary to do a spectral analysis. Figure 16 shows spectra for three coordinate directions corresponding to the predicted velocities shown in Figure 15. The spectra were obtained from the velocity plots by using a Fast-Fourier-Transform (FFT) algorithm in which the number of data points required for the algorithm must be a power of two. The velocities shown in Figure 15 were computed at every 0.0666 second for 100 seconds, which means that each velocity plot shown corresponds to about 1500 data points. It was only possible to use 1024 ($= 2^{10}$) points in the spectral analysis, which is equivalent to 68.1 seconds of a velocity plot. The frequencies shown in Figure 16 range from 0.0147 Hz to 7.4928 Hz in increments of 0.0147 Hz, i.e. $1/(0.0666 \times 1024)$ Hz, and the energy contribution at each frequency has been normalised by the total energy contribution summed over all frequencies. The spectra have not been smoothed in any way. It is apparent from the spectra that the dominant frequencies are below about 1 Hz. The spectra thus show that changes in the predicted

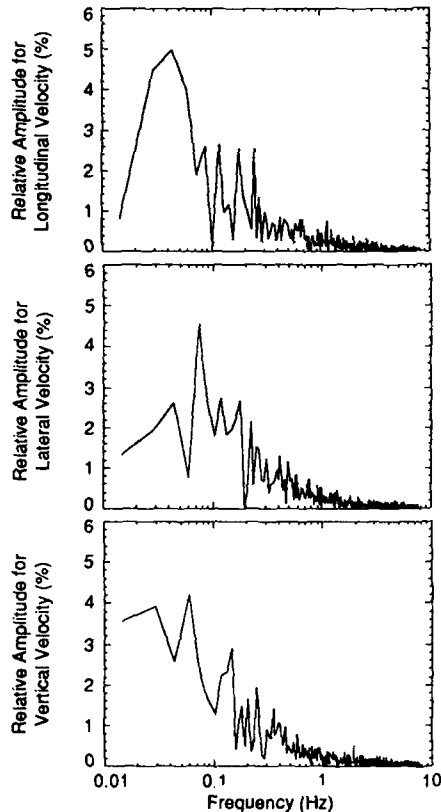


Figure 16. Frequency Spectra for Predicted Airwake Velocities

velocities occur predominantly at low frequencies.

The spectra plotted in Figure 17 are for the full-scale velocities shown in Figure 15. Once again, the spectra are based upon 1024 data points, but since the full-scale data were sampled at intervals of 0.05 second, and not 0.0666 second as previously, then the spectra now correspond to 51.2 seconds of a velocity plot, and the frequency range covered is now from 0.0195 Hz to 9.9805 Hz in increments of 0.0195 Hz. Because of these differences, spectra for full-scale velocities have not been superimposed on corresponding spectra for predicted velocities. From Figure 17 it can be seen that the dominant frequencies for the full-scale velocities are below about 1 Hz, as for the predicted velocities. Thus it is evident that although the mean-flow and fluctuating components of the predicted velocities often differ markedly from corresponding components for the full-scale velocities, the waveforms of the predicted velocities are realistic from a spectral viewpoint.

4.3 Preliminary Wind Tunnel Results

Typical wind tunnel results of the FFG-7 airwake are now

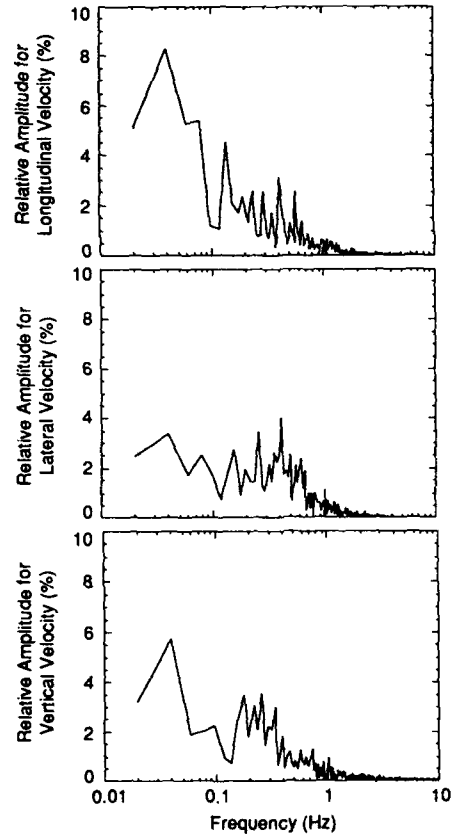


Figure 17. Frequency Spectra for Full-Scale Airwake Velocities

presented. The example illustrated in Figure 18 is for a freestream velocity of 50 m/s at an angle of yaw of 30 deg, and for $x = -800$ mm, y varying from -750 to 400 mm, and z varying from 0 to -350 mm (refer to Fig. 6 for corresponding dimensions on full-scale ship). Velocity vectors are projected onto the yz plane, defined in the wind tunnel coordinate system. The velocity vectors show that a large vortex exists in this region as a consequence of flow over the ship superstructure. Vectors are not given in some regions at the level of the flight deck because the flow angles incident on the probe are outside the range of the probe calibration. This problem is currently being investigated and it may be possible to extrapolate beyond the range of the calibration with little loss of accuracy; otherwise, it will be necessary to extend the range of calibration.

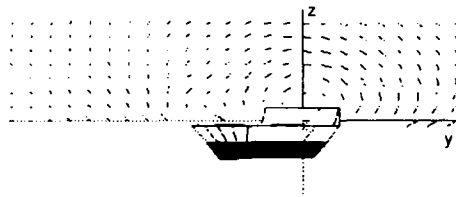


Figure 18. Typical Wind Tunnel Airwake Results

5. CONCLUDING REMARKS

An overview of the status of helicopter/ship dynamic interface modelling at ARL has been described, with the emphasis on undercarriage dynamics and studies of the airwake in the region of the flight deck. Validation of the undercarriage model has been of high priority because of the potential problems affecting clearance of the unique Australian radome. Improvements to the model have resulted from static trials, and further improvements are expected from planned dynamic trials. The full-scale airwake and ship motion trials are expected to provide a valuable data base for the FFG-7 frigate, once the parameter estimation techniques outlined here are applied, and the various corrections made to the data. With the wind tunnel airwake tests, it is recognised that there are limitations on the use of the data, e.g. only mean flow velocities are measured, disturbances are not generated in the tunnel upstream of the model to simulate atmospheric turbulence, and ship motion is not represented. However, these tests are expected to complement the full-scale measurements by providing data at locations beyond the flight deck, and they will provide a baseline set of measurements should it be decided that further, more realistic tests are worthwhile. As well as improving the Seahawk/FFG-7 simulation code by incorporating results obtained from these experimental programs, it is also planned to replace the actuator disc aerodynamic model for the main rotor with the blade-element representation of rotor aerodynamics found in the GENHEL code. This should allow more realistic modelling of airwake effects due to the presence of the ship superstructure.

ACKNOWLEDGEMENT

The authors are indebted to R.A. Feik for his assistance in the application of the parameter estimation program COMPAT to the problem of determining the unknown parameters of the ship motion.

REFERENCES

1. Arney, A.M., Blackwell, J., and Feik, R.A., "Modelling the Helicopter/Ship Dynamic Interface," *Proceedings of the Australian Aeronautical Conference*, Australian Institution of Engineers, National Conference Publication No. 89/14, October 1989.
2. Blackwell, J. and Feik, R.A., "A Mathematical Model of the On-Deck Helicopter/Ship Dynamic Interface," *ARL Aero. Tech. Memo 405*, September 1988.
3. Howlett, J.J., "UH-60A Black Hawk Engineering Simulation Program," Vols I and II, *NASA CR 166309 and 166310*, December 1981.
4. Sutton, C.W., "FFG-7 Extended Deck Ship Motion and Airwake Sea Trial (Trials Instruction for ARL Trial 1/89)," *ARL Flight Mech. Tech. Memo 414*, June 1989.
5. Blackwell, J., "Validation of a Seahawk Helicopter Undercarriage Model: Phase I - Using Static Load Deflection Measurements," *ARL Flight Mech. Tech. Memo* (to be published).
6. Toffoletto, R., "Calibration of a Rake of Velocity Vector Probes," *ARL Flight Mech. Tech. Memo* (to be published).
7. Maine, R.E. and Iliff, K.W., "Identification of Dynamic Systems," *AGARD-AG-300*, 1984.
8. Feik, R.A., "On the Application of Compatibility Checking Techniques to Dynamic Flight Test Data," *ARL Aero. Report 161*, June 1984.
9. Blackwell, J., "A Maximum Likelihood Parameter Estimation Program for General Non-Linear Systems," *ARL Aero. Tech. Memo 392*, January 1988.
10. Etkin, B., *Dynamics of Atmospheric Flight*, John Wiley and Sons, 1972.
11. Drinkrow, R., "A Solution to the Paired Gill Anemometer Response Function," *Journal of Applied Meteorology*, Vol. II, February 1972, pp. 76-80.

UNITED STATES NAVY SKI JUMP EXPERIENCE AND FUTURE APPLICATIONS

by

Mr. T. C. Lea, III
Mr. C. P. Senn

Mr. J. W. Clark, Jr.

STRIKE AIRCRAFT TEST DIRECTORATE
NAVAL AIR TEST CENTER
PATUXENT RIVER, MARYLAND 20670-5304
UNITED STATES OF AMERICA

AERO ANALYSIS DIVISION
NAVAL AIR DEVELOPMENT CENTER
WARMINSTER, PENNSYLVANIA 18974-5000
UNITED STATES OF AMERICA

SUMMARY

The United States Navy has been evaluating the performance benefits of using a ski jump during takeoff. The significant gains available with the use of Vertical and Short Takeoff and Landing (V/STOL) aircraft operating from a ski jump have been documented many times in the past; however, the U.S. Navy has expanded this concept to include Conventional Takeoff and Landing (CTOL) aircraft. This paper will present the results of a recent shipboard evaluation of the AV-8B aboard the Spanish ski jump equipped ship PRINCIPE DE ASTURIAS, and a shore based flight test evaluation of CTOL aircraft operating from a ski jump ramp. The analytical tools developed during the CTOL phase of testing are used to project the benefits which could be realized by combining the steam powered catapult and a "mini" ski jump ramp compatible with today's aircraft carriers.

NOMENCLATURE

AOA	-	Angle of Attack
CG	-	Aircraft Center of Gravity
CRAT	-	Catapult/Ramp Assisted Takeoff
CTOL	-	Conventional Takeoff and Landing
MIL	-	Military Thrust
Max A/B	-	Maximum Afterburner Thrust
ROC	-	Rate of Climb
STO	-	Short Takeoff
SLW	-	Short Lift Wet
V	-	Ramp Exit Airspeed (KEAS)
V_e	-	Ramp Exit Speed (kt)
VTOL	-	Vertical Takeoff and Landing
V/STOL	-	Vertical and Short Takeoff and Landing
W	-	Aircraft Gross Weight (lb)
W_h	-	Hover Weight (lb)
W/W_h	-	Hover Weight Ratio
WOD	-	Wind Over Deck

AV-8B SKI JUMP

Introduction

Flight tests were conducted aboard PRINCIPE DE ASTURIAS, a Spanish ship designed for Harrier operations with a 12 degree ski jump ramp, December 1988 to define operating procedures and limitations and document performance gains over conventional flat deck short takeoffs (STO's). A total of 89 STO's were conducted. PRINCIPE DE ASTURIAS proved to be an excellent platform for Harrier operations. The flight test program clearly demonstrated the performance gains, reduced pilot workload, and improved safety inherent in a ski jump assisted shipboard takeoff. WOD requirements were approximately 30 kt less than flat deck requirements, resulting in significant fuel savings and flight operations having less impact on ship's heading and speed. Deck run requirements were approximately 350 ft (107 m) less than flat

deck requirements, improving Harrier/helicopter interoperability. Maximum payload capability for a ski jump assisted launch is up to 53% greater than flat deck capability, allowing shipboard Harrier operations to the same takeoff gross weight as shore based. The heaviest Harrier to be launched from a ship to date was accomplished during the test program (31,000 lb). The ski jump launch always produced a positive rate of climb at ramp exit, the resulting altitude gain allowing aircrew more time to evaluate and react to an emergency situation. Pilot opinion is that the ski jump launch is the easiest and most comfortable way to takeoff in a Harrier.

Background

In the mid-1970's the British aerospace community identified the significant improvements in takeoff performance for vectored thrust aircraft obtained with the assistance of an upwardly inclined (ski jump) ramp and, as a result, incorporated ramps on existing Royal Navy carriers. In 1977, the Spanish Navy began construction of the first ship designed from the keel up to support Harrier operations. The basic ship design was modeled after the U.S. Navy sea control ship promoted by Admiral Zumwalt in the mid-1970's. A 12 degree ski jump ramp was incorporated to improve takeoff performance. Based on previous shore based ski jump testing and simulation efforts, a 12 degree ramp was found optimum for maximizing takeoff performance while maintaining aircraft structural loads within limits. The ramp profile is the same as that of HMS HERMES of the Royal Navy. Construction began in 1977 at the El Ferrol shipyard of Empresa Bazan Nacional. The ship was commissioned PRINCIPE DE ASTURIAS and delivered to the Spanish Navy 30 May 1988. Shortly thereafter, the Spanish Navy made an agreement with Naval Air Systems Command for Naval Air Test Center to conduct flight tests and engineering analysis required to publish an operating bulletin for AV-8B operations from the ship. Flight test objectives were to define operating procedures and limitations and document performance gains over conventional flat deck STO's.

Test Assets

Ship

PRINCIPE DE ASTURIAS can accommodate up to 36 aircraft consisting of both Harriers and helicopters. The flight deck is approximately 575 ft (175 m) long by 95 ft (29.0 m) wide. The ski jump ramp coordinates are presented in table 1. The maximum STO deck run length is 550 ft (168 m). The ship is stabilized in roll with four stabilizers. The ship has six VTOL spots. The flight deck including flight deck markings is illustrated in figure 1. A profile of the ship is presented in figure 2. The ship is equipped with SPN-35 radar for ground controlled approach, Harrier Approach Path Indicator (HAPI) and Deck Approach Projector Sight (DAPS) for glide slope information, and Hover Position Indicator (HPI) for height control. The ship has a 7,500

nautical mile range at 20 kt ship speed. The ship has a maximum speed of approximately 25 kt.

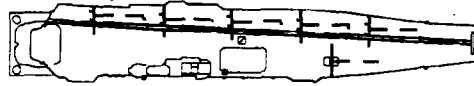


Figure 1
PRINCIPE DE ASTURIAS Flight Deck

Table 1
Ski Jump Ramp Coordinates

Distance Along Ramp		Ramp Height	
ft	(m)	ft	(m)
0.0	(0.0)	0.00	(0.00)
11.5	(3.5)	0.20	(0.06)
21.3	(6.5)	0.50	(0.15)
31.2	(9.5)	0.88	(0.27)
41.0	(12.5)	1.36	(0.41)
50.9	(15.5)	2.00	(0.61)
60.7	(18.5)	2.74	(0.84)
70.5	(21.5)	3.66	(1.12)
80.4	(24.5)	4.69	(1.43)
90.2	(27.5)	5.89	(1.80)
100.1	(30.5)	7.23	(2.20)
111.6	(34.0)	9.02	(2.75)
121.4	(37.0)	10.69	(3.26)
131.2	(40.0)	12.56	(3.83)
141.1	(43.0)	14.55	(4.43)
151.6	(46.2)	14.94	(4.55)

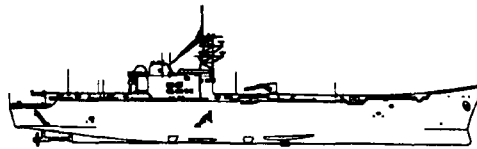


Figure 2
PRINCIPE DE ASTURIAS Profile

Test Aircraft

The AV-8B is a single place, single engine, tactical attack, vectored thrust, jet V/STOL aircraft built by McDonnell Aircraft Company (MCAIR). The aircraft has a shoulder mounted supercritical wing, four rotatable engine exhaust nozzles, and a lift improvement device system. The aircraft is powered by a Rolls Royce PEGASUS F-402-406A twin spool, axial flow, turbofan engine with an uninstalled sea level static short lift wet thrust rating of 21,500 lb (95,600 N). The primary flight controls consist of aerodynamic and reaction controls which are interlinked in all axes and hydraulically powered. The AV-8B is an excellent aircraft for ski jump takeoff due to its exceptional low-speed flying qualities. A three view drawing of the AV-8B is presented in figure 3.

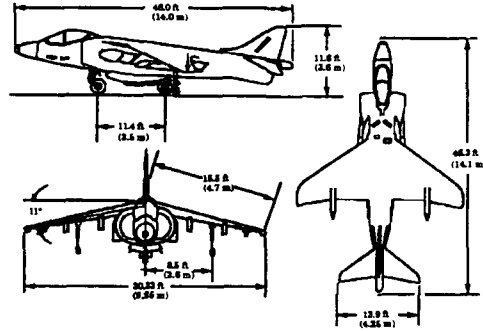


Figure 3
AV-8B Three View Drawing

Two aircraft were used for shipboard testing: a preproduction AV-8B which was instrumented for flying qualities and performance testing and nose and main landing gear strut positions, and a non-instrumented production AV-8B. Both aircraft were representative of production EAV-8B aircraft for the purpose of these tests.

Shipboard Tests

STO Launch Technique

A typical STO launch profile is illustrated in figure 4. Nozzles are positioned to 10 deg below fully aft for the deck run to reduce vibratory loads on the flaps and stabilator. The launch begins with application of full power with brake release as the tires begin to skid. The stick is guarded in the preset trim position throughout the deck run and nozzle rotation. As the aircraft exits the ramp, the pilot positions the nozzle lever to the preset STO stop. Ramp exit cues are both visual (nozzle rotation line) and physical (decrease in load factor as the aircraft leaves the ramp). After ramp exit, the pilot task is to maintain the aircraft pitch attitude achieved at ramp exit (approximately 18.5 deg) and monitor angle of attack (AOA). If AOA reaches 15 deg during the trajectory, the pilot decreases the aircraft pitch attitude as required to maintain AOA at or below 15 deg. Immediately after ramp exit, the velocity vector indicates a climb due to the upward velocity imparted by the ramp. This initial rate of climb is not a true indication of aircraft performance, and decreases to a minimum at an inflection point prior to the aircraft achieving a normal semi-jetborne climb. Prior to the inflection point, the aircraft normal acceleration is less than 1 g. The aircraft has a positive rate of climb due to the ramp induced vertical velocity, but rate of climb is decreasing due to insufficient lift. At the inflection point, the aircraft has accelerated to an airspeed at which aircraft normal acceleration is 1 g (lift=weight), and rate of climb is no longer decreasing. After the inflection point is reached, the aircraft begins a normal semi-jetborne climb (normal acceleration greater than 1 g), and rate of climb increases. At this point, the pilot gradually vectors the nozzles aft and accelerates to wingborne flight.

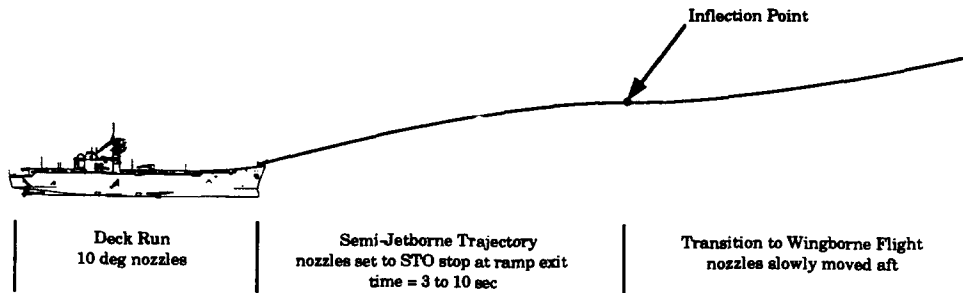


Figure 4
STO Launch Profile

STO Ramp Exit Speed

STO ramp exit speed must be accurately predicted to ensure ramp exit airspeed required is obtained and landing gear structural limits are not exceeded. Ramp exit speed is a function of aircraft hover weight ratio and deck run. Tests were conducted at deck runs from 200 to 550 ft (61 to 168 m). Actual Ramp exit speeds were obtained from infrared trips which were mounted at the end of the ramp. Ramp exit speed data was reduced to an exit speed parameter and plotted against deck run. The exit speed parameter is defined as $V^2(W/W_H)$ and its relationship to deck run is based on the dynamic relationship $V^2=2aS$ where "a" is the average acceleration and "S" is the deck run. STO ramp exit speed averaged one kt less than that of an identical flat deck launch due to the decelerating effects of the ramp. Ramp exit speed was predictable within 2.5 kt.

STO Landing Gear Structural Limits

During ski jump launch with no ship motion, loads are imparted on the landing gear due to aircraft gross weight, aerodynamic lift, vectored engine thrust, pitching moments, and inertial forces including centrifugal forces. Centrifugal forces are influenced by aircraft velocity and local ramp curvature. The primary dynamic response exhibited by the AV-8B during ski jump launch is in the aircraft heave mode. Dynamic response to aircraft pitch motion is small in comparison to heave.

STO maximum ramp exit speeds for landing gear structural limits were determined at gross weights of 26,000, 28,000, and 31,000 lb (11,793, 12,701, and 14,062 kg). Fatigue strength for 1,500 lifetime ski jump launches defined the limiting criteria for landing gear based on MCAIR analysis. Nose and main landing gear strut positions were instrumented and monitored real-time. Simulation data and previous ski jump testing indicated outrigger landing loads would not approach limiting criteria and were therefore not instrumented. Target ramp exit speed for the first launch at each gross weight was based on MCAIR simulation and was at least 10 kt below the predicted landing gear limit. The ramp exit speeds for successive launches were increased in increments of approximately three to five kt by increasing deck run until the limiting criteria were reached. A method suggested by MCAIR was used to account for ship motion. Load factor trends were incremented for sea state resulting in a shift in the aircraft gross weight vs maximum ramp exit velocity curve for given sea states. MCAIR correlated ship motion with sea state based on ship motion studies of similar type ships by David Taylor Ship

Research and Development Center. Worst case phasing of ship's pitch, heave, and coriolis effects were used to determine load factor increments due to sea state. The coriolis effect is the additional normal acceleration of the aircraft due to its increased velocity normal to the deck while it travels away from the ship's pitch center. Analytical results were verified with test data and are presented in figure 5.

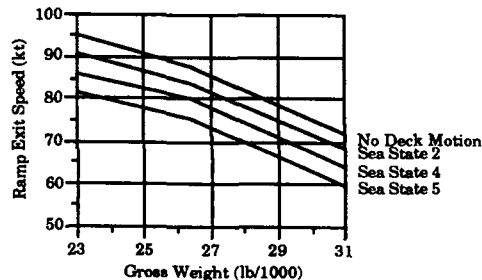


Figure 5
Landing Gear Structural Limits

STO Minimum Ramp Exit Airspeed

STO minimum ramp exit airspeed tests were conducted at hover weight ratios of 1.43, 1.52, and 1.60. The purpose of these tests was to define the minimum ramp exit airspeed required for a safe launch and to evaluate the sensitivity of reducing ramp exit airspeed when operating near the minimum. The minimum airspeed was approached by holding hover weight ratio constant while decreasing ramp exit airspeed for each successive launch. Ramp exit airspeed for the first launch at each hover weight ratio was based on MCAIR simulation and previous ski jump testing and targeted an airspeed approximately 15 kt above the predicted minimum. The ramp exit airspeeds for successive launches were reduced in decrements of approximately three to five kt by varying either deck run or WOD until the minimum ramp exit airspeed was reached. The limiting factor for ramp exit airspeed was zero rate of climb at the inflection point. Test results are presented in figure 6. Flying qualities at minimum ramp exit airspeeds were satisfactory. AOA was controllable with a maximum transient AOA of 17 deg. Lateral control was acceptable throughout the STO envelope. Longitudinal acceleration was acceptable for all launches, averaging two to four kt/sec for launches with rate of

climb from 200 to 1,000 ft/min (61 to 305 m/min). The minimum longitudinal acceleration achieved during the test program was 1.5 kt/sec.

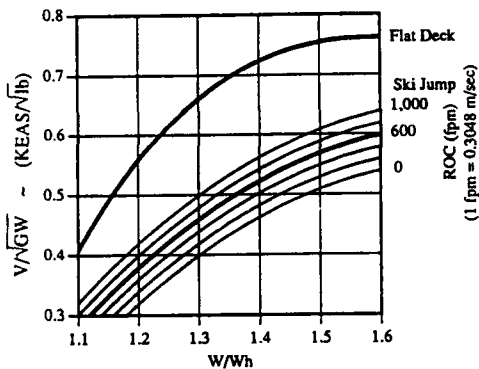


Figure 6
Takeoff Performance

Ski Jump/Flat Deck Comparison

Increased performance obtained from a ski jump assisted launch is realized through reduced WOD and/or deck run requirements and/or increased launch gross weight capability. The discussion in this section deals with the performance gains realized with the PRINCIPE DE ASTURIAS ramp. Performance gains obtained from different ramps will vary with ramp exit angle.

Ski jump launch WOD requirements are compared with flat deck requirements in figure 7. Required WOD for a ski jump assisted launch is approximately 30 kt less than a flat deck launch. Ski

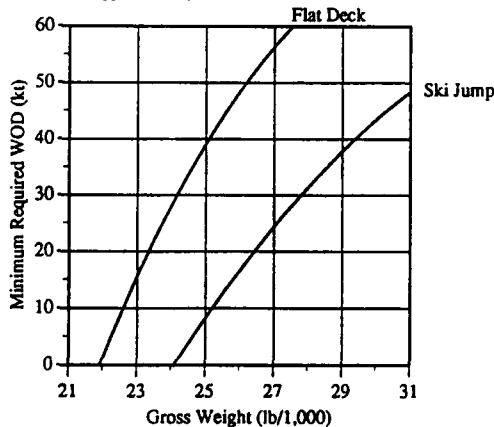


Figure 7
STO WOD Requirements
300 ft Deck Run
Standard Day, Nominal SLW Engine

jump launch operations are therefore not as dependent on natural winds for launch. As a result, normal launch operations do not dictate ship's heading, allowing the ship maneuvering flexibility and decreased operating area during flight operations. Reduced WOD requirements can be appreciated in fuel savings, as the ship can steam at the speed required for minimum steerage and not dictate ship's heading, allowing the ship maneuvering flexibility and decreased operating area during flight operations and still have the required WOD for normal launch operations. Reducing ship's speed from 25 to 7 kt decreases fuel consumption by approximately 80%.

Deck run requirements for ski jump launch are compared with flat deck requirements in figure 8. Instead of launching at lower WOD, ski jump launches can be conducted at the same WOD required for flat deck launches while reducing the deck run by approximately 350 ft (107 m). The result is improved interoperability between Harriers and helicopters. On flat deck ships, if a Harrier is to launch with a significant payload then the entire flight deck is often required for the deck run. This makes Harrier/helicopter interoperability extremely difficult. By reducing the required deck run with the assistance of a ski jump, Harriers can conduct takeoff and landing operations from the forward flight deck while helicopters operate concurrently and completely independently from the aft section. Vertical landing operations to the forward deck spots provide excellent visual cues due to the ramp height, offering significant improvement over vertical landing operations to forward deck spots on a flat deck ship. The ability to operate Harriers and helicopters at the same time from the same flight deck greatly enhances the efficiency of the amphibious assault force.

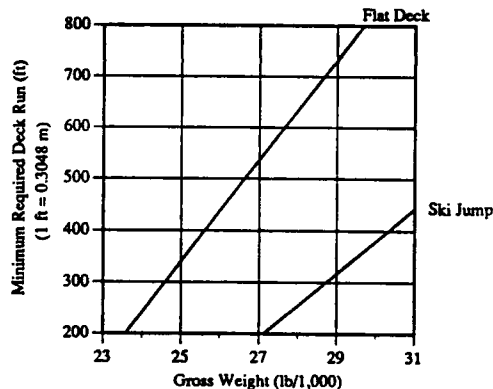


Figure 8
STO Deck Run Requirements
35 kt WOD
Standard Day, Nominal SLW Engine

Gross weight capability for a ski jump launch is compared with flat deck capability in figure 9. For a given WOD and deck run, an AV-8B can carry 3,000 to 5,900 lb more payload from a ski jump ship than from a flat deck ship. This equates to up to a 53% increase in takeoff payload capability. When operating from flat deck ships in tropical day conditions, AV-8B aircraft mission payload is limited by takeoff performance, which is not the case for operations from a ski jump ship. The efficiency of the close

air support mission is therefore enhanced by a ski jump assisted launch by allowing more payload per sortie.

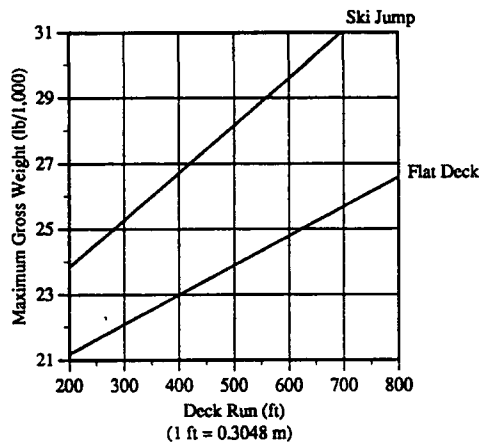


Figure 9
STO Gross Weight Capability
30 kt WOD
Tropical Day, Nominal SLW Engine

There are several safety enhancing characteristics inherent in a ski jump assisted launch. The tracking task during a ski jump launch is easier than during a flat deck launch because the tram lines are more prominent due to the height of the ramp. The ski jump launch produces no pitch-up tendencies at ramp exit and can be completely stick free for a few seconds after ramp exit. This reduces the tendency for pilot induced oscillations when attempting to capture a pitch attitude. The stick free characteristics inherent in a ski jump launch decrease pilot workload and allow more time for monitoring engine performance and critical launch parameters. The aircraft always has a positive rate of climb as it exits the ramp. The resulting additional altitude allows the aircrew more time to evaluate and react to emergency situations. The loss of an aircraft due to an emergency during a flat deck launch may be avoidable with the assistance of a ski jump. Pilot opinion is that the ski jump launch is the easiest and most comfortable way to takeoff in a Harrier.

Summary

PRINCIPE DE ASTURIAS proved to be an excellent platform for Harrier operations. The flight test program clearly demonstrated the performance gains, reduced pilot workload, and improved safety inherent in a ski jump assisted shipboard takeoff for Harrier aircraft when compared to that of a conventional flat deck. WOD requirements were approximately 30 kt less than flat deck requirements. Reduction in WOD requirements means significant fuel savings and flight operations having less impact on ship's heading. Deck run requirements were approximately 350 ft (107 m) less than flat deck requirements. Reduction in required deck run improves the Harrier/helicopter interoperability, allowing Harriers to use the forward half of the flight deck and helicopters the aft portion. Maximum payload capability for a ski

jump assisted launch is up to 53% greater than flat deck capabilities, allowing 3,000 to 5,900 lb more payload. The heaviest Harrier to be launched from a ship to date was accomplished during the test program (31,000 lb). Increased payload capability allows shipboard Harrier operations to the same takeoff gross weight as shore based. A ski jump launch always produces a positive rate of climb at ramp exit. The resulting altitude gain allows the aircrew more time to evaluate and react to emergency situations. The loss of an aircraft due to an emergency during a flat deck launch may be avoidable with the assistance of a ski jump. Pilot opinion is that the ski jump launch is the easiest and most comfortable way to takeoff in a Harrier.

CONVENTIONAL TAKEOFF AND LANDING (CTOL) AIRPLANE SKI JUMP EVALUATION

Background

The U. S. Navy has also evaluated ski jump takeoff as an alternative to shipboard catapult launch for conventional airplanes. The Naval Air Test Center conducted a ski jump takeoff test using a T-2C, an F-14A, and an F/A-18A operating from a variable geometry ski jump ramp to:

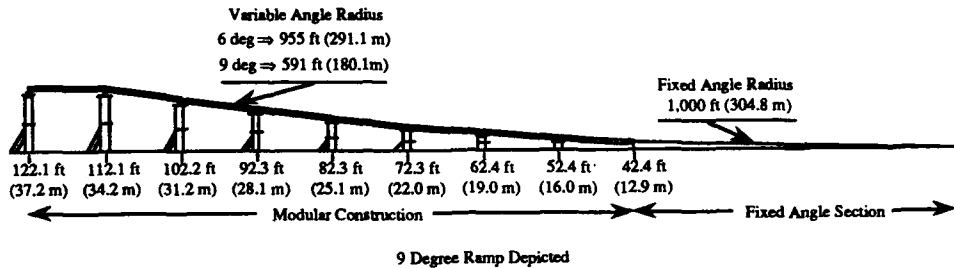
- Evaluate the feasibility of the concept.
- Define the operating limitations.
- Document performance gains.
- Verify and update aerodynamic and structural ski jump simulations.
- Propose airplane and ramp design considerations.

This section of this paper discusses the test program conducted with the F/A-18A airplane. Test results obtained with the T-2C and F-14A airplanes can be obtained from references 1 and 2. A more detailed discussion of the F/A-18A ski jump test program is presented in references 3 and 4.

Test Equipment

Ski Jump Ramp

The ski jump ramp, which was constructed at the Naval Air Test Center, was 60 ft (18.3 m) wide and 112.1 ft (34.2 m) or 122.1 ft (37.2 m) long, depending on the ramp angle. It was of modular steel construction of which the first 42 ft (12.8 m) was a fixed angle ramp with the remainder constructed of 10 x 30 ft (3.0 x 9.1 m) steel modules secured to steel pedestals. The heights of the steel pedestals was varied to give the desired ramp curvature. Figure 10 gives presents the general ramp arrangement and specific heights for the two ramp geometries. Leading into the ramp was a 60 ft (18.3 m) wide x 2,000 ft (609.6 m) long runway consisting of AM-2 matting. Centerline marking was two tram lines 2.5 ft (0.8 m) either side of the centerline. A modified holdback/release system was developed permitting stabilized thrust prior to the takeoff acceleration run. This system could be positioned anywhere along the runway to provide the desired ramp speed.



Distance Along Ramp ft (m)	Ramp Height ft (m)		Distance Along Ramp ft (m)	Ramp Height ft (m)	
	6 deg	9 deg		6 deg	9 deg
0	0	0	82.3 (25.1)	3.88 (1.18)	4.40 (1.34)
42.4 (12.9)	1.16 (0.35)	1.16 (0.35)	92.3 (28.1)	4.81 (1.47)	5.62 (1.71)
52.4 (16.0)	1.68 (0.51)	1.71 (0.52)	102.2 (31.2)	5.85 (1.78)	7.02 (2.14)
62.4 (19.0)	2.30 (0.70)	2.44 (0.74)	112.1 (34.2)	5.85 (1.78)	8.58 (2.62)
72.3 (22.0)	3.03 (0.92)	3.33 (1.01)	122.1 (37.2)	—	8.58 (2.62)

Figure 10
Ski Jump General Arrangement

Test Airplane

The F/A-18A airplane is a single-place, midwing, high performance, twin-engine strike fighter powered by two General Electric F404-GE-400 engines with an uninstalled thrust of 16,000 lb (71,171 N) each. The F/A-18 incorporates a digital fly-by-wire flight control system. The test airplane was aerodynamically and structurally representative of production airplanes. No modifications were made to the test airplane for the conduct of the tests. The following special flight test instrumentation installations were available:

- a) Magnetic tape and telemetry system to record/transmit all required parameters.
- b) Flight test instrumentation controls in the cockpit.
- c) Ballast was installed to simulate the weight and CG of production equipment not installed in the airplane.
- d) Radome mounted angle of sideslip vane which was displayed on the Head Up Display (HUD).
- e) Retro-reflectors near the tip of each vertical tail to provide LASER tracking spatial data.
- f) Landing gear instrumentation to obtain shock strut deflections and structural loads.

All build-up ground and flight tests and ski jump launch operations were conducted in the normal takeoff configuration. Table 2 details the test conditions. Two airplane gross weights were chosen to vary the thrust/weight ratio. External stores comprised two inert wingtip mounted AIM-9 (Sidewinder) and two inert nacelle mounted AIM-7 (Sparrow) missiles.

Table 2
Configuration Summary
F/A-18A Airplane

Takeoff Configuration	Gross Weight lb (kg)	Field Takeoff Airspeed KEAS	Thrust/Weight
Half Flaps (30 deg)	32,800 (14,878)	146	0.52 MIL 0.76 Max A/B
	37,000 (16,783)	154	0.46 MIL 0.67 Max A/B

Manned Simulation

Extensive simulation effort was expended prior to the first ski jump takeoff. Simulation included both an aerodynamic and a landing gear loads model. The simulations not only were used to predict performance gains and structural loads, but enabled the test team to develop a build-down procedure during actual ski jump

operations. Also, airplane single engine failure response characteristics and minimum safe ejection airspeeds in the event of an engine failure were established.

Early in the simulation effort, it was determined that additional performance gains could be realized by a "man in the loop" pitch attitude capture technique. Earlier simulation and all the ski jump takeoff tests with the T-2C and F-14A had been using the "stick free" technique. With these two airplanes, longitudinal trim was set to achieve the desired flyaway AOA. However, current F/A-18 flight control logic is such that a trim AOA is based on the initial stabilator trim position prior to the takeoff run. This AOA/trim schedule is shown in figure 11. Initial simulation runs at the higher ramp exit airspeeds permitted initial trim settings providing stick free flyaways at 12 deg AOA. However, as the ramp exit airspeed was reduced, the initial trim position had to be reduced to keep peak AOA's within limit (17 deg AOA true) during the initial rotation phase following ramp exit. This resulted in trim AOA's during the flyaway somewhat below any optimum for use during a ski jump takeoff. A pilot pitch capture technique was investigated which resulted in a significant decrease in the takeoff airspeed of approximately 15 kt below the stick free results. The technique was to allow the pitch attitude to increase during the initial rotation following ramp exit and peak at approximately 18 deg, at which time nose down pitch rate was generated as the flight control system attempted to acquire the commanded trim AOA. As the pitch attitude decreased to 15 deg the pilot commanded aft stick to maintain 15 deg pitch attitude. A target capture pitch attitude of 15 deg was chosen as the HUD pitch ladder is incremented every 5 deg and at zero rate of climb, a 2 deg AOA margin below the limit AOA was provided. During the flight test program, both the stick free and pitch capture techniques were evaluated.

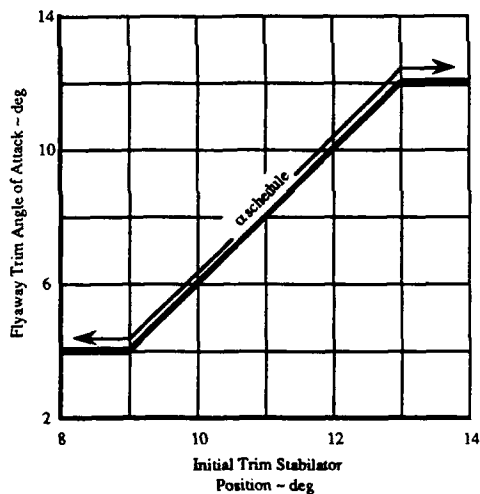


Figure 11
Trim Angle of Attack vs
Initial Stabilator Trim Position

Single Engine Airspeed Considerations

The reduced takeoff airspeeds attainable with ski jump operations are significantly below minimum controllability airspeeds in the event of a single engine failure. Simulation results allowed the test team to determine single engine airspeed boundaries and develop/employ aircrew procedures in event of an engine failure. Predicted F/A-18A minimum ski jump takeoff airspeeds were as much as 40 kt below dynamic single engine control airspeeds. Ski jump operations in this region mandated ejection should an engine failure occur at or shortly after ski jump ramp exit. F/A-18 safe ejection boundaries were established during simulation. With but one exception (32,800 lb with Max A/B on the 6 deg ramp), safe ejection airspeeds occurred at ramp exit airspeeds below the predicted two engine minimum takeoff airspeeds. For this one condition, testing was conducted only down to the safe ejection airspeed. For all tests, ejection was mandatory below 120 kt.

Build-up Test Operations

Prior to initial ski jump takeoffs, extensive build-up ground tests were performed. These included:

- Acceleration performance: Following thrust stand calibration, normal field takeoff tests were performed to equate ground roll and speed to airplane gross weight and thrust setting. The results provided ground roll requirements to provide the desired ramp speeds.
- Abort capability: The abort capability and pilot procedures were defined during simulated aborted takeoffs with the additional requirement of the pilot taxiing around the ski jump ramp (ramp simulated in position). During the takeoff ground roll at the desired groundspeed, the pilot retarded one engine to idle. After 1 sec, to simulate reaction time, the pilot retarded the other engine to idle and made aggressive lateral/directional inputs to the right on the runway. From these tests an abort location and speed could be determined. These data were provided to the pilot for each test event.
- Single engine-committed to takeoff: Once past the abort capable point, the airplane is committed to ramp takeoff. A single engine failure is the most critical from a standpoint of keeping the airplane within the 60 ft (18.3 m) width of the ski jump runway and ramp. As with the abort capability testing, engine failure during takeoff ground roll was simulated; however, the pilot task was to maintain runway centerline. The maximum lateral deviation recorded was 6 ft when using Max A/B. If an engine failure had occurred past the abort capable point, the airplane was controllable within the width of the runway and ramp.

Test Results

General

A total of 91 ski jump takeoffs were obtained with the F/A-18A operating from both the 6 and 9 deg ramps. Significant reductions in takeoff ground roll up to 66% with corresponding takeoff airspeed reductions of 64 kt were achieved. With the proper longitudinal trim set prior to the takeoff, a "hands off" takeoff during rotation and flyaway following ski jump ramp exit was possible. However, additional performance gains were obtained using the pilot pitch attitude capture technique described earlier.

Performance Gains

As the ski jump takeoff exit airspeed was decreased, the minimum rate of climb during the flyaway slowly decreased. The minimum rate of climb as a function of ramp exit airspeed for the 9 deg ramp is shown in figure 12. The minimum ski jump takeoff airspeed tested was dictated by zero rate of climb during takeoff. The minimum takeoff airspeeds achieved during tests are presented in table 3.

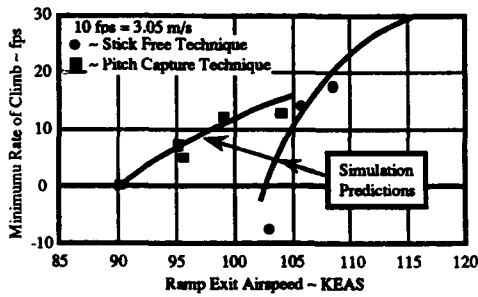


Figure 12
Minimum Rate of Climb during
9 Degree Ski Jump
F/A-18A Airplane
37,000 lb (16,783 kg) ~ Max A/B

Table 3
Ski Jump Minimum Takeoff Airspeeds

Thrust	Gross Weight lb (kg)	Minimum Takeoff Airspeed KEAS		Minimum Ground Roll ft (m)	
		6 deg ramp	9 deg ramp	6 deg ramp	9 deg ramp
MIL	32,800 (14,878)	102	98	1,075 (328)	850 (259)
	37,000 (16,783)	110	106	1,400 (427)	1,250 (381)
Max A/B	32,800 (14,878)	100	82	640 (195)	385 (117)
	37,000 (16,783)	99	90	700 (213)	575 (175)

NOTE: Minimum airspeed criteria: Proximity to zero rate of climb for all test points except 32,800 lb (14,878 kg) with Max A/B on 6 deg ramp which was limited by operation within safe ejection boundaries.

With the reduction in the ski jump takeoff airspeed was a corresponding reduction in the takeoff ground roll. F/A-18A ski jump reduction in takeoff distances for takeoff ground roll is presented in figure 13. The reduction in distance is related to the airplanes flight manual performance data for the test day conditions. The maximum reduction in takeoff ground roll relates to the

minimum takeoff airspeed, whether dictated by zero rate of climb or single engine safe ejection boundaries. For any takeoff where minimum ground roll is required and the takeoff trajectory is not critical, the lowest airspeed is necessary. Reductions in takeoff distances are summarized in table 4.

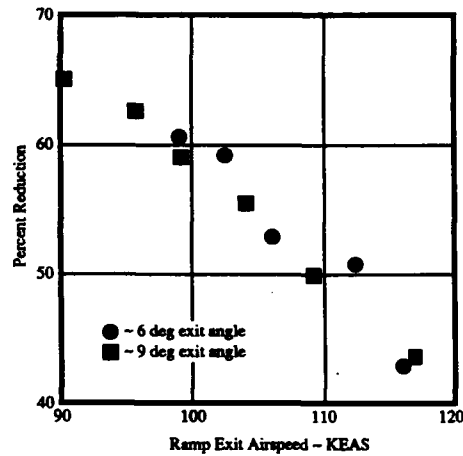


Figure 13
F/A-18A Reduction in Takeoff Distance
during Ski Jump Takeoff
37,000 lb (16,783 kg) ~ Max A/B

Table 4
Comparison of Reduction in Takeoff Distance
F/A-18A Ski Jump

Thrust	Gross Weight (lb)	% Reduction in Takeoff Ground Roll	
		6 Deg Ramp	9 Deg Ramp
MIL	32,800 (14,878)	51	51
	37,000 (16,783)	51	55
Max A/B	32,800 (14,878)	49	62
	37,000 (16,783)	61	66

Ground Handling and Flying Qualities

The ski jump takeoff commenced when the modified hold-back/release was activated. In both MIL and Max A/B thrust takeoffs, the initial acceleration was smooth with only a slight tendency towards pilot "head-jerk" at release. Although acceleration was more rapid in Max A/B, especially at the lower gross weight, the pilot had sufficient time to make pre-abort checks of engine performance. The airplane was not readily disturbed in its directional track by irregularities in the AM-2 matting; any small

deviations were easily controlled ± 2.5 ft (± 0.8 m) of runway centerline. No significant longitudinal airplane response (pitch oscillation, nosewheel bounce, etc.) was encountered after holdback release. Nosewheel lightening was experienced prior to going onto the ramp; however, it was not objectionable and did not affect directional control. The abort capability point within ± 50 ft (15.2 m) was recognized by the pilot visually and reinforced by scanning the INS display for the predetermined ground speed for abort. Once beyond the abort point and committed to takeoff, the pilot was able to monitor engine performance and maintain centerline tracking. An increase in normal acceleration of 2 to 4 g characterized the entry onto the ramp, with more onset rate perceived on the 6 deg ramp than the 9 deg ramp. Using the 6 deg ramp, a rapid and abrupt g-onset was encountered, feeling to the pilot as though the airplane had rolled over a small obstacle. Entry onto the 9 deg ramp was smooth with predictable g-onset building rapidly and without the "thump" associated with the 6 deg ramp. Duration of elevated g on the ramp was short, lasting 1/2 to 3/4 sec. The dynamic landing gear interface with the ramp allowed for predictable and satisfactory flying qualities upon ramp exit.

The inclination of the ramp established the initial pitch attitude off the ramp. Longitudinal trim settings, accurate to within ± 0.5 deg, produced comfortable, initial positive pitch rates of 6-8 deg/s.c. The trim setting was adjusted to obtain a peak pitch attitude of 18 ± 2 deg at less than the AOA limit of 17 deg. Pitch rates damped to zero or slightly positive during stick free takeoffs or were arrested to zero by pilot flight control input during pitch capture takeoffs. The airplane flew an arc with normal acceleration beginning at 0.25 g and increasing to 1 g over a 4 to 5 sec time frame. The 15 deg pitch capture was easily accomplished within ± 0.5 deg using longitudinal stick inputs of less than 2 inches (5 cm) and usually required only one stick input. No tendencies for longitudinal PIO were experienced during the pitch capture. The AOA peaked shortly after the peak pitch attitude and peaked a second time when the pilot captured 15 deg of pitch then smoothly decreased as the airplane accelerated.

Lateral control throughout the ski jump test program was excellent, even with a crosswind component. After departing the end of the runway, the airplane would yaw smoothly into the relative wind and little or no control input was required to maintain wings level attitude.

The F/A-18A digital flight control system eliminated any adverse flying qualities following takeoff from the ramp. The HUD information is sufficiently accurate for VMC and IFR conditions and would provide more than adequate information for night operations. The accurate and repeatable longitudinal trim system enhanced predictability for the ski jump takeoffs. All these factors made the F/A-18A ski jump takeoff, stick free or pilot-in-the-loop, easier than a field takeoff.

Structural Loads

Significant structural loads are imposed on an airplane during ski jump ramp transit. The stringent structural design requirements of US Navy carrier based airplanes provided the necessary strength for ski jump operations. The principle area of concern was landing gear loads. The desire to conduct initial ski jump takeoffs close to normal field takeoff airspeeds posed a dilemma in that the maximum loads were incurred during the first ski jump takeoffs. In general, main gear loads showed good agreement with simulation predictions; however, higher nose gear loads were obtained. A significant random variation in nose gear loads was experienced due to nose gear dynamics encountered prior to the start of the ramp. These nose gear dynamics were

attributable to the unloading of the nose gear during the acceleration run and the uneven surface of the AM-2 mating runway. Most notable to the pilot during ramp transit is the incremental normal acceleration. Peak incremental accelerations measured at the airplane CG are shown in figure 14. Accelerations experienced by the pilot were higher.

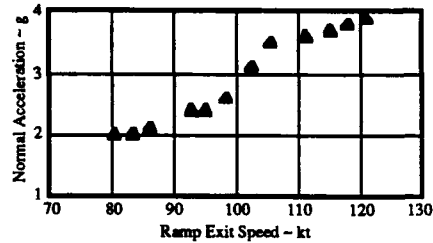


Figure 14
Maximum Normal Acceleration
During Ramp Transit
9 deg Exit Angle

A circular radius of curvature ramp, as tested, is not the optimum curvature profile for a ski jump ramp. Figure 15 depicts F/A-18A nose and main landing gear loads along the curvature of the ramp. High nose gear loads were encountered only during a small portion of the ramp. Ideally, landing gear loading should be equally distributed throughout ramp transit. This would permit attaining the desired ramp exit angle, ramp angle being the dominant factor in performance gains, using a minimum ramp size and still keeping the loads within limits. Simulation is the perfect tool to evaluate different ski jump ramp profiles to optimize nose and main landing gear loads.

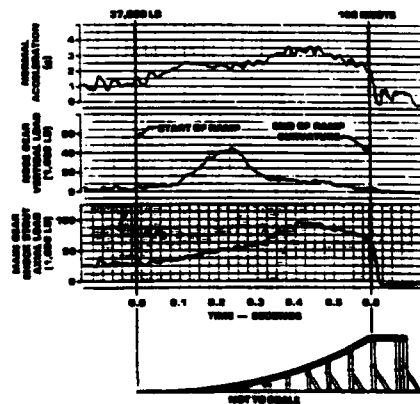


Figure 15
F/A-18A Nose and Main Landing Gear
Loading During Ramp Transit

Summary of CTOL Airplane Ski Jump Testing

Ski jump takeoff operations with current conventional fixed wing airplanes are possible. The significant performance gains, as exemplified by a 66% reduction in takeoff ground roll clearly demonstrates the potential of the ski jump concept. From a ground handling and flying qualities standpoint, a ski jump takeoff is an easier maneuver than a normal field takeoff. Longitudinal trim can be set to permit a stick free takeoff; however, additional performance gains were realized by the pilot using a pitch capture technique. Structural loads during ramp transit were well within the design limits of the test airplane.

CATAPULT/RAMP ASSISTED TAKEOFF

Introduction

The beneficial use of ramp assisted (Ski Jump) takeoff has been proven operationally by the British Navy, US Marine Corps and, most recently, by the Spanish Navy for AV-8B Harrier V/STOL aircraft. The US Navy test program described earlier in this paper demonstrated the feasibility of using Ski Jump to greatly reduce land-based takeoff distance requirements for CTOL aircraft as well. The analytical tools developed and validated during the US Navy CTOL program have been used to investigate potential benefits which might be derived from the use of Ski Jump for shipboard CTOL aircraft launch operations. A cross-section of operational US Navy carrier-based aircraft (F/A-18A, E-2C, A-6E, EA-6B, S-3A, F-14A) have been analyzed in conjunction with a modified mini-ramp geometry and steam catapult combination (Catapult/Ramp Assisted Takeoff (CRAT)). Aircraft performance, flying qualities, structural dynamics and piloting requirements were considered in determining possible required WOD reduction or allowable aircraft takeoff gross weight increase. Analytical results are presented which show potential reduction in WOD of from 5 to 35 kt for operational aircraft gross weights while keeping (1) maximum landing gear loads well below design limits and (2) minimum endspeeds above minimum aircraft control speed. A flight test program is planned to validate these results. The potential impact on aircraft carrier operations and possible operational problem areas are also discussed.

CRAT Concept and Ground Rules

The ski jump concept uses a ramp to rotate the aircraft flight path from horizontal to a positive climb angle at forward speeds less than those which are normally required to rotate the aircraft aerodynamically. The "early" rotation and lift-off provides an initial ROC and altitude margin which allows the aircraft to accelerate to flight speed while in a partially ballistic trajectory. A reduction in takeoff distance is achieved primarily as a result of lift-off speeds which may be considerably less than the stall speed of the aircraft.

CRAT uses the same concept as CTOL Ski Jump but replaces the free ground roll acceleration with a steam catapult assisted acceleration and the large ramp is replaced with a much smaller ramp due to deck space limitations. The lift-off speed reduction is applied to a reduction in catapult endspeed requirement for launch. In this case, takeoff distance is not reduced as it was in the previous CTOL Ski Jump effort but benefit is derived from:

- 1) Reduced WOD required for launch;
- 2) Increased takeoff gross weight at the conventionally required endspeed;

- (3) Some combination of 1) and 2).

For ease of analysis and initial flight test validation, the geometry of the "fixed" portion of the ramp used in the previous CTOL Ski Jump test program was used for analytical evaluation and will be used in flight test. The geometry is presented in figure 16 and represents the first 42.4 ft (12.9 m) of the ramp shown in figure 10. It has a reference radius of curvature of 1,000 ft (305 m), a departure angle of approximately 2.1 degrees and a maximum height above the first deck of 13.875 in (35 cm).

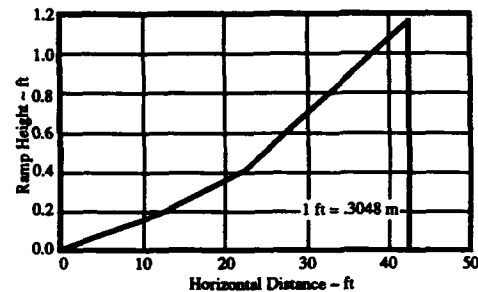


Figure 16
Mini-Ramp [42 ft (12.8 m)] Geometry

During a CRAT launch, the aircraft is assumed to leave the catapult (tow bar release) and immediately transition onto the ramp. Initial aircraft attitude, velocity, landing gear stroke, etc. are determined by the catapult stroke dynamics. Any stored energy in the landing gear due to strut compression during the catapult stroke will be released while the aircraft is on the ramp and resulting rotation is additive to that induced by the ramp. For the following analysis, each aircraft was assumed to enter onto the ramp with nominal end-of-catapult landing gear compression and aircraft pitch attitude (see table 5). Catapult endspeed was parametrically varied to evaluate performance benefits.

Table 5
Nominal Aircraft End-of-Catapult Conditions

Aircraft	Landing Gear Compression % Compressed		Pitch Attitude deg
	Nose	Main	
F/A-18A	80.7	75.0	-0.18
E-2C	0.0	83.5	1.35
A-6E	100.0	95.7	2.44
EA-6B	77.5	93.5	5.37
S-3A	96.0	84.5	1.10
F-14A	97.2	87.2	-2.13

"Minimum" Criteria Definition

The minimum launch airspeed for conventional aircraft catapult launch within the US Navy is defined as the minimum equivalent airspeed at the end of the catapult stroke for which the aircraft can safely fly away. Specifically, the minimum launch speed is set by a combination of related criteria which are described in reference 5 and are summarized here. The minimum launch airspeed is the highest of the following:

1) **Stall Speed** - The stall speed of the aircraft in the takeoff configuration or the speed at which stall warning first occurs if the warning does not significantly intensify as stall is approached.

2) **Minimum Satisfactory Flying Qualities Speed** - The speed below which the high AOA flying qualities of the configuration (e.g., damping, control response, etc.) become unsatisfactory.

3) **Minimum Level Acceleration Speed** - The speed at which sufficient thrust excess is available to provide at least 1 to 1.5 kt/sec of longitudinal acceleration.

4) **Minimum Engine Inoperative Speed** - The minimum airspeed for which there is sufficient lateral/directional control to counter an engine failure immediately following the catapult power stroke or for which single engine maximum rate of climb is attainable.

5) **Minimum Rotation/Sink-off-the-Bow Speed** - The speed below which aircraft pitch rotation is not sufficiently rapid or dynamic pressure is not great enough to provide enough lift (vertical acceleration) to arrest sink and establish level or climbing flight within some maximum acceptable amount of altitude loss; past experience indicates that this acceptable sink-off-the-bow is 15 to 20 ft (4.6 to 6.1 m).

The minimum conventional catapult end airspeed is typically defined by a combination of more than one of the preceding criteria over the takeoff gross weight range of a given aircraft. The **operational** minimum catapult end airspeed is set 15 kts higher than the previously defined minimum to allow for the negative effect of atmospheric disturbances, deck motion and non-optimum pilot technique, and to diminish (if not entirely remove) the probability of any sink-off-the-bow during normal launches.

Current practice for shipboard (AV-8A/B) ski jump operations is to define minimum launch speed such that the rate of climb during the flyaway does not become negative and available longitudinal acceleration does not become less than 1.5 kt/sec.

Additionally, the obvious criterion that flying qualities must remain satisfactory down to the launch speed is also enforced. These criteria (zero minimum rate of climb, 1.5 kt/sec minimum acceleration and satisfactory flying qualities) were also used successfully to safely establish the minimum ramp endspeed for the CTOL Ski Jump program described earlier in this paper.

Criteria for minimum endspeed for CRAT launches are not so clearly defined. Consider the possible flyaway trajectories of figure 17. When a ramp of any inclination is used to impart noseup rotation and rate of climb to a launching aircraft, the flyaway trajectory may be categorized into one of three classes. At higher speeds, comparable to conventional (flat deck) launch endspeeds, the trajectory exhibits positive rate of climb throughout (see trajectory 1 on the figure). As endspeed is decreased, the minimum rate of climb during the flyaway decreases until trajectory 2 is achieved with the rate of climb decreasing to zero but never becoming negative. This is equivalent to the minimum definition used for the previous CTOL programs. Finally, as endspeed is further decreased, the minimum rate of climb becomes increasingly negative and there is some minimum altitude (or maximum sink) achieved before rate of climb begins to increase (trajectory 3).

The likely candidate criteria for setting minimum endspeed are either 1) zero minimum rate of climb or 2) maximum allowable altitude loss. Zero minimum rate of climb has been proven for existing ski jump operations (both V/STOL and CTOL) and has the added benefit of always providing the pilot with a reassuring positive rate of climb. Maximum allowable altitude loss, on the other hand, is most like the current criteria for setting minimum endspeed for conventional catapult launch. Piloted flight simulation and perhaps even flight test is required to adequately choose one criterion or some compromise of the two (e.g., maximum rate of sink). Of course, conventional catapult launch criteria 2), 3), and 4) from above must still be satisfied. The analytical results which follow include potential performance improvements for both zero minimum rate of climb and maximum allowable altitude loss trajectories.

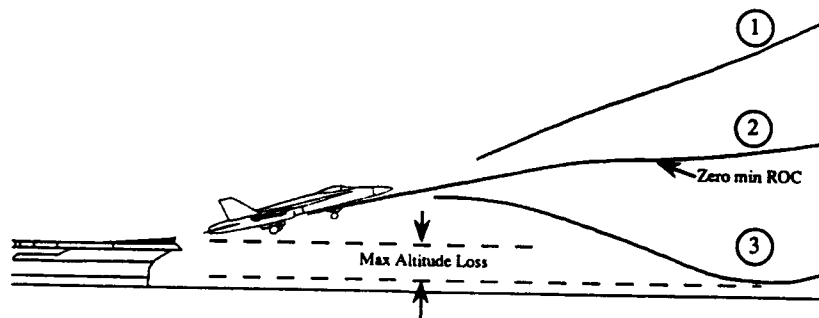


Figure 17
Possible CRAT Flyaway Trajectories

Analytical Results

The three degree of freedom (longitudinal, vertical and pitch dynamics) digital simulation model which was developed and validated during the CTOL Ski Jump program was used to analyze CRAT trajectories for a representative group of operational Navy aircraft. Table 6 list the aircraft configurations which were analyzed, including gross weights, thrust levels and flap settings. The models for each aircraft included nonlinear aerodynamic and thrust characteristics, nonlinear landing gear strut load and damping characteristics, and complete control system dynamics (see reference 6).

The analysis proceeded as follows. First, a conventional flat deck launch was simulated for each configuration at the minimum catapult endspeed and maximum altitude loss between 10 and 20 ft (3.1 and 6.1 m) was noted. These trajectories were used as a reference for comparison with the predicted CRAT launches. The ramp geometry of figure 16 was then simulated at the end of the catapult and the launch trajectories were recomputed for successively decreasing catapult endspeeds starting with the flat deck minimum and decreasing in 2-3 kt increments. Minimum rate of climb and altitude at zero rate of climb were recorded until the maximum altitude loss equalled or exceeded that for the flat deck launch. In all cases, nominal end of catapult conditions (landing gear strut compression, aircraft pitch attitude and CG height above deck) were assumed. Typical results are shown in figure 18 for the 46,000 lb (20,866 kg) F/A-18A with Max A/B Thrust. In this case, the flat deck minimum endspeed is 149 kt and the altitude loss at this speed is approximately 16 ft (4.9 m). With the ramp simulated, 16 feet of altitude loss occurs at an end speed of 129 kt providing a reduction in required catapult end airspeed of 20 kt. If the minimum were to be defined by zero minimum rate of climb instead of altitude loss, the minimum endspeed would be 137 kt providing a 12 kt reduction. Absolute minimum end airspeeds for all of the simulated configurations for flat deck launches with 15 to 20 ft (4.6 to 6.1 m) of sink and CRAT launches with comparable sink and zero minimum rate of climb are tabulated in table 7. Endspped reduction potential for each of the minimum criteria (sink or zero rate of climb) is compared in figure 19. The results of table 7 and figure 19 indicate that minimum catapult end airspeed (and therefore required WOD) can be reduced by anywhere from 5.5 to 34.0 kt depending on the aircraft/configuration. If zero minimum rate of climb is used as a criterion, minimum endspped reduction is decreased by a third to a half in most cases.

Table 6
Nominal Aircraft Configurations

Aircraft	Gross Weight lb (kg)	Thrust Setting
F/A-18A	46,000 (20,866)	MIL
	46,000 (20,866)	Max A/B
	52,000 (23,587)	MIL
	52,000 (23,587)	Max A/B
E-2C	53,000 (24,041)	MIL ⁽¹⁾
	53,000 (24,041)	MIL ⁽²⁾
A-6E	46,000 (20,866)	MIL
	58,600 (26,581)	MIL ⁽³⁾
EA-6B	50,000 (22,680)	MIL
	58,600 (26,581)	MIL
S-3A	44,000 (19,958)	MIL
	52,500 (23,814)	MIL
F-14A	59,000 (26,762)	MIL
	59,000 (26,762)	Max A/B
	69,800 (31,661)	Max A/B

- Notes: 1. 10 degree flap setting
2. 20 degree flap setting
3. With loaded Multiple Bomb Racks

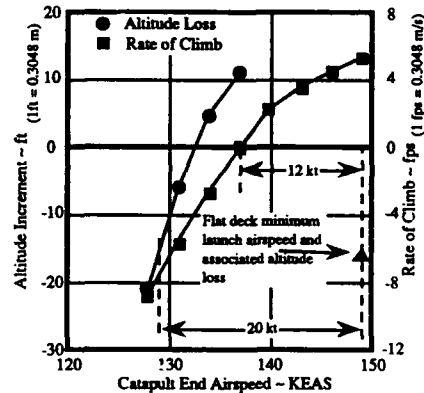


Figure 18
Altitude Loss and Minimum Rate of Climb vs. Endspped CRAT Launch of 46,000 lb (20,862 kg) F/A-18A with Max A/B

Table 7
CRAT Endspeed Summary

Aircraft	Configuration Wt - Thrust lb (kg)	Minimum Flat Deck Airspeed KEAS	Minimum Ramp Airspeed KEAS				Minimum Control Airspeed KEAS
			Altitude Loss		Zero Minimum ROC		
			Absolute KEAS	Δ kt	Absolute KEAS	Δ kt	
F/A-18A	46,000 (20,862) ~ MIL	152.0	138.5	-13.5	144.0	-8.0	120.0
	46,000 (20,862) ~ Max A/B	149.0	129.0	-20.0	137.0	-12.0	130.0
	52,000 (23,583) ~ MIL	164.0	150.5	-13.5	155.5	-8.5	120.0
	52,000 (23,583) ~ Max A/B	161.0	141.5	-19.5	150.0	-11.0	130.0
E-2C	53,000 (24,036) 10 deg flap	122.0	115.0	-7.0	122.0	0.0	97.0
	53,000 (24,036) 20 deg flap	108.0	102.5	-5.5	108.0	0.0	97.0
A-6E	46,000 (20,862)	115.0	105.5	-9.5	110.5	-4.5	* 105.0
	58,600 (26,576)	144.0	134.5	-9.5	138.5	-5.5	* 120.0
EA-6B	50,000 (22,676)	119.0	110.0	-9.0	114.0	-5.0	* 107.0
	58,600 (26,576)	129.0	119.0	-10.0	122.0	-7.0	* 120.0
S-3A	44,000 (19,955)	104.0	93.0	-11.0	102.0	-2.0	88.0
	52,500 (23,810)	115.0	106.0	-9.0	110.0	-5.0	88.0
F-14A	59,000 (26,757) ~ MIL	122.0	99.0	-23.0	111.0	-11.0	+ 88.0
	59,000 (26,757) ~ Max A/B	122.0	92.0	-30.0	105.0	-17.0	+ 103.0
	69,800 (31,655) ~ Max A/B	135.0	101.0	-34.0	112.0	-23.0	+ 103.0

* - 2 engine stall speed

- - Mid-Compression Bypass open, locked rotor, 10 deg sideslip

Aircraft Gross Weight and Configuration

F/A-18
46,000 lb (20,862 kg) ~ MIL
46,000 lb (20,862 kg) ~ Max A/B
52,000 lb (23,583 kg) ~ MIL
52,000 lb (23,583 kg) ~ Max A/B

E-2C
53,000 lb (24,036 kg) ~ 10 deg flaps
53,000 lb (24,036 kg) ~ 20 deg flaps

A-6E
46,000 lb (20,862 kg)
58,600 lb (26,576 kg)

EA-6B
50,000 lb (22,676 kg)
58,600 lb (26,576 kg)

S-3A
44,000 lb (19,955 kg)
52,500 lb (23,810 kg)

F-14A
59,000 lb (26,757 kg) ~ MIL
59,000 lb (26,757 kg) ~ Max A/B
69,800 lb (31,655 kg) ~ Max A/B

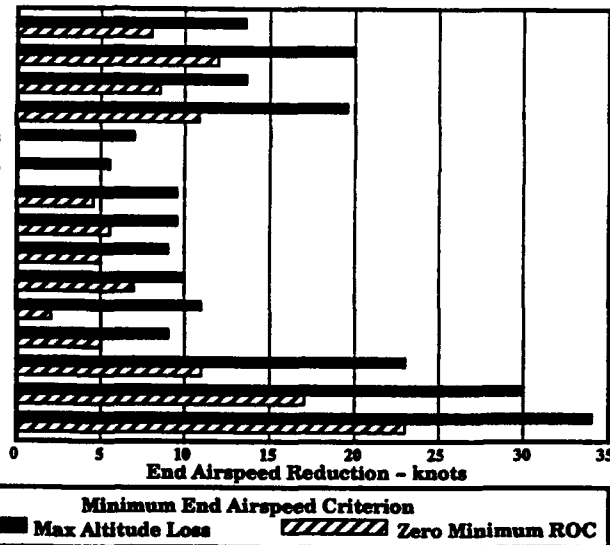


Figure 19
CRAT Endspeed Reduction Potential

The last column of table 7 indicates the minimum control speed for each of the configurations. This speed is determined from engine out control capability or aerodynamic stall speed of each configuration, whichever is most critical. The table shows that the minimum end airspeed with the ramp and using the altitude

loss criterion is significantly below the minimum control speed for only the F-14A Max A/B cases. Therefore, the wind over deck reduction potential for these case may be limited by minimum control speed restrictions. If the zero minimum rate of climb criterion is used, all of the predicted endspeeds are greater than the

corresponding minimum control speed. Table 8 summarizes the predicted maximum nose and main gear reaction loads and limit loads for each configuration for all speeds up to the current flat

deck minimum launch speeds. In all cases the predicted loads are well below the limit loads.

Table 8
CRAT Landing Gear Load Summary

Aircraft	Configuration Wt - Thrust lb (kg)	Landing Gear Reaction Load ~ 1,000 lb (kN)			
		Nose		Main	
		Maximum	Limit	Maximum	Limit
F/A-18A	46,000 (20,862) - MIL	53.2 (236.6)	80.0 (355.9)	48.3 (214.9)	77.0 (342.5)
	46,000 (20,862) - Max A/B	50.6 (225.1)	↓	46.4 (206.4)	↓
	52,000 (23,583) - MIL	66.7 (296.7)	↓	61.9 (275.3)	↓
	52,000 (23,583) - Max A/B	64.5 (286.9)	↓	59.6 (265.1)	↓
E-2C	53,000 (24,036) 10 deg flap	19.4 (86.3)	81.0 (360.3)	65.8 (292.7)	109.0 (484.9)
	53,000 (24,036) 20 deg flap	14.4 (64.1)	↓	46.4 (206.4)	↓
A-6E	46,000 (20,862)	41.9 (186.4)	64.0 (284.7)	38.4 (170.8)	88.0 (391.4)
	58,600 (26,576)	47.9 (213.1)	↓	54.3 (241.5)	↓
EA-6B	50,000 (22,676)	35.6 (158.4)	132.0 (587.12)	67.8 (301.6)	137.0 (609.4)
	58,600 (26,576)	41.7 (185.5)	↓	70.4 (313.2)	↓
S-3A	44,000 (19,955)	36.5 (162.4)	80.0 (355.9)	29.0 (129.0)	105.0 (467.1)
	52,500 (23,810)	38.3 (170.4)	↓	36.2 (161.0)	↓
F-14A	59,000 (26,757) - MIL	58.8 (261.6)	70.0 (311.4)	41.0 (182.4)	100.0 (444.8)
	59,000 (26,757) - Max A/B	58.8 (261.6)	↓	42.2 (187.7)	↓
	69,800 (31,655) - Max A/B	65.1 (289.6)	↓	52.5 (233.5)	↓

Operational Considerations

While the preceding simulation results indicate the strong potential for reducing WOD requirements for catapult launch from an aerodynamic performance viewpoint operational factors must still be considered. For example, is there sufficient usable space in front of existing catapult installations to accommodate a ramp of the required length? Should ramps be positioned in front of all catapults or just the bow catapults? If ramps are positioned in front of the waist catapults, what is the effect on bolter performance/characteristics and safety? Should operational launch speed be based on the minimum altitude criterion plus 15 kt excess, the zero minimum rate of climb criterion or some other criterion? These questions, as well as I'm sure others, must be answered before CRAT becomes an operational reality.

Plans

The current US Navy plan is to conduct pilot-in-the-loop simulation evaluation of F/A-18 shipboard CRAT performance and handling characteristics. This simulation would also investigate failure procedures (engine and other system failures) and piloting techniques prior to any flight test. Following successful simulation, a technology demonstration flight test program is planned using the existing 42 ft (12.8 m) mini ramp and the Naval Air Test Center TC-7 steam catapult installation. If the flight test successfully validates the CRAT concept, the simulation tools will be updated, if required, and CRAT compatibility with all US Navy carrier-based aircraft will be verified. Shipboard operational compatibility questions will be answered and, ultimately, a shipboard test program will be conducted.

Summary

In summary, non-real time simulation has indicated the potential to reduce WOD requirements for current US Navy carrier-based aircraft by as much as 35 kts using a combined catapult/ramp assisted launch. Maximum landing gear reaction loads remain well within acceptable limits and minimum airspeeds experienced are above the minimum aircraft control speeds. Based on the non-real time simulation, pilot-in-the-loop simulation followed by land-based demonstration flight test is planned to validate the concept. If the demonstration is successful, ramp shape, size, placement and construction will be optimized and the feasibility of carrier-based flight test will be investigated.

RELEASE

The conclusions concerning benefits of CRAT are the opinions of the authors and do not necessarily reflect those of the Naval Air Systems Command.

REFERENCES

1. Senn, C. P. and CDR J. A. Eastman, USN. "CONVENTIONAL TAKEOFF AND LANDING (CTOL) AIRPLANE SKI JUMP EVALUATION." Society of Flight Test Engineers 14th Annual Symposium Proceedings, 1983: Newport Beach, CA, August 15-19, 1983 pp. 3.5-1 to 3.5-10.
2. Eastman, CDR Jon A. USN, and C. Page Senn. "Conventional Takeoff and Landing (CTOL) Airplane Ski Jump Evaluation." Society of Experimental Test Pilots 27th Symposium Proceedings: Beverly Hills, CA, September 28 - October 1, 1983 pp. 269-288.

3. Senn, Carroll and LTCOL T. A. Wagner, USMC. "CONVENTIONAL TAKEOFF AND LANDING (CTOL) AIRPLANE SKI JUMP EVALUATION." Society of Flight Test Engineers 15th Annual Symposium Proceedings, 1984: St. Louis, MO, August 12-16, 1984 pp. 23-1 to 23-8.
4. Wagner, LTCOL Thomas A. USMC, and C. Page Senn. "F/A-18 Ski Jump Takeoff Evaluation." Society of Experimental Test Pilots Twenty-Eight Symposium Proceedings: Beverly Hills, CA, September 26-29, 1984 pp. 101-117.
5. Senn, C. P., "Flight Testing in the Aircraft Carrier Environment", Proceedings of the 16th Annual Society of Flight Test Engineering Symposium.
6. Clark, J. W., Jr. and Walters, M. M., "CTOL Ski Jump: Analysis, Simulation and Flight Test". Journal of Aircraft, Vol. 23, No. 5, pg. 382, May 1986.

HELICOPTER HANDLING: EXPERIENCE AND NEW DEVELOPMENTS

by

W.R.M. Reimering
RDM Technology
P O Box 913
3000 AX Rotterdam
The Netherlands

T. Craig
Mactaggart, Scott & Co., Ltd
Loanhead, Midlothian EH20 9SP
Scotland
United Kingdom

1. INTRODUCTION

Helicopter handling has developed in 25 years from a 'nice to have' extra to a virtual necessity in order to meet the present day mission requirements for operating helicopters from small ships. RDM (Rotterdam Dockyard) and MacTaggart Scott & Co. (Scotland) have been involved in developments from the early days of using helicopters on warships and present a survey of their experience and of new developments currently taking place.

The two companies provide the interface solutions demanded by the operators, bearing in mind the restrictions imposed by the airframe and ship's construction.

Whereas MTS concentrates on helicopter traversing systems, RDM is concerned with the landing grid and the design and construction of the decklock (sometimes referred to as the harpoon or talon). Much theoretical work has been carried out on ship characteristics which has given valuable input to the designers of the equipment, however, it must never be forgotten that, in the end, the sea and the air are the masters which require discipline and experience from the user.

2. GRIDS

The original grid was a series of bars mounted on the flight deck and between which the first generation decklock engaged. An example of this was used with the Alouette III. With the combined Anglo-French development of the Lynx helicopter, it was decided that a more refined system for securing the helicopter should be considered.

The decision resulted in the development of to-day's well-known landing grid (see photo 1) which is in operation with 23 Navies and Coast Guards

and installed on over 250 ships.

A major advantage of the grid landing system is that it can be used by different helicopters provided they are equipped with a decklock.

A typical grid has a diameter of 2.7 m and a height of 211 mm; it weighs approximately 1370 kg. The assembly consists of a top plate of a 28 mm thick special steel and in which a large number of holes are drilled at 120 degrees to each other. Each hole has a bell-mouth, such that nowhere is there a flat horizontal surface presented to the pointed beak of the decklock. The decklock is flexibly mounted and upon actuation the beak will be deflected by the bell-mouth and engaged with a hole. There are two beaks, one longer which enters a hole first with the shorter beak engaging in an adjacent hole. After the decklock is fully extended and the beaks have penetrated the grid, they grip the grid metal between the two engaged holes. The decklock can now be tensioned such that it pulls the helicopter against the flight deck. This increases the friction between the wheels and the deck to prevent sliding and at the same time provides security against toppling. The maximum pulling force on the decklock is therefore exerted on the 'bridge' between the two adjacent grid holes.

Careful selection was carried out to determine the optimum material for the top plate which had to combine substantial mechanical properties with high corrosion resistance.

RDM manufactures landing grids under an exclusive licence from DCN of Paris. With the advent of heavier ship-borne helicopters, which require higher decklock forces, both DCN and RDM carried out extensive calculations and physical testing to establish the maximum force

that could be exerted on the grid. The result of this analysis indicated a force of approximately 6.5 tonnes, which is sufficient for helicopters with an all-up-weight of approximately 10 tonnes or suitable for the Sea King, Super Puma and Sea Hawk range of helicopter.

In this upper range of pulling force some plastic deformation can take place especially if the decklock is not acting vertically, which could increase the possibility of stress corrosion.

RDM is currently investigating another design of beak for the decklock to permit higher pulling forces which will be discussed later.

With the 2.7 diameter grid being firmly established, DCN and RDM then considered other types of grids for different classes of vessel in order to make retrofitting easier.

One requirement, however, always remained and that was that the grids had to be capable of allowing cross-operation with all current decklock-fitted helicopters.

Out of this philosophy and discussions with customers and ship designers came a range of grids of lesser diameter (1.8 m) and height (100 mm) and of rectangular designs in order to simplify the integration of a grid landing system with different designs of ship. The 1.8 m grid weighs only 650 kg and is well suited for Coast Guard Cutters, Corvettes and Fast Patrol Boats. It can be mounted either on, or recessed flush with, the deck.

Summarising, the following points are emphasised:

1. It is a helicopter landing system which requires no crew on deck during landing or take off.
2. It holds the helicopter firmly on the deck and prevents sliding or toppling.
3. It provides a secure position for the helicopter to permit weapon's handling and from which traversing can be initiated.
4. The grid is light weight and of small volume in comparison to other systems, requires no ship board services and is of low cost.
5. Installation or retrofit of the grid is simple.
6. The maintenance requirements are minimal.
7. It is a proven system providing NATO Navies with a vital means of interoperability.
8. The decklock can be installed in a helicopter with a minimum weight penalty.

3. TRAVERSING AND WEAPON'S HANDLING

INTRODUCTION

Over the last three decades the use of helicopters on board warships has grown significantly and they now fulfill a wide variety of essential uses. In order to carry out its mission, a helicopter must be capable of operating in severe weather conditions. It is necessary therefore to be able to traverse the helicopter with security between the grid on the flight deck and the hangar, and vice-versa, with minimum hazard to the aircraft and personnel. In addition to landing and traversing the helicopter, a new requirement is to be able to re-arm and re-fuel the helicopter whilst on the grid in weather conditions as severe as for helicopter traversing. It can be appreciated that during a mission the helicopter might have to be re-fuelled and re-armed quickly in order that it can return to station with a minimum delay; hence the necessity of providing an effective weapon's handling system. This section of the paper deals with the factors involved in the design of an aircraft and weapon's handling system.

HISTORY

Approximately 30 years ago the Wasp Helicopter (5,500 lbs - 2.5 tonnes A.U.W.) started to operate from Royal Navy Frigates. It has a four wheel undercarriage and was moved manually between the Flight Deck and the hangar. It was capable therefore of being traversed in sea conditions of up to

Sea State 2. In order to enhance the operational capability, a three wire handling system (see photo 2) was introduced in 1962 and this allowed handling of the helicopter up to Sea State 3.

The Lynx (10,000 lbs - 4.5 tonnes A.U.W.) was introduced by the Royal Navy in the early 1970's. It was equipped with a decklock which could secure aircraft to the grid in up to Sea State 6. Since the bodywork of the Lynx could not withstand manual pushing forces (and bearing in mind its weight) it became mandatory to use a handling system. The capacity of the three winch system was uprated to take account of the heavier aircraft and with the inherent stability of the Lynx it was possible to handle the aircraft in up to Sea State 3/4. The three winch handling system gives good control over the aircraft when on the grid with each wire being displaced at approximately 120 degrees to each other. As the aircraft is pulled forward towards hangar the angle of athwartship's restraint offered by the two aft wires is reduced. It is this fact that limits the performance of the system at the hangar entrance where clearances are small. In order to improve the capability of the system, two additional restraining wires were added (see photo 3) each acting in a similar nature to a car seat belt, where the ratchet, when engaged, prevents unwanted athwartship's movement. The system is termed a five wire system and proved to be thoroughly effective in the South Atlantic in conditions of at least Sea State 5.

A wire handling system is appropriate for aircraft of up to 10,000 lbs weight (4.5 tonnes) and provides a simple, low cost and easily installed helicopter handling system. The aft wires can generally be attached to existing towing and tiedown points, with the hangar wire being attached to the manually controlled nose wheel steering arm. With the advent of larger helicopters, which are required to operate in Sea State 5 and above, it is necessary to

use a rail-guided handling system to provide the necessary security and two current examples will be described.

STATEMENT OF REQUIREMENTS

At this stage it is appropriate to review a typical statement of requirements for a combined aircraft and weapon's handling system. It is against this statement that the handling system must be designed and it should be emphasised that a collaboration in the initial stages between the helicopter user, the helicopter manufacturer and the ship designer is highly desirable in order that the handling designer can produce a correctly integrated system. In the past the handling system has usually been an after-thought with consequent compromise from an ideal solution. The aircraft manufacturer resists the inclusion of extra components and structure for a handling system with their associated weight penalty. In a similar way, the ship designer is unwilling to sacrifice space for the handling system with its attendant weight and structural penalties. Obviously both have to accommodate the needs of the handling system designer. A Statement of Requirements could cover the following points:

1. Grid landing system
2. Landing and traversing the aircraft in conditions up to Sea State 6
3. Wind velocity 50 knots
4. Ship course - any heading
5. Darkened ship
6. No men on deck for landing and traversing
7. Rotors running, re-arm and re-fuel on deck
8. Capability of handling other aircraft in reduced Sea States
9. Capable of integration into new and existing ships
10. Turnaround time.

In order to meet the above conditions it will be readily appreciated that the four interested parties must have a

close and sympathetic working relationship.

DESIGN PROCEDURE

The many advantages of using a grid landing system have been given, in particular the large area of grid which the pilot has as a target. This, however, requires that the handling system must pick up the helicopter from any point that the decklock may have been engaged in the grid. For small helicopters the wire system is ideal due to its flexibility; the wires are simply attached to strong points on the aircraft. Thereafter the wires are tensioned, the decklock and aircraft brakes released and the helicopter pulled into the hangar and guided accurately using the steering arm. With a rail guided handling system the helicopter, by definition, must be traversed along a predetermined path. Preliminary operations are required therefore to align the aircraft from any point on the grid to the rail system. These operations are termed 'centring' and consist of three movements: rotation, about the decklock or a point on the centre line of the main wheels; translation, a linear movement of the aircraft forward; and rotation, to align the helicopter to the rail system. Thereafter the helicopter can be traversed into the hangar.

LOADING

A thorough understanding of the loads present in handling the helicopter is necessary, not simply to establish component material sizes but to give guidance for the conceptual design. This might appear to be an obvious statement but designs can be stated where a lack of appreciation of the loading involved has led to badly designed equipment. A prerequisite of the handling system is to accommodate the reactive loads, provide security for the helicopter and present minimum loading to the airframe. It should be remembered that in general it is the helicopter that reacts against the

handling system and not the system loading the aircraft.

The Loads to be considered are:

1. Traction forces
2. Steering forces
3. Ship motion induced forces
 - 3.1. Athwartships sliding
 - 3.2. Rotary sliding (weather cocking)
 - 3.3. Vertical lifting (toppling)
 - 3.4. Centrifugal loading
 - 3.4.1. Athwartships sliding
 - 3.4.2. Vertical lifting (toppling)
4. Windforces

In order to determine the loading forces it is necessary to take account of the sea conditions and the response of the ship to them. Table 1 shows the sea state parameters in the North Atlantic and it is notable that in winter Sea State 5 and above is prevalent for 50 per cent of the time. This highlights the necessity of the ship having a helicopter handling system particularly when it is engaged in ASW. The maximum sea state where helicopter handling can safely be carried out by hand - perhaps 16 pairs of hands! - is Sea State 2/3. Table 2 shows ship motion for a typical Frigate using RMS values. In order to establish the actual motion, the RMS value is multiplied by a factor. For instance, if we are designing for the occurrence of a one in a million wave, then we might expect the magnitude to be 5.25 times the RMS value. As an example, in Sea State 6 with a head sea there is a one in the million chance that the vertical acceleration will exceed 7.875 m/s^2 (i.e. 1.5×5.25) or 0.8 g. The MacTaggart Scott ship motion programme treats the ship motion as being simple harmonic. This implies that maximum lateral acceleration occurs at maximum roll amplitude and that the maximum vertical up acceleration occurs at the maximum stern down pitch. Thus toppling effects due to roll are maximised, as is the aircraft weight, for towing up a gradient.

It is further assumed that roll and pitch are in phase in order that all the worst cases of body forces on the aircraft act simultaneously.

The MacTaggart Scott helicopter handling programme has been continuously developed since 1982 primarily for wire handling systems. The core algorithm to compute the statically indeterminate forces in wire ropes was written by The Heriot Watt University, Edinburgh.

The programme is designed to take given angular displacements and accelerations of the deck in global axes and refer these to the deck axes. The aircraft is also in the deck axes in the plane of the deck and is also given a yaw axis. The body forces on the aircraft can thus be calculated. The programme moves the aircraft iteratively against the wire ropes. The forces due to the incremental stretching of the wires is compared to the body forces on the aircraft. When a force balance is achieved, to within a preset accuracy, its iteration stops and a solution has been made.

The force balance also includes rolling resistance, deck friction, lateral tyre stiffness, wind loading, wheel reactions, minimum wire loads and constant tension wire loads. Oleo stiffness is not modelled.

The programme has the facility to print out both the global transformation and the force balance in ship and aircraft axes for manual verification.

Returning to the components of handling loads:

TRACTION FORCES

The net tractive force (hauling force less back-tension force) to cause the helicopter to move in a straight line rolling on its wheels is a function of the rolling resistance and the instantaneous weight plus wind resistance. The variation in tractive force in a Sea State 6 (and a one in a million chance of exceeding this value) is substantial.

At one point the stern is low (say, in a head sea) and accelerating vertically upwards with 0.8 g. The tractive force

to be applied therefore is equivalent to pulling a helicopter of 80% greater weight and up a sloping flight deck; in contrast when the stern is high, the aircraft will only weigh 20% of its normal weight and will require to be restrained from rolling down the flight deck.

STEERING FORCES

Ideally a straight rail should be used to guide the handling system between the flight deck and the hangar. This minimises the forces required to keep the helicopter to its predetermined path. Where a curved path is unavoidable a preferred solution is to provide a separate steering path or track for the single wheel, be it a nose wheel or a tail wheel, with the main wheels having pure rolling motion without side-slip or tyre scrub. MacTaggart Scott has developed software to describe the tractrix curve of the main wheels with either straight line or circular guidance for the third wheel. Of fundamental importance to a rail guided helicopter handling system is the provision of two points of attachment to the rail. If a single point of attachment only is provided it is possible for the aircraft to slew about this point due to ship motion and/or wind forces. The centre of gravity is seldom vertically coincident with the centre of pressure and a patch of low friction deck surface (due to ice or oil spillage for instance) could allow the aircraft to rotate out of control. Additionally, whereas it is possible to tow a nose wheel helicopter into a hangar from a single rail attachment point it is not possible to push the aircraft out from the hangar and guarantee that it will follow a straight path; ship motion and deck camber will readily deflect the aircraft from the intended path.

ATHWARTSHIPS LOADING

In addition to the above forces, the handling system must constrain the athwartships forces generated by the aircraft primarily due to roll and wind

reaction. Residual athwartships sliding forces are resisted by the handling system after assuming a coefficient of friction between the tyres and the deck and taking into account a simplified resistance due to tyre deflection.

ROTARY SLIDING

As the aircraft passes through the hangar door area the effect of wind assumes greater importance since unbalanced forces can be required to be restrained.

VERTICAL LIFTING

Once the athwartship's forces have been accommodated and further tendency to movement has been stopped by the handling system the aspect of aircraft toppling must be considered. Toppling is defined as the rotation of the aircraft about two wheels when the third wheel tends to become clear of the deck. To prevent this action vertical restraint must be applied to the helicopter.

CENTRIFUGAL LOADING

A final significant restraint must be provided to counteract the effects of centrifugal force due to the action of a sharp turn by the ship. The condition can be exacerbated when superimposed on the worst conditions of roll and associated vertical and horizontal accelerations and additional vertical and horizontal restraining of the aircraft will be required.

When the Statement of Requirements calls for 'no men on deck' to carry out aircraft landing and traversing it will readily be understood that in conditions of Sea State 6 the safety of men on the flight deck would be severely jeopardised.

EXAMPLES

Two examples of a rail-guided helicopter handling system are now described. In the first case the aircraft is in the 20,000 lbs (9 tonnes) weight category and is fitted with a freely casting tail wheel. The handling system

and grid are capable of being fitted on the deck of an existing ship. In contrast, the second example will describe the handling system for a 33,000 lbs (15 tonnes) helicopter with a non-casting nose wheel. This system has been designed to have a maximum height of 100 mm and is capable of being installed on an existing deck or to be built into a deck under construction.

Example 1: it is assumed that the aircraft has landed within an area equivalent to a landing grid; it is possible that one of the decklocks described previously could be installed and it is further assumed that the aircraft cannot rotate about the decklock. The handling system must be capable therefore of being attached to the aircraft after it has landed within the above defined area.

Photo 4 shows the aircraft landed with the handling system frame being brought out to the aircraft by the action of the outhaul winch and with the two inhaul winches providing back tension. Photo 5 shows the handling frame attached to the helicopter. The frame is moved manually from the rail-guided shuttle assembly. At this point the aircraft is secured to the landing grid through its decklock and additionally it is secured to the handling frame. The sequence of centring is now carried out and, as described before, consists of three steps; rotation, translation and rotation. The action of centring brings the aircraft from its landed position to the rail where it is rigidly guided, through the handling frame, at two points.

Photo 6 shows the rotation of the aircraft about an imaginary point between the helicopters main wheels. Rotation is carried out by using one of the two in-haul winches with the other on light back tension. The reaction of this load is taken by the outhaul winch brake and with the aft end of the handling frame assembly being prevented from horizontal movement via a reaction bar, the probe end of which is inserted in one of the grid holes.

Photo 7 shows the translation step where the aircraft and handling frame are pulled in a straight line towards the aft end of the shuttle by an inhaul winch. The movement is halted when the handling frame automatically engages with the aft end of the shuttle. The final step in centring is rotating the aircraft to align it with the rail. Rotation is caused by tensioning the second inhaul winch whilst maintaining tension on the other.

Photo 8 shows the aircraft centred and attached via the handling frame to the rail at two points. The above operation has maintained the security of the helicopter at all times after the handling frame has been attached and until the helicopter is housed in the hanger.

The second example illustrates the combined aircraft and weapon's handling system for the EH 101 or Merlin helicopter. The aircraft is very large and to appreciate the size one can compare the aircraft to four London double decker buses. The Statement of Requirements is substantially that which was described before, notably to land and traverse the helicopter with no men on deck. The sequence of handling the helicopter follows the same pattern as described in the first example, that is, a centring operation has to be carried out to align the aircraft with the rails.

The handling system has to be capable of being fitted to an existing deck, with no deck penetration and within a height of 100 mm.

Photo 9 shows the aircraft having landed with the decklock engaged. The first step, rotation, is carried out by the pilot who rotates the aircraft about the decklock in order to bring the nose wheel on to a small rail-guided platform or palm.

Photo 10 shows the nose wheel on the palm with the wheels pointing ahead, thus restraining the wheel from horizontal movement; no vertical restraint is provided and the pilot can take off if necessary by releasing the decklock.

Photo 11 illustrates the next step - translation - when the decklock is released and the aircraft pulled forward by the nose wheel to a predetermined spot at which point the main wheels are on a turntable. This operation is carried out during a quiescent phase and only takes a few seconds. At any time the pilot can re-engage the decklock and restore full security.

Photo 12 shows the aircraft with the main wheels on the turntable and ready to carry out the third phase of centring, namely rotation. A complete turntable is not needed and therefore two sections or arcuate plates are provided in order to rotate the aircraft about its nose wheel.

Photo 13 shows the aircraft completely aligned with the rails and with the decklock engaged. The aircraft is secure in this position and is ready for handling into the hangar or for re-arming or re-fuelling on the grid. The photograph also shows the main wheel shuttle engaged with the axle extension.

The rotors can be shut down and power folded after which the aircraft is ready to be traversed into the hangar by towing on the nose wheel and with restraint on the main wheel axle extensions.

4. DECKLOCKS

The current decklock designs from various manufacturers have been in operational service with excellent results.

RDM is developing improved decklock designs to provide extra potential:

DECKLOCK FOR SIKORSKY SH-60
a system to provide Sikorsky SH-60 'Seahawk' helicopters with a decklock whilst retaining their RAST capability. A number of Navies, including the U.S. Navy, have ships in service or under construction which do not or cannot incorporate the RAST system; alternatively they have the SH-60B in service or are considering its use. RDM therefore

first developed an insert to be lifted from the flight deck by the RAST messenger cable into the RAST probe on the Sea Hawk, thus giving a limited decklock capability as well. This design can be offered with some modification to the RAST probe. The weight penalty of this design is almost zero as the insert remains on the flight deck when the helicopter takes off. Traversing with this solution will not be possible.

RDM is now concentrating design efforts on a modified RAST probe giving the SH-60B 'Seahawk' both RAST and decklock capability. This will require more extensive modification. However, the interoperability between the two landing systems provides a distinct advantage. Additionally this solution solves a problem for the first series of DDG-51 Class Destroyers. It might also be a good proposal for some of the ships of our hosts in the Royal Spanish Navy in order to provide interoperability with other European Navies.

TULIP BEAK

a new beak called the 'Tulip' is now in the prototype stage.

Why a new beak? (see photo 14)

The very high pulling forces exerted by the decklock on the bridge between adjacent holes of the grid by large helicopters like the EH-101 was referred to above.

This has resulted in the choice of a very exotic, and hence very expensive, material for the top plate of the grid on the new Type 23 Frigate of the Royal Navy. The material, although having even better mechanical properties compared to the normal topplate material, has lower corrosion resistance.

An alternative to this solution is a new beak design whereby the decklock force exerted on the grid is transferred over a much larger contact area by expanding in a single hole. In this way no exotic materials for the topplate are required. The Tulip beak is now in the prototype stage and will be tested in the second half of 1991.

After it has been factory tested the beak will be fitted to a Lynx decklock and tested on board a ship.

The Tulip beak will retain the capability of rotation of the helicopter around the decklock (provided the decklock is located on a point of rotation of the airframe which is on the axis of the main wheels).

The value of this is, of course, the possibility of rotating the aircraft into the wind before take-off, as well as for lining up with the traversing system.

NEW DECKLOCK DESIGN

a new design of decklock for helicopters suitable for amongst others the Naval version of the NH-90, the SH-60 (Seahawk) and the SH-2F (Seasprite), minimises the weight penalty and incorporates the new Tulip beak. It will be offered for helicopters like the Naval NH-90 and the SH-2F (G) Kaman Seasprite. It can also be offered for the SH-60B in place of the RAST probe in which case the aircraft would lose the ability of operating with ships fitted with the RAST system. However, the decklock could be considered as an additional component and if fitted on the axis of the main wheels the aircraft would be able to make maximum use of both the grid landing system and the RAST system.

5. WEAPON HANDLING

With the increased capability of helicopters to act offensively a new requirement arises in the necessity to be able to re-arm the aircraft while secured to the grid and perhaps with rotors running. Incidents have been reported where deckhands handling or re-arming the aircraft, plus weapons, have been lost overboard in heavy weather. The difficulty of handling a weapon in these conditions can be fully appreciated.

The requirement is therefore to handle weapons with security and to place them accurately under the aircraft weapon pylons.

After landing, the aircraft will be centred as described above and the helicopter will then be accurately located at a predetermined spot. The main wheel shuttles are used as tractors to pull the weapon handler out to the aircraft. The weapon handler is rigidly guided by the rail. By inserting a suitable length of link between the shuttle and the handler, the weapon can be placed precisely under the pylon, due to the shuttle being stopped by the main wheel axle extension.

6. FUTURE

It is considered that a future requirement will be to land and traverse small unmmanned aircraft. This will introduce a new series of characteristics and associated challenges to the designer. It is anticipated that the aircraft will be of light weight and in order to provide reasonable endurance, the weight of aircraft mounted equipment for landing and traversing will have to be kept to the absolute minimum. For manned aircraft it is anticipated that weapon loading and re-fuelling will

become automated with no men on deck. In addition this will reduce manning requirements and enhance safety.

7. SUMMARY

This paper has covered the history and developments that the two companies, RDM and MTS, have been involved with for helicopter landing and traversing on board Warships. The use of the helicopter on board ship has evolved from simple beginnings to being a vital component of the ship's offence and defence capabilities. In conclusion we would like to reiterate the emphasis that has been placed on involving all the interested parties at the outset of design; the Navy, the helicopter manufacturer, the ship designer and the manufacturers of the landing and handling system. The landing and handling system is an important interface between the aircraft and the ship which must not be considered as an extra. It is an essential component which allows the helicopter to maximise its capability.

SEA STATE PARAMETERS IN NORTH ATLANTIC

OCCURENCE SEASTATE	SIGNIFICANT WAVE HEIGHT	PROBABILITY OF THIS SEASTATE OR WORSE	
		ANNUAL	WINTER
7	6-9 m	2%	15%
6	4-6 m	6%	30%
5	2.5-4 m	21%	50%
4	1.25-2.5 m	63%	
3	0.5-1.25 m	92%	
PERSISTENCE OF SEASTATE 6		PROBABILITY OF PERSISTING FOR LONGER THAN THIS PERIOD	
10 hours		55%	
30 hours		25%	
45 hours		15%	
70 hours		5%	

TABLE 1TYPICAL SHIP MOTION FOR A FRIGATE

SEA STATE	RELATIVE SEA DIRECTION	RMS SHIP MOTION PARAMETERS				FACTOR FOR PROBABILITY OF BEING EXCEEDED PER CYCLE			
		ROLL DGRS	PITCH DGRS	HORIZ ACCEL M/SEC-2	VERT ACCEL M/SEC-2	10E-3	10E-4	10E-5	10E-6
3	HEAD	0.35	0.3	0.05	0.30	3.7	4.3	4.8	5.25
	BEAM/QTR	0.75	0.2	0.10	0.15				
4	HEAD	0.75	0.6	0.10	0.60				
	BEAM/QTR	1.5	0.5	0.25	0.25				
5	HEAD	1.25	1.0	0.20	1.00				
	BEAM/QTR	2.5	0.8	0.40	0.40				
6	HEAD	2.0	1.6	0.20	1.60				
	BEAM/QTR	4.0	1.3	0.60	0.60				

TABLE 2

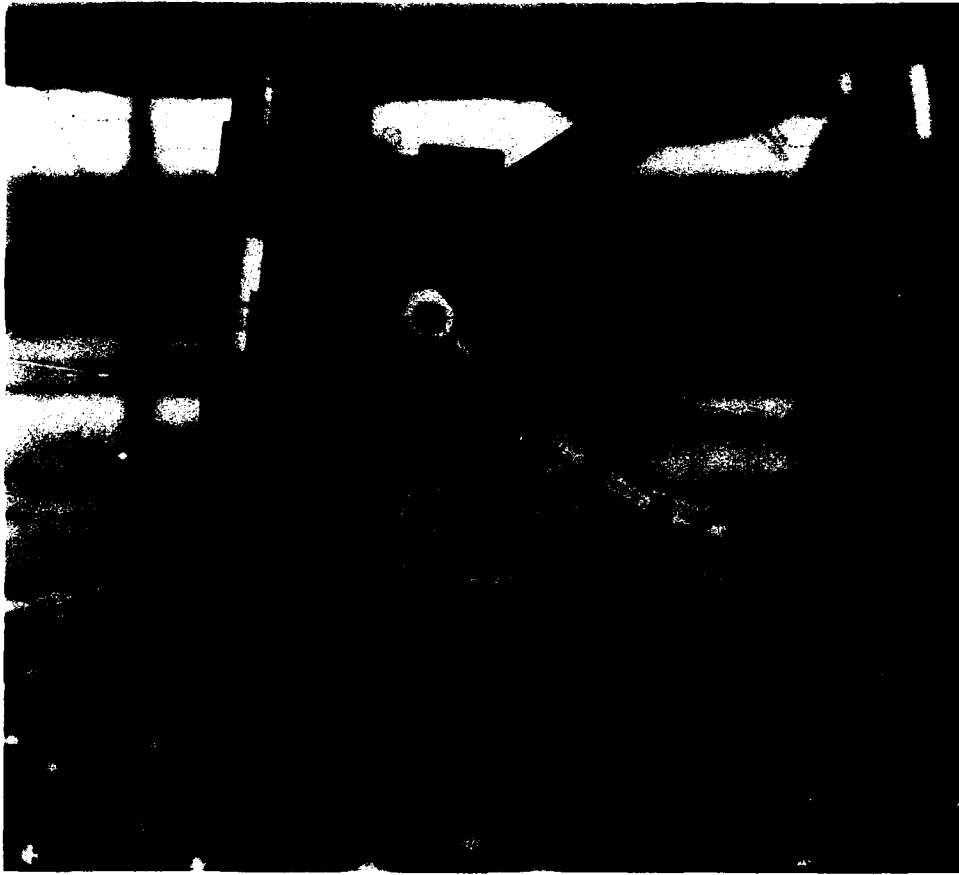
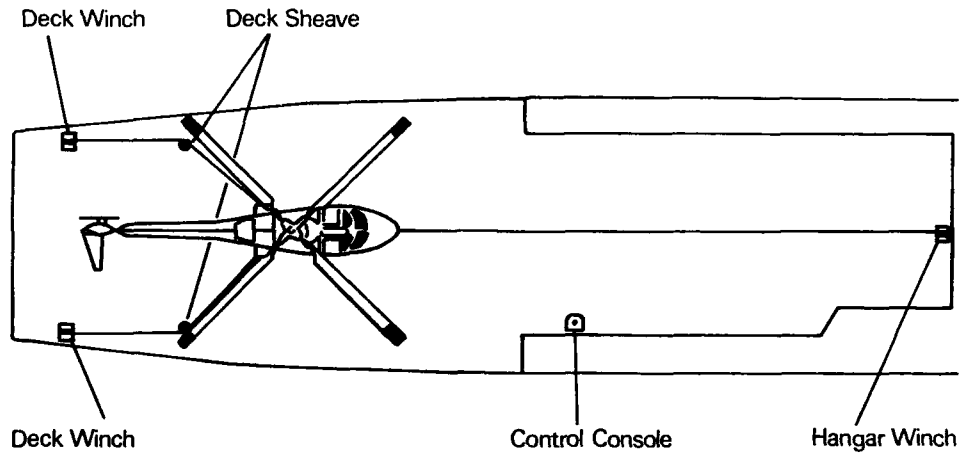
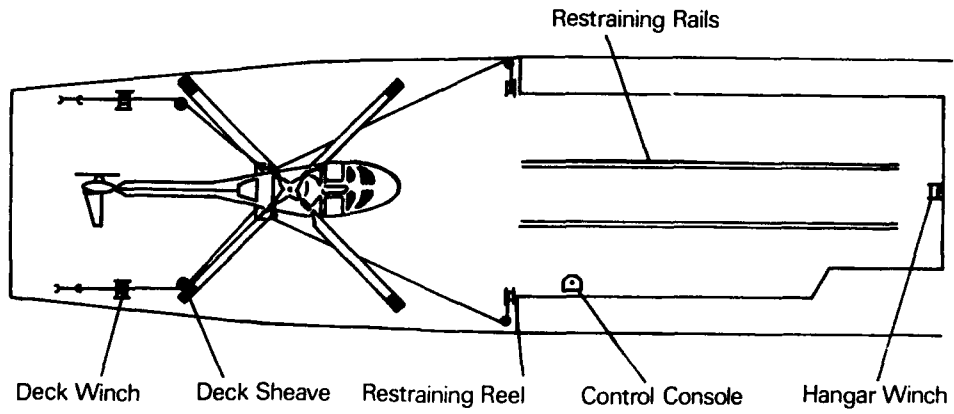


Photo 1



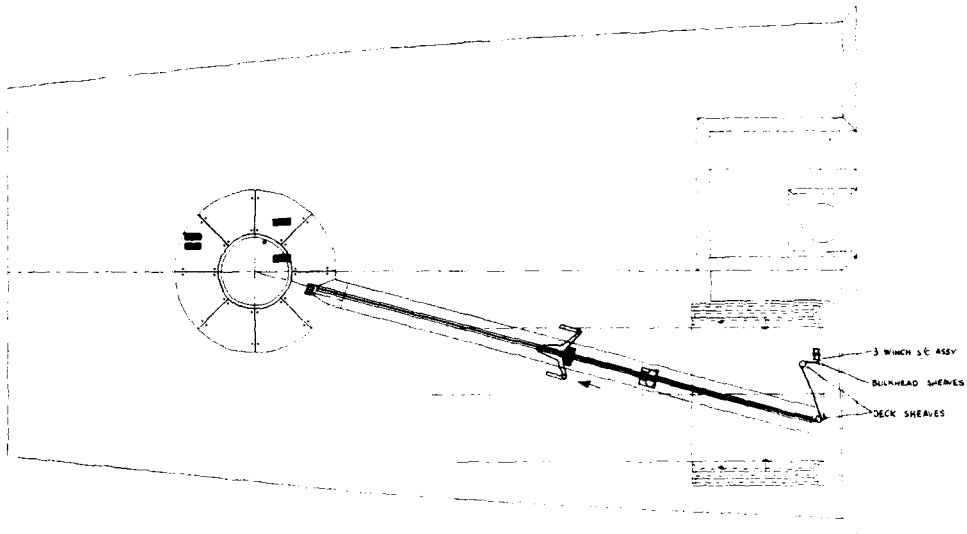
3 Winch Helicopter Handling System

Photo 2



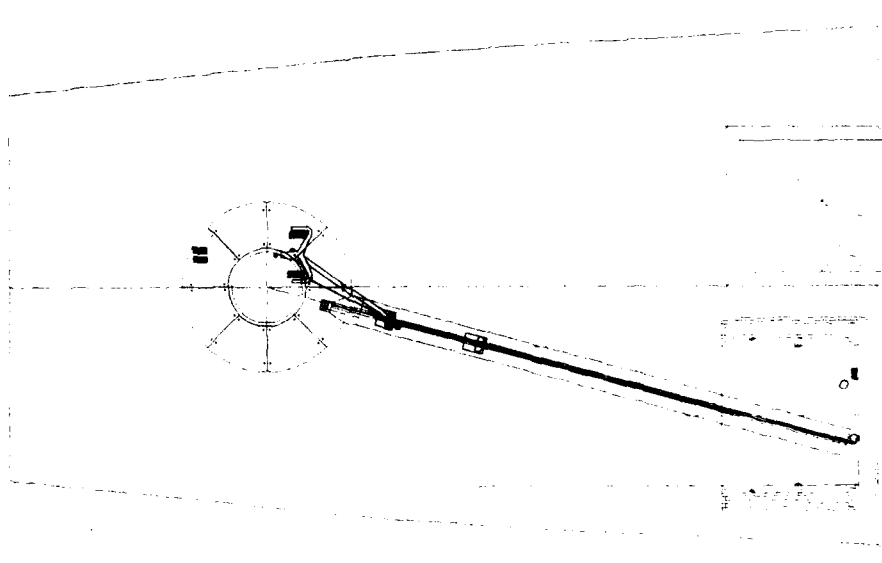
5 Wire Helicopter Handling System

Photo 3



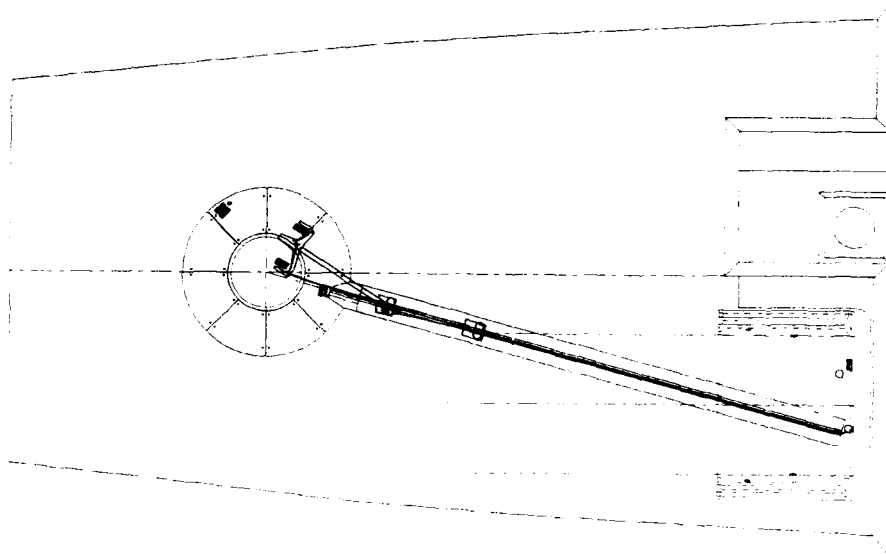
A/C LANDED DECKLOCK ENGAGED SHUTTLE MOVING AFT

Photo 4



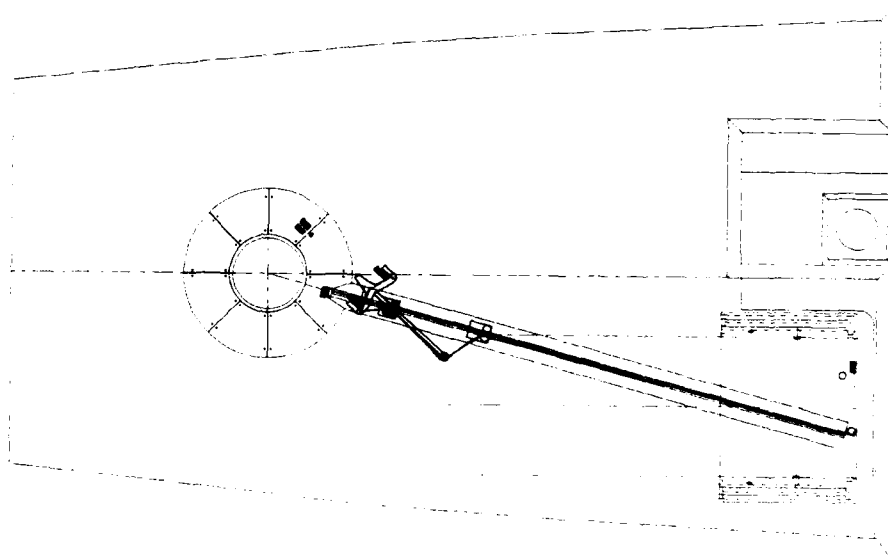
HANDLING FRAME ATTACHED TO A/C

Photo 5



A/C ROTATED BY FRAME

Photo 6



A/C PULLED INTO SHUTTLE

Photo 7

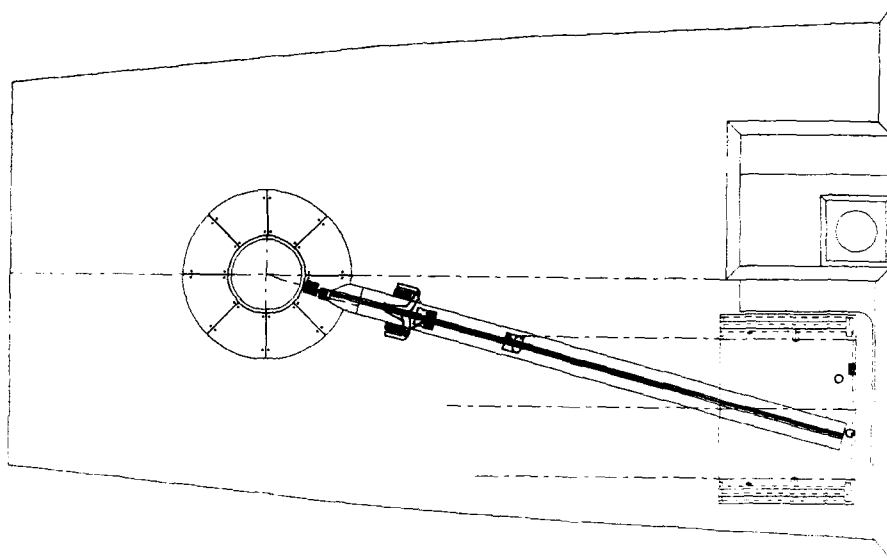


Photo 8



Photo 9

22-16

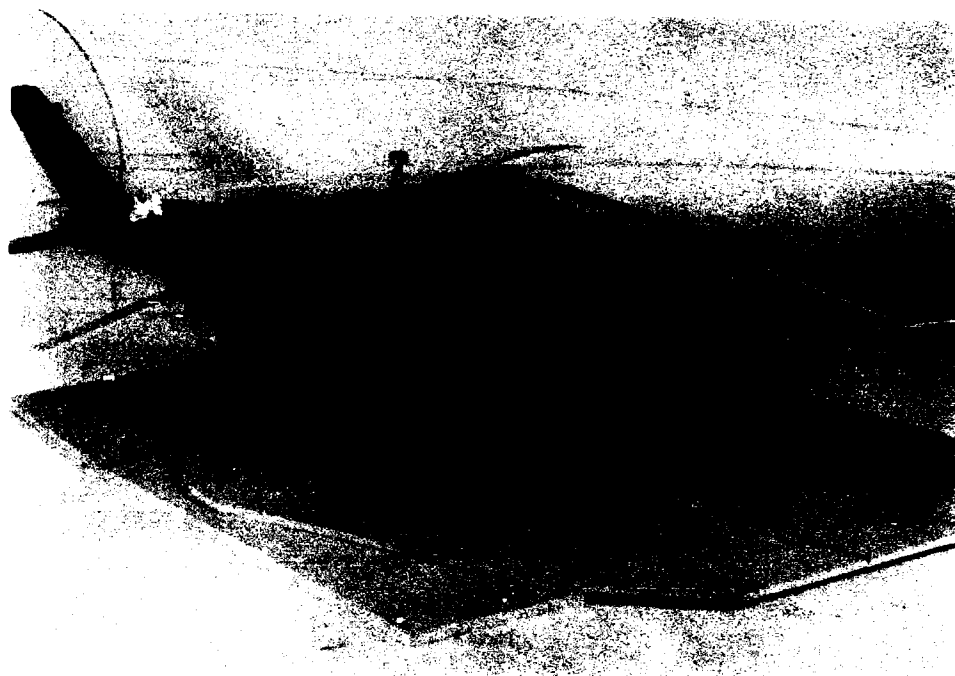


Photo 10

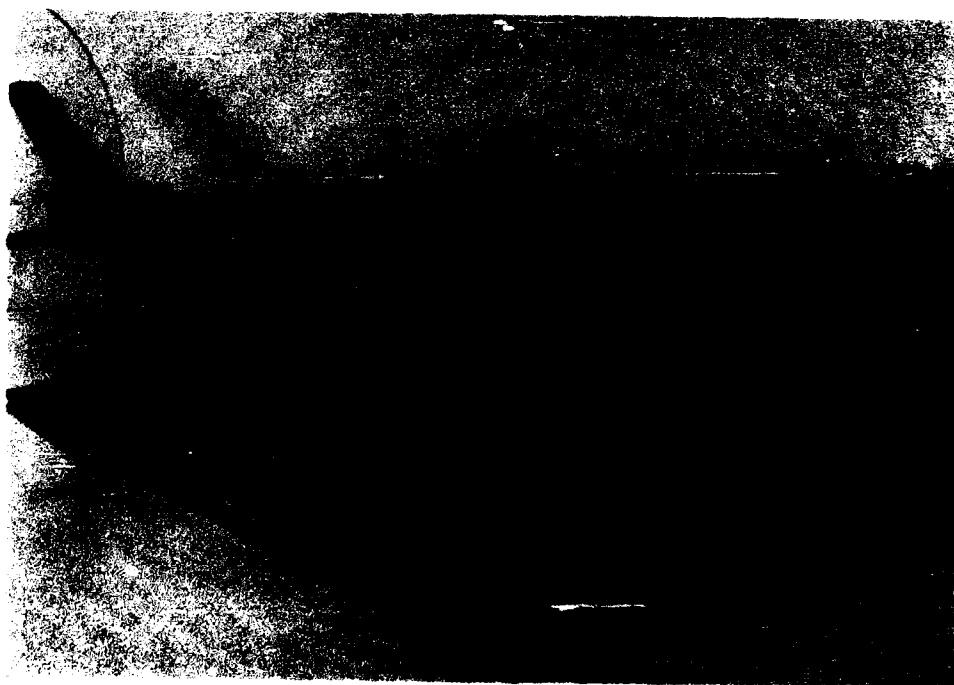


Photo 11

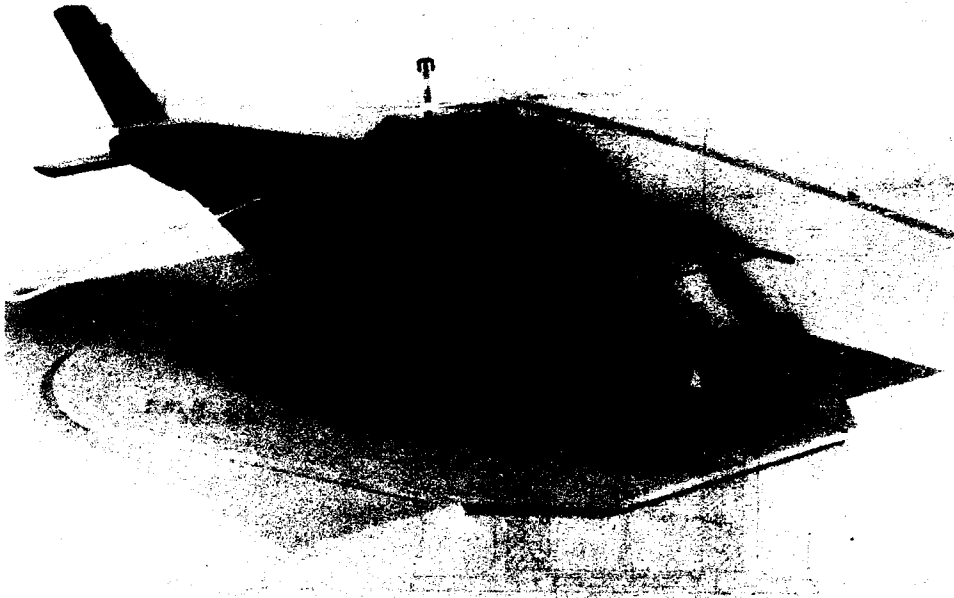


Photo 12

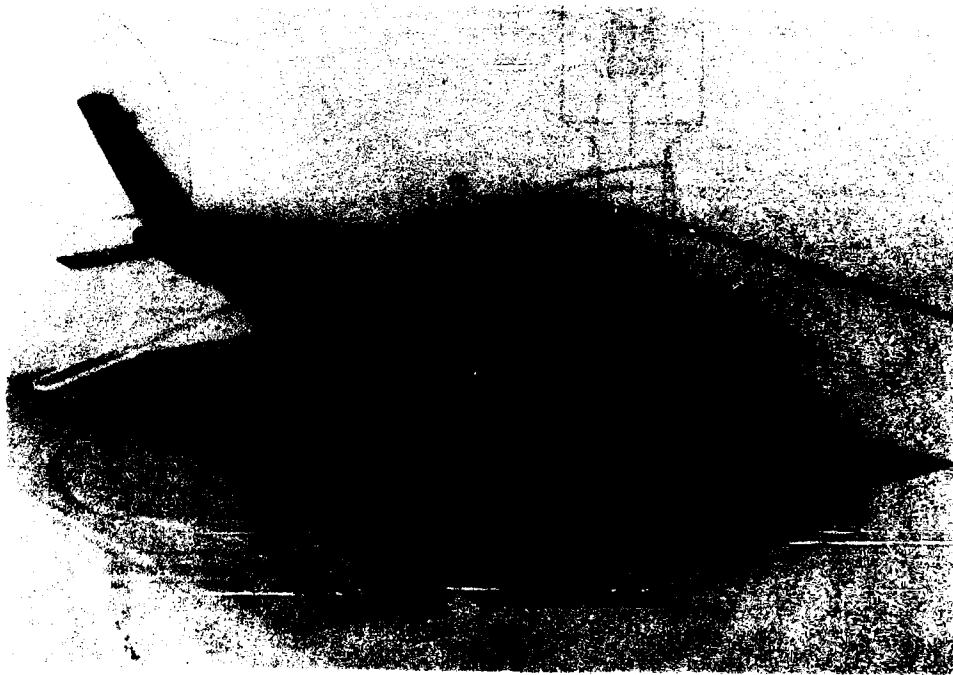


Photo 13

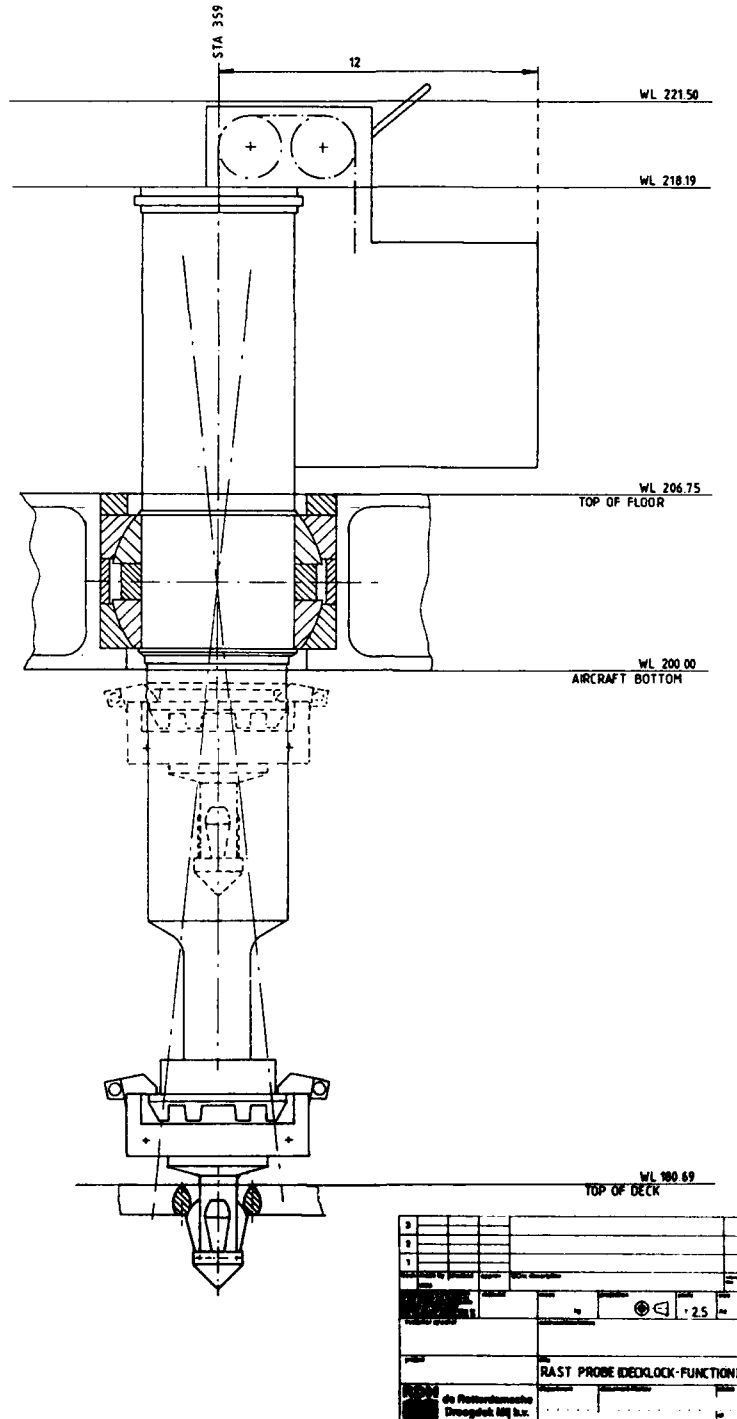


Photo 14

3					
2					
1					
0					
1	1	1	1	1	1
2	2	2	2	2	2
3	3	3	3	3	3
4	4	4	4	4	4
5	5	5	5	5	5
6	6	6	6	6	6
7	7	7	7	7	7
8	8	8	8	8	8
9	9	9	9	9	9
10	10	10	10	10	10
11	11	11	11	11	11
12	12	12	12	12	12
13	13	13	13	13	13
14	14	14	14	14	14
15	15	15	15	15	15
16	16	16	16	16	16
17	17	17	17	17	17
18	18	18	18	18	18
19	19	19	19	19	19
20	20	20	20	20	20
21	21	21	21	21	21
22	22	22	22	22	22
23	23	23	23	23	23
24	24	24	24	24	24
25	25	25	25	25	25
26	26	26	26	26	26
27	27	27	27	27	27
28	28	28	28	28	28
29	29	29	29	29	29
30	30	30	30	30	30
31	31	31	31	31	31
32	32	32	32	32	32
33	33	33	33	33	33
34	34	34	34	34	34
35	35	35	35	35	35
36	36	36	36	36	36
37	37	37	37	37	37
38	38	38	38	38	38
39	39	39	39	39	39
40	40	40	40	40	40
41	41	41	41	41	41
42	42	42	42	42	42
43	43	43	43	43	43
44	44	44	44	44	44
45	45	45	45	45	45
46	46	46	46	46	46
47	47	47	47	47	47
48	48	48	48	48	48
49	49	49	49	49	49
50	50	50	50	50	50
51	51	51	51	51	51
52	52	52	52	52	52
53	53	53	53	53	53
54	54	54	54	54	54
55	55	55	55	55	55
56	56	56	56	56	56
57	57	57	57	57	57
58	58	58	58	58	58
59	59	59	59	59	59
60	60	60	60	60	60
61	61	61	61	61	61
62	62	62	62	62	62
63	63	63	63	63	63
64	64	64	64	64	64
65	65	65	65	65	65
66	66	66	66	66	66
67	67	67	67	67	67
68	68	68	68	68	68
69	69	69	69	69	69
70	70	70	70	70	70
71	71	71	71	71	71
72	72	72	72	72	72
73	73	73	73	73	73
74	74	74	74	74	74
75	75	75	75	75	75
76	76	76	76	76	76
77	77	77	77	77	77
78	78	78	78	78	78
79	79	79	79	79	79
80	80	80	80	80	80
81	81	81	81	81	81
82	82	82	82	82	82
83	83	83	83	83	83
84	84	84	84	84	84
85	85	85	85	85	85
86	86	86	86	86	86
87	87	87	87	87	87
88	88	88	88	88	88
89	89	89	89	89	89
90	90	90	90	90	90
91	91	91	91	91	91
92	92	92	92	92	92
93	93	93	93	93	93
94	94	94	94	94	94
95	95	95	95	95	95
96	96	96	96	96	96
97	97	97	97	97	97
98	98	98	98	98	98
99	99	99	99	99	99
100	100	100	100	100	100

RAST PROBE (DECKLOCK-FUNCTION)

**COMPORTEMENT DYNAMIQUE D'UN AVION
SUR SES ATTERISSEURS : EXPERIMENTATION ET VALIDATION
PAR FRANCHISSEMENT D'UN DIEDRE**

par

D. Fleynac et E. Bourdais
Dassault Aviation — Direction Général Technique
78 quai Marcel Dassault
92214 Saint Cloud Cedex
France

1 - RESUME

Le rôle essentiel du comportement dynamique des atterrisseurs pour l'étude des phases de contact avec le sol et plus particulièrement pour l'analyse du catapultage des avions marins a justifié la volonté de valider, sur un avion existant, les modèles mis en oeuvre au stade de la conception.

Les travaux présentés consistent en la préparation, la réalisation, puis l'exploitation d'une campagne de décollages sur dièdre d'élanement d'un MIRAGE 2000.

Ces essais ont permis une identification détaillée du comportement des atterrisseurs dans une phase particulièrement dynamique, assez représentative de conditions d'utilisation au catapultage, ainsi que des efficacités aérodynamiques des gouvernes dans l'effet de sol.

2 - INTRODUCTION

Dans le cadre de l'étude des phases dites de "contact avec le sol", la Société DASSAULT AVIATION a développé, depuis plusieurs années, des moyens de simulation détaillée du comportement dynamique d'un avion sur ses atterrisseurs. Pour l'analyse du catapultage des avions marins, la capacité à représenter finement

ce comportement dynamique revêt un caractère particulièrement critique tant du point de vue de la définition des Systèmes de Contrôle du Vol (SCV), que de la conception de dispositifs visant à améliorer les performances de l'avion. On rappelle, à ce titre, que parmi les dispositifs envisagés, la solution d'un dièdre d'élanement de faibles dimensions a été retenue pour équiper les porte-avions à propulsion classique.

Le choix d'une modélisation adaptée de systèmes dynamiques complexes constitués d'un grand nombre d'éléments est fondé sur un certain nombre de considérations parmi lesquelles : le domaine de fonctionnement étudié, le niveau de qualité recherché dans la représentation du fonctionnement global ou/et interne du système, l'existence de couplages plus ou moins importants entre les différents éléments... Dans le cas particulier de l'étude du catapultage, le système dynamique considéré appelle un certain nombre d'observations :

- Les atterrisseurs sont soumis pendant la phase de catapultage à des sollicitations particulièrement dynamiques de compression et de détente rapides dont l'analyse nécessite la mise en oeuvre d'une modélisation fine et détaillée capable de représenter des comportements non-linéaires, hautes fréquences.

- Le Système de Contrôle du Vol (SCV) introduit un terme de couplage supplémentaire important entre les efforts train (et catapulte) et la dynamique avion. Sa conception, c'est-à-dire la définition des lois de contrôle, ne peut être dissociée de la conception générale du système Avion/Porte-avions.

Ces différentes constatations ont conduit à mettre en place des moyens de simulation complets, représentant le comportement dynamique de l'ensemble du système, et composés de modèles très détaillés des différents éléments intervenant au catapultage, notamment des atterrisseurs. La validation des différents éléments de modélisation peut être acquise par des moyens classiques (essais de chute, atterrissage, décollage...). Toutefois, il a semblé intéressant de procéder à une expérimentation spécifique visant à valider le modèle complet de simulation et, en particulier, les éléments déterminants tels que la modélisation des atterrisseurs et la modélisation d'effet de sol, dans des conditions aussi proches que possible de celles d'un catapultage.

C'est dans ce but qu'a été réalisée à Istres, une campagne de décollage sur dièdre d'un Mirage 2000. Cette expérimentation a été effectuée sous contrat du Ministère de la Défense, Délégation Générale de l'Armement, Service Technique des Programmes Aéronautiques.

Après une brève présentation de l'organisation des travaux et une description de la modélisation étudiée, l'objectif de cet exposé est de présenter la définition, la réalisation puis l'exploitation des essais. Nous concluons, enfin, sur l'intérêt présenté par cette expérimentation dans le cadre de la validation des modèles d'étude du comportement dynamique d'un avion sur ses atterrisseurs, en particulier, pour la simulation du catapultage des avions marins.

3 - ORGANISATION DES TRAVAUX

L'organisation générale des travaux est présentée figure 1.

La définition des essais par la même équipe, ayant en charge, au sein de la Direction Générale Technique, les activités de modélisation et d'étude des phases de contact avec le sol, a permis de mettre en place un protocole précis et adapté garantissant la complétude des essais et les moyens d'une identification, a posteriori, des éléments critiques de la modélisation.

La Direction des Essais en Vol, responsable de la mise en oeuvre et de la réalisation des essais, est intervenue au stade de la définition pour préciser les contraintes spécifiques à l'exécution de cette expérimentation.

4 - MODELISATION

4.1 - STRUCTURE DE MODELISATION

Les structures de modélisation détaillée développées pour représenter le comportement dynamique de l'avion peuvent être qualifiées de "modèles de connaissance" (par opposition à un modèle de comportement), c'est à dire des modélisations dont la structure fonctionnelle résulte directement des équations dynamiques du système physique représenté.

Le choix d'une telle structure, pouvant conduire à des modèles informatiques complexes, présente un certain nombre d'avantages :

- Les valeurs numériques des paramètres du modèle résultent alors, directement, des caractéristiques réelles de l'objet modélisé.
- La représentation fidèle des phénomènes physiques permet, au stade de la conception, d'évaluer directement l'effet de certains organes de réglage du système réel (par exemple, termes de laminage dans les atterrisseurs) sur son comportement dynamique.
- L'enrichissement progressif de la connaissance du système conduit à compléter, sans remettre en cause, la structure de modèle déjà établie.

4.2 - MODELE UTILISE POUR L'ETUDE

Pour l'étude de décollage sur dièdre du Mirage 2000 le système étudié est celui présenté figure 2. Le modèle complet de simulation comporte donc des représentations de :

- l'avion : sa modélisation aérodynamique est relativement précise elle émane des essais de soufflerie recalés des essais en vol. Ces bases aérodynamiques tiennent compte de l'effet de sol.
- Les capteurs dont les informations sont utilisées dans le SCV.
- Le calculateur du Système de Contrôle du Vol.
- Les servocommandes.
- Les moteurs avec leur dynamique propre.
- Les atterrisseurs : le modèle utilisé possède les caractéristiques essentielles suivantes :
 - * représentation de la dynamique de la partie non suspendue (roue et partie mobile de l'atterrisseur).
 - * Représentation de la configuration bi-chambre avec calcul de la position du piston séparateur fermant la chambre haute pression.
 - * Détermination des efforts de friction sur la partie mobile de l'atterrisseur en tenant compte de l'effet des efforts de frottement sec aux paliers (lesquels dépendent à leur tour de l'enfoncement de l'atterrisseur).
 - * Modification adéquate du système d'équations représentant le modèle lorsque le nombre de degrés de libertés mécaniques évolue (effet des butées mécaniques).
Une telle structure de modélisation permet de reconstituer le comportement dynamique de l'atterrisseur, qui est très fortement non linéaire, jusqu'à des fréquences de l'ordre de 30HZ.
 - * Représentation des pneumatiques et des efforts de contact pneumatiques/sol.

5 - DEFINITION DES ESSAIS

5.1 - OBJECTIFS - CONTRAINTES

5.1.1 - Objectifs des essais

Les essais réalisés sur Mirage 2000 s'inscrivaient dans un processus d'identification visant à valider et/ou recalibrer les modèles dans un domaine d'utilisation le plus proche possible d'un catapultage réel sur porte-avions. Le dièdre, de faibles dimensions (longueur 10 mètres, hauteur 0.25 m), était identique à celui actuellement prévu pour équiper les porte-avions à propulsion classique (figure 3). Son franchissement à des vitesses assez élevées permettait de solliciter les atterrisseurs dans des conditions particulièrement dynamiques de compression et de détente assez représentatives de celles observées au catapultage.

Le protocole d'essais, s'inscrivant dans le processus d'identification, devait fournir les éléments nécessaires à une identification fine des différents éléments du modèle et notamment du comportement dynamique des atterrisseurs et des efficacités de gouvernes dans l'effet du sol, ce qui pouvait être obtenu par un balayage adapté sur des sollicitations sensibilisantes telles que le braquage de gouvernes et la vitesse de franchissement du dièdre.

Par ailleurs, les différents essais devaient pouvoir être rejoués "fidèlement" hors temps réel ce qui impose de limiter le plus possible les facteurs de dispersions parmi lesquels le pilotage humain et les perturbations atmosphériques.

5.1.2 - Contraintes - cas de panne

La définition des conditions de l'expérimentation devait prendre en compte un certain nombre de contraintes liées notamment à la sécurité des essais :

- Avion :
 - . Efforts maximaux dans les atterrisseurs sur le dièdre et au rebond.
 - . Garde au sol sur piste et au passage du dièdre.

- Installation du dièdre

- Le dièdre devait être disposé en bout de piste pour faciliter son installation, ce qui limitait à 600 m la longueur de piste disponible avant le dièdre.

D'autre part, un certain nombre de cas de panne devaient être pris en compte au stade de la définition des essais parmi lesquels la panne moteur.

5.2 - DEFINITION DES ESSAIS

La réalisation d'un nombre important de simulations dans les conditions prévues de l'expérimentation, et notamment en introduisant, dans le modèle, le profil exact de la piste d'istres a permis de définir l'évolution des grandeurs contraignantes en fonction des conditions de franchissement du dièdre :

- vitesse de passage,
- braquage initial de gouvernes,
- poussée moteur.

Les résultats sont présentés figures 4,5,6. Les résultats de la figure 4 appellent un premier commentaire : selon la vitesse à l'entrée du dièdre, la garde au sol minimum est obtenue au décollage, au rebond, ou au franchissement du dièdre ce qui explique le caractère non-monotone des courbes présentées. On notera, par ailleurs, figure 5, que pour des Badin faibles (inférieurs à 40 kt) l'effort au rebond peut, sur le train auxiliaire, dépasser la charge limite. Ce résultat a conduit à définir des procédures particulièrement strictes d'expérimentation qui seront présentées au § 5.2.2.

L'analyse de ces résultats a permis de spécifier :

- les adaptations nécessaires du SCV.
- Les procédures à mettre en oeuvre pour couvrir les cas de panne ainsi que les consignes pilote éventuelles.
- Un programme d'essais approprié permettant une identification progressive et sûre du comportement du système.

Les adaptations du SCV et les procédures spécifiques de pilotage ont été validées et testées par les pilotes au simulateur de vol Temps-Réel.

5.2.1 - Adaptation du SCV

Quelques adaptations mineures du SCV, concernant exclusivement les réglages, ont été spécifiées.

L'autorité du trim de profondeur a été augmentée ce qui permettait au pilote d'afficher, à l'arrêt, un certain braquage initial d'élevons et de réaliser l'essai complet, jusqu'au passage éventuel du dièdre et au décollage, manche au neutre. Le pilote reprenait en main après décollage.

Le limiteur d'incidence a été adapté, en conséquence, dans la zone des basses vitesses.

Enfin certaines alarmes ont été désactivées.

5.2.2 - Procédures d'essais

Braquages maximaux de gouvernes

Le respect d'une garde au sol minimale de l'ordre de 0.5 m conduit à limiter les ordres à cabrer à des valeurs inférieures à 15° (figure 4).

Adaptation de la vitesse de franchissement du dièdre

La procédure d'accélération retenue consistait à attendre l'installation de la poussée pleins gaz secs, freins serrés, puis à lâcher les freins. La vitesse de franchissement du dièdre pouvait alors être adaptée :

- par la distance de lâcher des freins par rapport au dièdre,
- par la procédure de réduction des gaz et freinage éventuel à une certaine distance du dièdre.

Les efforts générés, au rebond, dans le train avant pouvant excéder les charges limites lors de franchissement du dièdre à des vitesses inférieures à 40 kt (figure 5), des modalités rigoureuses de mise en oeuvre de ces différentes procédures ont du être définies, tenant compte des cas de panne éventuels :

. En premier lieu, le lâcher des freins devait être réalisé à une distance suffisante du dièdre pour que, dans l'hypothèse d'une panne survenant à un Badin inférieur à 40 kt, l'avion puisse s'arrêter avant le dièdre. Cette distance minimale de lâcher des freins résulte directement de l'exploitation du diagramme d'accélération/décélération (figure 7) soit 160 mètres.

. Cette distance minimale de lâcher des freins conduit à des vitesses de franchissement en plein gaz sec supérieures à 80 kt (figure 7). Aussi, les vitesses de franchissement comprises entre 40 et 80 kt étaient-elles obtenues par réduction des gaz et freinage à une certaine distance du dièdre ce qui conduit à :

de 40 à 80 kt : passage au ralenti
au-delà de 80 kt : passage à pleins gaz secs.

. Enfin, pour chaque distance de lâcher des freins une distance de décision a pu être définie telle que, pour un cas de panne survenant en-deça, le pilote soit autorisé à réduire les gaz et freiner, l'arrêt se produisant alors avant le dièdre ; au-delà de cette distance de décision, le pilote avait pour consigne, en cas de panne, de continuer sur sa lancée sans freiner ni réduire les gaz, le franchissement du dièdre se faisant alors à un Badin supérieur à 40 kt (figure 8).

Une procédure d'évitement n'a pas été envisagée afin d'éviter un franchissement dissymétrique du dièdre.

5.2.3 - Protocole d'essais

La configuration avion retenue (masse légère) permettait, pour un braquage maximal autorisé des élévons de 15° à cabrer, de décoller dans la distance des 600 m précédant le dièdre. Cette masse légère permettait d'avoir une marge d'efforts importante sur les trains tout en assurant le pétrole suffisant pour faire un tour de piste en toute sécurité.

Le protocole d'essais visait à :

- assurer une certaine progressivité dans la criticité des essais réalisés.
- Fournir les éléments d'une première identification en "temps réel" permettant d'affiner à chaque étape les conditions exactes de la suivante.
- Garantir ainsi un certain niveau de sécurité notamment vis à vis des charges du train avant, vues plus haut.
- Constituer, enfin, une base de données suffisamment riche pour l'identification future des différentes caractéristiques du modèle.

En particulier, un balayage approprié sur les braquages de gouvernes et les vitesses de franchissement permettait d'évaluer la sensibilité du comportement du système à des variations élémentaires des entrées.

Le programme retenu comportait trois phases :

- a - Vérification des vitesses de lever de roulette et de décollage pour la configuration considérée.

Cette première étape permettait pour quelques valeurs de braquage initial d'élévons de mesurer les valeurs de vitesse de lever de roulette et de décollage et notamment de préciser la valeur de braquage telle que le décollage en pleins gaz secs se fasse dans la distance des 600 m tout en respectant une garde au sol suffisante.

b - Identification du comportement avion sur dièdre lors de passages "3 points".
 Cette étape visait à mesurer, pour une valeur de braquage donnée, les efforts générés dans les atterrisseurs par le franchissement du dièdre à différentes vitesses.

c - Identification du cas de décollage sur le dièdre avec et sans rebond.
 Compte-tenu des résultats acquis précédemment et notamment des vitesses de décollage mesurées au (a), cette étape consistait à parvenir à un décollage au passage sur dièdre, sans rebond.
 Autour du cas ainsi défini, un effet de vitesse (-2 m/s) et de braquage initial d'élèves (+2°) devait être réalisé.

Chaque essai devait être répété deux ou trois fois afin de réduire les effets des aléas de mesure.

6 - REALISATION DES ESSAIS

6.1 - DIEDRE - MONTAGE - DEMONTAGE

Le dièdre était constitué d'éléments démontables en construction mixte acier et béton et d'éléments en bois lamellé collé. Sa masse totale était de 16 T 5 et nécessitait donc une mise en oeuvre de grande ampleur aussi bien du point de vue personnel que matériel.

L'ensemble des panneaux était stocké sur un plateau semi-remorque. La manutention de ces panneaux s'effectuait grâce à deux chariots élévateurs équipés d'une poutre spéciale permettant de hisser les éléments avec deux élingues.

Son emplacement avait été défini de manière à limiter les travaux d'implantation sur la base.

6.2 - INSTALLATION D'ESSAIS

La mise en place d'une installation d'essais particulièrement complète assurait, pour la phase d'exploitation, la disponibilité de toutes les mesures nécessaires au bon déroulement du processus fin d'identification.

A l'installation normale d'essais comportant la télémétrie et un enregistreur magnétique, on avait ajouté des caméras sols, et des caméras embarquées pour filmer les trains, vérifier leur comportement au passage du dièdre et évaluer la garde au sol au cours de la rotation.

Les cinéthéodolites fournissaient la trajectographie au décollage et permettaient un recalage précis des informations avion.

Les trois trains étaient instrumentés pour enregistrer :

- les enfoncements des amortisseurs,
- les contraintes dans les fûts permettant, par étalonnage, de reconstituer les efforts,
- les accélérations (sur le fût et sur l'amortisseur).

Enfin, deux stations météo placées en amont du dièdre assuraient une mesure précise du vent (force et direction) indispensable d'une part pour ajuster la position initiale de l'avion en vue de franchir le dièdre à un badin donné et d'autre part pour permettre l'exploitation fine des résultats.

Afin de limiter les facteurs de dispersions, les essais n'avaient lieu que pour des conditions météo particulièrement calmes :

- vent de travers < 5 kt
- vent de face < 10 kt

6.3 - DEROULEMENT DES ESSAIS

Les essais, au nombre de 30, ont été effectués, tôt le matin (entre 6 et 8 heures), le montage du dièdre commençant de nuit.

Cet horaire matinal permettait, tout en respectant les contraintes de luminosité pour l'emploi des caméras et des cinéthéodolites, de réduire au minimum le temps d'immobilisation de la piste et d'avoir des conditions météo calmes.

Les essais ont nécessité une mise en oeuvre minutieuse. Avant chaque essai, le complément de plein était fait pour assurer la masse et le centrage souhaités. Le pilote alignait l'avion à une distance précise du dièdre, avec l'aide des cinéthéodolites, afin d'obtenir la vitesse de passage sur le dièdre déterminée.

Un premier recouplement, relativement bon, des essais avec les simulations a permis d'enchaîner les trois tranches d'essais en toute sécurité sans remettre en cause les conditions de l'expérimentation. (Décollage sans dièdre, rouleurs sur dièdre, décollage sur dièdre).

7 - EXPLOITATION DES ESSAIS

7.1 - PREMIERE ANALYSE EN COURS D'ESSAIS

La réalisation, au stade de la préparation des essais (§ 5.2), de simulations dans les conditions de l'expérimentation a fourni les moyens d'une première appréciation qualitative du modèle en cours d'essai.

Cette analyse "in-situ" visait notamment à assurer un niveau de sécurité suffisant dans l'enchaînement des différentes phases, et à procéder, le cas échéant, à une éventuelle adaptation des conditions d'essais.

7.2 - METHODOLOGIE D'IDENTIFICATION

La méthodologie suivie est une technique "classique" d'identification (figure 9).

Le processus réel considéré est constitué du système avion + atterrisseurs + SCV.

Les entrées efficaces consistent d'une part en la valeur du braquage initial de profondeur (ou position de trim) et d'autre part en la sollicitation générée par le franchissement du dièdre.

Par ailleurs, le système est soumis à un certain nombre de perturbations telles que la rugosité de la piste et la turbulence atmosphérique.

Les sorties consistent en l'ensemble des mesures enregistrées au cours des différents essais. Toutes ces informations peuvent être entachées d'un certain bruit de mesure.

Le modèle à identifier est le modèle complet de simulation présenté au § 4. Ce modèle, particulièrement riche, comporte un grand nombre de paramètres susceptibles d'être ajustés. Dans le cadre de l'opération décrite ici, l'attention était plus particulièrement portée sur les modèles dynamiques d'atterrisseurs et l'aérodynamique en effet de sol que l'opération visait à valider et/ou recalculer.

Enfin le critère retenu consiste :

- d'une part en un nombre limité de paramètres caractéristiques du roulage tels que la vitesse de lever de roulette et la vitesse de décollage.

- D'autre part, en l'appréciation "visuelle" de la comparaison des historiques mesurés en essais et de ceux obtenus par simulation sur les paramètres suivants :

- . paramètres avion :

- * vitesse sol
- * assiette
- * incidence
- * vitesse de tangage
- * vitesse verticale
- * accélération longitudinale
- * accélération normale

- . paramètres SCV :

- * position d'élèves

- . paramètres trains :

- * enfoncements des trois atterrisseurs,
- * efforts verticaux dans les trois atterrisseurs.

L'obtention d'un bon niveau de recouplement sur l'ensemble de ces paramètres assure la validation globale du modèle et sa bonne représentativité dans des conditions particulièrement dynamiques de fonctionnement.

L'adaptation des paramètres du modèle a été assurée "manuellement" compte-tenu du bon niveau de recouplement obtenu dès la première itération et du ch_x adapté du protocole d'essais assurant une bonne identifiabilité des paramètres importants du modèle.

7.3 - MISE EN OEUVRE DE LA PROCEDURE D'IDENTIFICATION

La procédure détaillée d'identification est présentée figure 10.

Les deux éléments de modélisation plus particulièrement susceptibles d'être adaptés étaient le modèle aérodynamique de l'avion (et notamment ses caractéristiques en effet de sol) et le modèle d'atterrisseurs.

Le protocole d'essais retenu (cf § 5.2.3) a permis une identification progressive de ces éléments.

7.3.1 - Introduction des conditions réelles d'essais

Cette étape a consisté, pour chaque essai, à introduire dans le modèle les conditions réelles de l'expérimentation.

La qualité de l'installation d'essais et les précautions prises lors de leur réalisation ont grandement facilité cette opération. Ainsi le relevé précis de la position initiale de l'avion a permis de prendre en compte dans le modèle le profil exact de la piste.

Toutefois un certain nombre de paramètres qui n'avaient pu être mesurés ont du être évalués. C'est le cas du centrage en X dont la mesure statique s'est révélée insuffisante. En effet, sous l'action de l'accélération longitudinale, le demi-plein de la nourrice fait reculer le centrage. De même, cette accélération fait bouger le manche de quelques mm soit quelques degrés de plus de gouvernes à cabrer.

7.3.2 - Problèmes de mesure

Quelques difficultés ont été rencontrées dans l'acquisition de certains paramètres : bruits de mesure, "trous de temps" dans les enregistrements...

Toutefois ces inconvénients ont pu être palliés grâce à la redondance des mesures d'une part, et à la répétitivité des essais prévus dans le protocole d'autre part.

7.3.3 - Ajustement du modèle aérodynamique de l'avion

L'exploitation de la première tranche d'essais (décollages sans tremplin) a mis en évidence un écart sur les vitesses de décollage, sur l'instant de début de rotation et sur la prise d'incidence.

Cette constatation a conduit à remettre en cause le calcul du moment aérodynamique de tangage et de l'effort de portance dans l'effet de sol et à procéder à leur ajustement.

Le modèle a été enrichi pour y introduire des termes complémentaires en portance et tangage relatifs à l'efficacité des gouvernes dans l'effet de sol soit :

$$\Delta C_{z\delta_m} \text{ et } \Delta C_m \delta_m$$

Ce complément de modélisation a permis d'obtenir un très bon niveau de recouplement sur les vitesses de décollage bien qu'il demeure un écart de l'ordre de 2 kt sur les vitesses de lever de roulette (figure 11).

Toutefois, cette adaptation s'est avérée insuffisante pour parvenir à un recouplement exact des vitesses de tangage au cours du décollage, celles-ci demeurant plus fortes en simulation que dans l'essai réel.

Une étude plus poussée de l'influence de l'effet de sol devrait permettre de restreindre encore ces écarts.

7.3.4 - Modèle d'atterrisseurs

Après ajustement du modèle aérodynamique (§ 7.3.3) l'exploitation exhaustive des trois tranches d'essais a été entreprise et a permis d'apprécier la qualité du modèle complet de simulation et d'évaluer, le cas échéant, les adaptations nécessaires du modèle d'atterrisseur.

En fait, le bon niveau de recouplement obtenu sur la restitution des efforts au passage du dièdre n'a pas justifié la volonté de procéder à un quelconque recalage du modèle.

7.4 - Résultats

7.4.1 - Exemples de rouleur sur dièdre et de décollage

Le niveau de recouplement essais-simulation obtenu après recalage du modèle aérodynamique peut-être apprécié sur les figures 12 et 13.

Exemple de rouleur sur dièdre :

figures 12-a à 12-f

Exemple de décollage sur dièdre avec rebond :

figures 13-a à 13-f

Les historiques présentés concernent les paramètres suivants :

- position des élevons
- vitesse de tangage
- accélération normale
- effort vertical train auxiliaire
- effort vertical train principal droit
- effort vertical train principal gauche

L'observation de ces résultats appelle un certain nombre de commentaires :

- En premier lieu, il convient de préciser qu'afin de faciliter l'appréciation visuelle des résultats, la fenêtre temporelle d'observation a été restreinte aux quelques secondes précédant et suivant le passage du dièdre, la synchronisation des historiques étant assurée en faisant coïncider les accélérations normales au franchissement du dièdre.
- Le niveau de recouplement obtenu sur les différents paramètres pendant les phases de roulage et de passage du dièdre peut-être qualifié d'excellent. On notera la bonne représentation des oscillations de l'avion sur ses trains pendant le roulage, en fréquence et en amplitude (vitesses de tangage, accélérations normales). De même, les efforts train et la réponse avion au franchissement du dièdre qui est la phase critique en ce qui concerne la validité des modèles dynamiques d'atterrisseurs sont parfaitement restitués.

- En revanche, les phases de rebond font apparaître un certain écart sur les valeurs d'accélération normale et d'efforts dans les atterrisseurs. Il est à noter que cet écart est croissant avec la vitesse de franchissement du dièdre (figures 12-C et 13-C). Cette constatation est cohérente avec le résultat du § 7.3.3. concernant la reconstitution imparfaite des vitesses de tangage au décollage. La prise d'incidence étant plus rapide en simulation, la portance est elle-même supérieure, et l'effort de rebond moindre. Toutefois, dans le cas du rouleur sur dièdre (vitesse de passage : 83 kt) on observe une bonne correspondance des efforts au rebond y compris pour le train avant.

7.4.2. - Synthèse des résultats

Les résultats présentés plus haut ont été obtenus sans recalage des modèles d'atterrisseurs.

Un ajustement complémentaire du modèle aérodynamique de l'avion aurait été nécessaire pour parfaire la reconstitution des rebonds.

Cependant, le bon recouplement observé au roulage et au passage du dièdre, n'a pas justifié la nécessité de procéder à une nouvelle itération dans le processus d'identification.

Il convient de souligner le caractère particulièrement représentatif des essais réalisés vis à vis d'un catapultage. Ainsi, le niveau d'accélération normale obtenue au franchissement du dièdre, de l'ordre de 2,5 g pour la vitesse de passage de 120 kt, est comparable à ceux obtenus au catapultage.

Aussi, la qualité du résultat obtenu, dans des conditions particulièrement dynamiques, permet-elle de conclure à la validité de la modélisation pour l'étude en simulation du comportement au catapultage d'un avion marin.

8 - CONCLUSION

L'opération qui vient d'être décrite a représenté un volume de travail assez important tant du point de vue de la définition des essais que de leur réalisation et de leur exploitation. Cette dernière étape a, toutefois, été grandement facilitée par le bon niveau de recouplement obtenu, après un simple ajustement de caractéristiques aérodynamiques, sur le comportement global du modèle étudié.

Le résultat obtenu consiste en la validation des modèles de simulation du comportement dynamique d'un avion sur ses atterrisseurs dans des conditions de fonctionnement particulièrement dynamiques proches de celles observées au catapultage. La mise en oeuvre d'une méthodologie rigoureuse, notamment dans la définition du programme d'essais, a permis d'identifier le comportement du système dans un large éventail de conditions d'utilisation, tout en tenant compte des contraintes très fortes de réalisation (garde au sol, efforts maximaux dans le train auxiliaire).

Ce résultat, obtenu sur MIRAGE 2000, permet d'avoir, aujourd'hui, un niveau de confiance relativement élevé dans les résultats de simulation de catapultage du RAFALE MARINE. La représentation fine du comportement dynamique de l'avion pendant cette phase critique est essentielle, non seulement pour la définition des Systèmes de Contrôle du Vol, mais plus généralement au stade de la conception avion, en particulier pour l'étude de dispositifs visant à améliorer les performances au catapultage.

La bonne représentativité de la modélisation actuelle pour l'étude du catapultage permettra de limiter le volume de la campagne d'essais sur base à terre du RAFALE MARINE et de réduire, ainsi, le délai de mise en service sur porte-avions.

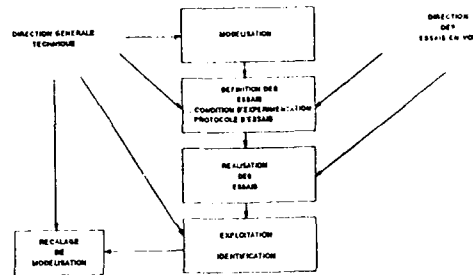


FIGURE 1 ORGANISATION DES TRAVAUX

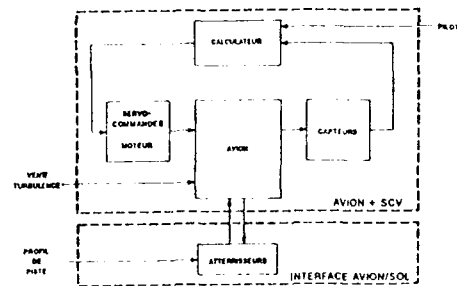


FIGURE 2 SYSTEMES DYNAMIQUES MIS EN JEU

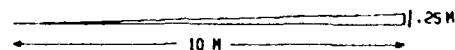


FIGURE 3 - COUPE DU DIEDRE D'ELANCEMENT

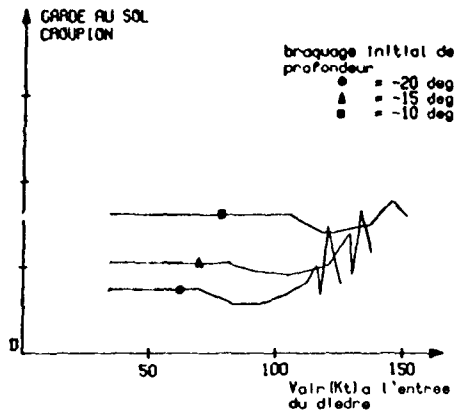


FIGURE 4 - EVOLUTION DE LA GARDE AU SOL

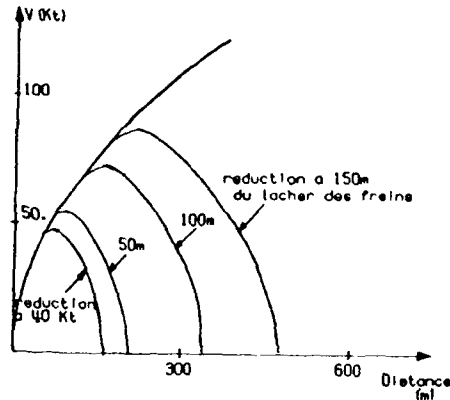


FIGURE 7

- DIAGRAMME ACCELERATION - DECELERATION

ACCELERATION - PLEIN GAZ SEC
 DECELERATION - REDUCTION MOTEUR EN 35 JUSQU'AU RALENTI
 - FREINAGE 15 APRES

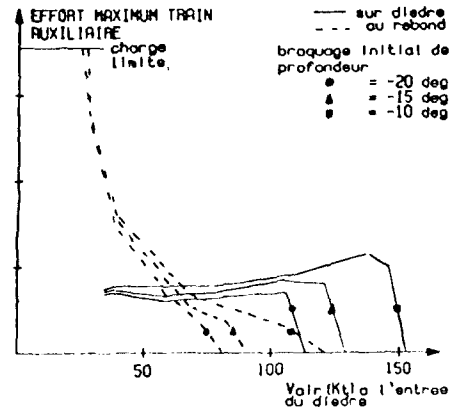


FIGURE 5 - EVOLUTION DE L'EFFORT MAXIMUM EN Z TRAIN AUXILIAIRE

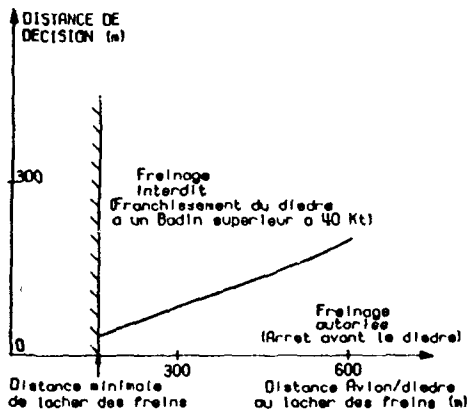


FIGURE 8 - CONSIGNES EN CAS DE PANNE

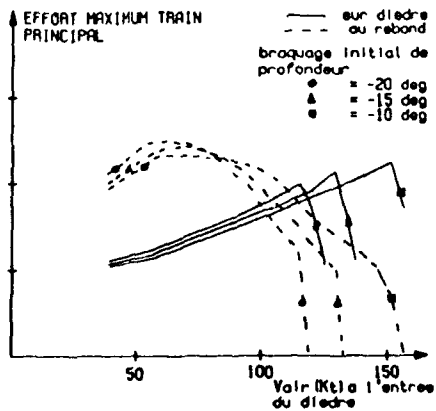


FIGURE 6 - EVOLUTION DE L'EFFORT MAXIMUM EN Z TRAIN PRINCIPAL

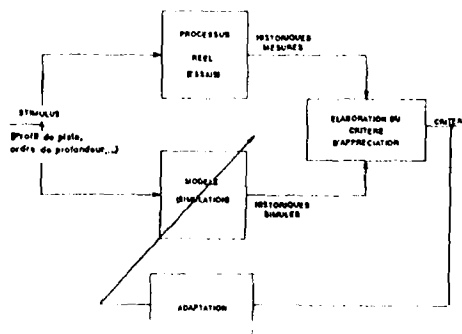


FIGURE 9 - PRINCIPE D'IDENTIFICATION

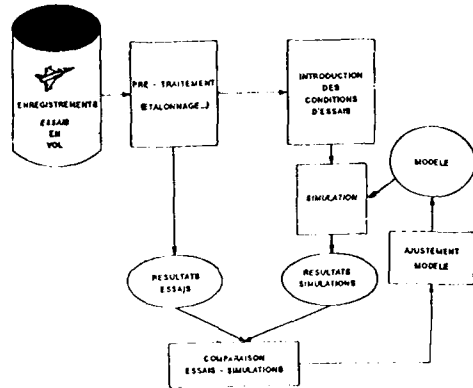


FIGURE 10 PROCEDURE D'IDENTIFICATION

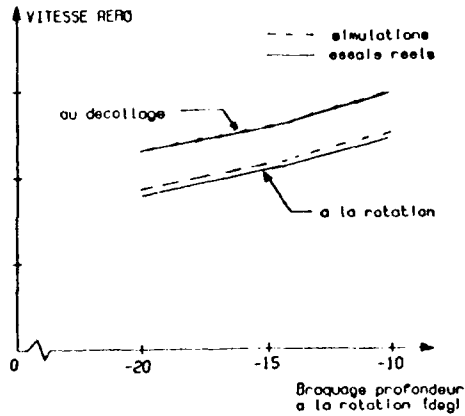


FIGURE 11 - COMPARAISON SIMULATIONS - ESSAIS REELS

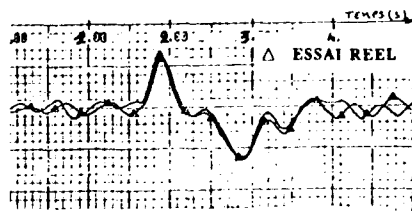


FIGURE 12 - ROULEUR SUR DIEDRE (Vitesse de passage 83k0)

a - position des elevons

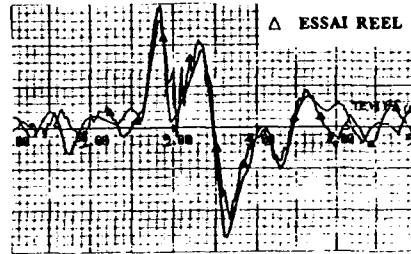


FIGURE 12 - ROULEUR SUR DIEDRE (Vitesse de passage 83k0)

b - vitesse de tangage

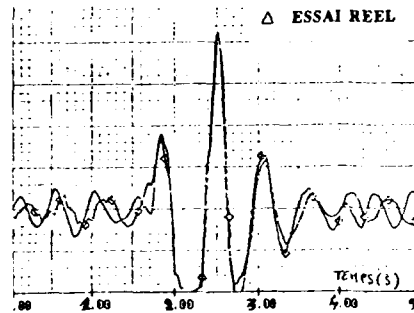


FIGURE 12 - ROULEUR SUR DIEDRE (Vitesse de passage 83k0)

c - accélération normale

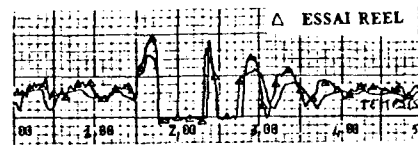


FIGURE 12 - ROULEUR SUR DIEDRE (Vitesse de passage 83k0)

d - effort vertical train auxiliaire

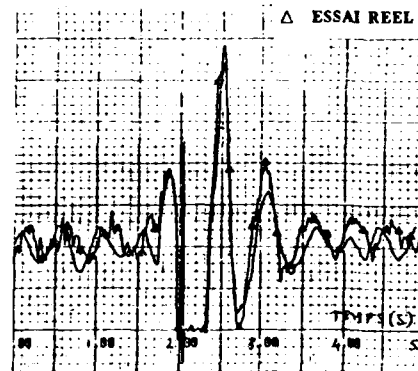


FIGURE 12 - ROULEUR SUR DIEDRE (Vitesse de passage 83k0)

e - effort vertical train principal droit

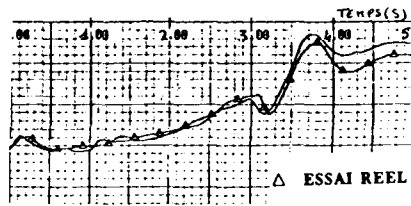


FIGURE 13 - DECOLLAGE SUR DIEDRE
(Vitesse de passage 120k)

a - position des élévons

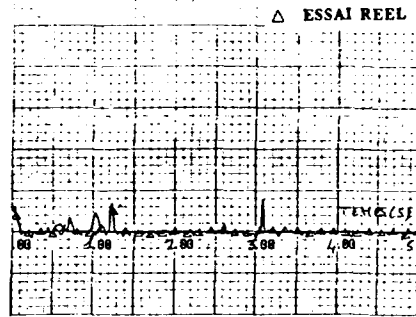


FIGURE 13 - DECOLLAGE SUR DIEDRE
(Vitesse de passage 120k)

d - effort vertical train auxiliaire

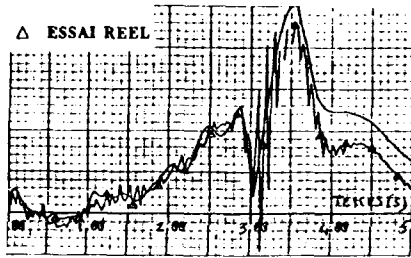


FIGURE 13 - DECOLLAGE SUR DIEDRE
(Vitesse de passage 120k)

b - vitesse de tangage

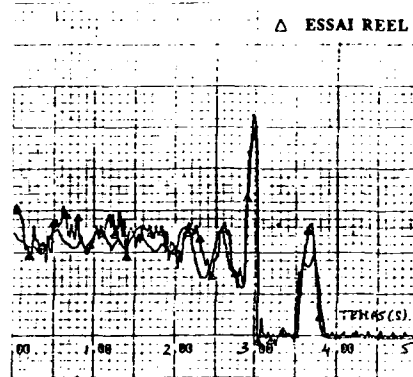


FIGURE 13 - DECOLLAGE SUR DIEDRE
(Vitesse de passage 120k)

e - effort vertical train principal droll

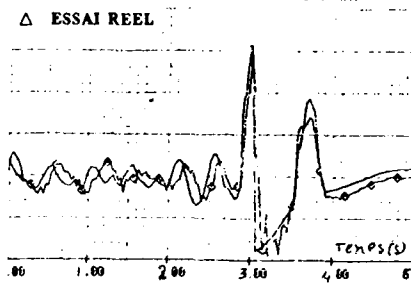


FIGURE 13 - DECOLLAGE SUR DIEDRE
(Vitesse de passage 120k)

c - accélération normale

**SOME IMPLICATIONS FOR ADVANCED STOVL
OPERATION FROM INVINCIBLE CLASS SHIPS**

by

K. Ainscow and P.G. Knott
Advanced Studies Department
British Aerospace (Military Aircraft) Ltd
Warton Aerodrome
Lancashire PR4 1AX
United Kingdom

SUMMARY

Replacing the Sea Harrier with a high performance Advanced STOVL design on the Invincible class ship has been studied. Four alternative ASTOVL propulsion concepts were included. The different concepts and their performance is described. The integration of these larger, heavier aircraft with the small ship, carrying EH101 helicopters, is discussed. It is shown that the constraints of the ship and the size and performance of the aircraft, require some changes in operational procedures by comparison with Sea Harrier practice. The higher take-off thrust to weight ratio and more hostile exhaust plumes suggest the use of the aft deck for recovery and a shorter deck run with the ski-ramp for launching, with a blast deflector between the two areas. A study of the deck environment generated by the ASTOVL aircraft indicates that a delicate balance between size, mass, performance and exhaust environment will need to be struck in future Sea Harrier replacement studies for small ship operation.

1 INTRODUCTION

The CAH-01, Invincible class ASW carriers were originally designed to operate rotary-wing aircraft in NATO waters, at least that was the official position. The fact that they had a 'through deck' and were capable of operating Harrier STOVL aircraft was played down. Various euphemisms were used to describe the ship at the time (ref. 1) of which 'See-Through Carrier' was probably the best indication of Naval intentions. It was fortunate for the Navy that the Sea King helicopter, and the Harrier were similar enough in terms of size and mass, Fig. 1, to allow a vessel designed for helicopter operations to be suitable for STOVL aircraft as well, provided there was sufficient deck length for a runway. (Fig. 2).

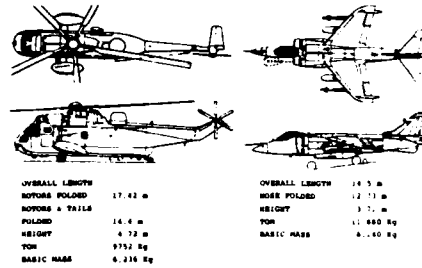


FIG. 1 COMPARISON OF SEA KING AND SEA HARRIER

The runway area is used for launching Harrier, even with aircraft parked by the island. It is used for the launch and recovery of Sea King and the recovery of both aircraft in combinations of up to four vehicles at a time (although it is not normal practice to mix types on recovery). The starboard area forward of the island is used for helicopter maintenance and as a parking area for aircraft. Starboard aft is used for helicopter launch and recovery, parking ready state Harriers, engine running and recovering Harriers.

All this activity needs crew and machinery on deck able to work quickly and efficiently in a noisy, wet and windy environment. The problems created by rotor downwash and high energy jet efflux are solved satisfactorily by operational procedures and special clothing such as ear defenders. Sea Harrier then, has the unique characteristic among fixed wing aircraft of being able to operate from the same platform as helicopters without requiring significant compromises on space or endangering ground crew. The introduction of ASTOVL aircraft needed to meet future threats will require changes to both operational procedures and possibly the ship itself. What are these changes and can they be incorporated without radical modifications?

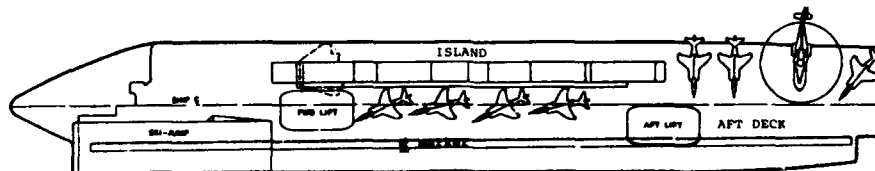


FIG. 2 FLIGHT DECK LAYOUT

An ASTOVL aircraft will not only be supersonic but will also have a greater payload and better range-endurance than Harrier. High levels of manoeuvrability will also be required for the aircraft to be competitive with future threats; and yet it must be operated from Invincible class carriers. Increased performance means increased aircraft weight as illustrated in Fig. 3.

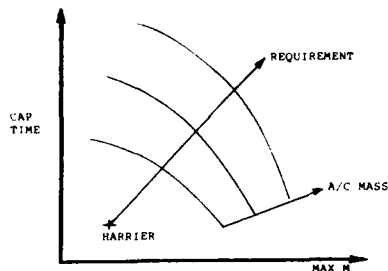


FIG. 3 MASS GROWTH WITH INCREASED PERFORMANCE

Supersonic requirements cause weight growth because the structure sees higher forces and needs to be stronger; while increased range-endurance requires extra volume to carry more fuel. Additionally efficient supersonic flight needs a slender fuselage and thin wing which again add weight. A slender fuselage demands an engine with a small cross section and high specific thrust, conflicting with the need for low specific thrust (to give a benign footprint) desirable for vertical landing.

The exercise reported here is an initial study to identify the compromises needed to the ship, the deck operating procedures and the ASTOVL aircraft for future operations based on Invincible class ships.

2 ASTOVL CONCEPTS

2.1 Design Considerations

There are three essential elements in any ASTOVL specification namely:-

- i) a robust, reversible transition from wing borne to thrust borne flight
- ii) a controllable vertical landing
- iii) true supersonic capability

In this exercise it was assumed that i) could be satisfied by a total thrust vectoring system with at least 120° to 60° range from HFD, ii) by a T/W ratio of 1.13 for the aircraft in landing configuration and iii) by a minimum Mach number of 1.6 in level flight with all weapons retained.

The aircraft were intended primarily for fleet defence work as is reflected in the design CAP mission shown on Fig. 4. Aircraft size was determined by the time required on station (effect of fuel volume) and the number of weapons carried, both were set at ambitious levels to test the limits imposed by the ship and to exaggerate any differences inherent in the chosen propulsion systems concepts.

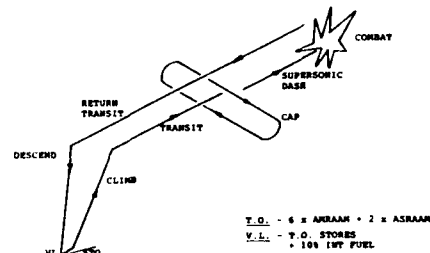


FIG. 4 DESIGN MISSION PROFILE

2.2 Propulsion Options

All the engines assume a technology level consistent with an in service date of 2000. They are hotter and have higher pressure ratios than Pegasus and, consequently, have a much improved thrust/weight ratio.

2.2.1 Remote Augmented Lift System (RALS)

The RALS system shown in Fig. 5, is based on a separate flow turbofan similar in concept to the Pegasus engine in Harrier, except that the bypass flow can be switched between a front (lift) nozzle and a rear (propulsive) nozzle. In lift mode the bypass air is ducted forward to a 2-dimensional nozzle capable of limited vectoring.

The concept allows flexibility in choosing an airframe configuration since the jet positions can be selected to match different platform shapes. It also offers pitch control during transition by modulating the front nozzle thrust and hence reducing long term Reaction Control System requirements.

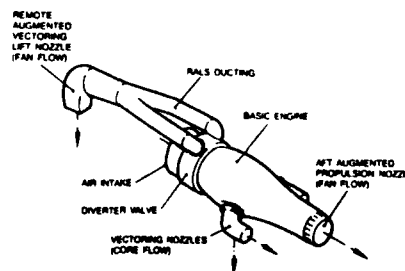


FIG. 5 REMOTE AUGMENTED LIFT SYSTEMS (RALS)

2.2.2 Tilt Engine

The tilt engine arrangement Fig. 6 allows the use of engines developed for a conventional fighter, such as EFA, rather than a specifically developed VSTOL engine. Aircraft control in the VSTOL mode is achieved through a combination of nacelle tilt, differential thrust and post exit thrust deflection, implying full flight and engine control system integration.

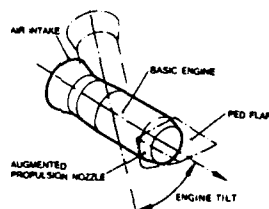


FIG. 6 MIXED FLOW TILT THRUST

2.2.3 Tandem Fan

This propulsion concept Fig. 7 offers a high specific thrust mixed turbofan for conventional flight but operates as a very high bypass ratio unmixed turbofan in the VSTOL mode thereby achieving some improvement in deck environmental conditions. This benefit has been maximised by designing for a vertical landing capability on dry thrust.

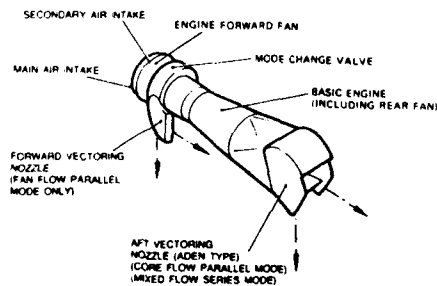


FIG. 7 TANDEM FAN

In the engine's parallel mode, used in the VSTOL regime, the main air intake feeds the forward fan which is discharged via a mode change valve to vectoring front nozzles. The rear fan is fed by a separate secondary intake, the discharge being split into a bypass stream and core flow as in a conventional low pressure ratio mixed flow turbofan.

In the series mode, the mode change valve is moved to allow the forward fan discharge to pass through to supercharge the rear fan and core; the secondary intake being closed and the forward nozzles faired to a low drag profile.

A twin engine layout was chosen for this concept because of difficulty experienced in installation of a single engine due to its length and the need to balance the split thrust about the CG.

2.2.4 Vectored Thrust

The vectored thrust concept presented here (Fig. 8) uses a separate flow turbofan engine and as such is essentially similar to current Pegasus applications. The high performance requirements lead to a high fan pressure ratio and thrust augmentation by Plenum Chamber Burning (pcb).

Some pitch trim capability is available by varying PCB temperature. The chosen configuration also uses a 2-bearing nozzle to effect vectoring of the core efflux via a single rear outlet.

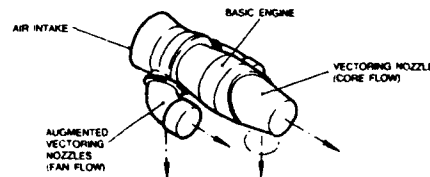


FIG. 8 SEPARATE FLOW VECTORED THRUST

2.2.5 Engine Comparison

Engine cycle and performance data are given in Table 1. The large advances in engine technology expected by the year 2000 should result in high specific thrust, high fan pressure ratio cycles being achievable to meet the flight requirements. These characteristics however, have an adverse effect on specific fuel consumption and consequently on mission fuel requirement. High overall engine pressure ratios are needed to minimise sfc.

TABLE 1 - ENGINE CYCLES AND PERFORMANCE

	RA15	TE	TF	AVT	SHAR
FAN PRESSURE RATIO	4.4	4.2	4.5	4.0	2.3
OVERALL PRESSURE RATIO	30	27	25	20	14
BYPASS RATIO	1.0	0.5	0.6	1.0	1.4
SLS UNINSTALLED PERFORMANCE					
TOTAL AIRFLOW (kg/s)	205	164	205	205	205
TOTAL THRUST AUGMENTED (kN)	202	217	260	200	0
TOTAL THRUST DRY (kN)	140	139	170	135	95.6

With the exception of the Tandem Fan concept, the deck environment has become less benign than Sea Harrier because of the increase in pressure and the use of fuel burning augmentation. Higher thrust/weight ratios give some compensation on take-off as very short deck runs can be used. The Tandem Fan aircraft was designed specifically to operate with low temperatures and pressures and was the only "dry lander" considered.

2.3 Aircraft Performance

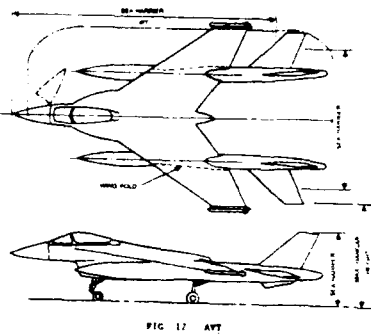
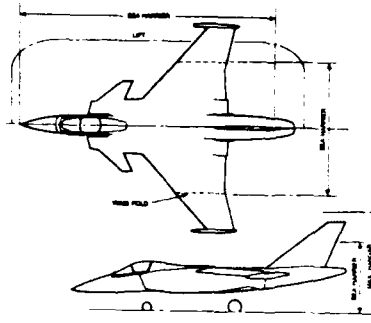
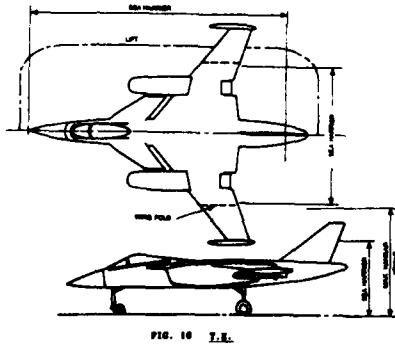
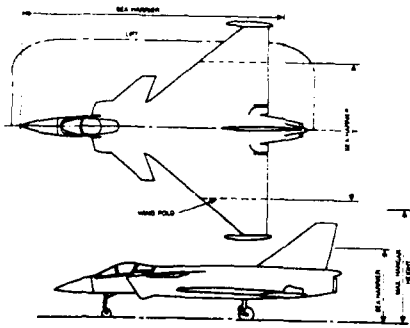
2.3.1 Aircraft Size

Line drawings of the four aircraft are shown in Figs. 9 to 12. On each, the span, length and height of the Sea Harrier is shown and the outline of the deck lift has also been marked. Maximum width, with wings folded and unfolded, length and height are listed in Table 2.

All aircraft are larger than Sea Harrier and need wing fold to fit on the lift.

TABLE 2 - AIRFRAME SIZE

GEOMETRY	RALS	TE	TF	AVT	SHAR
MAX WIDTH (WING FOLDED) (ft)	7.7	8.0	7.5	7.4	-
MAX WIDTH (WING UNFOLDED) (ft)	12.24	12.46	12.1	10.4	7.7
MAX LENGTH (ft)	14.0	15.74	15.74	17.33	14.52
MAX HEIGHT FROM DECK (ft)	5.46	5.0	5.17	3.78	-



2.3.2 Masses

The aircraft masses are shown relative to SHAR on Fig. 13.

The major reason for the increase in airframe size relative to Sea Harrier is the fuel mass which reflects the demanding nature of the CAP mission.

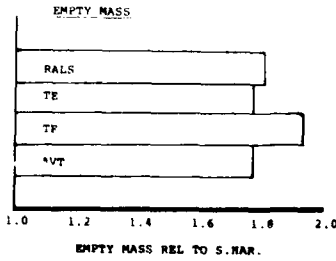
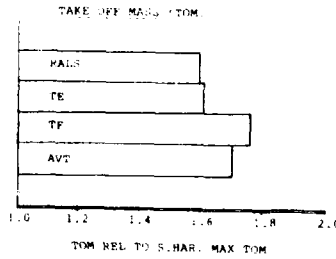


FIG. 13 AIRFRAME MASSES AT DESIGN MISSION RELATIVE TO SEA HARRIER

At take-off the aircraft are between 7 and 9 tonnes heavier than Sea Harrier. Fully fuelled and armed all aircraft exceed the maximum lift capacity.

At vertical landing, with design mission stores, the aircraft are between 6 and 7 tonnes heavier than Sea Harrier design landing mass. Assuming the same vertical descent velocity at touchdown the deck loads will be increased by about 80%.

2.3.3 Flight Performance

The relative design mission performance is illustrated in mass terms in Fig. 13.

Specific performance is shown in Fig. 14.

6 AMBAAM + 2 ADPAAM + 50% CAP MISSION FUEL

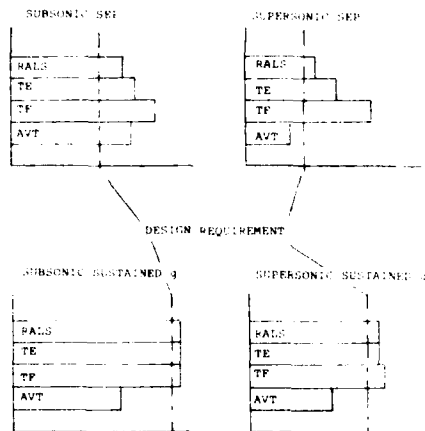


FIG. 14 SPECIFIC PERFORMANCE

2.3.4 Take-off and Landing

Ski jump take-offs with dry and augmented thrust are shown in Fig. 15. The TF takes-off dry as thrust augmentation is not available when used in parallel mode. The other aircraft use either full or partial augmentation and can take-off in 75m.

Using dry thrust for RALS, TE and AVT reduces thrust/weight at take-off by some 40-50% with a consequent increase in deck run and reduction in maximum take-off weight. At design mission weights the deck run is increased, to 70m for RALS, while TE needs a run of 90m.

Take-off estimates for RALS, TE and TF assume the aircraft are static, with full thrust, at the start of the take-off run. This is unlikely to be achieved in practice on brakes alone and therefore some restraining device will be necessary. If such a device is not used then the deck runs will be increased by 10-15m to allow the engine to run up to speed.

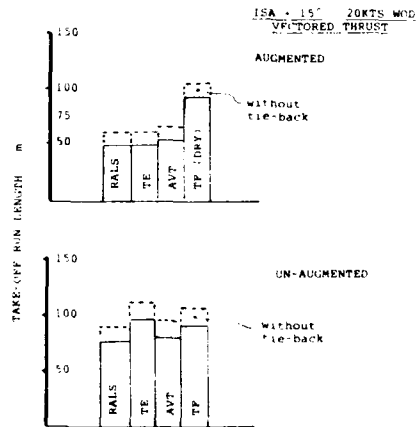
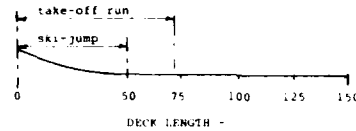


FIG. 15 SKI-JUMP TAKE-OFF PERFORMANCE AT DESIGN MISSION MASS

All aircraft are capable of vertical landing but with different degrees of environmental impact as discussed later.

Here landing performance is judged by the temperature of the bypass nozzle, or in the case of TE by the full exhaust front temperature. TF has been designed as a dry lander and therefore has the most benign temperature. RALS front jet temp has been limited to 1000°K as a design choice, but at design mission landing weight the engine is throttled back and the RALS temperature is only 880°K. TE has the smallest powerplant and has to use reheat on landing; the temperatures are consequently high at 1400°K, but this is approximately the same as the core jet temperatures of the RALS and AVT. The AVT also uses elevated front jet temperature by pcb but like the RALS these are reduced at design landing mass to about 700°K.

3 SHIP/AIRCRAFT INTEGRATION

Throughout the study it has been assumed that the ASTOVL aircraft would operate on board the Invincible class ship with EH101 helicopters rather than Sea King. When folded these two helicopters are not significantly different in size and hence this change does not actually influence the ASTOVL to ship integration.

3.1 Geometrical Constraints

The Invincible class ships impose shape, size and general layout constraints on the operation of VSTOL aircraft and helicopters. These constraints influence, differently in some respects, the way in which the ASTOVL aircraft and EH101 helicopter would be operated.

This section discusses these constraints and how the different aircraft might require, or benefit from, changes in the organisation on deck and in the hangar, together with minor alterations to the ships that might be considered.

Flight Deck

Fig. 2 shows the plan view of the flight deck with Sea Harrier and EH101 helicopters. The salient features are:-

- . The island
- . The ski-ramp
- . The take-off runway with centre line marker.
- . The aft deck

Take-off

During Harrier take-off the runway is only occupied by aircraft preparing to take off, which can include aircraft with a pilot in the cockpit and engines in idle at a safe distance behind the front aircraft. Between these aircraft and the island other aircraft may be armed and tied down. On the aft deck, but not on the runway aircraft and helicopters may be parked. The runway, culminating in the ski-ramp, has a centre line marking along its full length to help the pilot keep clear of parked aircraft during ground roll. On Harrier, deck clearances are about 2.7m from outriggers to port deck edge, and about 3m from the starboard wing tip to the parked aircraft.

The introduction of any of the ASTOVL configurations could require and benefit from three changes:-

- i) Since none of the proposed ASTOVL aircraft have outrigger gear, the runway centreline can be moved to port whilst maintaining a minimum clearance of approximately 2.2m from the port undercarriage to the port deck edge. Fig. 16. All the ASTOVL configurations have increased unfolded span hence this port movement of the centre line allows the maintenance of the starboard tip clearance. Typical movement of the centre line would be about 2.5 metres.

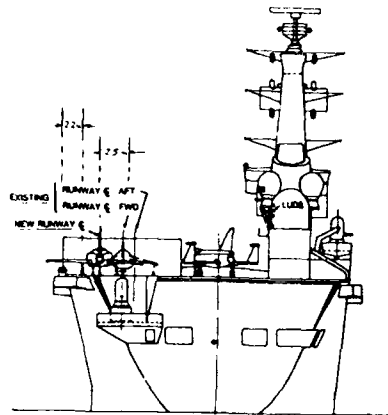


FIG 16 PROPOSED AND EXISTING RUNWAY CENTRELINES

- ii) All the candidate aircraft have higher installed thrust to weight at take-off which can be used to reduce the take-off deck length and thereby free all the aft deck for parking, landing operations and helicopter take-off. However, there is an increase in jet energy which will preclude the positioning of aircraft close behind the take-off vehicle. Thus the need arises to use a single blast deflector behind the take-off strip to protect the aft deck.
- iii) To maximise the short take-off performance, the aircraft needs to be held back against high thrust levels. Without such restraint, the take-off length would increase by some 10 to 15m, and the blast deflector should be located accordingly. The use of tie-back may also help to align the aircraft for the take-off.

All Invincible class ships are to be fitted with 12' ski-ramps as standard. With the narrower undercarriage track of the ASTOVL aircraft the width of the ski-ramp could be reduced to advantage.

Initial estimation of undercarriage dynamics on the ramp suggest the dynamic loading on the mainwheel may only exceed the static loads by some 10%.

Landing

In day-light and good weather, Harrier landings can take place at various locations along the deck. At night or in poor weather, only the aft deck can be used and then only when clear of parked aircraft. The candidate aircraft are all larger and heavier and it would seem likely that landings would necessarily be confined to the aft deck, which is in keeping with the suggested changes to take-off procedure.

Spotting and Ranging Assessment Aids

A one-hundredth scale model of Ark Royal was made to simply represent the upper four decks. The model was modular and the ski-jump, transparent flight deck and accommodation/workshops could be removed to give side and top access to the hangar floor level.

Simple models (plan and silhouette) of all candidate aircraft, with and without wing fold, were used to quickly assess numerous possible arrangements.

Deck Stowage

The following assumptions were made:

- As many aircraft and helicopters as possible are required to be placed on deck and all air vehicles are kept folded for all movements until just before take-off.
- Weapon stores are kept on deck and arming of the aircraft takes place on deck.
- If the wings fold for deck stowage it is a requirement that arming can take place with the wings folded.

No overall changes are envisaged to the above from the geometrical aspect, and the numbers of ASTOVL aircraft and EH101 helicopters which can be placed on deck is a function of the size and folding arrangements for each design. On deck in an operational condition and in the Hangar deck it was found that one less ASTOVL could be accommodated than Sea Harrier along with the EH101 i.e. 8 EH101 + 6 ASTOVL rather than 8 EH101 + 7 S.HAR. Fig. 17 shows a typical ASTOVL arrangement.

Lifts

The candidate aircraft have all been designed, in folded condition, to fit the existing lifts. The aircraft are also heavier than Harrier and exceed the current lift mass limits. Weapons and some fuel must therefore be removed before the lift is used.

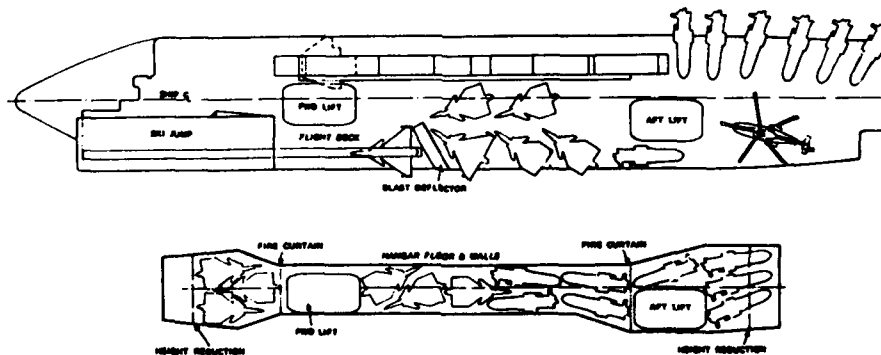


FIG. 17 FLIGHT AND HANGAR DECK SPOTTING

3.2 Deck Environment constraints

A major consideration in the operation of advanced STOVL vehicles on the Invincible class ships is the deck environment generated by the aircraft during the STO and VL manoeuvres.

Clearly the environment generated by Sea Harrier is acceptable and can thus conveniently form the basis or standard for evaluating ASTOVL. The extent to which this environment may be worsened by the introduction of advanced STOVL vehicles, which are larger and generally have more energetic engine exhaust plumes, has been briefly studied.

Fig. 18 shows the exhaust plume conditions at nozzle exit for the Sea Harrier and the 4 advanced concepts. Taking Sea Harrier rear jets as the worst current operating condition, it can be seen that all 4 ASTOVL concepts have rear jets with both higher temperatures and pressures, during STO & VL.

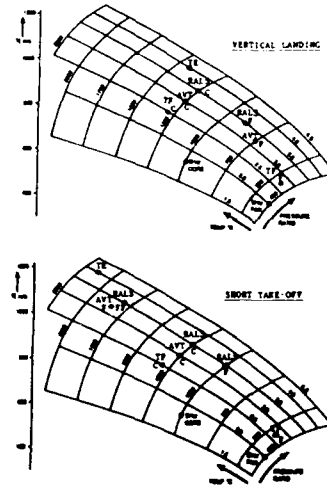


FIG. 18 JET EXHAUST PRESSURES AND TEMPERATURES

For the studies of the ASTOVL ship integration, a 30 metre radial distance from the aircraft during VL and a 15m side line distance during STO have been taken as locations for comparison. These distances were defined for the study and judged to be tolerable for personnel and equipment during Harrier operations. To put these distances into perspective Fig. 19 shows them relative to the Invincible class ship aft deck.

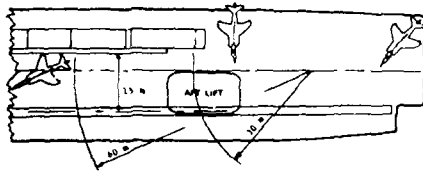


FIG. 19 DECK ENVIRONMENT STUDY

The aircraft generated environment on the ship is discussed under the following topic headings:-

- . Noise at the observer (30m/15m)
- . Radial ground sheet velocity and temperature at the observer
- . Deck surface damage (buckling and erosion)

The increased jet energy of the ASTOVL designs may also create adverse conditions for the aircraft relative to Harrier e.g. ingestion of hot gas into the inlet, acoustic and thermal environment for the airframe and weapons and increased noise in the cockpit, but these aspects are outside the scope of this paper.

3.2.1 Noise at the Observer

Table 3 shows some estimates of the peak noise level at 30 metres from the aircraft during a vertical landing. These suggest that the ASTOVL aircraft could be expected to be at least 7 to 9 dB(A) noisier than Harrier, partly due to increased jet size and partly due to increased jet energy.

At this 30m distance, ear protection is required for Harrier. The additional 7 to 9 dB(A) increase estimated for the ASTOVL concepts means that the attenuation of the ear protection needs to be more carefully considered, with the highest quality passive or possibly an active system employed. Alternatively the observer should be further away, but since 6 dB implies a doubling of distance this would effectively exclude crew from the flight deck. Whereas a good ear defender could probably cope with the ASTOVL noise increment at the ear, the levels are approaching that at which full body protection would be necessary.

TABLE 3
DECK ENVIRONMENT NOISE ESTIMATES DURING THE FINAL DESCENT IS GROUND EFFECT OF A VERTICAL LANDING
observer at 30 metres from the aircraft

CONFIGURATION	O.A.S.P.L. (dB(A))	INCREASE ABOVE HARRIER		
		Due to Size	Due to P. C	Due to Size
Sea Harrier	127	0	0	0
RAIS	135	4.5	3.5	8
TE	135.5	3.0	3.5	8.3
TF	136	4.0	3	9
AVT	136	5.0	2	7

During a STO ground roll, jet aft, the peak noise levels at 15m side-line distance are estimated to be some 4 to 5 dB(A) higher than the peak 30m VL levels. The exposure time to these peaks is very short however, nevertheless crew should not be exposed to such levels without the ear and body protection described and preferably should not be alongside the island during take-off.

3.2.2 Ground Sheet Velocities and Temperatures

During vertical landing with jets directed at the deck, the jet exhaust plumes impinge on the deck and spread out radially. This radial ground sheet decays in velocity and temperature inversely with radial distance. The multiple lift jets create a non-axisymmetric wall jet with peaks between the jets and reduced velocities and temperatures elsewhere. Each of the ASTOVL concepts are different due to differences in jet spacings, temperature and pressure. An example, the RALS concept, is shown on Fig. 20.

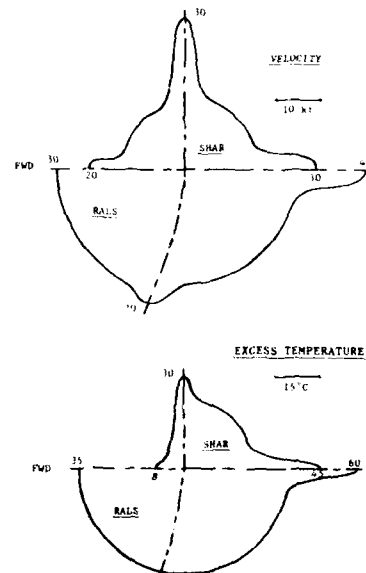


FIG. 20 PEAK GROUND SHEET VELOCITY AND EXCESS TEMPERATURE AT 10m FROM AIRCRAFT DURING VL

At 30m distance the RALS ASTOVL estimates suggest ground sheet velocities about 50% greater than Harrier. The peak velocities are equivalent to gale or near gale force on the Beaufort scale, and over a greater circumference than Harrier.

A similar increase in temperature is estimated but in particular the use of front jet augmentation makes the forward arc much more hostile.

During STO Ground roll the ASTOVL exhaust plumes will be far too hostile for the next aircraft to take-off to sit behind unprotected. A simple folding blast shield to deflect the hot, high velocity exhaust plume up and to port, placed aft of the longest take-off length normally required, is proposed. Fig. 21.

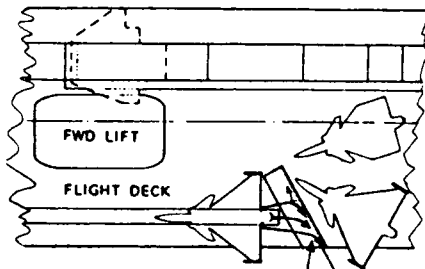


FIG. 21 BLAST DEFLECTOR

3.2.3 Deck Surface Damage

The Invincible class ship deck comprises a relatively thin (12mm) steel plate with an anti-skid surface paint. The anti-skid material "Camrex", is an epoxy resin base with fine grit particles and is painted on to a depth of about 1mm. The steel deck is attached to the ship structure such that intensive local heating can cause thermal expansion buckling. The steel has a relatively high thermal diffusivity but the Camrex diffusivity is low. Consequently the Camrex surface heats rapidly but acts as a partial thermal barrier to the steel. This serves as a useful purpose in reducing the risk of buckling. Despite the relatively low temperature of epoxy (100 to 150°C) the Camrex does withstand Harrier rear jet temperature well, with relatively few erosion problems in vertical landing operations.

Fig. 22 shows the presently defined boundary derived from rig tests. This is thought to be fairly conservative since it makes no allowance for vertical descent rate effects, and is based on rather limited data. It does however agree broadly with practical experience in that Harrier is on the "go" side, with acceptable residence times close to touchdown of about 20 seconds. The ASTOVL rear nozzle temperatures are, however, well beyond the material capability, based on these tests.

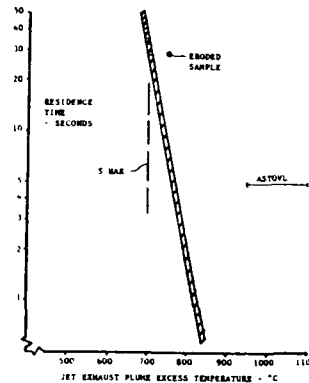


FIG. 22 SHIP DECK SURFACE EROSION LIMIT

For ASTOVL operation a higher temperature capable anti-skid thermal barrier surface coating will be needed, both to avoid surface erosion and deck buckling. The alternatives are to build raised gridded platforms, ducting hot exhaust over the edge of the ship or to limit nozzle exhaust temperatures. The former would have advantages with respect to the ground sheet deck wash, hot gas ingestion and lift loss. The latter approach would have implications on aircraft size and mass, or performance.

4. FURTHER AIRCRAFT DESIGN STUDIES

Under the umbrella of the US/UK ASTOVL memorandum of Understanding, further studies of ASTOVL concepts have been carried out. These studies, referred to in reference 2, included an "Ejector Augmentor" concept in which the front lift thrust was augmented by an ejector, thereby providing a benign footprint at the front end. This concept however did not strike the right balance between vehicle size and footprint conditions and, overall, the conclusions from those studies, for the way ahead, was for a concept with "conventional" mixed cycle engine in forward flight located in the aft fuselage and a powered lift arrangement which did not resort to thrust augmentation by fuel burning. An example of such a concept is shown on Fig. 23 and taken from reference 2. Studies are continuing on this concept.

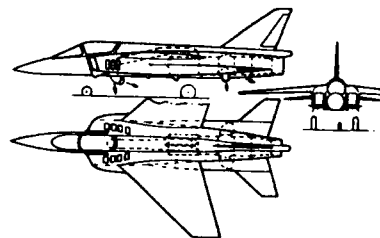


FIG. 23 ASTOVL AIRCRAFT CONFIGURATION WITH MIXED CYCLE ENGINE IN FORWARD FLIGHT

5. CONCLUSIONS

These ship integration studies indicate that introducing an ASTOVL vehicle, with greatly enhanced performance, to replace Sea Harrier on the small, Invincible class ships will have its problems. These problems are principally related to the worsening of the jet exhaust footprint environment during landing.

Whereas some propulsion system developments hold out the prospect of some size reduction and footprint improvement compared with the ASTOVL designs of this study, it is clear that significant reductions in jet exhaust pressure and temperature will have adverse impact on vehicle performance and/or size.

For satisfactory small ship integration further careful performance versus environment trade studies are required and a very delicate balance between size, mass performance and engine exhaust environment will need to be struck.

REFERENCES

1. Fozard J.W. "Harrier - Catalyst for change in Naval Airpower". 25th Sir Charles Kingsford-Smith Memorial Lecture. Sydney Branch Royal Aeronautical Society. 28th September 1983. Revised and reported January 1984.
2. Platt, J.T., Ainscow K., and Stott G. "Evolution of ASTOVL Aircraft Design "Paper II-10" in "International Powered Lift Conference" Royal Aircraft Establishment. 29-31 August 1990.

FIXED WING NIGHT CARRIER AEROMEDICAL CONSIDERATIONS

by

Cdr J.C. "Doc" Antonio
 Naval Weapons Center
 China Lake
 California 93555
 United States

The purpose of this brief is to discuss the emerging use of Night Vision Devices (NVDs) in USN/USMC fixed-wing aircraft, describe the NVD environment and identify areas of aeromedical concern associated with night carrier operations.

NVDs began their entrance into fixed wing upgrades (primarily A-6, FA-18, and AV-8) after a series of evaluations in the early 1980s. Although there are some differences in the application and design between airframes, the basic intent is the same and that is to improve or enhance the existing night capability. In the case of the A-6, which has a terrain following radar, NVDs are applied in the form of night vision goggles (NVGs) and design modifications to the cockpit lighting. This combination gives the A-6 an added capability under the right conditions and will enhance their terrain following mission. The FA-18 and AV-8 upgrades utilize both NVG (image intensification) and forward looking infrared or FLIR (thermal imaging) technologies to enhance their night capabilities.

For those not fully aware of NVDs the FA-18 NVD "system" will be briefly described. Components of the NVD system upgrade for the FA-18 include: a navigation FLIR (NAVFLIR), a raster capable heads-up display (HUD) to receive the NAVFLIR image, helmet mounted NVGs, NVG compatible lighting and a digital map set (DMS). By using both image intensification and thermal imaging technologies the system components complement each other during various portions of the flight and in varying environmental conditions. Enhancements to the FA-18 night strike mission provided by NVDs include:

1. Increased situational awareness (SA). Having a horizon and being able to maneuver using familiar daytime type tactics goes far in enhancing SA during the hours of darkness.
2. Enhanced night navigation. Visually identifying landmarks and "using the terrain" significantly adds to night navigation.
3. Threat avoidance. Terrain masking and other techniques are more readily available.
4. Multi/mixed aircraft tactics. Variations in tactical employment are broadened.
5. Air-to-ground delivery tactics normally reserved for daytime can be employed at night.
6. Night air-to-air tactics are significantly expanded, including the escort mission.

Some limitations to the FA-18 NVD mission include:

1. The system does not allow an all-weather capability. It is for clear air mass/under the weather only.
2. Low ambient light levels reduce maneuvering capability.

3. The system by itself offers limited targeting capability.
4. The full NVD system utilizes aircraft weapon stations.

These enhancements and limitations are specifically describing the impact of NVDs on the FA-18 mission but most are also applicable to the A-6 and AV-8.

As always, a picture is worth a thousand words, so the following video will offer an insight into the NVD world from the pilot's perspective. The video shows:

1. Inflight NVG video taken with an 8mm camcorder focused through an image intensifier tube from an AH-1, UH-1 and FA-18. Various scenes are shown to demonstrate the effects of terrain features, scan patterns, navigational cues, forward firing ordnance, and both internal and external lighting.
2. NAVFLIR video from an FA-18 to demonstrate thermal imaging information presented to the pilot.
3. Video showing split screen imaging from both NVGs and NAVFLIR to demonstrate the complimentary nature of NVD system components.
4. Video of a night low-level Sidewinder launch from an FA-18 taken with an IR camera to demonstrate an aspect of NVD utilization.

As can be seen from the the video and the description of the NVD mission, there are many aeromedical concerns involved; from hardware development, to training, to tactical employment. Comments will be limited, however, to those most obviously concerned with carrier operations. At present only one LHA has been modified with NVG compatible lighting to allow NVD capable aircraft to conduct night operations with aircrew wearing NVGs. This has allowed both the AH-1 Cobra helicopter and the AV-8 to evaluate shipboard lighting modifications and vertical night carrier operations while using NVGs. So far the results have been promising. Currently, no fast attack carrier supporting A6s and FA-18s has been modified for NVG operations. This is mostly due to the fact that present helmet mounted NVGs are not suitable for the forces encountered during launch and arrestment. However NVG night takeoffs and landings at shortbased facilities have proven to be very effective and certainly points towards a significant potential. As for now, all NVD capable aircraft will continue carrier launch and recovery in the usual manner at night. This of course means aircrew must put NVGs on after launch and remove them prior to recovery. This in itself brings up some areas of aeromedical concern.

The following lists a few areas needing research that are applicable to night carrier operations for aircrew using NVGs:

1. Vision testing:
 - a. Red/green discrimination. Does a minor deficiency manifest itself adversely in this environment?
 - b. Contrast sensitivity. Should this be looked at as a better tool in selection for this mission?
 - c. Visual activity. What role does it really play in this environment? Can training offset the loss?
 - d. Retinal saturation. What effect does wearing NVGs for long periods have on color discrimination or contrast sensitivity when they are removed prior to night carrier landing?

2. Hardware design and specification issues:
 - a. What is a physiological acceptable field-of-view for NVGs.
 - b. How can peripheral viewing be enhanced and how important is it?
 - c. What optical adjustments are necessary?
 - d. What impact does the transmissivity of visors, spectacles, laser eye protection, chemical/biological warfare equipment and canopies or windscreens have on the final image's resolution as perceived by the pilot?
3. Physiological issues:
 - a. What effects do long sortie lengths, extended night operations, and fatigue have on visual performance once NVGs are removed?
 - b. Are there spatial disorientation effects specific to post NVG use?

Some aeromedical issues have been researched but few of them specifically address night carrier operations. One notable exception was a study to determine the impact on depth perception after removing NVGs prior to night carrier landings.

The use of NVDs is fast becoming commonplace in the fixed wing, carrier based community and little research has been undertaken to help in its safe and effective employment. This type of capability is here to stay and it's only a matter of time before it will be used to enhance night carrier operations.

LIMITATIONS DES OPERATIONS DES HELICOPTERES DANS LE MILIEU AERONAVAL

par

Capitano di Corvetta D. Falcinelli
Stato Maggiore Marina
6 Reparto Aeromobili
Via Azuni,
00196 Roma
Italy

INTRODUCTION

La majeure partie de ceux qui participent ou qui se sont intéressés pour des raisons professionnelles à l'activité aéro-navale ont certainement déjà entendu parler des problèmes particuliers qui doivent être affrontés par les pilotes pendant l'activité de vol à bord des navires militaires et qui bien souvent limitent sensiblement la disponibilité des aéro-nefs.

Dans ce domaine beaucoup de choses ont été dites toutefois il me semble que les problèmes ont le plus souvent été traités de façon sectorielle et d'un point de vue relativement technique.

Je voudrais aujourd'hui profiter de cette occasion qui m'est offerte et je tiens à remercier de cela l'AGARD, pour Vous présenter ce thème de façon générale et surtout sous un angle légèrement différent, c'est à dire du point de vue de ceux qui comme moi en tant que pilotes ont du faire face à ces problèmes jour après jour pendant leur période de service à bord. Je ne prétends donc pas Vous fournir des explications techniques mais plutôt vous donner une vision générale des aspects plus importants du point de vue du pilotage ou plutôt ceux qui nous posent les problèmes majeurs, en espérant que cela puisse être utile à ceux qui sont chargés ou qui s'intéressent à rechercher des solutions dans ce domaine.

J'avoue que mon expérience est uniquement liée au domaine des hélicoptères, je pense toutefois que quelques aspects concernent les aéronefs en général.

Nous verrons quelles solutions dans les différents domaines ont été développées et adoptées pour faciliter les pilotes dans les phases les plus critiques de l'approche et de l'appontage.

Enfin, très brièvement, nous examinerons ensemble quelles sont en général les qualités requises des hélicoptères, toujours du point de vue des utilisateurs, et qui pourraient sensiblement améliorer leur activité à bord.

LIMITATIONS

Les limitations dues au milieu particulier qui caractérise les opérations de vol à bord des navires sont nombreuses et seule une profonde compréhension des facteurs qui sont en jeu peut permettre de réduire de façon satisfaisante les difficultés qui se présentent en augmentant ainsi la sécurité de l'aéronef et de son équipage.

Dans le milieu aéronautique en général le pilote est normalement entraîné à faire face à des phénomènes atmosphériques bien connus dont les principaux sont la réduite visibilité, les effets du vent et de la turbulence. Mais aussitôt que nous parlons d'activité de vol à bord il faut ajouter à tout cela les mouvements auxquels est sujet la zone d'atterrissage dus principalement à l'action de la mer et du vent sur le navire.

En général les dimensions réduites des ponts d'envol, les obstacles présents à bord du navire, qui ne font que diminuer l'espace à disposition, son mouvement et les conséquentes accélérations qui sont en jeu, requièrent de la part des pilotes un entraînement approfondi et surtout une longue expérience.

Le roulis et le tangage causent de sérieux problèmes pendant les différentes phases qui caractérisent les opérations de vol des hélicoptères embarqués et qui sont: la préparation de la mission assignée qui comporte le déplacement de l'hélicoptère du hangar au pont d'envol et toute l'activité du personnel technique autour de celui-ci; tous les contrôles et la mise en marche des moteurs et des systèmes de bord de la part des pilotes, le décollage et à fin de la mission l'approche au point d'atterrissage, l'acquisition du pont d'envol et l'appontage.

Il y a toutefois des phases qui du point de vue du pilote présentent des difficultés majeures comme par exemple l'appontage et le décollage. Pendant ces deux phases les repères visuels sont nécessaires pour le correct positionnement avant et pendant la phase de poser. La preuve en est que de gros efforts ont été faits dans le cadre de l'OTAN pour standardiser le marquage et le balisage des zones de poser à bord des bâtiments.

A cause des mouvements du navire, ces repères peuvent parfois disparaître du champ visuel du pilote qui peut donc se trouver dans une situation difficile qui peut mettre en danger la sécurité de l'hélicoptère et de son équipage. Naturellement ce problème est amplifié pendant l'activité nocturne lorsque la perception de la profondeur et la vision périphérique, facteurs fondamentaux pendant la phase de poser et de décollage, sont de fait réduits.

En outre si nous prenons en considération les dimensions de la majeure partie des ponts d'envol des Frégates et des Destroyers nous nous rendons compte que nous avons à faire à des dimensions plutôt limitées qui permettent des marges d'erreurs assez réduites. Par exemple les ponts d'envol des navires de la Marine Militaire Italienne ont des dimensions d'environ 24 mètres de long et 13 mètres de large pour les Destroyers et 21 mètres de long et 9 mètres de large pour les Frégates. Toutefois ces zones sont encore plus réduites pour des raisons de sécurité qui limitent la distance de l'hélicoptère des obstacles fixes présents sur le navire. En ce qui concerne enfin le point de poser, comme on peut l'imaginer, le marge d'erreur est ultérieurement réduit.

Cela requiert de la part des pilotes un continuel travail d'ajustement de la position de l'aéronef et donc une intense concentration due au continuel contrôle des repères et simultanément des indications à l'intérieur de la cabine de pilotage. Il faut donc acquérir une profonde expérience qui permettra une bonne et correcte évaluation des conditions en jeu permettant ainsi de déterminer le moment le plus favorable pour l'appontage.

Les mêmes difficultés sinon majeures se présentent lors de particulières missions comme par exemple l'évacuation de personnes à bord de petits bateaux qui ne disposent pas de points d'atterrissage ni de points de repères particuliers, ou pendant les opérations de ravitaillement vertical ou enfin pendant le ravitaillement en vol de carburant navire-hélicoptère.

A cela il faut ajouter les restrictions qui peuvent se vérifier de temps à autre et qui sont directement liées au scénario tactique dans lequel le navire se trouve comme par exemple la nécessité de sa part à maintenir un cap et une vitesse qui ne correspondent toujours pas aux meilleures conditions climatiques et de stabilité du pont d'envol, la partielle ou totale obscurité du navire et parfois, la réduction des communications hélicoptère/navire et des émissions radar, dans le but de ne pas être découverts, et qui ne font qu'augmenter les difficultés rencontrées par les équipages de vol.

Enfin le tangage et le roulis ne créent pas des problèmes qu'aux pilotes mais aussi aux constructeurs aéronautiques. En effet une fois l'hélicoptère posé sur le pont d'envol ces deux mouvements principaux se répercutent directement sur l'aéronef le soumettant à des accélérations verticales et latérales qui requièrent de leur part une particulière attention sur les efforts auxquels sont soumis les points d'ancrage et toute la structure de l'hélicoptère et qui doivent être dimensionnés de façon à supporter des accélérations plutôt élevées non sans tenir compte de la volonté de la part des utilisateurs de ne pas pénaliser outre mesure le poids de l'hélicoptère.

Avant de passer à d'autres limitations voyons quelles seront les capacités requises dans ce domaine aux futurs hélicoptères. En ce qui concerne le roulis il pourra être possible d'atterrir et de décoller avec un roulis de $\pm 15^\circ$ en considérant une accélération latérale d'environ 3m/sec^2 ; un tangage de $\pm 5^\circ$ en considérant une accélération verticale de 4m/sec^2 ; en ce qui concerne les capacités de déplacement de l'hélicoptère et d'hangarage le roulis envisagé sera de $\pm 20^\circ$ avec une accélération latérale de 3m/sec^2 , le tangage sera de $\pm 6^\circ$ avec une accélération verticale de 5m/sec^2 . Il y a bien sur des Marines qui ont la capacité d'opérer avec des valeurs de tangage et de roulis bien plus élevées non sans disposer de systèmes particuliers que nous verrons rapidement par la suite.

Nous avons vu jusqu'à ce point un des aspects, certainement le plus important, des limitations auxquelles doivent faire face les pilotes embarqués. Un autre facteur, sans doute limitatif du point de vue du pilotage aussi bien que pour l'aéronef lui-même est du aux effet de la turbulence sur le pont d'envol. En effet l'interaction du vent et des structures du navire créent dans la majeure partie, nous pourrions dire même dans la totalité des cas, des conditions de turbulence sur le pont d'envol, qui se différencient de navire a navire et qui affligent directement les caractéristiques aérodynamiques de l'hélicoptère. Il est souvent difficile sous cet aspect de quantifier toutes les données en jeu et d'évaluer l'effet résultant mais en même temps il est nécessaire d'avoir une idée plus ou moins correcte de ces interactions de façon à en prévoir les conséquences. Il est donc nécessaire d'effectuer des tests en mer de façon à obtenir une évaluation correcte et globale du problème et des effets qui peuvent dériver.

La présence de la turbulence ne fait qu'augmenter les capacités qui sont requises de la part des pilotes, et la nécessité de disposer d'hélicoptères dont les commandes de vol répondent immédiatement aux corrections de la part du pilote et aussi d'un bon marge de puissance à disposition.

Un autre facteur limitatif que nous devons considérer est le vent qui dans le milieu aéronaval se distingue en vent relatif et absolu. La capacité de supporter plus ou moins bien l'impact du vent est sensiblement liée aux caractéristiques du rotor de queue. Les limitations se différencient en fonction du secteur de provenance et a chaque secteur est liée une intensité maximale qui ne peut être dépassée. Là aussi les limitations majeures se vérifient au moment de l'appontage et décollage.

En effet suivant les cas il pourrait se créer des situations pendant lesquelles pour contraster les effets du vent le pilote pourrait avoir besoin d'effectuer des manoeuvres plutôt brusques et accentuées qui pourraient lui faire perdre la vision du point d'atterrissage ou qui pour les cas les plus extrême lui rendent impossible le contrôle de l'hélicoptère.

Pendant la phase de décollage le problème est plus ou moins le même toutefois il ne faut pas oublier que lorsque l'hélicoptère sort de l'effet du pont d'envol il perd de portance et si dans ce cas le vent absolu proviens des secteurs arrières le pilote pourrait se trouver dans des conditions assez critiques surtout si le marge de puissance à disposition est limité.

Le vent à similitude d'autres facteurs pose des problèmes, ou plutôt des limitations dans la phase de préparation au vol. Il suffit de penser qu'au delà d'une certaine intensité il peut être impossible de déplier le rotor principal ou même de l'engager.

Il faut enfin tenir compte des aspects, qui peuvent paraître secondaires mais dont toutefois il faut tenir compte comme par exemple les espaces réduits pour la mise en oeuvre de toutes les manutentions nécessaires à l'hélicoptère et de particulières interventions qui en général requièrent un certain espace à disposition tel que le changement d'un moteur, de la transmission ou d'une pale. Il y a aussi les effets plutôt négatifs que la salinité a sur la structure et tous les équipements de l'hélicoptère. Enfin, et non pas le moins important, la tenue de l'hélicoptère sur le pont et la nécessité, en cas de mer agitée, qu'il soit accroché sur le pont immédiatement après s'être posé.

Nous avons donc vu jusqu'à maintenant tous les principaux facteurs qui influencent plus ou moins négativement et donc limitent les opérations de vol a bord. Je voudrais donc Vous rappeler en quelques mots les efforts techniques qui sont faits ou qui ont été faits dans ce domaine pour la réalisation de systèmes de bord qui permettent de réduire l'impact de ces limitations et donc d'augmenter les capacités opératives des hélicoptères.

SYSTEMES D'AIDE AUX OPERATIONS DE VOL.

Compte tenu de toutes les difficultés que nous venons à peine de voir, il est nécessaire que les navires disposent de systèmes d'aide qui puissent en quelque sorte faciliter la tâche des pilotes.

Comme je Vous ai dit auparavant le moment le plus critique pour le pilote en cas de mouvements plutôt soutenus de la plateforme sur laquelle il doit se poser est celui de trouver l'instant le plus favorable pour atterrir et de gros efforts se font aussi dans ce domaine pour créer des systèmes qui puissent prévoir et fournir une correcte indication et information avant l'atterrissage tenu compte des majeurs facteurs qui influencent le mouvement du navire.

Les autres systèmes à disposition sont le balisage et repères visuels, les systèmes d'aide a l'appontage et au déplacement de l'hélicoptère sur le pont et les systèmes d'approche aussi bien à vue qu'instrumentales.

BALISAGE ET REPERES VISUELS

En dehors du cercle d'appontage qui indique la zone de poser, il existe plusieurs lignes de repères comme la ligne de dégagement avant qui est la ligne transversale indiquant la limite de la position avant de l'hélicoptère, dans certains cas on peut trouver une ligne de position avant/arrière qui n'est autre que la ligne de référence transversale permettant de déterminer la position avant/arrière de l'hélicoptère. Il existe en plus la ligne qui indique la trajectoire d'alignement et qui sert de repère pour la trajectoire que doit suivre l'axe avant/arrière de l'hélicoptère pour se poser dans la position correcte, et la ligne de position latérale qui indique la référence avant/arrière permettant de déterminer la position latérale de l'hélicoptère. En dehors de ces indications principales il en existe d'autres comme la ligne périphérique qui indique la zone claire d'obstacles, la ligne périphérique avant est généralement appelée ligne de dégagement avant. La ligne délimitant l'aire de manoeuvre ou de stationnement sur le pont qui indique l'endroit précis où l'hélicoptère doit stationner ou effectuer ses manoeuvres. En ce qui concerne la trajectoire d'alignement la ligne qui l'indique est parfois prolongée jusqu'à la façade et au sommet du hangar.

Voyons maintenant quels sont les principaux repères nocturnes utilisés par les pilotes. Il y a tout d'abord les feux d'axe d'approche qui indiquent l'alignement de l'hélicoptère pendant la phase d'approche. Il existe ensuite un certain nombre de projecteurs qui sont installés de façon à éclairer la façade du hangar améliorant ainsi la perception du pilote de la profondeur et lui montrent l'obstacle lui-même; d'autres éclairent le sommet du hangar toujours dans le but d'améliorer la perception de la profondeur et font ressortir un plus grand nombre de détails à l'horizon pour le cas où l'hélicoptère se trouvant au-dessus de la zone de poser, le pilote n'est pas en mesure d'apprécier clairement le pont d'envol éclairé. Il existe en plus des barres d'horizon et de tangage stabilisées pour donner aux pilotes des repères horizontaux précis. Il y a enfin d'autres feux qui fournissent des repères visuels supplémentaires comme par exemple l'éclairage des bords du pont, les trajectoires d'alignement et d'alignement prolongés, l'éclairage vertical (drop line), les feux d'axe d'approche, les trajectoires d'alignement a haute intensité, l'éclairage du pont de poser, les balises lumineuses de ralliement et les indicateurs de pente d'approche que nous examinerons plus tard.

Toutes ces indications peuvent sembler excessives toutefois les dimensions des ponts en jeu et la précision requise rendent ces indications nécessaires.

SYSTEMES D'APPONTAGE ET DE DEPLACEMENT

Je pense qu'un bon nombre d'entre Vous si ce n'est tous connaissent la grille Harpoon qui a résolu un problème important permettant d'assurer la tenue de l'hélicoptère sur le pont d'envol immédiatement après l'atterrissage, en évitant ainsi l'intervention de personnel externe et réduisant sensiblement le temps pendant lequel l'hélicoptère soumis au mouvement du navire pourrait difficilement maintenir sa position sur le pont.

Laissez moi Vous dire qu'en tant que pilote il n'est vraiment pas agréable de devoir attendre juste après l'atterrissage, et surtout en cas de mer agitée, que le personnel chargé d'assurer l'hélicoptère au pont vienne autour de l'hélicoptère pour effectuer ce genre d'opération. Ou bien dans le cas contraire pendant la phase de décollage lorsque trois sur quatre des points d'attache sont libérés et que le quatrième pour quelques raisons reste accroché et que l'hélicoptère commence à pivoter. Ce sont des situations dangereuses et qui ne donnent aux pilotes aucune possibilité d'intervention. Je vous assure que ceci peut se produire assez facilement surtout si l'on dispose d'hélicoptère avec un train d'atterrissage à patins et qui tendent plus facilement à glisser sur le pont quand les valeurs de roulis et de tangage sont proches des limites consenties.

Le Harpoon naturellement ne résoud que la partie finale du problème c'est à dire le problème de la stabilité de l'hélicoptère après l'atterrissage. Des progrès ont encore été faits et il existe actuellement des systèmes qui permettent l'accrochage de l'hélicoptère quand il est encore en vol stationnaire sur le pont et qui ont la capacité de pouvoir le guider ainsi dans la descente jusqu'au contact définitif avec le point d'atterrissage. Le même système peut par la suite être employé pour conduire l'hélicoptère à l'intérieur du hangar. Je Vous passe la description technique des principaux systèmes qui existent actuellement car il y a en a de toutes sortes et il semble qu'au moment actuel chaque Marine ait son propre système avec des solutions techniques souvent très différentes entre elles. Mais le problème est senti surtout pour ce qui concerne le déplacement de l'hélicoptère et la preuve en est que plusieurs Sociétés sont aventurées dans l'étude et la réalisation de ce genre de systèmes. Naturellement ceci ne favorisera pas l'interopérabilité tant souhaitée dans le cadre de l'OTAN.

SYSTEMES D'APPROCHE

En ce qui concerne enfin la phase d'approche de l'hélicoptère au navire de nuit les pilotes utilisent actuellement des systèmes lumineux pour visualiser et suivre le sentier de descente aussi bien que pour individuer l'exact alignement par rapport au navire même. Les sentiers lumineux indiquent généralement trois faisceaux lumineux qui sont le plus souvent de couleur ambre verte et rouge, ils sont stabilisés pour un mouvement du pont d'envol qui peut aller jusqu'à +/- 10 degrés de roulis et +/- 6 degrés de tangage. A l'exception du sentier correct de descente qui est le plus souvent de couleur verte, dans certains cas les autres faisceaux lumineux, généralement rouge (position au dessous du sentier) ou ambre (position au dessus du sentier), peuvent être intermittants indiquant ainsi une position de l'hélicoptère extrêmement élevée ou extrêmement basse par rapport au sentier de descente. La stabilisation a sensiblement diminué le problème qui se posait auparavant lorsque il était possible, à cause du mouvement de la plateforme, de perdre la vision du sentier lumineux.

Pour l'approche instrumentale plusieurs Marines utilisent le TACAN toutefois il se pourrait que dans un futur assez proche des systèmes d'approche du genre MLS soient disponibles à bord des bateaux militaires.

QUALITES REQUISES DES HELICOPTERES

Je voudrais avant de conclure examiner quelles sont les qualités requises ou du moins souhaitées de la part des pilotes pour faire face aux problèmes que nous venons d'examiner.

Naturellement, comme Vous pouvez le déduire de ce que nous avons vu auparavant, il est requis que l'hélicoptère ait une bonne stabilité quand soumis aux effets de la turbulence et aussi une immédiate réaction aux commandes pour ne pas dépasser outre mesure la charge de travail du pilote. Qu'il ne ressente pas ou du moins de façon limitée des effets du vent et ceci doit se refléter principalement dans les capacités du rotor de queue. Il est souhaité en outre que pendant les différentes manoeuvres il ne soit pas nécessaire d'effectuer des variations sensibles d'attitudes, qui pourraient faire perdre la vision des points de repère, et que le champ visuel de la cabine de pilotage soit le plus ample possible.

CONCLUSIONS

En conclusion, nous avons vu que les opérations des aéronefs et en particulier des hélicoptères présentent diverses limitations dues au particulier milieu aéronaval et qui sont en résumé les réduites dimensions de la place à disposition, les mouvements du pont d'envol, le vent et la turbulence. Une adéquate définition des caractéristiques nécessaires dans la phase de définition du projet de l'aéronef est certainement fondamentale à fin de réduire l'impact de ces limitations et faciliter ainsi les pilotes. Les efforts qui doivent être entrepris pour effectuer les opérations de vol à bord des navires peuvent être sensiblement diminués par une profonde préparation qui consiste à obtenir des informations détaillées sur les capacités aérodynamiques de l'hélicoptère, de l'interaction du vent et de la structure du bateau et des résultats qui en dérivent en effectuant des tests approfondis et une profonde et détaillée analyse des résultats.

REVOLUTION AT SEA: Aircraft Options for the Year 2030

James C. Biggers
ARC Professional Services Group
Atlantic Research Corporation
8201 Corporate Drive, Suite 350
Landover, Maryland 20785
and
Peter A. Silvia, U.S. Navy
Code 1261
David Taylor Research Center
Bethesda, Maryland 20084
U.S.A.

1. SUMMARY

Some innovative options for future aircraft and a revolutionary approach to the ships from which they operate are presented. Some options have been explored through the preliminary design stage, some are only at the conceptual design stage, and others are mere speculation. The limitations of the present fleet are noted, along with some possible solutions. All options assume the integration of ships and aircraft in more depth than previously. The objective of the paper is to create in the reader a vision of the future surface and air fleet that is significantly different from today's Navy, and to get the reader involved in bringing this vision to reality.

2. PREFACE

This paper is intended to stir up your thinking. It poses some ideas that may be controversial as it takes a new look at the roles of both ships and aircraft. Whether or not you agree with the ideas put forward, this paper will have accomplished its purpose if it results in a broader view of future possibilities. Because of the lead time in developing new classes of ships and aircraft, the future is NOW. We must begin immediately to make the decisions and accomplish the research for the systems that will be incorporated into Naval Aviation of the year 2030. We must address the questions of what aircraft will be needed, what will their missions be, and therefore what technologies must be developed.

3. FORCES FOR CHANGE

In Reference 1, the former U.S. Chief of Naval Operations, Admiral Carlisle Trost, laid out a number of principles central to the re-evaluation of the nation's naval strategy. His first point is that "responding to crises is a traditional naval mission". Admiral Trost goes on to say, "Naval forces enjoy particular advantages which make them ideal for responding to crisis situations." Whatever form the future may take, aircraft and ships will continue to be expected to provide these advantages as tools of national

policy. However, many factors already in operation will change the size, shape and structure of naval aviation. The primary forces for change are listed below.

FORCES FOR CHANGE

- CONTINUING SOVIET POWER
- THIRD WORLD POWER
- POLITICS & ECONOMICS
- TECHNOLOGY TRENDS

Table 3-1. Forces for change in the future fleet.

3.1 Continuing Soviet Power

Admiral Trost's second point is that "the Soviet Union, because of her geostrategic dominance of the Eurasian land mass and latent military power, will remain a power with which to reckon." Soviet hardware, the result of decades of investment of nearly 20% of their gross national product and half of their R&D money and manpower, will continue to pose a powerful threat to her neighbors and to the United States.

3.2 Third-World Power

The third and fourth points which Admiral Trost makes—that the most likely military engagement is "low intensity conflict", and that developing countries are armed with "First World" weapons—expand upon the range of possible military actions.

Three parallel evolutionary paths are operating to ensure the escalation of technology and lethality of low intensity conflict, also referred to as Contingency and Limited Objective Warfare (CALOW). First, the continual drive for "user friendliness" in computer-based systems means that high-tech weapons will become easier for third-world forces to operate. Second, industrial base considerations

and the economics of defense jobs around the world practically guarantee the accelerated transfer of ever more sophisticated weapons to the developing countries. Third, the export of high-tech manufacturing equipment means that third-world countries can build their own modern weapons systems. The reality of this threat is illustrated by Iraq importing technology from several countries to produce nuclear and chemical weapons of mass destruction.

3.3 Political and Economic Possibilities

In addition to what is ordinarily thought of as political instability in the "third" world, there is also the instability being created by major shifts in relative economic power in the "first" and "second" worlds. There is always the possibility that regional or national political and economic imperatives will drive a wedge between presently friendly high technology countries.

4. TECHNOLOGY TRENDS

Throughout history, the military organizations of the world have stimulated many technological advances. We have seen the results of today's military technology in the recent Persian Gulf conflict. Even as recently as ten years ago, few of us would have thought that such weapons would be so successful on such a wide scale. What have we to anticipate for the next 40 years?

4.1 Megatrends

Before examining the trends in technology, let us look at a broader perspective. In his prescient book, *Megatrends*³, John Naisbitt wrote of the rapid change away from the industrial society toward the information society. By this, he means the trend toward the processing and use of information, applying the growing capability of computer systems. In the more recent book, *Megatrends 2000*⁴, Naisbitt and Aburdene devote an entire chapter to the Pacific Rim and its expected growth in economic power, while expanding further on the information society trend in other parts of the book. This implies a changing threat for military systems, as we point out later. With these overall trends in mind, set us now examine the technologies applicable to military weapons. Figure 1 indicates the important technologies we must track for the future fleet.

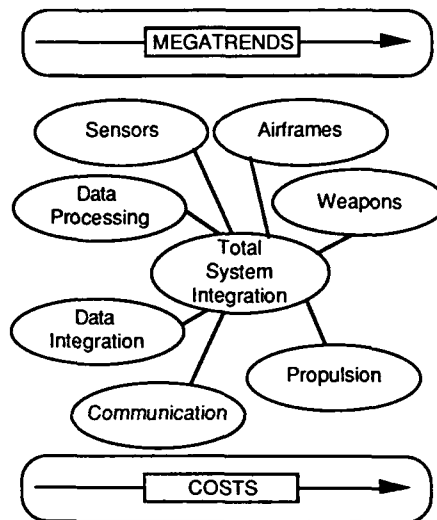


Figure 1. Important trends for future planning

4.2 Sensors

We have all recently seen news reports of the sensitive infrared and low light level vision systems used in the Persian Gulf. By the year 2030, further improvements in sensors will be available, with higher sensitivity, wider spectra, lower power requirements, automatic digitizing and built-in communication devices. Collecting data from numerous widely-spaced sensors will produce large apertures for further increasing sensitivity while providing directional information. Additional data processing will increase the ability to discriminate between targets and provide more information about each target.

One important new addition will be increasingly sensitive microphones and hydrophones. As future submarines become quieter, more sensitive hydrophones will be needed for detection and localization. As hydrophones become more sensitive, the aircraft designers will be forced to create much quieter air vehicles.

4.3 Data Processing

Development of smaller, faster computer chips will continue. Advanced memory devices will allow us to store vast amounts of information and access it very quickly. Detailed maps of virtually every place on Earth could be available for navigation systems. Already one can purchase charting chips for some commercial loran sets. These chips produce a chart on the screen that shows where the boat is located along with all the normal coastal chart information, including depth contours. Consider what could be done by combining aeronautical charts with the Global Positioning System! How long will it be until one of the chart makers produces a "You are here" system for aircraft navigation?

4.4 Data Integration

One application of the faster computer chips will be to combine the data from many sources. This will bring us the capability to integrate the output from many sensors and put the results into a full color, enhanced 3-dimensional image. The image would combine all the information from all sensors, and could include data from other sources through high-speed communication. Then using the high-speed computing capability, we can analyze the total situation, and indicate favorable options to the viewer.

4.5 Communication

Advanced communication systems will allow us to gather information from many widely-dispersed sensing systems as inputs to our image integration system. These systems might use low-power bursts, with wide spectrum transmission. Security of the information will be enhanced due to the low probability of intercept of the wide-spectrum signals as well as the additional encryption that wide-spectrum transmission offers.

4.6 Total System Integration

Using the above systems and integrating them into a single entity will permit collect data from a wide variety of sensors and sources, display the resulting image(s), analyze the situation, and develop options for success. With the processor speeds available, these actions can take place essentially in real time. Furthermore, the built-in testing features and redundant paths in the computer will allow self-diagnosis and repair. Furthermore, vehicle controls and navigation systems will be integrated into the total information systems. The resulting system could provide continual monitoring of all vehicle subsystems, diagnosis of problems, and possibly automatic compensation for failures.

4.7 Airframes

Integration of aerodynamics and stealth technology coupled with advances in composite structures is likely to lead to aircraft with very high performance and very low observables. The high speed microprocessors applied to "smart structures" technology will allow us to develop aircraft structures and contours that automatically adapt to rapid changes in flight condition and will compensate for damage or malfunctions.

New aircraft concepts such as the Tiptop⁵ unmanned air vehicle (UAV) and advanced applications of Tiltrotor technology will provide further options for air vehicles operating from small deck ships. To compensate for the growth of high performance aircraft, powered lift systems will be required for operation from aircraft carriers. The Short Takeoff, Vertical Landing (STOVL), tiltrotor and tilt wing developments could be very valuable for the future of Naval Aviation, especially when operating from smaller ships. Other high lift systems such as Circulation Control⁶ can be used to reduce the speed and hence the kinetic energy of carrier based aircraft as they approach the landing deck.

High performance fighter and attack aircraft will routinely cruise at supersonic speeds. Already we see the U.S. Advanced Tactical Fighter programs where, according to the aerospace press, supersonic cruise speeds are achieved without using afterburners.

Missile speeds will continue to increase. Hypersonic speeds will be necessary to intercept the high performance aircraft of the future. The future missiles may be able to out-maneuver the manned aircraft. It is even conceivable that missiles will be developed to intercept the air-to-air missiles, as well as air-to-surface missiles. Advanced structures and materials will play a strong part in making this possible.

4.8 Propulsion

Trends in propulsion systems suggest there will be continued advances in present systems, but new options will develop.

Gas turbines will continue to grow in power or thrust per unit of weight. New high temperature materials and cooling techniques will make it possible to obtain much higher performance and longer life from turbine engines.

Liquid hydrogen fuel, already planned for most Aerospace Planes, will be explored more fully, and offer much lower fuel weight, but higher volume, than present fuels. The resulting lower weight will decrease the induced drag of the aircraft and compensate for the higher fuel volume in many applications⁷. Use of hydrogen fuel can contribute to lower weight carrier aircraft, prolonging the life and utility of the large carriers. Furthermore, hydrogen fuel is much less polluting than hydrocarbons, so its increased usage may be dictated by environmental concerns.

Advances in hydrogen-oxygen and hydrogen-air fuel cells will offer the option of all-electric propulsion. This will be made more attractive by the efficient, light-weight electric motors now under development in many countries. This combination could also yield a system having a much lower infrared signature. Furthermore, electric propulsion may offer additional options for configuration design, since the fuel cell or generator can be located remotely from the propulsor. This approach has been taken in the design of the future ships discussed later.

4.9 Costs

We must be creative in reducing the enormous costs of military systems. As the military budgets come under increasing pressure, there may be much less funding for military research. Furthermore, there will be very few new weapon systems developed, hence even less opportunity for research to be done in conjunction with new military vehicle developments.

One approach is to adapt commercial products to military missions. Most of the technology trends discussed above are even more evident in the commercial sector. Also, commercial products rarely suffer from the long development cycle typical of the military procurement process. If we can find inexpensive ways to militarize the commercial products, we can obtain many of the benefits at very low cost.

5. TECHNOLOGY IMPLICATIONS FOR THE FLEET OF 2030.

What are the implications of the technology advances noted above? The detailed trends are noted in many of the scientific publications. However, without dwelling on

quantification of the advances, we can readily see some of the possibilities.

Air and sea vehicles can be developed to operate with a great deal of autonomy. Satellite and inertial navigation systems coupled with map information will allow such vehicles to go to specified locations using a programmed route. Onboard intelligence would allow the vehicle to modify the route, depending on what other events occurred. The sensors will allow a vast amount of data to be obtained. The communication systems will allow this data to be quickly transmitted to a base or ship for further processing and integration with information from other such vehicles. The computers will analyze the integrated information and present viable options and recommendations to the decision makers. Perhaps in that future time, the major cities will use computer technology to improve control of traffic!

The trends noted above are echoed in the following excerpts from the Century 21 panel's vision of the U.S. Navy 30 to 50 years hence⁸.

- o The Contest for information will dominate maritime warfare.
- o Surveillance that is global in scope will be a routine feature of military operations.
- o Significant portions of U.S. and opposing forces will incorporate stealth technology.
- o The "battle space" will continue to expand--forces will cover more area while becoming more integrated through the information system.

As weapon intelligence and range increases, the problem of detecting, classifying and targeting threats becomes greater. Battle damage assessment becomes more difficult. A stealthy threat multiplies the problem.

A naval task force spread over the ocean will depend upon communication links and offboard sensors for its overall effectiveness. As information networks improve, we will witness what Naisbitt³ calls the collapse of the "information float," the lag between the time when an event occurs and the time when "everyone" knows about it. In 2030, those to whom it is important will probably know where every ship, and possibly every aircraft, is at all times, anywhere in the world. The battle between stealth and deception versus detection will be intense.

5.1 Technological Obsolescence

Before discussing the future aircraft, we must consider the present aviation support ships and how they might evolve by the year 2030. The Forrestal class aircraft carriers have reached the practical limit of their evolutionary path. The forces of change may require a fresh start with a clean sheet of paper⁹.

In 1955 the USS Forrestal (CV-59) embodied all the features considered essential in top-of-the-line big-deck carriers: angled deck, deck-edge elevators, steam catapults, and four-wire arresting gear. Subsequently, other supercarriers were designed and built, each one a little larger. The arrival of the F-14 Tomcat in 1972 began to push the limits of the old Forrestal/Kitty Hawk design. In 1975, the USS Nimitz (CVN-68) design expanded the Forrestal concept to its maximum.

If the future evolution of top-of-the-line fighters continues along its present path, they will exceed even the capabilities of the Nimitz and her follow-ons. The problem is the continual rise of minimum controllable flying speed linked with increasing aircraft weight. This combination imposes increasing energy requirements on the catapults and arresting gear.

With catapult and arresting gear lengths essentially unchanged since 1955, the only way to handle higher flying speeds and greater weight is to increase acceleration for launching (and deceleration for landing) and the resulting forces imposed upon the airframe. The catapult tries to pull the aircraft's nose off, and the arresting gear tries to rip off its tail. In between, the airframe has to be heavily reinforced. So naval aircraft suffer a structural weight penalty. This limits our range and weapons payload compared to land-based threat aircraft which do not have to accommodate the structural abuse of carrier basing.

It is time to re-think the geometry and layout of the big-deck carrier. As launch and recovery speeds of the aircraft increase, the aircraft weights are increasing as well. To handle the resulting higher kinetic energy, we need longer catapults, or catapults combined with ski-jumps, and longer run-out for the arresting gear. This means redesigning the entire flight deck. While we are at it, we can make significant reductions in signature and in our ability to cope with contaminated environments. We can also change the whole shape of the battle force. However, this will take some innovative thinking and a willingness on the part of the naval aviation community to boldly break new ground.

5.2 Wild Cards

While re-thinking the battle force, here are two wild cards that further complicate matters:

First, as we conceive of ever more capable, innovative big-decks, reality reminds us of the "A" word: Affordability. How can we afford enough decks if the big ones must get bigger? Later in this paper we examine an alternative carrier battle force structure that allows us to make better use of our big deck carriers by offloading some of the less demanding missions to ships the size of LHDs. As budgets

get tighter, we will be forced to take some of the carriers out of service, so a lower cost alternative becomes inviting.

Second, there has been an evolution from manned aircraft to unmanned aircraft and missiles. Missiles do not care how many "g"s they pull. This will greatly increase the vulnerability of manned aircraft in the future, especially as missile speeds increase. In the Iraq campaign, the first systems that went in were very stealthy aircraft and cruise missiles and they did an excellent job of opening the skies for the venerable old B-52s.

Modern anti-aircraft weapons can make the skies too dangerous for any kind of manned aircraft. "Third world" weapons can be taken out with the planes and missiles we have now. Have we reached the end of the evolutionary development of manned aircraft? Once the smart missiles have neutralized the air defense, do we need anything higher tech than F/A-18s?

6. A REVOLUTIONARY APPROACH

By considering the battle force as a system to be designed as a whole rather than as individual ships and aircraft with specific missions, large improvements in military effectiveness and affordability can be achieved. What follows is a brief summary of one vision for the 2030 time period.

6.1 Present Surface Fleet

To help focus a vision, the shortcomings of the present surface Navy must be examined. In a paper presented in 1989 at the SNAME Ship Production Symposium¹⁰, the most significant shortcomings in the current surface Navy were noted as:

- o Highly observable ship signatures
- o Easily distinguished ship signatures
- o Logistically demanding fleet
- o Programmatically inefficient and expensive to acquire

The ships of the current surface navy are highly observable by radar, acoustic, infrared, magnetic, and electro-optical sensors. The result is that the enemy can, in most cases, engage our surface forces from outside the battle space of our own defensive weapon systems. This is shown graphically in Figure 2.

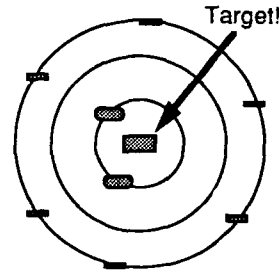


Figure 2. Appearance of Current Fleet.

Forty-two classes of surface ships currently operate in our carrier battle groups, surface action groups and other task forces and groups. Each of these ship classes has unique signatures that allow the enemy to discriminate between ships within a surface force. This allows an enemy to focus fire power on whatever type of ship their strategy identifies as important. Furthermore, all these specialized ships with minimum standardization are expensive to support and maintain. The new approach results in only three major ship classes.

6.2 The Future Battle Force and Its Ships

Investigations at David Taylor Research Center (DTRC) under the Technological Strategic Planning banner describe an alternative battle force architecture titled Distribute, Disperse, Disguise and Sustain (D³+S)¹¹, Figure 3. It should be noted that all of these ships are aviation ships, that is, we believe that aviation will be integrated into the ships just like other weapon systems, and are equally important!

THREE SHIP TYPES FOR D³+S

Distribute	}	New CVN+
Disperse		CLO, Carrier of Large Objects
Disguise		Scout Fighter (SF)
+		
Sustain	=	Design for sustainability

Figure 3. The new fleet types.

The D³+S alternative battle force is designed to:

- o promote increased force flexibility and mission survivability through the distribution of warfare and support functions among the ships of the

- o battle force,
- o disperse the fleet, making targets harder to associate with other ships,
- o be less detectable, less distinguishable and hence less targetable, through signature reduction and similarity,
- o be more sustainable by virtue of increased endurance, force-wide vertical onboard delivery and reduced parts inventory through extensive ship system similarity, and
- o retain the mobility features of our current force architecture.

A central feature of this architecture is a multi-function ship called the Carrier of Large Objects (CLO). One vision of the D3+S force architecture has been taken to a feasibility level of design wherein the CLO concept was expanded into the Carrier Dock Multimission (CDM). In the CDM adaptation of D3+S, published in reference 10, there are three basic ship classes: the Scout Fighter (SF), the Carrier Dock Multimission (CDM) and a new Big-deck Carrier (CVN+), as previously noted. Large objects include those listed in Table 6-1. The goals of this new ship are indicated in Figure 4.

LARGE OBJECTS FOR CLO

- AIRCRAFT AND AIRCREWS
- LOGISTICS SUPPLIES
- AMPHIBIOUS ATTACK GROUPS
- LARGE COMBAT SYSTEMS
- AUTONOMOUS VEHICLES
- OTHER (COMMAND, REPAIR, ETC.)

Table 6-1. Large objects to be carried by the CLO.

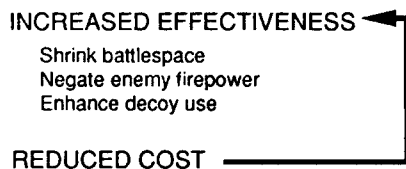


Figure 4. Goals of CDM.

The primary means of aviation power projection remains a carrier battle group centered around the big-deck aircraft carrier, but with CDMs accompanied by scout fighters instead of the present mix of cruisers, destroyers, frigates and logistics ships. The strike mission is supplemented by cruise missiles and Short Takeoff/Vertical Landing (STOVL) fighter/attack aircraft staged from aviation CDM variants. In the alternative battle force, the same number of

heavy strike aircraft are carried by a reduced number of Nimitz replacement new design big-deck aircraft carriers. This is possible due to the distribution of some aviation missions (namely long range anti-submarine warfare, airborne tanker duty and some surveillance) and their aircraft to the CDMs. Some CDM variants and the SF are shown in Figure 5.

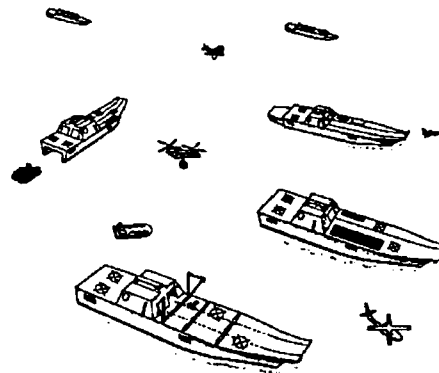


Figure 5. CDM, SF and aircraft.

The result of incorporating this new approach would transform the signatures and appearance of our navies as indicated on Figure 6. Not only would all signatures be reduced, but it would be fairly easy to disguise a Scout Fighter as a CLO, much to the surprise of an attacker.

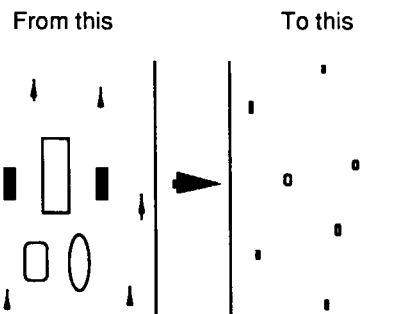


Figure 6. Transformation of the fleet.

6.2.1 The Scout Fighter

The Scout Fighter serves as the eyes and ears of the battle force. Its size is between that of a frigate and that of a destroyer--about 150 m (500 ft) long and 5000 tons displacement. Its concept is a more affordable outgrowth of the 1989 Battle Force Combatant (BFC). Its functions are to serve as the outer screen for anti-aircraft warfare (AAW)

and anti-submarine warfare (ASW). It has a 61 cell vertical launch missile system (VLS), a 155mm gun and two 30mm close-in weapons systems (CIWS). It tows a multi-line acoustic array. Its embarked aviation consists of vertical takeoff and landing (VTOL) unmanned air vehicles (UAVs). There is also the capability to refuel and rearm helicopters and STOVL aircraft. A sketch of the SF is shown in Figure 7.

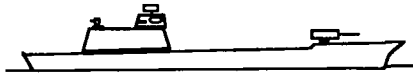


Figure 7. The Scout Fighter.

6.2.2 The Carrier Dock Multimission

The functions now concentrated on distinctive ships such as cruisers, amphibious assault ships, and logistics ships are performed by this one multi-purpose class of ships. CDMs are intended to carry the following large objects:

- o Aircraft, their operating and support equipment, and their personnel
- o Marines and their amphibious equipment
- o Logistics material and transfer equipment
- o In the future, autonomous vehicles (air, surface and

subsurface)

Each of the CDM variants is extremely similar externally to the others and all variants have the capability of short takeoff/vertical landing (STOVL) aviation. The variants differ in internal arrangement as required by the demands of the large objects carried, but they utilize similar subsystems such as the propulsion plant, crew quarters, ship controls, etc. to the maximum extent possible.

The CDM variants have many similarities to an LHD. They are about 235 m (770 ft) long and generally 30,000 to 40,000 long tons displacement (full load). They have a well deck aft for Landing Craft Air Cushions (LCACs) or other modular deployable vehicles for various surface and subsurface missions. In general appearance, a CDM has an aft deckhouse with a VTOL pad at the stern. Forward of the deckhouse is an unobstructed flight deck for short takeoff/vertical landing (STOVL) aircraft. The CDM topside configuration, although radically different from current air capable practice, has several advantages. The topside and superstructure of the ship would be clean, smooth and shaped for low signatures. There would be a hangar below the flight deck big enough to house all embarked aircraft during transit so there would be minimal clutter on the deck in order to reduce radar signature. The superstructure also has hangar space at its base for aircraft and aircraft handling gear. One variant of the CDM is shown in Figure 8.

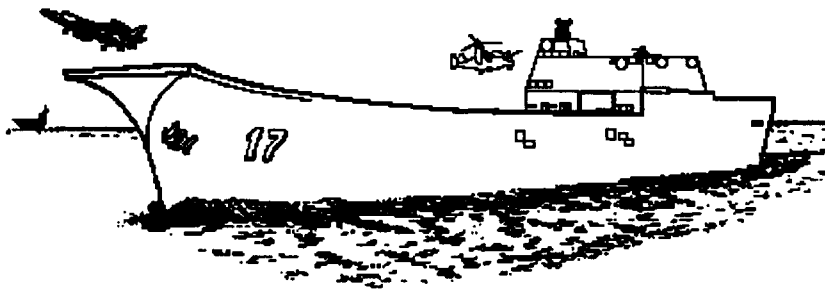


Figure 8. One CDM variant.

The typical CDM would operate helicopters and STOVL aircraft such as the current AV-8 Harrier, future V-22 Osprey and Advanced STOVL (ASTOVL). One through-deck CDM variant has been studied which typically operates ASTOVLs and V-22s but is also capable of landing, refueling, rearming and launching CTOL aircraft. This version has a

single electromagnetic catapult and three-wire arresting gear.

6.2.3 The New Big-Deck Carrier

Conventional takeoff and landing (CTOL) big-deck carriers will continue to exist, but in smaller numbers, and operate

only high-performance fighter and attack aircraft. To permit an all strike/interceptor airwing, the ASW, utility, COD and some AEW aircraft are offloaded to the CDMs. The big-deck carrier is envisioned to be a step beyond the present Nimitz class CVNs. These ships, which could be referred to as the CVN+, are designed for high-tempo operations with four catapults, three centerline aircraft elevators, and dual recovery decks clear of two of the

catapults. These would be the largest aviation capable ships and have the highest availability for air operations due to their good seakeeping. For the foreseeable future, these big-deck carriers will remain the best choice for large-scale air attack operations. The resulting design is sketched in Figure 9.

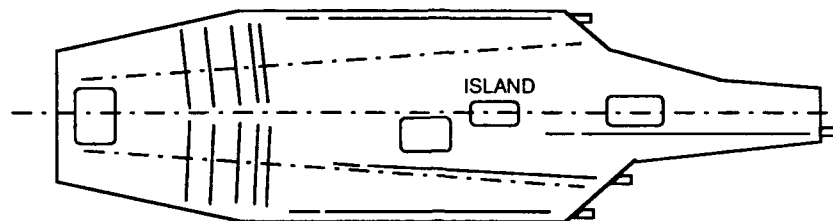


Figure 9. The CVN+ aircraft carrier.

6.2.4 The Combat Systems

All ships of the battle force would have related but not identical combat systems. The entire battle force is integrated for cooperative engagement. All of the sensors and all of the weapons in the force participate in the common information flow. At the heart of the combat system on each ship is an AEGIS-like combat system integration network. Each ship has one or more vertical launch missile magazines (VLS) and CIWS which provides at least two layers of AAW self defense (short range self defense gun and short range VLS missiles, four to each VLS cell). Long range anti-aircraft defense can be added in the form of long-range missiles in the VLS launcher and an airborne sensor, currently envisioned as a V-22 tiltrotor and/or a sea-launched High Altitude Long Endurance (HALE) aircraft.

A fourth AAW layer, that of the outer air battle, can be provided in several ways: (1) VLS launch of hypersonic missiles from any ship including the scout fighters; (2) STOVL aircraft, operable off any CDM; and (3) CTOL aircraft from the CVN+. ASW would be supported by both onboard and offboard sensors. ASW aviation is envisioned as a modularized V-22 to deploy and monitor active and passive sonobuoys and to prosecute contacts. These modularized V-22s have additional missions in airborne refueling, carrier onboard delivery, and vertical onboard delivery.

7. AVIATION REQUIREMENTS

7.1 Scout Fighter Aircraft Requirements

The Scout Fighters (SF), being small ships, will force their embarked aviation be able to cope with relatively large motions of the ship. Unless small waterplane area twin hull (SWATH) ships are developed for the SF role, seakeeping will be the governing limitation. VTOL operation will be required, probably assisted by a remote haul-down and traversing system. Hangar space and support facilities will be sized for a small number of embarked aircraft. It is conceivable that the SF would be used to extend the range of STOVL aircraft from the CDMs through refueling and rearming services plus very limited maintenance support.

Because of their small size, there will be less volume for hangars, storage and maintenance. On the other hand, the technology available may make it possible to operate with much smaller crews, which may free up some space for equipment and maintenance. More detailed studies are needed.

These design factors will impose restrictions on the air vehicles to operate from these small ships. The restricted volume available makes the small UAVs discussed earlier very attractive. If more detailed studies indicate the need for it, a new LAMPS-type ASW vehicle may be employed on the SF, too.

7.2 Carrier of Large Objects Aircraft Requirements

The CDM version of the Carrier of Large Objects (CLO) is primarily designed to accommodate rotorcraft and STOVL aircraft. If providing emergency landing facilities for CTOL aircraft becomes a requirement, the through-deck version can be pursued. The performance limitations imposed by the STOVL configuration can be mitigated by including a ski jump at the forward end of the flight deck. Any other type of VTOL aircraft can also be operated from the CDM.

A tiltrotor type of aircraft would be one good choice for a transport and long-range ASW platform. One STOVL is the AV-8 Harrier, currently in operation. A more advanced

ASTOVL is shown in Figure 10.

Since the CLO is an entirely different concept, its design is open to influence by the needs imposed by its embarked aircraft. One interesting example of this would be the modifications to the ship concept from a decision to sea-base a type of high altitude long endurance (HALE) AEW aircraft. A HALE typically has a very wide wingspan, wider than the beam of the ship. This aircraft would impose the elimination of the island control center from the flight deck. This reversion to the very earliest "flat top" configuration would require considerable ingenuity to find alternative means of providing the services now located in the island, especially the Primary Flight Control station (Pri-Fly).

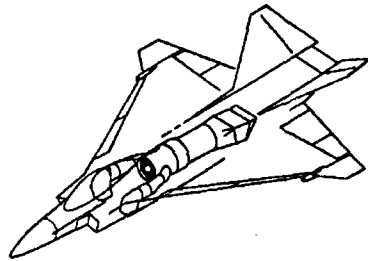


Figure 10. Advanced Short Takeoff and Landing aircraft (ASTOVL).

7.3 CVN+ Requirements

The opportunity to redesign the flight deck of the CVN+ opens up new possibilities for aircraft. The major requirements imposed on aviation would continue to be those related to the nose gear and tail hook. However, ski-jump bows and longer catapults and arresting gear would allow either lower stresses in the airframe or higher launch and approach speeds.

Another option to be considered for the large-deck carriers of the future is the use of powered lift to reduce the approach speeds and increase controllability. Systems like the ASTOVL designs and use of such techniques as circulation control could be applied to new fighter and attack aircraft. Lowering the approach speeds could be very effective in reducing the loads imposed on the catapults and arresting gear. The energy requirements of these items are linearly related to the kinetic energy of the aircraft at launch or recovery. Kinetic energy is related to the square of the speed, so small reductions in takeoff and landing speeds can result in large savings in the catapults and arresting gear.

7.4 Aircraft Missions

The new fleet we have been discussing will have a wide variety of missions, and this implies the embarked aircraft must also be capable of a wide variety of missions. Some of the aircraft missions might include the following:

- o Air Superiority
- o Long Range Attack
- o Surveillance
 - AEW (aircraft and ship targets)
 - ELINT
 - IR, visual
- o Localization and attack
 - Aircraft
 - Surface ships
 - Submarines
 - Over-the-horizon targeting (OTHT)
 - Midcourse guidance of missiles, torpedoes
- o Marine assault
 - Transport
 - Ground attack
 - Air superiority
- o Vertical Replenishment (VERTREP)

7.5 Aircraft Characteristics

The ship features and the variety of aircraft missions suggests the following characteristics will be desirable for the aircraft fleet of the year 2030.

- Smaller size aircraft (SF, CLO)
- Compact folding
- Ease of maintenance
- Low signatures
- Variety of sensors and weapons
- Need for hovering
 - dipping sonar (SF, CLO)
 - rescue
- Autonomous takeoff and landing
- Pilot associate functions
- Data link to ship
- Modular payloads for mission versatility

8. AIRCRAFT OPTIONS FOR THE YEAR 2030.

We have described the ships envisioned for the year 2030, the technical trends, the aircraft missions and the aircraft requirements. Now, what are the options for meeting all those restraints? A spectrum of several types and sizes of aircraft will be needed to carry out the complex missions of the future fleet.

One exciting concept is that of a partnership between manned and unmanned aircraft. The partners will operate as a team on many missions, with the manned aircraft providing instructions overall direction, and occasional guidance to the unmanned vehicle. We will focus on three types of manned aircraft and two types of unmanned air vehicle (UAV) to operate from the future CLOs and Scout Fighters. Long range planning is needed now so we will have time to identify and carry out the research and development required to make the fleet operational by the year 2030.

We believe the future air fleet will be comprised of families of integrated aircraft and UAVs designed to operate together in an effective manner. This includes the high performance aircraft for operation from aircraft carriers, the light attack

aircraft and transports designed for the CLO fleet, and the rotorcraft for operation from the smaller attack ships like the Scout Fighter.

The basic aircraft types include CTOL fighters and attack aircraft, new VTOL or STOVL vehicles, tiltrotors, helicopters, and VTOL UAVs. The tiltrotor concept has many attributes we need for this future fleet. Tiltrotors are heavier than helicopters, but fly much faster and farther. They are much more efficient for very low speed and hovering than jet-type VTOLs. We see, as noted earlier, the V-22 or its descendant operating as a modular payload vehicle, filling many roles, such as ASW, AEW, VOD, and carrying fuel for the other aircraft.

8.1 Scout Fighter Based Air Vehicles.

First, let us examine the options for aircraft for operation from the smaller Scout Fighter type ships. Assuming a manned aircraft is required, we envision a future air vehicle similar in purpose to the Light Airborne Multipurpose System Mark III (LAMPS III) of today. Of course, we do not mean an SH-60 will still be around then, but the approach to developing that system will be valid for the future fleet. The approach is to design an air vehicle capable of several missions, integrated into the ship systems as intimately as the ship's weapons and sensors. This vehicle will probably be a rotorcraft, to obtain efficient hovering and low speed capability and the inherent controllability required for operating from the small ships.

The primary mission will be ASW, just as in the present LAMPS vehicle. Because the future submarines will be very quiet, dipping sonar will probably be required, even with the more sensitive hydrophones. Thus the LAMPS 2030 will have to hover for dipping sonar as well as for personnel rescue.

This aircraft will also carry other sensors such as sonobuoys, infrared sensors, radar, and electronic intelligence gathering systems. All sensors will be data linked to the ship for further processing and integration with other data. Also, sensor processing will take place on the LAMPS air vehicle, and the processed data will be sent to the ship as well.

Although the present LAMPS helicopters carry torpedoes, the LAMPS 2030 will not. Instead, it will employ missile-boosted torpedoes from the ship's vertical launch tubes. It could also call for an anti-air missile or an anti-surface missile, and provide mid-course guidance to any of them. Eliminating the requirement to carry torpedoes and missiles will allow the vehicle to be smaller, matching the space requirements of the small Scout Fighter ship on which it is based.

The companion unmanned air vehicle for the LAMPS 2030 might be the Tipjet concept, shown in Figures 11 and 12. The Tipjet UAV, described in Reference 5, is a convertible rotorcraft. It takes off and lands like a helicopter, but converts to an airplane in flight by stopping the rotor. The rotor then becomes a high aspect ratio wing having excellent altitude and endurance capability. If high speed is desired, the wing may be swept, as in the oblique wing concept, allowing operation at much higher Mach number without the wave drag of the straight wing.

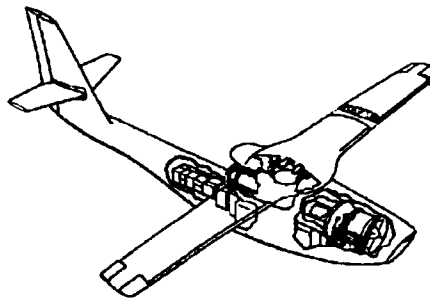


Figure 11. The Tipjet Unmanned Air Vehicle.

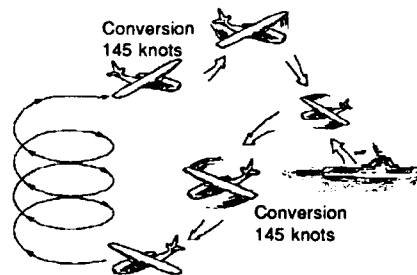


Figure 12. Tipjet UAV operation.

Other UAV concepts include the tiltrotor, already under investigation in a small flight test vehicle, tilt wing, or any VTOL design. However, it should be noted that jet VTOLs may not be compatible with these small ships.

As mentioned earlier, the SF could also be a temporary base for other types of VTOL aircraft, including a VTOL fighter/attack machine. This would give a group of SF ships an air superiority role in a limited engagement.

8.2 CLO-Based Aircraft

For the CLO, we need several different types of aircraft. For many of the missions of these ships, we will need a transport, like the present V-22. The transport missions would include carrier onboard delivery (COD) and replenishment duties. The same airframe could be adapted to the long-range ASW role offloaded from the CVs. Also, this airframe could be used in an aerial tanker configuration to refuel the fighters and transports.

The CLO will need an air superiority aircraft that will operate from this smaller flight deck. The ASTOVL designs now being investigated are good candidates for this fighter/attack mission. This aircraft can be considered the replacement of the current AV-8 fleet, with improved high speed performance and air-to-air missile capability.

A possible companion UAV for the ASTOVL fighter/attack aircraft would be a smaller version of the same concept. One manned aircraft might be accompanied by several of the UAVs, carrying close-in guns and missiles. This group of aircraft would be very deadly adversaries to an enemy.

The UAVs could also be used for long range attack of very dangerous targets or radar systems, and be controlled from the manned aircraft. Onboard computers would allow the UAVs to simply be directed, rather than requiring the manned vehicle pilot to provide detailed control.

Finally, the CLO will be a base for the future LAMPS 2030 system and its companion UAV as well, to supplement the SF based aircraft.

8.3 CVN+ Based Aircraft

For the future CVN+, we will need excellent air superiority and attack aircraft. The supercarrier will still be the vehicle for bringing to bear the massive firepower and air superiority for which current carriers are used. As stated earlier, we expect many of the missions to be offloaded to the CLO fleet.

For short range attack and air superiority, we expect to see the ATF, now under development, for many years. It should be noted that historically, airframes are typically kept in service through several generations of avionics equipment. Examine any example in the current inventory and you will find the older aircraft are operating their fourth or fifth set of avionics.

By the year 2030, we expect to see a new replacement for the A-6, to take over the heavy attack role. It is regrettable that the A-12 was cancelled, because we believe lower radar signatures are very important for future aircraft. With high-lift and/or powered lift systems, perhaps the catapults and arresting gear can handle the weight growth trend of future attack aircraft.

A recent announcement in the aviation press indicated a joint Navy/NASA program to investigate a Mach 5 carrier based aircraft.¹² Its projected takeoff weight is 36,300 kg (80,000 pounds). This Mach 5 vehicle could be used for numerous purposes. It might be configured for high altitude surveillance, air superiority, or other missions. However, without powered lift systems, it is unlikely that this aircraft could operate even from the future carriers. Careful attention must be paid to launch and takeoff configuration to reduce the required speeds and keep the kinetic energy within the limits of the catapults and arresting gear.

9. TRANSITION TO THE FUTURE

We have shown an innovative approach to the future Navy, and how to increase its effectiveness. We hope we have stimulated you to think creatively about that future. Please note that this effort was very limited, and did not examine many variations or options. Clearly, there are advantages to this approach, but much additional work is necessary to fully explore the potential of a revolution at sea. Now, how can we get there from here?

First, we must recognize that ships and aircraft take a long time from when an operational requirement is established to when the first few vehicles are out there in the fleet and fully operational. Based on recent history of actual procurement of new major weapon systems, this process takes about twenty years, based on an average of numerous procurement actions by all three of the U.S. Navy systems commands. The official actions required can be performed much faster, but this number includes the effects of all the delaying factors such as the budget process.

Second, we must recognize that present vehicles are kept operating for a long time, typically twenty or more years. Overhauls, service life extensions, and other such programs stretch the life of our weapon systems. Otherwise, they would not be affordable. This means that we cannot quickly replace all the ships and aircraft at once, but must use a long, gradual process.

Taken together, these facts make us look forty years ahead to define the fleet and the resulting vehicle requirements. Figure 13 shows the present fleet, the future fleet, and a transition period. The transition period is where the old ships are being gradually replaced by the new designs. As you can see, the transition is long. This is both for affordability and practical reasons like availability of shipyards and other manufacturing facilities. Also, training will be needed, so one must include simulators and other training systems in the plans.

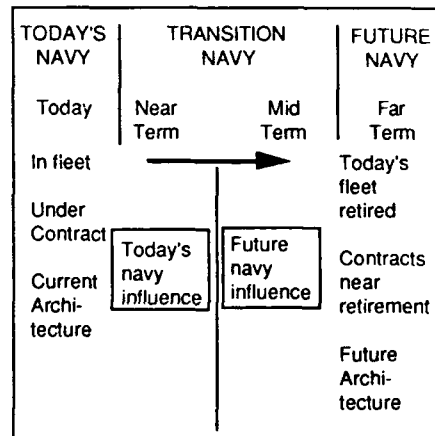


Figure 13. Transition to the future.

The conclusion of this schedule examination is that the future is NOW! If we are to make an impact, we must begin now to perform the studies that define the specific concepts to be pursued. That in turn defined the research required to bring the technology along, so it will be ready for the

designers when they need it.

10. CONCLUSIONS

- o Re-thinking naval aviation and the Carrier battle force is clearly a worthwhile effort. Significant gains are achievable at lower costs than today's fleet.
- o Many opportunities such as SWATH alternative hull forms and Super-cruise aircraft remain to be investigated.
- o Computer models are available in both the aviation and surface communities to do a credible job of assessing cost and effectiveness of alternate ships and aircraft.
- o System-wide studies integrating ships and aircraft in a combined force architecture are more difficult because of the historical separation of the lines of development.
- o The CDM⁵ and the FANGS⁴ efforts represent only a beginning. These approaches should be expanded upon in the future.
- o Aviation research is needed, targeted toward the missions and scenarios shown in this paper. More detailed studies are needed to define the research requirements.
- o Unmanned Air Vehicles are promising, and should be examined in more detail.
- o You are invited to contribute support and ideas.

Acknowledgment: Much of the work on ship design reported here has been adapted from a paper by LCDR Michael Bosworth, Aileen G. Kleiman and Steven C. Matz which was presented to the American Society of Naval Engineers in May of 1991⁵. Several related briefing packets and an unpublished FANGS paper⁴ by the same authors were also drawn upon for material. The ASNE source paper gives technical information on the ships presented here.

Disclaimer: This paper is an opinion piece by the authors. The views expressed herein are those of the authors and are not endorsed by the U.S. Department of Defense, the Department of the Navy, David Taylor Research Center, nor the Atlantic Research Corporation.

11. REFERENCES

1. Admiral Carlisle A.H. Trost, USN, "The Necessity for Naval Power in the 1990s," 30 December 1989, Open distribution copy of CNO (OP-OOK) Memorandum, citations are from pages 3-6 of the 11-page document, quoted at length in Inside The Navy, 4 March 1991, page 10.
2. Fuhrman, Peter, "The Soviet Army's Angst," Forbes

Magazine, 1 April 1991, pp. 42-43.

3. Naisbitt John, "Megatrends," Warner Books, New York, NY, 1982.
4. Naisbitt, John and Aburdene, Patricia, "Megatrends 2000," William Morrow & Co., New York, NY, 1990.
5. Schwartz, Alan R., Reader, Kenneth R., and Rogers, Ernest O., "An Unmanned Air Vehicle Concept with Tipjet Drive," American Helicopter Society and National Aeronautics and Space Administration, Specialists Meeting on Vertical Lift Aircraft Design, San Francisco, California, January 1990.
6. Nielsen, Jack N. and Biggers, James C.: *Recent Progress in Circulation Control Aerodynamics*. AIAA 25th Aerospace Sciences Meeting, Reno, Nevada, January 12-15, 1987.
7. Bryant, William R. Jr., "Hydrogen Fueled Aircraft in the USA," presented at 1991 SAE Aerospace Atlantic, April 22-26, 1991, Dayton, Ohio.
8. Etzold, Hon. Thomas H., "Strategy in the 21st Century," Center for Naval Warfare Studies and Naval Surface Warfare Center, January 1990.
9. Graham, Captain Clark, USN, and Bosworth, LCDR Michael L., USN, "Designing the Future U.S. Naval Surface Fleet for Effectiveness and Producibility", SNAME 1989 Ship Production Symposium, Arlington, Virginia, 13-15 September 1989.
10. Series of working papers and reports under the title "FANGS--Future Aircraft for Next Generation Ships", prepared for the Surface Ship and Aviation Technology Block Managers, Office of Naval Technology, by a team of representatives from the Naval Air Development Center, the Naval Air Engineering Center and David Taylor Research Center, 1989 and 1990.
11. Bosworth, LCDR Michael L., USN, Kleiman, Aileen G. and Matz Steven C., "Multimission Ship Design for an Alternative Fleet Concept," American Society of Naval Engineers Journal vol. 103, no. 3, May 1991, pp. 91-106.
12. Phillips, Edward H., "Langley Develops Thermal Management Concept for Hypersonic Aircraft," Aviation Week and Space Technology, McGraw Hill, April 15, 1991.

REPORT DOCUMENTATION PAGE															
1. Recipient's Reference	2. Originator's Reference	3. Further Reference	4. Security Classification of Document												
	AGARD-CP-509	ISBN 92-835-0641-3	UNCLASSIFIED												
5. Originator	Advisory Group for Aerospace Research and Development North Atlantic Treaty Organization 7 rue Ancelle, 92200 Neuilly sur Seine, France														
6. Title	AIRCRAFT SHIP OPERATIONS														
7. Presented at	the Flight Mechanics Panel Symposium held in Seville, Spain from 20th—23rd May 1991.														
8. Author(s)/Editor(s)	Various		9. Date November 1991												
10. Author's/Editor's Address	Various		11. Pages 348												
12. Distribution Statement	This document is distributed in accordance with AGARD policies and regulations, which are outlined on the back covers of all AGARD publications.														
13. Keywords/Descriptors	<table border="0"> <tr> <td>Aircraft carriers</td> <td>Shipboard landing</td> </tr> <tr> <td>Carrier based aircraft</td> <td>Flight tests</td> </tr> <tr> <td>Helicopters</td> <td>Computerized simulation</td> </tr> <tr> <td>Antisubmarine warfare</td> <td>Vertical takeoff aircraft</td> </tr> <tr> <td>Ship motion</td> <td>Search and rescue</td> </tr> <tr> <td>Guidance and control</td> <td>Amphibious operations</td> </tr> </table>			Aircraft carriers	Shipboard landing	Carrier based aircraft	Flight tests	Helicopters	Computerized simulation	Antisubmarine warfare	Vertical takeoff aircraft	Ship motion	Search and rescue	Guidance and control	Amphibious operations
Aircraft carriers	Shipboard landing														
Carrier based aircraft	Flight tests														
Helicopters	Computerized simulation														
Antisubmarine warfare	Vertical takeoff aircraft														
Ship motion	Search and rescue														
Guidance and control	Amphibious operations														
14. Abstract	<p>The interest in the use of shipborne aircraft is widespread among NATO countries. Major weapons systems like aircraft carriers with conventional fixed-wing aircraft, VSTOL aircraft or helicopters embarked, are operated by the United States, the United Kingdom, France, Italy and Spain. Nearly all NATO countries employ various classes of smaller ships as helicopter platforms for amphibious assault, anti-submarine warfare or search and rescue.</p> <p>The deployment of aircraft on board ships presents unusual and difficult technical and operational problems. Considering the multi-national interest in aircraft/ship operations it was considered meaningful and timely for the Flight Mechanics Panel to sponsor a symposium on this topic. This symposium considered problems of mutual interest connected with fixed and rotary wing aircraft operations from ships, and the application of new technology to enhance such operations.</p> <p>The Symposium reviewed and assessed the current problems and possible future progress in:</p> <ul style="list-style-type: none"> — The ship environment in terms of wind, temperature, precipitation, turbulence and deck motion; — Guidance, Controls and Displays, primarily in the approach and landing phase; — Flight Test and Simulation Techniques; — Launch, Recovery and Handling Systems Developments; — Operational/Pilot Views; and — Future Developments. 														

<p>AGARD Conference Proceedings 509 Advisory Group for Aerospace Research and Development, NATO AIRCRAFT SHIP OPERATIONS Published November 1991 348 pages</p> <p>The interest in the use of shipborne aircraft is widespread among NATO countries. Major weapons systems like aircraft carriers with conventional fixed-wing aircraft, VSTOL aircraft or helicopters embarked, are operated by the United States, the United Kingdom, France, Italy and Spain. Nearly all NATO countries employ various classes of smaller ships as helicopter platforms for amphibious assault, anti-submarine warfare or search and rescue.</p> <p>P.T.O.</p>	<p>AGARD-CP-509</p> <p>Aircraft carriers Carrier based aircraft Helicopters Antisubmarine warfare Ship motion Guidance and control Shipboard landing Flight tests Computerized simulation Vertical takeoff aircraft Search and rescue Amphibious operations</p>	<p>AGARD Conference Proceedings 509 Advisory Group for Aerospace Research and Development, NATO AIRCRAFT SHIP OPERATIONS Published November 1991 348 pages</p> <p>The interest in the use of shipborne aircraft is widespread among NATO countries. Major weapons systems like aircraft carriers with conventional fixed-wing aircraft, VSTOL aircraft or helicopters embarked, are operated by the United States, the United Kingdom, France, Italy and Spain. Nearly all NATO countries employ various classes of smaller ships as helicopter platforms for amphibious assault, anti-submarine warfare or search and rescue.</p> <p>P.T.O.</p>	<p>AGARD-CP-509</p> <p>Aircraft carriers Carrier based aircraft Helicopters Antisubmarine warfare Ship motion Guidance and control Shipboard landing Flight tests Computerized simulation Vertical takeoff aircraft Search and rescue Amphibious operations</p>
<p>AGARD Conference Proceedings 509 Advisory Group for Aerospace Research and Development, NATO AIRCRAFT SHIP OPERATIONS Published November 1991 348 pages</p> <p>The interest in the use of shipborne aircraft is widespread among NATO countries. Major weapons systems like aircraft carriers with conventional fixed-wing aircraft, VSTOL aircraft or helicopters embarked, are operated by the United States, the United Kingdom, France, Italy and Spain. Nearly all NATO countries employ various classes of smaller ships as helicopter platforms for amphibious assault, anti-submarine warfare or search and rescue.</p> <p>P.T.O.</p>	<p>AGARD-CP-509</p> <p>Aircraft carriers Carrier based aircraft Helicopters Antisubmarine warfare Ship motion Guidance and control Shipboard landing Flight tests Computerized simulation Vertical takeoff aircraft Search and rescue Amphibious operations</p>	<p>AGARD Conference Proceedings 509 Advisory Group for Aerospace Research and Development, NATO AIRCRAFT SHIP OPERATIONS Published November 1991 348 pages</p> <p>The interest in the use of shipborne aircraft is widespread among NATO countries. Major weapons systems like aircraft carriers with conventional fixed-wing aircraft, VSTOL aircraft or helicopters embarked, are operated by the United States, the United Kingdom, France, Italy and Spain. Nearly all NATO countries employ various classes of smaller ships as helicopter platforms for amphibious assault, anti-submarine warfare or search and rescue.</p> <p>P.T.O.</p>	<p>AGARD-CP-509</p> <p>Aircraft carriers Carrier based aircraft Helicopters Antisubmarine warfare Ship motion Guidance and control Shipboard landing Flight tests Computerized simulation Vertical takeoff aircraft Search and rescue Amphibious operations</p>

<p>The deployment of aircraft on board ships presents unusual and difficult technical and operational problems. Considering the multi-national interest in aircraft/ship operations it was considered meaningful and timely for the Flight Mechanics Panel to sponsor a symposium on this topic. This symposium considered problems of mutual interest connected with fixed and rotary wing aircraft operations from ships, and the application of new technology to enhance such operations.</p> <p>The Symposium reviewed and assessed the current problems and possible future progress in:</p> <ul style="list-style-type: none"> — The ship environment in terms of wind, temperature, precipitation, turbulence and deck motion. — Guidance, Controls and Displays, primarily in the approach and landing phase. — Flight Test and Simulation Techniques. — Launch, Recovery and Handling Systems Developments. — Operational/Pilot Views. — Future Developments. <p>ISBN 92-835-0641-3</p>	<p>The deployment of aircraft on board ships presents unusual and difficult technical and operational problems. Considering the multi-national interest in aircraft/ship operations it was considered meaningful and timely for the Flight Mechanics Panel to sponsor a symposium on this topic. This symposium considered problems of mutual interest connected with fixed and rotary wing aircraft operations from ships, and the application of new technology to enhance such operations.</p> <p>The Symposium reviewed and assessed the current problems and possible future progress in:</p> <ul style="list-style-type: none"> — The ship environment in terms of wind, temperature, precipitation, turbulence and deck motion. — Guidance, Controls and Displays, primarily in the approach and landing phase. — Flight Test and Simulation Techniques. — Launch, Recovery and Handling Systems Developments. — Operational/Pilot Views. — Future Developments. <p>ISBN 92-835-0641-3</p>
<p>The deployment of aircraft on board ships presents unusual and difficult technical and operational problems. Considering the multi-national interest in aircraft/ship operations it was considered meaningful and timely for the Flight Mechanics Panel to sponsor a symposium on this topic. This symposium considered problems of mutual interest connected with fixed and rotary wing aircraft operations from ships, and the application of new technology to enhance such operations.</p> <p>The Symposium reviewed and assessed the current problems and possible future progress in:</p> <ul style="list-style-type: none"> — The ship environment in terms of wind, temperature, precipitation, turbulence and deck motion. — Guidance, Controls and Displays, primarily in the approach and landing phase. — Flight Test and Simulation Techniques. — Launch, Recovery and Handling Systems Developments. — Operational/Pilot Views. — Future Developments. <p>ISBN 92-835-0641-3</p>	<p>The deployment of aircraft on board ships presents unusual and difficult technical and operational problems. Considering the multi-national interest in aircraft/ship operations it was considered meaningful and timely for the Flight Mechanics Panel to sponsor a symposium on this topic. This symposium considered problems of mutual interest connected with fixed and rotary wing aircraft operations from ships, and the application of new technology to enhance such operations.</p> <p>The Symposium reviewed and assessed the current problems and possible future progress in:</p> <ul style="list-style-type: none"> — The ship environment in terms of wind, temperature, precipitation, turbulence and deck motion. — Guidance, Controls and Displays, primarily in the approach and landing phase. — Flight Test and Simulation Techniques. — Launch, Recovery and Handling Systems Developments. — Operational/Pilot Views. — Future Developments. <p>ISBN 92-835-0641-3</p>

AGARD

NATO  OTAN

7 RUE ANCELLE · 92200 NEUILLY-SUR-SEINE
FRANCE

Téléphone (1)47.38.57.00 · Télex 610 176
Télécopie (1)47.38.57.99

DIFFUSION DES PUBLICATIONS
AGARD NON CLASSIFIEES

L'AGARD ne détient pas de stocks de ses publications, dans un but de distribution générale à l'adresse ci-dessus. La diffusion initiale des publications de l'AGARD est effectuée auprès des pays membres de cette organisation par l'intermédiaire des Centres Nationaux de Distribution suivants. A l'exception des Etats-Unis, ces centres disposent parfois d'exemplaires additionnels; dans les cas contraire, on peut se procurer ces exemplaires sous forme de microfiches ou de microcopies auprès des Agences de Vente dont la liste suit.

CENTRES DE DIFFUSION NATIONAUX

ALLEMAGNE

Fachinformationszentrum,
Karlsruhe
D-7514 Eggenstein-Leopoldshafen 2

BELGIQUE

Coordonnateur AGARD-VSL
Etat-Major de la Force Aérienne
Quartier Reine Elisabeth
Rue d'Evere, 1140 Bruxelles

CANADA

Directeur du Service des Renseignements Scientifiques
Ministère de la Défense Nationale
Ottawa, Ontario K1A 0K2

DANEMARK

Danish Defence Research Board
Ved Idraetsparken 4
2100 Copenhagen Ø

ESPAGNE

INTA (AGARD Publications)
Pintor Rosales, 34
28008 Madrid

ETATS-UNIS

National Aeronautics and Space Administration
Langley Research Center
M/S 180
Hampton, Virginia 23665

FRANCE

O.N.E.R.A. (Direction)
29, Avenue de la Division Leclerc
92320, Châtillon sous Bagneux

GRECE

Hellenic Air Force
Air War College
Scientific and Technical Library
Dekelia Air Force Base
Dekelia, Athens TGA 1010

ISLANDE

Director of Aviation
c/o Flugrad
Reykjavik

ITALIE

Aeronautica Militare
Ufficio del Delegato Nazionale all'AGARD
Aeroporto Pratica di Mare
00140 Pomezia (Roma)

LUXEMBOURG

Voir Belgique

NORVEGE

Norwegian Defence Research Establishment
Att: Biblioteket
P.O. Box 25
N-2007 Kjeller

PAYS-BAS

Netherlands Delegation to AGARD
National Aerospace Laboratory NLR
Kluyverweg 1
2629 HS Delft

PORTUGAL

Portuguese National Coordinator to AGARD
Gabinete de Estudos e Programas
CLAPA
Base de Alfragide
Alfragide
2700 Amadora

ROYAUME UNI

Defence Research Information Centre
Kentigern House
65 Brown Street
Glasgow G2 8EX

TURQUIE

Milli Savunma Başkanlığı (MSB)
ARGE Daire Başkanlığı (ARGE)
Ankara

LE CENTRE NATIONAL DE DISTRIBUTION DES ETATS-UNIS (NASA) NE DETIENT PAS DE STOCKS
DES PUBLICATIONS AGARD ET LES DEMANDES D'EXEMPLAIRES DOIVENT ETRE ADRESSEES DIRECTEMENT
AU SERVICE NATIONAL TECHNIQUE DE L'INFORMATION (NTIS) DONT L'ADRESSE SUIT.

AGENCES DE VENTE

National Technical Information Service
(NTIS)
5285 Port Royal Road
Springfield, Virginia 22161
Etats-Unis

ESA/Information Retrieval Service
European Space Agency
10, rue Mario Nikis
75015 Paris
France

The British Library
Document Supply Division
Boston Spa, Wetherby
West Yorkshire LS23 7BQ
Royaume Uni

Les demandes de microfiches ou de photocopies de documents AGARD (y compris les demandes faites auprès du NTIS) doivent comporter la dénomination AGARD, ainsi que le numéro de série de l'AGARD (par exemple AGARD-AG-315). Des informations analogues, telles que le titre et la date de publication sont souhaitables. Veuillez noter qu'il y a lieu de spécifier AGARD-R-*nnn* et AGARD-AR-*nnn* lors de la commande de rapports AGARD et des rapports consultatifs AGARD respectivement. Des références bibliographiques complètes ainsi que des résumés des publications AGARD figurent dans les journaux suivants:

Scientific and Technical Aerospace Reports (STAR)
publié par la NASA Scientific and Technical
Information Division
NASA Headquarters (NTT)
Washington D.C. 20546
Etats-Unis

Government Reports Announcements and Index (GRA&I)
publié par le National Technical Information Service
Springfield
Virginia 22161
Etats-Unis
(accessible également en mode interactif dans la base de
données bibliographiques en ligne du NTIS, et sur CD-ROM)



Imprimé par Specialised Printing Services Limited
40 Chigwell Lane, Loughton, Essex IG10 3TZ

AGARD

NATO  OTAN

7 RUE ANCELLE · 92200 NEUILLY-SUR-SEINE
FRANCE

Telephone (1)47.38.57.00 · Telex 610 176
Telefax (1)47.38.57.99

DISTRIBUTION OF UNCLASSIFIED
AGARD PUBLICATIONS

AGARD does NOT hold stocks of AGARD publications at the above address for general distribution. Initial distribution of AGARD publications is made to AGARD Member Nations through the following National Distribution Centres. Further copies are sometimes available from these Centres (except in the United States), but if not may be purchased in Microfiche or Photocopy form from the Sales Agencies listed below.

NATIONAL DISTRIBUTION CENTRES

BELGIUM

Coordonnateur AGARD - VSL
Etat-Major de la Force Aérienne
Quartier Reine Elisabeth
Rue d'Evere, 1140 Bruxelles

LUXEMBOURG

See Belgium

NETHERLANDS

Netherlands Delegation to AGARD
National Aerospace Laboratory NLR

CANADA

Director Scientific
Dept of National
Ottawa, Ontario



National Aeronautics and
Space Administration

Washington, DC. **SPECIAL FOURTH CLASS MAIL
BOOK**
20546

Postage and Fees Paid
National Aeronautics and
Space Administration
NASA-451

Official Business
Penalty for Private Use \$300



DENMARK

Danish Defence R
Ved Idrætsparke
2100 Copenhagen

FRANCE

O.N.E.R.A. (Direc
29 Avenue de la D
92320 Châtillon

GERMANY

Fachinformationsz
Karlsruhe
D-7514 Eggenstein

GREECE

Hellenic Air Force
Air War College
Scientific and Techn
Dekelia Air Force B
Dekelia, Athens TG.

ICELAND

Director of Aviation
c/o Flugrad
Reykjavik

ITALY

Aeronautica Militare
Ufficio del Delegato Nazionale all'AGARD
Aeroporto Pratica di Mare
00040 Pomezia (Roma)

UNITED KINGDOM

Defence Research Information Centre
Kentigern House
65 Brown Street
Glasgow G2 8EX

UNITED STATES

National Aeronautics and Space Administration (NASA)
Langley Research Center
M/S 180
Hampton, Virginia 23665

THE UNITED STATES NATIONAL DISTRIBUTION CENTRE (NASA) DOES NOT HOLD
STOCKS OF AGARD PUBLICATIONS, AND APPLICATIONS FOR COPIES SHOULD BE MADE
DIRECT TO THE NATIONAL TECHNICAL INFORMATION SERVICE (NTIS) AT THE ADDRESS BELOW.

SALES AGENCIES

National Technical
Information Service (NTIS)
5285 Port Royal Road
Springfield, Virginia 22161
United States

ESA/Information Retrieval Service
European Space Agency
10, rue Mario Nikis
75015 Paris
France


The British Library
Document Supply Centre
Boston Spa, Wetherby
West Yorkshire LS23 7BQ
United Kingdom

Requests for microfiches or photocopies of AGARD documents (including requests to NTIS) should include the word 'AGARD' and the AGARD serial number (for example AGARD-AG-315). Collateral information such as title and publication date is desirable. Note that AGARD Reports and Advisory Reports should be specified as AGARD-R-*nnn* and AGARD-AR-*nnn*, respectively. Full bibliographical references and abstracts of AGARD publications are given in the following journals:

Scientific and Technical Aerospace Reports (STAR)
published by NASA Scientific and Technical
Information Division
NASA Headquarters (NTT)
Washington D.C. 20546
United States

Government Reports Announcements and Index (GRA&I)
published by the National Technical Information Service
Springfield
Virginia 22161
United States

(also available online in the NTIS Bibliographic
Database or on CD-ROM)


Printed by Specialised Printing Services Limited
40 Chigwell Lane, Loughton, Essex IG10 3TZ

ISBN 92-835-0641-3